

Developing an amplitude level approach to radiative processes in quantum chromodynamics



The University of Manchester

Jack L.R. Holguin

Theoretical Particle Physics Group
School of Physics & Astronomy
Faculty of Science & Engineering
The University of Manchester

A thesis submitted for the degree of
Doctor of Philosophy

June 2021

Contents

1	Introduction	12
	References	13
2	Background	15
2.1	Quantum field theory	15
2.1.1	Dirac fields	17
2.1.2	The Maxwell Lagrangian	19
2.1.3	Electrodynamics	20
2.1.4	Gauge theories and Yang-Mills theory	21
2.1.5	Path integral quantisation	23
2.1.5.1	Gauge fixing with vector fields in $SU(N)$	25
2.2	Quantum chromodynamics	28
2.2.1	Chromodynamics	28
2.2.2	Quantum Lagrangian	30
2.2.3	The LSZ reduction formula and S-matrix	30
2.2.3.1	Feynman rules in momentum space without renormalisation	33
2.2.3.2	Gauge dependent terms and gluon propagators	36
2.2.4	BRST symmetries and Ward identities	39
2.2.5	Renormalised quantum action	43
2.2.6	The running coupling	46
2.3	Current frontiers of particle phenomenology	49
2.3.1	The Standard Model	49
2.3.2	Phenomenology at the Large Hadron Collider	51
	References	52
3	Quantum chromodynamics in the infra-red limit	56
3.1	A maths toolbox for kinematic factors in amplitudes	56
3.1.1	The method of regions	56
3.1.2	The KLN theorem	60

3.1.3	Spinor-helicity methods	63
3.2	A maths toolbox for colour factors in amplitudes	67
3.2.1	Basis independent colour charge operators	67
3.2.2	The colour flow basis	69
3.2.3	$1/N_c$ expansion	73
3.3	One diverging emission or loop	75
3.3.1	The soft limit of a loop	76
3.3.2	The soft limit of a real emission	84
3.3.3	The collinear limit of a loop	86
3.3.4	The collinear limit of a real emission	89
3.3.5	Generalisations	96
3.4	Resummation	99
3.4.1	Sudakov factors	100
3.4.1.1	Anomalous dimension matrices	102
3.4.2	Computing observables	103
3.4.2.1	Factorisation theorems	106
3.4.2.2	DGLAP evolution of a proton	109
3.4.2.3	Resummation of an observable	111
3.5	Parton showers	115
	References	117
4	Publication: Parton branching at amplitude level	122
4.1	Preface	122
4.2	Introduction	128
4.3	The algorithm	130
4.3.1	Parton branching with interleaved soft and collinear evolution (A)	132
4.3.2	Parton branching using complete collinear splitting functions (B)	137
4.3.3	Collinear subtractions and the ordering variable	140
4.3.4	A local recoil prescription	143
4.3.4.1	A LL_Σ recoil prescription	146
4.3.5	A manifestly infra-red finite reformulation	147
4.4	Collinear factorisation	149
4.4.1	Factorisation on hard legs without Coulomb interactions	149
4.4.1.1	The details	154
4.4.1.2	Recovering the ‘plus prescription’	155
4.4.2	Complete collinear factorisation without Coulomb interactions	156

4.4.3	Partial collinear factorisation with Coulomb interactions	161
4.4.4	Observations on factorisation	163
4.5	Phenomenology and resummations	164
4.5.1	DGLAP evolution	164
4.5.2	Example resummations	166
4.5.2.1	Thrust	167
4.5.2.2	Hemisphere jet mass	168
4.5.2.3	Gaps-between-jets	169
4.6	Conclusions	170
4.7	Appendix: Splitting functions	170
4.8	Appendix: Connecting to other work on spin	176
	References	181
5	Publication: Comments on a new ‘full colour’ parton shower	185
5.1	Preface	185
5.2	Introduction	188
5.3	Summary of the new ‘full colour’ parton shower	189
5.4	The problem with Sudakovs	190
5.5	Conclusions	193
	References	193
6	Publication: Building a consistent parton shower	195
6.1	Preface	195
6.2	Introduction	199
6.3	Evolution equations	200
6.3.1	Amplitude evolution overview	200
6.3.2	Angular ordered shower	203
6.3.3	Dipole shower	206
6.4	Improving recoil in dipole showers	209
6.4.1	NLC and NLL accuracy of the global recoil	213
6.5	Conclusions	217
6.6	Appendix: The evolution equations supplementary material	217
6.6.1	Amplitude evolution detailed definitions	217
6.6.1.1	Computing observables	220
6.6.2	Derivation of the angular ordered shower	220
6.6.2.1	Observable dependence and logarithmic accuracy	223
6.6.2.2	Azimuthal averaging	225

6.6.3	Derivation of the dipole shower	229
6.7	Appendix: Spin averaging	234
6.8	Appendix: Dipole shower with spectator recoil	235
6.8.1	NLC and NLL accuracy of the spectator recoil	236
6.9	Appendix: Further checks	237
6.9.1	Thrust with NLL accuracy using global recoil	237
6.9.2	Generating functions for jet multiplicity using global recoil	240
	References	242
7	Publication: Improvements on dipole shower colour	246
7.1	Preface	246
7.2	Introduction	251
7.3	A recap of the $\mathcal{O}(\alpha_s^2)$ QCD squared matrix element	253
7.4	Computing the squared matrix element with the dipole shower	256
7.4.1	$\mathcal{O}(\alpha_s^2)$ with emissions ordered in angle	258
7.4.2	$\mathcal{O}(\alpha_s^2)$ with emissions unordered in angle	260
7.4.3	Summary	261
7.5	Colour factors for emissions unordered in angle	263
7.5.1	The effects of momentum conservation	265
7.6	Errors in other dipole showers	267
7.7	Conclusions	270
7.8	Appendix: Drawing planar diagrams at arbitrary order	271
7.9	Appendix: Current limitations of our dipole shower	272
	References	274
8	Publication: Coulomb gluons will generally destroy coherence	278
8.1	Preface	278
8.2	Introduction	281
8.2.1	Case study: gaps between jets	281
8.3	General considerations	283
8.4	The logarithmic order of coherence violation	285
8.5	Conclusions	289
	References	289
9	Conclusions and outlook	292

A	Definitions and identities	297
A.1	Dirac algebra and polarisation sums	297
A.2	Spinor-helicity identities	298
A.3	Sudakov decompositions, kinematic variables and phase-space measures	299
A.4	Dimensional regularisation	300
	References	302

Word count: 65658

Abstract

This thesis details studies into soft and collinear radiation dressing QCD hard process amplitudes. Primarily, we present a formalism which reduces the computation of arbitrary multiplicities of soft and collinear QCD radiation in the massless limit, dressing any QCD hard process, to a single Markovian evolution equation. We present the evolution equation at leading logarithmic order, with complete spin correlations, and notably without approximating the QCD colour charge; though our formalism can be systematically extended beyond this order. We investigate the formalism and find that it can be used to study the accuracy of modern day parton showers, motivate new parton showers with increased accuracy, and study the factorisation properties of QCD processes in hadron colliders. From our studies, we introduce a new form of dipole shower, constructed to inherit the accuracy of an angular-ordered shower without losing the benefits and generalised applicability of a traditional dipole shower. We also study observables which suffer from coherence violating logarithms in proton evolution at hadron colliders. We arrive at the conclusion that almost all observables at hadron colliders will violate coherence to some degree. Only observables entirely insensitive to wide-angle soft physics remain completely safe.

This thesis consists of five individual publications and supplementary material providing context and greater detail. This thesis is also supplemented with an extended discussion of introductory material on quantum chromodynamics and quantum field theories more broadly.

Declaration

No portion of the work referred to in this thesis has been submitted in support of an application for another degree or qualification of this or any other university or other institute of learning.

This is a journal format thesis. It is constructed from five original publications by this thesis's author and collaborators. Each publication is presented with a preface providing context to the research. Before each publication there is also a declaration, making clear the author's contributions and the originality of the work. This thesis also contains three chapters before the presentation of these publications. These chapters cover much of the academic background and necessary prerequisite knowledge needed to understand the publications.

Copyright

1. The author of this thesis (including any appendices and/or schedules to this thesis) owns certain copyright or related rights in it (the “Copyright”) and s/he has given The University of Manchester certain rights to use such Copyright, including for administrative purposes.
2. Copies of this thesis, either in full or in extracts and whether in hard or electronic copy, may be made only in accordance with the Copyright, Designs and Patents Act 1988 (as amended) and regulations issued under it or, where appropriate, in accordance with licensing agreements which the University has from time to time. This page must form part of any such copies made.
3. The ownership of certain Copyright, patents, designs, trademarks and other intellectual property (the “Intellectual Property”) and any reproductions of copyright works in the thesis, for example graphs and tables (“Reproductions”), which may be described in this thesis, may not be owned by the author and may be owned by third parties. Such Intellectual Property and Reproductions cannot and must not be made available for use without the prior written permission of the owner(s) of the relevant Intellectual Property and/or Reproductions.
4. Further information on the conditions under which disclosure, publication and commercialisation of this thesis, the Copyright and any Intellectual Property and/or Reproductions described in it may take place is available in the University IP Policy (see <http://documents.manchester.ac.uk/DocuInfo.aspx?DocID=24420>), in any relevant Thesis restriction declarations deposited in the University Library, The University Library’s regulations (see <http://www.library.manchester.ac.uk/about/regulations/>) and in The University’s policy on Presentation of Theses.

Acknowledgements

There are many people who deserve thanks for helping me complete my studies and this thesis. Chief amongst them is my PhD supervisor, Prof. Jeff Forshaw. Jeff's patient guidance has helped lead me from one interesting research project to the next and facilitated my growth as a scientist. His teachings, from my undergraduate studies through to my PhD, deserve a large amount of the credit for what I have achieved as a physicist, and for any ability I now have to convey my achievements. I also would like to thank Dr. Simon Plätzer who I have worked closely with throughout my PhD. Simon has been both a colleague and a mentor to me. In no particular order, I am also indebted to Dr. Agni Bethani, Dr. Aditya Pathak, Matthew De Angelis, Jack Helliwell, Chris Shepherd, and Keiran Finn for their friendship, collaboration and overall helping to keep my PhD as enjoyable as possible. Thanks too to the Manchester Particle Physics group.

On a personal note, I would like to thank my parents, Helen and Simon, and my sisters, Amy and Nina. It is through their care and encouragement that I am who I am today. My wider family, grandparents, aunts and uncles, also deserve credit for this. Thanks too to my partner Lorna who has brightened the years of my life since we met and has done an admirable job putting up with me throughout my PhD and a pandemic. An honourable mention goes to my lock-down bubble: Ciaran, Jemma, and Phil. Despite multiple PhD's being undertaken and theses being written, I think we did a pretty good job staying sane during a global crisis. I would also like to acknowledge the role that the climbing crews at Rockover, the Depot Manchester, and MCC have played in making my many years living in Manchester so enjoyable. Between my friends, colleagues, the climbing community, the music and queer scenes, I cannot imagine a place I would rather have studied my PhD than Manchester. Finally, I would like to thank my secondary school maths and physics teachers, particularly Mr. G., without whom I might not have gone down the path I have.

Preface

I have written this thesis with two goals, other than the thesis being suitable to attain a PhD. Firstly I have tried to provide a sufficiently detailed summary of the research, prior to my own, so that someone else working in QCD theory can read my work with minimal effort. This is the purpose of Chapter 3 and the prefaces provided before each paper. Secondly, I have covered some of the relevant foundations of QCD and QFT that underpin my work. In my experience so far, the people who benefit most from reading theses are those who are new to the field of research. Perhaps a graduate student near the start of their studies. My aim is that a graduate student with a mathematical inclination, some experience of particle physics, QFT, and of group theory (such as I at the start of my doctoral studies) would also benefit from reading this thesis and would be able to understand my work (though perhaps with a little more than minimal effort). To this end, I have also included Chapter 2. This chapter aims to concisely cover much of the necessary foundations needed to work specifically on the problems I have studied. Most of Chapter 2 would typically be left out of a doctoral thesis and instead can be found scattered across some famous hefty textbooks. My hope is that presenting this information in a concise form is helpful to somebody (or at least myself in the future).

I would like to give a brief comment on writing style. I recognise that the ability to write compelling and articulate prose is not a talent of mine - rather something I must work hard on. To aid me, this thesis is largely written in the plural first person, such as is common in scientific literature. During my studies I have become accustomed to writing in this style and it is the style in which my included publications are written. However, I will also sometimes employ singular first person when making comments directly to the reader.

Chapter 1

Introduction

“It’s a dangerous business, Frodo, going out your door. You step onto the road, and if you don’t keep your feet, there’s no knowing where you might be swept off to.”

— Bilbo Baggins, J.R.R. Tolkien, *The Fellowship of the Ring*

In the modern era, the phenomenology of particle physics is predominantly studied by exploring the properties of quantum fields. However, whilst theories of quantum fields have provided some of the most accurate predictions physicists have ever made, quantum fields are notoriously complicated. Quantum chromodynamics (QCD) is simultaneously one of the most experimentally tested quantum field theories (QFTs) and also one of the most difficult to use. In this thesis, we aim to address pertinent questions on how to accurately extract predictions from QCD in collider experiments.

QCD is the mathematical formulation underpinning the currently prevailing theory of the strong nuclear force. It describes the interaction of fundamental quantum fields for quarks and gluons, and the particles that emerge from these fields. In principle, QCD describes a huge range of phenomena: from the internal structure of nuclei within atoms, to the degeneracy pressure of a neutron star, and to properties of the primordial plasma less than a second after the big bang. QCD is unified with theories for electromagnetism and the weak nuclear force (responsible for radiative decay) to give the Standard Model. The Standard Model, as a QFT, [1] and Einstein’s general relativity [2] together form the present frontier of experimentally verified fundamental physics. However, it is known that this picture is incomplete.

The detailed study of data from collider experiments (such as the LHC [3], HERA [4], LEP [5] and the Tevatron [6]) has provided some of most significant advancements in fundamental physics in the last several decades. This thesis aims to help continue this paradigm. Until recently, relatively few processes with significant contributions from QCD have been

studied at collider experiments with percent level precision. A large hurdle in achieving precise predictions from QCD has been accurately describing the large multiplicities of QCD radiation produced at collider experiments. To this end, this thesis studies QCD radiation. The goal of this thesis is to present a new unified formalism for the computation of QCD radiation, applicable to any process at a collider experiment where large amounts of momentum is transferred by particles in an inelastic collision. Studying this formalism is interesting in its own right, however we also endeavour to use the formalism to derive improvements to other, currently used, descriptions of QCD radiation.

This thesis is structured as follows. Chapter 2 presents an overview of QFTs with a focus on deriving many of the elementary properties of QCD. A reasonably complete description of QFTs and QCD would necessarily be far too extensive for inclusion in a single thesis. Therefore, Chapter 2 reflects the biases of the author. It consists of only a selection of the fundamental aspects of QCD that I consider most essential to the study of high energy radiation in collider experiments, and the elementary building blocks of QFTs underpinning QCD. Chapter 3 builds further on the foundations in Chapter 2, presenting many of the foundational results used in the study of QCD radiation. To aid the reader, Chapter 3 starts with a ‘maths toolbox’ presenting mathematical techniques useful to the study of QCD amplitudes. Chapter 4 presents the formalism we develop for the computation of QCD radiation. We refer to the formalism as ‘parton branching at amplitude level’. We study the formalism and from it re-derive several seminal results describing QCD at collider experiments, most notably we study the collinear factorisation of QCD amplitudes with and without Coulomb/Glauber gluons. Following this, Chapters 5, 6, and 7 use insight from our parton branching formalism to highlight errors in and improvements to other widely used descriptions of QCD radiation. Chapter 8 builds on insight from our study of collinear factorisation to evaluate the significance of ‘coherence-violating logarithms’ in observables one might measure at hadron collider experiments. Chapters 4 through 8 are presented in the journal format. Finally, we conclude our findings in Chapter 9 and discuss prospects for future research. An Appendix is included covering common and useful definitions.

References

- [1] S. Weinberg, “A Model of Leptons”, *Phys. Rev. Lett.* **1967**, *19*, 1264–1266.
- [2] A. Einstein, “Die Feldgleichungen der Gravitation”, *Sitzungsberichte der Königlich Preussischen Akademie der Wissenschaften (Berlin)* **1915**, 844–847.
- [3] “LHC Machine”, *JINST* **2008**, *3*, (Eds.: L. Evans, P. Bryant), S08001.
- [4] H. Abramowicz, A. Caldwell, “HERA collider physics”, *Rev. Mod. Phys.* **1999**, *71*, 1275–1410, arXiv: [hep-ex/9903037](https://arxiv.org/abs/hep-ex/9903037).

- [5] S. Myers, “The LEP collider, from design to approval and commissioning”, **1991**, DOI [10.5170/CERN-1991-008](https://doi.org/10.5170/CERN-1991-008).
- [6] R. R. Wilson, “The Tevatron”, *Phys. Today* **1977**, *30N10*, 23–30.

Chapter 2

Background

“If there’s any kind of magic in this world it must be in the attempt of understanding” ... “I know, it’s almost impossible to succeed ... but who cares really? The answer must be in the attempt.”

— Celine, Before Sunrise

2.1 Quantum field theory

Quantum field theory is a broad theoretical framework that combines quantum mechanics and classical field theory. Since its birth, it has seen a great deal of applications over many fields in physics. It has been successfully applied to solid state physics, where it is used to imbue the macroscopic properties of a material with quantum phenomena. A quintessential example is the quantisation of the magnetic field of a ferromagnet. The quantum magnetic field contains bosonic pseudo-particle excitations known as magnons; the superposition of their wave functions generating the macroscopic magnetic field. In this situation the quantum field theory is not fundamental but is an ‘effective field theory’ that describes the system when viewed at an appropriate scale, the fundamental theory is provided by atomic theory. However, there are also quantum field theories that are considered fundamental - at least so far as experimental verification is concerned. These are the quantum field theories of particle physics and the Standard Model. This chapter will provide an overview of these theories with a particular focus on the fundamentals of quantum chromodynamics.

The starting point for quantum field theory was the development of the Klein-Gordon [1, 2] equation describing the dynamics of both free scalar fields and particles;

$$(\partial^\mu \partial_\mu + m^2)\varphi(x) = 0, \tag{2.1}$$

where $\varphi(x)$ is either a relativistic scalar field or the wave function of a relativistic scalar particle, and m is the mass of the field/particle. The Klein-Gordon equation is constructed

so that in momentum space it gives the Einstein relation

$$(-E^2 + \mathbf{p}^2 + m^2)\varphi(p) = 0. \quad (2.2)$$

Quantum field theory connects the relativistic Klein-Gordon scalar field with the relativistic Klein-Gordon particle by quantising the field: the field quanta are the particles. We will illustrate this very quickly using canonical quantisation, initially in the Schrödinger picture.¹ The Klein-Gordon Lagrangian and Hamiltonian densities for a real scalar field are

$$\mathcal{L}_{\text{KG}} = \frac{1}{2}\partial^\mu\varphi\partial_\mu\varphi - \frac{1}{2}m^2\varphi^2, \quad \mathcal{H}_{\text{KG}} = \frac{1}{2}\pi^2 + \frac{1}{2}(\nabla\varphi)^2 + \frac{1}{2}m^2\varphi^2, \quad \pi = \frac{\partial\mathcal{L}}{\partial(\partial_t\varphi)}, \quad (2.3)$$

where π is the conjugate field. The canonical quantisation conditions come from promoting the field to being operator valued, $\varphi \rightarrow \hat{\varphi}$. On top of this, Poisson brackets of the field and its conjugate are promoted to commutators of the operators;

$$[\hat{\varphi}(\mathbf{x}), \hat{\pi}(\mathbf{y})] = i\delta^3(\mathbf{x} - \mathbf{y}), \quad [\hat{\varphi}(\mathbf{x}), \hat{\varphi}(\mathbf{y})] = [\hat{\pi}(\mathbf{x}), \hat{\pi}(\mathbf{y})] = 0. \quad (2.4)$$

We can solve the system for $\hat{\varphi}(\mathbf{x})$ by making use of a Fourier decomposition

$$\hat{\varphi}(\mathbf{x}) = \int \frac{d^3\mathbf{p}}{(2\pi)^3} e^{i\mathbf{p}\cdot\mathbf{x}} \hat{\varphi}(\mathbf{p}). \quad (2.5)$$

By applying the Klein-Gordon equation to $\hat{\varphi}(\mathbf{x})$ and imposing the quantisation commutation relations, it can be found that

$$e^{i\mathbf{p}\cdot\mathbf{x}} \hat{\varphi}(\mathbf{p}) = \frac{e^{i\mathbf{p}\cdot\mathbf{x}}}{\sqrt{2(\mathbf{p}^2 + m^2)^{\frac{1}{2}}}} \hat{a}(\mathbf{p}) + \frac{e^{-i\mathbf{p}\cdot\mathbf{x}}}{\sqrt{2(\mathbf{p}^2 + m^2)^{\frac{1}{2}}}} \hat{a}^\dagger(\mathbf{p}), \quad (2.6)$$

where $\hat{a}(\mathbf{p})$ and $\hat{a}^\dagger(\mathbf{p})$ are ladder operators obeying the same commutation relations as in the quantum harmonic oscillator:

$$[\hat{a}(\mathbf{p}), \hat{a}^\dagger(\mathbf{q})] = (2\pi)^3 \delta^3(\mathbf{p} - \mathbf{q}). \quad (2.7)$$

The ladder operators therefore act as creation and annihilation operators $\hat{a}(\mathbf{p})|\mathbf{p}\rangle = |\emptyset\rangle$ and $\hat{a}^\dagger(\mathbf{p})|\emptyset\rangle = |\mathbf{p}\rangle$.² The state $|\mathbf{p}\rangle$ is a particle quantum, in the field $\hat{\varphi}(\mathbf{x})$, with 3-momentum \mathbf{p} and obeys the Klein-Gordon equation in operator form

$$(-\hat{E}^2 + \hat{\mathbf{p}}^2 + m^2)|\mathbf{p}\rangle = 0. \quad (2.8)$$

¹In the Schrödinger picture operators are time independent and states are time dependent. Conversely, Heisenberg picture operators are time dependent and states are time independent.

²It is worth noting that the commutation relation for $\hat{a}(\mathbf{p})$ and $\hat{a}^\dagger(\mathbf{p})$ does not have a Lorentz invariant normalisation. Consequently, neither does the bracket $\langle\mathbf{p}|\mathbf{q}\rangle = (2\pi)^3 \delta^3(\mathbf{p} - \mathbf{q})$. A Lorentz invariant delta function is given by $(2\pi)^3 2E_{\mathbf{p}} \delta^3(\mathbf{p} - \mathbf{q})$. Some authors choose to normalise the ladder operators as $\hat{a}(\mathbf{p}) \rightarrow \hat{a}(\mathbf{p})/\sqrt{2E_{\mathbf{p}}}$, ensuring brackets and commutators have Lorentz invariant normalisations. In practice the choice of normalisation is largely aesthetic.

In the Schrödinger picture, the time evolution of a state is given by $|\varphi(t)\rangle = \hat{U}(t)|\varphi(0)\rangle$ where $\hat{U}(t) = \exp(i\hat{H}t)$ and \hat{H} is the Hamiltonian. Heisenberg picture operators, at a time t , can be found from Schrödinger picture operators via $\hat{O}_H(t) = \hat{U}(t)\hat{O}_S\hat{U}(t)^{-1}$.

This is the only discussion of canonical quantisation in this thesis. Later we will need to study quantisation in the context of gauged field theories and gauge fixing. In these discussions we will employ the more sophisticated approach of path integral quantisation. However, for each of the theories we discuss the two approaches are equivalent. Remembering the canonical approach can be a helpful to guide intuition.

2.1.1 Dirac fields

The Klein-Gordon equation was a first attempt at relativistically covariant formulation for quantum mechanics, however it had several limitations. The equation showed promise in providing a description for the quantum mechanics of bosonic systems but it seemed incompatible with fermionic systems and spin. Also, the equation was second order making it difficult to solve. This motivated Dirac to find a linear equation. We will now give an overview of the equation Dirac found [3, 4], from a modern perspective.³

In the previous section we summarised the quantum field theory of free Lorentz scalar fields. Under active Lorentz transformations scalar fields transform as

$$\Lambda : \varphi(x) \mapsto \varphi'(x) = \varphi(\Lambda^{-1}x), \quad \text{where } \Lambda \in \text{SO}(1, 3), \quad (2.9)$$

where the same transformation sends coordinates $x \mapsto x' = \Lambda x$.⁴ Let us now consider a general field ϕ in some representation of the Lorentz group. This field must transform as

$$\Lambda : \phi(x) \mapsto \phi'(x) = D(\Lambda)\phi(\Lambda^{-1}x), \quad \text{where } \Lambda \in \text{SO}(1, 3) \text{ and } D(\Lambda) \in \text{repSO}(1, 3), \quad (2.10)$$

where $\text{repSO}(1, 3)$ is some representation of the Lorentz group. In the following section we will discuss the special case in which $D(\Lambda) = \Lambda$, i.e. the field is a vector field. In this section we will explore the spinor representation.

Continuous transformations can be constructed by the exponentiation of group generators. A helpful parametrisation of a general transformation in the Lorentz group is

$$D(\Lambda) = e^{\frac{1}{2}\Omega_{\rho\tau}S^{\rho\tau}} \quad \text{for} \quad \Lambda = e^{\frac{1}{2}\Omega_{\rho\tau}M^{\rho\tau}}, \quad (2.11)$$

³The following discussion is based on those in [5, 6].

⁴Passive transformations are equivalent to co-ordinate redefinitions. Active transformations transform the frame in which an object is defined: i.e. $\varphi(x)$ which must be equal to $\varphi'(x')$ under an active transformation, hence it is necessary that $\varphi'(x) = \varphi(\Lambda^{-1}x)$.

where $\Omega_{\rho\tau}$ are the parameters defining the transformation, $M^{\rho\tau}$ are the six $\text{SO}(1,3)$ group generators and $S^{\rho\tau}$ are the six $\text{repSO}(1,3)$ group generators. They are anti-symmetric matrices that are members of the Lorentz Lie algebra;

$$[S^{\rho\tau}, S^{\sigma\nu}] = g^{\rho\nu} S^{\tau\sigma} - g^{\sigma\nu} S^{\tau\rho} + g^{\tau\sigma} S^{\rho\nu} - g^{\rho\tau} S^{\nu\sigma}, \quad (2.12)$$

where $g = \text{Diag}(1, -1, -1, -1)$ is the Minkowski metric. The question of finding a representation effectively reduces to finding a set of matrices $\{S^{\rho\tau}\}$ that satisfy the above commutation relations. One such representation is the spinor representation, for which $S^{\rho\tau}$ can be constructed using a Clifford algebra. The Clifford algebra is defined by the anti-commutator

$$\{\gamma^\mu, \gamma^\nu\} = 2g^{\mu\nu}1. \quad (2.13)$$

A useful basis for the algebra is the chiral basis;

$$\gamma^\mu = \begin{pmatrix} 0 & \sigma^\mu \\ \bar{\sigma}^\mu & 0 \end{pmatrix}, \quad (2.14)$$

where $\sigma^0 = 1$, $\bar{\sigma}^i = -\sigma^i$, and σ^i are the Pauli spin matrices. Using the Clifford algebra we can define $S^{\rho\tau} = \frac{1}{4}[\gamma^\rho, \gamma^\tau]$; it can be checked that this satisfies the Lorentz Lie algebra.

Now let us briefly explore the properties of a field that transforms under the spinor representation of the Lorentz group. First let us look at rotations in space; the $\text{SO}(3)$ subgroup of $\text{SO}(1,3)$. Let's consider rotations by angle θ around an axis \mathbf{n} ; i.e. $\Lambda = R(\mathbf{n}, \theta) \in \text{SO}(3)$. Three of the $\text{SO}(1,3)$ generators form the Lie algebra of the $\text{SO}(3)$ subgroup. These generators generate the rotation by θ , in doing so fixing $\Omega_{\rho\tau}$. In turn $\Omega_{\rho\tau}$ can then be used as input to find $D(\Lambda)$. We obtain $D(R(\mathbf{n}, \theta)) = R(\mathbf{n}, \theta/2)$. This is the transformation rule for the rotation of a fermion.

As with a scalar field, we can insist that our new found fermion field also obeys Einstein's relation by setting

$$(\partial^\mu \partial_\mu + m^2)\phi(x) = 0. \quad (2.15)$$

We can use the Clifford algebra to manipulate this expression. Note that

$$g^{\mu\nu} \partial_\mu \partial_\nu = \frac{1}{2} \{\gamma^\mu, \gamma^\nu\} \partial_\mu \partial_\nu = \gamma^\mu \gamma^\nu \partial_\mu \partial_\nu.$$

Using this we can factorise the Klein-Gordon equation;

$$(i\gamma^\mu \partial_\mu + m)(i\gamma^\nu \partial_\nu - m)\phi(x) = 0. \quad (2.16)$$

As the second order differential operator on ϕ factorises, the set of solutions to the first order differential equation $(i\gamma^\nu \partial_\nu - m)\phi(x) = 0$ necessarily obey Einstein's relation. Solutions

to the linear equation are traditionally labelled $\psi(x)$ and are named Dirac fields. Thus we arrive at the famous Dirac equation for a Dirac field,

$$(i\gamma^\mu\partial_\mu - m)\psi(x) = 0. \quad (2.17)$$

The Dirac equation is Lorentz covariant, not invariant like the Klein Gordon equation. To build Lorentz invariants we must introduce a conjugate field $\bar{\psi}(x) = \psi^\dagger(x)\gamma^0$. Using $\bar{\psi}(x)$ we can write a Lorentz invariant Lagrangian density consistent with the Dirac equation;

$$\mathcal{L}_D = \bar{\psi}(x)(i\cancel{\partial} - m)\psi(x), \quad (2.18)$$

where $\cancel{\partial} = \gamma^\mu\partial_\mu$. The Dirac field can be canonically quantised in the Schrödinger picture using techniques similar to the quantisation of the Klein-Gordon field; the techniques modified for fermionic degrees of freedom. Specifically, it's required for fermionic fields that commutators get replaced by anti-commutators

$$\{\hat{\psi}_\alpha(\mathbf{x}), \hat{\pi}_{\psi\beta}(\mathbf{y})\} = i\delta^3(\mathbf{x} - \mathbf{y}), \quad \{\hat{\psi}_\alpha(\mathbf{x}), \hat{\psi}_\beta(\mathbf{y})\} = \{\hat{\pi}_{\psi\alpha}(\mathbf{x}), \hat{\pi}_{\psi\beta}(\mathbf{y})\} = 0, \quad (2.19)$$

where α and β are spinor indices. The quantised free Dirac field in the Schrödinger picture has the form

$$\hat{\psi}_\alpha(\mathbf{x}) = \sum_s \int \frac{d^3\mathbf{p}}{(2\pi)^3} \frac{1}{\sqrt{2}(\mathbf{p}^2 + m^2)^{\frac{1}{4}}} \left(e^{i\mathbf{p}\cdot\mathbf{x}} u^s(\mathbf{p}) \hat{b}^s(\mathbf{p}) + e^{-i\mathbf{p}\cdot\mathbf{x}} v^s(\mathbf{p}) \hat{c}^{s\dagger}(\mathbf{p}) \right), \quad (2.20)$$

where $u^s(\mathbf{p})$ and $v^s(\mathbf{p})$ are the spinor solutions of spin s to the Dirac equation in momentum space. $\hat{b}^s(\mathbf{p})$ and $\hat{c}^{s\dagger}(\mathbf{p})$ are ladder operators for fermionic and anti-fermionic degrees of freedom respectively, with spin s .⁵

2.1.2 The Maxwell Lagrangian

In the previous sections we discussed the construction of relativistically covariant field theories. To build a field theory for fermions we had to employ some quite heavy mathematical machinery; representation theory and new algebras. By contrast, the classical description of electromagnetism is a manifestly Lorentz covariant field theory from the outset. In fact classical electrodynamics motivated the first study of the Lorentz group. In this section we will review some key features of electromagnetism. However, we will leave the quantisation of the theory to a later section.

⁵It is important to note that when spinor indices are dropped, it is implicit that (anti-)commutators of spinor fields refer only to the (anti-)commutation of operators in the field's definition so that both terms produced by the (anti-)commutator have the same dimension: i.e. $\hat{\psi}\hat{\pi}_\psi$ is a rank $\binom{1}{1}$ tensor whilst $\hat{\pi}_\psi\hat{\psi}$ is a scalar. For instance $\{u^s\hat{b}^s, u^{s\dagger}\hat{b}^{s\dagger}\} = \{\hat{b}^s, \hat{b}^{s\dagger}\}u^s u^{s\dagger}$.

A free electromagnetic field is described by the Maxwell Lagrangian density:

$$\mathcal{L}_{\text{Mx}} = -\frac{1}{4}F_{\mu\nu}F^{\mu\nu}, \quad \text{where} \quad F_{\mu\nu} = \partial_\mu A_\nu - \partial_\nu A_\mu. \quad (2.21)$$

A_μ is a vector potential for the electromagnetic field. Maxwell's equations are obtained from the equations of motion,

$$\frac{\partial \mathcal{L}_{\text{Mx}}}{\partial(\partial_\mu A_\nu)} = -\partial_\mu F^{\mu\nu} = 0, \quad \rightarrow \quad (g_{\mu\nu}\partial_\sigma\partial^\sigma - \partial_\mu\partial_\nu)A^\nu = 0, \quad (2.22)$$

and the Bianchi identity (a consequence of our definition of $F_{\mu\nu}$),

$$\partial_{[\mu}F_{\nu\sigma]} = 0. \quad (2.23)$$

The Maxwell Lagrangian is invariant under a gauge transformation

$$A_\mu \rightarrow A_\mu + \partial_\mu\alpha(x), \quad (2.24)$$

for all reasonable functions $\alpha(x)$ (functions that are continuous and decay suitably fast as $x \rightarrow \infty$). At this stage, the gauge symmetry makes canonical quantisation tricky since it causes the equations of motion to not be invertible. We will give the symmetry both a geometric interpretation and tackle quantisation properly later (Sections 2.1.4 and 2.1.5).

2.1.3 Electrodynamics

Let us now put the work of our previous sections together and couple the electromagnetic field to matter fermionic fields. The Lagrangian density for electrodynamics (EM fields coupled to a charged current) is given by

$$\mathcal{L}_{\text{ED}} = -\frac{1}{4}F_{\mu\nu}F^{\mu\nu} - ej^\mu A_\mu, \quad (2.25)$$

where j^μ is some vector current and e is the coupling strength. There is only one bilinear of Dirac spinors with the same mass dimension as j^μ that transforms as a vector; $\bar{\psi}\gamma^\mu\psi$. Putting the Maxwell Lagrangian together with the Dirac Lagrangian, with this coupling term, we find the bare Lagrangian for quantum electrodynamics

$$\mathcal{L}_{\text{QED}} = -\frac{1}{4}F_{\mu\nu}F^{\mu\nu} + \bar{\psi}(x)(i\not{\partial} - e\gamma^\mu A_\mu - m)\psi(x). \quad (2.26)$$

We can make a few observations. Firstly, the coupling between the vector field and the Dirac field has broken the individual gauge invariance of the vector field. Secondly, the Lagrangian is symmetric under a global U(1) symmetry; $\psi(x) \rightarrow e^{i\alpha}\psi(x)$. If we apply Noether's theorem [7] (or see [8] for a more accessible discussion) we find that the global symmetry ensures that the current $j^\mu = \bar{\psi}\gamma^\mu\psi$ is conserved ($\partial_\mu j^\mu = 0$). Thirdly, the Lagrangian does have a gauge symmetry, however it is constructed from the composition of a local U(1) transformation, $\psi(x) \rightarrow e^{-ie\alpha(x)}\psi(x)$, and a gauge transformation of the vector field, $A_\mu \rightarrow A_\mu + \partial_\mu\alpha(x)$. In the next section, we will argue that this composite transformation is a local U(1) gauge transformation of the combined theory.

2.1.4 Gauge theories and Yang-Mills theory

Let us think more about the implications of \mathcal{L}_{QED} 's gauge symmetry. It is easy to see that $\psi(x)$ is transforming locally under the fundamental representation of $U(1)$, but what is governing how A_μ transforms?

Think back to general relativity. The covariant derivative of a field $\phi^a(x)$ in an arbitrary representation of the Lorentz group is given by

$$\nabla_\mu \phi^a(x) = \partial_\mu \phi^a(x) + \Gamma_{\mu c}^a \phi^c(x);$$

μ, ν are indices in the fundamental representation of the Lorentz group and roman indices are indices over the representation in which $\phi^a(x)$ transforms. $\Gamma_{\mu c}^a$ is the connection on the space-time manifold of the theory. This derivative transforms covariantly under co-ordinate transformations $x \rightarrow J(x)x$ and $\phi^a(x) \rightarrow D_b^a(x; J)\phi^b(J(x)x)$; i.e.

$$\nabla_\mu \phi^a(x) \rightarrow D_b^a(x; J)J_\mu^\nu(x)\nabla_\nu \phi^b(J(x)x).$$

This is ensured by the connection, $\Gamma_{\mu c}^a$, which is an object defined in the tangent space⁶ to the space-time manifold in which $\phi^a(x)$'s basis exists that acts to compensate for the variation of said basis. Dropping the arguments, the connection transforms as

$$\Gamma_{\mu c}^a \rightarrow J_\mu^\nu D_b^a \Gamma_{\nu d}^b (D^{-1})_c^d - J_\mu^\nu (D^{-1})_c^b \partial_\nu D_b^a.$$

Now consider a situation where $J = 1$ but our representation of $\phi^a(x)$ is degenerate over some isometries (gauge transformations). We can re-parametrise $\phi^a(x)$ by a gauge transformation $\phi^a(x) \rightarrow D_b^a(x)\phi^b(x)$ where $D_b^a(x) \in G$ the isometry group of our representation. Under this transformation $\nabla_\mu \phi^a(x) \rightarrow D_b^a(x)\nabla_\mu \phi^b(x)$ and

$$\Gamma_{\mu c}^a \rightarrow D_b^a \Gamma_{\mu d}^b (D^{-1})_c^d - (D^{-1})_c^b \partial_\mu D_b^a.$$

In the previous section we saw that \mathcal{L}_{QED} was invariant under a local $U(1)$ transformation of the Dirac field, $\psi(x) \rightarrow e^{-ie\alpha(x)}\psi(x)$, if the electromagnetic field also transformed via a gauge transformation as $A_\mu \rightarrow A_\mu + \partial_\mu \alpha(x)$. The transformation of the EM field can be written in an alternative form,

$$A_\mu \rightarrow e^{-ie\alpha(x)} A_\mu e^{ie\alpha(x)} + \frac{i}{e} e^{ie\alpha(x)} \partial_\mu e^{-ie\alpha(x)}.$$

This is exactly how the connection transforms under a $U(1)$ gauge transformation, up to the factor $\frac{i}{e}$ which arises from the normalisation pre-factors to A_μ . This gives us intuition

⁶Strictly speaking, the connection is defined in the principal fibre bundle of the space-time manifold as it 'connects' the tangent space at a point, x , on the manifold to the tangent spaces at the points in the infinitesimal neighbourhood of x .

for what is going on. The fermion field is defined in a representation of the gauge group, in this case the fundamental representation of $U(1)$ which is trivial - hence why we didn't have to consider its gauge group representation when putting \mathcal{L}_D together. The vector field is defined in the tangent space (strictly the tangent bundle) of our gauge group and plays the role of a connection. Hence, this field is defined in a representation of the Lie algebra of the group, also trivial for $U(1)$. Therefore the gauge transformations that leave \mathcal{L}_{QED} invariant are local $U(1)$ transformations for which $\psi(x)$ transforms in the fundamental representation of $U(1)$ and A_μ transforms in the fundamental representation of the Lie algebra of $U(1)$ (denoted $\mathfrak{u}(1)$). This motivates naming A_μ a gauge field.

Let us now consider generalising the Maxwell Lagrangian. We can do so by introducing a gauge field defined in the Lie algebra of a more complicated group. Let us pick $SU(N)$. Now our gauge field is of the form $\vec{A}_\mu = A_\mu^a T^a$ where T^a are the generators of $SU(N)$ in the fundamental representation. The generators are $N \times N$ matrices, there are $N^2 - 1$ of them, and they are elements of the group Lie algebra $\mathfrak{su}(N)$. To build a Lagrangian for \vec{A}_μ first we must generalise $F_{\mu\nu}$ to $SU(N)$. $F_{\mu\nu}$ is gauge covariant. We can rewrite its definition in such a way as to make this manifest; $F_{\mu\nu} = -\frac{i}{e}[D_\mu, D_\nu]$ where D_μ is the gauge covariant derivative of a field transforming in the fundamental representation of $U(1)$, $D_\mu = (\partial_\mu + ieA_\mu)$.⁷ Written in this form, it is easy to see that a gauge transformation on $F_{\mu\nu}$ gives $e^{-ie\alpha(x)}F_{\mu\nu}e^{ie\alpha(x)} = F_{\mu\nu}$. We can extend this definition to an $SU(N)$ gauge theory by defining an appropriate $SU(N)$ gauge derivative,

$$D_\mu = (1_N \partial_\mu - ig\vec{A}_\mu). \quad (2.27)$$

This derivative is gauge covariant when acting on any field, ϕ , that transforms in the fundamental representation of $SU(N)$; i.e. if $\phi \rightarrow U(x)\phi$ then $D_\mu\phi \rightarrow U(x)D_\mu\phi$ where $U(x) \in SU(N)$. Now by analogy to the $U(1)$ case we can introduce a field strength tensor

$$\vec{F}_{\mu\nu} = \frac{i}{g}[D_\mu, D_\nu], \quad (2.28)$$

where $(\vec{F}_{\mu\nu})_{ij} = F_{\mu\nu}^a T_{ij}^a$. By construction the field strength tensor transforms under an $SU(N)$ gauge transformation as $\vec{F}_{\mu\nu} \rightarrow U(x)\vec{F}_{\mu\nu}U(x)^{-1}$. Now we have $\vec{F}_{\mu\nu}$ we can define a gauge invariant Lagrangian for the $SU(N)$ gauge field - the Yang-Mills Lagrangian. The Lagrangian density is

$$\mathcal{L}_{\text{YM}} = -\frac{1}{2}\text{Tr}(\vec{F}_{\mu\nu}\vec{F}^{\mu\nu}) = -\frac{1}{4}F_{\mu\nu}^a F^{\mu\nu a}. \quad (2.29)$$

⁷Continuing our analogies to general relativity, we can see that $F_{\mu\nu}$ is just the curvature tensor in another guise.

This Lagrangian now comes equipped with two self interaction terms between the gauge fields (these terms are given at the head of Section 2.2.1) and a global $SU(N)$ symmetry. This global symmetry results in a conserved current of gauge fields. We will come back to the interaction terms and current later in the context of QCD. The Lagrangian has a gauge symmetry under the transformations

$$\vec{A}_\mu \rightarrow U(x)\vec{A}_\mu U(x)^{-1} - \frac{i}{g} (\partial_\mu U(x)) U(x)^{-1}, \quad \text{where } U(x) \in SU(N). \quad (2.30)$$

Finally, we have given the definition of a gauge covariant derivative when acting on a field transforming in a representation of $SU(N)$. However, it is helpful to also define the covariant derivative of objects which are defined in $\mathfrak{su}(N)$, the Lie algebra of $SU(N)$; objects such as the field tensor and the gauge fields. It can be checked that $D_\sigma \vec{F}_{\mu\nu} = \partial_\sigma \vec{F}_{\mu\nu} - ig[\vec{A}_\sigma, \vec{F}_{\mu\nu}]$ transforms as required, $D_\sigma \vec{F}_{\mu\nu} \rightarrow U(x)D_\sigma \vec{F}_{\mu\nu} U(x)^{-1}$. Using this gauge derivative, the equations of motion are

$$D_\mu \vec{F}^{\mu\nu} = 0, \quad D_{[\mu} \vec{F}_{\nu\sigma]} = 0. \quad (2.31)$$

2.1.5 Path integral quantisation

In this section we will review some of the important features of the path integral for quantum fields. We will not derive the path integral since a derivation would be both lengthy and wholly unnecessary for our work.⁸

When working with a quantum theory, we are interested in (in terms of making predictions) the overlap of a state at a time t_i with another state at a later time t_f . An alternative approach to quantisation is to simply define how to compute this transition. This is the approach of path integral quantisation. The basic path integral for a transition in a general quantum field theory from a state Ω at time t_i to state Ω' at time t_f has the form

$$\langle \Omega'(t_f) | \Omega(t_i) \rangle = N \int_{b,c} \mathcal{D}[\{\phi\}] \exp \left(i \int_{t_i}^{t_f} dt \int d^{d-1}x \mathcal{L}(\{\phi\}) \right). \quad (2.32)$$

The set $\{\phi\}$ is the set of quantum degrees of freedom of the field theory; i.e. the fields. The measure $\mathcal{D}[\{\phi\}]$ integrates over every possible configuration of the degrees of freedom between times t_i and t_f with the boundary conditions that the configurations corresponding to states at times $t_{i,f}$ are fixed as $|\{\phi(t_i)\}\rangle = |\Omega(t_i)\rangle$ and $|\{\phi(t_f)\}\rangle = |\Omega'(t_f)\rangle$. N is a normalisation factor, often compensating for divergences in the path integral itself.

⁸Furthermore, for some field theories (with non-linear kinetic terms or complicated non-polynomial potentials) the path integral cannot be derived by the usual methods employed by physicists but instead must be postulated. Moreover, a mathematician might argue that path integrals in quantum field theory cannot be rigorously derived (except in some special cases). On this we will choose to bury our head in the sand.

The path integral effectively assigns a phase to each configuration $|\{\phi(t)\}\rangle$, computes their superposition and then projects the outcome onto the $|\Omega'(t_f)\rangle$ state.

Eq. (2.32) is entirely obtuse as to how path integrals actually work. To help, let us re-write the equation with all the limits in place in (1+1)D and with a single field $\phi(x)$,

$$\langle \Omega'(t_f) | \Omega(t_i) \rangle = \lim_{a \rightarrow 0} N(a) \int_{b.c} \prod_{x_{k,k'}} d\phi(x_{k,k'}) \exp \left(i \sum_{t_k \in [t_i, t_f]} \sum_{\text{all } x_{k'}} \mathcal{L}_d(\phi(x_{k,k'})) a^2 \right), \quad (2.33)$$

where $x_{k,k'} = (t_k, x_{k'})^T$ is a general point in latticed space-time with a lattice spacing a ; i.e. $x_{k+n,k'+m} - x_{k,k'} = (na, ma)^T$. \mathcal{L}_d is the discretised Lagrangian density; built by making substitutions of the form $\phi(x) \rightarrow \phi(x_{k,k'})$ and $\partial_t \phi(x) \rightarrow (\phi(x_{k,k'}) - \phi(x_{k-1,k'}))/a$.⁹ Notice that if the Lagrangian depends on derivatives then the phase, $e^{ia^2 \mathcal{L}(\phi(x_{k,k'}))}$, assigned to each field configuration $\phi(x_{k,k'})$ is also dependent on adjacent field configurations $\phi(x_{k\pm 1, k'\pm 1})$. This propagates a dependence on the boundary conditions throughout the whole integral.

We will now itemise a few key points in the study of path integrals. Firstly the partition function of a theory is defined as

$$Z = \lim_{T \rightarrow \infty(1-i\epsilon)} \langle \Omega(T) | \Omega(-T) \rangle = \lim_{T \rightarrow \infty(1-i\epsilon)} N \int_{b.c} \mathcal{D}[\{\phi\}] \exp \left(i \int_{-T}^T dt \int d^{d-1}x \mathcal{L}(\{\phi\}) \right), \quad (2.34)$$

where $|\Omega(t)\rangle$ is the ground (or vacuum) state of the theory at a time t . From now on we will treat the $T \rightarrow \infty(1-i\epsilon)$ limit as implicit in a $d^d x$ measure. Relatedly, the generating partition functional is defined as

$$Z[\{J_\phi\}] = N \int_{b.c} \mathcal{D}[\{\phi\}] \exp \left(i \int d^d x \mathcal{L}(\{\phi\}) + i S_{\text{gen}}[\{J_\phi\}, \{\phi\}] \right), \quad (2.35)$$

so that $Z[\{0\}] = Z$ and

$$\frac{\delta Z[\{J_\phi\}]}{\delta J_\phi(x_1)} = N \int_{b.c} \mathcal{D}[\{\phi\}] i\phi(x_1) \exp \left(i \int d^d x \mathcal{L}(\{\phi\}) + i S_{\text{gen}}[\{J_\phi\}, \{\phi\}] \right), \quad (2.36)$$

where $\frac{\delta}{\delta J_\phi(x)}$ is a functional derivative;

$$\frac{\delta J_\phi(y)}{\delta J_\phi(x)} = \delta^d(x-y),$$

and where $S_{\text{gen}}[\{J_\phi\}, \{\phi\}]$ is defined so that $Z[\{J_\phi\}]$ has the properties given. For example, if the theory is of a single scalar field, $\{\phi\} = \varphi$, then $S_{\text{gen}}[\{J_\phi\}, \{\phi\}] = \int d^d x J(x)\varphi(x)$. The

⁹There can be some ambiguity in defining the discretised Lagrangian. These ambiguities can have consequences whenever one tries to evaluate the path integral at finite a , either with the intention of finding an approximate solution or with the intention to take the limit at a later stage. This affects research into lattice QCD and other latticed field theories but it shan't be discussed further in this thesis.

generating function can be used to compute correlation functions:

$$\lim_{T \rightarrow \infty(1-i\epsilon)} \left\langle \Omega(T) \left| \mathbb{T}\{\hat{\phi}_a(x_1) \dots \hat{\phi}_b(x_n)\} \right| \Omega(-T) \right\rangle = \frac{(-i)^n}{Z} \frac{\delta^n Z[\{J_\phi\}]}{\delta J_{\phi_a}(x_1) \dots \delta J_{\phi_b}(x_n)} \Big|_{\text{all } J_\phi=0}, \quad (2.37)$$

where $\mathbb{T}\{\dots\}$ time-orders the operators in the braces; i.e.

$$\mathbb{T}\{\hat{\phi}_a(x_1)\hat{\phi}_b(x_2)\} = \hat{\phi}_a(x_1)\hat{\phi}_b(x_2)|_{t_1>t_2} \pm \hat{\phi}_b(x_2)\hat{\phi}_a(x_1)|_{t_2>t_1},$$

where the plus sign is for bosonic fields and the minus for fermionic. Notice that the normalisation factor cancels between the numerator and denominator, thus it is typical to ignore the factor and set $N = 1$. Finally a fermionic degree of freedom, $\psi_a(x)$, appears in path integrals as a Grassmann field. Grassmann fields can be decomposed as $\psi_a(x) = \sum_i \Psi_a^{(i)}(x)\omega_i$ where each $\Psi_a^{(i)}(x)$ is a complex (not Grassmann) field with index a and each ω_i is a Grassmann number. We can get a feel for why Grassmann numbers emerge by looking at one of their properties: Grassmann numbers anti-commute. This means that $\{\omega_i, \omega_j\} = 0$ which can be compared with the commutator for ‘normal’ numbers $[a, b] = 0$. As the quantisation of fermionic fields is dependent on anti-commutators, the necessity for Grassmann numbers arises naturally. Algebra with Grassmann numbers is both interesting and important to quantum field theory but we point the reader to other literature for more details [8].

2.1.5.1 Gauge fixing with vector fields in $SU(N)$

Up to now, we have avoided the issue of the quantisation of a gauge field. This was with good reason. If we tried to apply the approach of canonical quantisation we would quickly run into a stumbling block. In this approach it is necessary for us to constrain the form of the field operator by taking the Fourier transform and ensuring that the field solves the equations of motion for the theory in momentum space. However, the equations of motion for a gauge field are not invertible: since the equations are covariant under gauge transformations, they have a spectrum of gauge equivalent solutions. This prevents us from uniquely specifying a consistent quantisation of the theory via a naive canonical quantisation approach.¹⁰

Instead, let us consider quantising the theory via the path integral formalism. The partition function for an $SU(N)$ Yang-Mills theory is given by

$$Z = \int \mathcal{D}[A] \exp\left(-i \int d^d x \frac{1}{4} F_{\mu\nu}^a F_a^{\mu\nu}\right). \quad (2.38)$$

¹⁰The following discussion is based on that in [9].

If we tried to evaluate this partition function we would rapidly come across divergences. Intuitively, divergences emerge because for every physical field configuration we include we must also integrate over the infinite spectrum of unphysical degenerate configurations, equivalent up to a gauge transformation. This is the same issue that made our equations of motion not invertible. However, the partition function itself isn't what matters to us when trying to use a theory (under most circumstances). It is just a tool to compute correlators of operators

$$\langle \Omega | T \{ \hat{O}(A) \} | \Omega \rangle = Z^{-1} \int \mathcal{D}[A] O(A) \exp \left(-i \int d^d x \frac{1}{4} F_{\mu\nu}^a F_a^{\mu\nu} \right), \quad (2.39)$$

where $\hat{O}(A)$ is a gauge invariant operator built from the field operators \hat{A} . If we were to fix the gauge we work in, it might allow the divergent gauge degrees of freedom to cancel in the computation of correlators. This is the essence of the Faddeev and Popov trick [10] for gauge fixing.

Consider a possible gauge fixing condition $G(A) = 0$. We want to try and 'sneak' this into our Lagrangian in such a way that correlators remain unchanged. As a simple example, consider trying to evaluate $\int dx dy f(x, y)$ when we know that the condition $y = w(x)$ will make the integral much simpler. We could try multiplying by

$$1 = \int dw \delta(w(x) - y).$$

Here it is important to note that the integrand is actually independent of y as x can always adjust itself to compensate and that $w(x)$ must be integrated over the same range as y . Thus we are able to write

$$\int dx dy f(x, y) = \int dw \delta(w(x) - y) dx dy f(x, y) = Y \int dx dy \delta(w(x) - y) f(x, w(x)),$$

where Y is the total volume of the y integration, it now acts a global factor. The Faddeev and Popov trick [10] is essentially the same procedure. It uses a gauge fixing condition, $G(A) = 0$, to factorise the integration over degenerate gauge configurations out from the partition function.

To begin the trick, we make an infinitesimal gauge transformation so that $A_\mu^a \mapsto {}^\alpha A_\mu^a = A_\mu^a + \frac{1}{g} D_\mu \alpha^a(x)$ and use this as input to a generalisation of the Dirac delta function:

$$1 = \int \mathcal{D}[\alpha] \delta^\infty(G({}^\alpha A)) \det \left(\frac{\delta G({}^\alpha A)}{\delta \alpha} \right). \quad (2.40)$$

Applying this to Eq. (2.39), we find

$$\int \mathcal{D}[A] O(A) e^{iS[A]} = \int \mathcal{D}[\alpha] \int \mathcal{D}[{}^\alpha A] O({}^\alpha A) e^{iS[{}^\alpha A]} \delta^\infty(G({}^\alpha A)) \det \left(\frac{\delta G({}^\alpha A)}{\delta \alpha} \right). \quad (2.41)$$

Where we used that $\mathcal{D}[\alpha A] = \mathcal{D}[A]$, $O(\alpha A) = O(A)$, and $S[\alpha A] = S[A]$ since they each are individually invariant under gauge transformations. Now let us assume a form for our gauge fixing so that $G(\alpha A) \rightarrow G(\alpha A) - w(x)$ where $w(x)$ has no dependence on α . We can also multiply Eq. (2.39) by a Gaussian integral over $w(x)$ that is normalised to 1,

$$\int \mathcal{D}[A] O(A) e^{iS[A]} = N(\xi) \int \mathcal{D}[w] \exp\left(-i \int d^d x \frac{w^2}{2\xi}\right) \int \mathcal{D}[\alpha A] O(\alpha A) e^{iS[\alpha A]}. \quad (2.42)$$

Using this expression in conjunction with Eq. 2.41, we can write

$$\begin{aligned} & \int \mathcal{D}[A] O(A) e^{iS[A]} \\ &= N(\xi) \int \mathcal{D}[w, \alpha, \alpha A] O(\alpha A) \exp\left(iS[\alpha A] - i \int d^d x \frac{w^2}{2\xi}\right) \delta^\infty(G(\alpha A)) \det\left(\frac{\delta G(\alpha A)}{\delta \alpha}\right). \end{aligned} \quad (2.43)$$

Now we can perform the integral over $w(x)$ using the delta function

$$\begin{aligned} & \int \mathcal{D}[A] O(A) e^{iS[A]} \\ &= N(\xi) \int \mathcal{D}[\alpha, \alpha A] O(\alpha A) \exp\left(iS[\alpha A] - i \int d^d x \frac{G(\alpha A)^2}{2\xi}\right) \det\left(\frac{\delta G(\alpha A)}{\delta \alpha}\right). \end{aligned} \quad (2.44)$$

The gauge fixing condition has now been integrated into the same exponent as the action and could be absorbed into the definition of a quantum action. Finally, noting the following identity with Grassmann fields, c and \bar{c} ,

$$\int \mathcal{D}[c] \mathcal{D}[\bar{c}] \exp\left(-i \int d^d x \bar{c} B c\right) = \det(B), \quad (2.45)$$

we remove the determinant and write

$$\begin{aligned} & \int \mathcal{D}[A] O(A) e^{iS[A]} \\ &= N(\xi) \int \mathcal{D}[\alpha, \alpha A, \bar{c}, c] O(\alpha A) \exp\left[iS[\alpha A] - i \int d^d x \left(\frac{G(\alpha A)^2}{2\xi} + \bar{c} \frac{\delta G(\alpha A)}{\delta \alpha} c\right)\right]. \end{aligned} \quad (2.46)$$

As every configuration of αA is integrated over, it is no more than a dummy variable and we can safely relabel $\alpha A \rightarrow A$. Finally, if we pick $G(A)$ so that it is a linear operation on $\alpha(x)$, then the Grassmann term does not depend on $\alpha(x)$. As such, the integral over α factorises out as a global prefactor, just as Y did in our toy example. Applying what has been derived to Eq. (2.39), the matrix element can now be written as

$$\begin{aligned} \langle \Omega | T \{ \hat{O}(A) \} | \Omega \rangle &= \frac{N(\xi) \int \mathcal{D}[\alpha] \int \mathcal{D}[A, \bar{c}, c] O(A) \exp\left[iS[A] - i \int d^d x \left(\frac{G(A)^2}{2\xi} + \bar{c} \frac{\delta G(A)}{\delta \alpha} c\right)\right]}{N(\xi) \int \mathcal{D}[\alpha] \int \mathcal{D}[A, \bar{c}, c] \exp\left[iS[A] - i \int d^d x \left(\frac{G(A)^2}{2\xi} + \bar{c} \frac{\delta G(A)}{\delta \alpha} c\right)\right]}, \\ &= \frac{\int \mathcal{D}[A, \bar{c}, c] O(A) \exp\left[iS[A] - i \int d^d x \left(\frac{G(A)^2}{2\xi} + \bar{c} \frac{\delta G(A)}{\delta \alpha} c\right)\right]}{\int \mathcal{D}[A, \bar{c}, c] \exp\left[iS[A] - i \int d^d x \left(\frac{G(A)^2}{2\xi} + \bar{c} \frac{\delta G(A)}{\delta \alpha} c\right)\right]}. \end{aligned} \quad (2.47)$$

This procedure has fixed the gauge, removing the immediate problems with quantising the theory. However, the procedure has introduced two new terms that must be incorporated into the Lagrangian, one of which introduces new unphysical Grassmann fields known as ‘ghosts’.¹¹ We can define a quantum partition function incorporating these new terms;

$$Z = \int \mathcal{D}[A, \bar{c}, c] \exp \left[i \int d^d x \left(-\frac{1}{4} F_{\mu\nu}^a F_a^{\mu\nu} - \frac{G(A)^2}{2\xi} - \bar{c} \frac{\delta G(A)}{\delta \alpha} c \right) \right]. \quad (2.48)$$

The terms in the parentheses can be identified as a quantum Lagrangian density. If we use this Lagrangian we can canonically quantise without issue, as we did with scalar and Dirac fields.

2.2 Quantum chromodynamics

2.2.1 Chromodynamics

Quantum chromodynamics (QCD) is the theory of quarks and the strong nuclear force. The strong force is carried by the gluon field; an SU(3) Yang-Mills gauge field (with the properties discussed in Section 2.1.4). Quarks are Dirac fermions; they come in six flavours and are oscillations in the six quark fields. The quark fields are also gauged and transform in the fundamental representation of SU(3). As a consequence of the SU(3) gauging each quark field comes in three ‘colours’; red, green, and blue, one for each dimension of the fundamental representation. Similarly there are eight components to the gluon field, often indexed by colour anti-colour pairs, one for each generator of the fundamental representation. The quark and gluon fields are coupled by a covariant derivative. Without further ado, the Lagrangian density is given by

$$\mathcal{L}_{\text{QCD}} = -\frac{1}{4} G_{\mu\nu}^a G_a^{\mu\nu} + \sum_f \bar{\psi}_f i (i \not{D}_{ij} - \delta_{ij} m_f) \psi_f, \quad (2.49)$$

where f indexes the six species of quark and where

$$\begin{aligned} D_{ij}^\mu \psi_j &= (\delta_{ij} \partial^\mu - i g_s t_{ij}^a A^{\mu a}) \psi_j, & D^{\mu ac} A_\nu^c &= (\delta^{ac} \partial^\mu - i g_s f^{abc} A^{\mu b}) A_\nu^c, \\ G_{\mu\nu}^a t_{ij}^a \psi_j &= \frac{i}{g_s} [D_\mu, D_\nu]_{ij} \psi_j, & t^a \in \mathfrak{su}(3)_{\text{fund}} &\text{ and } f^{abc} \in \mathfrak{su}(3)_{\text{adj}}. \end{aligned} \quad (2.50)$$

More explicitly, the field tensor is equal to

$$G_{\mu\nu}^a = \partial_\mu A_\nu^a - \partial_\nu A_\mu^a + g_s f^{abc} A_\mu^b A_\nu^c. \quad (2.51)$$

¹¹Depending on the gauge choice and representation of the gauge fields, the operator $\frac{\delta G(A)}{\delta \alpha}$ may actually require the ghost fields to also be in a rep of SU(3) or its Lie algebra, and therefore the ghost term should strictly speaking be inside a trace. However, the trace is easily performed for the QCD ghost Lagrangian and so not usually included.

Indices i and j are indices over the dimension of $\mathfrak{su}(3)_{\text{fund}}$, they are in the set $\{1, 2, 3\}$ and are often labelled with colours red, green, and blue. Indices $a, b,$ and c index the eight generators, or equivalently the dimension of $\mathfrak{su}(3)_{\text{adj}}$.

By construction, the QCD Lagrangian is invariant under $SU(3)$ gauge transformations

$$\psi_f \rightarrow U(x)\psi_f, \quad \vec{A}_\mu \rightarrow U(x)\vec{A}_\mu U(x)^{-1} - \frac{i}{g_s} (\partial_\mu U(x)) U(x)^{-1}, \quad \text{where } U(x) \in SU(N). \quad (2.52)$$

QCD is also subject to many global symmetries, some of which we will now summarise with their consequences.

- QCD is trivially invariant under a global $SU(3)$ transformation. This gives a conserved Noether current of $j^{\mu a} = \bar{\psi}_f i\gamma^\mu t_{ij}^a \psi_{fj}$.
- QCD is invariant under transformations in the Poincaré group. This gives the conservation of the energy-momentum tensor.
- QCD is invariant under a global $U(1)$ transformation $\psi_f \rightarrow e^{i\theta}\psi_f$. This gives conservation of baryon number, $B = \frac{1}{3}(n_q - n_{\bar{q}})$ where n_q is the number of quarks in a process and $n_{\bar{q}}$ the number of anti-quarks.
- QCD is invariant under each of C (charge conjugation $\psi_f \rightarrow \psi_f^c = i\gamma_2\psi_f^*$ in the chiral basis and $\vec{A}_\mu \rightarrow -\vec{A}_\mu$), P (parity inversion $\mathbf{x} \rightarrow -\mathbf{x}$), and T (time inversion $t \rightarrow -t$).
- In the limit that n quarks are massless or have the same mass, QCD is invariant under a global $SU(n)$ rotation between the quarks of $\psi_f \rightarrow U_{f'f}\psi_f$ where f and f' are indices over the flavours of the n quarks. This gives a conserved current and charge which, when $n = 2$, is known as isospin.
- In the massless limit there are also chiral and axial symmetries. These involve independent unitary rotations on chiral right and left states ($\psi_{R/L} = (1 \pm \gamma^5)\psi$ where $\gamma^5 = i\gamma^0\gamma^1\gamma^2\gamma^3$). Both symmetries give rise to conserved currents, though the conserved chiral current is anomalously broken by quantum corrections.

In reality, each quark has a distinct non-zero mass. As a result the latter two bullet points describe approximate symmetries of QCD.

The equations of motion and continuity equations for chromodynamics are

$$\begin{aligned} D_\mu^{ac} G^{\mu\nu c} &= -g_s \sum_f \bar{\psi}_f i\gamma^\nu t_{ij}^a \psi_{fj}, & (i\not{D}_{ij} - \delta_{ij}m_f) \psi_{fj} &= 0, \\ \partial_\mu \bar{\psi}_f i\gamma^\mu t_{ij}^a \psi_{fj} &= 0, & D_{[\mu} \vec{G}_{\nu\sigma]} &= 0. \end{aligned} \quad (2.53)$$

The QCD Lagrangian can be partitioned into kinetic terms and interaction terms; respectively those that survive as $g_s \rightarrow 0$ and those that don't. Note that the gluon field has self interaction terms (in contrast to the photon which does not). A typical approach to solving problems in QCD is to use perturbation theory, expanding in g_s . The perturbative series for cross-sections/probabilities only depends on even powers of g_s , and so it is usual to express the series in terms of $\alpha_s = g_s^2/4\pi$.

2.2.2 Quantum Lagrangian

The QCD Lagrangian presented in the previous section is not yet suitable for quantum computations. The gluon fields need gauge fixing and the theory must be quantised. We can follow the gauge fixing procedure given in Section 2.1.5.1 and define a gauge fixed quantum Lagrangian density:

$$\mathcal{L}_{\text{qQCD}}(A, \psi, \bar{\psi}, c, \bar{c}) = \mathcal{L}_{\text{QCD}} - \frac{G(A)^2}{2\xi} - \bar{c} \frac{\delta G(A)}{\delta \alpha} c, \quad (2.54)$$

where $G(A) = 0$ is our gauge fixing condition, ξ is a gauge fixing parameter, and c and \bar{c} are Grassmann ghost fields.

We can quantise QCD by giving its generating partition functional:

$$Z[\{J\}] = \int \mathcal{D}[A, \psi, \bar{\psi}, c, \bar{c}] \exp \left(i \int d^d x \mathcal{L}_{\text{qQCD}}(A, \psi, \bar{\psi}, c, \bar{c}) + i S_{\text{gen}}[\{J\}, \{\phi\}] \right), \quad (2.55)$$

where $\{J\} = \{J_A^{\mu a}, \bar{J}_{\psi_f}, J_{\bar{\psi}_f}, \bar{J}_c, J_{\bar{c}}\}$ and where

$$S_{\text{gen}}[\{J\}, \{\phi\}] = \int d^d x \left(\sum_f \bar{J}_{\psi_f i} \psi_{f i} + \sum_f \bar{\psi}_{f i} J_{\bar{\psi}_f i} + \bar{J}_c c + \bar{c} J_{\bar{c}} + J_A^{\mu a} A_\mu^a \right). \quad (2.56)$$

Note that \bar{J}_{ψ_f} , $J_{\bar{\psi}_f}$, \bar{J}_c , and $J_{\bar{c}}$ are Grassmann valued.

2.2.3 The LSZ reduction formula and S-matrix

In this thesis we are interested in the computation of scattering amplitudes in QCD. These are described by the QCD S-matrix. So far we have introduced QCD and quantised it so that we can compute correlation functions of operators. We will now introduce S-matrices and link their computation to the calculation of correlation functions.

S-matrices (scattering matrices) describe the transition by scattering of well separated, localised in momentum space, particles from the distant past into well separated, localised in momentum space, particles in the distant future. The S-matrix is defined by

$$\lim_{t \rightarrow \infty(1+i\epsilon)} \langle p_1, \dots, p_n; t | k_1, \dots, k_m; -t \rangle = \langle p_1, \dots, p_n | \hat{S} | k_1, \dots, k_m \rangle \quad (2.57)$$

where states on the left hand side are in the Schrödinger picture (they are time, t , dependent)¹² and states on the right are both defined at a common time (they can be taken to be in any picture, Heisenberg, Schrödinger, or interaction picture).¹³ The S-matrix can be viewed as a time evolution operator on the space of states that are well separated and localised in momentum space. It is usual to decompose the S-matrix as $\hat{S} = 1 + i\hat{T}$ where \hat{T} is the transition matrix (the identity term corresponds to the possibility that nothing happens). As all amplitudes corresponding to physical states necessarily conserve momentum, it is typical to pull out a momentum conserving delta function and define the matrix element

$$\mathcal{M}(\{k\} \rightarrow \{p\}) \delta^d \left(\sum_i p_i - \sum_j k_j \right) = (2\pi)^{-d} \langle p_1, \dots, p_n | \hat{T} | k_1, \dots, k_m \rangle. \quad (2.58)$$

The work presented in this thesis contributes to the body of research looking to understand properties of QCD matrix elements.

The LSZ reduction formula relates S-matrix elements to correlation functions. Therefore, let us start by providing more detail on 2-point correlation functions,

$$-\frac{1}{Z} \frac{\delta^2 Z[\{J\}]}{\delta \bar{J}_{\psi_{f_i}} \delta J_{\psi_{f'_j}}} \Big|_{\text{all } J_\phi=0} = \langle \Omega | T \{ \hat{\psi}_{f_i}(x) \hat{\psi}_{f'_j}(y) \} | \Omega \rangle. \quad (2.59)$$

Consider inserting an identity operator $1 = |\Omega\rangle \langle \Omega| + \sum_\lambda |\lambda\rangle \langle \lambda|$, where λ is an arbitrary (not necessarily one particle) state, into the correlator. We can use the Lorentz invariance of the theory to let

$$1 = |\Omega\rangle \langle \Omega| + \sum_\lambda \int \frac{d^{d-1}p}{(2\pi)^3 2E_{\lambda_{\mathbf{p}}}} |\lambda_{\mathbf{p}}\rangle \langle \lambda_{\mathbf{p}}|,$$

where $\lambda_{\mathbf{0}}$ is a state of zero total momentum and $\lambda_{\mathbf{p}}$ is the same state boosted to have total momentum \mathbf{p} . Inserting this identity and using a little complex analysis we find¹⁴

$$\langle \Omega | T \{ \hat{\psi}_{f_i}(x) \hat{\psi}_{f'_j}(y) \} | \Omega \rangle = \sum_\lambda \int \frac{d^d p}{(2\pi)^4} \frac{i \langle \Omega | \hat{\psi}_{f_i}(x) | \lambda_{\mathbf{p}} \rangle \langle \lambda_{\mathbf{p}} | \hat{\psi}_{f'_j}(y) | \Omega \rangle}{p^2 - m_\lambda^2 + i\epsilon}. \quad (2.60)$$

To finish computing the correlator we just need to evaluate $\langle \Omega | \hat{\psi}_{f_i}(x) | \lambda_{\mathbf{p}} \rangle$. A proper treatment of this bracket is complicated, we will handle it a little heuristically. To see what

¹²It is entirely possible to define the S-matrix in a Lorentz covariant fashion using the Heisenberg picture for states. In this picture operators take on time dependence and unitary operators are inserted to control for the observation of the particles being ‘free states’ in the distance past and distance future. The two definitions for the S-matrix are thus related by a unitary transformation [11].

¹³We have not labelled each particle in the state with its quantum numbers or species, rather just its momenta. We did this just to save space.

¹⁴Note that the time ordering has disappeared from the right hand side of the expression. Summing over both possible orderings of the left hand side gives the right.

is going on, we can compute the bracket in the free theory ($\alpha_s = 0$). In the free theory, we can set $|\lambda_{\mathbf{p}}\rangle = |\mathbf{p}; s\rangle$, a single particle state of definite momentum and spin.¹⁵ Therefore,

$$\langle \Omega | \hat{\psi}_{fi}(x) | \mathbf{p}; s \rangle \Big|_{\alpha_s=0} = e^{-ip \cdot x} u_{fi}^s(\mathbf{p}). \quad (2.61)$$

This result was found by using the expression for the canonically quantised free Dirac field Eq. (2.19). u^s is a free space spinor solution to the Dirac equation with spin s . In the free theory, m_λ^2 can be identified with the mass of the fermion. If we assume the correlator is dominated by the single particle limit (we don't pick up multi-particle resonances so $|\lambda_{\mathbf{p}}\rangle \equiv |\mathbf{p}; s\rangle$) then, by analogy to the free space solution, we can let

$$\langle \Omega | \hat{\psi}_{fi}(x) | \lambda_{\mathbf{p}} \rangle = e^{-ip \cdot x} \sqrt{Z_2} u_{fi}^{\lambda}(\mathbf{p}),$$

and let m_λ^2 remain the mass of the fermion f .¹⁶ $\sqrt{Z_2}$ plays the role of an unspecified normalisation that comes from our lack of knowledge of the 'inner workings' of $|\lambda_{\mathbf{p}}\rangle$ in the full theory. The sum over λ now acts as a sum over the quantum numbers involved, i.e. spin. We can remove this sum by employing the identity $\sum_s u_{fi}^s(\mathbf{p}) \bar{u}_{f'j}^s(\mathbf{p}) = (\not{p} + m) \delta_{ij} \delta_{ff'}$. Hence we find

$$\langle \Omega | T \{ \hat{\psi}_{fi}(x) \hat{\psi}_{f'j}(y) \} | \Omega \rangle = \int \frac{d^d p}{(2\pi)^4} e^{-ip \cdot (x-y)} \frac{i Z_2 (\not{p} + m) \delta_{ij} \delta_{ff'}}{p^2 - m^2 + i\epsilon}. \quad (2.62)$$

This is the position space quark propagator. This procedure can be repeated to find the gluon and ghost propagators which are given in the next section with the rest of the QCD Feynman rules.¹⁷ It should be clear that in the free theory $Z_2 = 1$. In the full theory it is typical to handle Z_2 perturbatively so that $Z_2 = 1 + \mathcal{O}(\alpha_s)$. Absorbing the factor $\sqrt{Z_2}$ into the fields provides the basis for field renormalisation, which we will summarise in Section 2.2.5.

So far, we have outlined the computation of a 2-point correlator in the full theory. When working with canonical quantisation, Wick's theorem can be used to reduce all n -point correlators to sums over products of 2-point correlators [8]. Alternatively, the same result can be achieved via applying the chain rule to functional derivatives in the path integral formalism. 2-point correlators often are represented as lines linking the two points. The products of 2-point correlators come with various pre-factors found by expanding

$$\frac{(-i)^n}{Z} \frac{\delta^n Z[\{\phi\}, \{J\}]}{\delta J_{\phi_j} \cdots \delta J_{\phi_i}} \Big|_{\text{all } J_\phi=0}$$

¹⁵For all other $|\lambda_{\mathbf{p}}\rangle$ the bracket $\langle \Omega | \hat{\psi}_{fi}(x) | \lambda_{\mathbf{p}} \rangle$ is either proportional to $\langle \Omega | \lambda'_{\mathbf{p}'} \rangle = 0$, where $\lambda'_{\mathbf{p}'}$ is non-vacuum state of total momentum \mathbf{p}' , or $\hat{\psi}_{fi}(x) | \lambda_{\mathbf{p}} \rangle = 0$.

¹⁶The entire discussion in this section can be achieved without this assumption, however doing so complicates matters. Chapter 7 of [8] provides a relatively complete and accessible discussion.

¹⁷In the case of gluons extra care must be taken since canonical quantisation is muddled by the issue of gauge fixing. Instead of splitting the 2 point correlator into brackets of single canonically quantised fields, the gluon propagator is typically found working directly with the partition functional where the propagator emerges as the Green's function that inverts the equation of motion.

perturbatively for small couplings. The pre-factors can be given a diagrammatic interpretation as coming from vertices linking the 2-point correlators. This interpretation forms the foundations for Feynman diagrams discussed in the following section.

As we mentioned at the head of this section, the LSZ reduction formula reduces the computation of S-matrices to that of n -point correlators. We will now outline how this is achieved. However, the full LSZ formula for QCD is unwieldy. Therefore we will instead only describe the LSZ formula in momentum space for a theory with a single scalar field. Whilst being more algebraically lengthy, the QCD formula is not dramatically different. By inserting an identity ($1 = |\Omega\rangle\langle\Omega| + \sum_{\lambda} |\lambda\rangle\langle\lambda|$) into an n -point correlator and using the same manipulations as we used above for the 2-point correlator, we find the relation

$$\begin{aligned} \int d^d x_1 e^{ix_1 \cdot p_1} \langle\Omega| T\{\varphi(x_1)\dots\varphi(x_n)\varphi(y_1)\dots\varphi(y_m)\} |\Omega\rangle \Big|_{x_1^0 > x_i^0 \forall i > 1} \\ = \frac{i\sqrt{Z}}{p_i^2 - m^2 + i\epsilon} \langle\mathbf{p}_1| T\{\varphi(x_2)\dots\varphi(x_n)\varphi(y_1)\dots\varphi(y_m)\} |\Omega\rangle, \end{aligned} \quad (2.63)$$

where we have defined that for a scalar field with only single particle resonances,

$$\langle\Omega| \varphi(x_1) |\mathbf{p}_1\rangle \Big|_{\alpha_s=0} = e^{-ip \cdot x} \sqrt{Z}. \quad (2.64)$$

Just as with Dirac fields, we have introduced \sqrt{Z} to parametrise our ignorance of the full theory.¹⁸ Equivalent relations can be found for the other possible time orderings. Repeated application of this identity gives the LSZ reduction formula:

$$\langle p_1, \dots, p_n | \hat{S} | k_1, \dots, k_m \rangle = \left(\prod_{i=1}^n \frac{i\sqrt{Z}}{p_i^2 - m^2 + i\epsilon} \prod_{j=1}^m \frac{i\sqrt{Z}}{p_j^2 - m^2 + i\epsilon} \right)^{-1} \tilde{G}_{n,m}, \quad (2.65)$$

where

$$\tilde{G}_{n,m} = \prod_{i=1}^n \int d^d x_i e^{ip_i \cdot x_i} \prod_{j=1}^m \int d^d y_j e^{-ik_j \cdot y_j} \langle\Omega| T\{\varphi(x_1)\dots\varphi(x_n)\varphi(y_1)\dots\varphi(y_m)\} |\Omega\rangle. \quad (2.66)$$

2.2.3.1 Feynman rules in momentum space without renormalisation

In the previous section we illustrated how elements of the QCD S-matrix can be computed via correlators over operators. In turn, those multi-point correlators can be computed by re-arranging them into sums over products of 2-point correlators. These sums over products of 2-point correlators can be computed perturbatively using Feynman diagrams. Ignoring ghost fields, which are gauge dependent and discussed in the next section, momentum space Feynman diagrams for QCD (without renormalisation) are constructed with the following rules:

¹⁸ \sqrt{Z} is not the square root of the partition function, despite both sharing the same label. Though this labelling might be confusing, it is the commonly accepted notation in the literature [8, 9].

- With vertices time-ordered from left and to right, 2-point correlators in the free theory ($g_s = 0$) are given by propagators

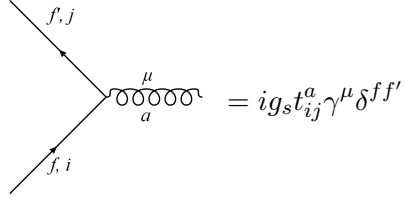
$$\overrightarrow{f,i} \longrightarrow \overrightarrow{f,j} = \int d^d x \langle \Omega | T \{ \hat{\psi}_{f,i}(x) \hat{\psi}_{f',j}(y) \} | \Omega \rangle e^{ip \cdot (y-x)} = \frac{i(\not{p} + m_f) \delta^{ij} \delta^{ff'}}{p^2 - m_f^2 + i\epsilon}, \quad (2.67)$$

and

$$\overrightarrow{\mu} \text{---} \overrightarrow{\nu} = \int d^d x \langle \Omega | T \{ \hat{A}_\mu^a(x) \hat{A}_\nu^b(y) \} | \Omega \rangle e^{iq \cdot (y-x)} = \frac{-i d_{\mu\nu} \delta^{ab}}{q^2 + i\epsilon}, \quad (2.68)$$

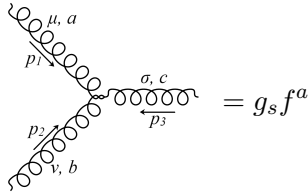
where $d_{\mu\nu}$ is a gauge dependent function of q and will be given in the following section. Anti-quarks have an arrow in the opposite direction (pointing backwards in time).

- Three point vertices are given by



$$= i g_s t_{ij}^a \gamma^\mu \delta^{ff'}, \quad (2.69)$$

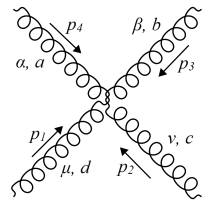
and



$$= g_s f^{abc} [g^{\mu\nu} (p_1 - p_2)^\sigma + g^{\nu\sigma} (p_2 - p_3)^\mu + g^{\sigma\mu} (p_3 - p_1)^\nu], \quad (2.70)$$

where each vertex is implicitly momentum conserving.

- The four point vertex is given by



$$= -g_s^2 \begin{bmatrix} f^{eab} f^{ecd} (g_{\mu\beta} g_{\nu\alpha} - g_{\mu\alpha} g_{\nu\beta}) \\ + f^{eac} f^{edb} (g_{\mu\alpha} g_{\beta\nu} - g_{\mu\nu} g_{\beta\alpha}) \\ + f^{ead} f^{ebc} (g_{\mu\nu} g_{\beta\alpha} - g_{\mu\beta} g_{\nu\alpha}) \end{bmatrix}, \quad (2.71)$$

where, once again, this vertex is momentum conserving.

- The external leg factors are:

- $u(p, s)$ for an initial state fermion with momentum p and spin s ,
- $\bar{u}(p, s)$ for a final state fermion with momentum p and spin s ,

- $\bar{v}(p, s)$ for an initial state anti-fermion with momentum p and spin s ,
- $v(p, s)$ for a final state anti-fermion with momentum p and spin s ,
- $\epsilon_\lambda(p)$ for an initial state vector boson with momentum p and polarisation λ ,
- $\epsilon_\lambda^*(p)$ for a final state vector boson with momentum p and polarisation λ ,

where u, v, ϵ are the usual free Dirac spinors and gauge polarisation vectors respectively, functional forms are given in Section 3.1.3.

- An unconstrained momentum p in a loop should be integrated over using the measure $\int \frac{d^d p}{(2\pi)^4}$.
- A symmetry factor should be included for the exchange of identical particles. The symmetry factors cancel for the exchange of fermion lines so only become relevant when gluon lines are exchanged. However, two diagrams which are equivalent up to the exchange of two fermion lines will have a relative minus sign between them.
- Include any necessary ghost lines and vertices. These are gauge dependent and are discussed in the subsequent sections.

The amplitude for a Feynman diagram is built up by following the arrows on fermion lines in reverse, as you go including the relevant terms from the list above. Terms relating to gluon lines commute and so can be included in any order provided the indices match up.¹⁹ An n -point correlator is computed by summing over every possible permutation of Feynman diagrams with n initial/final state particles of which there are the same number of initial/final state quarks/gluons as there are quark/gluon fields in the correlator.²⁰ When computing a correlator, every line should be treated as internal and no external leg factors should be included. S-matrices are computed by including external leg factors for initial/final state particle lines instead of including a propagator; i.e. look at Eq. (2.65), all propagators for initial or final state lines are divided out and replaced with an external leg factor (which is unity for scalar fields).

¹⁹Note that the colour algebra does not commute, however we have given the Feynman rules in terms of elements of the colour matrices which do commute.

²⁰Note that

$$\overset{f,i}{\longrightarrow} \longrightarrow \overset{f,j}{\longrightarrow} = \int d^d x \langle \Omega | T \{ \hat{\psi}_{f,i}(x) \hat{\psi}_{f',j}(y) \} | \Omega \rangle e^{ip \cdot (y-x)}$$

has one incoming quark and one outgoing (even though they are both the same quark).

2.2.3.2 Gauge dependent terms and gluon propagators

To complete our set of Feynman rules we must select a gauge. We will discuss two common gauge choices, both of which will be used in the thesis.

The Lorenz gauge condition is given by $G(A) = \partial^\mu \vec{A}_\mu = 0$. Firstly, let us look at the effect gauge fixing has on the gauge sector: in this gauge $G(A)^2 = \partial^\mu A_\mu^a \partial^\nu A_\nu^a$. This gauge has several advantages: it is explicitly Lorentz covariant and gives the simplest form of the gauge boson propagator. In this gauge, the equation of motion for a free gluon field is

$$(g_{\mu\nu} \partial_\sigma \partial^\sigma - (1 - \xi^{-1}) \partial_\mu \partial_\nu) \vec{A}^\nu = 0. \quad (2.72)$$

The gluon propagator, $\Delta_{ab}^{\nu\sigma}$, is the Green's function for the equation of motion in momentum space. Thus $\Delta_{ab}^{\nu\sigma}$ is the solution to

$$(-g_{\mu\nu} q^2 + (1 - \xi^{-1}) q_\mu q_\nu) \Delta_{ab}^{\nu\sigma}(q) = i \delta_\mu^\sigma \delta_{ab}, \quad (2.73)$$

which gives

$$\Delta_{ab}^{\mu\nu}(q) = \frac{-i d^{\mu\nu} \delta_{ab}}{q^2 + i\epsilon} = \frac{-i}{q^2 + i\epsilon} \left(g^{\mu\nu} - (1 - \xi) \frac{q^\mu q^\nu}{q^2} \right) \delta_{ab}. \quad (2.74)$$

$\xi = 1$ is known as the Feynman gauge and letting $\xi \rightarrow 0$ the Landau gauge (despite the singularity in the equation of motion, in most situations one can set $\xi = 0$ without need for extra care). Keeping ξ unspecified is known as an R_ξ gauge.

Now, let us evaluate the ghost Lagrangian in Lorenz gauge:

$$\frac{\delta G(A)}{\delta \alpha^a} = \frac{\delta}{\delta \alpha^a} \left(\partial_\mu \vec{A}^\mu + \frac{1}{g_s} \partial_\mu D^\mu \vec{\alpha} \right) = \frac{t^c}{g_s} \partial_\mu D^{\mu ca}. \quad (2.75)$$

This is an operator on fields defined in the Lie algebra of $SU(3)$, such as the gauge fields. It's therefore required that $c \rightarrow \vec{c}$ and $\mathcal{L}_{\text{ghost}} \rightarrow \text{Tr} \mathcal{L}_{\text{ghost}}$. Explicitly labelling the gauge group indices on the ghost fields, this gives the following ghost Lagrangian,

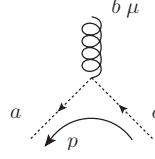
$$\mathcal{L}_{\text{ghost}}^{\text{Lorenz}} = -\vec{c}^a \partial_\mu \left(\delta^{ac} \partial^\mu - i g_s f^{abc} A^{\mu b} \right) c^c, \quad (2.76)$$

where the extra factor of g_s has been absorbed into the normalisation of the ghost fields. In the Lorenz gauge the ghost Lagrangian couples the ghost and gluon fields. Ghosts are unphysical and so can only appear as internal lines in Feynman diagrams. They contribute to the Feynman rules:

- Two point ghost correlators are given by the ghost propagator

$$\begin{array}{c} a \\ \cdots \cdots \cdots \longrightarrow \cdots \cdots \cdots \\ b \end{array} = \int d^d x \langle \Omega | T \{ \hat{c}^a(x) \hat{c}^b(y) \} | \Omega \rangle e^{ip \cdot (y-x)} = \frac{i \delta^{ab}}{p^2 + i\epsilon}, \quad (2.77)$$

- A three point ghost vertex is given by



$$= -g_s f^{abc} p^\mu, \quad (2.78)$$

where the vertex is momentum conserving.

An alternative gauge choice is an axial-like gauge. This gauge is defined by $G(A) = |\mathbf{n}|^{-1} n^\mu \vec{A}_\mu = 0$ where n^μ is an arbitrary 4-vector. In context, the axial ghost Lagrangian is

$$\begin{aligned} \frac{\delta G(A)}{\delta \alpha^a} &= \frac{\delta}{\delta \alpha^a} \left(\frac{n_\mu}{|\mathbf{n}|} \vec{A}^\mu + \frac{1}{g_s} \frac{n^\mu}{|\mathbf{n}|} D^\mu \vec{\alpha} \right) = \frac{t^c}{g_s} \frac{n_\mu}{|\mathbf{n}|} D^{\mu ca}, \\ \therefore \mathcal{L}_{\text{ghost}}^{\text{axial}} &= -\bar{c}^a \frac{n^\mu}{|\mathbf{n}|} \delta^{ac} \partial_\mu c^c. \end{aligned} \quad (2.79)$$

Thus we see that in the axial gauge the ghost fields are not coupled to the gluon or quark fields. As a result, the ghost fields factorise out the partition function integrals into the normalisation pre-factor and therefore cancel in the computation of amplitudes.

Now let us give the form of the gluon propagator, $\Delta_{ab}^{\mu\nu}(q)$; found by solving the equations of motion. The propagator is given by

$$\Delta_{ab}^{\mu\nu}(q) = \frac{-i d^{\mu\nu} \delta_{ab}}{q^2 + i\epsilon} = \frac{-i}{q^2 + i\epsilon} \left(g^{\mu\nu} - \frac{n^\mu q^\nu + q^\mu n^\nu}{n \cdot q} + \frac{(n^2 + \xi q^2) q^\mu q^\nu}{(n \cdot q)^2} \right) \delta^{ab}, \quad (2.80)$$

where we have assumed n is normalised so that $n^2 = \pm 1$ or 0 . It is usual to choose n^μ to be light-like and to set $\xi = 0$ in order to kill the last term. This is known as a light-cone gauge choice. In a light-cone gauge $d^{\mu\nu}(q) \equiv \sum_{p,p'} \epsilon_p(q) \epsilon_{p'}^*(q)$ where ϵ_p is a physical polarisation vector with polarisation p . This property makes the light-cone gauge particularly useful for our purposes later on in this thesis as it allows amplitudes with virtual gluons to be expressed in terms the same functions and kinematics as on-shell gluons.

The discussion of gauge fixing in QCD that we just provided is entirely sufficient for our purposes in this thesis. However, there are subtleties that we glossed over (for instance Gribov ambiguities and gauge orbits [12]). One such subtly we hid behind some choice wording, ‘‘In context, the axial ghost Lagrangian is...’’ Let us elucidate this statement a bit further by recalculating the axial Lagrangian,

$$\frac{\delta G(A)}{\delta \alpha^a} = \frac{t^c}{g_s} \frac{n_\mu}{|\mathbf{n}|} D^{\mu ca}, \quad \therefore \mathcal{L}_{\text{ghost}}^{\text{axial}} = -\bar{c}^a \frac{n^\mu}{|\mathbf{n}|} \left(\delta^{ac} \partial_\mu - i g_s f^{abc} A_\mu^b \right) c^c. \quad (2.81)$$

In order to arrive at the Lagrangian given in Eq. (2.79) we employed the gauge fixing condition $n^\mu \vec{A}_\mu = 0$, removing the second term. However, readers paying close attention might be troubled by this step. In order to exponentiate the gauge fixing condition we

set $n \cdot \vec{A}(x) = \vec{w}(x)$ and convoluted the $\vec{w}(x)$ dependence with a Gaussian. Therefore the gauge fixing condition does not simply remove the second term, rather we integrate over every field configuration for the second term weighted by a Gaussian. So let us analyse the ghost Lagrangian with this term intact. First an observation, $n^\mu D_\mu^{ac} c^c = 0$ is not a wave equation. Therefore the ghost fields do not propagate and so, if they contribute anything to the Feynman rules, they must contribute a contact term. Now, let us return to the Faddeev Popov trick. We showed that

$$\int \mathcal{D}[A] O(A) e^{iS[A]} = \int \mathcal{D}[\alpha] \int \mathcal{D}[A] O(A) e^{iS[A]} \delta^\infty(G(A)) \det \left(\frac{\delta G(A)}{\delta \alpha} \right). \quad (2.82)$$

As it stands, the $\delta^\infty(G(A))$ dependence does enforce the $n^\mu \vec{A}_\mu = 0$ gauge fixing condition. Let us exponentiate the gauge fixing condition via an alternate means such that we preserve the delta function, $\delta^\infty(G(A))$. For this we can use the following analytic continuation of a delta function

$$\delta(x) = \lim_{\xi \rightarrow i0^-} \frac{e^{-\frac{x^2}{2\xi}}}{\sqrt{2\pi i \xi}}. \quad (2.83)$$

Thus we find

$$\int \mathcal{D}[A] O(A) e^{iS[A]} = \lim_{\xi \rightarrow i0^-} N(\xi) \int \mathcal{D}[\alpha] \det \left(\frac{\delta G(A)}{\delta \alpha} \right) \int \mathcal{D}[A] O(A) e^{iS[A] - i \int d^d x \frac{G(A)^2}{2\xi}}. \quad (2.84)$$

Where the front factor and gauge integral cancel as usual in the computation of correlators. The $\xi \rightarrow i0^-$ limit seems subtle but it is simple for all amplitudes that are holomorphic functions of ξ , in which case we can set $\xi = 0$ and ghosts decouple. Let us now compare the computation of amplitudes in QCD in the axial gauge using Eq. (2.84) with the computation of amplitudes in QCD in the axial gauge using Eq. (2.48),

$$\begin{aligned} Z[\{J\}] &\equiv \int \mathcal{D}[A, \bar{c}, c] \exp \left[iS[\{J\}, \{\phi\}] - i \int d^d x \left(\frac{G(A)^2}{2\xi} + \bar{c} \frac{\delta G(A)}{\delta \alpha} c \right) \right] \\ &\equiv \lim_{\xi \rightarrow i0^-} \int \mathcal{D}[A] \exp \left[iS[\{J\}, \{\phi\}] - i \int d^d x \frac{G(A)^2}{2\xi} \right], \end{aligned} \quad (2.85)$$

where $S[\{J\}, \{\phi\}] = S_{\text{QCD}}[\{\phi\}] + S_{\text{gen}}[\{J\}, \{\phi\}]$. The equivalence sign is used as shorthand for $Z[\{J\}]/Z[\{0\}]$ is the same when computed with each expression. As the ghost Lagrangian is independent of ξ and the equivalence holds for all values of ξ in the first line, the two lines are only consistent if ghosts decouple and cancel in the computation of amplitudes. Thus, in the axial gauge ghosts decouple from the computation of QCD amplitudes. This is what we meant by ‘‘In context, the axial ghost Lagrangian is...’’ The argument in this section implicitly assumes that amplitudes are holomorphic in ξ , however

it can be argued that ghost fields decouple more generally. This can be achieved through the Slavnov-Taylor identities, discussed in Section 2.2.4, or by studying gauge orbits in the partition function and noting that the partition function must be independent of $\vec{w}(x)$ for a fixed $\vec{w}(x)$ [12].

2.2.4 BRST symmetries and Ward identities

Gauge fixing removes the explicit SU(3) gauge symmetry of the QCD quantum action. However, the action does still have symmetries.²¹ In particular, the BRST (Becchi, Rouet, Stora [15], and Tyutin [16]) symmetry. The BRST symmetry is a ‘tuned’ infinitesimal SU(3) gauge symmetry and so let us start by recapping how each field transforms under an infinitesimal SU(3) gauge transformation. To begin, we can re-write the gauge fixing term using an auxiliary field, $\vec{B}(x)$,

$$\mathcal{L}_{\text{GF}} = -\frac{G(A)^2}{2\xi} \equiv \frac{\xi}{2} \text{Tr } \vec{B}^2 - \text{Tr } \vec{B}G(A). \quad (2.86)$$

When B^a is integrated out of the path integral the standard gauge fixing term is recovered (B^a can be thought of as a Lagrange multiplier). An infinitesimal gauge transformation acts as,

$$\begin{aligned} U : \phi &\mapsto \phi + \delta\phi \quad \text{for } U = \exp(i\epsilon g_s \vec{\alpha}), \text{ where } U \in \text{SU}(3) \text{ and } \epsilon \rightarrow 0, \\ \delta \vec{A}_\mu &= \epsilon D_\mu \vec{\alpha}, \quad \delta\psi_f = i\epsilon g_s \vec{\alpha}\psi_f, \quad \delta\bar{\psi}_f = -i g_s \bar{\psi}_f \epsilon \vec{\alpha}, \\ \delta \vec{c} &= i[\vec{c}, \epsilon \vec{\alpha}], \quad \delta \bar{\vec{c}} = i[\bar{\vec{c}}, \epsilon \vec{\alpha}], \quad \delta \vec{B} = i[\vec{B}, \epsilon \vec{\alpha}]. \end{aligned} \quad (2.87)$$

As \vec{B} is an auxiliary field we are free to define $\vec{B} = [\vec{c}, \vec{\alpha}]$, and following this definition the Jacobi identity can be employed so that $\delta \vec{B} = 0$. \mathcal{L}_{QCD} is invariant under this transformation for arbitrary ϵ , however generally $\mathcal{L}_{\text{GF}} + \mathcal{L}_{\text{ghost}}$ is not. The important observation by BRST is that $\mathcal{L}_{\text{GF}} + \mathcal{L}_{\text{ghost}}$ is invariant under the transformation if ϵ is a Grassman number and if $\vec{\alpha}$ obeys fermionic statistics. The combination $\epsilon\alpha^a$ commutes with the fields (despite ϵ and α^a individually anti-commuting) meaning this is still a SU(3) transformation. BRST set $g_s \vec{\alpha} = i\vec{c}$, thus ensuring that $\vec{\alpha}$ is fermionic. The BRST transformations are

$$\begin{aligned} \text{BRST} : \phi &\mapsto \phi + \epsilon(Q, \phi) \quad \text{where } Q : \phi \mapsto (Q, \phi) = \epsilon^{-1} \delta\phi, \\ \epsilon^{-1} \delta \vec{A}_\mu &= [Q, \vec{A}_\mu] = \frac{i}{g_s} D_\mu \vec{c}, \\ \epsilon^{-1} \delta\psi_f &= \{Q, \psi_f\} = -\vec{c}\psi_f, \quad \epsilon^{-1} \delta\bar{\psi}_f = \{Q, \bar{\psi}_f\} = -\bar{\psi}_f \vec{c}, \\ \epsilon^{-1} \delta \vec{c} &= \{Q, \vec{c}\} = \frac{i}{2g_s} \{\vec{c}, \vec{c}\}, \quad \epsilon^{-1} \delta \bar{\vec{c}} = \{Q, \bar{\vec{c}}\} = -\frac{i}{g_s} \vec{B}, \quad \delta \vec{B} = 0, \end{aligned} \quad (2.88)$$

²¹The discussion in this section is based on [8, 13, 14].

where Q is a fermionic generator that generates the transformations of the BRST symmetry, and $(Q, \phi) = \{Q, \phi\}$ for ϕ a fermionic field and $(Q, \phi) = [Q, \phi]$ for ϕ a bosonic field.

Let us now consider applying a BRST transformation twice, i.e. $(Q, (Q, \phi))$. It can be checked that this gives

$$[Q, \{Q, \text{fermionic field}\}] = \{Q, [Q, \text{bosonic field}]\} = 0. \quad (2.89)$$

By the Jacobi identity we see that the BRST symmetry is nilpotent, i.e. $\frac{1}{2}\{Q, Q\}\phi = Q^2\phi = 0$. We can use the nilpotency of Q to show that $\mathcal{L}_{\text{GF}} + \mathcal{L}_{\text{ghost}}$ is invariant under the BRST symmetry. We can write $\mathcal{L}_{\text{GF}} + \mathcal{L}_{\text{ghost}} = \{Q, \Psi\}$ where

$$\Psi = 2i \text{Tr} \left(\vec{c} \left(\frac{\xi}{2} \vec{B} - G(A) \right) \right), \quad (2.90)$$

hence²²

$$Q : \mathcal{L}_{\text{GF}} + \mathcal{L}_{\text{ghost}} \mapsto [Q, \{Q, \Psi\}] = Q^2\Psi = 0.$$

Thus, as we stated at the head of this section, $\mathcal{L}_{\text{qQCD}}$ (Eq. (2.54)) is invariant under BRST transformations. Similarly it can be checked that the path integral measure is invariant under BRST transformations (i.e. the symmetry is not anomalously broken by quantum corrections).

Let us now introduce Ward identities. If a theory has a symmetry ($\{\phi\} \rightarrow \{\phi'\}$) that preserves the partition function, i.e. both the quantum action (as discussed in Section 2.2.2) and the integration measure over all fields are invariant under the symmetry, then necessarily

$$\frac{(-i)^n \delta^n Z[\{\phi\}, \{J\}]}{Z[\{\phi\}] \delta J_{\phi_j} \cdots \delta J_{\phi_i}} \Big|_{\text{all } J_\phi=0} = \frac{(-i)^n \delta^n Z[\{\phi'\}, \{J\}]}{Z[\{\phi'\}] \delta J_{\phi_j} \cdots \delta J_{\phi_i}} \Big|_{\text{all } J_\phi=0}, \quad (2.91)$$

where $\phi_i, \phi_j \in \{\phi\}$. In terms of expectation values of operators, this means that

$$\langle \Omega | T \{ O_1(\{\phi(x_1)\}) \cdots O_n(\{\phi(x_n)\}) \} | \Omega \rangle = \langle \Omega | T \{ O_1(\{\phi'(x_1)\}) \cdots O_n(\{\phi'(x_n)\}) \} | \Omega \rangle, \quad (2.92)$$

where $O_1(\{\phi\}), \dots, O_n(\{\phi\})$ are operators built from the fields $\{\phi\}$. This is a Ward identity and these relations constrain the form of all non-zero correlators in a theory. For a simple example, let us consider the Poincaré symmetries of a theory. Firstly, translational invariance $\{\phi(x)\} = \{\phi(x+a)\}$. Dropping the field dependencies in favour of just position dependencies, the Ward identity gives

$$\langle \Omega | T \{ O_1(x_1) \cdots O_n(x_n) \} | \Omega \rangle = \langle \Omega | T \{ O_1(x_1+a) \cdots O_n(x_n+a) \} | \Omega \rangle, \quad (2.93)$$

²²This argument assumes that $G(A)$ is a linear function of \vec{A} .

from which we can deduce that correlators are only functions of relative distances, i.e. $x_i - x_j$. Looking to the Lorentz subgroup, if we have the symmetry $\{\phi(x)\} = \{J\phi(\Lambda x)\}$ for $\Lambda \in \text{SO}(1, 3)$ and $J \in \text{repSO}(1, 3)$, the Ward identities require that

$$\langle \Omega | T\{O_1(x_1) \cdots O_n(x_n)\} | \Omega \rangle = \langle \Omega | T\{O_1(\Lambda x_1) \cdots O_n(\Lambda x_n)\} | \Omega \rangle, \quad (2.94)$$

where we have assumed the operators $O_1(\{\phi\}), \dots, O_n(\{\phi\})$ are Lorentz scalars. Consequently, correlators of Lorentz scalar operators can only be functions of Lorentz invariants. Between this constraint and the previous, we know these operators must only be functions of squares of relative distances, i.e. $(x_i - x_j)^2$.

The insight gained from the Ward identities of the Poincaré symmetry may seem almost trivial. However, Ward identities are found for every symmetry of the partition function and can give powerful insight into the structure of correlators. Let us now look the Slavnov-Taylor identities, which are the Ward identities from the BRST symmetry. The Slavnov-Taylor identities are the non-Abelian generalisations of the Takahashi-Ward identities which ensure that in QED unphysical modes (photons with longitudinal polarisations) always cancel in observable states. The Slavnov-Taylor identities are given by

$$\langle \Omega | T\{O(\{\psi_f, \vec{A}_\mu, \vec{c}\})\} | \Omega \rangle = \langle \Omega | T\{O(\{\psi_f + \delta\psi_f, \vec{A}_\mu + \delta\vec{A}_\mu, \vec{c} + \delta\vec{c}\})\} | \Omega \rangle, \quad (2.95)$$

where $O(\{\psi_f, \vec{A}_\mu, \vec{c}\})$ is any operator in QCD. The identities are typically re-arranged into the form

$$\begin{aligned} & \langle \Omega | T\{O(\{\psi_f + \delta\psi_f, \vec{A}_\mu + \delta\vec{A}_\mu, \vec{c} + \delta\vec{c}\})\} | \Omega \rangle - \langle \Omega | T\{O(\{\psi_f, \vec{A}_\mu, \vec{c}\})\} | \Omega \rangle \\ & = \langle \Omega | T\{\delta_{\text{BRST}}O(\{\psi_f, \vec{A}_\mu, \vec{c}\})\} | \Omega \rangle = 0. \end{aligned} \quad (2.96)$$

This is the so called “master equation” for the Slavnov-Taylor identities. Let us see an implication of this identity. Consider the correlator

$$\langle \Omega | T\{\vec{c}(y)\vec{A}_{\mu_1}(x_1)\vec{A}_{\mu_2}(x_2) \cdots \vec{A}_{\mu_n}(x_n)\} | \Omega \rangle = 0, \quad (2.97)$$

where the dots represent $n - 3$ more gluon fields. This correlator is zero as there is no vertex in the theory which can produce a single ghost field. Using the “master equation” we have

$$\begin{aligned} & \langle \Omega | T\{\delta_{\text{BRST}}(\vec{c}(y)\vec{A}_{\mu_1}(x_1)\vec{A}_{\mu_2}(x_2) \cdots \vec{A}_{\mu_n}(x_n))\} | \Omega \rangle \\ & = \epsilon \langle \Omega | T\{(Q, \vec{c}(y))\vec{A}_{\mu_1}(x_1)\vec{A}_{\mu_2}(x_2) \cdots \vec{A}_{\mu_n}(x_n)\} | \Omega \rangle \\ & \quad + \epsilon \langle \Omega | T\{\vec{c}(y)(Q, \vec{A}_{\mu_1}(x_1))\vec{A}_{\mu_2}(x_2) \cdots \vec{A}_{\mu_n}(x_n)\} | \Omega \rangle + \cdots \\ & = 0, \end{aligned} \quad (2.98)$$

where the dots indicate summing over the application of Q to each successive gluon field. Let us look only at terms with the same pole structure as the second line and contract the

expression with $\epsilon^{\mu_1} \dots \epsilon^{\mu_n}$ where each ϵ^{μ_i} is a physical transverse polarisation state. Only the first term is non-zero: the other terms with the same pole structure either vanish for the same reason as Eq. (2.97) (they contain a vertex with an odd number of ghosts) or are proportional to ∂_{μ_i} which contracts with ϵ^{μ_i} to give zero. Therefore

$$\begin{aligned} & \epsilon^{\mu_1} \dots \epsilon^{\mu_n} \langle \Omega | T \{ (Q, \vec{c}(y)) \vec{A}_{\mu_1}(x_1) \vec{A}_{\mu_2}(x_2) \dots \vec{A}_{\mu_n}(x_n) \} | \Omega \rangle \\ &= -\frac{i}{g_s} \epsilon^{\mu_1} \dots \epsilon^{\mu_n} \langle \Omega | T \{ \vec{B}(y) \vec{A}_{\mu_1}(x_1) \vec{A}_{\mu_2}(x_2) \dots \vec{A}_{\mu_n}(x_n) \} | \Omega \rangle = 0. \end{aligned} \quad (2.99)$$

Looking back to the definition of \vec{B} in Eq. (2.86), we can remove the auxiliary field from the theory by setting²³

$$\vec{B} = \frac{G(A)}{\xi}. \quad (2.100)$$

Thus we find that

$$\epsilon^{\mu_1} \dots \epsilon^{\mu_n} \langle \Omega | T \{ G(A(y)) \vec{A}_{\mu_1}(x_1) \vec{A}_{\mu_2}(x_2) \dots \vec{A}_{\mu_n}(x_n) \} | \Omega \rangle = 0. \quad (2.101)$$

In the Lorenz gauge, and in momentum space, this gives

$$q^\nu \epsilon^{\mu_1} \dots \epsilon^{\mu_n} \langle \Omega | T \{ \vec{A}_\nu(q) \vec{A}_{\mu_1}(p_1) \vec{A}_{\mu_2}(p_2) \dots \vec{A}_{\mu_n}(p_n) \} | \Omega \rangle = 0. \quad (2.102)$$

Thus the Slavnov-Taylor identities require that amplitudes with ‘unphysical’ longitudinally polarised gluons in the final or initial state go to zero. Although we have only demonstrated this for purely gluonic amplitudes, it is not too difficult to generalise the procedure to including quarks and more ghost fields. Using an axial gauge, one also finds that

$$n^\nu \epsilon^{\mu_1} \dots \epsilon^{\mu_n} \langle \Omega | T \{ \vec{A}_\nu(q) \vec{A}_{\mu_1}(p_1) \vec{A}_{\mu_2}(p_2) \dots \vec{A}_{\mu_n}(p_n) \} | \Omega \rangle = 0, \quad (2.103)$$

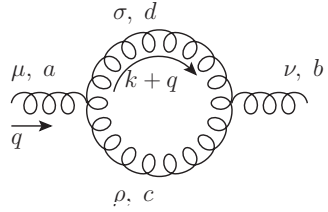
where n^ν is the axial gauge vector.

The Slavnov-Taylor identities have a lot of applications. From them it can also be shown that: QCD amplitudes are fully gauge invariant under $SU(3)_c$ despite that $\mathcal{L}_{\text{qQCD}}$ is not, amplitudes with initial/final state ghosts always cancel to zero, amplitudes computed via perturbative QCD obey unitarity (to all orders 2-point correlators never diverge faster than p^{-2} and cross-sections obey the Froissart bound [17] so that $\sigma < \ln^2 s$ for a centre of mass energy s), and the theory is renormalisable.

²³Handling the field \vec{B} more carefully and integrating it out of theory achieves exactly this result.

2.2.5 Renormalised quantum action

So far we have introduced the quantum action for QCD and we have set up the computation of QCD S-matrix elements via Feynman rules. However, there is a problem lurking in our discussion so far. When computing S-matrix elements beyond tree-level (or zeroth order), the Feynman amplitudes diverge. Ultra-violet divergences (divergences due to arbitrarily large momenta) are caused by unconstrained momenta in loops. For instance, consider the gluon self energy diagram,



$$= \frac{g_s^2}{2} f^{acd} f^{bcd} \int \frac{d^4k}{(2\pi)^4} \frac{-i}{k^2 + i\epsilon} \frac{-i}{(k+q)^2 + i\epsilon} N^{\mu\nu}, \quad (2.104)$$

where $N^{\mu\nu}$ is the numerator coming from the two triple gluon vertices

$$N^{\mu\nu} = [g^{\mu\rho}(q-k)^\sigma + g^{\rho\sigma}(2k+q)^\mu - g^{\sigma\mu}(k+2q)^\rho] \\ \times [\delta_\rho^\nu(k-q)_\sigma - g_{\rho\sigma}(2k+q)^\nu + \delta_\sigma^\nu(k+2q)_\rho]. \quad (2.105)$$

Simple power counting lets us see that this integral has parts which diverge logarithmically and parts which diverge quadratically as $E_k^2 + \mathbf{k}^2 \rightarrow \infty$, though it transpires that the quadratic divergences cancel.

Divergences are unphysical. In reality we expect there to be something, as yet unknown, limiting the loop integrals so that infinite energy/momentum modes are not included. If our theory is to be usable in its current form, divergences should cancel in the computation of any physically observable quantity, when expressed entirely in terms of other observable quantities. We could attempt to cancel divergences term by term in every computation that we undertake. However, this would be laborious and perhaps a better approach can be found. This motivates us to consider renormalisation.²⁴

Renormalisation is the process of substituting the ‘bare’ fields and parameters defining the quantum action with ‘physical’ ones. The basic idea is that, at a given energy density (or some other relevant scale), quantum fields will always come with an associated amount of quantum noise. If we were to measure a quark, really we would be measuring the quark plus the characteristic amount of QCD noise (in the form of real and virtual particles) dressing the quark at the given scale. This will shift our measurement of its mass (or charge) away from the ‘bare’ parameter in our Lagrangian. Similarly, the quantum noise overlaying each quantum field will shift its value at each point in space-time away from the

²⁴The following discussion is based on that found in [9] and uses results from [8].

‘bare’ field in the Lagrangian. Every time we use the bare fields and parameters to compute something physical, we are required to recompute the quantum noise. The computation of the noise requires us to integrate over all possible modes, introducing dependence on the unphysical infinite energy modes into each of our calculations. By substituting ‘bare’ parameters and fields for ‘physical’ ones, we aim to only compute the noise once - when doing the substitution. If the theory is renormalisable, the UV divergences should all be absorbed into this computation and no more should appear. Fortunately, QCD is renormalisable [18, 19].

The renormalisation procedure is necessarily not unique. Firstly we must define what ‘physical’ is. This will be a choice known as the renormalisation scheme. This is particularly hard for QCD, where confinement ensures the physically observable objects are hadrons, not the quarks and gluons present in the Lagrangian. On top of this, we are absorbing divergences into redefinitions of the ‘bare’ parameters and so this will depend on the regularisation scheme we have used for these divergences. We will be using dimensional regularisation (see Appendix A.4). Fortunately, upon the completion of a computation, the differences between renormalisation schemes will always appear as a correction one order higher than the accuracy of the computation (this is shown in Chapter 1 of [9]).

In our discussion of the LSZ reduction formula (Section 2.2.3), we have already come across a parameter for our lack of knowledge of the quantum noise surrounding the propagation of a fermion, Z'_2 :

$$\langle \Omega | T \{ \hat{\psi}_{f i}(x) \hat{\bar{\psi}}_{f' j}(y) \} | \Omega \rangle = Z'_2 \langle \Omega | T \{ \hat{\psi}_{f i}(x) \hat{\bar{\psi}}_{f' j}(y) \} | \Omega \rangle \Big|_{g_s=0}. \quad (2.106)$$

A similar parameter emerges when one looks at the propagation of a gluon, Z'_3 :

$$\langle \Omega | T \{ A_\mu^a(x) A_\nu^b(y) \} | \Omega \rangle = Z'_3 \langle \Omega | T \{ A_\mu^a(x) A_\nu^b(y) \} | \Omega \rangle \Big|_{g_s=0}. \quad (2.107)$$

As does a parameter, \tilde{Z}'_2 , when we look at the propagation of ghost fields.²⁵ Inspired by this, we can introduce parameters Z_2 , \tilde{Z}_2 , and Z_3 to define our renormalised fields. It is typical to give bare (not renormalised) fields a 0 subscript. We define the renormalised fields as

$$\sqrt{Z_2} \psi = \psi_0, \quad \sqrt{\tilde{Z}_2} c = c_0, \quad \text{and} \quad \sqrt{Z_3} A_\mu^a = A_{0\mu}^a. \quad (2.108)$$

If we let $Z_i = Z'_i$ we have effectively made the choice that a ‘physical’ quark/gluon is one which, between interactions, propagates like a free particle – this is known as an on-shell scheme. Other schemes can be introduced by letting each Z'_i , which multiply correlators in Eqs. (2.106) and (2.107), differ from the Z_i renormalising the field. The difference can

²⁵We have added primes to each Z to avoid confusion later.

be computed perturbatively. A common alternative choice is to let each Z_i equal one plus the divergent part of Z'_i : this is a minimal subtraction (MS) scheme and is equivalent to saying a ‘physical’ parameter is just the ‘bare’ one with divergences removed. We must also define a renormalised quark mass and strong coupling. Akin to how we handled fields²⁶, we introduce

$$g_s = Z_g^{-1} \mu^{-\epsilon} g_{s0}, \quad \text{and} \quad m = Z_m^{-1} m_0. \quad (2.109)$$

The factor $\mu^{-\epsilon}$ is included so that the Lagrangian is consistently defined in $d = 4 - 2\epsilon$ dimensions with a dimensionless coupling. μ is the renormalisation scale. The gauge fixing parameter also needs renormalising. It is usual to choose

$$\xi = Z_3^{-1} \xi_0, \quad (2.110)$$

so that the gauge fixing term is independent of the renormalisation when one uses a covariant gauge.²⁷ The renormalised quantum Lagrangian in the Lorenz gauge, and at a fixed renormalisation scale μ , is

$$\begin{aligned} \mathcal{L}_{\text{eff}}^{\text{renorm}} = & -\frac{1}{4} Z_2 \left(\partial_\mu A_\nu^a - \partial_\nu A_\mu^a + Z_3 Z_g^{-1} \mu^\epsilon g_s f^{abc} A_\mu^b A_\nu^c \right)^2 \\ & + \sum_f Z_{2f} \bar{\psi}_{fi} \left(i\gamma_\mu (\delta_{ij} \partial^\mu - i Z_3 Z_g \mu^\epsilon g_s t_{ij}^a A^{\mu a}) - \delta_{ij} Z_{mf} m_f \right) \psi_{fj} \\ & - \frac{(\partial^\mu \vec{A}_\mu)^2}{2\xi} - \tilde{Z}_2 \bar{c}^a \partial_\mu \left(\delta^{ac} \partial^\mu - i Z_3 Z_g \mu^\epsilon g_s f^{abc} A^{\mu b} \right) c^c. \end{aligned} \quad (2.111)$$

In Section 2.2.3, we have already argued that $Z'_2 = 1 + \mathcal{O}(\alpha_s)$, corresponding to the free theory plus perturbations. This is true for all Z'_i and Z_i . Therefore it is typical to expand each Z_i as $Z_i = 1 + \Delta Z_i$ where each ΔZ_i is computable from perturbation theory. As mentioned earlier, the form of ΔZ_i will be dependent on the renormalisation and regularisation scheme. In an MS scheme ΔZ_i absorbs only the divergent pieces from

²⁶The following relations can be tied back to 3-point correlators, such as

$$\langle \Omega | T \{ \hat{\psi}_{fi}(x) \hat{\psi}_{f'j}(x) A_\mu^a(x) \} | \Omega \rangle,$$

just as Z_2 and Z_3 were tied to 2-point correlators.

²⁷Not covariant gauges require the components of \vec{A}_μ to be renormalised with more care due to the presence of external reference vectors. This forces the gauge fixing term to depend on the renormalisation procedure.

the 2-point and 3-point correlators. For instance, at order α_s ,

$$\begin{aligned}
& \int d^d x e^{iq \cdot (y-x)} \langle \Omega | T \{ \hat{\psi}_{f i 0}(x) \hat{\psi}_{f' j 0}(y) \} | \Omega \rangle \\
&= \int d^d x e^{iq \cdot (y-x)} \langle \Omega | T \{ \hat{\psi}_{f i 0}(x) \hat{\psi}_{f' j 0}(y) \} | \Omega \rangle \Big|_{\alpha_s=0} \\
&\quad + \frac{i^2 (\not{q} + m_{f0})}{(q^2 - m_{f0}^2 + i\epsilon)^2} \left[\begin{array}{c} \text{---} \xrightarrow{q} \text{---} \\ \text{---} \text{---} \text{---} \text{---} \text{---} \text{---} \end{array} \right] (\not{q} + m_{f0}), \\
&= \frac{i(\not{q} + m_{f0}) \delta^{ij} \delta^{ff'}}{q^2 - m_{f0}^2 + i\epsilon} \left(1 + \frac{g_{s0}^2 C_F}{(4\pi)^2} \frac{1}{\epsilon} (3m_{f0} - \xi(\not{q} - m_{f0})) \frac{(\not{q} + m_{f0})}{(q^2 - m_{f0}^2 + i\epsilon)} + \mathcal{O}(\epsilon^0) \right), \tag{2.112}
\end{aligned}$$

where $C_F = (N_c^2 - 1)/2N_c$. This can be compared against the same 2-point correlator computed with renormalised fields, expanded to first order in ΔZ_i ,

$$\begin{aligned}
& \int \frac{d^d p}{(2\pi)^4} e^{iq \cdot (y-x)} \langle \Omega | T \{ \sqrt{Z_2} \hat{\psi}_{f i}(x) \sqrt{Z_2} \hat{\psi}_{f' j}(y) \} | \Omega \rangle \\
&= \delta_{ij} \delta_{ff'} \frac{i(1 + \Delta Z_{2f})(\not{q} + m_{f0}) - i\Delta Z_{mf} m_{f0} \frac{\not{q} + m_{f0}}{\not{q} - m_{f0}}}{q^2 - m_{f0}^2 + i\epsilon}. \tag{2.113}
\end{aligned}$$

Hence, in the MS scheme,

$$\Delta Z_{2f} = -\frac{g_s^2 C_F \xi}{(4\pi)^2} \frac{1}{\epsilon} \quad \text{and} \quad \Delta Z_{mf} = -\frac{3g_s^2 C_F}{(4\pi)^2} \frac{1}{\epsilon}. \tag{2.114}$$

By considering other 2- and 3-point correlators, it can also be found that

$$\begin{aligned}
\Delta \tilde{Z}_2 &= \frac{g_s^2 C_A}{4(4\pi)^2} (3 - \xi) \frac{1}{\epsilon}, \quad \Delta Z_3 = -\frac{g_s^2}{(4\pi)^2} \frac{1}{\epsilon} \left(C_A \frac{3\xi - 13}{6} + \frac{2n_f}{3} \right), \\
\text{and } \Delta Z_g &= -\frac{g_s^2}{(4\pi)^2} \frac{1}{\epsilon} \left(C_A \frac{11}{6} - \frac{n_f}{3} \right), \tag{2.115}
\end{aligned}$$

where $C_A = N_c$ and n_f is the total number of fermions.²⁸

2.2.6 The running coupling

As we discussed in the previous section, there was a lot of arbitrariness in our choice of renormalisation and regularisation schemes. Furthering the arbitrariness, the scheme we specified for regularisation introduced a new, seemingly unconstrained, scale to the QCD Lagrangian, μ , with the dimensions of an energy/momentum.²⁹ Some of the arbitrariness

²⁸Note that Z_i are functions of g_s not g_{s0} . At tree level the bare and renormalised couplings are equal and so they appear interchangeable at the level of analysis we have discussed. However, at higher orders they differ. The MS scheme is defined around removing divergences from the renormalised Lagrangian; these divergences are multiplied by factors of the renormalised coupling, hence Z_i are functions of the renormalised coupling.

²⁹Whilst this may seem like a consequence of our decision to use dimensional regularisation, a new scale would have been introduced regardless of the scheme used. For instance an ultra-violet cut-off would introduce the UV cut-off scale into each Z_i .

is removed by noting that the renormalisation scheme dependence cancels from calculations order-by-order. However, the dependence on the new, currently unconstrained, scale remains.³⁰ To address this, it is of interest to understand how the theory changes as we vary the scale. Changing the scale from one value to another can be achieved by renormalising the theory a second time at the new value. The action of repeated renormalisations of the theory forms a group (where the elements of the group are the functions/functors specifying the renormalisation procedure). Thus studying the variation of a theory under a change in scale is known as studying the renormalisation group. The effect of an infinitesimal change in scale μ is computable from the renormalisation group equations. Here we will only introduce the renormalisation group equation for the variation of the strong coupling with scale.

In the previous section we renormalised the strong coupling (with dimensional regularisation) as

$$g_s(\mu) = Z_g^{-1} \mu^{-\epsilon} g_{s0}. \quad (2.116)$$

We now wish to find how g_s varies with μ and eliminate its dependence on g_{s0} . Note that g_{s0} is independent of μ . Therefore

$$\frac{dg_s(\mu)}{d\mu} = -Z_g^{-2} \frac{dZ_g}{d\mu} \mu^{-\epsilon} g_{s0} - \epsilon Z_g^{-1} \mu^{-1-\epsilon} g_{s0}, \quad (2.117)$$

which can be re-arranged to give

$$\frac{d \ln g_s}{d \ln \mu} = -\epsilon - g_s \frac{d \ln Z_g}{dg} \frac{d \ln g_s}{d \ln \mu}, \quad (2.118)$$

which is equal to

$$\frac{d \ln g_s}{d \ln \mu} = \frac{-\epsilon}{1 + g_s \frac{d \ln Z_g}{dg_s}}. \quad (2.119)$$

In the minimal subtraction scheme, ΔZ_g only absorbs terms with poles. Consequently Z_g has the expansion

$$Z_g = 1 + \sum_{n=1}^{\infty} \frac{Z_g^{(n)}}{\epsilon^n}, \quad \text{where} \quad Z_g^{(n)} = \sum_{k=n}^{\infty} c_k^{(n)} g_s^{2k}. \quad (2.120)$$

Now note that $\frac{d \ln g_s}{d \ln \mu}$ is finite and therefore all pole terms must cancel as $\epsilon \rightarrow 0$. We can expand it in g_s ,

$$\frac{d \ln g_s}{d \ln \mu} = -\epsilon \left(1 - g_s \epsilon^{-1} \frac{dZ_g^{(1)}}{dg_s} + \mathcal{O}(g_s^2) \right). \quad (2.121)$$

³⁰Though, as we will see in Eq. (2.125), varying the scale also appears as a correction one order higher than the accuracy of the computation.

Importantly, all terms $\mathcal{O}(g_s^2)$ have poles and so must cancel to zero. Therefore, as $\epsilon \rightarrow 0$,

$$\frac{d \ln g_s}{d \ln \mu} = g_s \frac{dZ_g^{(1)}}{dg_s} = \beta(g_s). \quad (2.122)$$

Finally, we can expand $\beta(g_s)$ in powers of g_s ,

$$\beta(g_s) = - \sum_{n=0}^{\infty} \beta_n \left(\frac{\alpha_s}{4\pi} \right)^n, \quad (2.123)$$

and β_0 can be read off from Eq. (2.115),

$$\beta_0 = \frac{11}{3} N_c - \frac{2}{3} n_f. \quad (2.124)$$

Thus we can solve for $g_s(\mu)$ with the lowest order β function, although the solution is more elegantly expressed in terms of α_s ,

$$\alpha_s(\mu) = \frac{\alpha_s(\mu_0)}{1 + \frac{\alpha_s(\mu_0)}{4\pi} \beta_0 \ln \left(\frac{\mu^2}{\mu_0^2} \right)}, \quad (2.125)$$

where $\alpha_s(\mu_0)$ is a boundary condition.

There are a couple of things to note about $\alpha_s(\mu)$. Most importantly, as

$$\mu^2 \rightarrow \mu_0^2 e^{-4\pi/\alpha_s(\mu_0)\beta_0}$$

the coupling diverges and as $\mu^2/\mu_0^2 \rightarrow \infty$ the coupling goes to zero. The latter property is called asymptotic freedom [20, 21], when μ is large (corresponding to short distances) the coupling is small. In an MS scheme in $d = 4 - 2\epsilon$ dimensions, for each order in α_s the dependence on μ can typically be written in a form similar to

$$\alpha_s \int_0^\infty \frac{\mu^{2\epsilon} p^{-2\epsilon} dp^2}{p^2 + M^2} - \alpha_s \int_{\mu^2}^\infty \frac{\mu^{2\epsilon} p^{-2\epsilon} dp^2}{p^2} \sim \alpha_s \ln \frac{M^2}{\mu^2},$$

where the first term represents a contribution from a divergent loop and the second term a contribution from a ΔZ_i (cancelling the $p^2 \rightarrow \infty$ pole). M is a physical mass/energy scale which is characteristic of the process being computed. Generally, the perturbative series will converge fastest for $M^2 \sim \mu^2$, minimising the logarithm. This motivates choosing μ to be a scale which characterises the phenomenon being studied (see Section 1.11 of [9] for an extended discussion and [22] for an example of choosing μ for processes dominated by IR QCD radiation). Therefore, asymptotic freedom implies QCD becomes increasingly perturbative as we study processes which probe smaller and smaller distances. Conversely, the coupling becoming large at large scales in position space implies that the theory becomes

non-perturbative.³¹ There are two key scales in the discussion of $\alpha_s(\mu)$: the scale where $\alpha_s(\mu) \sim 1$, at which the theory is becoming non-perturbative; and the scale at which $\alpha_s(\mu)$ diverges, signalling complete break down of our perturbative approach, defined to be at $\mu = \Lambda_{\text{QCD}}$. Hadrons are non-perturbative bound states, therefore we expect them to have masses near Λ_{QCD} . We can solve (2.122) a second time to express $\alpha_s(\mu)$ in terms of Λ_{QCD} ,

$$\ln\left(\frac{\mu}{\Lambda_{\text{QCD}}}\right) = -\int_{g_s(\mu)}^{\infty} \frac{dg_s}{g_s\beta(g_s)}, \quad (2.126)$$

which at lowest order gives

$$\alpha_s(\mu) = \frac{4\pi}{\beta_0 \ln\left(\frac{\mu^2}{\Lambda_{\text{QCD}}^2}\right)}. \quad (2.127)$$

From this we find that $\alpha_s(\mu) \sim 1$ for $\mu \sim \Lambda_{\text{QCD}} e^{2\pi/\beta_0} \approx 4\Lambda_{\text{QCD}}$, assuming 3 active light quarks at scales of order Λ_{QCD} . Λ_{QCD} must be found by fitting to experimental data. Such fits vary depending on the renormalisation schemes used and the assumptions used to obtain the fits. Typically Λ_{QCD} is in the range of 200MeV to 300MeV [23].

2.3 Current frontiers of particle phenomenology

2.3.1 The Standard Model

There are four known fundamental forces of nature: the electromagnetic force (mediated by photons), the strong interaction (mediated by gluons), the weak interaction (mediated by W and Z bosons) and gravitation (perhaps mediated by gravitons). Quantum electrodynamics is the theory of electromagnetism and quantum chromodynamics is the theory of the strong interaction. The Standard Model (SM) [24] unifies QED and the weak interaction to form the electroweak interaction. It also describes how all matter fields (including quarks) interact with the unified electroweak force. As a part of the unification process, the SM includes the Higgs mechanism [25–28] which describes how W and Z bosons become massive, and how matter fields (including quarks) gain mass through the Yukawa couplings. It is not currently known how to correctly unify the SM and gravity.

The Standard Model is a $\text{SU}(3) \times \text{SU}(2) \times \text{U}(1)$ gauge theory of fermions and bosons. The $\text{SU}(3)$ sub-group is that of QCD. The $\text{SU}(2) \times \text{U}(1)$ subgroup is that of the unified electroweak interaction. Without the Higgs mechanism, the electroweak interaction has four

³¹The diverging coupling also hints at QCD confinement, where viewed at large distances quarks and gluons are bound into non-perturbative colour singlet states known as baryons. Quarks and gluons are never seen individually. The growing coupling gives an intuitive explanation for this property. As quarks/gluons are pulled apart, it becomes increasingly likely that a new particle/anti-particle pair will appear from the vacuum forming bound states from the separated coloured particles.

massless bosons for the four group generators, an $SU(2)$ field \vec{W}_μ and a $U(1)$ field B_μ . The Higgs mechanism causes spontaneous symmetry breaking to occur around the electroweak scale (in the range of $0.1 - 1\text{TeV}$). This breaks the $SU(2) \times U(1)$ group to $SU(2)$. The component of the $SU(2) \times U(1)$ fields which has the broken generator becomes a Goldstone boson [29, 30]. Superpositions of the \vec{W}_μ and B_μ fields with unbroken generators form the W , Z and photon fields. The W and Z fields absorb the Goldstone field and in doing so become massive. The Yukawa couplings couple the Higgs field and the matter fields. Spontaneous symmetry breaking causes the Yukawa couplings to generate a mass term for each fermion, proportional to the strength of their Yukawa coupling and the Higgs vacuum expectation value. Consequently the Higgs field couples to matter fields proportionally to their mass. The Yukawa couplings and the gauge couplings do not share the same eigenbasis for the quark fields. The two are related by a unitary transformation mapping the mass basis (from the Yukawa couplings) to the flavour basis (from the electroweak gauge couplings), parametrised by the CKM mixing matrix [31, 32]. Pure QCD is usually only expressed in the mass basis, as it is otherwise symmetrical under the exchange of flavour, and so the CKM matrix is irrelevant (furthermore massless QCD does not distinguish between the two bases). The CKM matrix only becomes of important when considering the weak interaction, which couples to the flavour basis.

As we mentioned above, the SM does not include gravity, this alone would be motivation for looking at theories which go beyond the Standard Model (BSM). However, there are yet more known problems with the Standard Model. Chief amongst these problems, the SM does not contain good candidates for explaining dark matter or dark energy. BSM model-building tends to centre on finding dark matter candidates, as more is known about the properties of any prospective dark matter candidate particle (i.e. the ranges of allowed masses and relative coupling strengths to SM fields [33]). Popular models include, minimally supersymmetric standard models (MSSMs) [34], axions [35], and sterile neutrinos [36, 37] (often via a seesaw model), amongst others [38]. Models which are popular tend to be so because they address multiple problems at the same time. Other known problems with the SM include

1. Neutrino mixing: it has been experimentally verified that the neutrino mass and flavour bases differ in a fashion similar to that described by the CKM matrix. However, the relative weakness of the neutrino Yukawa couplings (due to the small, possibly even zero, neutrino masses), and the absence of mixing between electrons, muons, and taus (beyond small corrections due to the weak interaction), precludes the SM from naturally explaining the mixing. Currently neutrino mixing is introduced in the SM by the ad hoc inclusion of the PMNS mixing matrix [39, 40].

2. The hierarchy and naturalness problems: the Higgs mass is unstable due to quantum corrections originating from the Higgs quartic self coupling. Consequently, if one tries to imagine the SM interacting with gravity, it is hard to see how the Higgs mass would remain stable at the electroweak scale and not cascade 19 orders of magnitude towards the Planck mass. This is the hierarchy problem and it is closely related to the naturalness problem. The naturalness problem is simply that it is hard to explain, without fine tuning, why the fundamental constants of nature present in the SM and gravity span such a large range of magnitudes, from meV (or less) for the lightest neutrino to 10^{19} GeV for the Planck mass.

3. The strong CP problem: the strong CP problem relates to the fine tuning of the QCD vacuum. A careful study of the QCD vacuum leads to finding that topological particles (instantons) are present, which require the addition of a new term to the quantum action (the θ term) [41]. A similarly careful study of quantum corrections to the QCD action finds that the axial symmetry is anomalously broken, also resulting in a new term being added to the quantum Lagrangian [42]. The two terms cancel each other when a parameter (θ) describing the QCD vacuum is fine tuned, however without fine tuning they persist. The new terms are CP violating, and therefore can be constrained experimentally by looking for CP violation in the strong interaction. Experimental measurements of the neutron magnetic moment find no CP violation, requiring θ to be fine tuned to the order 10^{-9} [43].

Sterile neutrinos are typically introduced as a dark matter candidate whilst also explaining neutrino mixing [36, 37]. Axions were originally motivated to solve the strong CP problem whilst also giving a dark matter candidate [35, 41, 42]. MSSMs have many attractive features to theorists and have been used in attempts to solve all three of the above problems [34] (though they are becoming highly constrained experimentally [38]). Supersymmetry is often also used as a framework through which quantum fields and gravity can be unified (whether by supersymmetric string theories [44] or other theories of everything [38]). However, these theories all lack experimental validation. Further constraining the SM and theories BSM requires increasingly precise and high energy experiments. With these experiments, more precise predictions from theory are needed. It is here where studying QCD plays a vital role.

2.3.2 Phenomenology at the Large Hadron Collider

The Large Hadron Collider (LHC) is the most powerful particle accelerator built to date. After the first long shutdown, the collider accelerated bunches of protons (and separately

ions) to 6.5TeV (2.56TeV/u for ions) inducing collisions at 4 detector sites [45]. These collisions were produced and recorded between June 2015 and October 2018, a period referred to as ‘run 2’. At full operation, during run 2, there were approximately 1 billion 13TeV proton collisions per second. Since it first began operation in 2008, the LHC has been the source of many of major experimental discoveries in particle physics: the discovery of the Higgs boson [46, 47], precision measurements of the top quark [48, 49], measurement of the Yukawa couplings [50], observations of exotic hadrons [51], precision measurements of rare decays [52–54], and more [38]. On top of this, the LHC has been the source of many new constraints on BSM models.

At the time of writing this thesis, the LHC is being further upgraded to the ‘high-luminosity LHC’. Run 3 of data taking with the LHC is set to begin in March 2022 and the high-luminosity LHC is to begin operation by the end of 2027 [55]. The goal of the upgrade is to greatly increase the amount of data taken, increasing the precision of measurements made. To match this, theoretical predictions must also become more precise. QCD is an inescapable background to physics at the LHC, even when not being measured directly since protons provide the initial state to every process. Furthering the importance of QCD, the LHC produces huge amounts of QCD radiation. The non-perturbatively bound hadrons observed in detectors are typically produced at scales near Λ_{QCD} , three to four orders of magnitude lower than the energy of proton collisions. Consequently, the particles produced in the proton collisions continually radiate, losing energy and momentum until they reach the scale of hadronisation. A detailed account of QCD radiation is crucial to producing precise predictions from theory. Starting from the following chapter, this thesis is dedicated to the study of QCD radiation within the context of high energy particle colliders.

References

- [1] O. Klein, “Quantentheorie und fünfdimensionale Relativitätstheorie”, *Zeitschrift für Physik* **1926**, *37*, 895–906.
- [2] W. Gordon, “Der Comptoneffekt nach der Schrödingerschen Theorie”, *Zeitschrift für Physik* **1926**, *40*, 117–133.
- [3] P. Dirac, “The quantum theory of the electron”, *Proc. R. Soc. Lond. A* **1928**, *117*, 610–624.
- [4] P. Dirac, “A theory of electrons and protons”, *Proc. R. Soc. Lond. A* **1930**, *126*, 360–365.
- [5] D. Tong, Lecture notes, University of Cambridge, UK, available at <https://www.damtp.cam.ac.uk/user/tong/qft/qft.pdf>, **2021**.
- [6] S. Weinberg, *The Quantum Theory of Fields, Vol. 1*, Cambridge University Press, **1995**.

- [7] E. Noether, “Invariant Variation Problems”, *Gott. Nachr.* **1918**, 1918, 235–257, arXiv: [physics/0503066](https://arxiv.org/abs/physics/0503066).
- [8] M. E. Peskin, D. V. Schroeder, *An Introduction to quantum field theory*, Addison-Wesley, Reading, USA, **1995**.
- [9] B. L. Ioffe, V. S. Fadin, L. N. Lipatov, *Quantum chromodynamics: Perturbative and nonperturbative aspects, Vol. 30*, Cambridge Univ. Press, **2010**.
- [10] V. N. Popov, L. D. Faddeev, “English translation: Perturbation theory for gauge-invariant fields”, *Kiev Inst. Theor. Phys. Acad. Sci.* **1972**, *NAL-THY-57*.
- [11] S. Weinberg, *The Quantum theory of fields. Vol. 1: Foundations*, Cambridge University Press, **2005**.
- [12] N. Vandersickel, D. Zwanziger, “The Gribov problem and QCD dynamics”, *Phys. Rept.* **2012**, 520, 175–251, arXiv: [1202.1491](https://arxiv.org/abs/1202.1491) [[hep-th](https://arxiv.org/abs/hep-th)].
- [13] H. Paukkunen, Lecture notes, University of Jyväskylä, Finland, available at <http://users.jyu.fi/~htpaukku/QFTII>, **2021**.
- [14] D. Skinner, Lecture notes, University of Cambridge, UK, available at <http://www.damtp.cam.ac.uk/user/dbs26/AQFT/>, **2021**.
- [15] C. Becchi, A. Rouet, R. Stora, “Renormalization of gauge theories”, *Annals of Physics* **1976**, 98, 287–321.
- [16] I. V. Tyutin, “Gauge Invariance in Field Theory and Statistical Physics in Operator Formalism”, **1975**, arXiv: [0812.0580](https://arxiv.org/abs/0812.0580) [[hep-th](https://arxiv.org/abs/hep-th)].
- [17] M. Froissart, “Asymptotic Behavior and Subtractions in the Mandelstam Representation”, *Phys. Rev.* **1961**, 123, 1053–1057.
- [18] G. ’t Hooft, “Renormalization of Massless Yang-Mills Fields”, *Nucl. Phys. B* **1971**, 33, 173–199.
- [19] G. ’t Hooft, “Renormalizable Lagrangians for Massive Yang-Mills Fields”, *Nucl. Phys. B* **1971**, 35, (Ed.: J. C. Taylor), 167–188.
- [20] D. J. Gross, F. Wilczek, “Ultraviolet Behavior of Nonabelian Gauge Theories”, *Phys. Rev. Lett.* **1973**, 30, (Ed.: J. C. Taylor), 1343–1346.
- [21] H. D. Politzer, “Reliable Perturbative Results for Strong Interactions?”, *Phys. Rev. Lett.* **1973**, 30, (Ed.: J. C. Taylor), 1346–1349.
- [22] S. Catani, B. Webber, G. Marchesini, “QCD coherent branching and semi-inclusive processes at large x ”, *Nuclear Physics B* **1991**, 349, 635–654.
- [23] A. Deur, S. J. Brodsky, G. F. de Teramond, “The QCD Running Coupling”, *Nucl. Phys.* **2016**, 90, 1, arXiv: [1604.08082](https://arxiv.org/abs/1604.08082) [[hep-ph](https://arxiv.org/abs/hep-ph)].
- [24] S. Weinberg, “A Model of Leptons”, *Phys. Rev. Lett.* **1967**, 19, 1264–1266.
- [25] P. W. Anderson, “Plasmons, Gauge Invariance, and Mass”, *Phys. Rev.* **1963**, 130, 439–442.
- [26] F. Englert, R. Brout, “Broken Symmetry and the Mass of Gauge Vector Mesons”, *Phys. Rev. Lett.* **1964**, 13, 321–323.
- [27] P. W. Higgs, “Broken Symmetries and the Masses of Gauge Bosons”, *Phys. Rev. Lett.* **1964**, 13, 508–509.

- [28] G. S. Guralnik, C. R. Hagen, T. W. B. Kibble, “Global Conservation Laws and Massless Particles”, *Phys. Rev. Lett.* **1964**, *13*, 585–587.
- [29] Y. Nambu, “Quasi-Particles and Gauge Invariance in the Theory of Superconductivity”, *Phys. Rev.* **1960**, *117*, 648–663.
- [30] J. Goldstone, “Field theories with ”superconductor” solutions”, *Nuovo Cimento* **1960**, *19*, 154–164.
- [31] N. Cabibbo, “Unitary Symmetry and Leptonic Decays”, *Phys. Rev. Lett.* **1963**, *10*, 531–533.
- [32] M. Kobayashi, T. Maskawa, “CP Violation in the Renormalizable Theory of Weak Interaction”, *Prog. Theor. Phys.* **1973**, *49*, 652–657.
- [33] J. L. Feng, “Dark Matter Candidates from Particle Physics and Methods of Detection”, *Ann. Rev. Astron. Astrophys.* **2010**, *48*, 495–545, arXiv: [1003.0904](https://arxiv.org/abs/1003.0904) [[astro-ph.CO](#)].
- [34] H. P. Nilles, “Supersymmetry, Supergravity and Particle Physics”, *Phys. Rept.* **1984**, *110*, 1–162.
- [35] J. E. Kim, G. Carosi, “Axions and the Strong CP Problem”, *Rev. Mod. Phys.* **2010**, *82*, [Erratum: *Rev. Mod. Phys.* 91, 049902 (2019)], 557–602, arXiv: [0807.3125](https://arxiv.org/abs/0807.3125) [[hep-ph](#)].
- [36] K. N. Abazajian et al., “Light Sterile Neutrinos: A White Paper”, **2012**, arXiv: [1204.5379](https://arxiv.org/abs/1204.5379) [[hep-ph](#)].
- [37] M. Drewes et al., “A White Paper on keV Sterile Neutrino Dark Matter”, *JCAP* **2017**, *01*, 025, arXiv: [1602.04816](https://arxiv.org/abs/1602.04816) [[hep-ph](#)].
- [38] P. A. Zyla et al., “Review of Particle Physics”, *PTEP* **2020**, *2020*, 083C01.
- [39] B. Pontecorvo, “Inverse beta processes and nonconservation of lepton charge”, *Zh. Eksp. Teor. Fiz.* **1957**, *34*, 247.
- [40] Z. Maki, M. Nakagawa, S. Sakata, “Remarks on the unified model of elementary particles”, *Prog. Theor. Phys.* **1962**, *28*, 870–880.
- [41] R. D. Peccei, H. R. Quinn, “CP Conservation in the Presence of Instantons”, *Phys. Rev. Lett.* **1977**, *38*, 1440–1443.
- [42] R. D. Peccei, H. R. Quinn, “Constraints Imposed by CP Conservation in the Presence of Instantons”, *Phys. Rev. D* **1977**, *16*, 1791–1797.
- [43] R. D. Peccei, “The Strong CP problem and axions”, *Lect. Notes Phys.* **2008**, *741*, (Eds.: M. Kuster, G. Raffelt, B. Beltran), 3–17, arXiv: [hep-ph/0607268](https://arxiv.org/abs/hep-ph/0607268).
- [44] M. Nakahara, *Geometry, topology and physics*, **2003**.
- [45] LHC Season 2 facts and figures, available at https://home.cern/sites/home.web.cern.ch/files/2018-07/factsandfigures-en_0.pdf, **2021**.
- [46] G. Aad et al., “Observation of a new particle in the search for the Standard Model Higgs boson with the ATLAS detector at the LHC”, *Phys. Lett. B* **2012**, *716*, 1–29, arXiv: [1207.7214](https://arxiv.org/abs/1207.7214) [[hep-ex](#)].
- [47] S. Chatrchyan et al., “Observation of a New Boson at a Mass of 125 GeV with the CMS Experiment at the LHC”, *Phys. Lett. B* **2012**, *716*, 30–61, arXiv: [1207.7235](https://arxiv.org/abs/1207.7235) [[hep-ex](#)].
- [48] “First combination of Tevatron and LHC measurements of the top-quark mass”, **2014**, arXiv: [1403.4427](https://arxiv.org/abs/1403.4427) [[hep-ex](#)].

- [49] G. Aad et al., “Measurement of Spin Correlation in Top-Antitop Quark Events and Search for Top Squark Pair Production in pp Collisions at $\sqrt{s} = 8$ TeV Using the ATLAS Detector”, *Phys. Rev. Lett.* **2015**, *114*, 142001, arXiv: [1412.4742 \[hep-ex\]](#).
- [50] G. Aad et al., “Evidence for the Higgs-boson Yukawa coupling to tau leptons with the ATLAS detector”, *JHEP* **2015**, *04*, 117, arXiv: [1501.04943 \[hep-ex\]](#).
- [51] R. Aaij et al., “Observation of $J/\psi p$ Resonances Consistent with Pentaquark States in $\Lambda_b^0 \rightarrow J/\psi K^- p$ Decays”, *Phys. Rev. Lett.* **2015**, *115*, 072001, arXiv: [1507.03414 \[hep-ex\]](#).
- [52] R. Aaij et al., “First observation of CP violation in the decays of B_s^0 mesons”, *Phys. Rev. Lett.* **2013**, *110*, 221601, arXiv: [1304.6173 \[hep-ex\]](#).
- [53] R. Aaij et al., “Observation of CP Violation in Charm Decays”, *Phys. Rev. Lett.* **2019**, *122*, 211803, arXiv: [1903.08726 \[hep-ex\]](#).
- [54] R. Aaij et al., “Test of lepton universality in beauty-quark decays”, **2021**, arXiv: [2103.11769 \[hep-ex\]](#).
- [55] “Longer term LHC schedule, available at <https://lhc-commissioning.web.cern.ch/schedule/LHC-long-term.htm>”, **2021**.

Chapter 3

Quantum chromodynamics in the infra-red limit

“How do you go on, when in your heart you begin to understand... there is no going back?”

—Frodo Baggins, J.R.R. Tolkien, *The Return of the King*

In the previous chapter we gave an introduction to QCD and its place in modern theoretical physics. By considering experiments at the LHC, we motivated the importance of studying large multiplicities of QCD radiation in detail. This chapter builds on the previous by delving further into the details of QCD amplitudes. QCD radiation is dominated by radiation emitted into and around points in phase-space where the amplitudes for QCD particles diverge or become large. Ultra-violet divergences, such as we renormalised in the previous chapter, are generally screened by phase-space boundaries (a proton of finite energy cannot emit a real infinite energy gluon) and so are less relevant for the computation of real radiation. The divergences of interest to us are infra-red divergences. We will particularly be studying amplitudes in the neighbourhood of divergences due to particles emitted at arbitrarily low energies or small angles. To aid us, we will first devote two sections to introducing some mathematical methods that are useful to the study of amplitudes. Following these sections, we will derive many of the elementary results in the study of infra-red QCD radiation.

3.1 A maths toolbox for kinematic factors in amplitudes

3.1.1 The method of regions

The method of regions is an approach to systematically expanding integrals around various limits.¹ These limits are usually associated with poles in the integrand or boundary condi-

¹The discussion in this section is based around those in [1, 2].

tions on the integration. One can use the method of regions to expand either amplitudes or the QCD partition function. When approached systematically, both applications are in correspondence with each other. The expanded partition function constructs an effective field theory [3, 4], the Feynman diagrams from which reconstruct the expanded QCD amplitudes. We will largely focus on the expansion of amplitudes directly.

To illustrate the fundamentals of the method of regions, let us do a toy example. Consider the integral

$$I = \int_0^\infty dk \frac{k}{(k^2 + m^2)(k^2 + M^2)} = \frac{\ln(m/M)}{m^2 - M^2}, \quad (3.1)$$

in the limit $m \ll M$. As $m/M \rightarrow 0$, I diverges. Around this limit, I has the expansion

$$I \approx -\frac{\ln(m/M)}{M^2} \left(1 + \frac{m^2}{M^2} + \dots\right). \quad (3.2)$$

The first term is completely dominant in this limit, as it goes to infinity whilst the other terms go to zero. Thus computing only this term would serve as a good approximation. We could have more easily computed the expansion by dividing the integral into two regions

$$I_M = \int_\Lambda^\infty dk \frac{k}{(k^2 + m^2)(k^2 + M^2)}, \quad I_m = \int_0^\Lambda dk \frac{k}{(k^2 + m^2)(k^2 + M^2)}, \quad (3.3)$$

where we impose that $m \ll \Lambda \ll M$. In I_M the domain of integration is always such that $k \gg m$ and so we can use such an expansion

$$I_M \approx \int_\Lambda^\infty dk \frac{k}{k^2(k^2 + M^2)} \left(1 - \frac{m^2}{k^2} + \dots\right). \quad (3.4)$$

Similarly, in I_m the domain is such that $k \ll M$. Thus

$$I_m \approx \int_0^\Lambda dk \frac{k}{M^2(k^2 + m^2)} \left(1 - \frac{k^2}{M^2} + \dots\right). \quad (3.5)$$

At this point we can make an important observation: Λ regulates divergences in both I_M and I_m . Had we applied either the $k \gg m$ or $k \ll M$ limits without partitioning the integral domain we would have been faced with a need to introduce a regulator. We can integrate both our expressions for I_M and I_m and find

$$\begin{aligned} I_M &\approx \frac{1}{2M^2} \ln\left(1 + \frac{M^2}{\Lambda^2}\right) \approx -\frac{\ln(\Lambda/M)}{M^2} + \frac{\Lambda^2}{2M^4}, \\ I_m &\approx \frac{M^2 + m^2}{2M^4} \ln\left(1 + \frac{\Lambda^2}{m^2}\right) - \frac{\Lambda^2}{2M^4} \approx -\frac{\ln(m/\Lambda)}{M^2} - \frac{\Lambda^2}{2M^4}. \end{aligned} \quad (3.6)$$

Thus

$$I = I_m + I_M \approx -\frac{\ln(m/M)}{M^2} + \mathcal{O}\left(\frac{m^2 \ln(m/M)}{M^4}\right). \quad (3.7)$$

This is in agreement with the first term in the correct expansion we previously computed in Eq. (3.2).

Our toy example illustrates the basic technique of the method of regions: identify all useful expansions of an integrand and partition the domain of the integral so that the expansions are always well defined. Though the method of regions seems a little laborious in this example, as integrals become more complicated the method becomes very powerful. Our toy model highlights a key feature, if the scale Λ is well chosen the complete answer can be found from either I_m or I_M individually (by letting $\Lambda \approx M$ or m respectively). With QCD, it is often the case that we can only compute one of the two complimentary expansion regions, thus Λ will remain as a parameter in our calculation for which we will need to choose an appropriate scale. Sometimes it is possible to find the correct value for Λ by matching to other calculations, other times the variation due to Λ will remain as an error on the theoretical prediction.

Now let us examine a generic QCD amplitude and identify the regions we will be expanding in QCD. We will be working with QCD in the massless limit, for which all amplitudes have the form

$$\mathcal{A}_{abc\dots} = \mathcal{C}_{abc\dots} \prod_i \int \frac{d^4 q_i}{2\pi} \frac{N(\{q\}, \{p\}, \{\epsilon(p)\})}{\prod_j [l_j^2(\{q\}, \{p\}) + i\epsilon]}, \quad (3.8)$$

where “ $abc\dots$ ” are colour indices, $\mathcal{C}_{abc\dots}$ is a colour factor, $N(\{q\}, \{p\}, \{\epsilon(p)\})$ is a numerator, $\{q\}$ is a set of loop momenta, $\{p\}$ is a set of initial/final state momenta, $\{\epsilon(p)\}$ is a set of polarisation vectors, and each l_j is a linear combination of momenta in the sets $\{q\}$ and $\{p\}$. The ultraviolet divergences, renormalised in the previous chapter, occur when $N(\{q\}, \{p\}, \{\epsilon(p)\})$ diverges faster than the denominator for large momenta. Infra-red divergences are pinched singularities found when the denominator vanishes faster than the numerator.² It is in the regions of phase-spaces around these pinched divergences where amplitudes for QCD radiation can become arbitrarily large, dominating the distribution of the radiation. Therefore we wish to apply the method of regions to expand around the pinched divergences.

The denominator only vanishes if at least one of l_j^2 goes to zero. We can analyse the routes l_j^2 has to zero by power counting. From this analysis we will be able to apply the method of regions to expand in the neighbourhood of these routes to zero. Let $l_j^2 = \lambda^2 L_j^2$ where L_j^2 is finite whilst $\lambda^2 \rightarrow 0$ and let us express l_j in a light-cone basis,

$$l_j^\mu = l_j^+ n^\mu + l_j^- \bar{n}^\mu + l_{j\perp} n_\perp^\mu, \quad (3.9)$$

²‘Pinched’ meaning that a suitable complex contour cannot be deformed in such a way as to avoid the singularities.

where n, \bar{n}, n_\perp are auxiliary vectors which obey: $n^2 = \bar{n}^2 = 0$, $n \cdot \bar{n} = 2$, $n \cdot n_\perp = \bar{n} \cdot n_\perp = 0$, and where both n, \bar{n} are normalised against their zeroth component. Thus

$$l_j^2 = 2l_j^+ l_j^- + (l_{j\perp})^2 n_\perp^2. \quad (3.10)$$

Following this, one usually defines a positive scalar $k_\perp^2 = -(l_{j\perp})^2 n_\perp^2$ to help simplify expressions. In order for $l_j^2 = \lambda^2 L_j^2$, one of the following must be the case:

$$l_j^+ l_j^- = \lambda^2 L_j^+ L_j^- \quad \text{and} \quad l_{j\perp} = \lambda L_{j\perp}, \quad (3.11)$$

$$\text{or} \quad l_j^+ l_j^- = L_j^+ L_j^- \mathcal{O}(\lambda^3) \quad \text{whilst} \quad l_{j\perp} = \lambda L_{j\perp}, \quad (3.12)$$

$$\text{or} \quad l_j^+ l_j^- = \lambda^2 L_j^+ L_j^- \quad \text{whilst} \quad l_{j\perp} = L_{j\perp} \mathcal{O}(\lambda^2), \quad (3.13)$$

where each of the light-cone components of L_j are finite. If l_j is constrained to be a near on-shell momentum, both $l_j^+ l_j^-$ and k_\perp^2 must go to zero at the same rate. This constrains the scalings of the components of l_j to being of the first form. There are three scalings of the components of l_j consistent with this

$$(l_j^+, l_j^-, l_{j\perp}) = (L_j^+, \lambda^2 L_j^-, \lambda L_{j\perp}), \quad (3.14)$$

$$(l_j^+, l_j^-, l_{j\perp}) = (\lambda^2 L_j^+, L_j^-, \lambda L_{j\perp}), \quad (3.15)$$

$$(l_j^+, l_j^-, l_{j\perp}) = \lambda(L_j^+, L_j^-, L_{j\perp}). \quad (3.16)$$

Regions of phase-space with these scalings are typically known as the collinear, anti-collinear, and soft regions respectively. If l_j can be off-shell a fourth region becomes relevant:

$$(l_j^+, l_j^-, l_{j\perp}) = (\lambda^2 L_j^+, \lambda^2 L_j^-, \lambda L_{j\perp}), \text{ or } (\lambda^2 L_j^+, \lambda L_j^-, \lambda L_{j\perp}), \text{ or } (\lambda L_j^+, \lambda^2 L_j^-, \lambda L_{j\perp}). \quad (3.17)$$

This is of the form shown in Eq. (3.12) and is known as the Coulomb (or Glauber) region. Scalings of the form Eq. (3.13) are ultra-collinear and tend not to be relevant.³ Sometimes it is necessary to distinguish between two l_j and $l_{j'}$ that are both going to zero but at differing rates: $l_j^2 = \lambda^2 L_j^2$ and $l_{j'}^2 = \lambda^4 L_{j'}^2$. This gives rise to three further regions

$$(l_{j'}^+, l_{j'}^-, l_{j'\perp}) = \lambda(L_{j'}^+, \lambda^2 L_{j'}^-, \lambda L_{j'\perp}), \quad (3.18)$$

$$(l_{j'}^+, l_{j'}^-, l_{j'\perp}) = \lambda(\lambda^2 L_{j'}^+, L_{j'}^-, \lambda L_{j'\perp}), \quad (3.19)$$

$$(l_{j'}^+, l_{j'}^-, l_{j'\perp}) = \lambda^2(L_{j'}^+, L_{j'}^-, L_{j'\perp}). \quad (3.20)$$

These are the soft-collinear, soft-anti-collinear, and ultra-soft regions respectively.

In order to use the method of regions we must relate λ back to physical quantities in the problem we are trying to solve. Usually this is achieved by letting $\lambda = \mu/Q$ where μ is

³Their scaling ensures that they would only be present in self-energy-like diagrams where the infra-red safety of QCD ensures ultra-collinear poles are not present (at least at the accuracy considered in this thesis).

some low scale, it could be taken to zero or some physical observable dependent value, and where Q is the ‘hard’ scale, typically the transverse momentum or centre of mass energy of the QCD process the radiation is originating from (for instance the transverse momentum of a jet). The correct scales (μ and Q) can either be found by matching to complete fixed order calculations or our lack of knowledge of the correct scales remains as an uncertainty on our calculations.

3.1.2 The KLN theorem

The QCD S-matrix has infra-red divergences, as we highlighted in Section 3.1.1. So far we have taken it for granted that these divergences will cancel. Understanding the mechanism behind the cancellation of IR divergences is important to the study of QCD radiation, for which we have argued the distribution of radiation is dominated by regions of phase-space near the divergences. In this section we review the KLN (Kinoshita [5], Lee and Nauenberg [6]) theorem, which proves that all logarithmic IR divergences in QCD and Standard Model cross-sections do cancel. We take the approach of Lee and Nauenberg [6].

Let us start by recapping the QCD S-matrix

$$\lim_{t \rightarrow \infty(1+i\epsilon)} \langle p_1, \dots, p_n; t | k_1, \dots, k_m; -t \rangle = \langle p_1, \dots, p_n | \hat{S} | k_1, \dots, k_m \rangle, \\ \text{where } \lim_{t \rightarrow \infty(1+i\epsilon)} \hat{S} = \hat{U}(t_0, t) \hat{U}^\dagger(-t, t_0), \quad (3.21)$$

where $\hat{U}(t_0, t)$ is the time evolution operator of the theory from a common time t_0 to t . For what follows we assume the states $|k_1, \dots, k_m\rangle$ and $|p_1, \dots, p_n\rangle$ are in the Heisenberg picture. Consider diagonalising the theory. To do so we introduce two unitary transformations \hat{U}_+ and \hat{U}_- which diagonalise the Hamiltonian $\hat{H}(t)$ at times $t = \infty + i\epsilon$ and $-\infty - i\epsilon$ respectively. By definition, and dropping the explicit time dependence,

$$\hat{U}_\pm^\dagger (\hat{H}_0 + g_s \hat{H}_1) \hat{U}_\pm = \hat{E}, \quad (3.22)$$

where $\hat{H}_0 + g_s \hat{H}_1 = \hat{H}$. \hat{H}_0 is the free theory Hamiltonian and is diagonal (we assume $|k_1, \dots, k_m\rangle$ and $|p_1, \dots, p_n\rangle$ are eigenstates of the free theory). \hat{E} is the diagonalised full theory Hamiltonian, it projects out the energy of eigenstates states in the full theory. With these we can write

$$\lim_{t \rightarrow \infty(1+i\epsilon)} \langle p_1, \dots, p_n; t | k_1, \dots, k_m; -t \rangle = \langle p_1, \dots, p_n | \hat{U}_+^\dagger \hat{U}_+ \hat{S} \hat{U}_-^\dagger \hat{U}_- | k_1, \dots, k_m \rangle. \quad (3.23)$$

$\hat{U}_+ \hat{S} \hat{U}_-^\dagger = \lim_{t \rightarrow \infty+i\epsilon} \exp(-i \int_{-t}^t dt' \hat{E}(t'))$ is diagonal and acting on $\hat{U}_- |k_1, \dots, k_m\rangle$ becomes a phase which cancels, thus $\hat{S} \equiv \hat{U}_+^\dagger \hat{U}_-$. Now let us look at perturbatively expanding \hat{U}_\pm . We can re-arrange its defining relation to give

$$(g_s \hat{H}_1 + \hat{H}_0 - \hat{E}) \hat{U}_\pm = [\hat{U}_\pm, \hat{E}], \quad (3.24)$$

from which we can derive a perturbative expansion for the elements of \hat{U}_\pm :

$$\langle i | \hat{U}_\pm | j \rangle = (\hat{U}_\pm)_{ij} = \delta_{ij} + \frac{g_s(1 - \delta_{ij})(\hat{H}_1)_{ij}}{E_j - E_i \mp i\epsilon} + \mathcal{O}(g_s^2), \quad (3.25)$$

where i and j index states in the theory and $E_{ij} = \delta_{ij}E_j$.⁴ We assume the theory has an infra-red regulator which ensures that no states are degenerate with each other: i.e. an IR cut-off or equivalent which regulates the soft and collinear divergences discussed in the previous section, including gluon and quark masses would achieve this. If the theory contains states that become degenerate as the infra-red regulator goes to zero⁵ (some $E_i \rightarrow E_j$) the theory will have diverging S-matrix elements proportional to negative powers of $(E_j - E_i \mp i\epsilon)$.

The key observation by Lee and Nauenberg (LN) is that as the IR regulator goes to zero, despite the S-matrix diverging, the following sum is finite for arbitrary fixed a, b :

$$\begin{aligned} & \sum_{i' \in i + \text{degen.}} (\hat{U}_\pm)_{ai'} (\hat{U}_\pm^*)_{bi'} \\ &= \sum_{i' \in i + \text{degen.}} \left(\delta_{i'a} \delta_{i'b} + \delta_{i'b} \frac{g_s(1 - \delta_{i'a})(\hat{H}_1)_{ai'}}{E_a - E_{i'} \mp i\epsilon} - \delta_{i'a} \frac{g_s(1 - \delta_{i'b})(\hat{H}_1)_{i'b}}{E_{i'} - E_b \mp i\epsilon} + \mathcal{O}(g_s^2) \right), \end{aligned} \quad (3.26)$$

where the sum over “ $i' \in i + \text{degen.}$ ” is over all states degenerate to i (including i). We can quickly check this case by case: if i is degenerate with a but not b ,

$$\begin{aligned} \sum_{i' \in i + \text{degen.}} (\hat{U}_\pm)_{ai'} (\hat{U}_\pm^*)_{bi'} &= \delta_{ib} \frac{g_s(1 - \delta_{ia})(\hat{H}_1)_{ab}}{E_a - E_b \mp i\epsilon} \\ &+ \delta_{ab} - \frac{g_s(1 - \delta_{ab})(\hat{H}_1)_{ab}}{E_a - E_b \mp i\epsilon} + \mathcal{O}(g_s^2), \end{aligned} \quad (3.27)$$

which is explicitly finite (there is no $E_a - E_i$ denominator). Here the first line came from $i' = i$ and the second from $i' = a$. A similar result is found when i and b are degenerate but a is not. Next if i, a , and b are degenerate,

$$\sum_{i' \in i + \text{degen.}} (\hat{U}_\pm)_{ai'} (\hat{U}_\pm^*)_{bi'} = 2\delta_{ab} - \frac{g_s(1 - \delta_{ab})(\hat{H}_1)_{ab}}{E_a - E_b \mp i\epsilon} + \frac{g_s(1 - \delta_{ab})(\hat{H}_1)_{ab}}{E_a - E_b \mp i\epsilon} + \mathcal{O}(g_s^2). \quad (3.28)$$

Finally, when $i = a = b$ the sum is equal to $1 + \mathcal{O}(g_s^2)$. Including more states degenerate to i does not change matters. The probability for a transition from j to i is given by

$$P_{ij} = |\langle i | \hat{S} | j \rangle|^2 = \sum_{a,b} (\hat{U}_+^*)_{ai} (\hat{U}_+)_{bi} (\hat{U}_-)_{aj} (\hat{U}_-^*)_{bj}. \quad (3.29)$$

⁴The $i\epsilon$ comes from defining U_\pm at a complexified time. E_j are energies of the system and so also become complexified.

⁵Each of the routes to zero for l_j discussed in the previous section describe a way through which a linear combination of momenta can become degenerate. For instance a state with no zero-energy-gluons is equivalent to a state with an infinite number of zero-energy-gluons. The presence of a zero energy gluon in a loop gives rise to propagators which have a soft scaling in the denominator. Regulating the l_j divergence removes the degeneracy, for instance by removing zero-energy-gluons.

Using the finite sum above, we can recognise that a finite probability, P , is returned by summing over the states degenerate to i and j :

$$P = \sum_{i' \in i + \text{degen.}} \sum_{j' \in j + \text{degen.}} P_{i'j'} = \sum_{a,b} \sum_{i' \in i + \text{degen.}} (\hat{U}_+^*)_{ai'} (\hat{U}_+)_{bi'} \sum_{j' \in j + \text{degen.}} (\hat{U}_-)_aj' (\hat{U}_-^*)_{bj'}. \quad (3.30)$$

Note that this is an incoherent sum. It only makes sense to sum over degenerate states at the level of computing probabilities not amplitudes. Amplitudes of degenerate states cannot be made IR finite. This result, that P is finite, is the KLN theorem. Though we have only demonstrated the KLN theorem to first order in the coupling, LN showed inductively that it applies to all orders in perturbation theory. Kinoshita found this result independently by directly studying the divergences of Feynman diagrams.

To all orders, the precise statement of the KLN theorem is: if we can introduce an infrared regulator, μ , (either a IR cut-off or mass scale) to the theory, which completely removes IR degeneracies by introducing logarithmic dependence on the regulator (i.e. $(E_i - E_j)^{-1} \sim \ln^p \mu$ for some power p), then LN probabilities

$$P(\mu) = \sum_{i' \in i + \text{degen.}} \sum_{j' \in j + \text{degen.}} P_{i'j'}(\mu), \quad (3.31)$$

do not depend logarithmically on μ and so are finite in the limit $\mu \rightarrow 0$.

Practically speaking, there are two main sources of IR divergences, loops and the integration over the phase-space of external particles. The KLN theorem tells us that if we sum inclusively over the IR divergences that appear at each order in perturbation theory, all logarithmic divergences will cancel. To illustrate this, consider the computation of an n particle QCD matrix element, \mathcal{M}_n . At tree level, this matrix element ($\mathcal{M}_n^{(0)}$) is finite, as are the n particle differential cross-sections we can compute from it. If we were to compute the first order correction to \mathcal{M}_n due to one loop, which we label $\mathcal{M}_n^{(1)}$, the matrix element will diverge. This is because $\mathcal{M}_n^{(1)}$ is degenerate with the tree level matrix element in the limit that the loop transfers no momentum (i.e. the loop momenta has a soft or collinear scaling). Therefore, when computing a cross-section we must add to $\mathcal{M}_n^{(1)}$ any other $\mathcal{O}(\alpha_s)$ corrections to \mathcal{M}_n which are also degenerate with $\mathcal{M}_n^{(0)}$. There is only one other $\mathcal{O}(\alpha_s)$ degenerate correction to \mathcal{M}_n , which is $\mathcal{M}_{n+1}^{(0)}$ where one of the $n+1$ particles has a soft or collinear scaling relative to another of the $n+1$ particles. The KLN theorem states that the LN probability, P , is finite

$$P \propto (\mathcal{M}_n^{(0)})^* \mathcal{M}_n^{(0)} + \int d\Pi_{n+1} \mathcal{M}_{n+1}^* \mathcal{M}_{n+1} + (\mathcal{M}_n^{(1)})^* \mathcal{M}_n^{(0)} + (\mathcal{M}_n^{(0)})^* \mathcal{M}_n^{(1)}, \quad (3.32)$$

where $d\Pi_{n+1}$ is the phase-space measure of the soft or collinear particle. We will make substantial use of this relation, mostly re-written into the form

$$\text{Pole} \left\{ \int d\Pi_{n+1} \mathcal{M}_{n+1}^* \mathcal{M}_{n+1} + (\mathcal{M}_n^{(1)})^* \mathcal{M}_n^{(0)} + (\mathcal{M}_n^{(0)})^* \mathcal{M}_n^{(1)} \right\} = 0, \quad (3.33)$$

where ‘Pole’ is the operation to extract the pole terms from the bracketed expression. Note that, for first order corrections, soft and collinear divergences can be independently regularised with separate IR cut-offs⁶. Therefore the KLN theorem requires that soft divergences cancel independently of collinear divergences and vice versa.

3.1.3 Spinor-helicity methods

The computation of Feynman diagrams is often complicated and algebraically tedious. However, in stark contrast, cross-sections and ‘bottom-line answers’ tend to appear surprisingly simple. This leads to the common speculation that perhaps the Feynman diagram approach, in its generality, is obscuring the potential simplicity of amplitudes. One particularly fruitful approach to solving this dichotomy is the spinor-helicity formalism [7, 8].⁷

The spinor-helicity formalism aims to make manifest the Poincaré symmetries of a scattering amplitude so that they can be better exploited. Transformations in the Poincaré group can be crudely divided into two separate sub-groups: the group of transformations that map a given momentum, k , on to another, p ; and the ‘little group’ of transforms which map a given momentum, k , onto itself. Transformations which rotate one spin or polarisation state into another, whilst preserving individual momenta, necessarily must be in the little group. The representation of the little group for a particle state with momentum, k , and spin, s , depends on its spin statistics:

$$U |k; s\rangle = |k; s'\rangle, \quad U \in \text{rep. of little group.} \quad (3.34)$$

If the particle transforms as a vector in the Lorentz group, finding the little group and its representation reduces to finding the set of transformations for which

$$U^{\mu\nu} k^\nu = k^\nu. \quad (3.35)$$

If k is massive then $U \in \text{SO}(3)$, and if k is massless $U \in \text{Eu}(2)$ (the group of 2D Euclidean isometries). In practice we focus on the $\text{SO}(2)$ subgroup of $\text{Eu}(2)$ for massless particles as these transformations have a physical interpretation of rotating the spin of a definite helicity state within the plane orthogonal to its polarisation. In the computation of amplitudes

⁶For instance a cut-off on the loop energy regularises the soft divergences but not the collinear divergences.

⁷The discussion in this section is based on those in [7, 9–11].

for the scattering of vector particles, the internal properties of each particle are well represented by the $SO(1,3)$ Lorentz indices on the particle's momenta. However, for fermions the situation is more complex. Just as fermions transform under a different representation of the Lorentz group compared to vector particles, fermions also transform under different representations of the massive and massless little groups. The little group for massive Dirac fermions is $SU(2) \oplus \overline{SU}(2) \simeq SO(3)$ ⁸, since these transformations map a Dirac spinor of a space-like momentum k onto another Dirac spinor also of momentum k . Little group transformations for massless Dirac fermions are elements of $U(1) \oplus \overline{U}(1) \simeq SO(2)$. Typical approaches to the calculation Feynman diagrams of fermionic amplitudes involve spin averaging, or otherwise extracting 4-vectors from the Dirac spinors, reducing the amplitude to products of 4-vectors with $SO(1,3)$ Lorentz indices. This can obscure information on spin and the internal symmetries of particles in the amplitude since 4-vectors do not transform in the same representation of the little group as the fermions themselves. The spinor-helicity formalism is a set of techniques to elegantly re-write amplitudes directly in terms of spinors which do transform in the fermionic little group. We will now introduce the formalism, beginning quite generally then focusing on developing these methods for massless particles.

There are two starting observations from which spinor-helicity methods are derived. Firstly a Dirac spinor can be decomposed into two 'chiral spinors'. Each chiral spinor transforms individually in the spinor rep of $SO(1,3)$. The decomposition is as follows:

$$\psi_{\pm} = \frac{1}{2}(1 \pm \gamma_5)\psi, \quad \psi = \psi_+ + \psi_-, \quad \text{where } \gamma^5 = i\gamma^0\gamma^1\gamma^2\gamma^3. \quad (3.36)$$

This decomposition is particularly insightful in the chiral basis where,

$$\psi_+ = \begin{pmatrix} 0 \\ \tilde{\chi} \end{pmatrix}, \quad \psi_- = \begin{pmatrix} \chi \\ 0 \end{pmatrix}. \quad (3.37)$$

Here $\chi, \tilde{\chi}$ are two component spinors known as a Weyl spinors. Working more abstractly, we can write the Dirac spinor as $\psi = \chi \oplus \tilde{\chi}$. In this notation it is perhaps clear that we can partition the little group so that χ transforms under $SU(2)$ (or $U(1)$ if massless) and $\tilde{\chi}$ under the conjugate group $\overline{SU}(2)$ (or $\overline{U}(1)$ if massless). To make their independent transformation properties explicit the spinors are given indices as χ_{α} and $\tilde{\chi}^{\dot{\alpha}}$. Undotted indices index the space on the left of the direct sum, dotted the space on the right. Note that undotted covariant indices represent vectors whereas dotted contravariant indices represent

⁸Here the $\overline{SU}(2)$ transformations are conjugate to the $SU(2)$ transformations in the fundamental representation and don't represent individual degrees of freedom.

vectors.⁹ The two Weyl spinor representations are related by $\chi_{\dot{\alpha}} = \chi_{\alpha}^* = (\epsilon_{\alpha\beta}\chi^{\beta})^*$, note that $\epsilon_{\alpha\beta} = -\epsilon^{\alpha\beta}$.

We can introduce a helicity operator which is the operator for the projection of angular momentum (due to spin) along the direction of momentum: $\hat{h} = \frac{i}{2}\epsilon_{ijk}\hat{p}_i J_{jk}$ where $J_{jk} \in \mathfrak{so}(3)$ and $\hat{\mathbf{p}}$ is the 3-momentum operator. In the massless limit $[\gamma_5, \hat{h}] = 0$ and so each chiral state is also a state of definite helicity. Thus we can label each massless Weyl spinor with a definite spin state projected onto the direction of motion; $\chi_{\alpha}(p) \equiv \chi_{\alpha}(p, -)$ and $\tilde{\chi}(p)^{\dot{\alpha}} \equiv \tilde{\chi}(p, +)^{\dot{\alpha}}$, respectively referred to as left and right handed. In the free massless case, ψ_+ and ψ_- both independently solve the Dirac equation $\not{p}\psi_{\pm} = 0$. Written in terms of the spinors this gives $p^{\mu}\sigma_{\mu}\chi = 0$ and $p^{\mu}\bar{\sigma}_{\mu}\tilde{\chi} = 0$. Therefore we can deduce that $\det(p_{\mu}\sigma^{\mu}) = \det(p_{\mu}\bar{\sigma}^{\mu}) = 0$ for $p^2 = 0$. The degeneracy includes the U(1) little group phase that can be given to each Weyl spinor. These phases can be independently fixed as the two spinors independently satisfy the Dirac equation. The complete free Dirac equation has the solutions

$$u(p, s) = \begin{pmatrix} \chi(p, s)_{\alpha} \\ \tilde{\chi}(p, s)^{\dot{\alpha}} \end{pmatrix} |E > 0, \quad v(p, s) = \begin{pmatrix} \tilde{\chi}(p, s)_{\alpha} \\ \chi(p, s)^{\dot{\alpha}} \end{pmatrix} |E < 0, \quad (3.38)$$

given that χ and $\tilde{\chi}$ are positive energy Weyl spinors satisfying $p^{\mu}\sigma_{\mu}\chi = 0$, $p^{\mu}\bar{\sigma}_{\mu}\tilde{\chi} = 0$, and $\chi_{\alpha}(p, +) = \tilde{\chi}(p, -)^{\dot{\alpha}} = 0$. If we take $p^{\mu}\sigma_{\mu}\chi = 0$, and act on it with a parity transformation, we find that

$$P : (p^{\mu}\sigma_{\mu}\chi = 0) \mapsto (p^{\mu}\bar{\sigma}_{\mu}P\chi = 0).$$

Therefore $P\chi = \tilde{\chi}$ up to transformations in the little group. In other words, we can freely set $u(p, s) = v(p, -s)$. This sets $\tilde{\chi}(p)^{\dot{\alpha}} = \chi(p)^{\dot{\alpha}}$ for free massless Weyl spinors. Solutions to $p^{\mu}\sigma_{\mu}\chi = 0$ can be expressed in many ways, one of the most common is

$$\chi = \sqrt{2E} \begin{pmatrix} -e^{-i\phi} \sin \frac{\theta}{2} \\ \cos \frac{\theta}{2} \end{pmatrix}, \quad (3.39)$$

for momentum $p = E(1, \cos \phi \sin \theta, \sin \phi \sin \theta, \cos \theta)^{\text{T}}$.

The second observation is that a null 4-vector k can be uniquely expressed as $k_{\alpha\dot{\alpha}} = \sigma_{\alpha\dot{\alpha}}^{\mu}k_{\mu}$.¹⁰ The null condition is encoded by $k^2 = \det(k_{\mu}\sigma^{\mu}) = 0$. Thus $k_{\alpha\dot{\alpha}}$ must be degenerate and so can be expressed as the tensor product of two equal momentum free massless Weyl spinors, $k_{\alpha\dot{\alpha}} = \chi(k)_{\alpha}\tilde{\chi}(k)_{\dot{\alpha}}$.¹¹ The basic tenet of the spinor-helicity formalism

⁹The Clifford algebra can be interpreted as linking the left and right spaces. If we look to the Dirac equation in terms of Weyl spinors, $p^{\mu}\sigma_{\mu}\chi = m\tilde{\chi}$ and $p^{\mu}\bar{\sigma}_{\mu}\tilde{\chi} = m\chi$, we can see that necessarily σ_{μ} receives indices as $\sigma_{\mu}^{\dot{\alpha}\alpha}$ and similarly $\bar{\sigma}_{\mu}$ as $\bar{\sigma}_{\mu}^{\alpha\dot{\alpha}}$.

¹⁰The relationship $k_{\alpha\dot{\alpha}} = \sigma_{\alpha\dot{\alpha}}^{\mu}k_{\mu}$ can be inverted as $k^{\mu} \propto \frac{1}{2}\chi(k)^{\alpha}\sigma_{\alpha\dot{\alpha}}^{\mu}\tilde{\chi}(k)^{\dot{\alpha}}$. The final relation is proportional up to the little group phase that can be chosen to be unity.

¹¹This follows since a 2×2 degenerate matrix has 3 degrees of freedom. Each Weyl spinor has 2 degrees of freedom but the pair are constrained to be of equal momentum, removing 1 degree of freedom. Now we can check $\det(\chi(k)_{\alpha}\tilde{\chi}(k)_{\dot{\alpha}}) = \epsilon^{\alpha\dot{\alpha}}\chi(k)_{\alpha}\tilde{\chi}(k)_{\dot{\alpha}} = \chi(k)_{\alpha}\tilde{\chi}(k)^{\alpha} \propto k \cdot k$, which is zero. Hence we see the equal momentum constraint enforces degeneracy on the matrix.

is that amplitudes of fermions can be better expressed in terms of products of Weyl spinors of the fermion momenta rather than momentum vectors, since the transformation properties of spinors better encapsulates the symmetries of a fermionic system. To aid us, let us introduce some further notation:

$$|k\rangle^{\dot{\alpha}} = \tilde{\chi}(k)^{\dot{\alpha}}, \quad |k]_{\alpha} = \chi(k)_{\alpha}, \quad \langle k|_{\dot{\alpha}} = \epsilon_{\dot{\alpha}\beta} \tilde{\chi}(k)^{\dot{\beta}} = \tilde{\chi}(k)_{\dot{\alpha}}, \quad [k]^{\alpha} = \epsilon^{\alpha\beta} \chi(k)_{\beta} = \chi(k)^{\alpha}, \quad (3.40)$$

from which we define the brackets

$$\langle qk \rangle = \tilde{\chi}(q)_{\dot{\alpha}} \tilde{\chi}(k)^{\dot{\alpha}}, \quad [qk] = \chi(q)^{\alpha} \chi(k)_{\alpha}. \quad (3.41)$$

Using the representation given in Eq. (3.39) we can compute these brackets for momenta $k = E_k(1, \cos \phi \sin \theta, \sin \phi \sin \theta, \cos \theta)^T$ and $q = E_q(1, 0, 0, 1)^T$. We find

$$\langle qk \rangle = \sqrt{2q \cdot k} e^{i\phi}, \quad [qk] = \sqrt{2q \cdot k} e^{-i\phi + i\pi}. \quad (3.42)$$

Here we see these U(1) little group phases due to rotations in the plane perpendicular to the spin axis emerge, parametrised by ϕ . We can also readily see that $\langle qk \rangle = -\langle kq \rangle$ and $[qk] = -[kq]$, a consequence of Weyl spinors anti-commuting. Finally $\langle qk \rangle^* = [kq]$, which means that $\langle qk \rangle [kq] = 2q \cdot k$. Further spinor identities are given in Appendix A.2.

As previously stated, our goal in employing this formalism is to completely express amplitudes of fermions in terms of spinors. However, fermions in the Standard Model interact via gauge bosons. These introduce polarisation vectors to our amplitudes. Therefore we must now introduce a decomposition for the polarisation vectors in terms of spinors. Physical polarisation vectors must satisfy:

$$p \cdot \epsilon_{\pm}(p) = 0, \quad q \cdot \epsilon_{\pm}(p) = 0, \quad \epsilon_{\lambda}(p) \cdot \epsilon_{\lambda'}^*(p) = -\delta_{\lambda\lambda'}, \quad (3.43)$$

where q is an arbitrary auxiliary vector chosen to fix the gauge. The following two ansatz satisfy these requirements,

$$\epsilon_{+}^{\mu}(p) = \frac{1}{\sqrt{2}} \frac{\langle q | \sigma^{\mu} | p \rangle}{\langle qp \rangle}, \quad \epsilon_{-}^{\mu}(p) = -\frac{1}{\sqrt{2}} \frac{[q | \bar{\sigma}^{\mu} | p \rangle}{[qp]}. \quad (3.44)$$

We can check that, given this representation for polarisation vectors, a shift in the reference vector, $q \rightarrow q'$, is equivalent to a gauge transformation:

$$\begin{aligned} \frac{1}{\sqrt{2}} \frac{\langle q' | \sigma^{\mu} | p \rangle}{\langle q'p \rangle} &= -\frac{1}{\sqrt{2}} \frac{\langle q' | \sigma^{\mu} p_{\nu} \bar{\sigma}^{\nu} | q \rangle}{\langle qp \rangle \langle q'p \rangle} = \frac{1}{\sqrt{2}} \frac{\langle q' | p_{\nu} \sigma^{\nu} \bar{\sigma}^{\mu} | q \rangle}{\langle qp \rangle \langle q'p \rangle} + \frac{1}{\sqrt{2}} \frac{\langle q' | 2p_{\nu} g^{\mu\nu} | q \rangle}{\langle qp \rangle \langle q'p \rangle}, \\ &= \frac{1}{\sqrt{2}} \frac{\langle q'p \rangle [p | \bar{\sigma}^{\mu} | q \rangle}{\langle qp \rangle \langle q'p \rangle} + \frac{\sqrt{2} \langle q'q \rangle p^{\mu}}{\langle qp \rangle \langle q'p \rangle} = \frac{1}{\sqrt{2}} \frac{\langle q | \sigma^{\mu} | p \rangle}{\langle qp \rangle} + \mathcal{O}(p^{\mu}). \end{aligned} \quad (3.45)$$

Here we have made use of identities given in Appendix A.2. Terms linear in p^{μ} are gauge transformations that vanish thanks to the BRST symmetry, see Section 2.2.4.

We will make extensive use of the spinor-helicity formalism throughout this and later chapters. As such we will withhold giving an example until Section 3.3.

3.2 A maths toolbox for colour factors in amplitudes

3.2.1 Basis independent colour charge operators

Matrix elements in $SU(N_c)$ gauge theories are typically defined to carry the $SU(N_c)$ group structure of the particles involved as colour indices; i.e.

$$\mathcal{M}_{i_1 \dots i_m}^{a_1 \dots a_n}$$

where $i_1 \dots i_m$ are indices in the fundamental representation of $SU(N_c)$, corresponding to m external quarks, and $a_1 \dots a_n$ are indices in the adjoint representation of $SU(N_c)$, corresponding to n external gluons. In the QCD amplitudes we have looked at so far, colour matrices have always been implicitly given in the $SU(3)$ Gell-Mann basis – the most commonly used basis for $\mathfrak{su}(3)_{\text{fund}}$. However, it can be helpful to compute matrix elements using other representations of $SU(3)$. To aid us changing basis let us define

$$\mathcal{M}_{i_1 \dots i_m}^{a_1 \dots a_n} = \langle a_1 \dots a_n; i_1 \dots i_m | \mathcal{M}_{n+m} \rangle, \quad (3.46)$$

where $|\mathcal{M}_{n+m}\rangle$ is a state vector for an amplitude involving m external (anti-)quarks and n external gluons. $|a_1 \dots a_n; i_1 \dots i_m\rangle$ is a basis vector in an $n + m$ dimensional product space of vectors in the Gell-Mann basis. It projects out the Gell-Mann basis representation of the amplitude $|\mathcal{M}_{n+m}\rangle$. There are many different bases which could be used to represent the $SU(3)$ product space in which $|\mathcal{M}_{n+m}\rangle$ resides. We will now look to generalise the colour charge so that it is an operator acting on $|\mathcal{M}_{n+m}\rangle$. This will prove useful in its own right, as well as making it easier to change basis.¹²

To begin, let us define a colour charge in the Gell-Mann basis for the emission of a gauge boson with colour a :

$$(T_i^a)_{dc} = \begin{cases} t_{dc}^a & i = \bar{u}, \\ t_{dc}^a & i = \bar{v}, \\ -t_{cd}^a & i = u, \\ -t_{dc}^a & i = v, \\ if^{dac} & i = \epsilon, \\ -if^{cad} & i = \epsilon^*. \end{cases} \quad (3.47)$$

Here the index i indexes the particle line which the colour charge is associated with - the line of the ‘emitter’. For example an incoming fermion emitting a gauge boson would have a colour charge $(T_u^a)_{dc} = -t_{cd}^a$. In a general Feynman amplitude there is an ambiguity as to what exactly is meant for one particle to emit another - which is the emitter, which is the emitted? The answer one chooses does not matter provided it can be consistently applied throughout the calculation. We will be using the colour charge for the computation of soft

¹²This thesis follows the definitions used in [12–14], though alternative definitions can be found [15].

and collinear limits of amplitudes where the emitter is unambiguous. Usually the lower indexes on the colour charge can be dropped, instead assuming matrix multiplication along a given particle line. Finally $T_i^{a\dagger}T_i^a \equiv T_i \cdot T_i = C_i \mathbb{1}_d$ is the Casimir matrix in the same representation as particle i (i.e. $d = 3$ and $C_i = C_F$ if i is a quark, whilst $d = 8$ and $C_i = C_A$ if i is a gluon).

We can use the Gell-Mann basis colour charge to define a colour charge operator:

$$\begin{aligned} \langle d_i | \mathbb{T}_i^a | c_i \rangle &= (T_i^a)_{d_i c_i}, \\ \langle d_1, \dots, d_i, \dots, d_n | \mathbb{T}_i^a | c_1, \dots, c_i, \dots, c_n \rangle &= \delta_{d_1 c_1} \dots (T_i^a)_{d_i c_i} \dots \delta_{d_n c_n}, \end{aligned} \quad (3.48)$$

where $|c_i\rangle$ and $|d_i\rangle$ are basis vectors for the Gell-Mann basis.¹³ This colour operator has the familiar properties,

$$[\mathbb{T}_i^a, \mathbb{T}_j^b] = \begin{cases} if^{abc}\mathbb{T}_i^c & i = j, \\ 0 & i \neq j. \end{cases} \quad (3.49)$$

$$\mathbb{T}_i \cdot \mathbb{T}_i = C_i \mathbb{1}. \quad (3.50)$$

\mathbb{T}_i^a is a ‘rectangular operator’, increasing the dimension of the colour product-space in which an amplitude resides by adding the index a . Often we will drop the upper index on the colour operator, in which case it should be understood that it is an operator that increases the dimension of the SU(3) product space of an amplitude by 1 (i.e. in the Gell-Mann basis $\langle d_i, a | \mathbb{T}_i | c_i \rangle = (T_i^a)_{d_i c_i}$). Finally, we know from the Slavnov-Taylor identities (Section 2.2.4) that a physical amplitude $|\mathcal{M}\rangle$ is invariant under SU(3) gauge transformations:

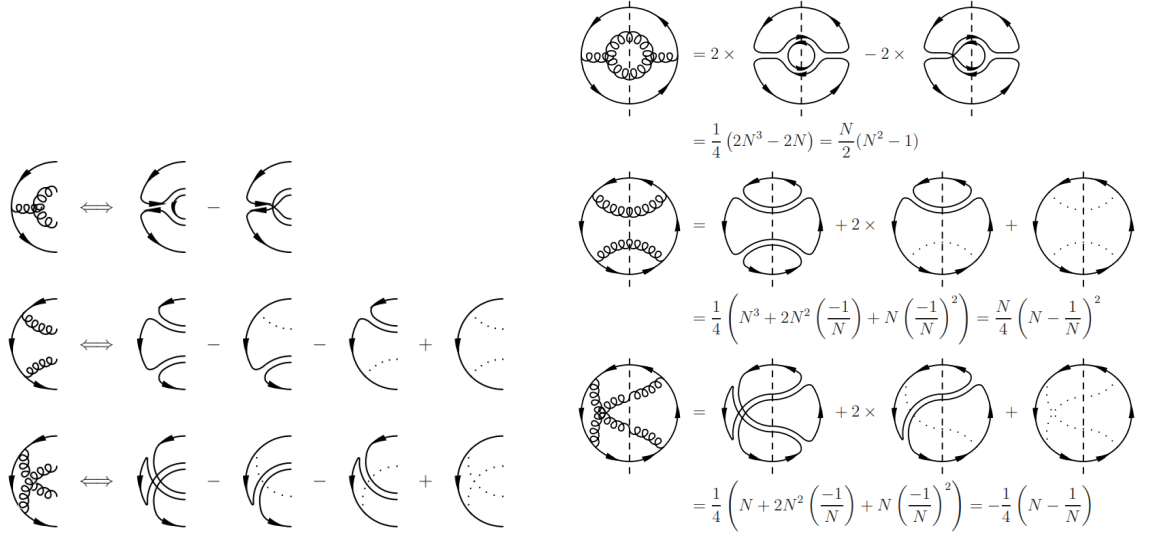
$$e^{i\alpha^a \sum_i \mathbb{T}_i^a} |\mathcal{M}\rangle = |\mathcal{M}\rangle, \quad (3.51)$$

which is a gauge transformation applied consistently across each of the i th SU(3) sub-spaces. Expanding to first order we find a final identity,

$$\sum_i \mathbb{T}_i^a |n\rangle = 0. \quad (3.52)$$

This is known as colour conservation (by analogy to charge conservation in QED for which the sum over all charges in a process is an invariant). When discussing soft-currents we will see that colour conservation is related to the cancellation of unphysical longitudinal polarisations of gluons. This should not be surprising as the SU(3) gauge symmetry of an amplitude and the cancellation of longitudinal gluons are both consequences of the BRST symmetry and its Ward identities.

¹³Sometimes we will write the colour charge operator as \mathbf{T}_i^a . Generally speaking an amplitude has both a colour and spin structure. We give operators that act individually on either the colour space or spin space in the \mathbb{O} style, whilst composite operators acting in both spaces we give in the \mathbf{O} style. Spin averaged amplitudes have a trivial spin space and so we can use \mathbf{T}_i^a interchangeably with \mathbb{T}_i^a .



(a) Some topologies contributing to the amplitude for $\gamma^* \rightarrow q\bar{q}gg$ and their representation in terms of colour flows.

(b) Topologies contributing to the computation of $\gamma^* \rightarrow q\bar{q}gg$ at cross-section level, their representation in terms of colour flows and corresponding colour factors in terms of the number of colours N . The amplitude is drawn to the left of the dashed line, the conjugate amplitude is drawn to the right. Final state particles are represented by lines bisected by the dashed line.

Figure 3.1: Colour factors for $\gamma^* \rightarrow q\bar{q}gg$ computed using colour flow diagrams derived from the Fierz identity. The virtual photon has no colour charge and so has not been included on the diagrams, it could be attached at any point along the quark/anti-quark lines. These diagrams were first presented in [16].

3.2.2 The colour flow basis

The colour flow basis is a powerful alternative to the Gell-Mann basis for amplitudes in $SU(N_c)$ gauge theories. It is found by using Fierz identity,

$$\sum_a t_{ij}^a t_{kl}^a = \frac{1}{2} \left(\delta_{il} \delta_{kj} - \frac{1}{N_c} \delta_{ij} \delta_{kl} \right) \equiv \frac{1}{2} \left(\begin{array}{c} i \longrightarrow l \\ j \longleftarrow k \end{array} \right) - \frac{1}{2N_c} \left(\begin{array}{c} i \\ j \end{array} \right) \left(\begin{array}{c} l \\ k \end{array} \right), \quad (3.53)$$

to decompose the colour structure of an amplitude into (anti)-colour lines which follow the contraction of indices on Kronecker deltas. Using this approach, we can compute colour factors diagrammatically by exchanging gluon and quark lines in Feynman diagrams with colour and anti-colour lines, see Figure 3.1. For a complete set of rules for colour flow diagrams in QCD see [16]. When computing a cross-section, every colour/anti-colour line will close to form a loop. Each loop corresponds to a factor of $\delta_{ii} = N_c$. Summing over all the colour topologies gives the colour factor associated with the squared Feynman amplitudes under consideration.

With this diagrammatic approach we can think of $|\mathcal{M}\rangle$ as being a vector in a product space $V_1 \otimes V_2 \otimes \dots \otimes V_n$, for $2n$ (anti-)colour lines, where each V_i is a vector space in a representation of $SU(N_c)$ for each colour line anti-colour line pair¹⁴. The colour flow basis (CFB) is a spanning set used to parametrise the product space $V_1 \otimes V_2 \otimes \dots \otimes V_n$ of colour line anti-colour line pairs (or colour flows). It represents a particular permutation of colour line anti-colour lines pairs by a vector $|\sigma_n\rangle$ where σ_n is an element of the permutation group S_n . The most common convention for the colour flow basis is to index the colour lines in an order corresponding to particle indices and relative to that labelling the permutations of connected anti-colour by σ (see Figure 3.2). The complete CFB spanning set is

$$\{|\sigma_n\rangle\}; \quad \sigma_n \in S_n. \quad (3.54)$$

The CFB is defined to have the bracket

$$\langle \sigma_n | \tau_n \rangle = N_c^{n-T(\sigma_n, \tau_n)}; \quad \sigma_n, \tau_n \in S_n \quad (3.55)$$

where $T(\sigma, \tau)$ counts the minimum number of transpositions separating σ and τ in the permutation group. Note that this bracket means the CFB is not orthonormal. The bracket encodes the Fierz identity into the colour flow algebra and therefore ensures each element of the CFB represents a colour flow diagram as one would find using the Fierz identity. The CFB grows factorially with the number of colour flows (pairs of lines), meaning that it is over-complete – hence why it is a spanning set.¹⁵

The problem with not orthonormal spanning sets

As previously mentioned, the CFB is not orthonormal. A typical way to approach a non-orthogonal basis is to construct a dual basis, $\{|\sigma'_n\rangle\}$, defined so that

$$[\sigma_n | \sigma'_n \rangle = \delta_{\sigma_n, \sigma'_n}. \quad (3.56)$$

This is the approach presented in [14]. With such a dual basis an identity operator,

$$\sum_{\sigma_n} |\sigma_n\rangle [\sigma_n| = \sum_{\sigma_n} [\sigma_n| \langle \sigma_n| = \mathbb{1}, \quad (3.57)$$

and projection operators can be constructed. However there is a problem with employing this approach naively. It is not possible to construct a dual basis for an over-complete

¹⁴We employ crossing symmetry to represent incoming colour lines as outgoing anti-colour lines. Consequently, the colour/anti-colour lines of any gauge invariant amplitude can always be grouped into connected pairs.

¹⁵Systematically and efficiently finding complete sets of basis tensors in an arbitrarily large $SU(N)$ product space is a well studied but still fairly open problem ([17, 18] and references therein). However, it is known that the number of basis tensors grows slower than the factorial of the product space's dimension [18].

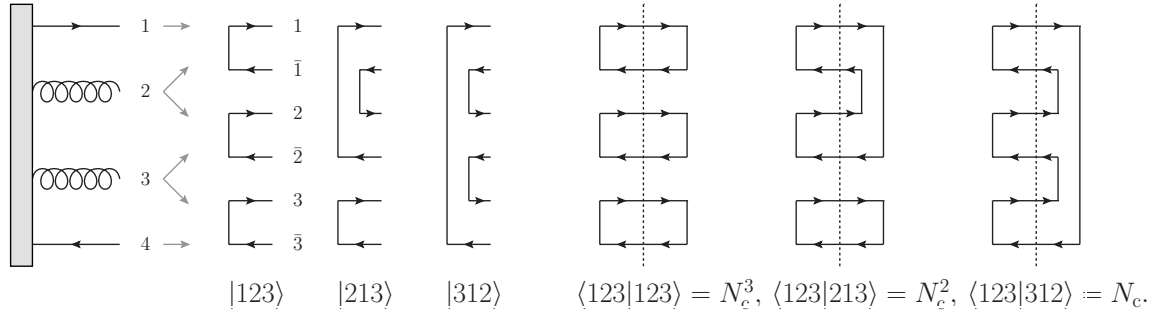


Figure 3.2: Diagrammatic representation of colour flow basis states and their inner products. The left half of the figure shows three out of the six basis tensors required for a $qg\bar{g}\bar{q}$ state, originating from some process in the grey rectangle. The grey arrows indicate how leg labels $i = 1, \dots, 4$ are mapped onto colour and anti-colour indices. The right hand part of the figure illustrates how inner products relate to powers of N_c depending on how many loops are formed after contraction, or equivalently the number of permutations between the two colour-flow basis vectors as per Eq. (3.55). Figure based on the diagrams presented in [14].

spanning set. This is because for a spanning set to be over-complete the following must be true:

$$\sum_{\sigma_n} \lambda_{\sigma_n} |\sigma_n\rangle = 0 \mid \exists \lambda_{\sigma_n} \neq 0. \quad (3.58)$$

However we can see that if a dual basis exists

$$\forall \sigma'_n, \quad [\sigma'_n | \sum_{\sigma_n} \lambda_{\sigma_n} |\sigma_n\rangle = \lambda_{\sigma'_n} = 0. \quad (3.59)$$

This is contradictory. However, despite this contradiction, a more sophisticated construction does allow for a dual basis to be used in conjunction with the CFB.

Embedding-space trick

We can express $|\mathcal{M}_m\rangle$, where m is the number of colour flows, using the following expansion in the CFB

$$|\mathcal{M}_m\rangle = \sum_{\sigma_m} \mathcal{M}_{\sigma_m} |\sigma_m\rangle, \quad \sigma_m \in S_m. \quad (3.60)$$

This expansion is not unique, due to the basis being over-complete, however we do not need the expansion to be unique for the following discussion. Thus we can compute ‘squared amplitudes’ as

$$\langle \mathcal{M}'_m | \mathcal{M}_m \rangle = \sum_{\sigma'_m, \sigma_m} \mathcal{M}'_{\sigma'_m} \mathcal{M}_{\sigma_m} \langle \sigma'_m | \sigma_m \rangle. \quad (3.61)$$

Let us introduce a new larger colour flow vector

$$|\tau_m^n\rangle = |\sigma_m, m+1, m+2, \dots, n\rangle; \quad (3.62)$$

i.e. if $\sigma_4 = 4, 2, 3, 1$ then $\tau_4^n = 4, 2, 3, 1, 5, 6, \dots, n$ (we require that $n > m$). Note that

$$\{|\tau_m^n\rangle\} \subset \{|\sigma_n\rangle\}, \quad (3.63)$$

and that S_m is a subgroup of S_n . Now, consider the limit $n \rightarrow \infty$. We denote the over-complete basis over an uncountably infinite number of colour flows as $\{|\sigma_\infty\rangle\}$ ¹⁶ and the complete basis over the countable (finite) subset of colour flows as $\{|\tau_m^\infty\rangle\}$. It is the case that

$$\lim_{n \rightarrow \infty} \{|\tau_m^n\rangle\} := \{|\tau_m^\infty\rangle\} \subset \{|\sigma_\infty\rangle\}, \quad (3.64)$$

spans a subspace equivalent to that of $\{|\sigma_m\rangle\}$. Following these observations, we have the bracket

$$\langle \sigma'_m | \sigma_m \rangle = \frac{\langle \tau_m'^n | \tau_m^n \rangle}{N_c^{n-m}}. \quad (3.65)$$

As this expression evaluates to being independent of n we can take the limit

$$\langle \sigma'_m | \sigma_m \rangle = \lim_{n \rightarrow \infty} \frac{\langle \tau_m'^n | \tau_m^n \rangle}{N_c^{n-m}}. \quad (3.66)$$

We can define a dual basis by embedding our representation of the CFB within the space spanned by $\{|\tau_m^\infty\rangle\}$, using this bracket and exploiting the $n \rightarrow \infty$ limit.¹⁷ We can find a representation for such a dual basis:

$$|\tau_m^n\rangle = N_c^{n-m} \sum_{\sigma'} N_c^{T(\sigma'_m, \sigma_m) - n} n^{-T(\sigma'_m, \sigma_m)} |\tau_m'^n\rangle, \quad (3.67)$$

which satisfies

$$[\tau_m'^n | \tau_m^n] = N_c^{n-m} \delta_{\tau_m', \tau_m} + N_c^{n-m} (1 - \delta_{\tau_m', \tau_m}) \mathcal{O}(n^{-T(\sigma'_m, \sigma_m)}). \quad (3.68)$$

We can note that $\delta_{\tau_m', \tau_m} \equiv \delta_{\sigma'_m, \sigma_m}$. Thus we can employ a dual basis so that

$$[\sigma'_m | \sigma_m] \equiv \lim_{n \rightarrow \infty} \frac{[\tau_m'^n | \tau_m^n]}{N_c^{n-m}} = \delta_{\sigma'_m, \sigma_m}. \quad (3.69)$$

We can use Eq. (3.65) as a new but essentially equivalent definition for a dot-product/bracket in the CFB (replacing Eq. (3.55)). The outcome of this trick is that we can use a dual basis

¹⁶The number of basis tensors for an infinite product space of $SU(N)$ is countably infinite [18].

¹⁷Formally this dual basis should be considered a dual set as it does not form a basis over the dual vector space. Rather than forming a basis, the dual set exploits the structure of the CFB to define an operator which acts as a dual to a state $|\sigma_n\rangle$. Specifically, we are exploiting that $T(\sigma'_m, \sigma_m) = 0$ only when $\sigma'_m = \sigma_m$ and that terms for which $T(\sigma'_m, \sigma_m) \neq 0$ can be associated with a suppression.

i	c_i	\bar{c}_i	λ_i	$\bar{\lambda}_i$
quark	yes	no	$\sqrt{T_R}$	0
gluon	yes	yes	$\sqrt{T_R}$	$\sqrt{T_R}$
anti-quark	no	yes	0	$\sqrt{T_R}$

Table 3.1: The colour index specifications for the three types of QCD particle (quark, anti-quark, and gluons). If the particle has a colour line index c_i then the column is marked with yes, likewise for an anti-colour line index \bar{c}_i . $T_R = 1/2$ is the usual normalisation factor of $SU(N)$ group generators.

quite freely whilst performing computations in the colour flow basis; with the knowledge that we are relying on the existence of this embedding and that if a representation of the dual basis is ever explicitly needed then the embedding must be explicitly used.¹⁸ For our purposes, a representation is never necessary as the dual basis mostly plays the roll of providing formal underpinning to the book-keeping of large colour flow diagrams, as per the approach in [14].

3.2.3 $1/N_c$ expansion

Now we have introduced the colour-flow basis and discussed some formalities associated with its usage, let us give some direct examples leading us towards the $1/N_c$ expansion. We begin by expressing amplitude density matrices as

$$|M_n\rangle \langle M_n| = \mathbf{A} = \sum_{\tau, \sigma} \mathcal{A}_{\tau\sigma} |\tau\rangle \langle \sigma|. \quad (3.70)$$

Here on we drop the labels on τ and σ and assume they are both elements of the permutation group S_n . The coefficients $\mathcal{A}_{\tau\sigma}$ are not simply the elements of the amplitude density matrix, \mathbf{A} , as one might find in the Gell-Mann basis, since the colour flow basis is not orthonormal. Rather, the coefficients are related to \mathbf{A} through a dual basis for which

$$[\tau|\mathbf{A}|\sigma] \equiv \mathcal{A}_{\tau\sigma}. \quad (3.71)$$

In order to work directly with the elements of an amplitude density matrix, a scalar product matrix $S_{\tau\sigma} = \langle \tau|\sigma \rangle$ has to be introduced:

$$\text{Tr}[\mathbf{A}] = \text{Tr}[\mathcal{A}S] = \sum_{\tau, \sigma} [\tau|\mathbf{A}|\sigma] \langle \sigma|\tau \rangle. \quad (3.72)$$

¹⁸Unlike a dual basis, a dual set is in fact not unique. Therefore other constructions will exist and could also be used.

By carefully studying the Fierz identity's application to the QCD Feynman rules, we can decompose the colour charge operator associated to an external particle i as

$$\mathbb{T}_i = \lambda_i \mathfrak{t}_{c_i} - \bar{\lambda}_i \bar{\mathfrak{t}}_{\bar{c}_i} - \frac{1}{N_c}(\lambda_i - \bar{\lambda}_i) \mathfrak{s} , \quad (3.73)$$

where the factors λ_i and $\bar{\lambda}_i$ are defined in Table 3.1, and where the colour-line operators \mathfrak{t} , $\bar{\mathfrak{t}}$ and \mathfrak{s} are defined through their action on the basis states, i.e.

$$\mathfrak{t}_\alpha |\sigma\rangle = \mathfrak{t}_\alpha \left| \begin{array}{cccccc} 1 & \cdots & \alpha & \cdots & n & \\ \sigma(1) & \cdots & \sigma(\alpha) & \cdots & \sigma(n) & \end{array} \right\rangle = \left| \begin{array}{cccccc} 1 & \cdots & \alpha & \cdots & n & n+1 \\ \sigma(1) & \cdots & n+1 & \cdots & \sigma(n) & \sigma(\alpha) \end{array} \right\rangle , \quad (3.74)$$

and

$$\bar{\mathfrak{t}}_{\bar{\alpha}} |\sigma\rangle = \mathfrak{t}_{\sigma^{-1}(\bar{\alpha})} |\sigma\rangle , \quad (3.75)$$

for the inverse permutation σ^{-1} for which $\tau = \sigma^{-1}(\sigma(\tau))$, and

$$\mathfrak{s} |\sigma\rangle = \mathfrak{s} \left| \begin{array}{cccccc} 1 & \cdots & \cdots & n & & \\ \sigma(1) & \cdots & \cdots & \sigma(n) & & \end{array} \right\rangle = \left| \begin{array}{cccccc} 1 & \cdots & \cdots & n & n+1 & \\ \sigma(1) & \cdots & \cdots & \sigma(n) & n+1 & \end{array} \right\rangle . \quad (3.76)$$

It can be checked from the above relations that colour charge operators cannot map two distinct basis tensors $|\sigma\rangle$ and $|\tau\rangle$ into the same tensor $|\rho\rangle$.

Colour-line operators and their products, such as $\mathfrak{t}_\alpha \cdot \mathfrak{t}_\beta = \mathfrak{t}_\beta \cdot \mathfrak{t}_\alpha$, are referred to as ‘colour reconnectors’ in [19]. It is helpful to note that $\mathfrak{s} \cdot \mathfrak{t}_\alpha = \mathfrak{t}_\alpha \cdot \mathfrak{s} = \mathbb{1}$ and $\mathfrak{s} \cdot \mathfrak{s} = N_c \mathbb{1}$. For more details on expressing colour charges in the colour flow basis see [14].

An important limit for QCD amplitudes is the large- N_c (planar) limit, first introduced by ’t Hooft [20], from which we can define a large- N_c expansion (or $1/N_c$ expansion). The limit is formally defined by letting $N_c \rightarrow \infty$ whilst holding $g_s^2 N_c$ finite, referred to as the ’t Hooft coupling. By considering the possible contractions of colour indices, it should be clear that the largest powers of N_c contributing to QCD cross-sections go as $(\alpha_s N_c)^n$ ¹⁹, and so the large N_c limit defines an expansion in the colour structures of an amplitude: leading colour $((\alpha_s N_c)^n)$, next-to-leading colour $((\alpha_s N_c)^n / N_c)$, NNL colour $((\alpha_s N_c)^n / N_c^2)$, and so forth. QCD colour structures can become very complicated to compute for large multiplicities of radiation. However, often the leading colour terms (see dipole showers in Section 3.5) or terms up to the NNL colour (see angular-ordered showers in Section 3.5) can be remarkably simple. The colour flow basis provides a natural framework in which the large- N_c expansion can be made. To this end we introduce the operation

$$\text{Leading}_{g_{\tau\sigma}}^{(l)} [\mathbf{A}] = \sum_{k=0}^l \mathcal{A}_{\tau\sigma} \Big|_{1/N_c^k} \delta_{T(\tau,\sigma),l-k} , \quad (3.77)$$

¹⁹For a loop to contract non-trivially, a colour line must loop back on itself as an anti-colour line. This only happens at vertices in Feynman diagrams. Hence every non-trivial colour loop comes with at least one vertex and so at least one power of α_s in the cross-section.

where

$$\mathcal{A}_{\tau\sigma}\Big|_{1/N_c^k} \tag{3.78}$$

indicates to pick terms from $\mathcal{A}_{\tau\sigma}$ which are suppressed by a factor of $1/N_c^k$ with respect to the leading power of N_c in $\mathcal{A}_{\tau\sigma}$. As per the previous sections, $T(\sigma, \tau)$ counts the minimum number of transpositions separating σ and τ . Contributions from $\mathcal{A}_{\tau\sigma}\Big|_{1/N_c^k}$ to the trace of \mathbf{A} all give an enhancement or a suppression by a single global power of N_c . Consequently, if we set the 't Hooft coupling to be unitary (i.e. let $\alpha_s = N_c^{-1}$), then

$$\text{Tr} \left[\text{Leading}^{(l)}[\mathbf{A}] \right] \propto N_c^{-l} . \tag{3.79}$$

The leading colour piece is therefore found from

$$\text{Leading}_{\tau\sigma}^{(0)}[\mathbf{A}] = \mathcal{A}_{\tau\sigma}\Big|_{1/N_c^0} \delta_{\tau,\sigma} . \tag{3.80}$$

This has the property that colour flows τ and σ must equal each other. In other words, only products of matrix elements with conjugate matrix elements of the same colour structure contribute to leading colour cross-sections. All quantum mechanical interference between differing colour flows is sub-leading. This motivates the possibility of using a classical branching process for the computation of leading colour QCD radiation (again see Section 3.5). In Chapter 6 we do just this and derive a description of leading colour QCD which is a classical Markov chain. For more details on the colour expansion in the colour flow basis see [14, 19].

3.3 One diverging emission or loop

In this section we will compute limits of two perturbative QCD amplitudes: $|n+1\rangle$, the tree level amplitude for the scattering of $n+1$ well separated on-shell massless quarks and gluons; and $|n^{(1)}\rangle$, the $\mathcal{O}(\alpha_s)$ 1-loop correction to $|n\rangle$.²⁰ We allow for each of the n external particles in $|n\rangle$ to be either incoming or outgoing, however we always assume that the external particle of interest in $|n+1\rangle$ is outgoing. This section is organised as follows:

1. We compute the limit that an internal gluon line which forms a part of a loop becomes soft. We show that, in this limit, the leading behaviour of $|n^{(1)}\rangle$ factorises as $|n^{(1)}\rangle \approx \ln \bar{\mathbf{V}}_{a,b}^n |n\rangle$ where $\ln \bar{\mathbf{V}}_{a,b}^n$ is an operator that dresses the amplitude with a soft loop. The reason for the log in its definition will become clear in Section 3.4.

²⁰This section is based around an amalgam of the seminal texts [7, 21–26].

2. Next we consider the limit that one of the outgoing external particles in $|n+1\rangle$ is soft. We show that, in this limit, the leading behaviour of $|n+1\rangle$ factorises as $|n+1\rangle = \mathbf{S}_{n+1}|n\rangle$ where \mathbf{S}_{n+1} is an operator for emitting a soft gluon. This computation is greatly simplified by the application of the KLN theorem, which necessitates

$$\int_a^b d\Pi_{n+1} \mathbf{S}_{n+1}^\dagger \mathbf{S}_{n+1} = -2\text{Re}\{\ln \bar{\mathbf{V}}_{a,b}^n\},$$

where $d\Pi_{n+1}$ is the phase-space measure for the soft particle and a, b limit the energy of the soft particle in the laboratory frame. This relation ensures the cancellation of logarithmic IR divergences as the energy of the soft particle is allowed to go to zero ($a \rightarrow 0$).

3. Following this we show that in the limit that an internal line which forms a part of a loop becomes collinear to a line joined to it through a vertex, the amplitude factorises as $|n^{(1)}\rangle \approx \ln \tilde{\mathbf{V}}_{a,b}^n |n\rangle$ where $\ln \tilde{\mathbf{V}}_{a,b}^n$ is an operator that dresses the amplitude with a collinear loop.
4. After this, we show that in the limit that one of the outgoing external particles in $|n+1\rangle$ becomes collinear to another particle in $|n+1\rangle$, the amplitude's leading behaviour factorises as $|n+1\rangle = \mathbf{C}_{n+1}|n\rangle$ where \mathbf{C}_{n+1} is an operator for emitting a collinear particle. Again, this computation will be simplified by the application of the KLN theorem.
5. Finally, we study some generalisations: divergences associated with higher powers of α_s , combining the emission/loop operators into a single object, and the unitarity of said object.

We present this discussion assuming a fixed coupling (i.e. without UV renormalisation).

3.3.1 The soft limit of a loop

Let us now compute the leading behaviour of $|n^{(1)}\rangle$ in the limit that one of the internal lines that makes up the loop has momentum $k^\mu = \lambda q^\mu$ where $\lambda \rightarrow 0$ and q is a finite 4-momentum. This is a soft scaling as discussed in Section 3.1.1. We will perform this computation using spin-averaged amplitudes since the soft limit is insensitive to spin, which we show in the following section. There are 3 distinct groups of Feynman diagram topologies we can consider: the momenta flowing through the vertices at the end of the soft line are distinct and on-shell, one or both of the momentum flowing through the vertices at the end of the line are distinct and off-shell, and the loop is self-energy-like. For each group of topologies we also consider every permutation of the lines involved being gluonic, fermionic, or ghosts.

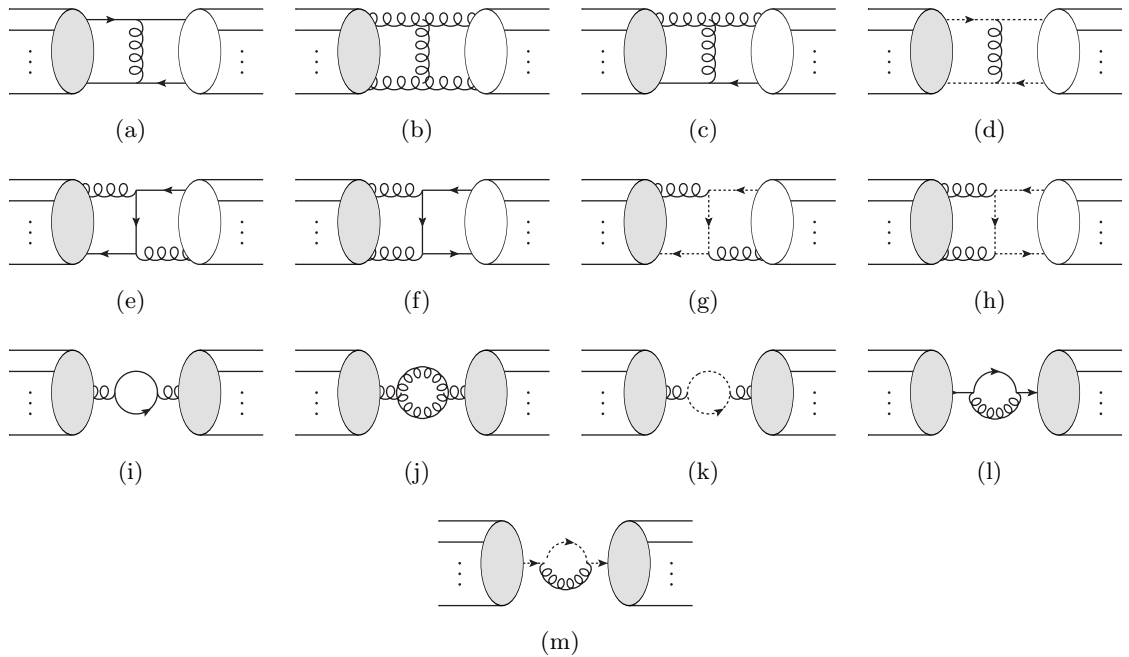


Figure 3.3: The Feynman diagrams contributing to $|n^{(1)}\rangle$. We have not separated incoming lines from outgoing, which means external lines to the left and right can be in either the initial or final state. External solid lines are allowed to be fermionic or gluonic. The graphs are in this style so that the loop momentum can be isolated as depicted. The ovals contain the remaining lines and vertices in the graph. The grey ovals represent connected graphs whilst the white ovals can be separated into two disconnected sub-graphs. In graphs (a)-(h) we have singled out the (vertical) line which is becoming soft (or collinear in the subsequent sections) and the loop closes in the grey oval. We refer to the loops in graphs (i)-(m) as self-energy-like. In graphs (i)-(m) the grey ovals only depend on on-shell momenta. We have omitted drawing every asymmetric permutation of gluon/fermion/ghost lines linking the grey oval and the white oval.

The relevant graphs are shown in Figure 3.3. In this section we will primarily focus on the calculation of graph 3.3(a), culminating in the factorised form given in Eq. (3.93). Following this, we will observe that graphs 3.3(b) and 3.3(c) are functionally the same as graph 3.3(a) due to the universality of the soft gluon limit, and we will argue that all other graphs give a sub-leading contribution in the soft limit.

We will now compute the soft limit of graph 3.3(a). We can write the amplitude for a gluon line, in the Feynman gauge, joining two fermion lines (A and B) to form a loop inside

$|n^{(1)}\rangle$ as

$$\begin{aligned}
\left|n^{(1)} : f_A g f_B\right\rangle &= g_s^2 \int \frac{d^4k}{(2\pi)^4} \frac{i u_s^\alpha(p_A) \bar{u}_s^\beta(p_A)}{p_A^2 + i\epsilon} i \gamma_{\beta\gamma}^\mu T_{ij}^c \frac{i u_s^\gamma(p_A - k) \bar{u}_s^\delta(p_A - k)}{(p_A - k)^2 + i\epsilon} \\
&\quad \times \frac{i u_{s'}^{\alpha'}(p_B) \bar{u}_{s'}^{\beta'}(p_B)}{p_B^2 + i\epsilon} i \gamma_{\beta'\gamma'}^\nu T_{lk}^c \frac{i u_{s'}^{\gamma'}(p_B + k) \bar{u}_{s'}^{\delta'}(p_B + k)}{(p_B + k)^2 + i\epsilon} \\
&\quad \times \frac{-i g^{\mu\nu}}{k^2 + i\epsilon} |\overline{w+2}\rangle_\alpha^i |z+2\rangle_{\alpha'}^l |\overline{n-w-z}\rangle_{\delta\delta'}^{jk}, \quad (3.81)
\end{aligned}$$

where the label $f_A g f_B$ singles out the topology where a loop gluon is exchanged between fermion particle lines A and B (see Figure 3.4). $|\overline{n-w-z}\rangle_{jk}^{\delta\delta'}$ is an ‘incomplete’ tree-level $(n-w-z)$ particle amplitude, it is a function of $p_A - k$ and $p_B + k$. Similarly $|\overline{w+2}\rangle_i^\alpha$ $|\overline{z+2}\rangle_l^{\alpha'}$ are ‘incomplete’ tree-level $w+2$ and $z+2$ particle amplitudes; they are functions of p_A and p_B respectively but not k . The ‘incomplete’ amplitudes are related to complete spin-averaged amplitudes for the scattering of on-shell particles by

$$|\overline{n-w-z}\rangle = \sum_{\bar{s}, \bar{s}'} \bar{u}_{\bar{s}}^\delta(p_A - k) \bar{u}_{\bar{s}'}^{\delta'}(p_B + k) |\overline{n-w-z}\rangle_{\delta\delta'}, \quad (3.82)$$

given $p_A - k$ and $p_B + k$ are on-shell 4-momenta, and

$$|\overline{w+2}\rangle = \sum_s u_s^\alpha(p_A) |\overline{w+2}\rangle_\alpha, \quad |z+2\rangle = \sum_{s'} u_{s'}^{\alpha'}(p_B) |z+2\rangle_{\alpha'}, \quad (3.83)$$

given p_A and p_B are on-shell 4-momenta. We have chosen to express the colour charge operators for the emission from fermionic legs A and B in the Gell-Mann basis ($\mathbb{T}_A \mapsto T_{ij}^c$ and $\mathbb{T}_B \mapsto T_{lk}^c$) whilst keeping the rest of the colour structures abstracted. We do this so that it is easier to see in which $SU(N)$ sub-space each operator acts and apply the Feynman rules given in Section 2.2.3. $\alpha, \beta, \gamma, \delta$ are 4-component spinor indices and summation over paired indices is implicit. We have assumed all momenta are outgoing, however this was without loss of generality. To treat p_A as incoming we need only systemically exchange $u_s^\alpha(p_A) \rightarrow v_{-s}^\alpha(p_A)$ and $p_A \rightarrow -p_A$.

Firstly let us consider the case where p_A and p_B are on-shell. In this limit

$$\sum_s \frac{u_s^\alpha(p_A)}{p_A^2 + i\epsilon} |\overline{w+2}\rangle_\alpha^i \rightarrow \begin{cases} 1 & \text{if } w = 0, \\ \infty & \text{if } w > 0, \end{cases} \quad (3.84)$$

as momentum conservation requires that if $w > 0$ then w of those particles must be either exactly soft or exactly collinear to p_A . The same is true for $|\overline{z+2}\rangle_{\alpha'}^l$. We wish to study the limit where exactly one of the particle lines (i.e. the one with momentum k) is soft and

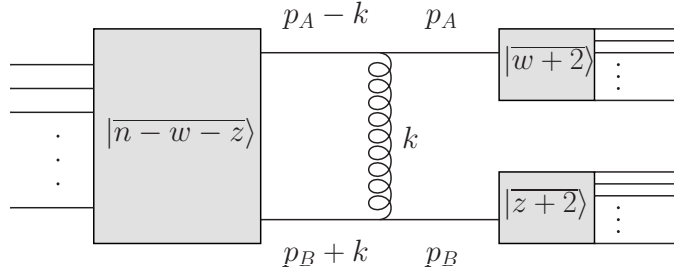


Figure 3.4: The topology contributing to $|n^{(1)}\rangle$ considered in Eq. (3.81). The grey boxes represent incomplete amplitudes defined by the relations below Eq. (3.81). The loop with momentum k is completed in $|\overline{n-w-z}\rangle$. Just as in Figure 3.3, incoming lines have not been separated from outgoing. External lines to the left and right can be in either the initial or final state.

there are no other IR divergences. Hence, we find

$$\begin{aligned}
\left|n^{(1)} : f_A g f_B\right\rangle_{p_A^2=p_B^2=0} &= \sum_{s,s'} g_s^2 \int \frac{d^4 k}{(2\pi)^4} \bar{u}_s^\beta(p_A) i\gamma_{\beta\gamma}^\mu T_{ij}^c \frac{i u_s^\gamma(p_A - k) \bar{u}_s^\delta(p_A - k)}{-2p_A \cdot k + i\epsilon} \\
&\quad \times \bar{u}_{s'}^{\beta'}(p_B) i\gamma_{\beta'\gamma'}^{\nu} T_{lk}^c \frac{i u_{s'}^{\gamma'}(p_B + k) \bar{u}_{s'}^{\delta'}(p_B + k)}{2p_B \cdot k + i\epsilon} \\
&\quad \times \frac{-ig^{\mu\nu}}{k^2 + i\epsilon} |\bar{n}\rangle_{\delta\delta'}^{jk}. \tag{3.85}
\end{aligned}$$

Now we can employ the soft limit so that $u_s(p_A - k) = u_s(p_A) + \mathcal{O}(\lambda)$. We can use the relation $\bar{u}_s(p)\gamma^\mu u_{s'}(p) = 2p^\mu \delta_{ss'}$ ²¹ so that

$$\begin{aligned}
\left|n^{(1)} : f_A g f_B\right\rangle_{p_A^2=p_B^2=0} &= g_s^2 \int \frac{d^4 k}{(2\pi)^4} \frac{i^2 2p_A^\mu}{-2p_A \cdot k + i\epsilon} \frac{-ig_{\mu\nu}}{k^2 + i\epsilon} \frac{i^2 2p_B^\nu}{2p_B \cdot k + i\epsilon} \\
&\quad \times \mathbb{T}_A \cdot \mathbb{T}_B |n\rangle + \mathcal{O}(\lambda), \tag{3.86}
\end{aligned}$$

where we have restored the complete colour charge operators. Thus we can see that in the limit we are considering the 1-loop n particle amplitude factorises into a tree-level n particle amplitude and a colour space operator acting on that amplitude.

Before further proceeding, let us get a few technical details out the way. Firstly, we are integrating over k and so in order to correctly approximate around the limit that $k^\mu = \lambda q^\mu$ where $\lambda \rightarrow 0$ we must use the method of regions. This means splitting the domain of integration into regions defined around some Lorentz invariant ‘hard scale’ $Q^2 \sim (p_A + p_B)^2$ so that we can define $\lambda = k^0/Q$. There are 4 relevant regions for us; where $k^0 < Q$ and $\mathbf{k}^2 < Q^2$, where $k^0 < Q$ and $\mathbf{k}^2 > Q^2$ or vice versa, and where $k^0 > Q$ and $\mathbf{k}^2 > Q^2$. Note that only the first and last regions listed allow for k to be on-shell and that only the first region contains an infra-red pole, this is what we have computed. Following the method of

²¹Useful relations for free Dirac spinors are itemised in Appendix A.1.

regions carefully, the domain of integration in Eq. (3.86) should be restricted so that $k^0 < Q$ and $\mathbf{k}^2 < Q^2$. As we discussed in Section 3.1.1, computing the other non-pole regions is needed to know the correct value for Q^2 . This is not possible in the completely general case but for specific cases can be found by matching to fixed order computations. We'll discuss this more at the end of this section.

Eq. (3.86) was derived assuming both A and B are outgoing. Let us now give the relations allowing for incoming particles:

$$\left| n^{(1)} : f_A g f_B \right\rangle \Big|_{p_A^2=p_B^2=0} = g_s^2 \int \frac{d^4 k}{(2\pi)^4} \frac{i^2 2p_A^\mu}{-2p_A \cdot k + i\epsilon} \frac{-ig_{\mu\nu}}{k^2 + i\epsilon} \frac{i^2 2p_B^\nu}{-2p_B \cdot k + i\epsilon} \times \mathbb{T}_A \cdot \mathbb{T}_B |n\rangle + \mathcal{O}(\lambda), \quad (3.87)$$

if A is outgoing and B is incoming, and

$$\left| n^{(1)} : f_A g f_B \right\rangle \Big|_{p_A^2=p_B^2=0} = g_s^2 \int \frac{d^4 k}{(2\pi)^4} \frac{i^2 2p_A^\mu}{2p_A \cdot k + i\epsilon} \frac{-ig_{\mu\nu}}{k^2 + i\epsilon} \frac{i^2 2p_B^\nu}{-2p_B \cdot k + i\epsilon} \times \mathbb{T}_A \cdot \mathbb{T}_B |n\rangle + \mathcal{O}(\lambda), \quad (3.88)$$

if both A and B are incoming.

Now all that remains is to perform the integration. This is most easily done by decomposing the integral measure in the A, B zero-momentum frame as $dk^4 \rightarrow dk^0 d^2\mathbf{k}_\perp^{(A,B)} d\theta$ where k^0 is the energy of k , $\mathbf{k}_\perp^{(A,B)}$ is the transverse momentum of k , and θ is the angle between k and p_A (or p_B).²² First looking at Eq. (3.87), the k^0 integral can be performed by the residue theorem: we pick up a pole from the gluon propagator with an accompanying requirement that $k^2 = 0$. The trivial azimuth in the $d^2\mathbf{k}_\perp^{(A,B)}$ integral can also be easily performed. The final two integrals provide a non-integrable double pole, hence we will leave them undone. We find that

$$\text{Eq. (3.87)} = \frac{g_s^2}{4\pi^2} \int_0^\infty \frac{dk_\perp^{(A,B)}}{dk_\perp^{(A,B)}} \int_0^\pi \frac{d\theta}{\sin\theta} \Theta(k_\perp^{(A,B)} < Q) \Theta(k^0 < Q) \mathbb{T}_A \cdot \mathbb{T}_B |n\rangle + \mathcal{O}(\lambda). \quad (3.89)$$

Here the theta functions come from our application of the method of regions. The same result is found when letting A be incoming and B be outgoing. Turning to Eq. (3.86), the k^0 integral can again be performed by the residue theorem. The same gluon propagator pole is found, and a second pole is also picked up from fermion B 's propagator. The gluon-propagator-pole term integrates to the same form as Eq. (3.89), however the fermion propagator pole introduces a second term that is purely imaginary, known as the Coulomb/Glauber term²³.

²²Useful relations for decomposing phase-space measures are given in Appendix A.3.

²³Technically the gluon loop momentum has a Coulomb/Glauber scaling when we pick up the residue from the pole.

All together,

$$\begin{aligned} \text{Eq. (3.86)} &= \frac{g_s^2}{4\pi^2} \int_0^\infty \frac{dk_\perp^{(A,B)}}{dk_\perp^{(A,B)}} \int_0^\pi \frac{d\theta}{\sin\theta} \Theta(k_\perp^{(A,B)} < Q) \Theta(k^0 < Q) \mathbb{T}_A \cdot \mathbb{T}_B |n\rangle \\ &\quad - \frac{g_s^2}{4\pi^2} \int_0^\infty \frac{dk_\perp^{(A,B)}}{dk_\perp^{(A,B)}} i\pi \Theta(k_\perp^{(A,B)} < Q) \mathbb{T}_A \cdot \mathbb{T}_B |n\rangle + \mathcal{O}(\lambda). \end{aligned} \quad (3.90)$$

The same is found when both p_A and p_B are incoming. We can combine Eq. (3.89) and Eq. (3.90) as

$$\left| n^{(1)} : f_A g f_B \right\rangle \Big|_{p_A^2=p_B^2=0} \approx \frac{\alpha_s}{\pi} \int_0^Q \frac{dk_\perp^{(A,B)}}{dk_\perp^{(A,B)}} \left(\int_0^\pi \frac{d\theta}{\sin\theta} \Theta(k^0 < Q) - i\pi \tilde{\delta}_{AB} \right) \mathbb{T}_A \cdot \mathbb{T}_B |n\rangle, \quad (3.91)$$

where $\tilde{\delta}_{AB} = 1$ when A, B are both outgoing or both incoming and $\tilde{\delta}_{AB} = 0$ otherwise.

Now let us consider what happens when either p_A or p_B (or both) are relatively off-shell ($p_{A/B}^2 \gg p_{A/B} \cdot k$).²⁴ We can again start from Eq. (3.81) and, to be concrete, let p_A be off-shell. If we expand around the soft limit we find

$$\begin{aligned} \left| n^{(1)} : f_A g f_B \right\rangle &\approx g_s^2 \int \frac{d^4k}{(2\pi)^4} \frac{i u_s^\alpha(p_A) \bar{u}_s^\beta(p_A)}{p_A^2 + i\epsilon} i \gamma_{\beta\gamma}^\mu T_{ij}^c \frac{i u_s^\gamma(p_A) \bar{u}_s^\delta(p_A)}{p_A^2 + i\epsilon} \\ &\quad \times \frac{i u_{s'}^{\alpha'}(p_B) \bar{u}_{s'}^{\beta'}(p_B)}{p_B^2 + i\epsilon} i \gamma_{\beta'\gamma'}^\nu T_{lk}^c \frac{i u_{s'}^{\gamma'}(p_B) \bar{u}_{s'}^{\delta'}(p_B)}{2p_B \cdot k + i\epsilon} \\ &\quad \times \frac{-i g^{\mu\nu}}{k^2 + i\epsilon} \left| \overline{w+2} \right\rangle_\alpha^i \left| \overline{z+2} \right\rangle_{\alpha'}^l \left| \overline{n-w-z} \right\rangle_{\delta\delta'}^{jk}. \end{aligned} \quad (3.92)$$

This term is linear in λ and so vanishes in the exact soft-limit. Therefore, at the accuracy we are considering, we treat it as sub-leading and so set it to zero. Allowing both p_A and p_B to be relatively off-shell gives a contribution cubic in λ and so is even further suppressed in the soft limit.

Summing Eq. (3.91) and Eq. (3.92) gives the complete soft limit of graph 3.3(a). However, before we give the final result, let us consider when the soft gluon loop is self-energy-like and attached to fermion vertices (graph 3.3(1)). We can once again start from Eq. (3.81) and set $p_A = p_B$. In the case that p_A is relatively off-shell the diagram is cubic in λ , as we argued in the previous paragraph, and is therefore negligible. In case where p_A is on-shell, the diagram is proportional to p_A^2 and so is also equal to zero; see Eq. (3.87). Thus, we can combine the self-energy-like graph with graph 3.3(a) and find the complete leading contribution from soft gluon lines forming loops attached to fermion vertices:

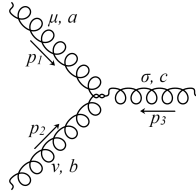
$$\left| n^{(1)} : f g f \right\rangle \approx \frac{\alpha_s}{\pi} \sum_{\text{pairs}(A,B)} \int_0^Q \frac{dk_\perp^{(A,B)}}{dk_\perp^{(A,B)}} \left(\int_0^\pi \frac{d\theta}{\sin\theta} \Theta(k^0 < Q) - i\pi \tilde{\delta}_{AB} \right) \mathbb{T}_A \cdot \mathbb{T}_B |n\rangle, \quad (3.93)$$

²⁴The case where $p_{A/B}^2 < p_{A/B} \cdot k$ but non-zero reduces to the same form where $p_{A/B}$ is exactly on-shell.

where A and B are on-shell fermions in the amplitude $|n\rangle$. The subscripts on fgf have been dropped since pairs of fermion lines A and B are summed over.

To complete our discussion of the leading behaviour of $|n^{(1)}\rangle$, as a loop momentum becomes soft, we must do two things. Firstly, compute the other possible loop topologies: a loop gluon line becoming soft which is attached via vertices to other gluon lines (graphs 3.3(b) and 3.3(j)), a loop gluon line becoming soft which is attached via vertices to another gluon line and another fermion line (graph 3.3(c)), a loop fermion line becoming soft (graphs 3.3(e), 3.3(f), 3.3(i), 3.3(l)), and graphs with ghost lines in the loop (the remaining graphs in Figure 3.3). As we will shortly argue, we have already done all the hard work and these topologies can be easily deduced from $|n^{(1)} : fgf\rangle$. And secondly, we must complete our application of the method of regions by discussing the contributions from non-pole regions.

The soft gluon limit is universal, regardless whether the gluon is emitted from a quark or gluon the factorised soft operator is the same. This can be quickly seen by noting that the triple vertex in a Feynman diagram with a gluon in the soft limit can be replaced by



$$= g_s f^{abc} [g^{\mu\nu} (p_1 - p_2)^\sigma + g^{\nu\sigma} (p_2 - p_3)^\mu + g^{\sigma\mu} (p_3 - p_1)^\nu],$$

$$\equiv 2g_s \mathbb{T}_1 g^{\mu\nu} p_1^\sigma + \mathcal{O}(\lambda) \equiv -2g_s \mathbb{T}_2 g^{\mu\nu} p_2^\sigma + \mathcal{O}(\lambda), \quad (3.94)$$

where p_3 is soft. This leads to the numerator for a Feynman diagram with a soft gluon being independent of whether the gluon is attached to other quarks or gluons; remember that the soft limit leads to numerators of the form $\bar{u}_s(p_A + k) g_s \gamma^\mu \mathbb{T}_A u_{s'}(p_A) = 2g_s \mathbb{T}_A p_A^\mu \delta_{ss'} + \mathcal{O}(\lambda)$ when the gluon is connected to a quark. Thus $|n^{(1)} : fgf\rangle \approx |n^{(1)} : fgg\rangle \approx |n^{(1)} : ggg\rangle$ to first order in λ .²⁵ Also note that an (anti-)quark becoming soft does not contribute to the leading behaviour of an amplitude in the IR limit since the diagrams have the same denominator structure as those of a soft gluon but the fermion propagator numerator scales linearly in λ . Therefore soft fermion amplitudes (graphs 3.3(e), 3.3(f), 3.3(i), 3.3(l)) are linear in λ . All together, the amplitude for topologies in the form of graph 3.3(c) is

$$|n^{(1)} : fgg\rangle \approx \frac{\alpha_s}{\pi} \sum_{\text{pairs}(A,B)} \int_0^Q \frac{dk_\perp^{(A,B)}}{dk_\perp^{(A,B)}} \left(\int_0^\pi \frac{d\theta}{\sin\theta} \Theta(k^0 < Q) - i\pi \tilde{\delta}_{AB} \right) \mathbb{T}_A \cdot \mathbb{T}_B |n\rangle, \quad (3.95)$$

²⁵This is not accidental and can be attributed to an approximate supersymmetry of QCD. At tree-level and ignoring colour charges, massless QCD amplitudes are equivalent to those of a super-symmetric Yang-Mills theory with gluinos playing the role of quarks. This supersymmetry constrains the soft gluon limit to being universal at tree level [25, 27] and therefore by the KLN theorem it must also be universal at one loop.

where A is an on-shell fermion in $|n\rangle$ and B an on-shell gluon in $|n\rangle$. The amplitude for topologies in the form of graph 3.3(c) is

$$\left|n^{(1)} : ggg\right\rangle \approx \frac{\alpha_s}{\pi} \sum_{\text{pairs}(A,B)} \int_0^Q \frac{dk_{\perp}^{(A,B)}}{dk_{\perp}^{(A,B)}} \left(\int_0^{\pi} \frac{d\theta}{\sin \theta} \Theta(k^0 < Q) - i\pi \tilde{\delta}_{AB} \right) \mathbb{T}_A \cdot \mathbb{T}_B |n\rangle, \quad (3.96)$$

where both A and B are on-shell gluons in $|n\rangle$, and the leading behaviour of an amplitude containing a soft fermion line is

$$\left|n^{(1)} : \text{soft } f\right\rangle \approx 0. \quad (3.97)$$

Finally, ghosts also do not provide a leading contribution. To see this, consider recreating the generalised Feynman amplitude, Eq. (3.81), however letting either the momenta p_A or p_B (or both) be the momentum of a ghost line. Depending on the diagram topology, the loop momentum k will either be associated to a gluon or a ghost line. In both cases it is not possible to place either p_A or p_B on-shell as this would require the ghosts to be in either the final or initial state particles. Therefore, p_A and p_B must be off-shell, forcing the diagram to be sub-leading – as was the case when the fermion momenta were off-shell. For an alternative derivation, we can consider recreating Eq. (3.81) and let both lines associated with momenta $p_A - k$ or $p_B + k$ be ghost lines. Again, depending on the diagram topology, loop momentum k will either be associated to a gluon or a ghost line. The case where k is associated with a gluon line is sub-leading following the same argument as we provided for the other ghost diagrams considered in this paragraph. In the case where k is associated with a ghost line, the diagram obeys the same scaling in λ as that of a soft fermion loop and so is also sub-leading. Hence

$$\left|n^{(1)} : \text{ghosts}\right\rangle \approx 0. \quad (3.98)$$

In total, the leading behaviour of a general one-loop amplitude where one of the loop lines becomes soft is given by

$$\begin{aligned} \left|n^{(1)}\right\rangle &= \left|n^{(1)} : fgf\right\rangle + \left|n^{(1)} : fgg\right\rangle + \left|n^{(1)} : ggg\right\rangle \\ &+ \left|n^{(1)} : (g \rightarrow f)f(g \rightarrow f)\right\rangle + \left|n^{(1)} : \text{ghosts}\right\rangle \approx \ln \bar{\mathbf{V}}_{0,Q}^n |n\rangle, \end{aligned} \quad (3.99)$$

where

$$\ln \bar{\mathbf{V}}_{a,b}^n = \frac{\alpha_s}{\pi} \sum_{\text{pairs}(A,B)} \int_a^b \frac{dk_{\perp}^{(A,B)}}{dk_{\perp}^{(A,B)}} \left(\int_0^{\pi} \frac{d\theta}{\sin \theta} \Theta(k^0 < Q) - i\pi \tilde{\delta}_{AB} \right) \mathbb{T}_A \cdot \mathbb{T}_B, \quad (3.100)$$

and where A and B are on-shell particles in $|n\rangle$. Note that since gauge transformations cannot alter the scaling properties of an amplitude, and both $|n\rangle$ and $|n^{(1)}\rangle$ are independently gauge invariant, $\ln \bar{\mathbf{V}}_{a,b}^n$ must be a gauge invariant operator. Though we derived it using the Feynman gauge, the same result would be found using any other gauge.

To conclude, let us finish our discussion of the application of the method of regions. As we mentioned previously, it is not generally possible to compute the other complimentary regions and cancel the Q dependence. This is because the other regions do not factorise from the amplitude in a process-independent way, as $\ln \bar{\mathbf{V}}_{a,b}^n$ did. This implies that the scale Q is process-dependent. Complete fixed order calculations of various processes typically find that Q should be a Lorentz invariant quantity describing the largest momentum transfer in the process [28]. It is often the centre of mass energy, or the transverse momentum away from the plane of a collision or interaction, or a characteristic Mandelstam variable. The majority of the work in this thesis is process independent and so Q is left as a free parameter. The approximated amplitude varies logarithmically with Q and so when Q can not be precisely determined our usage of the method of regions has an error proportional to a power of $\ln Q/Q'$ where Q' is the correct hard scale. It is usually assumed that $Q/Q' \sim \mathcal{O}(1)$ and so the error will be small.

3.3.2 The soft limit of a real emission

We have computed the soft limit of a single loop and seen that the soft factor factorises from the amplitude. We know from the KLN theorem that the logarithmic divergences from a soft loop must cancel against those from the integration over the phase-space of a single soft external particle. As we mentioned when outlining this section, should soft emissions factorise as $|n+1\rangle = \mathbf{S}_{n+1} |n\rangle$, the KLN theorem leads to the following operator relation

$$\int_a^b d\Pi_{n+1} \mathbf{S}_{n+1}^\dagger \mathbf{S}_{n+1} = -2\text{Re}\{\ln \bar{\mathbf{V}}_{a,b}^n\}, \quad (3.101)$$

where $d\Pi_{n+1}$ is the phase-space measure for the soft particle. In the previous section we showed that only soft loops between external on-shell particles contribute to $\bar{\mathbf{V}}_{a,b}^n$. We also found that the form of $\bar{\mathbf{V}}_{a,b}^n$ was independent of the number of quarks or gluons in $|n\rangle$, rather only depending on the total number of coloured particles. Therefore, Eq. (3.101) informs us that to compute \mathbf{S}_{n+1} we only need to consider a when $|n+1\rangle$ contains a soft gluon, j , emitted from an external on-shell quark, i .²⁶ The matrix element for this topology is

$$|n+1; s_i, \lambda_j\rangle = ig_s \epsilon_\mu^*(p_j, \lambda_j) \bar{u}(p_i, s_i) \mathbb{T}_i \gamma^\mu \frac{i(\not{p}_i + \not{p}_j)}{(p_i + p_j)^2 + i\epsilon} |\hat{n}\rangle, \quad (3.102)$$

²⁶We could have chosen i to be a gluon however this would have entailed slightly more algebra.

where s_i is the spin of quark i , λ_j is the polarisation of gluon j , and where

$$\bar{u}(p_i + p_j, s_{ij}) |\hat{n}\rangle = |n; s_{ij}\rangle. \quad (3.103)$$

Here s_{ij} is the spin of the quark before emitting the gluon j . Now we take the soft limit, $p_j^\mu = \lambda q^\mu$ where $\lambda \rightarrow 0$ and q is a finite 4-momentum, and keep only the leading terms:

$$|n + 1; s_i, \lambda_j\rangle = -g_s \epsilon_\mu^*(p_j, \lambda_j) \bar{u}(p_i, s_i) \mathbb{T}_i \gamma^\mu \frac{\not{p}_i}{2p_i \cdot p_j + i\epsilon} |\hat{n}\rangle + \mathcal{O}(\lambda^0). \quad (3.104)$$

Now note that in the massless limit we can use the relation (see Appendix A.1),

$$\bar{u}(p_i, s_i) \gamma^\mu \not{p}_i \approx \bar{u}(p_i, s_i) \gamma^\mu \sum_{s_{ij}} u(p_i + p_j, s_{ij}) \bar{u}(p_i + p_j, s_{ij}) \approx 2p_i^\mu \bar{u}(p_i + p_j, s_{ij}) \delta_{s_i, s_{ij}}, \quad (3.105)$$

where the approximately equal to means to first order in the soft limit. Thus

$$|n + 1; s_i, \lambda_j\rangle = -g_s \mathbb{T}_i \frac{\epsilon^*(p_j, \lambda_j) \cdot p_i}{p_i \cdot p_j + i\epsilon} |n; s_{ij}\rangle \delta_{s_i, s_{ij}} + \mathcal{O}(\lambda^0). \quad (3.106)$$

This has the important property that the soft limit of the emitted gluon is independent of the spin of the particle from which it was emitted. Thus, summing over all the possible particles, i , from which j could of been emitted,

$$|n + 1\rangle = \mathbf{S}_{n+1} |n\rangle \delta_{s_i, s_{ij}} + \mathcal{O}(\lambda^0), \quad (3.107)$$

where

$$\mathbf{S}_{n+1} = - \sum_{\lambda_j} \sum_i g_s \mathbb{T}_i \frac{\epsilon^*(p_j, \lambda_j) \cdot p_i}{p_i \cdot p_j + i\epsilon}. \quad (3.108)$$

\mathbf{S}_{n+1} is known as the eikonal current. As per the previous discussion on $\ln \bar{\mathbf{V}}_{a,b}^n$, the phase-space for p_j should be restricted in accordance with the method of regions (so that $E_j < E_i$ or an equivalent boundary). It can be checked that the current is gauge invariant by letting $\epsilon^* \rightarrow \epsilon^* + \alpha p_j$, which we know via the Slavnov-Taylor identities is equivalent to a BRST gauge transformation:

$$- \sum_{\lambda_j} \sum_i g_s \mathbb{T}_i \frac{(\epsilon^*(p_j, \lambda_j) + \alpha p_j) \cdot p_i}{p_i \cdot p_j + i\epsilon} = - \sum_{\lambda_j} \sum_i g_s \mathbb{T}_i \frac{\epsilon^*(p_j, \lambda_j) \cdot p_i}{p_i \cdot p_j + i\epsilon} - 2\alpha g_s \sum_i \mathbb{T}_i = \mathbf{S}_{n+1}, \quad (3.109)$$

where we used colour conservation so that $\sum_i \mathbb{T}_i |n\rangle = 0$. Finally, we can check the KLN theorem,

$$\begin{aligned} \mathbf{S}_{n+1}^\dagger \mathbf{S}_{n+1} &= g_s^2 \sum_{\lambda_j} \sum_{i'} \frac{\epsilon(p_j, \lambda_j) \cdot p_{i'}}{p_{i'} \cdot p_j - i\epsilon} \sum_{\lambda_j} \sum_i \mathbb{T}_{i'} \cdot \mathbb{T}_i \frac{\epsilon^*(p_j, \lambda_j) \cdot p_i}{p_i \cdot p_j + i\epsilon}, \\ &= -g_s^2 \sum_{i \neq i'} \mathbb{T}_{i'} \cdot \mathbb{T}_i \frac{p_{i'} \cdot p_i}{(p_{i'} \cdot p_j)(p_i \cdot p_j)}. \end{aligned} \quad (3.110)$$

Noting that

$$\frac{2(p_{i'} \cdot p_j)(p_i \cdot p_j)}{p_{i'} \cdot p_i} = (p_{j\perp}^{(i',i)})^2, \quad (3.111)$$

the squared transverse momentum of j in the (i', i) zero-momentum frame, it can be checked by re-labelling dummy indices for the summation over external particles that

$$\int_a^b d\Pi_{n+1} \mathbf{S}_{n+1}^\dagger \mathbf{S}_{n+1} = -2\text{Re}\{\ln \overline{\mathbf{V}}_{a,b}^n\}.$$

3.3.3 The collinear limit of a loop

Having studied the soft limit, we will now study the collinear limit. The procedure is similar to that of a soft particle but with two key differences: we will be using an axial gauge, which simplifies the analysis by removing ghosts, and we will be expanding around the collinear limit with the scaling given in Section 3.1.1.

To begin our analysis, let us consider a gluon loop with loop momentum going collinear to one of (or both of if the loop is self-energy-like) the momenta flowing through the vertices to which it is attached. We can start from Eq. (3.85), derived in our discussion of soft gluons. At this point we had not yet taken the soft limit but had argued that when the loop was between off-shell momenta it was sub-leading in the IR limit. Eq. (3.85) was for a gluon loop between two fermion lines in the Feynman gauge: replacing the Feynman gauge propagator for the axial gauge,

$$\begin{aligned} |n^{(1)} : f_A g f_B \rangle &= \sum_{s,s'} g_s^2 \int \frac{d^4 k}{(2\pi)^4} \bar{u}_s^\beta(p_A) i\gamma_{\beta\gamma}^\mu T_{ij}^c \frac{i u_s^\gamma(p_A - k) \bar{u}_s^\delta(p_A - k)}{-2p_A \cdot k + i\epsilon} \\ &\quad \times \bar{u}_{s'}^{\beta'}(p_B) i\gamma_{\beta'\gamma'}^\nu T_{lk}^c \frac{i u_{s'}^{\gamma'}(p_B + k) \bar{u}_{s'}^{\delta'}(p_B + k)}{2p_B \cdot k + i\epsilon} \\ &\quad \times \frac{-i d^{\mu\nu}(q)}{k^2 + i\epsilon} |\bar{n}\rangle_{\delta\delta'}^{jk}. \end{aligned} \quad (3.112)$$

where $d^{\mu\nu}(q)$ is the axial gauge numerator (Eq. (2.80)) with an auxiliary vector q .

Now let us consider the limit that k is collinear to p_A and that $p_A \neq p_B$ (graph 3.3(a)). To help us, we use a Sudakov decomposition (Appendix A.3):

$$\begin{aligned} p_A^\mu &= zP^\mu + \frac{k_\perp^2}{z2P \cdot q} q^\mu + k_\perp^\mu, \\ k^\mu &= (1-z)P^\mu + \frac{k_\perp^2}{(1-z)2P \cdot q} q^\mu - k_\perp^\mu, \end{aligned} \quad (3.113)$$

where $k_\perp^\mu \sim \mathcal{O}(\lambda)$, $\lambda \rightarrow 0$, and $P = k + p + \mathcal{O}(\lambda^2)$.²⁷ q^μ is an auxiliary reference vector used to define the decomposition. We have chosen q^μ to coincide with the auxiliary vector in the

²⁷Technically before using this decomposition we should have performed one of the k integrals, the residue of the ϵ pole places k on-shell which the Sudakov decomposition exploits. However this does not effect the power counting argument.

numerator of the axial gauge gluon propagator. Power counting lets us see that the integral measure is cubic in λ and denominators are quadratic. Once simplified, the numerator will necessarily have the form

$$\text{numerator} = (\alpha p_A^\mu + \beta k^\mu) d_{\mu\nu}(q) (\alpha' p_B^\mu + \beta' k^\mu) \quad (3.114)$$

where $\alpha, \beta, \alpha', \beta'$ are Lorentz invariant products of momenta. Note that in the axial gauge $k^\mu d_{\mu\nu}(q) = 0$, and as k is going collinear to p_A it is also the case that $p_A^\mu d_{\mu\nu}(q) = \mathcal{O}(\lambda^2)$. Therefore the configuration from Eq. (3.85) is sub-leading in the collinear limit (it is $\mathcal{O}(\lambda)$).

In order to get a configuration which is leading in the collinear limit, we require that $p_A = p_B$. In the previous section we have argued that $p_A = p_B$ can only occur at our level of accuracy for self-energy-like topologies, where A and B are the same particle (graphs such as 3.3(1)). Therefore, in the axial gauge, a collinear gluon loop joined by vertices to quarks is only leading for self-energy-like topologies. This is a general feature of the axial gauge, and using a similar approach to the one above it can be shown that only self-energy-like topologies of loops dressing on-shell particles contribute to the leading collinear limit.

Let us now focus on a self-energy-like gluon loop dressing an on-shell quark (A) in the amplitude $|n^{(1)}\rangle$ (graph 3.3(1) either of the two ovals removed). The amplitude for this is

$$\begin{aligned} |n^{(1)} : q_A g q_A\rangle &= \sum_s g_s^2 \int \frac{d^4 k}{(2\pi)^4} \bar{u}_s^\beta(p_A) i\gamma_{\beta\gamma}^\mu T_{ij}^c \frac{i u_s^\gamma(p_A - k) \bar{u}_s^\delta(p_A - k)}{-2p_A \cdot k + i\epsilon} \\ &\quad \times i\gamma_{\delta\gamma'}^\nu T_{jk}^c \frac{i u_{s'}^{\gamma'}(p_A) \bar{u}_{s'}^{\delta'}(p_A) - id^{\mu\nu}(q)}{p_A^2 + i\epsilon} \frac{-id^{\mu\nu}(q)}{k^2 + i\epsilon} |\bar{n}\rangle_{\delta'}^k. \end{aligned} \quad (3.115)$$

We can re-express this as

$$\begin{aligned} |n^{(1)} : q_A g q_A\rangle &= \sum_s g_s^2 \int \frac{d^4 k}{(2\pi)^4} \bar{u}_s^\beta(p_A) i\gamma_{\beta\gamma}^\mu \frac{i u_s^\gamma(p_A - k) \bar{u}_s^\delta(p_A - k)}{-2p_A \cdot k + i\epsilon} \\ &\quad \times i\gamma_{\delta\gamma'}^\nu \frac{i u_{s'}^{\gamma'}(p_A) - id^{\mu\nu}(q)}{p_A^2 + i\epsilon} \mathbb{T}_A^2 |n\rangle. \end{aligned} \quad (3.116)$$

Performing the residue integral over k^0 picks up a pole forcing k on-shell. We can use the Sudakov decomposition so that (after some lengthy algebra which is shown in more detail in the next section²⁸) the leading part is given by

$$|n^{(1)} : q_A g q_A\rangle = -\frac{\alpha_s}{\pi} \int \frac{dk_\perp}{k_\perp} \int \frac{dz d\phi}{8\pi} \mathcal{P}_{qq}(z) \Theta(k) \mathbb{T}_A^2 |n\rangle, \quad (3.117)$$

where $\mathcal{P}_{qq}(z)$ is the $q \rightarrow qq$ splitting function:

$$\mathcal{P}_{qq}(z) = \frac{1+z^2}{1-z}. \quad (3.118)$$

²⁸Better yet, the algebra can be quickly performed in a bespoke computer program such as Mathematica.

$\Theta(k)$ is a theta function, ensuring that k is integrated only over a region consistent with the method of regions, i.e. $k_\perp < Q$ some hard scale and $z < 1$ ensuring both p_A and k are on-shell.

As we previously explained, leading collinear terms come from loops which are self-energy-like. There are two further self-energy-like diagrams we can consider: $g \rightarrow q\bar{q} \rightarrow g$ (graph 3.3(i)), and $g \rightarrow gg \rightarrow g$ (graph 3.3(j)). There is no further subtlety in computing these loops, rather one must just “turn the handle” and get through the algebra. As we go through the algebra in the next section on collinear external particles, we will just state the answer for now. For $g \rightarrow q\bar{q} \rightarrow g$,

$$\left| n^{(1)} : g_A q g_A \right\rangle = -\frac{\alpha_s}{\pi} \int \frac{dk_\perp}{k_\perp} \int \frac{dz d\phi}{8\pi} \mathcal{P}_{qg}(z) \Theta(k) |n\rangle, \quad (3.119)$$

where

$$\mathcal{P}_{qg}(z) = n_f T_R (1 - 2z(1 - z)). \quad (3.120)$$

Here n_f is the number of light quarks (which can be approximated as massless), typically taken as 3 for QCD. $T_R = 1/2$ is the usual group theory normalisation constant for SU(3) generators in the fundamental representation. For $g \rightarrow gg \rightarrow g$,

$$\left| n^{(1)} : g_A g g_A \right\rangle = -\frac{\alpha_s}{\pi} \int \frac{dk_\perp}{k_\perp} \int \frac{dz d\phi}{8\pi} \mathcal{P}_{gg}(z) \Theta(k) \mathbb{T}_A^2 |n\rangle, \quad (3.121)$$

where²⁹

$$\mathcal{P}_{gg}(z) = \left(z(1 - z) + \frac{z}{1 - z} + \frac{1 - z}{z} \right). \quad (3.122)$$

Concluding this section, the collinear limit of a single loop factorises from a one loop amplitude as

$$\left| n^{(1)} \right\rangle \approx \ln \tilde{\mathbf{V}}_{0,Q}^n |n\rangle, \quad (3.123)$$

where

$$\ln \tilde{\mathbf{V}}_{a,b}^n = -\frac{\alpha_s}{\pi} \sum_A \int_a^b \frac{dk_\perp}{k_\perp} \int \frac{dz d\phi}{8\pi} \Theta(k) \left(\mathcal{P}_{qg}(z) \mathbb{T}_A^2 \delta_A^{(g)} + \mathcal{P}_{qg}(z) \delta_A^{(g)} + \mathcal{P}_{gg}(z) \mathbb{T}_A^2 \delta_A^{(g)} \right), \quad (3.124)$$

and where A is an external particle in $|n\rangle$, and $\delta_A^{(g)} = 1$ when A is a quark and zero otherwise (vice versa for $\delta_A^{(g)}$).

²⁹Often \mathcal{P}_{gg} is defined with an additional factor of two. This is in relation to its role in initial state radiation from hadrons, discussed in Section 3.4.2.2. It is also with relation to initial state radiation that the splitting functions \mathcal{P} are labelled with indices, therefore for final state particles $\mathcal{P}_{x \rightarrow x'+y} \equiv \mathcal{P}_{x'x}$.

3.3.4 The collinear limit of a real emission

We will now compute the leading behaviour of $|n+1\rangle$ in the limit where one of the external particles becomes collinear to the momentum of the particle line to which it is connected by a vertex. We will assume that all particles in $|n+1\rangle$ are outgoing as this simplifies matters by removing flux factors and symmetry factors for initial state particles (discussed in Section 3.4.2.2). The KLN theorem requires that the logarithmic divergences from the integration over the phase-space of the collinear external particle are exactly equal and opposite to those from a collinear loop, which factorised as

$$|n^{(1)}\rangle \approx \ln \tilde{\mathbf{V}}_{a,b}^n |n\rangle. \quad (3.125)$$

Therefore $|n+1\rangle$ must also factorise in the collinear limit so that

$$|n+1\rangle \approx \mathbf{C}_{n+1} |n\rangle, \quad (3.126)$$

where

$$\int_a^b d\Pi_{n+1} \mathbf{C}_{n+1}^\dagger \mathbf{C}_{n+1} = -2\text{Re}\{\ln \tilde{\mathbf{V}}_{a,b}^n\}, \quad (3.127)$$

and where $d\Pi_{n+1}$ is the phase-space measure for the collinear particle. a and b limit the transverse momentum of the collinear particle.³⁰ We know that $\ln \tilde{\mathbf{V}}_{a,b}^{n+1}$ has a colour structure proportional to a Casimir operator, originating from self-energy-like loops on external legs. \mathbf{C}_{n+1} must also have this structure and so we only need look at Feynman diagrams for collinear particles attached to other external legs and can assume that interference terms give sub-leading contributions to the overall cross-section.³¹

$q \rightarrow qg$

First, let us consider the case that the collinear particle is a gluon and is connected to an external quark. We can think of this as a $1 \rightarrow 2$ particle transition where the quark splits into a quark and a collinear gluon, hence this process is labelled as a $q \rightarrow qg$ splitting. The matrix element, assuming the quark and gluon are in the final state, is

$$|n+1; s_i, \lambda_j\rangle = ig_s \epsilon_\mu^*(p_j, \lambda_j) \bar{u}(p_i, s_i) \mathbb{T}_{ij} \gamma^\mu \frac{i(\not{p}_i + \not{p}_j)}{(p_i + p_j)^2 + i\epsilon} |\hat{n}\rangle, \quad (3.128)$$

³⁰Note that in Eq. (3.101) a and b limited the energy of the emission, whereas here a and b limit the transverse momentum. This is because an infra-red cut-off on energy regularises soft divergences but not collinear divergences. Whereas transverse momentum regularises collinear divergences. In fact, transverse momentum can also be used to regularise soft divergences, however we chose to use energy in the initial presentation of \mathbf{S}_{n+1} as it gives the intuitive picture that soft radiation comes from low energy gluons.

³¹These statements rely on the fact we are using the same axial gauge to compute $|n+1\rangle$ as we did to compute $|n^{(1)}\rangle$. Other gauges are less simple as they allow for Casimir operators to appear from interference between not-self-energy-like terms.

where p_j is the gluon momentum, p_i the quark momentum after splitting to produce the gluon, and where

$$\bar{u}(p_i + p_j, s_{ij}) |\hat{n}\rangle \approx z^{-1/2} \bar{u}(p_i, s_{ij}) |\hat{n}\rangle = |n; s_{ij}\rangle. \quad (3.129)$$

s_{ij} is the spin of the combined ij particle, and \mathbb{T}_{ij} the colour charge of the combined ij particle. Here, and throughout this section, the approximately-equal-to sign means to first order in the collinear limit where p_j goes collinear to p_i with collinear scaling given in Section 3.1.1. We are using the same Sudakov decomposition as in the previous section and as given in Appendix A.3, note that $z \approx E_i/(E_i + E_j)$. Looking only at terms with Lorentz/spin structure in the numerator of Eq. (3.128):

$$\begin{aligned} \mathfrak{L} &\doteq \epsilon_\mu^*(p_j) \bar{u}(p_i) \gamma^\mu (\not{p}_i + \not{p}_j) |\hat{n}\rangle = \epsilon_\mu(p_j, \lambda_j) \bar{u}(p_i, s_i) \gamma^\mu \sum_{s_{ij}} u(p_{ij}, s_{ij}) \bar{u}(p_{ij}, s_{ij}) |\hat{n}\rangle, \\ &= \epsilon_\mu^*(p_j, \lambda_j) \left(\tilde{\chi}^\alpha(p_i, s_i), \chi_{\dot{\alpha}}^\dagger(p_i, s_i) \right) \begin{pmatrix} 0 & \sigma_{\alpha\dot{\beta}}^\mu \\ \bar{\sigma}^{\mu\dot{\alpha}\beta} & 0 \end{pmatrix} \\ &\quad \times \sum_{s_{ij}} \begin{pmatrix} \chi_\beta(p_{ij}, s_{ij}) \\ \tilde{\chi}^{\dagger\dot{\beta}}(p_{ij}, s_{ij}) \end{pmatrix} \left(\tilde{\chi}^\gamma(p_{ij}, s_{ij}), \chi_{\dot{\gamma}}^\dagger(p_{ij}, s_{ij}) \right) |\hat{n}\rangle_{\dot{\gamma}}, \end{aligned} \quad (3.130)$$

where $p_{ij} = p_i + p_j$. Taking the massless limit of the Weyl spinors,

$$\mathfrak{L} = \epsilon_\mu^*(p_j, \lambda_j) \tilde{\chi}^\alpha(p_i, \frac{1}{2}) \sigma_{\alpha\dot{\beta}}^\mu \tilde{\chi}^{\dagger\dot{\beta}}(p_{ij}, \frac{1}{2}) (\tilde{\chi}^\gamma(p_{ij}, \frac{1}{2}), 0) |\hat{n}\rangle_\gamma \delta_{s_i}^{(+\frac{1}{2})} \quad (3.131)$$

$$+ \epsilon_\mu^*(p_j, \lambda_j) \chi_{\dot{\alpha}}^\dagger(p_i, -\frac{1}{2}) \bar{\sigma}^{\mu\dot{\alpha}\beta} \chi_\beta(p_{ij}, -\frac{1}{2}) \left(0, \chi_{\dot{\gamma}}^\dagger(p_{ij}, -\frac{1}{2}) \right) |\hat{n}\rangle_{\dot{\gamma}} \delta_{s_i}^{(-\frac{1}{2})}. \quad (3.132)$$

where $\delta_s^{(\pm\frac{1}{2})}$ is unity when spin $s = \pm\frac{1}{2}$ and is zero otherwise. Looking term by term at each separate combination of spins, labelling \mathfrak{L} and $|n\rangle$ appropriately, and using the spinor helicity notation from Section 3.1.3,

$$\mathfrak{L}_{+i+j} = [p_i]^\alpha \epsilon^*(p_j, +) \cdot \sigma_{\alpha\dot{\beta}} [p_{ij}]^{\dot{\beta}} (\tilde{\chi}^\gamma(p_{ij}, \frac{1}{2}), 0) |\hat{n}\rangle_\gamma = \sqrt{2} \frac{[p_i p_j]}{\langle q p_j \rangle} \langle q p_{ij} | n; +\frac{1}{2} ij \rangle, \quad (3.133)$$

and

$$\mathfrak{L}_{+i-j} = [p_i]^\alpha \epsilon^*(p_j, -) \cdot \sigma_{\alpha\dot{\beta}} [p_{ij}]^{\dot{\beta}} (\tilde{\chi}^\gamma(p_{ij}, \frac{1}{2}), 0) |\hat{n}\rangle_\gamma \approx \sqrt{2z} \frac{[p_i q]}{[q p_j]} \langle p_j p_i | n; +\frac{1}{2} ij \rangle. \quad (3.134)$$

As in Section 3.1.3, q is a reference vector used to specify ϵ^* . Changes in q are equivalent to gauge transformations. By the CP invariance of QCD, $\mathfrak{L}_{s_i s_j} = \mathfrak{L}_{-s_i -s_j}^*$ ³², we can immediately find

$$\mathfrak{L}_{-i-j} = -\sqrt{2} \frac{\langle p_i p_j \rangle}{[q p_j]} [q p_{ij}] |n; -\frac{1}{2} ij\rangle, \quad (3.135)$$

³²Depending on the sign convention for spinor v , this could also read $\mathfrak{L}_{s_i s_j} = -\mathfrak{L}_{-s_i -s_j}^*$.

$$\mathfrak{L}_{-i+j} \approx -\sqrt{2z} \frac{\langle p_i q \rangle}{\langle q p_j \rangle} [p_j p_i] |n; -\frac{1}{2}ij\rangle. \quad (3.136)$$

Each $\mathfrak{L}_{s_i s_j}$ can quickly be expressed as a function of z and single spinor bracket of p_i and p_j , and the colour algebra can be reduced, by applying the KLN theorem to match our calculation back to the loop calculation in the previous section. Note the following gauge invariant ratios,

$$\begin{aligned} \frac{\langle n; +\frac{1}{2}ij | \mathfrak{L}_{+i-j}}{\langle n; +\frac{1}{2}ij | \mathfrak{L}_{+i+j}} &\approx -z \frac{\langle p_j p_i \rangle}{[p_i p_j]} \equiv -ze^{i\theta_{+i\mp j}}, \\ \frac{\langle n; -\frac{1}{2}ij | \mathfrak{L}_{-i+j}}{\langle n; +\frac{1}{2}ij | \mathfrak{L}_{+i+j}} &\approx -\sqrt{z} \frac{\langle p_i q \rangle [p_j p_i] \langle q p_j \rangle}{[p_i p_j] \langle q p_i \rangle \langle q p_j \rangle} \approx z, \\ \frac{\langle n; -\frac{1}{2}ij | \mathfrak{L}_{-i-j}}{\langle n; +\frac{1}{2}ij | \mathfrak{L}_{+i+j}} &\approx -\frac{\langle p_i p_j \rangle}{[p_i p_j]} \equiv -e^{i\theta_{+i\mp j}}. \end{aligned} \quad (3.137)$$

where $e^{i\theta_{+i\mp j}}$ is a complex phase that can be found using the representation given in Eq. (3.39) to compute the spinor products. The squared matrix element for the $q \rightarrow qq$ splitting is

$$\langle n+1 | n+1 \rangle = \frac{g_s^2 \mathbb{T}_i \cdot \mathbb{T}_i}{(2p_i \cdot p_j)^2} \left(\mathfrak{L}_{+i+j}^\dagger \mathfrak{L}_{+i+j} + \mathfrak{L}_{+i-j}^\dagger \mathfrak{L}_{+i-j} + \mathfrak{L}_{-i+j}^\dagger \mathfrak{L}_{-i+j} + \mathfrak{L}_{-i-j}^\dagger \mathfrak{L}_{-i-j} \right). \quad (3.138)$$

Inserting an identity operator, $\sum_{s_{ij}} |n; +s_{ij}\rangle \langle n; +s_{ij}|$, between each $\mathfrak{L}_{s_i s_j}^\dagger \mathfrak{L}_{s_i s_j}$, and using the ratios just given, we find that

$$\langle n+1 | n+1 \rangle \approx \frac{g_s^2 \mathbb{T}_i \cdot \mathbb{T}_i}{2(p_i \cdot p_j)^2} (1+z^2) \left(\langle n; +\frac{1}{2}ij | \mathfrak{L}_{+i+j} \right)^2, \quad (3.139)$$

Applying the KLN theorem to the cross-section, it is required that

$$\left(\langle n; +\frac{1}{2}ij | \mathfrak{L}_{+i+j} \right)^2 \approx \frac{2p_i \cdot p_j}{\mathcal{C}_F(1+z^2)} \mathcal{P}_{qq}. \quad (3.140)$$

From this we can write the complete spin dependent $q \rightarrow qq$ splittings:

$$|n+1; +\frac{1}{2}ij \rightarrow +\frac{1}{2}i+1j\rangle \approx g_s \sqrt{\frac{\mathcal{P}_{qq}}{\mathcal{C}_F(1+z^2)}} \frac{1}{\langle p_j p_i \rangle} \mathbb{T}_{ij} |n; +\frac{1}{2}ij\rangle, \quad (3.141)$$

$$|n+1; -\frac{1}{2}ij \rightarrow -\frac{1}{2}i+1j\rangle \approx g_s \sqrt{\frac{z^2 \mathcal{P}_{qq}}{\mathcal{C}_F(1+z^2)}} \frac{1}{\langle p_j p_i \rangle} \mathbb{T}_{ij} |n; -\frac{1}{2}ij\rangle, \quad (3.142)$$

$$|n+1; +\frac{1}{2}ij \rightarrow +\frac{1}{2}i-1j\rangle \approx g_s \sqrt{\frac{z^2 \mathcal{P}_{qq}}{\mathcal{C}_F(1+z^2)}} \frac{1}{[p_i p_j]} \mathbb{T}_{ij} |n; +\frac{1}{2}ij\rangle, \quad (3.143)$$

$$|n+1; -\frac{1}{2}ij \rightarrow -\frac{1}{2}i-1j\rangle \approx g_s \sqrt{\frac{\mathcal{P}_{qq}}{\mathcal{C}_F(1+z^2)}} \frac{1}{[p_i p_j]} \mathbb{T}_{ij} |n; -\frac{1}{2}ij\rangle, \quad (3.144)$$

where we have labelled the spin/helicity states of each particle involved after the semi-colon. All other combinations of spins and helicities are 0. This was derived for the case of a quark emitting a gluon, however the functions $\bar{q} \rightarrow \bar{q}g$ functions are easily retrieved by letting $\bar{s} = -s$ (an application of crossing symmetry and CP invariance).

$q \rightarrow gq$

The $q \rightarrow gq$ splitting can be evaluated by making the combined transformation ($p_i \leftrightarrow p_j$) \wedge ($z \mapsto 1 - z$) on the $q \rightarrow qq$ splitting:

$$|n + 1; +\frac{1}{2}ij \rightarrow +1_i + \frac{1}{2}j\rangle \approx g_s \sqrt{\frac{\mathcal{P}_{gq}}{\mathcal{C}_F(2 - 2z + z^2)}} \frac{1}{\langle p_i p_j \rangle} \mathbb{T}_{ij} |n; +\frac{1}{2}ij\rangle, \quad (3.145)$$

$$|n + 1; -\frac{1}{2}ij \rightarrow +1_i - \frac{1}{2}j\rangle \approx g_s \sqrt{\frac{(1 - z)^2 \mathcal{P}_{gq}}{\mathcal{C}_F(2 - 2z + z^2)}} \frac{1}{\langle p_i p_j \rangle} \mathbb{T}_{ij} |n; -\frac{1}{2}ij\rangle, \quad (3.146)$$

$$|n + 1; +\frac{1}{2}ij \rightarrow -1_i + \frac{1}{2}j\rangle \approx g_s \sqrt{\frac{(1 - z)^2 \mathcal{P}_{gq}}{\mathcal{C}_F(2 - 2z + z^2)}} \frac{1}{[p_j p_i]} \mathbb{T}_{ij} |n; +\frac{1}{2}ij\rangle, \quad (3.147)$$

$$|n + 1; -\frac{1}{2}ij \rightarrow -1_i - \frac{1}{2}j\rangle \approx g_s \sqrt{\frac{\mathcal{P}_{gq}}{\mathcal{C}_F(2 - 2z + z^2)}} \frac{1}{[p_j p_i]} \mathbb{T}_{ij} |n; -\frac{1}{2}ij\rangle. \quad (3.148)$$

All other combinations of spins and helicities are 0. Antiparticles are handled in the same fashion as the $q \rightarrow qq$ splitting functions, by letting $\bar{s} = -s$.

$g \rightarrow q\bar{q}$

Now let us consider when the collinear particle is a quark and it is connected to an external anti-quark. This is thought of as a $1 \rightarrow 2$ particle transition where a gluon splits into an anti-quark and a collinear quark, labelled as a $g \rightarrow \bar{q}q$ splitting. The matrix element, assuming the quarks are in the final state, is

$$\begin{aligned} |n + 1; s_i, s_j\rangle &= ig_s t^a \bar{u}(p_j, s_j) \gamma^\mu v(p_i, s_i) \frac{\delta^{ad} d_{\mu\nu}(p_i + p_j)}{(p_i + p_j)^2 + i\epsilon} |\hat{n}\rangle_d^\nu, \\ &= ig_s t^a \left(\tilde{\chi}^\alpha(p_j, s_j), \chi_{\dot{\alpha}}^\dagger(p_j, s_j) \right) \begin{pmatrix} 0 & \sigma_{\alpha\dot{\beta}}^\mu \\ \bar{\sigma}^{\mu\dot{\alpha}\beta} & 0 \end{pmatrix} \begin{pmatrix} \tilde{\chi}_\beta(p_i, s_i) \\ \chi^{\dagger\dot{\beta}}(p_i, s_i) \end{pmatrix} \sum_{\lambda_{ij}} \frac{\epsilon_\mu(p_{ij}, \lambda_{ij})}{2p_i \cdot p_j} |n; \lambda_{ij}\rangle^a, \end{aligned} \quad (3.149)$$

where $d_{\mu\alpha}(p_i + p_j)$ is the numerator of the gluon propagator in the axial gauge with a light-like reference vector, see Eq. (2.80), and where

$$\epsilon_\nu^*(p_{ij}, \lambda_{ij}) |\hat{n}\rangle^\nu = |n; \lambda_{ij}\rangle. \quad (3.150)$$

Again, looking just at the Lorentz/spin structure of the numerator of Eq. (3.149) in the massless limit:

$$\begin{aligned}
\mathfrak{L}^a &= \tilde{\chi}^\alpha(p_j, s_j) \sigma_{\alpha\dot{\beta}}^\mu \chi^{\dot{\beta}}(p_i, s_i) \sum_{\lambda_{ij}} \epsilon_\mu(p_{ij}, \lambda_{ij}) |n; \lambda_{ij}\rangle^a \\
&\quad + \chi_{\dot{\alpha}}^\dagger(p_j, s_j) \bar{\sigma}^{\mu\dot{\alpha}\beta} \tilde{\chi}_\beta(p_i, s_i) \sum_{\lambda_{ij}} \epsilon_\mu(p_{ij}, \lambda_{ij}) |n; \lambda_{ij}\rangle^a, \\
&= \sum_{\lambda_{ij}} [p_j | \sigma \cdot \epsilon(p_{ij}, \lambda_{ij}) | p_i \rangle |n; \lambda_{ij}\rangle^a \delta_{s_i}^{(+\frac{1}{2})} \delta_{s_j}^{(+\frac{1}{2})} + \sum_{\lambda_{ij}} \langle p_j | \bar{\sigma} \cdot \epsilon(p_{ij}, \lambda_{ij}) | p_i \rangle |n; \lambda_{ij}\rangle^a \delta_{s_i}^{(-\frac{1}{2})} \delta_{s_j}^{(-\frac{1}{2})},
\end{aligned} \tag{3.151}$$

which can be split apart by spin state and simplified as

$$\mathfrak{L}_{+ij+i} \approx \sqrt{2(1-z)} \frac{[p_j q] \langle p_j p_i \rangle}{[p_{ij} q]} |n; +1_{ij}\rangle, \tag{3.152}$$

$$\mathfrak{L}_{-ij+i} \approx \sqrt{2z} \frac{[p_j p_i] \langle q p_i \rangle}{\langle p_{ij} q \rangle} |n; -1_{ij}\rangle, \tag{3.153}$$

$$\mathfrak{L}_{+ij-i} \approx \sqrt{2z} \frac{\langle p_j p_i \rangle [q p_i]}{[p_{ij} q]} |n; +1_{ij}\rangle, \tag{3.154}$$

$$\mathfrak{L}_{-ij-i} \approx \sqrt{2(1-z)} \frac{\langle p_j q \rangle [p_j p_i]}{\langle p_{ij} q \rangle} |n; -1_{ij}\rangle. \tag{3.155}$$

By CP symmetry $\mathfrak{L}_{+ij+i} = \mathfrak{L}_{-ij-i}^*$ and $\mathfrak{L}_{-ij+i} = \mathfrak{L}_{+ij-i}^*$. Again, we can use the KLN theorem to express these splittings in Sudakov variables:

$$|n+1; +1_{ij} \rightarrow +\frac{1}{2}i + \frac{1}{2}j\rangle \approx g_s \sqrt{\frac{(1-z)^2 \mathcal{P}_{qg}}{1-2z(1-z)}} \frac{1}{[p_i p_j]} |n; +1_{ij}\rangle, \tag{3.156}$$

$$|n+1; -1_{ij} \rightarrow +\frac{1}{2}i + \frac{1}{2}j\rangle \approx g_s \sqrt{\frac{z^2 \mathcal{P}_{qg}}{1-2z(1-z)}} \frac{1}{\langle p_j p_i \rangle} |n; -1_{ij}\rangle, \tag{3.157}$$

$$|n+1; +1_{ij} \rightarrow -\frac{1}{2}i - \frac{1}{2}j\rangle \approx g_s \sqrt{\frac{z^2 \mathcal{P}_{qg}}{1-2z(1-z)}} \frac{1}{[p_i p_j]} |n; +1_{ij}\rangle, \tag{3.158}$$

$$|n+1; -1_{ij} \rightarrow -\frac{1}{2}i - \frac{1}{2}j\rangle \approx g_s \sqrt{\frac{(1-z)^2 \mathcal{P}_{qg}}{1-2z(1-z)}} \frac{1}{\langle p_j p_i \rangle} |n; -1_{ij}\rangle. \tag{3.159}$$

Here we derived the $g \rightarrow \bar{q}q$ splitting functions. The $g \rightarrow q\bar{q}$ splitting functions can be found by the combined transformations $(p_i \leftrightarrow p_j) \wedge (z \mapsto 1-z)$.

$g \rightarrow gg$

Finally we consider when the collinear particle is a gluon and it is connected to an external gluon. This configuration can either originate from a gluon triple vertex or quadruple vertex. Quadruple vertices are sub-leading in the collinear limit as they necessarily have

fewer divergent propagators.³³ Thus we are looking to compute the matrix element for a $g \rightarrow gg$ splitting via a triple gluon vertex. As we have now laid down the foundations for these calculations several times, we shall skip straight to

$$\mathfrak{L} = \epsilon_\alpha^*(p_i, \lambda_i) \epsilon_\beta^*(p_j, \lambda_j) \left(g^{\alpha\beta} (p_j - p_i)^\gamma - g^{\beta\gamma} (2p_j + p_i)^\alpha + g^{\gamma\alpha} (2p_i + p_j)^\beta \right) \sum_{\lambda_{ij}} \epsilon_\gamma(p_{ij}, \lambda_{ij}) |n; \lambda_{ij}\rangle, \quad (3.160)$$

$$= \epsilon^*(p_i, \lambda_i) \cdot \epsilon^*(p_j, \lambda_j) \sum_{\lambda_{ij}} (p_j - p_i) \cdot \epsilon(p_{ij}, \lambda_{ij}) |n; \lambda_{ij}\rangle \quad (1)$$

$$- 2\epsilon^*(p_i, \lambda_i) \cdot p_j \sum_{\lambda_{ij}} \epsilon^*(p_j, \lambda_j) \cdot \epsilon(p_{ij}, \lambda_{ij}) |n; \lambda_{ij}\rangle \quad (2)$$

$$+ 2\epsilon^*(p_j, \lambda_j) \cdot p_i \sum_{\lambda_{ij}} \epsilon^*(p_i, \lambda_i) \cdot \epsilon(p_{ij}, \lambda_{ij}) |n; \lambda_{ij}\rangle. \quad (3) \quad (3.161)$$

We can express each line in terms of spinor products,

$$\begin{aligned} \mathfrak{L}_{\pm ij \rightarrow +i+j}^{(1)} &= \frac{1}{2\sqrt{2}} \left(\frac{\langle p_i | \bar{\sigma}^\mu | q \rangle \langle p_j | \bar{\sigma}_\mu | q \rangle}{[p_i q] [p_j q]} \right)^* (p_j - p_i) \cdot \epsilon(p_{ij}, \pm 1_{ij}) |n; \pm 1_{ij}\rangle = 0, \\ \mathfrak{L}_{\pm ij \rightarrow -i-j}^{(1)} &= \frac{1}{2\sqrt{2}} \left(\frac{[p_i | \sigma^\mu | q] [p_j | \sigma_\mu | q]}{\langle p_i q \rangle \langle p_j q \rangle} \right)^* (p_j - p_i) \cdot \epsilon(p_{ij}, \pm 1_{ij}) |n; \pm 1_{ij}\rangle = 0, \end{aligned} \quad (3.162)$$

by the Fierz identities (see Appendix A.2). Similarly

$$\mathfrak{L}_{+ij \rightarrow \pm i-j}^{(2)} = \mathfrak{L}_{-ij \rightarrow \pm i+j}^{(2)} = \mathfrak{L}_{+ij \rightarrow -i\pm j}^{(3)} = \mathfrak{L}_{-ij \rightarrow +i\pm j}^{(3)} = 0.$$

Consequently, $\mathfrak{L}_{\mp ij \rightarrow \pm i\pm j} = 0$. Continuing with this line-by-line and term-by-term approach,

$$\mathfrak{L}_{\pm ij \rightarrow +i-j}^{(1)} = \frac{1}{\sqrt{2}} \frac{\langle p_{ij} \mp | (p_j - p_i) \cdot \sigma_\mp | q \mp \rangle}{\langle p_{ij} \pm | q \mp \rangle} |n; \pm 1_{ij}\rangle. \quad (3.163)$$

$$\mathfrak{L}_{-ij \rightarrow +i-j}^{(2)} = -\sqrt{2} \frac{\langle q | p_j \cdot \bar{\sigma} | p_i]}{\langle p_i q \rangle} |n; -ij\rangle. \quad (3.164)$$

$$\mathfrak{L}_{+ij \rightarrow +i-j}^{(3)} = \sqrt{2} \frac{[q | p_i \cdot \sigma | p_j \rangle}{[p_j q]} |n; +ij\rangle, \quad (3.165)$$

³³We can also argue that quadruple vertices are sub-leading by looking to the KLN theorem,

$$\int d\Pi_{n+1} \mathbf{C}_{n+1}^\dagger \mathbf{C}_{n+1} = -2\text{Re}\{\ln \tilde{\mathbf{V}}_{a,b}^{n+1}\}.$$

The right-hand-side is $\mathcal{O}(\alpha_s)$ whilst including a quadruple vertex into \mathbf{C}_{n+1} would generate an $\mathcal{O}(\alpha_s^2)$ term on left-hand-side.

where the first line borrows notation from Appendix A.2. Therefore

$$\begin{aligned}\mathfrak{L}_{+ij \rightarrow +i-j} &\approx \left[\sqrt{\frac{z}{2}} \frac{\langle p_i p_j \rangle [p_j q]}{[p_{ij} n]} - \sqrt{\frac{1-z}{2}} \frac{\langle p_j p_i \rangle [p_i q]}{[p_{ij} n]} + \sqrt{2} \frac{[q p_i] \langle p_i p_j \rangle}{[p_j q]} \right] |n; +1_{ij}\rangle, \\ &\approx \sqrt{\frac{2z^3}{1-z}} \langle p_i p_j \rangle |n; +1_{ij}\rangle.\end{aligned}\quad (3.166)$$

$$\begin{aligned}\mathfrak{L}_{-ij \rightarrow +i-j} &\approx \left[\sqrt{\frac{z}{2}} \frac{[p_i p_j] \langle p_j q \rangle}{\langle p_{ij} q \rangle} - \sqrt{\frac{1-z}{2}} \frac{[p_j p_i] \langle p_i q \rangle}{\langle p_{ij} q \rangle} - \sqrt{2} \frac{\langle q p_j \rangle [p_j p_i]}{\langle p_i q \rangle} \right] |n; -1_{ij}\rangle, \\ &\approx \sqrt{\frac{2(1-z)^3}{z}} [p_i p_j] |n; -1_{ij}\rangle.\end{aligned}\quad (3.167)$$

Again using CP invariance, $\mathfrak{L}_{\lambda_{ij} \rightarrow \lambda_i \lambda_j} = \mathfrak{L}_{-\lambda_{ij} \rightarrow -\lambda_i -\lambda_j}^*$, and therefore

$$\mathfrak{L}_{-ij \rightarrow -i+j} \approx -\sqrt{\frac{2z^3}{1-z}} [p_i p_j] |n; -1_{ij}\rangle. \quad (3.168)$$

$$\mathfrak{L}_{+ij \rightarrow -i+j} \approx -\sqrt{\frac{2(1-z)^3}{z}} \langle p_i p_j \rangle |n; +1_{ij}\rangle. \quad (3.169)$$

Finally, by applying the same approach we also find that

$$\mathfrak{L}_{+ij \rightarrow +i+j} \approx \sqrt{\frac{2}{z(1-z)}} [p_i p_j] |n; +i_j\rangle. \quad (3.170)$$

And so, the full spin dependent $g \rightarrow gg$ splittings are

$$|n+1; +1_{ij} \rightarrow +1_i + 1_j\rangle \approx g_s \sqrt{\frac{1}{z(1-z)}} \frac{1}{\langle p_j p_i \rangle} \mathbb{T}_{ij} |n; +1_{ij}\rangle, \quad (3.171)$$

$$|n+1; +1_{ij} \rightarrow -1_i - 1_j\rangle \approx 0, \quad (3.172)$$

$$|n+1; +1_{ij} \rightarrow +1_i - 1_j\rangle \approx g_s \sqrt{\frac{z^3}{1-z}} \frac{1}{[p_j p_i]} \mathbb{T}_{ij} |n; +1_{ij}\rangle, \quad (3.173)$$

$$|n+1; +1_{ij} \rightarrow -1_i + 1_j\rangle \approx g_s \sqrt{\frac{(1-z)^3}{z}} \frac{1}{[p_i p_j]} \mathbb{T}_{ij} |n; +1_{ij}\rangle, \quad (3.174)$$

$$|n+1; -1_{ij} \rightarrow -1_i - 1_j\rangle \approx g_s \sqrt{\frac{1}{z(1-z)}} \frac{1}{[p_i p_j]} \mathbb{T}_{ij} |n; -1_{ij}\rangle, \quad (3.175)$$

$$|n+1; -1_{ij} \rightarrow +1_i + 1_j\rangle \approx 0, \quad (3.176)$$

$$|n+1; -1_{ij} \rightarrow +1_i - 1_j\rangle \approx g_s \sqrt{\frac{(1-z)^3}{z}} \frac{1}{\langle p_j p_i \rangle} \mathbb{T}_{ij} |n; -1_{ij}\rangle, \quad (3.177)$$

$$|n+1; -1_{ij} \rightarrow -1_i + 1_j\rangle \approx g_s \sqrt{\frac{z^3}{1-z}} \frac{1}{\langle p_i p_j \rangle} \mathbb{T}_{ij} |n; -1_{ij}\rangle. \quad (3.178)$$

We now have everything we need to provide a complete definition for \mathbf{C}_{n+1} . However, due to the large number of relevant spin states and transitions, the final expression for \mathbf{C}_{n+1} is lengthy. It is given in full in Section 4.7.

3.3.5 Generalisations

Higher orders

Thus far we have derived the leading singularity structure for first order corrections to an n particle tree-level amplitude, $|n\rangle$. We saw that the IR³⁴ singularities factorise from $|n\rangle$ and can be handled as operators which act on $|n\rangle$ to ‘dress’ the amplitude with the leading corrections from QCD radiation. The operators are related to each other by the KLN theorem, ensuring poles cancel once first order corrections are inclusively summed over. It is now pertinent for us to discuss the generalisation to higher order corrections to $|n\rangle$ from QCD radiation.

We begin by looking at $|n^{(2)}\rangle$, the two loop correction to $|n\rangle$. In our previous discussions on soft and collinear loops we argued that loops between relatively off-shell particles are sub-leading in the soft and collinear limits since the off-shell momenta screened the propagator divergences. Consequently, $\ln \bar{\mathbf{V}}_{a,b}^n$ and $\ln \tilde{\mathbf{V}}_{a,b}^n$ only recieved contributions from loops between on-shell external legs. This argument holds regardless of the number of additional loops included in the internal structure of $|n\rangle$ provided those loops are also relatively off-shell. Therefore, to analyse $|n^{(2)}\rangle$ we must make further use of the method of regions. Let the two loop-momenta in $|n^{(2)}\rangle$ be k_1 and k_2 . We must divide the regions of the loop integral as

$$\int \frac{d^4 k_1}{(2\pi)^4} \int \frac{d^4 k_2}{(2\pi)^4} = \int \frac{d^4 k_1}{(2\pi)^4} \int \frac{d^4 k_2}{(2\pi)^4} \Theta(k_{1\perp} < k_{2\perp}) + \int \frac{d^4 k_1}{(2\pi)^4} \int \frac{d^4 k_2}{(2\pi)^4} \Theta(k_{2\perp} < k_{1\perp}), \quad (3.179)$$

where $k_{1\perp}$ and $k_{2\perp}$ are transverse momenta which parametrise the divergences from the propagators in each loop (i.e. placing a IR cut-off on both these transverse momenta regularises the IR divergences). We use transverse momenta as they have consistent scalings between both soft and collinear divergences and so the dicussion in this section can be applied to both limits (see Section 3.1.1 where in both cases transverse momenta are linear in λ). $\Theta(k_{2\perp} < k_{1\perp})$ is step function.

There are three sets of topologies we must consider when analysing $|n^{(2)}\rangle$: when both loops k_1 and k_2 are attached with vertices to relatively off-shell particles, when only one of k_1 and k_2 are attached to vertices to on-shell particles, and when both k_1 and k_2 are attached to on-shell particles. The first case, when all loop vertices involve off-shell momenta, is sub-leading following our previous arguments. The second case is most interesting. Assume k_1 is attached to on-shell momenta and k_2 is not. Only the $\Theta(k_{1\perp} < k_{2\perp})$ term is leading

³⁴Some authors refer to the class of singularities we have studied thus far as IR and collinear (IRC), reserving the term IR for just soft singularities. As all IRC singularities can be regulated with a shared IR cut-off (i.e. gluon and quark masses or a transverse momentum cut-off), we are not so careful and will use the terms IR and IRC somewhat interchangeably.

as when $k_{2\perp} < k_{1\perp}$ the IR divergences are regularised for finite $k_{2\perp}$. If both $k_{2\perp}$ and $k_{1\perp}$ go to zero at the same rate then the loop integrand in the $k_{2\perp} < k_{1\perp}$ region can diverge (as $k_{1\perp}$ is allowed to go to zero) but the region of phase-space where this can happen is infinitely smaller than the region where $k_{2\perp}$ and $k_{1\perp}$ go to zero individually.³⁵ This combats the divergence forcing the $k_{2\perp} < k_{1\perp}$ term to be sub-leading, for example

$$\int_x^y \frac{dk_{1\perp}}{k_{1\perp}} \int_{k_{1\perp}}^y dk_{2\perp} = y \ln \frac{y}{x} + x - y, \quad (3.180)$$

diverges logarithmically as $x \rightarrow 0$, whilst

$$\int_x^y dk_{2\perp} \int_{k_{2\perp}}^y \frac{dk_{1\perp}}{k_{1\perp}} = (y-x) \ln y + (y-x) + x \ln \frac{x}{y^{y/x}}, \quad (3.181)$$

does not diverge as $x \rightarrow 0$.³⁶ Finally, in the third case where both loop momenta k_1 and k_2 flow through vertices of on-shell particles both regions are leading. In this case our labelling of k_1 and k_2 was arbitrary and so if we sum with the contribution where the two loops were oppositely labelled a factor of 1/2 must be included. We can additionally note that when the integrand is symmetrical under the exchange of labels 1 and 2,

$$\frac{1}{2} \int \frac{d^4 k_1}{(2\pi)^4} \int \frac{d^4 k_2}{(2\pi)^4} = \int \frac{d^4 k_1}{(2\pi)^4} \int \frac{d^4 k_2}{(2\pi)^4} \Theta(k_{1\perp} < k_{2\perp}). \quad (3.182)$$

In all, summing over all the possible topologies for the loops (of which only loops from on-shell particles are leading), applying the method of regions between the two loops, and consistently re-labelling the most divergent loop momentum as k_s and the less divergent loop momentum k_h (i.e. so that $k_{s\perp} < k_{h\perp}$), we find that in the soft loop limit the leading divergences are given by

$$\left| n^{(2)} \right\rangle \approx \ln \bar{\mathbf{V}}_{0,Q}^n(k_{s\perp}) \Theta(k_{s\perp} < k_{h\perp}) \left| n^{(1)} \right\rangle, \quad (3.183)$$

where $\ln \bar{\mathbf{V}}_{0,Q}^n(k_{s\perp})$ is found by substituting k for k_s in $\ln \bar{\mathbf{V}}_{0,Q}^n$. Similarly, in the collinear limit,

$$\left| n^{(2)} \right\rangle \approx \ln \tilde{\mathbf{V}}_{0,Q}^n(k_{s\perp}) \Theta(k_{s\perp} < k_{h\perp}) \left| n^{(1)} \right\rangle. \quad (3.184)$$

Applying the results of the previous sections, in the limit that both loops are soft,

$$\left| n^{(2)} \right\rangle \approx \ln \bar{\mathbf{V}}_{0,Q}^n(k_{s\perp}) \ln \bar{\mathbf{V}}_{0,Q}^n(k_{h\perp}) \Theta(k_{s\perp} < k_{h\perp}) |n\rangle = \ln \bar{\mathbf{V}}_{0,Q}^n(k_{s\perp}) \ln \bar{\mathbf{V}}_{k_{s\perp},Q}^n(k_{h\perp}) |n\rangle, \quad (3.185)$$

³⁵In fact the region is one dimension lower, $k_{2\perp}$ and $k_{1\perp}$ going to zero at the same rate defines a line through phase-space whilst each going individually is a plane (of which the line is just one path across).

³⁶In QCD amplitudes it is often the case that terms equivalent to $k_{2\perp} < k_{1\perp}$ do diverge, however they never contribute to the leading divergence because of the argument we have given.

and in the collinear limit,

$$\left|n^{(2)}\right\rangle \approx \ln \tilde{\mathbf{V}}_{0,Q}^n(k_{s\perp}) \ln \tilde{\mathbf{V}}_{0,Q}^n(k_{h\perp}) \Theta(k_{s\perp} < k_{h\perp}) |n\rangle = \ln \tilde{\mathbf{V}}_{0,Q}^n(k_{s\perp}) \ln \tilde{\mathbf{V}}_{k_{s\perp},Q}^n(k_{h\perp}) |n\rangle. \quad (3.186)$$

This is known as ‘strong ordering’. Here a transverse momentum is used an ‘ordering variable’ (i.e. it appears in the step function because of our application of regional methods), however at leading-order any kinematic quantity which parametrises the divergence and scales with λ could be used. Strong ordering extends simply to higher orders, i.e. the leading soft divergences from $|n^{(m)}\rangle$ are given by

$$\left|n^{(m)}\right\rangle \approx \ln \bar{\mathbf{V}}_{0,Q}^n(k_{m\perp}) \ln \bar{\mathbf{V}}_{k_{m\perp},Q}^n(k_{m-1\perp}) \dots \ln \bar{\mathbf{V}}_{k_{3\perp},Q}^n(k_{2\perp}) \ln \bar{\mathbf{V}}_{k_{2\perp},Q}^n(k_{1\perp}) |n\rangle. \quad (3.187)$$

Strong ordering also extends naturally to consecutive soft or collinear external particles.

Combining soft and collinear operators

We have derived operators for dressing an amplitude $|n\rangle$ with the soft and collinear pole structures from higher order QCD corrections. It is natural to ask if we can combine these operators into a single operator. The definition of such an operator is a central part of the discussion in Chapter 4 and so here we will only outline a key feature of the procedure: double counting. We have introduced two operators for 1-loop IR divergences: $\ln \bar{\mathbf{V}}_{0,Q}^n$ which handles soft poles, and $\ln \tilde{\mathbf{V}}_{0,Q}^n$ which handles collinear divergences. However, it is possible for a loop to become simultaneously soft and collinear. This limit gives the double pole in both $\ln \bar{\mathbf{V}}_{0,Q}^n$ and $\ln \tilde{\mathbf{V}}_{0,Q}^n$. A combined operator $\ln \mathbf{V}_{0,Q}^n$ for both soft and collinear divergences should have three parts:

$$\ln \mathbf{V}_{0,Q}^n \sim \text{soft not collinear} + \text{collinear not soft} + \text{soft and collinear}. \quad (3.188)$$

Therefore, to avoid double counting,

$$\ln \mathbf{V}_{0,Q}^n = \ln \bar{\mathbf{V}}_{0,Q}^n + \ln \tilde{\mathbf{V}}_{0,Q}^n - \text{soft and collinear}. \quad (3.189)$$

The ‘soft and collinear’ piece can be found by either expanding $\ln \tilde{\mathbf{V}}_{0,Q}^n$ to leading order in the soft limit or by expanding $\ln \bar{\mathbf{V}}_{0,Q}^n$ to leading order in the collinear limit. Subtracting off the ‘soft and collinear’ piece is sometimes referred to as a zero-bin subtraction since the ‘soft and collinear’ piece integrates to zero when one uses an analytic continuation in dimensional regulation where UV poles are cancelled against IR poles [1]. However, more generally the ‘soft and collinear’ piece does not vanish and is the most divergent part of the amplitude, thus providing the leading contribution to many processes one might wish to compute.

Unitarity

Let us consider an operator \mathbf{E} which dresses an amplitude $|n\rangle$ with all the leading IR poles from radiative corrections to the amplitude. Necessarily $\mathbf{E}^\dagger\mathbf{E}$ has the α_s expansion

$$\begin{aligned} \mathbf{E}^\dagger\mathbf{E} = & 1 + \int \Pi_{n+1} \left(\mathbf{C}_{n+1}^\dagger \mathbf{C}_{n+1} + \mathbf{S}_{n+1}^\dagger \mathbf{S}_{n+1} \right) \\ & + \ln \bar{\mathbf{V}}_{0,Q}^{n\dagger} + \ln \bar{\mathbf{V}}_{0,Q}^n + \ln \tilde{\mathbf{V}}_{0,Q}^{n\dagger} + \ln \tilde{\mathbf{V}}_{0,Q}^n + \mathcal{O}(\alpha_s^2). \end{aligned} \quad (3.190)$$

where we have ignored the double counting of soft and collinear poles which does not effect this discussion. The $\mathcal{O}(\alpha_s^2)$ piece can be constructed by summing over every $\mathcal{O}(\alpha_s^2)$ strongly ordered permutation of the $\mathcal{O}(\alpha_s)$ operators: i.e. it will contain terms such as

$$\int \Pi_{n+1} \mathbf{C}_{n+1}^\dagger \mathbf{C}_{n+1} \ln \tilde{\mathbf{V}}_{p_{n+1\perp},Q}^n$$

and $\ln \bar{\mathbf{V}}_{0,Q}^{n\dagger}(k_2) \ln \tilde{\mathbf{V}}_{k_{2\perp},Q}^n$. Applying the KLN theorem to $\mathbf{E}^\dagger\mathbf{E}$ we find that it is required that $\mathbf{E}^\dagger\mathbf{E} = 1$. This is expected since $\langle n | \mathbf{E}^\dagger\mathbf{E} | n \rangle$ sums over all states degenerate with $|n\rangle$, thus it is a physical LN probability, and we defined \mathbf{E} to only contain terms with the leading poles and therefore it only depends logarithmically on a cut-off scale regulating the divergences. Consequently, if we integrate inclusively over all IR radiation dressing an amplitude, the operator \mathbf{E} must be unitary. Therefore the application of the KLN theorem to QCD radiation is often referred to as using unitarity. Some approaches to QCD radiation take the unitarity of operators as a guiding principle and use it to help ‘bootstrap’ (reverse engineer) a description of QCD radiation [29, 30]. It is important to note that unitarity is an operator level relationship. By making further approximations (which we summarise in Section 3.5 and discuss in detail in Chapter 5) similar relationships, often referred to as parton shower unitarity, can be found between the traces of the operators.

3.4 Resummation

The core methodology explored by this thesis, for the computation of QCD amplitudes, is perturbation theory. However, perturbation theory comes with an inherent problem: the strong coupling is not particularly small and so the convergence of the perturbative series is often slow at best.³⁷ Furthering this problem, the strong coupling runs, becoming large at low scales. At the high scales of the large hadron collider $\alpha_s(100\text{GeV to }1\text{TeV}) \sim 0.1$ ³⁸ implying each order in the perturbation series gives a correction at least 10% of the previous,

³⁷Here we ignore that formally the radius of convergence is zero and that a QCD perturbation series actually forms an asymptotic series [31]. The point still stands as corrections to the asymptotic series can remain large at high powers in the coupling.

³⁸ $\alpha_s(M_Z \approx 91.1\text{GeV}) = 0.117 \pm 0.002$ [32].

and at the scale of the hadrons seen in a detector $\alpha_s \sim 1$. Also, as we have demonstrated, the matrix elements for QCD radiation diverge in the IR limit, with higher order terms in the perturbation series diverging faster than lower order terms. Though poles cancel from physical quantities by the KLN theorem, matrix elements and cross-sections can remain large in the regions of phase-space around poles. The relative size of the matrix elements in the neighbourhoods of poles, and the lack of a small expansion parameter, is such that higher order terms in the perturbation series can become as dominant as lower order terms. We will formalise this statement in Section 3.4.2 when we introduce the logarithmic expansion of an observable. However, for now we will just take it as motivation to resum the perturbative series we have studied so far.

The basic resummation procedure is as follows:

1. Study an n th order correction to a matrix element, \mathcal{M} , (or cross-section, σ) due QCD radiation and, at that order, isolate the most dominant part of the matrix element by using various approximations in limits relevant to the process being studied.
2. Write the dominant n th order correction in a closed form, factorised from the rest of the matrix element (or cross-section), so that we can sum the radiative corrections as

$$\sum_n (\textit{nth order correction}).$$

3. Find a special function, F , whose expansion gives the sum over the dominant n th order corrections and for which the expansion converges for $\alpha_s < 1$.
4. ‘Resum’ the radiative corrections to \mathcal{M} (or σ) by defining the resummed matrix element (or cross-section) as $F\mathcal{M}$ (or $F\sigma$). This resummed matrix element (cross-section) will now have an extended radius of convergence as α_s approaches unity.³⁹

This recipe is somewhat of an oversimplification, and there can be a tremendous amount of work required between each step. However, it does illustrate the basic approach to resummation in perturbative QCD.

3.4.1 Sudakov factors

The first step we will take towards the resummation of QCD radiative corrections is the resummation of soft and collinear loops. In Section 3.3 we showed that m soft loops factorise at leading order as

$$\left| n^{(m)} \right\rangle \approx \ln \overline{\mathbf{V}}_{0,Q}^n(k_{m\perp}) \ln \overline{\mathbf{V}}_{k_{m\perp},Q}^n(k_{m-1\perp}) \dots \ln \overline{\mathbf{V}}_{k_{3\perp},Q}^n(k_{2\perp}) \ln \overline{\mathbf{V}}_{k_{2\perp},Q}^n(k_{1\perp}) |n\rangle. \quad (3.191)$$

³⁹As we mentioned in the previous footnote, formally the radius of convergence is still zero but $F\mathcal{M}$ is a term in a new asymptotic series for which higher order corrections are smaller over a larger domain.

This achieves point one of our recipe for resummation. In this case, point two is simple. We can sum over the corrections to all orders by defining an operator

$$\bar{\mathbf{V}}_{0,Q}^n = \sum_{m=0}^{\infty} \ln \bar{\mathbf{V}}_{0,Q}^n(k_{m\perp}) \ln \bar{\mathbf{V}}_{k_{m\perp},Q}^n(k_{m-1\perp}) \dots \ln \bar{\mathbf{V}}_{k_{3\perp},Q}^n(k_{2\perp}) \ln \bar{\mathbf{V}}_{k_{2\perp},Q}^n(k_{1\perp}). \quad (3.192)$$

We have chosen notation which is suggestive of the corresponding special function. The series expansion for a path ordered exponential is given by

$$\begin{aligned} \text{Pexp} \left(\int_a^b dx \mathbf{A}(x) \right) := & 1 + \int_a^b dx \mathbf{A}(x) + \int_a^b dx_1 \int_{x_1}^b dx_2 \mathbf{A}(x_1) \mathbf{A}(x_2) \\ & + \int_a^b dx_1 \int_{x_1}^b dx_2 \int_{x_2}^b dx_3 \mathbf{A}(x_1) \mathbf{A}(x_2) \mathbf{A}(x_3) + \dots, \end{aligned} \quad (3.193)$$

where $\mathbf{A}(x)$ is matrix (operator) valued. It can be checked that in the limit $[\mathbf{A}(x), \mathbf{A}(y)] = 0$ the path ordered exponential is equivalent to the usual definition for matrix (operator) exponentiation. Comparing Eq. (3.192) and Eq. (3.193) we see that strongly ordered soft loops can be resummed as

$$\bar{\mathbf{V}}_{a,b}^n = \text{Pexp} \left(\ln \bar{\mathbf{V}}_{a,b}^n \right). \quad (3.194)$$

In Eq. (3.193) the integral over the operator and the operator are factorised. To express $\bar{\mathbf{V}}_{a,b}^n$ in the same factorised fashion we define

$$\begin{aligned} \ln \bar{\mathbf{V}}_{a,b}^n &= \frac{\alpha_s}{\pi} \int_a^b \frac{dk_{\perp}}{dk_{\perp}} \sum_{\text{pairs}(A,B)} \left(\int_0^{\pi} \frac{d\theta}{\sin \theta} \theta(k, p_A, p_B) - i\pi \tilde{\delta}_{AB} \right) \mathbb{T}_A \cdot \mathbb{T}_B \\ &\equiv -\frac{\alpha_s}{\pi} \int_a^b \frac{dk_{\perp}}{dk_{\perp}} \bar{\Gamma}^n(k_{\perp}), \end{aligned} \quad (3.195)$$

where $\theta(k, p_A, p_B) = \Theta(p_A \cdot p_B - p_A \cdot k) \Theta(p_A \cdot p_B - p_B \cdot k)$, which is a Lorentz invariant phase-space boundary equivalent at our accuracy to requiring $k^0 < E_A, E_B$ (the boundary we inherited from the application of the method of regions). $\bar{\Gamma}^n(k_{\perp})$ is known as the soft anomalous dimension matrix. Therefore, soft loops dressing an amplitude $|n\rangle$ can be resummed as

$$\sum_{m=0}^{\infty} |n^{(m)}\rangle \approx \bar{\mathbf{V}}_{0,Q} |n\rangle = \text{Pexp} \left(-\frac{\alpha_s}{\pi} \int_0^Q \frac{dk_{\perp}}{dk_{\perp}} \bar{\Gamma}(k_{\perp}) \right) |n\rangle, \quad (3.196)$$

where we have dropped the n superscript on operators as is usual in the literature. $\bar{\mathbf{V}}_{a,b}$ is an amplitude level soft Sudakov factor.

By following the same procedure, collinear loops can be resummed into an amplitude level collinear Sudakov factor

$$\tilde{\mathbf{V}}_{a,b} = \text{Pexp} \left(\ln \tilde{\mathbf{V}}_{a,b}^n \right) \equiv \text{Pexp} \left(-\frac{\alpha_s}{\pi} \int_a^b \frac{dk_{\perp}}{dk_{\perp}} \tilde{\Gamma}(k_{\perp}) \right), \quad (3.197)$$

where $\tilde{\Gamma}(k_{\perp})$ is the collinear anomalous dimension matrix.

3.4.1.1 Anomalous dimension matrices

Anomalous dimension matrices arise naturally when we resum loops in the IR limit. However, they also appear in the renormalisation of amplitudes, affording them two complementary interpretations. Consider an n particle amplitude, dimensionally regularised at a scale Q ,

$$|N(\epsilon, Q)\rangle = \sum_m |n^{(m)}(\epsilon, Q)\rangle.$$

We know from the KLN theorem that IR ϵ poles must cancel in the computation of a physical cross-section. Just like UV poles, the IR poles have the interpretation of coming from a universal background of quantum noise, only this time it is the low frequency modes causing the amplitudes themselves to diverge. In Section 2.2.5 we renormalised QCD to remove the diverging UV modes from our calculations.⁴⁰ Now we consider renormalising $|N(\epsilon, Q)\rangle$ at a renormalisation scale $\mu < Q$ in a minimal subtraction scheme so that the renormalised amplitude has no IR divergences. We define the renormalised amplitude⁴¹ as

$$|N(\epsilon, Q, \mu)\rangle = \mathbf{Z}^{-1}(\epsilon, \mu) |N(\epsilon, Q)\rangle, \quad (3.198)$$

where we know that \mathbf{Z} will cancel from any LN probability which is fully inclusive over radiation up to the scale Q . \mathbf{Z} has a perturbative expansion

$$\mathbf{Z}(\epsilon, \mu) = 1 + \sum_{n=1}^{\infty} \left(\frac{\alpha_s}{\pi}\right) \mathbf{Z}^{(n)}(\epsilon, \mu), \quad (3.199)$$

which can be computed Feynman diagrammatically. For instance, it is clear from our prior discussions that $\mathbf{Z}^{(1)}(\epsilon, \mu)$ can be read off from dimensionally regularising $\ln \bar{\mathbf{V}}_{a,b}^n$ and $\ln \tilde{\mathbf{V}}_{a,b}^n$.

Let us compute the variation in the renormalised amplitude as we vary the renormalisation scale,

$$\frac{d |N(\epsilon, Q, \mu)\rangle}{d \ln \mu} = -\frac{d \ln \mathbf{Z}(\epsilon, \mu)}{d \ln \mu} |N(\epsilon, Q, \mu)\rangle. \quad (3.200)$$

This leads to the defining relation for an anomalous dimension matrix

$$\mathbf{\Gamma}(\mu, \epsilon) = -\frac{d \ln \mathbf{Z}(\epsilon, \mu)}{d \ln \mu}. \quad (3.201)$$

Note that $\mathbf{\Gamma}(\mu, \epsilon)$ is necessarily finite in the limit $\epsilon \rightarrow 0$. Expanding to first order in the coupling

$$\frac{d |N(\epsilon, Q, \mu)\rangle}{d \ln \mu} = -\frac{1}{\pi} \frac{d \alpha_s \mathbf{Z}^{(1)}(\epsilon, \mu)}{d \ln \mu} |N(\epsilon, Q, \mu)\rangle. \quad (3.202)$$

⁴⁰Remember that in a renormalisable theory the UV modes can be fully absorbed into diverging bare parameters in the Lagrangian to leave all amplitudes finite.

⁴¹The following discussion is based off that which is presented in [33].

From which it can be shown that if \mathbf{Z} renormalises only soft divergences then at one loop $\Gamma(\mu, \epsilon) = \frac{\alpha_s}{\pi} \bar{\Gamma}(\mu)$, and if \mathbf{Z} renormalises only collinear divergences then at one loop $\Gamma(\mu, \epsilon) = \frac{\alpha_s}{\pi} \tilde{\Gamma}(\mu)$. Assuming the following boundary conditions,

$$\mu < Q, \quad \text{and} \quad |N(\epsilon, Q, \mu = Q)\rangle = |n(\epsilon, Q)\rangle, \quad (3.203)$$

Eq. (3.200) has the solution

$$|N(\mu)\rangle = \text{Pexp} \left(- \int_{\mu}^Q \frac{d\mu'}{\mu'} \Gamma(\mu') \right) |n(Q)\rangle, \quad (3.204)$$

where the ϵ dependence has been dropped since each term is finite without a regulator and the dependence on the hard scale prior to renormalisation has also been dropped from $|N(\mu)\rangle$. This affords a new interpretation to $\bar{\mathbf{V}}_{\mu, Q}$ (and $\tilde{\mathbf{V}}_{\mu, Q}$). It renormalises an n particle amplitude from a hard scale Q to a lower scale μ by dressing the amplitude with the quantum noise from soft (collinear) modes that span the two scales. The anomalous dimension matrices are interpreted as generators for the evolution of amplitudes through the renormalisation group along paths that preserve particle number. In the preface to Chapter 4 we give a generalisation of Eq. (3.200) to include generators for the evolution of amplitudes along renormalisation group flows which do not preserve particle number. Chapter 4 explores the properties of this generalisation.

3.4.2 Computing observables

Up to this point, this thesis has concerned itself with the computation of QCD matrix elements using perturbation theory. Now we will make the connection to observables: quantities measurable in experiments. At a collider experiment, an integrated observable is computed from the cross-section σ for a process $X \rightarrow Y$ as

$$\Sigma(\{v_i\}) = \prod_i \int dw_i \frac{d\sigma(X \rightarrow Y)}{\prod_j dw_j} u(\{w_i\}, \{v_i\}), \quad (3.205)$$

where Σ is the cross-section for the observable, w_i are functions of the kinematics, v_i are parameters defining the observable, and u is a function enforcing the observable on the phase-space. The simplest observable is the total integrated cross-section, for which $u = 1$ and $\Sigma = \sigma$. Another simple observable is a weighted cross-section known as the energy-energy correlation [34–36]:

$$\Sigma(\alpha) = \sum_{i, j \in Y} \int d\theta_{ij} \frac{d\sigma(X \rightarrow Y)}{d\theta_{ij}} \frac{E_i E_j}{Q^2} \Theta(\theta_{ij} > \alpha). \quad (3.206)$$

Here i and j index hadrons measured in the final state, Y , and θ_{ij} is the angle between them in the laboratory frame. $\Sigma(\alpha)$ is the cross-section for seeing an event in the detector

with hadrons in the final state separated by an angle greater than α , weighted by the energy of the separated hadrons, i.e. this observable is large for an event containing high energy hadrons separated by angles greater than α , it is small for an event containing low energy hadrons separated by angles greater than α , and zero for an event containing only hadrons separated by angles less than α .

Broadly speaking, observables fall into three categories:

1. Event shape observables: these have the general form $u(\{w_i\}, \{v_i\}) = \Theta(F(\{w_i\}, \{v_i\}))$ for some function F . Event shapes tend to be some of the most simple and best studied observables [37–41] and will be the most discussed in this thesis.
2. Weighted cross-sections: these have the general form

$$u(\{w_i\}, \{v_i\}) = \sum_k G_k(\{w_i\}) \Theta(F_k(\{w_i\}, \{v_i\})),$$

for some functions F_k and G_k . Energy-energy correlations between various multiplicities of particles are an example. [36]

3. Jet observables: these are algorithmically applied cuts to the phase-space of a differential cross-section and sometimes re-weightings of the cross-section. They can be challenging to express as single functions $u(\{w_i\}, \{v_i\})$ but are widely used in collider phenomenology and experiments. [42]

In this chapter, we have extensively discussed the KLN theorem, which necessitates that whenever we compute a physically measurable quantity we must sum over all contributing degenerate states. If we do not, cross-sections and probabilities will unphysically diverge. The requirement to sum over degenerate states puts constraints on which observables are ‘valid’. Chief amongst these constraints is infra-red and collinear safety (IRC safety), which requires that an observable is inclusive over exactly collinear and zero energy particles, ensuring the cancellation of IR poles. Let us re-express $u(\{w_i\}, \{v_i\}) \equiv u(\{p_1, p_2, \dots\}, \{v_i\})$ where $\{p_1, p_2, \dots\}$ is the set of particle momenta on which the fully differential cross-section $d\sigma$ depends. IRC safety requires that

$$u(\{p_1, p_2, \dots, p_i, \dots, p_j, \dots\}, \{v_i\}) \rightarrow u(\{p_1, p_2, \dots, p_i + p_j, \dots, p_{j-1}, p_{j+1}, \dots\}, \{v_i\}), \quad (3.207)$$

in the collinear limit where $p_i + p_j \rightarrow \frac{E_i + E_j}{E_i} p_i$, and that

$$u(\{p_1, p_2, \dots, p_i, \dots\}, \{v_i\}) \rightarrow u(\{p_1, p_2, \dots, p_{i-1}, p_{i+1}, \dots\}, \{v_i\}), \quad (3.208)$$

in the soft limit where $p_i^\mu \rightarrow 0$. For example, consider the energy-energy correlation:

$$u(\{p_1, p_2, \dots\}, \alpha) = \sum_{i,j \in Y} \frac{E_i E_j}{Q^2} \Theta(\theta_{ij} > \alpha). \quad (3.209)$$

In the limit that particle k is soft, $E_k \rightarrow 0$, we find that

$$\begin{aligned} u(\{\dots, p_k, \dots\}, \alpha) &= \sum_{i \in Y} \frac{E_i E_k}{Q^2} \Theta(\theta_{ik} > \alpha) + \sum_{i,j \in Y | i,j \neq k} \frac{E_i E_j}{Q^2} \Theta(\theta_{ij} > \alpha) \\ &\rightarrow \sum_{i,j \in Y | i,j \neq k} \frac{E_i E_j}{Q^2} \Theta(\theta_{ij} > \alpha) = u(\{\dots, p_{k-1}, p_{k+1}, \dots\}, \alpha). \end{aligned} \quad (3.210)$$

Similarly, in the collinear limit $p_k + p_l \rightarrow \frac{E_k + E_l}{E_k} p_k$,

$$\begin{aligned} &u(\{\dots, p_k, \dots, p_l, \dots\}, \alpha) \\ &= E_k \sum_{i \in Y} \frac{E_i}{Q^2} \Theta(\theta_{ik} > \alpha) + E_l \sum_{i \in Y} \frac{E_i}{Q^2} \Theta(\theta_{il} > \alpha) + \sum_{i,j \in Y | i,j \neq k,l} \frac{E_i E_j}{Q^2} \Theta(\theta_{ij} > \alpha) \\ &\rightarrow \sum_{i \in Y} \frac{E_i (E_k + E_l)}{Q^2} \Theta(\theta_{ik} > \alpha) + \sum_{i,j \in Y | i,j \neq k,l} \frac{E_i E_j}{Q^2} \Theta(\theta_{ij} > \alpha) \\ &= u(\{\dots, p_k + p_l, \dots, p_{l-1}, p_{l+1}, \dots\}, \alpha). \end{aligned} \quad (3.211)$$

IRC safety ensures that IR poles from QCD radiation cancel and that amplitudes are finite. However, it does not prevent QCD radiation from having a big effect. As we have discussed previously, divergences from QCD radiation are logarithmic, consequently even after cancelling they can leave large logarithms. To illustrate this, consider a process with a hard scale Q to which we apply an IRC safe observable defined so that u is zero if the total energy of the particles in the final state is greater than E_0 and unity otherwise. When computing the observable's cross-section we will find integrals of the form,

$$\underbrace{\alpha_s \int_0^Q \frac{dE}{E}}_{\text{from a soft loop}} - \underbrace{\alpha_s \int_0^{E_0} \frac{dE}{E}}_{\text{from a soft external particle}} = \alpha_s \ln \left(\frac{Q}{E_0} \right). \quad (3.212)$$

As E_0 is reduced the logarithm gets larger and so the soft radiation generates an increasing contribution to the amplitude. By looking at the structure of the anomalous dimension matrices, $\Gamma(\mu)$, in the limit $\mu \rightarrow 0$, it is easy to convince yourself that each order in α_s sees two new logarithmic IR divergences emerge (one soft and one collinear). Therefore, the n th order perturbative correction to a simple one-parameter (v) observable, which diverges in the limit that $v \rightarrow 0$, will have the form,

$$\Sigma^{(n)}(v) = \alpha_s^n \Sigma^{(0)}(v) \sum_{m=0}^{2n} C_m^n(v) (\ln v)^{2n-m}, \quad (3.213)$$

where $C_m^n(v) \sim \mathcal{O}(1)$ or 0 in the limit $v \rightarrow 1$. Provided that every $C_m^n(v)$ is finite, the leading term in the limit that $v \rightarrow 1$ is the $\alpha_s^n C_0^n(v)(\ln v)^{2n}$ piece, which originates from n simultaneously soft and collinear (soft-collinear) gluons dressing the zeroth order cross-section.⁴² For small v , where $v \sim e^{-\alpha_s^{-1}}$, $\alpha_s^n C_0^n(v)(\ln v)^{2n}$ and $\alpha_s^{n+1} C_0^{n+1}(v)(\ln v)^{2n+2}$ give comparable contributions to the cross-section and therefore need resumming. To this end, we re-organise the perturbative series to the observable as

$$\frac{\Sigma(v)}{\Sigma^{(0)}(v)} = \left(\underbrace{\sum_{n=0}^{\infty} \alpha_s^n C_0^n(v)(\ln v)^{2n}}_{\text{leading expansion}} + \underbrace{\sum_{n=1}^{\infty} \alpha_s^n C_1^n(v)(\ln v)^{2n-1}}_{\text{NL expansion}} + \underbrace{\sum_{n=1}^{\infty} \alpha_s^n C_2^n(v)(\ln v)^{2n-2} + \dots}_{\text{NNL expansion}} \right), \quad (3.214)$$

where NL stands for next-leading, NNL next-to-next-to-leading, and $C_0^0 = 1$. Often this organising of the perturbative series is referred to as the logarithmic accuracy in the expansion of the observable [40] and is abbreviated as leading log in the expansion (LL_Σ), next-to-leading log in the expansion (NLL_Σ), and so forth.

The goal of resummation is to resum as much of the logarithmic expansion as possible into a special function which converges over the full range of $\alpha_s < 1$. However, we have a hurdle to cross before we can do this. Throughout this thesis we have deferred off dealing with an important part of the physics. QCD is non-perturbative at lower scales and the particles we observe in detectors are low-scale non-perturbative hadrons. Just as resummation becomes important when accurately computing an observable with low scale particles, so does non-perturbative physics become important at even lower scales. Along with the resummation of QCD radiation, dealing with the non-perturbative aspects of QCD is a substantial hurdle in the complete computation of an observable. In the following section we discuss the factorisation of non-perturbative physics from perturbative physics. This key feature of QCD cross-sections will allow us to compute observables using the resummed perturbative physics that we have been developing so far.

3.4.2.1 Factorisation theorems

There are many factorisation theorems useful to the study of QCD. We have already seen one example of factorisation when in Section 3.3 we derived the factorisation of soft and collinear currents at first order. One of the fundamental factorisation theorems in the study of perturbative QCD is Collins, Soper and Sterman [43–45] (CSS) factorisation. CSS showed

⁴²Some observables are constructed such that they are insensitive to soft radiation [36] or insensitive to collinear radiation [15]. In which case $C_m^n(v) \rightarrow 0$ in the limit $v \rightarrow 1$ for $m < n$ since the KLN cancellation of double poles can go ahead without leaving a large logarithm.

that for e^+e^- collisions, deep inelastic scattering, and Drell-Yan processes non-perturbative physics will factorise into distributions which can be independently evaluated from perturbatively computed cross-sections of partons (QCD particles which later hadronise to become ‘parts’ of hadrons).

The proto-typical CSS factorisation formula is that for Drell-Yan,

$$\frac{d\sigma_{\text{DY}}}{dydQ^2} = \sum_{a,b} \int_{x_A}^1 d\xi_A \int_{x_B}^1 d\xi_B \frac{d\hat{\sigma}_{\text{DY}}^{ab}\left(\frac{x_A}{\xi_A}, \frac{x_B}{\xi_B}, Q; \frac{\mu}{Q}, \alpha_s(\mu)\right)}{dydQ^2} f_{a/A}(\xi_A, \mu) f_{b/B}(\xi_B, \mu) + \mathcal{O}\left(\frac{\Lambda_{\text{QCD}}^2}{Q^2}\right), \quad (3.215)$$

where $d\sigma_{\text{DY}}$ is the complete differential Drell-Yan cross-section for two protons A, B and $d\hat{\sigma}_{\text{DY}}^{ab}$ is the partonic Drell-Yan cross-section for two partons a, b . $f_{a/A}(\xi_A, \mu)$ is a parton distribution function (PDF) and can be interpreted as the probability density for a parton a to be found inside a hadron A carrying a fraction of the total hadron’s momentum ξ_A (we make this more precise in the following section). Q is the hard scale, here the observed invariant mass of the leptonic final state.

$$y = \frac{1}{2} \ln \left(\frac{q \cdot P_A}{q \cdot P_B} \right),$$

where q is the total momentum of the final state (i.e. $q^2 = Q^2$) and $P_{A,B}$ are the momenta of hadrons A, B , and

$$x_A = e^y \sqrt{\frac{Q^2}{(P_A + P_B)^2}}, \quad x_B = e^{-y} \sqrt{\frac{Q^2}{(P_A + P_B)^2}}.$$

Finally μ is a renormalisation scale at which the factorisation is defined (i.e. the scale of the PDFs).

The factorisation formula for deep-inelastic scattering shares the same basic structure

$$\frac{d\sigma_{\text{DIS}}(x, Q^2)}{dx dQ^2} = \sum_a \int_{x_A}^1 d\xi \frac{d\hat{\sigma}_{\text{DIS}}^a(x_A/\xi, Q^2)}{dx dQ^2} f_{a/A}(\xi_A, \mu) + \mathcal{O}\left(\frac{\Lambda_{\text{QCD}}^2}{Q^2}\right), \quad (3.216)$$

where $d\sigma_{\text{DIS}}$ is the differential deep inelastic scattering cross-section a proton A and $d\hat{\sigma}_{\text{DIS}}^a$ is the partonic deep inelastic scattering differential cross-section for an incoming parton a . The similarity between these formulas (and other known factorisation formulas [45, 46]) leads to two of the core assumptions in perturbative QCD:

1. Non-perturbative physics factorises from perturbative physics as

$$d\sigma(X \rightarrow Y) = d\sigma(x \rightarrow y) \otimes (f_{x/X}(\mu) f_{y/Y}(\mu)) + \mathcal{O}\left(\frac{\Lambda_{\text{QCD}}}{\mu}\right), \quad (3.217)$$

where X is hadronic initial state and Y a hadronic final state. [46] $\hat{\sigma}(x \rightarrow y)$ is a partonic cross-section for an initial ensemble of partons x and final state ensemble y (i.e. quarks and gluons). f are probability distributions for finding the parton ensemble x (y) in the hadronic state X (Y). Typically f_X is a product of PDFs and f_Y a product of fragmentation functions (PDFs but defined for outgoing particles). The ‘ \otimes ’ represents a convolution over parameters shared between $d\sigma(x \rightarrow y)$ and $f_{x/X}f_{y/Y}$, as well as a sum over all relevant partonic states x, y . This relation is thought to hold up to corrections $\mathcal{O}\left(\frac{\Lambda_{\text{QCD}}}{\mu}\right)$ which are known as ‘power suppressed corrections’. Operators suppressed by powers of the scale can correspond to larger transfers of angular momentum [47] or other non-perturbative effects [48].

2. A PDF for a parton a typically appears entirely independent of a PDF for parton b , this motivates the principle of parton-hadron duality. This principle states that the process of hadronisation is localised in phase-space space and consequently does not effect the basic ‘shape’ of the energy flows of a process up to corrections $\mathcal{O}\left(\frac{\Lambda_{\text{QCD}}}{\mu}\right)$. This leads to the following: let \hat{Y} be an operator which, up to power suppressed corrections, maps a partonic state y onto a hadronic state Y :

$$\hat{Y} |y; p_{Y_1}, p_{Y_2}, \dots\rangle = |Y; p_{Y_1}, p_{Y_2}, \dots\rangle + \mathcal{O}\left(\frac{\Lambda_{\text{QCD}}}{\mu}\right), \quad (3.218)$$

where p_{Y_i} is the total momenta of the cluster of partons in the region of phase-space in which hadron $Y_i \in Y$ is found. It is implicit that the state $|y\rangle$ sums over all y that could hadronise to produce Y . Summing over all possible states Y forces \hat{Y} to act as identity operator on $|y; p_{Y_1}, p_{Y_2}, \dots\rangle$, hence

$$\begin{aligned} \sum_Y d\sigma_{X \rightarrow Y} &\sim \sum_Y |\langle Y | \hat{S} | X \rangle|^2 = \sum_Y |\langle y | \hat{Y}^\dagger \hat{S} | X \rangle|^2 + \mathcal{O}\left(\frac{\Lambda_{\text{QCD}}}{\mu}\right) \\ &= |\langle y | \hat{S} | X \rangle|^2 + \mathcal{O}\left(\frac{\Lambda_{\text{QCD}}}{\mu}\right) \sim d\sigma_{X \rightarrow y} + \mathcal{O}\left(\frac{\Lambda_{\text{QCD}}}{\mu}\right). \end{aligned} \quad (3.219)$$

Consequently, parton-hadron duality implies that if we sum inclusively over the species of hadrons in the final state of a process, then an observable computed on the process can be equivalently computed from the partonic cross-section (using CSS factorisation).

These statements follow directly from CSS factorisation in e^+e^- collisions, deep inelastic scattering, and Drell-Yan processes. CSS have also shown [44] that for suitably inclusive observables these assumptions are also valid in proton-proton processes, such as at the LHC. However, beyond these processes there are not currently any general proofs for the assumptions. In this thesis we go with general consensus (for instance see these prevailing

approaches to QCD resummation [39, 40]) by assuming the validity of these assumptions to arbitrary processes with the caveat that μ is always less than some, observable dependent, inclusivity scale⁴³. This caveat ensures CSS' work on proton-proton processes applies. In Section 4.4.3 and later in Chapter 8 we show that if we assume Eq. (3.217) for μ less some inclusivity scale, factorisation of the form in Eq. (3.217) does not follow simply for μ greater than the inclusivity scale.

Another key factorisation theorem is that of hard process factorisation [45, 49]. This is the factorisation of infra-red⁴⁴ singular terms in $d\hat{\sigma}$ into a hard process defined without low scale QCD radiation and an operator containing the IR singularities. In this chapter we have already done much of the groundwork towards proving this for leading singularities by deriving the factorised soft and collinear currents at $\mathcal{O}(\alpha_s)$ and arguing for the generalisation of these currents to higher orders by using strong ordering. More generally, hard process factorisation is closely linked to the IR renormalisation, and factorisation, of Wilson loops in amplitudes (see [1, 33, 50] and references therein for a more detailed accounts).

3.4.2.2 DGLAP evolution of a proton

In the previous section we introduced parton distribution functions (PDFs) to describe the non-perturbative physics of hadrons at a given scale. Let us now briefly expand on the definition of the PDFs and summarise how they evolve with changes in scale, following the approach in [45]. The bare (not renormalised) unpolarised (spin averaged) PDFs are formally defined as

$$f_{a/A}(\xi)d\xi = \sum_s \frac{d(\xi P_A^+)}{\xi P_A^+} \int dk_\perp \langle P_A | \hat{b}_{a,s}^\dagger(\xi P_A^+, k_\perp) \hat{b}_{a,s}(\xi P_A^+, k_\perp) | P_A \rangle, \quad (3.220)$$

where $f_{a/A}(\xi)$ is the PDF for finding a parton a inside a hadron A . P_A is the momentum of hadron A . P_A^+ is a light-cone component of P_A , and is defined so that $P_A^- = m_A^2/2P_A^+$ and $P_A^2 = 2P_A^+P_A^- = m_A^2$. ξ is the fraction of momentum P_A^+ carried by a . $\hat{b}_{a,s}^\dagger(\xi P_A^+, k_\perp)$ is a creation operator for parton a with spin s and with momentum in light-cone coordinates $(k^+, k^-, k_\perp) = (\xi P_A^+, \frac{k_\perp^2}{2\xi P_A^+}, k_\perp)$. The combined operator $\hat{b}_{a,s}^\dagger \hat{b}_{a,s}$ is the number density operator (the continuous spectrum analogue to the harmonic oscillator number operator). It is implicit that this correlation function is time-ordered with an 'out state' on the left and 'in state' on the right.

Though the state $|P_A\rangle$ represents a non-perturbative hadron, the operator structure inside the correlator can be computed perturbatively provided we assume $\alpha_s < 1$ and

⁴³An inclusivity scale is a scale for which all radiation emitted into regions of phase-space below the scale is integrated/summed over completely; correspondingly leading terms from the radiation fully cancel, as per the KLN theorem.

⁴⁴Sometimes further specified as infra-red and collinear (IRC).

therefore the scale we renormalise the theory at is $\mu \gg \Lambda_{\text{QCD}}$. The calculation itself requires a fair amount of work (see [28, 45, 51], ordered in accessibility), however the bottom line answer in $d = 4 - 2\epsilon$ dimensions has the form

$$f_{a/A}(\xi) = \delta_{aA}\delta(1-\xi) - \frac{1}{\epsilon} \frac{\alpha_s}{\pi} C_A S \mathcal{P}_{aA}(\xi) + \frac{1}{\epsilon} \frac{\alpha_s}{\pi} C_A \sum_{bA \in \{qq, gq, gg\}} \int d\xi' \mathcal{P}_{bA}(\xi') \delta_{aA} \delta(1-\xi) + \mathcal{O}(\alpha_s^2, \epsilon^0). \quad (3.221)$$

Here A is assumed to be purely partonic⁴⁵, \mathcal{P}_{Aa} is an appropriate collinear splitting function determined by the colour charge of A (derived in Section 3.3), C_A is the Casimir colour factor that comes with each splitting function, and S is a symmetry factor that originates from particles which are considered indistinguishable in the final state being distinguishable in the initial state⁴⁶. The zeroth order term corresponds to when hadron A is parton a . The first order term has two parts, the first part comes from hadron A being identified as a parton which has emitted another parton into the final state – in doing so A transitions so that it contains parton a with a momentum fraction ξ . The second part of the first order correction (proportional to $\delta(1-\xi)$) is the one-loop correction to hadron A being parton a . Ultra-violet divergences have been renormalised and cancelled from the calculation. Importantly, there is one uncancelled IR divergence of collinear origin (the soft limit is found when $\xi \rightarrow 1$, and the soft divergences cancel in this limit). The origin of this divergence is a failure of the KLN theorem, which was perturbatively derived. In the KLN theorem, loop divergences cancelled divergences from external particles because the external particles were indistinguishable. However, in this calculation the symmetry factor S has appeared and $f_{a/A}$ is sensitive to the momentum fraction of a even in the exact collinear limit, spoiling indistinguishability. Both these properties prevent the cancellation of the collinear pole. It is typical to re-write the first order correction in the form

$$f_{a/A}(\xi) = \delta_{aA}\delta(1-\xi) - \frac{1}{\epsilon} \frac{\alpha_s}{\pi} P_{aA}(\xi) + \mathcal{O}(\alpha_s^2, \epsilon^0). \quad (3.222)$$

where $P_{aA}(\xi)$ are the Altarelli-Parisi splitting functions [23]:

$$\begin{aligned} P_{qq}(\xi) &= \mathcal{C}_F \left(\frac{1+\xi^2}{1-\xi} \right)_+ \equiv \mathcal{C}_F \left[\frac{1+\xi^2}{(1-\xi)_+} + \frac{3}{2} \delta(1-\xi) \right], \\ P_{gg}(\xi) &= 2\mathcal{C}_A \left(\frac{\xi}{(1-\xi)_+} + \xi(1-\xi) + \frac{1-\xi}{\xi} \right) + \frac{1}{6} (11\mathcal{C}_A - 4n_f T_R) \delta(1-\xi), \\ P_{gq}(\xi) &= \mathcal{C}_F \mathcal{P}_{gq}(\xi), \quad P_{qg}(\xi) = \mathcal{P}_{qg}(\xi). \end{aligned} \quad (3.223)$$

⁴⁵i.e. A is an ensemble of exactly collinear quarks and gluons with a combined colour charge equivalent to that of either a quark or gluon.

⁴⁶i.e. after a $1 \rightarrow 2$ parton transition it matters which parton is in hadron A or was emitted from hadron A , whereas in the final state switching the two partons is nothing more than a re-labelling. Hence, for a transition $g \rightarrow gg$, $S = 2$.

Here we have used the ‘plus prescription’ which acts as a distribution on a function g defined by the relation $f(\xi)_+g(\xi) = f(\xi)g(\xi) - f(\xi)g(1)$.

The single uncanceled IR divergence can be removed by renormalising the PDFs, leading to the scale dependent PDFs used in the factorisation theorems of the previous section. The renormalised PDFs obey a renormalisation group equation called the DGLAP equation (after Dokshitzer [27], Gribov [52], Lipatov, and Altarelli & Parisi [23]). The DGLAP equation is

$$\mu \frac{df_{a/A}(\xi, \mu)}{d\mu} = \sum_b \int_\xi^1 \frac{dz}{z} \frac{\alpha_s(\mu)}{\pi} P_{ab}(z) f_{b/A}(\xi/z, \mu). \quad (3.224)$$

In Section 4.5 we provide a re-derivation of the DGLAP equation (with a fixed coupling constant) from the formalism we develop in the following chapters. We can see from Eq. (3.224), which only depends on collinear splitting functions, that the DGLAP equation is only resumming the collinear radiation surrounding the hadrons. To this end, CSS factorisation is often referred to as collinear factorisation since the factorisation formulas can be interpreted as collinear radiation surrounding hadrons factorising from the rest of the cross-section. For inclusive processes, it is typical to let $\mu \sim Q$, the hard scale of a process, which has the effect of resumming all the collinear radiation dressing the initial hadrons into the PDFs. This scale choice allows one to think of the initial state hadrons as coherent wave packets which interact in the hard process, and has the effect of minimising logarithms in μ/Q that emerge from the renormalisation procedure and reducing the size of power suppressed corrections.

3.4.2.3 Resummation of an observable

Now we have discussed the factorisation of non-perturbative physics from perturbative physics, we can proceed to discuss the resummation of large logarithms in the perturbative expansion of an observable. We have already seen that loop contributions can be resummed into exponential functions (Sudakov factors). We have also studied the KLN theorem, which required the logarithmic divergences from loops to cancel against those of external particles. Let us look at the effect this has on the computation of an observable at first order:

$$\begin{aligned} & \prod_i \int dw_i \frac{d\sigma_n}{\prod_j dw_j} u(\{w_i\}, \{v_i\}) \\ & \approx \prod_i \int dw_i \frac{d\sigma_n^{(0)}}{\prod_j dw_j} \left(1 + \frac{\int \frac{d\Phi_{n+1}}{\prod_j dw_j} |M_{n+1}^{(0)}|^2}{\int \frac{d\Phi_n}{\prod_j dw_j} |M_n^{(0)}|^2} \right. \\ & \quad \left. + \frac{2 \int \frac{d\Phi_n}{\prod_j dw_j} \text{Re}\{M_n^{(0)*} M_n^{(1)}\}}{\int \frac{d\Phi_n}{\prod_j dw_j} |M_n^{(0)}|^2} + \mathcal{O}(\alpha_s^2) \right) u(\{w_i\}, \{v_i\}), \quad (3.225) \end{aligned}$$

where $M_{n+p}^{(m)}$ is an n particle matrix element with m loops and dressed with p soft or collinear real particles, and $d\Phi_n$ is the n parton phase-space measure. $d\sigma_n^{(0)}$ is often referred to as the hard process cross-section (so called because it is without soft and collinear radiation). On the RHS we have only kept the leading divergent pieces of the matrix elements, these are the pieces that will produce large logs: i.e. the third line will be proportional to an anomalous dimension, $\text{Re}\{\int \frac{dk_\perp}{k_\perp} \Gamma(k_\perp)\}$. Let us assume that the observable factorises as $u_0(\{w_i\}, \{v_i\})u_m(\{w_i\}, \{v_i\})$ so that

$$\begin{aligned} & \prod_i \int dw_i \frac{d\sigma_n^{(0)}}{\prod_j dw_j} u_0(\{w_i\}, \{v_i\}) \int \frac{d\Phi_{n+m}}{\prod_j dw_j} u_m(\{w_i\}, \{v_i\}) \\ & = \Sigma^{(0)}(\{v_i\}) \prod_i \int dw_i \int \frac{d\Phi_{n+m}}{\prod_j dw_j} u_m(\{w_i\}, \{v_i\}), \end{aligned} \quad (3.226)$$

where $\Sigma^{(0)}(\{v_i\})$ is the zeroth order (Born) cross-section of the observable. If this is the case, then the KLN theorem can be used so that the first order correction is written as

$$\begin{aligned} & \Sigma^{(0)}(\{v_i\}) \prod_i \int dw_i \left(\frac{\int \frac{d\Phi_{n+1}}{\prod_j dw_j} |M_{n+1}^{(0)}|^2}{\int \frac{d\Phi_n}{\prod_j dw_j} |M_n^{(0)}|^2} + \frac{2 \int \frac{d\Phi_n}{\prod_j dw_j} \text{Re}\{M_n^{(0)*} M_n^{(1)}\}}{\int \frac{d\Phi_n}{\prod_j dw_j} |M_n^{(0)}|^2} \right) u_1(\{w_i\}, \{v_i\}) \\ & = -\Sigma^{(0)}(\{v_i\}) \prod_i \int dw_i \frac{\int \frac{d\Phi_{n+1}}{\prod_j dw_j} |M_{n+1}^{(0)}|^2}{\int \frac{d\Phi_n}{\prod_j dw_j} |M_n^{(0)}|^2} (1 - u_1(\{w_i\}, \{v_i\})). \end{aligned} \quad (3.227)$$

If u_1 is unity in some allowed regions of phase-space and zero elsewhere (for example u is an event shape observable), this relation implies that the first order correction to the observable can be computed by integrating the soft/collinear loop contribution over the regions of phase-space not allowed by the observable. As we have shown, logarithmically divergent terms from loops exponentiate – resumming their large logs. Therefore, should this pattern continue to higher perturbative orders, we can postulate an ansatz that perturbative contributions to the resummed observable exponentiate in the following form:

$$\prod_i \int dw_i \frac{d\sigma_n}{\prod_j dw_j} u(\{w_i\}, \{v_i\}) \approx \Sigma^{(0)}(\{v_i\}) e^{-\prod_i \int dw_i \frac{\int \frac{d\Phi_{n+1}}{\prod_j dw_j} |M_{n+1}^{(0)}|^2}{\int \frac{d\Phi_n}{\prod_j dw_j} |M_n^{(0)}|^2} (1 - u_1(\{w_i\}, \{v_i\}))}. \quad (3.228)$$

For many observables this is indeed the case and this ansatz correctly resums the LL_Σ logarithms, sometimes referred to as doubly logarithmic (DL) accuracy in the resummation. In Section 4.5 we demonstrate that the ‘thrust distribution’ [37] resums in this fashion at DL accuracy for an e^+e^- hard process and discuss observables for which this approach to resummation fails. Shortly we will describe a broad class of event shape observables (rIRC

safe observables) which resum in this fashion at DL accuracy for e^+e^- and proton-proton hard processes.⁴⁷

The generalisation of the ansatz for the resummation of a one-parameter event shape observable in Eq. (3.228), to arbitrary logarithmic order, is

$$\begin{aligned}\Sigma(v) &= \prod_i \int dw_i \frac{d\sigma(X \rightarrow Y)}{\prod_j dw_j} u(\{w_i\}, v_i) \\ &= \prod_i \int dw_i \frac{d\sigma_0(X \rightarrow Y)}{\prod_j dw_j} F_{X \rightarrow Y}(\alpha_s, L) u_0(\{w_i\}, v),\end{aligned}\quad (3.229)$$

where $L = \ln(1/v)$, and where

$$F_{X \rightarrow Y}(\alpha_s, L) = (1 + C(\alpha_s)) e^{Lg_1(\alpha_s L) + g_2(\alpha_s L) + \sum_{n>0} \alpha_s^n g_{n+2}(\alpha_s L)} (1 + S(\alpha_s L) + D(v)).\quad (3.230)$$

Each function on the right-hand-side of this expression goes to zero as their argument goes to zero. $S(\alpha_s L)$ resums non-exponentiating terms, the most common of which are ‘non-global logarithms’. An exponentiating observable is one for which $S = 0$. $Lg_1(\alpha_s L)$ is the leading-log piece (LL). It resums all of the LL_Σ terms and sometimes other sub-leading terms in the expansion. $g_2(\alpha_s L)$ is the next-to-leading-log (NLL) piece. In exponentiating observables, the LL term plus the NLL together resum the LL_Σ and NLL_Σ terms as well as many further sub-leading terms in the expansion. $D(v)$ is a ‘remainder’ function that does not contribute logarithms to the resummation.

We can let X be a hadronic state with n hadrons and use the CSS factorisation of non-perturbative physics so that

$$\Sigma(v) = \prod_i \int dw_i \frac{d\sigma_0(x \rightarrow Y)}{\prod_j dw_j} \otimes \left(\left[\prod_{i=1}^n f_i(x_i, \mu_F) \right] F_{x \rightarrow Y}(\alpha_s, L, \mu_F, x_i) \right) u_0(\{w_i\}, v),\quad (3.231)$$

where $f_i(x_i, \mu_F)$ is a PDF for the i th hadron at a factorisation scale $\mu_F \sim Q$, the hard scale of $\sigma_0(x \rightarrow Y)$, and ‘ \otimes ’ is the usual convolution over momentum fractions, x_i . $F_{x \rightarrow Y}$ has been modified so that functions $g_{j>1}$ gain contributions from the running of the PDFs,

$$\sum_{j=0} \alpha_s^j g_{j+2}(\alpha_s L) \supset \sum_{i=1}^n \ln \frac{f_i(x_i, V(v)\mu_F)}{f_i(x_i, \mu_F)},\quad (3.232)$$

where $V(v)$ is some function of v that enforces the phase-space boundaries from the observable restricting collinear radiation from the initial state.⁴⁸ Note that only collinear divergences contribute to the renormalisation of the PDFs, hence they contribute only single

⁴⁷The thrust distribution is an rIRC safe observable [53].

⁴⁸Restricting the phase-space of collinear radiation from the initial state changes the first term on the second line of Eq. (3.221) and therefore modifies the renormalisation of the PDFs.

logarithms (at most $\mathcal{O}(\alpha_s^m L^m)$) as double logarithms come from soft-collinear divergences. Therefore the running of the PDFs does not contribute to $Lg_1(\alpha_s L)$.⁴⁹

We have presented the ansatz for an exponentiating observable without giving a statement on which observables it is applicable to. This is because a general statement on which observables will or will not resum into this form, at an arbitrary accuracy, is not known. However, it has been shown that a broad class of observables, known as continuously-global recursively IRC (rIRC) safe observables, exponentiate in this form at NNLL $_{\Sigma}$ accuracy [39, 40] for proton-proton hard processes⁵⁰ and will have this form at NNLL accuracy for e^+e^- hard processes [41]. The precise definition of IRC safety is technical⁵¹. However, in summary, continuously-global rIRC safety defines a class of one parameter event shape observables which have the form $u(\{w_i\}, v) = \Theta(V(\{w_i\}) - v)$ where

- $V(\{w_i\})$ is global, meaning that it is sensitive to radiation emitted into all parts of phase-space.
- Following globalness, $V(\{w_i\})$ must be continuously-global. This requires that $V(\{w_i\})$ has a uniform scaling across all parts of phase-space under the variation of the transverse momenta of soft and collinear radiation: i.e. for an arbitrary soft or collinear particle i , across the i 's complete phase-space $V(\{w_i\}) \sim k_{i\perp}^a$ for some constant power a .
- rIRC safety requires two things: that $V(\{w_i\})$ has the same scaling properties under the variation of the momenta of multiple soft and collinear partons as it does under the variation of the momentum of one soft or collinear particle, and that there exists some scale ϵv for which radiation satisfying $V(\{w_i\}) < \epsilon v$ does not significantly contribute to the observable $\Sigma(v)$, i.e. a phase-space restriction $V(\{w_i\}) > \epsilon v$ can be consistently applied as an IR cut-off below which the KNL theorem would ensure the complete cancellation of radiation.

In Sections 4.5, 6.4.1, 6.9, and Chapter 8 we give example resummations and fixed order computations of both continuously-global rIRC safe observables and not-continuously-global not-rIRC safe observables using the formalism we develop.

⁴⁹This all hinges on the validity of non-perturbative factorisation for all scales $\mu_F < Q$. In Chapter 8 we demonstrate that this assumption is not valid for many observables and the PDFs can source contributions to $Lg_1(\alpha_s L)$ via ‘coherence violating’ logarithms.

⁵⁰We stress that the arguments demonstrating this accuracy all rest of the assumption of CSS factorisation in proton-proton processes, though [40] does attempt to count for the possibility of CSS factorisation failing and argue that the NNLL $_{\Sigma}$ accuracy remains untarnished.

⁵¹The precise definition is given in [39]. We point the reader to [54] for a simple overview and example resummations.

3.5 Parton showers

Parton showers provide an alternative to analytical resummation. They are the basis for all purpose computer programs which can be used to compute an observable by Monte Carlo integration. The programs simulate the distribution of partons one would see in a detector by approximating the squared matrix elements for large multiplicities of QCD radiation with classical branching algorithms and producing events (configurations of partons) with weights proportional to the squared matrix elements.⁵² An observable is computed by placing selection cuts on events (or re-weighting the events), corresponding to the action of $u(\{w_i\}, \{v_i\})$ across that phase-space of the partons, and then summing over the events whilst normalising the distribution against the luminosity, approximating the limit that the number of events goes to infinity. This approximates the Monte-Carlo integration of

$$\frac{\Sigma_L(\{v_i\})}{L} = \lim_{L' \rightarrow \infty} \frac{1}{L'} \prod_i \int dw_i \frac{d\sigma_{L'}(X \rightarrow Y)}{\prod_j dw_j} u(\{w_i\}, \{v_i\}),$$

where L is the luminosity, $\Sigma_L(\{v_i\})$ is the observable cross-section at luminosity L , and $d\sigma_{L'}(X \rightarrow Y)$ the differential cross-section at luminosity L' .

There are multiple parton shower models on the market at the moment – each different model using a different methodology to approximate the the squared matrix elements of QCD radiation. Two of the most prevalent models are angular-ordered showers [57], and dipole showers [58–60]. We provide complete derivations for these models in Chapter 6 and then give further details in Chapter 7. These derivations are performed with the goal of finding improvements to these models; however, sufficient introductory material is also given. Therefore, in this section we will only give a qualitative description of the models. Other models, not discussed in this thesis, do also exist: i.e. antenna showers [61], and hybrid models which combine approaches [62].

Angular-ordered showers

Angular-ordered showers are based around simulating the description of QCD radiation used by a formalism for resummation known as coherent branching. Coherent branching exploits a property known as coherence. When radiation is emitted from a charge distribution (whether gravitational, EM or QCD) if the charge distribution is viewed from a sufficiently large distance away the radiation interferes with itself such that it appears to have been emitted ‘incoherently’ from the combined distribution: viewed from a distance a hydrogen

⁵²Classical branching algorithms are used since, generally speaking, as the multiplicity of QCD radiation increases the number of interference terms contributing to a cross-section grows factorially. Historically, this has rendered the simulation of interference terms impractical. However, some modern approaches have made substantial progress in attempts to simulate the full matrix elements [55, 56].

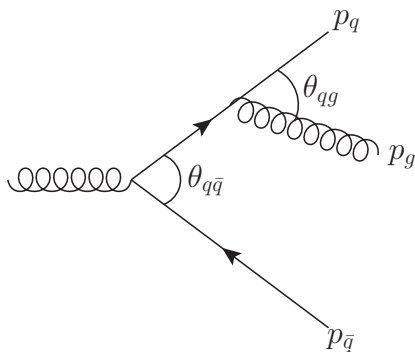


Figure 3.5: The labelling of particle momenta and angles for the $g \rightarrow q\bar{q}$ charge distribution which emits further radiation (the gluon).

atom is electrically neutral. Only when viewed at a finer resolution scale can the individual components of the distribution be resolved and so the radiation is emitted ‘coherently’ from the components.

Let us make this intuition from coherence a little more concrete, following the approach of [25]. Let the charge distribution be a freely propagating gluon which decayed into a quark anti-quark pair. We want to compute the QCD radiation emitted from this distribution, i.e. computing the emission of a soft gluon. We will begin by assuming the gluon is emitted from the quark (see Figure 3.5). Before emitting the gluon, the quark is off-shell with a momentum $(p_q + p_g)$; all other momenta are on-shell and we assume the quarks are massless. We can use the Heisenberg uncertainty relation to find the amount of time after the $g \rightarrow q\bar{q}$ transition at which the second gluon is emitted:

$$\Delta t \approx \frac{E_q}{M_{\text{virtual}}^2} = \frac{E_q}{(p_q + p_g)^2} \approx \frac{1}{E_g \theta_{qg}^2}. \quad (3.233)$$

We can express Δt in terms of the wavelength of the gluon by substituting $E_g \theta_{qg} \approx k_{\perp} = \lambda_{\perp}^{-1}$, where λ_{\perp} is the transverse wavelength of the emitted gluon. The gluon can only resolve the $q\bar{q}$ pair when its transverse wavelength is less than the separation between the two quarks (the usual diffraction limit of a wave). The separation s at a time Δt after the $g \rightarrow q\bar{q}$ transition is given by $s \approx \theta_{q\bar{q}} \Delta t$. Therefore, radiation emitted from the distribution can only resolve the distribution for $\lambda_{\perp} < s$ which necessitates that the radiation is emitted at angles $\theta_{qg} < \theta_{q\bar{q}}$ (or $\theta_{\bar{q}g} < \theta_{q\bar{q}}$). Radiation emitted at angles larger than the angular separation of the $q\bar{q}$ pair only resolve the combined distribution, equivalent to that of the gluon present before the $g \rightarrow q\bar{q}$ transition.

Coherent branching and angular-ordered showers use coherence to compute squared matrix elements from a Markov chain of collinearly emitted radiation ordered in angle: i.e. radiation is emitted proportionally to collinear splitting functions (see 3.3) with the

associated Casimir colour factors. First the widest angle radiation is emitted and then radiation at successively smaller angles which builds up the unresolved sub-structure of the charge distribution. We discuss the accuracy of the approach in detail in Chapter 6 and then with particular focus on the accuracy of colour factors in Chapter 7. However, in summary, the coherent branching formalism is sufficient to accurately compute the NLL_Σ terms for most observables, failing for observables with strong dependence on angular correlations or for hard processes which do not form a colour singlet, and it can be used to resum many continuously-global 2-jet observables at NLL accuracy [37, 39].

Dipole showers

Dipole showers are defined around the leading colour limit of QCD. They exploit that

$$\text{Leading}^{(0)} \left[\langle M_n | \mathbf{S}_{n+1}^\dagger \mathbf{S}_{n+1} | M_n \rangle \right] = 2\pi\alpha_s N_c \sum_{\sigma} \sum_{(i,j) \text{ c.c.} \in \sigma} w_{ij}^{(n+1)} |M_n^\sigma|^2, \quad (3.234)$$

where $\text{Leading}^{(0)}$ is the operation for extracting the leading colour piece (introduced in Section 3.2.3), \mathbf{S}_{n+1} is the eikonal current (see Section 3.3), M_n^σ is a matrix element for a given colour flow σ , and the summation over ‘ $(i, j) \text{ c.c.} \in \sigma$ ’ is a sum over pairs of partons i, j which are connected by a colour line in the colour flow σ . $w_{ij}^{(n+1)}$ is the eikonal/soft antenna function

$$w_{ij}^{(n+1)} = \frac{p_i \cdot p_j}{p_{n+1} \cdot p_i p_{n+1} \cdot p_j}. \quad (3.235)$$

Dipole showers approximate the squared matrix elements for QCD radiation by taking the leading colour limit and using Monte-Carlo methods to sum over strongly ordered radiation with emission kernels proportional to Eq. (3.234). This gives dipole showers broad LC and LL accuracy since they compute squared matrix elements in the immediate neighbourhood of soft and collinear poles with complete LC accuracy⁵³. Addressing how the accuracy of a dipole shower can be systematically improved beyond this is the purpose of Chapters 6 and 7.

References

- [1] T. Becher, A. Broggio, A. Ferroglia, *Introduction to Soft-Collinear Effective Theory, Vol. 896*, Springer, 2015, arXiv: 1410.1892 [hep-ph].

⁵³It is tempting to believe that dipole showers should also correctly compute LC squared matrix elements in the immediate neighbourhood of soft wide-angle poles, as these poles are captured by Eq. (3.234). As we discuss in Chapters 6, and was first demonstrated in [63], accuracy in this region of phase-space can be complicated by momentum conservation.

- [2] T. Coughlin, PhD thesis, School of Physics and Astronomy, The University of Manchester, UK, available at <http://www.hep.manchester.ac.uk/u/forshaw/Tim-Thesis.pdf>, **2009**.
- [3] C. W. Bauer, S. Fleming, M. E. Luke, “Summing Sudakov logarithms in $B \rightarrow X_s + \gamma$ in effective field theory”, *Phys. Rev.* **2000**, *D63*, 014006, arXiv: [hep-ph/0005275](https://arxiv.org/abs/hep-ph/0005275) [[hep-ph](#)].
- [4] C. W. Bauer, S. Fleming, D. Pirjol, I. W. Stewart, “An Effective field theory for collinear and soft gluons: Heavy to light decays”, *Phys. Rev.* **2001**, *D63*, 114020, arXiv: [hep-ph/0011336](https://arxiv.org/abs/hep-ph/0011336) [[hep-ph](#)].
- [5] T. Kinoshita, “Mass singularities of Feynman amplitudes”, *J. Math. Phys.* **1962**, *3*, 650–677.
- [6] T. D. Lee, M. Nauenberg, “Degenerate Systems and Mass Singularities”, *Phys. Rev.* **1964**, *133*, (Ed.: G. Feinberg), B1549–B1562.
- [7] L. J. Dixon in QCD and beyond. Proceedings, Theoretical Advanced Study Institute in Elementary Particle Physics, TASI-95, Boulder, USA, June 4-30, 1995, **1996**, pp. 539–584, arXiv: [hep-ph/9601359](https://arxiv.org/abs/hep-ph/9601359) [[hep-ph](#)].
- [8] H. K. Dreiner, H. E. Haber, S. P. Martin, “Two-component spinor techniques and Feynman rules for quantum field theory and supersymmetry”, *Phys. Rept.* **2010**, *494*, 1–196, arXiv: [0812.1594](https://arxiv.org/abs/0812.1594) [[hep-ph](#)].
- [9] A. Ochirov, “Helicity amplitudes for QCD with massive quarks”, *JHEP* **2018**, *04*, 089, arXiv: [1802.06730](https://arxiv.org/abs/1802.06730) [[hep-ph](#)].
- [10] H. K. Dreiner, H. E. Haber, S. P. Martin, “Two-component spinor techniques and Feynman rules for quantum field theory and supersymmetry”, *Phys. Rept.* **2010**, *494*, 1–196, arXiv: [0812.1594](https://arxiv.org/abs/0812.1594) [[hep-ph](#)].
- [11] D. Tong, Lecture notes, University of Cambridge, UK, available at <https://www.damtp.cam.ac.uk/user/tong/qft/qft.pdf>, **2021**.
- [12] R. Ángeles-Martínez, J. R. Forshaw, M. H. Seymour, “Coulomb gluons and the ordering variable”, *JHEP* **2015**, *12*, 091, arXiv: [1510.07998](https://arxiv.org/abs/1510.07998) [[hep-ph](#)].
- [13] R. Ángeles Martínez, J. R. Forshaw, M. H. Seymour, “Ordering multiple soft gluon emissions”, *Phys. Rev. Lett.* **2016**, *116*, 212003, arXiv: [1602.00623](https://arxiv.org/abs/1602.00623) [[hep-ph](#)].
- [14] R. Ángeles Martínez, M. De Angelis, J. R. Forshaw, S. Plätzer, M. H. Seymour, “Soft gluon evolution and non-global logarithms”, *JHEP* **2018**, *05*, 044, arXiv: [1802.08531](https://arxiv.org/abs/1802.08531) [[hep-ph](#)].
- [15] J. R. Forshaw, A. Kyrieleis, M. H. Seymour, “Super-leading logarithms in non-global observables in QCD: Colour basis independent calculation”, *JHEP* **2008**, *09*, 128, arXiv: [0808.1269](https://arxiv.org/abs/0808.1269) [[hep-ph](#)].
- [16] W. Kilian, T. Ohl, J. Reuter, C. Speckner, “QCD in the Color-Flow Representation”, *JHEP* **2012**, *10*, 022, arXiv: [1206.3700](https://arxiv.org/abs/1206.3700) [[hep-ph](#)].
- [17] S. Keppeler, M. Sjö Dahl, “Hermitian Young Operators”, *J. Math. Phys.* **2014**, *55*, 021702, arXiv: [1307.6147](https://arxiv.org/abs/1307.6147) [[math-ph](#)].
- [18] J. Alcock-Zeilinger, H. Weigert, “A simple counting argument of the irreducible representations of $SU(N)$ on mixed product spaces”, *Journal of Algebraic Combinatorics* **2018**, *50*, 281–291.

- [19] S. Plätzer, “Summing Large- N Towers in Colour Flow Evolution”, *Eur. Phys. J.* **2014**, *C74*, 2907, arXiv: [1312.2448 \[hep-ph\]](#).
- [20] G. 't Hooft, “A Planar Diagram Theory for Strong Interactions”, *Nucl. Phys. B* **1974**, *72*, (Ed.: J. C. Taylor), 461.
- [21] A. Bassetto, M. Ciafaloni, G. Marchesini, “Jet Structure and Infrared Sensitive Quantities in Perturbative QCD”, *Phys. Rept.* **1983**, *100*, 201–272.
- [22] Z. Bern, V. Del Duca, W. B. Kilgore, C. R. Schmidt, “The infrared behavior of one loop QCD amplitudes at next-to-next-to leading order”, *Phys. Rev.* **1999**, *D60*, 116001, arXiv: [hep-ph/9903516 \[hep-ph\]](#).
- [23] G. Altarelli, G. Parisi, “Asymptotic freedom in parton language”, *Nuclear Physics B* **1977**, *126*, 298–318.
- [24] S. Catani, M. H. Seymour, “A General algorithm for calculating jet cross-sections in NLO QCD”, *Nucl. Phys.* **1997**, *B485*, [Erratum: *Nucl. Phys.*B510,503(1998)], 291–419, arXiv: [hep-ph/9605323 \[hep-ph\]](#).
- [25] Y. L. Dokshitzer, V. A. Khoze, A. H. Mueller, S. I. Troian, *Basics of perturbative QCD*, **1991**.
- [26] J. R. Forshaw, A. Kyrielleis, M. H. Seymour, “Gaps between jets in the high energy limit”, *JHEP* **2005**, *06*, 034, arXiv: [hep-ph/0502086](#).
- [27] Y. L. Dokshitzer, “Calculation of the Structure Functions for Deep Inelastic Scattering and e^+e^- Annihilation by Perturbation Theory in Quantum Chromodynamics.”, *Sov. Phys. JETP* **1977**, *46*, [Zh. Eksp. Teor. Fiz.73,1216(1977)], 641–653.
- [28] R. K. Ellis, W. J. Stirling, B. R. Webber, “QCD and collider physics”, *Camb. Monogr. Part. Phys. Nucl. Phys. Cosmol.* **1996**, *8*, 1–435.
- [29] Z. Nagy, D. E. Soper, “What is a parton shower?”, *Phys. Rev.* **2018**, *D98*, 014034, arXiv: [1705.08093 \[hep-ph\]](#).
- [30] S. Höche, D. Reichelt, “Numerical resummation at sub-leading color in the strongly ordered soft gluon limit”, **2020**, arXiv: [2001.11492 \[hep-ph\]](#).
- [31] F. J. Dyson, “Divergence of perturbation theory in quantum electrodynamics”, *Phys. Rev.* **1952**, *85*, 631–632.
- [32] T. Becher, M. D. Schwartz, “A precise determination of α_s from LEP thrust data using effective field theory”, *JHEP* **2008**, *07*, 034, arXiv: [0803.0342 \[hep-ph\]](#).
- [33] T. Becher, M. Neubert, “Infrared singularities of scattering amplitudes in perturbative QCD”, *Phys. Rev. Lett.* **2009**, *102*, [Erratum: *Phys.Rev.Lett.* 111, 199905 (2013)], 162001, arXiv: [0901.0722 \[hep-ph\]](#).
- [34] F. V. Tkachov, “Measuring multi - jet structure of hadronic energy flow or What is a jet?”, *Int. J. Mod. Phys. A* **1997**, *12*, 5411–5529, arXiv: [hep-ph/9601308](#).
- [35] D. M. Hofman, J. Maldacena, “Conformal collider physics: Energy and charge correlations”, *JHEP* **2008**, *05*, 012, arXiv: [0803.1467 \[hep-th\]](#).
- [36] H. Chen, I. Moulton, X. Zhang, H. X. Zhu, “Rethinking jets with energy correlators: Tracks, resummation, and analytic continuation”, *Phys. Rev. D* **2020**, *102*, 054012, arXiv: [2004.11381 \[hep-ph\]](#).

- [37] S. Catani, L. Trentadue, G. Turnock, B. Webber, “Resummation of large logarithms in e^+e^- event shape distributions”, *Nucl. Phys.* **1993**, *B407*, 3.
- [38] G. P. Korchemsky, G. F. Sterman, “Power corrections to event shapes and factorization”, *Nucl. Phys. B* **1999**, *555*, 335–351, arXiv: [hep-ph/9902341](#).
- [39] A. Banfi, G. P. Salam, G. Zanderighi, “Principles of general final-state resummation and automated implementation”, *JHEP* **2005**, *03*, 073, arXiv: [hep-ph/0407286 \[hep-ph\]](#).
- [40] A. Banfi, G. P. Salam, G. Zanderighi, “Phenomenology of event shapes at hadron colliders”, *JHEP* **2010**, *06*, 038, arXiv: [1001.4082 \[hep-ph\]](#).
- [41] A. Banfi, H. McAslan, P. F. Monni, G. Zanderighi, “A general method for the resummation of event-shape distributions in $e+e^-$ annihilation”, *JHEP* **2015**, *05*, 102, arXiv: [1412.2126 \[hep-ph\]](#).
- [42] G. P. Salam, “Towards Jetography”, *Eur. Phys. J. C* **2010**, *67*, 637–686, arXiv: [0906.1833 \[hep-ph\]](#).
- [43] J. C. Collins, D. E. Soper, “The Theorems of Perturbative QCD”, *Ann. Rev. Nucl. Part. Sci.* **1987**, *37*, 383–409.
- [44] J. C. Collins, D. E. Soper, G. F. Sterman, “Soft Gluons and Factorization”, *Nucl. Phys.* **1988**, *B308*, 833–856.
- [45] J. C. Collins, D. E. Soper, G. F. Sterman, “Factorization of Hard Processes in QCD”, *Adv. Ser. Direct. High Energy Phys.* **1989**, *5*, 1–91, arXiv: [hep-ph/0409313](#).
- [46] M. D. Schwartz, “Quantum Field Theory and the Standard Model”, *Cam. Press* **2014**.
- [47] M. E. Peskin, D. V. Schroeder, *An Introduction to quantum field theory*, Addison-Wesley, Reading, USA, **1995**.
- [48] M. Beneke, “Renormalons”, *Phys. Rept.* **1999**, *317*, 1–142, arXiv: [hep-ph/9807443](#).
- [49] B. R. Webber, “Monte Carlo Simulation of Hard Hadronic Processes”, *Ann. Rev. Nucl. Part. Sci.* **1986**, *36*, 253–286.
- [50] A. Grozin, J. M. Henn, G. P. Korchemsky, P. Marquard, “Three Loop Cusp Anomalous Dimension in QCD”, *Phys. Rev. Lett.* **2015**, *114*, 062006, arXiv: [1409.0023 \[hep-ph\]](#).
- [51] Y. Dokshitzer, D. Dyakonov, S. Troyan, “Hard processes in quantum chromodynamics”, *Physics Reports* **1980**, *58*, 269–395.
- [52] V. N. Gribov, L. N. Lipatov, “Deep inelastic $e p$ scattering in perturbation theory”, *Sov. J. Nucl. Phys.* **1972**, *15*, [Yad. Fiz.15,781(1972)], 438–450.
- [53] A. Banfi, G. P. Salam, G. Zanderighi, “Resummed event shapes at hadron - hadron colliders”, *JHEP* **2004**, *08*, 062, arXiv: [hep-ph/0407287 \[hep-ph\]](#).
- [54] G. Luisoni, S. Marzani, “QCD resummation for hadronic final states”, *J. Phys. G* **2015**, *42*, 103101, arXiv: [1505.04084 \[hep-ph\]](#).
- [55] Z. Nagy, D. E. Soper, “Parton showers with more exact color evolution”, **2019**, arXiv: [1902.02105 \[hep-ph\]](#).
- [56] M. D. Angelis, J. R. Forshaw, S. Plätzer, “Resummation and simulation of soft gluon effects beyond leading colour”, **2020**, arXiv: [2007.09648 \[hep-ph\]](#).

- [57] S. Gieseke, P. Stephens, B. Webber, “New formalism for QCD parton showers”, *JHEP* **2003**, *12*, 045, arXiv: [hep-ph/0310083](#) [hep-ph].
- [58] T. Sjöstrand, S. Ask, J. R. Christiansen, R. Corke, N. Desai, P. Ilten, S. Mrenna, S. Prestel, C. O. Rasmussen, P. Z. Skands, “An Introduction to PYTHIA 8.2”, *Comput. Phys. Commun.* **2015**, *191*, 159–177, arXiv: [1410.3012](#) [hep-ph].
- [59] S. Plätzer, S. Gieseke, “Dipole Showers and Automated NLO Matching in Herwig++”, *Eur. Phys. J.* **2012**, *C72*, 2187, arXiv: [1109.6256](#) [hep-ph].
- [60] F. Krauss, A. Schalicke, G. Soff, “APACIC++ 2.0: A Parton cascade in C++”, *Comput. Phys. Commun.* **2006**, *174*, 876–902, arXiv: [hep-ph/0503087](#) [hep-ph].
- [61] N. Fischer, S. Prestel, M. Ritzmann, P. Skands, “Vincia for Hadron Colliders”, *Eur. Phys. J.* **2016**, *C76*, 589, arXiv: [1605.06142](#) [hep-ph].
- [62] Z. Nagy, D. E. Soper, “Parton showers with quantum interference: Leading color, with spin”, *JHEP* **2008**, *07*, 025, arXiv: [0805.0216](#) [hep-ph].
- [63] M. Dasgupta, F. A. Dreyer, K. Hamilton, P. F. Monni, G. P. Salam, “Logarithmic accuracy of parton showers: a fixed-order study”, *JHEP* **2018**, *09*, 033, arXiv: [1805.09327](#) [hep-ph].

Chapter 4

Publication: Parton branching at amplitude level

“The world is indeed full of peril, and in it there are many dark places; but still there is much that is fair...”

— Haldir of Lórien, J.R.R. Tolkien, *The Fellowship of the Ring*

4.1 Preface

In this section we present work, by the author, on constructing an algorithm that evolves hard processes at the amplitude level by dressing them iteratively with (massless) quarks, gluons and loops. The algorithm is constructed by interleaving collinear emissions with soft emissions and includes Coulomb/Glauber exchanges. The work was published as a self contained research paper in 2019. After giving a small amount of background and motivation, we present the work in the form it was published.

The research paper builds on a large body of work developing algorithms for dressing hard processes with soft gluons [1–4]. Consequently, it jumps straight into the construction of the algorithm. We will now give an overview of the assumptions used in the paper and the prior work [1–4].

The primary assumption is that non-perturbative physics can be factorised from perturbative physics in the following form:

$$\int d\sigma_{\text{total}}(\mu) = \int d\sigma_{\text{partonic}}(\mu) \circ f(\mu) \left(1 + \mathcal{O} \left(\left(\frac{\Lambda_{\text{QCD}}}{\mu} \right)^p \right) \right), \quad (4.1)$$

where $\mu \gg \Lambda_{\text{QCD}}$ is a resolution scale above which physics can be considered perturbative in the high energy limit, and $f(\mu)$ is a function describing the non-perturbative physics (i.e. usually a product of parton distribution functions and/or fragmentation functions). ‘ \circ ’ represents a convolution over shared kinematics. The boundaries on the phase-space

integrals are process dependent, as is the positive constant p which parameterises the sensitivity of the process to non-perturbative physics at the scale μ . Maximising μ , given the constraints of the observable, minimises the effect of non-perturbative physics which is not adequately described by $f(\mu)$. For inclusive processes, colour singlet hard processes (i.e. e^+e^- and Drell-Yan), and deep inelastic scattering, this factorisation is a very rudimentary application of the factorisation theorems by Collins, Soper, and Sterman (CSS) [5, 6] where μ is typically taken to be the lowest scale relevant to the computation of the observable (see the factorised cross-sections given in Section 3.4.2). For more complex processes, such as proton-proton scattering producing QCD jets with an exclusive observable, it is an assumption that CSS factorisation holds in exclusive regions of phase-space [6, 7]. Whenever possible, we require that μ is less than or equal to a global inclusivity scale¹ for an observable. This requirement strengthens the validity of our use of CSS factorisation for complicated processes since it removes the need to assume factorisation in exclusive regions (as discussed in Section 3.4).

The algorithm we developed is for the computation of $d\sigma_{\text{partonic}}(\mu)$ (for which we now drop the subscript). Our next assumption is hard-process factorisation given a hard scale $Q \gg \mu$,

$$\int d\sigma(\mu) \approx \int d\Pi_{\text{born}}(\mu) \text{Tr}(E(Q, \mu, \{p; \mu\}_0, \{p; Q\}_0) \cdot \mathbf{H}(Q; \{p; Q\}_0)). \quad (4.2)$$

$\mathbf{H}(Q)$ is the hard process density matrix and E is an operator for dressing the hard process with IRC singular terms from QCD radiation at a scale much lower than Q . Non-singular terms ($\mathcal{O}(\mu^0/Q^0)$) from radiation have been dropped. The set $\{p; \mu\}_n$ is the set of hard process momenta, and the momenta of n lower scale partons dressing the hard process, as measured at a scale μ . The boundary condition $E(Q, Q) = 1$ is used and ‘.’ represents a convolution over the shared hard process momenta $\{p; Q\}_0$. Hard process factorisation has been proven for all inclusive QCD processes computed at leading-twist [8], and has been shown to hold at least at leading-log accuracy for generalised exclusive processes in inelastic collisions [9] (which is sufficient for our purposes). We can expand the partonic cross-section in parton multiplicity

$$\int d\sigma(\mu) = \int \sum_n d\sigma_n(\mu) \quad (4.3)$$

¹An inclusivity scale is a characteristic scale for a process (for instance an energy or k_t) below which, at a given logarithmic accuracy, all real radiation cancels completely against loops as per the KLN theorem (Section 3.1.2). The existence of an inclusivity scale is a requirement of infra-red safety. In principle an inclusivity scale can be arbitrarily small, however safety against uncontrolled non-perturbative physics requires that the scale be much greater than Λ_{QCD} . Continuously global event shape observables typically have inclusivity scales proportional to the hard process scale whilst exclusive processes typically have an inclusivity scale proportional to a scale determining acceptance into exclusive regions (see Chp. 8 for more details).

and from this define

$$d\sigma_n = d\Pi_{\text{born}}(\mu) \text{Tr}(E_n(Q, \mu) \cdot \mathbf{H}(Q)) = d\Pi_{\text{born}}(\mu) \text{Tr} \left(\mathbf{E}_n(Q, \mu) \mathbf{H}(Q) \mathbf{E}_n^\dagger(Q, \mu) \right), \quad (4.4)$$

and

$$\mathbf{E}_n(Q, \mu) \mathbf{H}(Q; \{p; Q\}_0) \mathbf{E}_n^\dagger(Q, \mu) = \mathbf{A}_n(\mu; \{p; \mu\}_n) \prod_{i=1}^n d\Pi_i, \quad (4.5)$$

where $\mathbf{A}_0(Q; \{p\}_0) = \mathbf{H}(Q)$. This re-arrangement and set of definitions have been introduced so that we can work with amplitude density matrices $\mathbf{A}_n \equiv |M_n\rangle \langle M_n|$ which have computable perturbative expansions (the limits of the matrix elements computed in Section 3.3).

We wish to find an evolution equation for $\mathbf{A}_n(\mu; \{p\}_n)$. For two reasons, we are well motivated to believe the evolution of $\mathbf{A}_n(\mu; \{p\}_n)$ under the variation of the scale, μ , should be Markovian. Firstly the repeated application of hard process factorisation, separating lower scale radiation from higher scale, generates a Markov series: i.e.²

$$E(Q, \mu, \{p; \mu\}_0, \{p; Q\}_0) \mapsto E(Q_1, \mu, \{p; \mu\}_0, \{p; Q_1\}_0) \cdot E(Q, Q_1, \{p; Q_1\}_0, \{p; Q\}_0). \quad (4.6)$$

Secondly, renormalisation group equations are Markovian and $E(Q, \mu)$ has the form of a renormalisation group operator on $\mathbf{H}(Q)$ (see Section 3.4). Therefore, assuming a Markovian evolution equation for the variation of $\mathbf{A}_n(\mu; \{p\}_n)$ as μ decreases gives the following ansatz:

$$\begin{aligned} \mu \frac{\partial \mathbf{A}_n(\mu; \{p\}_n)}{\partial \mu} = & \Gamma_n(\mu) \mathbf{A}_n(\mu; \{p\}_n) + \mathbf{A}_n(\mu; \{p\}_n) \Gamma_n^\dagger(\mu) \\ & - \sum_{i=1}^n \int dR_n^i \mathbf{D}_n^i(\mu_n) \mathbf{A}_{n-i}(\mu_n; \{p\}_{n-i}) \mathbf{D}_n^{i\dagger}(\mu_n) \mu \delta(\mu - \mu_n). \end{aligned} \quad (4.7)$$

$\mathbf{D}_n^i(\mu_n)$ is an operator for dressing $\mathbf{A}_{n-i}(\mu_n; \{p\}_{n-i})$ with i lower scale partons. $\Gamma_n(\mu)$ is an anomalous dimension matrix: it acts as a ‘non-emission operator’ which dresses $\mathbf{A}_n(\mu; \{p\}_n)$ with loops at the scale μ . Integration over the measure dR_n^i handles momentum conservation. In the limit $\mu/Q \ll 1$, fixed order calculations motivate the correct resolution scale for the ansatz being a carefully chosen transverse momentum, q_\perp [1, 3, 10]. The detailed definition of q_\perp is discussed in the paper.

Expanding the operators to first order in α_s gives

$$\begin{aligned} q_\perp \frac{\partial \mathbf{A}_n(q_\perp; \{p\}_n)}{\partial q_\perp} = & \Gamma_n^{(0)}(q_\perp) \mathbf{A}_n(q_\perp; \{p\}_n) + \mathbf{A}_n(q_\perp; \{p\}_n) \Gamma_n^{(0)\dagger}(q_\perp) \\ & - \int dR_n^{1(0)} \mathbf{D}_n^{1(0)}(q_{n\perp}) \mathbf{A}_{n-1}(q_{n\perp}; \{p\}_{n-1}) \mathbf{D}_n^{1(0)\dagger}(q_{n\perp}) q_\perp \delta(q_\perp - q_{n\perp}). \end{aligned} \quad (4.8)$$

²The following equation is schematic and is abusing the trace in Eq. (4.2) to simplify matters. Each E should be separated into an operator acting to the left and an operator acting to the right of the hard process, just as in Eq. (4.4).

The operators on the RHS are computable from Feynman amplitudes by studying the $\mathcal{O}(\alpha_s)$ corrections to n -parton amplitudes which are singular in the limit $q_\perp/Q \rightarrow 0$, giving the leading power expansion of the operators (again see Section 3.3). The limit $q_\perp/Q \rightarrow 0$ exposes both soft and collinear poles. Therefore the operators describe the emission of real and virtual, soft and collinear partons.

Throughout the rest of this thesis we drop the upper indices and always work with the first-order, leading-power operators. The evolution equation is solved by the Markov series

$$\mathbf{A}_n(q_\perp; \{p\}_n) = \int dR_n \mathbf{V}_{q_\perp, q_{n\perp}} \mathbf{D}_n \mathbf{A}_{n-1}(q_{n\perp}; \{p\}_{n-1}) \mathbf{D}_n^\dagger \mathbf{V}_{q_\perp, q_{n\perp}}^\dagger \Theta(q_\perp \leq q_{n\perp}), \quad (4.9)$$

where $\mathbf{V}_{a,b}$ evolves a state $\mathbf{A}_n(b; \{p\}_n)$ to a state at a lower scale $\mathbf{A}_n(a; \{p\}_n)$. It is an amplitude level Sudakov factor, defined as

$$\mathbf{V}_{a,b} = \text{Pexp} \left(- \int_a^b \frac{dq_\perp}{q_\perp} \mathbf{\Gamma}_n(q_\perp) \right). \quad (4.10)$$

It is in this form that we present the Parton Branching algorithm in the following paper.³

A comment on context and the current ‘state of the art’

The following paper was originally published in 2019 and this thesis is now being written in 2021. The field has progressed significantly since 2019 and several questions discussed in the paper, which were unanswered, have now been answered. Most notably, since 2019 there has been extended discussions in the literature on how to achieve NLL accuracy in parton shower algorithms [11–13] and successful implementations have been demonstrated for e^+e^- hard processes [12, 14]. Small amendments have been made to what follows so as to make discussions consistent with the most recent literature in 2021.

References

- [1] J. R. Forshaw, A. Kyrieleis, M. H. Seymour, “Super-leading logarithms in non-global observables in QCD: Colour basis independent calculation”, *JHEP* **2008**, 09, 128, arXiv: [0808.1269](#) [[hep-ph](#)].
- [2] J. R. Forshaw, M. H. Seymour, A. Siódmok, “On the Breaking of Collinear Factorization in QCD”, *JHEP* **2012**, 11, 066, arXiv: [1206.6363](#) [[hep-ph](#)].
- [3] R. Ángeles-Martínez, J. R. Forshaw, M. H. Seymour, “Coulomb gluons and the ordering variable”, *JHEP* **2015**, 12, 091, arXiv: [1510.07998](#) [[hep-ph](#)].
- [4] R. Ángeles Martínez, M. De Angelis, J. R. Forshaw, S. Plätzer, M. H. Seymour, “Soft gluon evolution and non-global logarithms”, *JHEP* **2018**, 05, 044, arXiv: [1802.08531](#) [[hep-ph](#)].

³In the following publication we pull apart dR_n into the product of a Lorentz invariant measure $\prod_{i=1}^{n_H+1} d^4 p_i$ and recoil functions absorbed into the definition of \mathbf{D}_n .

- [5] J. C. Collins, D. E. Soper, “The Theorems of Perturbative QCD”, *Ann. Rev. Nucl. Part. Sci.* **1987**, *37*, 383–409.
- [6] J. C. Collins, D. E. Soper, G. F. Sterman, “Soft Gluons and Factorization”, *Nucl. Phys.* **1988**, *B308*, 833–856.
- [7] J. R. Forshaw, A. Kyrieleis, M. H. Seymour, “Super-leading logarithms in non-global observables in QCD”, *JHEP* **2006**, *08*, 059, arXiv: [hep-ph/0604094](#) [[hep-ph](#)].
- [8] J. C. Collins, D. E. Soper, G. F. Sterman, “Factorization of Hard Processes in QCD”, *Adv. Ser. Direct. High Energy Phys.* **1989**, *5*, 1–91, arXiv: [hep-ph/0409313](#).
- [9] B. R. Webber, “Monte Carlo Simulation of Hard Hadronic Processes”, *Ann. Rev. Nucl. Part. Sci.* **1986**, *36*, 253–286.
- [10] R. Ángeles Martínez, J. R. Forshaw, M. H. Seymour, “Ordering multiple soft gluon emissions”, *Phys. Rev. Lett.* **2016**, *116*, 212003, arXiv: [1602.00623](#) [[hep-ph](#)].
- [11] G. Bewick, S. Ferrario Ravasio, P. Richardson, M. H. Seymour, “Logarithmic Accuracy of Angular-Ordered Parton Showers”, **2019**, arXiv: [1904.11866](#) [[hep-ph](#)].
- [12] M. Dasgupta, F. A. Dreyer, K. Hamilton, P. F. Monni, G. P. Salam, G. Soyez, “Parton showers beyond leading logarithmic accuracy”, **2020**, arXiv: [2002.11114](#) [[hep-ph](#)].
- [13] J. R. Forshaw, J. Holguin, S. Plätzer, “Building a consistent parton shower”, *JHEP* **2020**, *09*, 014, arXiv: [2003.06400](#) [[hep-ph](#)].
- [14] K. Hamilton, R. Medves, G. P. Salam, L. Scyboz, G. Soyez, “Colour and logarithmic accuracy in final-state parton showers”, **2020**, arXiv: [2011.10054](#) [[hep-ph](#)].
- [15] D. Binosi, L. Theussl, “JaxoDraw: A Graphical user interface for drawing Feynman diagrams”, *Comput. Phys. Commun.* **2004**, *161*, 76–86, arXiv: [hep-ph/0309015](#) [[hep-ph](#)].

Declaration

The subsequent work is mine and my collaborators. It is without plagiarism. Specifically, every section in the paper (withholding Section 4.3.3) is my own research. Section 4.3.3 is the work of Dr. Simon Plätzer later amended by myself and Prof. Jeff Forshaw.

This work has received funding from the UK Science and Technology Facilities Council (grant no. ST/P000800/1), the European Union's Horizon 2020 research and innovation programme as part of the Marie Skłodowska-Curie Innovative Training Network MCnetITN3 (grant agreement no. 722104). JRF thanks the Institute for Particle Physics Phenomenology in Durham for the award of an Associateship and the Particle Physics Group of the University of Vienna for financial support and kind hospitality. JH thanks the UK Science and Technology Facilities Council for the award of a studentship. SP acknowledges partial support by the COST actions CA16201 PARTICLEFACE and CA16108 VBSCAN. We would like to thank Matthew De Angelis for extensive discussions. We would also like to thank Mrinal Dasgupta, Jack Helliwell and Mike Seymour for helpful discussions and comments on the manuscript. Figures have been prepared using JaxoDraw [15].

Parton Branching at amplitude level

Authors: Jack Holguin, Jeffrey R. Forshaw, Simon Plätzer

Abstract

We present an algorithm that evolves hard processes at the amplitude level by dressing them iteratively with (massless) quarks and gluons. The algorithm interleaves collinear emissions with soft emissions and includes Coulomb/Glauber exchanges. It includes all orders in N_c , is spin dependent and is able to accommodate kinematic recoils. Although it is specified at leading logarithmic accuracy, the framework should be sufficient to go beyond. Coulomb exchanges make the factorisation of collinear and soft emissions highly non-trivial. In the absence of Coulomb exchanges, we show how factorisation works out and how a partial factorisation is manifest in the presence of Coulomb exchanges. Finally, we illustrate the use of the algorithm by deriving DGLAP evolution and computing the resummed thrust, hemisphere jet mass and gaps-between-jets distributions in e^+e^- .

4.2 Introduction

Modern day experimental particle physics is often performed at hadron colliders. As an unavoidable consequence, QCD corrections play a large role. Contributions from coloured radiation, when evaluated Feynman diagrammatically, diverge at multiple points in the phase space. When regularised and cancelled, the divergences may leave behind large logarithms. The accurate inclusion of logarithmically enhanced corrections is of importance to both the theoretical and experimental communities. Historically there have been two main approaches to dealing with QCD radiative corrections: resummations and parton showers.

Resummations look to re-organise the perturbative expansion by classifying the large logarithms and then summing the perturbation series such that the most dominant logarithmically enhanced terms are included. Towers of logarithms may be further simplified by making the leading colour (LC) approximation. The re-organised expansions are referred to by their logarithmic accuracy; leading log (LL), next-to-leading log (NLL), etc. This

procedure has recently been further formalised by work in soft-collinear effective field theories [1–4]. From this perspective, resummations are renormalisation group flows that evolve ‘safe’ perturbative predictions into regions of phase space where perturbative expansions would be otherwise ‘unsafe’.

In contrast, parton showers may be thought of as providing an all-purpose approximation to the resummation procedure. Modern parton showers generate an evolving, classical system of partons whilst cleverly encoding quantum interference effects (made possible by working in the LC approximation). The majority of currently available parton showers claim LL accuracy using the LC approximation [5–11]. The quest to better understand the data from the LHC is a major driver for increasingly precise parton showers. At present, there is a growing list of phenomena that parton showers do not encapsulate. This includes effects sub-leading in colour, Coulomb/Glauber exchanges, super-leading logarithms [12–14] and the violation of QCD coherence (or collinear factorisation) [15, 16]. Moreover, recent fixed-order studies have cast further doubt on the accuracy of modern parton showers. It has been shown in [17] that the PYTHIA [10, 11] and DIRE [8] showers suffer from both incorrect next-to-leading logarithms at leading colour and incorrect contributions from sub-leading colour (NLC) at LL. Although these showers never claim NLL or NLC accuracy, the findings of Dasgupta et al questions the fruitfulness of attempts to extend conventional parton showers beyond LL and LC in general.⁴ In recent years, there has been movement towards finding new constructions for partons showers; constructions more suited to including NLC or NLL corrections [9, 21–28]. However, as of yet, success has been limited.

The algorithm we present here aims to provide a framework for the development of future parton showers, enabling them to be systematically improved. We hope it will also help make more rigorous the link between resummations and parton showers. Our starting point is the soft-gluon evolution algorithm explored in [27], which we refer to as the FKS algorithm. The evolution generated by the FKS algorithm is systematic to all orders in colour and it accounts for the leading soft logarithms. The FKS algorithm was originally used to derive the super-leading logarithms that may occur in hadron-hadron collisions [12, 13]. It has been analytically verified for a general hard process dressed with up to two soft real emissions and one loop [29, 30]. It has also been shown to generate the BMS equation [31] (it presumably also includes the NLC corrections to it) and it correctly accounts for the leading non-global logarithms for various observables [27]. The main goal of this paper is to improve the FKS algorithm by including collinear emissions, spin dependence and kinematic

⁴As of 2021, multiple conventional parton showers have been proposed which correctly resum LC NLLs for observables with colour singlet hard processes [18, 19] and progress has been made towards implementing sub-leading colour for global observables into parton showers [20]. However, extending this accuracy to proton-proton hard processes remains elusive.

recoil. The algorithm we present is Markovian and can be solved iteratively, making it well suited for use as a parton shower.

The remainder of the paper is organised as follows. In the next section, we introduce the algorithm in a form we refer to as variant A, in which we interleave soft and collinear emissions. Variant A has the virtue of being a simple extension of the FKS algorithm, though it suffers from unnecessarily complex colour evolution in the soft-collinear sector. It also suffers from the fact that we cannot uniquely identify a parent parton in the case of soft-gluon emission, which complicates the issue of longitudinal momentum conservation. We are thus motivated to re-cast the algorithm in a more convenient form, which we refer to as variant B. Specifically, in variant B we manipulate the colour structures of variant A to isolate the full collinear splitting functions, after which we are able to implement longitudinal momentum conservation in a simple way. We also spend some time illustrating how recoils may be included in both variants, though this will only be relevant beyond the LL approximation. As it stands, either variant A or B could be used to create a fully functioning parton shower, though B will be computationally more efficient. In Section 4.3.5 we present a manifestly infra-red finite version of the algorithm. This reformulation is particularly useful for the resummation of specific observables, though it is not so well suited for use as a general purpose parton shower. This is because the infra-red singularities are regularised by the explicit inclusion (and exponentiation) of a measurement function.

The second half of the paper is devoted to issues of collinear factorisation and to providing examples to illustrate how the algorithm is used. In Section 4.4 we discuss the factorisation of collinear physics from soft physics. We start by considering the case when Coulomb/Glauber exchanges are turned off (such as would be the case in e^+e^- collisions). After this we discuss how Coulomb exchanges can be introduced one-by-one. We will see that collinear factorisation occurs below the scale of the last Coulomb exchange. This discussion shows consistency between our approach and the proofs of collinear factorisation by Collins, Soper and Sterman [32, 33]. After this, we show how DGLAP evolution for the parton distribution functions emerges [34–36]. We finish the paper by illustrating the use of the algorithm; by calculating the thrust, hemisphere jet mass, and gaps-between-jets distributions in e^+e^- . We leave an extensive discussion of spin correlations to an appendix.

4.3 The algorithm

In this section we present the algorithm. It is Markovian and interleaves soft emissions and virtual corrections with collinear emissions and virtual corrections, see Figure 4.1. Successive real emissions are strongly ordered in an appropriately defined transverse momentum. We will present two variants of the algorithm, which we refer to as A and B. The two differ

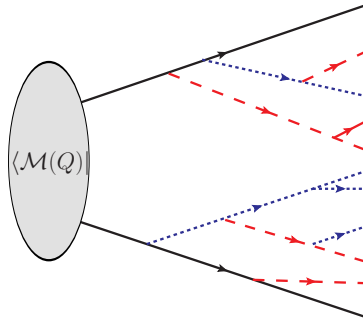


Figure 4.1: A term contributing to evolution of the conjugate amplitude (it contributes to \mathbf{A}_9). Red dashed lines represent the emission of soft gluons and collinear partons are represented by blue dotted lines. Loops (Sudakov factors) have been neglected to avoid clutter. We draw all particles heading to the right, away from the hard process, including incoming particles. In contrast, evolution of the amplitude will have all particles drawn heading to the left and away from the hard process.

only in where we put the soft-collinear emissions: in A they are in the soft sector and in B they are in the collinear sector. The second approach allows us to exploit the colour-diagonal nature of collinear emissions and it makes kinematic recoil more straightforward to implement. Variant A has the virtue that it is an almost trivial extension of the purely soft evolution presented in [27]. We present both A and B with the momentum mappings after each real emission parametrised into two initially unspecified functions. This is so the algorithm is able to accommodate partonic recoil. Later, in Section 4.3.4, we discuss specific examples of recoil in action. For processes with coloured incoming partons, the algorithm should be convoluted with parton distributions functions. We leave a full description of how to do this to Section 4.5.

Before plunging in, we should explain the theoretical basis for what follows. Our algorithm is based on Feynman diagram calculations [13, 27, 29, 34, 37–39] and, in its present form, captures all of the logarithms associated with the leading amplitude-level singularities. It uses a fixed coupling as effects from the running coupling are considered beyond the scope of this paper. Therefore the algorithm captures leading logarithms from wide-angle soft emissions, hard-collinear emissions and simultaneously soft and collinear emissions. This means the algorithm is guaranteed to capture only the most leading logarithms in the expansion of the cross-section (LL_Σ) to any observable. That said, it is also able to capture the leading single non-global logarithms, even if the global part is double-logarithmic, as is the case with the hemisphere jet mass for example (see Section 4.5). For any process involving incoming hadrons or measured outgoing hadrons, the single logarithms from DGLAP evolution are recovered as well (i.e. parton distribution function and by a simple extension fragmentation function evolution). Correctly capturing these logarithms requires the inclu-

sion of kinematic recoil into the algorithm, which is typically considered sub-leading for the computation of LLs. We believe our framework to be sufficiently flexible that we can, in the future, extend it beyond the LL_Σ approximation. The algorithm is fully differential in parton kinematics making the extension to a running coupling simple and we have set up the algorithm so that the complete conservation of momentum can be simply implemented.

4.3.1 Parton branching with interleaved soft and collinear evolution (A)

The algorithm evolves a hard-scattering matrix, $\mathbf{H}(Q; \{p\})$, which is defined at some hard scale Q and is a function of the hard-particle four-momenta, $\{p\}$. It does so by dressing with successive soft and/or collinear real emissions and virtual corrections. $\mathbf{H}(Q; \{p\})$ is a tensor in the product space of colour and helicity⁵, defined as $\mathbf{H}(Q; \{p\}) \equiv (|\text{colour}\rangle \otimes |\text{spin}\rangle) \otimes (\langle \text{colour}| \otimes \langle \text{spin}|)$. The hard-scattering matrix is defined so that $\text{Tr} \mathbf{H}(Q; \{p\})$ is the hard matrix element squared, summed over colour and spin⁶. Successive real emissions are added via ‘rectangular’ operators, which act as a map increasing the dimension of the representation of $SU(3) \times E(2)$ in which $\mathbf{H}(Q; \{p\})$ resides. The virtual evolution operators are ‘square’ and preserve the representation of $\mathbf{H}(Q; \{p\})$. Specifically,

$$\begin{aligned} d\sigma_0 &= \text{Tr} \left(\mathbf{V}_{\mu, Q} \mathbf{H}(Q; \{p\}) \mathbf{V}_{\mu, Q}^\dagger \right) = \text{Tr} \mathbf{A}_0(\mu; \{p\}), \\ d\sigma_1 &= \int \prod_{i=1}^{n_H+1} d^4 p_i \text{Tr} \left(\mathbf{V}_{\mu, q_{1\perp}} \mathbf{D}_1 \mathbf{V}_{q_{1\perp}, Q} \mathbf{H}(Q; \{p\}) \mathbf{V}_{q_{1\perp}, Q}^\dagger \mathbf{D}_1^\dagger \mathbf{V}_{\mu, q_{1\perp}}^\dagger \right) d\Pi_1 \\ &= \text{Tr} \mathbf{A}_1(\mu; \{\tilde{p}\} \cup q_1) d\Pi_1, \\ d\sigma_n &= \text{Tr} \mathbf{A}_n(\mu; \{p\}_n) \prod_{i=1}^n d\Pi_i, \end{aligned} \quad (4.11)$$

where

$$\mathbf{A}_n(q_\perp; \{\tilde{p}\}_{n-1} \cup q_n) = \int \prod_{i=1}^{n_H+n} d^4 p_i \mathbf{V}_{q_\perp, q_{n\perp}} \mathbf{D}_n \mathbf{A}_{n-1}(q_{n\perp}; \{p\}_{n-1}) \mathbf{D}_n^\dagger \mathbf{V}_{q_\perp, q_{n\perp}}^\dagger \Theta(q_\perp \leq q_{n\perp}). \quad (4.12)$$

At each step, the emission operators (\mathbf{D}_n) add one new particle, of four-momentum q_n , to the set $\{p\}_{n-1}$, to produce the set $\{p\}_n$. We use $p_j \in \{p\}_n = \{P_1, P_2, \dots, P_{n_H}, q_1, \dots, q_n\}$ to denote the momentum of the j^{th} parton and $1 < j < n_H + n$, where n_H is the number of partons associated with the original hard process and n is the number of emitted partons. Hidden in the emission operators is a map from $\{p\}_{n-1}$ to a new set, $\{\tilde{p}\}_{n-1}$. The difference between these two sets is determined by the way we implement energy-momentum conservation (i.e. the recoil prescription) and it is why there is an extra integral over p_i (it is not

⁵This paper only concerns itself with massless partons and so all particles have a definite helicity.

⁶We may also choose to include averaging factors, a flux factor and the hard process phase-space, so that it is then the hard-process differential cross section.

a phase-space integral). The virtual evolution operators $\mathbf{V}_{a,b}$ encode the loop corrections. To avoid cumbersome notation we write $\{p\}_n = \{\tilde{p}\}_{n-1} \cup \{q_n\}$ is the set of n momenta including the last emission, q_n . We have not yet defined the ordering variable, $q_{i\perp}$; we will do that shortly. A generalised observable Σ , with measurement function $u_n(q_1, \dots, q_n)$, is then given by⁷

$$\begin{aligned}\Sigma(\mu) &= \int \sum_n d\sigma_n u_n(q_1, \dots, q_n), \\ &= \int \sum_n \left(\prod_{i=1}^n d\Pi_i \right) \text{Tr} \mathbf{A}_n(\mu; \{p\}_n) u_n(q_1, \dots, q_n),\end{aligned}\quad (4.13)$$

where $d\Pi_i$ is the phase-space for the i^{th} emission (see below). μ should be taken either to 0 or to the scale below which the observable is inclusive over all radiation. The virtual (Sudakov) evolution operator is⁸

$$\begin{aligned}\mathbf{V}_{a,b} = & \text{Pexp} \left[-\frac{\alpha_s}{\pi} \sum_{i < j} \int_a^b \frac{dk_{\perp}^{(ij)}}{k_{\perp}^{(ij)}} (-\mathbb{T}_i^g \cdot \mathbb{T}_j^g) \left\{ \int \frac{dy d\phi}{4\pi} (k_{\perp}^{(ij)})^2 \frac{\tilde{p}_i \cdot \tilde{p}_j}{(\tilde{p}_i \cdot k)(\tilde{p}_j \cdot k)} \theta_{ij}(k) - i\pi \tilde{\delta}_{ij} \right\} \right. \\ & \left. \times \mathcal{R}_{ij}^{\text{soft}}(k, \{\tilde{p}\}) - \frac{\alpha_s}{\pi} \sum_i \int_a^b \frac{dk_{\perp}^{(i\bar{n})}}{k_{\perp}^{(i\bar{n})}} \sum_{v \in \{q,g\}} \mathbb{T}_i^{\bar{v}2} \int \frac{dz d\phi}{8\pi} \overline{\mathcal{P}}_{vv_i}^{\circ}(z) \theta_i(k) \mathcal{R}_i^{\text{coll}}(k, \{\tilde{p}\}) \right],\end{aligned}\quad (4.14)$$

where i and j run over all external legs (those from the initial hard process and also previous emissions in the evolution). $\tilde{\delta}_{ij} = 1$ if both partons i, j are incoming or both outgoing and $\tilde{\delta}_{ij} = 0$ otherwise. $\theta_{ij}(k) = \Theta(p_i \cdot p_j - k \cdot (p_j + p_i))$ and ensures that the phase space of the integration corresponds to that of a real gluon. Likewise, the z integral is over the range⁹

$$z \in \left[\frac{\alpha}{2} - \frac{1}{2} \sqrt{\alpha^2 - \frac{4k_{\perp}^{(i\bar{n})2}}{(n \cdot p)^2}}, \frac{\alpha}{2} + \frac{1}{2} \sqrt{\alpha^2 - \frac{4k_{\perp}^{(i\bar{n})2}}{(n \cdot p)^2}} \right], \quad \alpha = \frac{2p \cdot p_i + p_i \cdot n p \cdot n}{(p \cdot n)^2}, \quad (4.15)$$

which can be expressed via a single theta function

$$\theta_i(k) = \Theta((n \cdot p_i - n \cdot k)n \cdot p + 2p \cdot p_i - 2p \cdot k).$$

The vectors p and $n = (1, \vec{n})$ will be defined shortly: to LL $_{\Sigma}$ accuracy $p = p_i$ and $\alpha = 1$. $v_i, v \in \{q, g\}$ label parton species. $\bar{v} = g$ in all cases except when $v_i = g$ and $v = q$, then $\bar{v} = q$. $\overline{\mathcal{P}}_{vv_i}^{\circ}$ is the $v_i \rightarrow v$ hard-collinear splitting function and it is defined in Appendix 4.7 along with the conventions we use for helicity states and antiparticles.

⁷For fixed Born-level kinematics. Generally the measurement function will depend upon the hard process momenta P_j , which we do not show explicitly.

⁸The path ordering ensures that the operators are ordered in $k_{\perp}^{(ij)}$ with the largest to the right.

⁹We specify the range corresponding to emission off a final state particle, for emission off an initial state particle exchange $p_i \rightarrow \tilde{p}_i$.

$\mathcal{R}_{ij}^{\text{soft}}(k, \{p\})$ and $\mathcal{R}_i^{\text{coll}}(k, \{p\})$ are concerned with the recoil prescription and are included to preserve unitarity, they are defined in (4.21) and (4.22) below. $k_{\perp}^{(ij)}$ and y are the transverse momentum and rapidity in the ij zero-momentum frame. To make the (unitarity) link to the real emissions more explicit, we choose not to use the substitution

$$(k_{\perp}^{(ij)})^2 \frac{\tilde{p}_i \cdot \tilde{p}_j}{(\tilde{p}_i \cdot k)(\tilde{p}_j \cdot k)} = 2. \quad (4.16)$$

The real-emission operator is built using two operators:

$$\begin{aligned} \mathbf{S}_i &= \sum_j \left(\frac{q_{i\perp}^{(j\vec{m})}}{2\tilde{p}_j \cdot q_i} \mathbb{T}_j^g \otimes (\tilde{p}_j \cdot \epsilon_+^*(q_i) \mathbb{S}^{1_i} + \tilde{p}_j \cdot \epsilon_-^*(q_i) \mathbb{S}^{-1_i}) \right) \mathfrak{R}_{ij}^{\text{soft}}(\{p\}, \{\tilde{p}\}, q_i), \\ \mathbf{C}_i &= \sum_j \frac{q_{i\perp}^{(j\vec{m})}}{2\sqrt{z_i}} \Delta_{ij} \bar{\mathbf{P}}_{ij} \mathfrak{R}_{ij}^{\text{coll}}(\{p\}, \{\tilde{p}\}, q_i), \end{aligned} \quad (4.17)$$

such that \mathbf{D}_i acts as

$$\dots \mathbf{D}_i \mathcal{O} \mathbf{D}_i^\dagger \dots = \dots \mathbf{S}_i \mathcal{O} \mathbf{S}_i^\dagger \dots + \dots \mathbf{C}_i \mathcal{O} \mathbf{C}_i^\dagger \dots \quad (4.18)$$

j again runs over all external legs and i labels the emitted parton. \mathbf{S}_i generates soft emissions and \mathbf{C}_i hard-collinear emissions. The symbol Δ_{ij} is defined so that $\Delta_{ij} \Delta_{ik} = \delta_{jk}$ and δ_j^{final} ($\delta_j^{\text{initial}}$) is unity when parton j is in the final (initial) state and zero otherwise. $\bar{\mathbf{P}}_{ij}$ are the amplitude-level hard-collinear splitting functions and are defined in Appendix 4.7. The splitting functions encode DGLAP evolution [34–36] including the spin-dependence. \mathbb{T}_i^g is a basis independent colour charge operator. We have indexed each \mathbb{T}_i^g with the leg on which it acts, i , and by whether it corresponds to the emission of a gluon or not (i.e. the index g refers to a $g \rightarrow q\bar{q}$ splitting). \mathbb{S}^{s_i} updates the helicity state by adding the helicity of the emitted parton, s_i . The operators \mathbb{S} and \mathbb{T} are also defined in Appendix 4.7.

In the soft sector we have introduced an auxiliary vector \vec{m} . It is uniquely determined, but only at cross-section level, since we require $q_{\perp}^{(i\vec{m})} q_{\perp}^{(j\vec{m}')} |_{p_i \neq p_j} = (q_{\perp}^{(ij)})^2$, which corresponds to choosing \vec{m} to lie in the direction of j and \vec{m}' (the corresponding vector in the conjugate amplitude) in the direction of i . It is only ever this combination that appears at cross-section level. In the collinear sector, the momentum fraction z_i is defined by (see Figure 4.2):

$$\begin{aligned} z_i &= \frac{\tilde{p}_j \cdot n}{p \cdot n} \quad \text{for final-state emissions} \\ \text{and} \quad z_i &= \frac{p_j \cdot n}{p \cdot n} \quad \text{for initial-state emissions,} \end{aligned} \quad (4.19)$$

where the light-like four-vector n satisfies $n \cdot q_{i\perp}^{(j\vec{m})} = 0$. The light-like four-vector p satisfies $p \cdot q_{i\perp}^{(j\vec{m})} = 0$. Neglecting terms suppressed by the transverse momentum of the emission

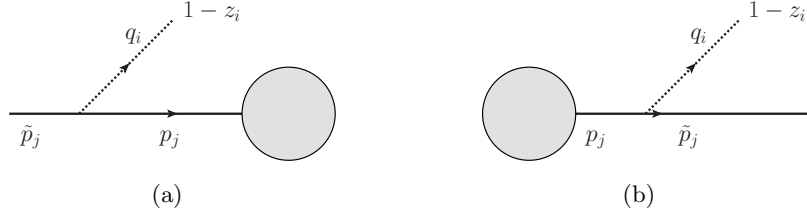


Figure 4.2: Defining the kinematics: (a) q_i is emitted off an incoming leg; (b) q_i is emitted off an outgoing leg.

(which is permissible in the LL_Σ approximation) we may take $p = p_j$ for final-state emissions and $p = \tilde{p}_j$ for initial-state emissions, in which case z_i is the light-cone momentum fraction. The precise definition of p is dependent on the recoil prescription, as we illustrate in Section 4.3.4.

Now we can define the ordering variable, i.e. the definition of a and b in the Sudakov operator $\mathbf{V}_{a,b}$. We use transverse momentum ordering, where the transverse momentum should be defined by the parent partons of the emitted parton. Doing this means that we really ought not to sum over partons in (4.17) and we should replace (4.12) by

$$\mathbf{A}_n = \sum_{j_n, j'_n} \int \prod_{i=1}^{n_{\text{H}}+n} d^4 p_i \mathbf{V}_{q_\perp, q_{n\perp}} \mathbf{D}_n^{j_n} \mathbf{A}_{n-1} \mathbf{D}_n^{j'_n \dagger} \mathbf{V}_{q_\perp, q_{n\perp}}^\dagger \Theta(q_\perp \leq q_{n\perp}) \quad (4.20)$$

where $\mathbf{D}_n^{j_n}$ is defined by

$$\mathbf{D}_n = \sum_{j_n} \mathbf{D}_n^{j_n} .$$

The ordering variable is then $q_{n\perp} = q_n^{(j_n, j'_n)}$ if the emission is soft or $q_{n\perp} = q_n^{(j_n, \vec{n})}$ if the emission is collinear. At LL_Σ , this choice of ordering variable is somewhat arbitrary but being a transverse momentum it is able to generate the super-leading logarithms correctly [29]. That said, it is not equivalent to the ordering indicated by the results in [29, 30], which is based on fixed-order Feynman diagram calculations. We have not yet figured out a way to implement the latter ordering to all orders. In the remainder of the paper, we will use the simpler (though potentially misleading) notation of equation (4.12).

The recoil functions, $\mathfrak{R}_{ij}^{\text{soft}*} \mathfrak{R}_{ij'}^{\text{soft}}$ and $\mathfrak{R}_{ij}^{\text{coll}*} \mathfrak{R}_{ij'}^{\text{coll}}$, encode the maps that implement energy-momentum conservation. As the algorithm proceeds, each $\mathfrak{R}_{ij}^{\text{soft}}$ and $\mathfrak{R}_{ij}^{\text{coll}}$ will always collect into the pairs just given. The functions only ever appear singularly to aid book keeping¹⁰. The recoil functions should be constructed out of delta functions and algebraic

¹⁰Singular definitions would require \mathfrak{R} functions to contain integrals of delta functions which independently evolve momenta in the amplitude and similarly for \mathfrak{R}^* in the conjugate amplitude. The external momentum integrals, $\int \prod_k d^4 p_k$, would be used to force the two separately evolving momenta to coincide. Giving these definitions provides an entirely unnecessary extra complexity.

pre-factors relating the momentum from the current step in the algorithm, $\{p\}$, to the momentum that will be carried forwards to the next step of the algorithm, $\{\tilde{p}\}$ and q_i . $\mathcal{R}_{ij}^{\text{soft}}$ and $\mathcal{R}_i^{\text{coll}}$ are fixed by $\mathfrak{R}_{ij}^{\text{soft}*}$ and $\mathfrak{R}_{ij}^{\text{coll}}$, i.e.

$$\int \prod_k d^4 p_k \mathfrak{R}_{ij}^{\text{soft}*}(\{p\}, \{\tilde{p}\}, q_i) \mathfrak{R}_{ij'}^{\text{soft}}(\{p\}, \{\tilde{p}\}, q_i) = \mathcal{R}_{jj'}^{\text{soft}}(q_i, \{\tilde{p}\}), \quad (4.21)$$

and

$$\int \prod_k d^4 p_k \mathfrak{R}_{ij}^{\text{coll}*}(\{p\}, \{\tilde{p}\}, q_i) \mathfrak{R}_{ij'}^{\text{coll}}(\{p\}, \{\tilde{p}\}, q_i) = \mathcal{R}_j^{\text{coll}}(q_i, \{\tilde{p}\}). \quad (4.22)$$

In the LL_Σ approximation, $\mathcal{R}_{jj'}^{\text{soft}} = \mathcal{R}_j^{\text{coll}} = 1$. \mathbf{S}_i generates soft emissions and one might suppose that a suitable choice of recoil (to LL_Σ accuracy) is

$$\mathfrak{R}_{ij}^{\text{soft}} \mathfrak{R}_{ij'}^{\text{soft}*} = \prod_k \delta^4(p_k - \tilde{p}_k). \quad (4.23)$$

We will shortly see that things are not quite so simple, and that this requires modification. \mathbf{C}_i generates hard-collinear emissions, however only the longitudinal component of the recoil is hard. Therefore, in the LL_Σ approximation, we may implement recoils in the collinear sector via

$$\mathfrak{R}_{ij}^{\text{coll}*} \mathfrak{R}_{ij}^{\text{coll}} = \left(\delta^4(p_j - z_i^{-1} \tilde{p}_j) \delta_j^{\text{final}} + \delta^4(p_j - z_i \tilde{p}_j) \delta_j^{\text{initial}} \right) \prod_{k \neq j} \delta^4(p_k - \tilde{p}_k). \quad (4.24)$$

Finally, the phase-space is included via

$$d\Pi_i = \frac{2\alpha_s}{\pi^2 q_{i\perp}^2} \frac{d^3 q_i}{2E_i}. \quad (4.25)$$

The pre-factor has been included to simplify the definitions of \mathbf{S}_i and \mathbf{C}_i , as well as to make each term in the algorithm dimensionless and keep explicit dependence on the ordering variable in \mathbf{D}_i . To simplify the notation, in (4.25) and elsewhere, we will drop the dipole labels on transverse momenta. It should be clear from the context which partons are intended. In the case of (4.25), it means we should use the transverse momentum defined by the parent parton and the vector \vec{n} in the case of collinear emissions or $q_\perp^{(ij)}$ in the case of soft emissions. It is often useful to note that

$$d\Pi_i = \frac{2\alpha_s}{\pi} \frac{dq_{i\perp}}{q_{i\perp}} \frac{dz_i}{1-z_i} \frac{d\phi_i}{2\pi} = \frac{2\alpha_s}{\pi} \frac{dq_{i\perp}}{q_{i\perp}} \frac{dy d\phi}{2\pi}, \quad (4.26)$$

where y is the rapidity in the frame defining $q_{i\perp}$. Using these last two relations the link between real emissions and virtual corrections is clear, i.e. the square of the emission operators $\int \mathbf{D}_i^\dagger \mathbf{D}_i d\Pi_i$ is, for e^+e^- collisions¹¹, equal to minus twice the real part of the exponent in (4.14).

¹¹This caveat is necessary to avoid complications associated with emissions off coloured incoming legs.

Using the naive recoil prescription of (4.23) and (4.24), the array of parton momenta gets modified after a collinear emission, generated by $\bar{\mathbf{P}}_{ij}$, but not after a soft emission (except to add one new soft gluon of course). Specifically, this means acting with $\bar{\mathbf{P}}_{ij}\mathfrak{R}_{ij}^{\text{coll}}$ maps $p_j \mapsto \tilde{p}_j = z_i p_j + \mathcal{O}(q_\perp)$ (for final state partons), and a parton with momentum $q_i = (1-z)p_j + \mathcal{O}(q_\perp)$ is added. As usual, p_j is the momentum of parton j prior to the action of $\bar{\mathbf{P}}_{ij}\mathfrak{R}_{ij}^{\text{coll}}$. A more careful treatment of momenta is not required to reproduce the leading logarithms for many observables. However, any observable dependent upon parton distribution functions or fragmentation functions will be incorrectly calculated because this naive recoil prescription does not reproduce DGLAP evolution. This is because the terms with soft-collinear poles are handled in the ‘soft side’ of the algorithm and do not conserve longitudinal momentum. This manifests as DGLAP evolution with an incorrect plus prescription, i.e.

$$\left(\frac{1+z^2}{1-z}\right)_+ = \left(\frac{2}{1-z}\right)_+ - (1+z)_+ \xrightarrow{\text{variant A}} -(1+z)_+, \quad (4.27)$$

as the soft poles have been removed from the hard-collinear splitting functions defining $\bar{\mathbf{P}}_{ij}$. On the flip side, the algorithm works well for event shape observables in e^+e^- collisions. We will refer to the framework in this section as variant A of the algorithm. Within variant A, this problem could be solved by implementing a universal recoil for all emissions, soft and collinear, i.e.

$$\int \prod_k d^4 p_k \mathfrak{R}_{ij}^{\text{coll}} \mathfrak{R}_{ij}^{\text{coll}*} = \int \prod_k d^4 p_k \sum_{j'} \mathfrak{R}_{ij}^{\text{soft}} \mathfrak{R}_{ij'}^{\text{soft}*}. \quad (4.28)$$

We will not consider universal recoils in this paper and will instead solve this ‘plus prescription problem’ another way; by putting the soft-collinear emissions in the collinear sector of the algorithm. Doing this will lead us to variant B of the algorithm. In Section 4.3.4, we will use the insight gained from formulating B to show how to solve the plus-prescription problem within the framework of A.

4.3.2 Parton branching using complete collinear splitting functions (B)

Soft-collinear poles can be exchanged reasonably simply between eikonal currents and collinear splitting functions. We will now define variant B of our algorithm, which restores the soft-collinear poles in the collinear splitting functions and removes them from the eikonal currents. This is a good thing to do for two reasons:

1. Collinear evolution is generated by unit operators in colour space. Making this manifest for the soft-collinear poles simplifies the colour evolution of the algorithm.

2. Putting the soft-collinear poles into the collinear ‘side’ of the algorithm simplifies the recoil prescription because every collinear emission has a uniquely identifiable parent.

Variant B is very similar in form to variant A:

$$\begin{aligned}\mathbf{S}_i &= \sum_j \left(\frac{q_{i\perp}^{(j\vec{n})}}{2\tilde{p}_j \cdot q_i} \mathbb{T}_j^g \otimes (\tilde{p}_j \cdot \epsilon_+^*(q_i) \mathbb{S}^{1_i} + \tilde{p}_j \cdot \epsilon_-^*(q_i) \mathbb{S}^{-1_i}) \right) \mathfrak{R}_{ij}^{\text{soft}}(\{p\}, \{\tilde{p}\}, q_i), \\ \mathbf{C}_i &= \sum_j \frac{q_{i\perp}^{(j\vec{n})}}{2\sqrt{z_i}} \Delta_{ij} \mathbf{P}_{ij} \mathfrak{R}_{ij}^{\text{coll}}(\{p\}, \{\tilde{p}\}, q_i),\end{aligned}\quad (4.29)$$

with

$$\dots \mathbf{D}_i \mathcal{O} \mathbf{D}_i^\dagger \dots = \dots \mathbf{S}_i \mathcal{O} \mathbf{S}_i^\dagger \mathfrak{f}_{jj'}(q_i, \{p\}, \{\tilde{p}\}) \dots + \dots \mathbf{C}_i \mathcal{O} \mathbf{C}_i^\dagger \dots \quad (4.30)$$

The form of \mathbf{S}_i is the same as in A and the Sudakov changes as

$$\begin{aligned}\mathbf{V}_{a,b} = & \text{Pexp} \left[-\frac{\alpha_s}{\pi} \sum_{i < j} \int_a^b \frac{dk_{\perp}^{(ij)}}{k_{\perp}^{(ij)}} (-\mathbb{T}_i^g \cdot \mathbb{T}_j^g) \left\{ \int \frac{dy d\phi}{4\pi} (k_{\perp}^{(ij)})^2 \frac{\tilde{p}_i \cdot \tilde{p}_j}{(\tilde{p}_i \cdot k)(\tilde{p}_j \cdot k)} \theta_{ij}(k) \right. \right. \\ & \left. \left. \times \mathcal{F}_{ij}(k, \{\tilde{p}\}) - i\pi \tilde{\delta}_{ij} \right\} \mathcal{R}_{ij}^{\text{soft}} - \frac{\alpha_s}{\pi} \sum_i \int_a^b \frac{dk_{\perp}^{(i\vec{n})}}{k_{\perp}^{(i\vec{n})}} \sum_v \mathbb{T}_i^{v2} \int \frac{dz d\phi}{8\pi} \mathcal{P}_{vv_i}^\circ \theta_i(k) \mathcal{R}_i^{\text{coll}} \right].\end{aligned}$$

The only changes relative to variant A are the appearance of $\mathfrak{f}_{jj'}(q_i, \{p\}, \{\tilde{p}\})$ and $\mathcal{F}_{ij}(k, \{\tilde{p}\})$, which specify the prescription for the subtraction of soft-collinear poles from the eikonal currents, and the replacement of $\bar{\mathbf{P}}_{ij}$ with \mathbf{P}_{ij} . Explicit dependence on \mathbf{P}_{ij} in \mathbf{C}_i means that $\mathbf{C}_i \mathcal{O} \mathbf{C}_i^\dagger$ now contains the full spin-dependent DGLAP splitting functions [40]. Unitarity requires that

$$\int \prod_i d^4 p_i \mathfrak{f}_{jj'}(q_i, \{p\}, \{\tilde{p}\}) \mathfrak{R}_{ij}^{\text{soft}*} \mathfrak{R}_{ij'}^{\text{soft}} = \mathcal{F}_{jj'}(q_i, \{p\}, \{\tilde{p}\}) \mathcal{R}_{ij}^{\text{soft}}(q_i, \{\tilde{p}\}). \quad (4.31)$$

The functional forms of $\mathfrak{f}_{jj'}(q_i, \{p\}, \{\tilde{p}\})$ and $\mathcal{F}_{jj'}(q_i, \{\tilde{p}\})$ are uniquely fixed by the choice of $\mathfrak{R}_{ij}^{\text{coll}}$ and $\mathfrak{R}_{ij}^{\text{soft}}$ once we have fixed \mathbf{P}_{ij} . Specifically, we can derive variant B from A by adding and subtracting a function:

$$\mathbf{S}_i^{\text{B}} \mathcal{O} \mathbf{S}_i^{\text{B}\dagger} d\Pi_i + \mathbf{C}_i^{\text{B}} \mathcal{O} \mathbf{C}_i^{\text{B}\dagger} d\Pi_i = \underbrace{\mathbf{S}_i^{\text{A}} \mathcal{O} \mathbf{S}_i^{\text{A}\dagger} d\Pi_i - \mathbf{s}_i \mathcal{O} \mathbf{s}_i^\dagger}_{\equiv \mathbf{S}_i^{\text{B}} \mathcal{O} \mathbf{S}_i^{\text{B}\dagger} d\Pi_i} + \underbrace{\mathbf{C}_i^{\text{A}\dagger} \mathcal{O} \mathbf{C}_i^{\text{A}} d\Pi_i + \mathbf{s}_i \mathcal{O} \mathbf{s}_i^\dagger}_{\equiv \mathbf{C}_i^{\text{B}} \mathcal{O} \mathbf{C}_i^{\text{B}\dagger} d\Pi_i}, \quad (4.32)$$

where we have labelled each operator with a superscript indicating which variant it corresponds to and where \mathcal{O} is some general operator in colour and spin. The subtraction term was constructed so that

$$\mathbf{s}_i \mathcal{O} \mathbf{s}_i^\dagger \equiv \sum_j \frac{(q_{i\perp}^{(j\vec{n})})^2}{4z_i} (\mathbf{P}_{ij} \mathcal{O} \mathbf{P}_{ij}^\dagger - \bar{\mathbf{P}}_{ij} \mathcal{O} \bar{\mathbf{P}}_{ij}^\dagger) \mathfrak{R}_{ij}^{\text{coll}} \mathfrak{R}_{ij}^{\text{coll}*} d\Pi_i \quad (4.33)$$

and after some manipulation is equal to

$$\begin{aligned} \mathbf{s}_i \mathcal{O} \mathbf{s}_i^\dagger &= \frac{2\alpha_s}{\pi} \sum_j \mathbb{T}_j^g \otimes \left(\frac{\mathbb{S}^{1_i}}{\langle q_i \tilde{p}_j \rangle} + \frac{\mathbb{S}^{-1_i}}{[q_i \tilde{p}_j]} \right) \mathcal{O} \mathbb{T}_j^{g\dagger} \otimes \left(\frac{\mathbb{S}^{1_i}}{\langle q_i \tilde{p}_j \rangle} + \frac{\mathbb{S}^{-1_i}}{[q_i \tilde{p}_j]} \right)^\dagger \\ &\quad \times q_i \cdot \tilde{p}_j \frac{dq_{i\perp}^{(j\vec{n})}}{q_{i\perp}^{(j\vec{n})}} \frac{dy d\phi}{2\pi} \theta_j(q_i) (\delta_j^{\text{final}} + \delta_j^{\text{initial}}(\tilde{p}_j \leftrightarrow p_j)) \mathfrak{R}_{ij}^{\text{coll}} \mathfrak{R}_{ij}^{\text{coll}*}. \end{aligned} \quad (4.34)$$

$\langle q_i \tilde{p}_j \rangle$ and $[q_i \tilde{p}_j]$ are Weyl products in the spinor-helicity formalism [41]. Also note, $\mathbf{s}_i \mathcal{O} \mathbf{s}_i^\dagger$ is equal to the collinear limit of $\mathbf{S}_i^A \mathcal{O} \mathbf{S}_i^{A\dagger} d\Pi_i$ with $q_{i\perp}^{(j\vec{n})} \approx q_{i\perp}^{(j\vec{n})}$. To see the equality we express polarisation vectors using spinor products,

$$e^\mu(q_i, \pm 1) = \frac{1}{\sqrt{2}} \frac{\langle q_i \mp | \sigma_\mp^\mu | n \mp \rangle}{\langle q_i \pm | n \mp \rangle}, \quad (4.35)$$

where $\sigma_\mp^\mu = (\mathbb{1}, \mp \sigma_1, \mp \sigma_2, \mp \sigma_3)^T$ are vectors of Pauli matrices and n is an auxillary light-like vector (best chosen to be either p_j or $p_{j'}$).

To complete the definition of variant B we must compute $\mathfrak{f}_{jj'}(q_i, \{p\}, \{\tilde{p}\})$ and $\mathcal{F}_{jj'}(q_i, \{\tilde{p}\})$. Note that $\mathbf{s}_i^\dagger \mathbf{s}_i$ is proportional to the unit operator in colour and helicity. After taking the trace over helicity space, (4.32) leads to

$$\begin{aligned} &\sum_{j,j'} \mathbb{T}_j^g \mathcal{O} \mathbb{T}_{j'}^{g\dagger} \frac{dq_{i\perp}^{(jj')}}{q_{i\perp}^{(jj')}} \frac{dy d\phi}{4\pi} \theta_{jj'}(q_i) \mathfrak{R}_{ij}^{\text{soft}} \mathfrak{R}_{ij'}^{\text{soft}*} \mathfrak{f}_{jj'}(q_i, \{p\}, \{\tilde{p}\}) = \\ &\sum_{j,j'} \mathbb{T}_j^g \mathcal{O} \mathbb{T}_{j'}^{g\dagger} \frac{dq_{i\perp}^{(jj')}}{q_{i\perp}^{(jj')}} \frac{dy d\phi}{4\pi} \theta_{jj'}(q_i) \mathfrak{R}_{ij}^{\text{soft}} \mathfrak{R}_{ij'}^{\text{soft}*} + \sum_j \mathbb{T}_j^g \mathcal{O} \mathbb{T}_j^{g\dagger} \frac{dq_{i\perp}^{(j\vec{n})}}{q_{i\perp}^{(j\vec{n})}} \frac{dy d\phi}{4\pi} \theta_j(q_i) \mathfrak{R}_{ij}^{\text{coll}} \mathfrak{R}_{ij}^{\text{coll}*}. \end{aligned} \quad (4.36)$$

We can use colour conservation to factorise the colour operators and simplify the second term on the right-hand side, i.e.

$$\mathfrak{f}_{jj'}(q_i, \{p\}, \{\tilde{p}\}) = 1 - \frac{dq_{i\perp}^{(j\vec{n})}}{dq_{i\perp}^{(jj')}} \frac{q_{i\perp}^{(jj')}}{q_{i\perp}^{(j\vec{n})}} \theta_j(q_i) \frac{\mathfrak{R}_{ij}^{\text{coll}*} \mathfrak{R}_{ij}^{\text{coll}}}{\mathfrak{R}_{ij}^{\text{soft}*} \mathfrak{R}_{ij'}^{\text{soft}}} \quad (4.37)$$

and

$$\mathcal{F}_{jj'}(q_i, \{p_j\}) = 1 - \frac{dq_{i\perp}^{(j\vec{n})}}{dq_{i\perp}^{(jj')}} \frac{q_{i\perp}^{(jj')}}{q_{i\perp}^{(j\vec{n})}} \theta_j(q_i) \frac{\mathcal{R}_j^{\text{coll}}}{\mathcal{R}_{jj'}^{\text{soft}}}. \quad (4.38)$$

For a universal recoil it is possible to employ colour conservation and write

$$\sum_j \mathbb{T}_j^g \mathcal{O} \mathbb{T}_j^{g\dagger} \frac{dq_{i\perp}^{(j\vec{n})}}{q_{i\perp}^{(j\vec{n})}} \frac{dy d\phi}{4\pi} \theta_j(q_i) \mathfrak{R}_{ij}^{\text{coll}} \mathfrak{R}_{ij}^{\text{coll}*} = \sum_{j,j'} \mathbb{T}_j^g \mathcal{O} \mathbb{T}_{j'}^{g\dagger} \frac{dq_{i\perp}^{(j\vec{n})}}{q_{i\perp}^{(j\vec{n})}} \frac{dy d\phi}{4\pi} \theta_j(q_i) \mathfrak{R}_{ij}^{\text{soft}} \mathfrak{R}_{ij'}^{\text{soft}*}, \quad (4.39)$$

which enables us to re-write (4.37) as

$$f_{jj'}(q_i, \{p\}, \{\tilde{p}\}) = 1 - \frac{dq_{i\perp}^{(j\bar{n})}}{dq_{i\perp}^{(jj')}} \frac{q_{i\perp}^{(jj')} \theta_j(q_i)}{q_{i\perp}^{(j\bar{n})} \theta_{jj'}(q_i)}. \quad (4.40)$$

In the case of a universal recoil prescription, the effects of the recoil can be factorised out of the emission operators and into a redefinition of the phase space measure. Recoil schemes that may be universal include the more ‘true to Feynman diagrams’ global prescriptions which put momenta of partons higher in the chain of emissions off-shell (e.g. see [42] and references therein) and schemes which democratically share recoil across a jet or every parton in the shower. Depending on their implementation, such schemes can be universal since they globally redistribute momentum across the whole event as a $n \rightarrow n + 1$ parton processes. We leave the specification a universal recoil scheme to future work. For now we re-iterate that it is only when considering effects beyond LL_Σ that (4.40) and (4.37) differ.

Our implementation of recoil is not unique, and it remains to be seen (by performing analytic calculations at NLL and beyond) the extent to which we will eventually be able to capture the salient sub-leading logarithms in the framework of our algorithm. A slightly different approach would be to start with variant B (recall we started from variant A above) and assume (4.40) holds true. Variant A could then be constructed but it would now include subtraction functions akin to $f_{jj'}$. In the case of universal recoils, none of this matters of course.

4.3.3 Collinear subtractions and the ordering variable

Before moving on, we’d like to present a slightly more general approach to subtracting the soft-collinear contribution. This calculation will shed some light on the role played by the ordering variable. We start by writing¹²

$$\ln \mathbf{V}_{ab} = \frac{\alpha_s}{2\pi} \sum_{i < j} \mathbb{T}_i^g \cdot \mathbb{T}_j^g \int_{a^2}^{b^2} \frac{dq^2}{q^2} \int \frac{d^3k}{2E} \frac{K^2(p_i, p_j; k)}{\pi} \frac{p_i \cdot p_j}{p_i \cdot k p_j \cdot k} \delta(q^2 - K^2(p_i, p_j; k)) \theta_{ij}(k), \quad (4.41)$$

which holds for a general definition of the ordering variable, $K^2(p_i, p_j, k)$. In order to isolate the collinear divergence, we should first expose, and factor, the soft divergence. To do this, it is sufficient to consider any scaling which is linear in the emitted gluon’s momentum components, such that we can re-write

$$\ln \mathbf{V}_{ab} = \frac{\alpha_s}{2\pi} \sum_{i < j} \mathbb{T}_i^g \cdot \mathbb{T}_j^g \int_{a^2}^{b^2} \frac{dq^2}{q^2} \int \frac{d^3k}{2E} \frac{K^2(p_i, p_j; k)}{\pi (S \cdot k)^2} \frac{n_i \cdot n_j}{n_i \cdot n n_j \cdot n} \delta(q^2 - K^2(p_i, p_j; k)) \theta_{ij}(k), \quad (4.42)$$

¹²We ignore ignore hard-collinear corrections and the effects of recoil in this section.

where $n_i = q_i/(S \cdot q_i)$, $n = k/(S \cdot k)$ and S is any time-like four-vector, which we choose to satisfy $S^2 = 1$. The soft divergence is now isolated from the eikonal term, which is singular only in the collinear limits $n_{i,j} \cdot n \rightarrow 0$. The collinear divergences can be subtracted. We want the ordering variable to become independent of the other parton's direction in the collinear limit, such that the entire collinear divergence can be moved into a jet factor that is trivial in colour space.

We choose to re-write the virtual evolution as $\ln \mathbf{V}_{ab} = \ln \mathbf{W}_{ab} + \ln \mathbf{K}_{ab}$, where

$$\begin{aligned} \ln \mathbf{W}_{ab} = & \frac{\alpha_s}{2\pi} \sum_{i < j} \mathbb{T}_i^g \cdot \mathbb{T}_j^g \int_{a^2}^{b^2} \frac{dq^2}{q^2} \int \frac{d^3k}{2E} \frac{1}{\pi (S \cdot k)^2} \\ & \left(K^2(p_i, p_j; k) \frac{n_i \cdot n_j}{n_i \cdot n \ n \cdot n_j} \delta(q^2 - K^2(p_i, p_j; k)) \theta_{ij}(k) \right. \\ & \left. - \frac{K^2(p_i; k)}{n_i \cdot n} \delta(q^2 - K^2(p_i; k)) \theta_i(k) - \frac{K^2(p_j; k)}{n_j \cdot n} \delta(q^2 - K^2(p_j; k)) \theta_j(k) \right), \end{aligned} \quad (4.43)$$

and colour conservation can now be used to obtain

$$\ln \mathbf{K}_{ab} = \frac{\alpha_s}{2\pi} \sum_i (\mathbb{T}_i^g)^2 \int_{a^2}^{b^2} \frac{dq^2}{q^2} \int \frac{d^3k}{2E} \frac{2}{\pi (S \cdot k)^2} \frac{K^2(p_i; k)}{n_i \cdot n} \delta(q^2 - K^2(p_i; k)) \theta_i(k). \quad (4.44)$$

This factor contains the ordering variable in terms of a single emitter direction, which is the limiting case of the dipole-type definition in each collinear limit, i.e. $K^2(p_i, p_j, k) \rightarrow K^2(p_i; k)$ as $n_i \cdot n \rightarrow 0$. Given the Lorentz invariance of the virtual evolution and the integration measure we can choose $S = (1, \vec{0})$.

In the case of energy ordering, we obtain the following for the subtracted soft evolution:

$$\begin{aligned} \ln \mathbf{W}_{ab} \Big|_{\text{energy}} &= \frac{\alpha_s}{\pi} \sum_{i < j} \mathbb{T}_i^g \cdot \mathbb{T}_j^g \int_a^b \frac{dE}{E} \int \frac{d\Omega}{4\pi} \left(\frac{n_i \cdot n_j - n_i \cdot n - n_j \cdot n}{n_i \cdot n \ n \cdot n_j} \right) \\ &= \frac{\alpha_s}{\pi} \sum_{i < j} \mathbb{T}_i^g \cdot \mathbb{T}_j^g \int_a^b \frac{dE}{E} \ln \frac{n_i \cdot n_j}{2} \end{aligned} \quad (4.45)$$

where the angular integral can be performed using the same integral that gives rise to angular ordering. And for the collinearly divergent factor:

$$\ln \mathbf{K}_{ab} \Big|_{\text{energy}} = \frac{\alpha_s}{\pi} \sum_i (\mathbb{T}_i^g)^2 \int_a^b \frac{dE}{E} \int \frac{d\Omega}{4\pi} \frac{2}{n_i \cdot n}. \quad (4.46)$$

There is no need for θ_{ij} since this simply enforces that the emitted gluon should have energy smaller than $\sqrt{\frac{1}{2} p_i \cdot p_j}$ in the ij zero momentum frame, which is automatically satisfied since $a < E < b$.

Now let us consider the case of transverse momentum ordering. This can be implemented through

$$K^2(p_i, p_j; k) = (k_{\perp}^{(ij)})^2 = \frac{2 p_i \cdot k k \cdot p_j}{p_i \cdot p_j}, \quad (4.47)$$

and

$$K^2(p; k) \sim 2p \cdot k \quad (4.48)$$

where the similarity sign refers to any function which approaches unity in the limit $p \cdot k \rightarrow 0$. Making the minimal choice, the full evolution becomes

$$\ln \mathbf{V}_{ab} \Big|_{k_T} = \frac{\alpha_s}{\pi} \sum_{i < j} \mathbb{T}_i^g \cdot \mathbb{T}_j^g \int_a^b \frac{dk_{\perp}}{k_{\perp}} \int \frac{dz}{1-z} \frac{d\phi}{2\pi} \theta_{ij}(k) \quad (4.49)$$

and

$$\begin{aligned} \ln \mathbf{K}_{ab} \Big|_{k_T} &= \frac{\alpha_s}{2\pi} \sum_i (\mathbb{T}_i^g)^2 \int_a^b \frac{dk_{\perp}}{k_{\perp}} \int_{\alpha}^1 \frac{dz}{1-z+\alpha} \int \frac{d\phi}{2\pi} \\ &= \frac{\alpha_s}{2\pi} \sum_i (\mathbb{T}_i^g)^2 \int_a^b \frac{dk_{\perp}}{k_{\perp}} \int_0^{1-\alpha} \frac{dz}{1-z} \int \frac{d\phi}{2\pi} \end{aligned} \quad (4.50)$$

where $\alpha = k_{\perp}^2 / (2S \cdot p_i)^2$. This is the same as the subtraction prescription we introduced in the last section, with the only difference being that the lower limit on the z integral is (approximately) equal to α in that case. Finally, using colour conservation we can compute $\ln \mathbf{V}_{ab} - \ln \mathbf{K}_{ab}$ and get

$$\begin{aligned} \ln \mathbf{W}_{ab} \Big|_{k_T} &= \frac{\alpha_s}{\pi} \sum_{i < j} \mathbb{T}_i^g \cdot \mathbb{T}_j^g \int_a^b \frac{dk_{\perp}}{k_{\perp}} \int \frac{dy d\phi}{2\pi} (\theta_{ij}(k) - \theta_i(k)), \\ &= \frac{\alpha_s}{\pi} \sum_{i < j} \mathbb{T}_i^g \cdot \mathbb{T}_j^g \int_a^b \frac{dk_{\perp}}{k_{\perp}} \int \frac{dy d\phi}{2\pi} \mathcal{F}_{ij}(k) \theta_{ij}(k), \\ &\approx \frac{\alpha_s}{\pi} \sum_{i < j} \mathbb{T}_i^g \cdot \mathbb{T}_j^g \int_a^b \frac{dk_{\perp}}{k_{\perp}} \ln \frac{n_i \cdot n_j}{2}, \end{aligned} \quad (4.51)$$

where the second line illustrates the equivalence with the subtraction scheme presented in the previous section (recall we are ignoring recoil in this section). The approximately-equal-to sign is because we neglect terms suppressed by powers of k_{\perp}^2 . As expected, this finite term is the same as the energy ordering case in equation (4.45). The form factor $\exp(\ln \mathbf{W})$ captures all of the truly wide-angle soft-gluon physics and is essentially the same as the fifth form factor introduced by Dokshitzer & Marchesini [43].

4.3.4 A local recoil prescription

Next we will show how a more sophisticated recoil prescription (than (4.23) and (4.24)) can be implemented. The recoil we choose is based on the one in [44, 45], but extended to work with colour off-diagonal evolution. The dipole recoil is itself based on Catani-Seymour dipole factorisation and furthers the work in [46] so that recoil can be implemented in a dipole parton shower. As a result, this recoil scheme shares similarities with the spectator recoil prescriptions used in modern dipole showers such as PYTHIA and DIRE [8, 11]. The idea is not to present a definitive recoil prescription but rather to illustrate how one can be implemented in our algorithm. To that end, we calculate \mathcal{F}_{ij} and $\mathfrak{R}_{ij}^{\text{coll}}$. We also provide a short discussion on the successes and limitations of the prescription. We then go on to show that, at LL, the recoil prescription can be reduced to the naive recoil prescription when implemented in variant B (but not variant A).

To keep things as simple as possible, we will consider the dipole recoil scheme in the case of only coloured final-state partons. The extension to coloured initial-state partons is straightforward and can be found by following Section 3.2 of [45]. First we will summarise the dipole recoil for colour-diagonal evolution. It works by adding a spectator particle to the standard description of a $1 \rightarrow 2$ collinear splitting ($p_j \rightarrow \tilde{p}_j, q_i$). This spectator particle absorbs the recoil from the splitting, which would otherwise put p_j off-shell. The spectator particle has a second function: to specify the frame in which the transverse momentum of the emission is computed. In [45] it was shown that one can obtain the correct colour-diagonal evolution by choosing the parton that is colour connected to parton j as the spectator. We will denote the momentum of the spectator parton by $p_{j\text{LR}}$ (the reason for the LR subscript will become clear). The Sudakov decomposition is

$$\begin{aligned} \tilde{p}_j &= z_i p_j - k_\perp + \frac{(q_\perp^{(jj\text{LR})})^2}{z_i} \frac{p_{j\text{LR}}}{2p_j \cdot p_{j\text{LR}}}, & (q_\perp^{(jj\text{LR})})^2 &= -k_\perp^2, \\ q_i &= (1 - z_i) p_j + k_\perp + \frac{(q_\perp^{(jj\text{LR})})^2}{1 - z_i} \frac{p_{j\text{LR}}}{2p_j \cdot p_{j\text{LR}}}, \\ \tilde{p}_{j\text{LR}} &= \left(1 - \frac{(q_\perp^{(jj\text{LR})})^2}{z_i(1 - z_i)} \frac{1}{2p_j \cdot p_{j\text{LR}}} \right) p_{j\text{LR}}, & k_\perp \cdot p_j &= k_\perp \cdot p_{j\text{LR}} = 0. \end{aligned} \quad (4.52)$$

This now defines a $2 \rightarrow 3$ splitting ($p_j, p_{j\text{LR}} \rightarrow q_i, \tilde{p}_j, \tilde{p}_{j\text{LR}}$) in which q_i is emitted collinear to p_j . The prescription is momentum conserving, i.e.

$$p_j + p_{j\text{LR}} = q_i + \tilde{p}_j + \tilde{p}_{j\text{LR}}$$

and it ensures that all particles are on-shell at each stage in the evolution. One can check that this Sudakov decomposition does not change the functional form of the leading-order

collinear splitting functions. Comparing to (4.19), we see that p and n are now fixed: $p = p_j$ and $n = p_{j\text{LR}}$. Working in the LC approximation, the effect of this prescription amounts to a correction to the single-particle emission phase space [45], i.e.

$$d\sigma(q_i, \tilde{p}_j, \tilde{p}_{j\text{LR}}) = \frac{\alpha_s}{2\pi} d\sigma(p_j, p_{j\text{LR}}) \frac{dq_{\perp}^{(jj\text{LR})}}{q_{\perp}^{(jj\text{LR})}} dz_i \mathcal{P}_{v_i v_j}(z_i) \left(1 - \frac{(q_{\perp}^{(jj\text{LR})})^2}{z_i(1-z_i)} \frac{1}{2p_j \cdot p_{j\text{LR}}} \right). \quad (4.53)$$

This correction contributes soft-collinear NLLs and hard-collinear NNLLs [45].

The dipole recoil prescription was developed for a leading N_c shower and as such is not completely sufficient for our purposes. That is because, beyond the LC approximation, the left evolution (of the amplitude) and right evolution (of the conjugate amplitude) are independent, which means they can evolve to produce colour off-diagonal terms. These are terms for which the parton j is colour connected to different partons in the left and right evolution. In such a case $p_{j\text{LR}}$ cannot be defined. Instead, we must introduce parton $p_{j\text{L}}$, which is the colour connected parton to j in the left evolution, and parton $p_{j\text{R}}$, which is colour connected to j in the right evolution. We will now construct a recoil prescription that extends the dipole recoil to include colour off-diagonal terms but collapses back to the dipole recoil in the LC approximation.

To begin, we define a Sudakov decomposition for a $3 \rightarrow 4$ splitting ($p_j, p_{j\text{L}}, p_{j\text{R}} \rightarrow q_i, \tilde{p}_j, \tilde{p}_{j\text{L}}, \tilde{p}_{j\text{R}}$). We aim to construct the decomposition so that recoil is shared equally between $p_{j\text{L}}$ and $p_{j\text{R}}$. We also wish to leave the collinear splitting functions unchanged. Finally, we also require all partons involved to be on-shell. These constraints are fulfilled by the decomposition:

$$\begin{aligned} \tilde{p}_j &= z_i p_j - k_{\perp} + \frac{(q_{\perp}^{(j\bar{n})})^2}{z_i} \frac{n}{2p_j \cdot n}, \\ q_i &= (1-z_i)p_j + k_{\perp} + \frac{(q_{\perp}^{(j\bar{n})})^2}{1-z_i} \frac{n}{2p_j \cdot n}, \\ n &= p_{j\text{L}} + p_{j\text{R}}(1 - \delta_{j\text{L},j\text{R}}) - \sqrt{\frac{2p_{j\text{L}} \cdot p_{j\text{R}}}{\hat{n}^2}} \hat{n}, \\ \tilde{p}_{j\text{L}} &= (1-\gamma)p_{j\text{L}} + \gamma \sqrt{\frac{p_{j\text{L}} \cdot p_{j\text{R}}}{2\hat{n}^2}} \hat{n} + \gamma l(1 - \delta_{j\text{L},j\text{R}}), \\ \tilde{p}_{j\text{R}} &= (1-\gamma)p_{j\text{R}} + \gamma \sqrt{\frac{p_{j\text{L}} \cdot p_{j\text{R}}}{2\hat{n}^2}} \hat{n} - \gamma l(1 - \delta_{j\text{L},j\text{R}}), \end{aligned} \quad (4.54)$$

where

$$\begin{aligned}
(q_{\perp}^{(j\vec{n})})^2 &= -k_{\perp}^2, & 2q \cdot \tilde{p}_j &= \frac{(q_{\perp}^{(j\vec{n})})^2}{z_i(1-z_i)}, & \hat{n} \cdot p_{jL} &= \hat{n} \cdot p_{jR} = 0, \\
\gamma &= \frac{(q_{\perp}^{(j\vec{n})})^2}{z_i(1-z_i)} \frac{1}{2p_j \cdot n}, & k_{\perp} \cdot p_j &= k_{\perp} \cdot n = 0, \\
l^2 &= \frac{p_{jL} \cdot p_{jR}}{2}, & l \cdot \left((1-\gamma)(p_{jL} + p_{jR}) + \gamma \sqrt{\frac{p_{jL} \cdot p_{jR}}{2\hat{n}^2}} \hat{n} \right) &= 0,
\end{aligned} \tag{4.55}$$

where $\delta_{jL,jR}$ is the usual Kronecker delta symbol. Note that $p_j + p_{jL} + p_{jR} = q_i + \tilde{p}_j + \tilde{p}_{jL} + \tilde{p}_{jR}$, and so momentum is conserved in the $3 \rightarrow 4$ splitting. Also note that when $j^L = j^R = j^{LR}$, i.e. the emission is colour-diagonal, this reduces to the dipole $2 \rightarrow 3$ scattering with $p_j + p_{jLR} = q_i + \tilde{p}_j + \tilde{p}_{jLR}$. Finally, note that every new term relative the dipole recoil is accompanied by a factor γ , which is two orders higher than the leading terms in the collinear limit and one order higher in the soft limit. Using this decomposition, the recoil prescription for collinear emissions is

$$\begin{aligned}
\mathfrak{R}_{ij}^{\text{coll}*} \mathfrak{R}_{ij}^{\text{coll}} &= z_i (\mathcal{J}_{ij}(z_i, q_{i\perp}^{(j\vec{n})}, p_{jL}, p_{jR}, l, \hat{n}))^2 \delta^4 \left(\tilde{p}_j - z_i p_j + k_{\perp} - \frac{(q_{\perp}^{(j\vec{n})})^2}{z_i} \frac{n}{2p_j \cdot n} \right) \\
&\times \delta^4 \left(\tilde{p}_{jL} - (1-\gamma) p_{jL} - \gamma \sqrt{\frac{p_{jL} \cdot p_{jR}}{2\hat{n}^2}} \hat{n} - \gamma l (1 - \delta_{jL,jR}) \right) \\
&\times \delta^4 \left(\tilde{p}_{jR} - (1-\gamma) p_{jR} - \gamma \sqrt{\frac{p_{jL} \cdot p_{jR}}{2\hat{n}^2}} \hat{n} + \gamma l (1 - \delta_{jL,jR}) \right) \prod_{k \neq j, j^L, j^R} \delta^4(p_k - \tilde{p}_k),
\end{aligned} \tag{4.56}$$

where the Jacobian, \mathcal{J}_{ij} , can (in principle) be evaluated using

$$\begin{aligned}
\mathcal{J}_{ij} &= \left[\int d^4 p'_{jL} d^4 p'_{jR} \delta^4 \left(\tilde{p}_{jL} - (1-\gamma') p'_{jL} - \gamma' \sqrt{\frac{p'_{jL} \cdot p'_{jR}}{2\hat{n}'^2}} \hat{n}' - \gamma' l (1 - \delta_{jL,jR}) \right) \right. \\
&\times \delta^4 \left(\tilde{p}_{jR} - (1-\gamma') p'_{jR} - \gamma' \sqrt{\frac{p'_{jL} \cdot p'_{jR}}{2\hat{n}'^2}} \hat{n}' + \gamma' l (1 - \delta_{jL,jR}) \right) \left. \right]^{-1} + \mathcal{O} \left(\left(q_{i\perp}^{(j\vec{n})} / Q \right)^3 \right), \\
&= 1 + \mathcal{O}(\gamma).
\end{aligned} \tag{4.57}$$

One factor of $z_i \mathcal{J}_{ij}$ ensures that the integral over the delta functions is correctly normalised whilst the additional factor of \mathcal{J}_{ij} encodes the recoil corrections. This is the factor that was absorbed into the phase-space in [45], i.e.

$$d\sigma(q_i, \tilde{p}_j, \tilde{p}_{jL}, \tilde{p}_{jR}) = \frac{\alpha_s}{2\pi} d\sigma(p_j, p_{jL}, p_{jR}) \frac{dq_{i\perp}^{(j\vec{n})}}{q_{i\perp}^{(j\vec{n})}} dz_i \mathcal{P}_{v_i v_j}(z_i) \mathcal{J}_{ij}. \tag{4.58}$$

We can extend this prescription to the soft sector using Catani-Seymour dipole factorisation [46]. The dipole factorisation provides a unique way to split the parent dipole of a soft emission into two halves, identifiable by their separate collinear poles:

$$\frac{\tilde{p}_{j'} \cdot \tilde{p}_j}{(q_i \cdot \tilde{p}_{j'}) (\tilde{p}_j \cdot q_i)} = \frac{\tilde{p}_{j'} \cdot \tilde{p}_j}{q_i \cdot (\tilde{p}_{j'} + \tilde{p}_j) \tilde{p}_j \cdot q_i} + \frac{\tilde{p}_{j'} \cdot \tilde{p}_j}{\tilde{p}_{j'} \cdot q_i (\tilde{p}_{j'} + \tilde{p}_j) \cdot q_i}.$$

This provides the means to implement a local recoil using the parton contributing to the collinear pole in each half of the dipole. Thus we can write

$$\mathfrak{R}_{ij'}^{\text{soft}} * \mathfrak{R}_{ij}^{\text{soft}} = \frac{(q_{i\perp}^{(jj')})^2 \tilde{p}_{j'} \cdot \tilde{p}_j}{2q_i \cdot (\tilde{p}_{j'} + \tilde{p}_j) (\tilde{p}_j \cdot q_i)} \mathfrak{R}_{ij}^{\text{coll}} * \mathfrak{R}_{ij'}^{\text{coll}} + \frac{(q_{i\perp}^{(jj')})^2 \tilde{p}_{j'} \cdot \tilde{p}_j}{2(\tilde{p}_{j'} \cdot q_i) (\tilde{p}_{j'} + \tilde{p}_j) \cdot q_i} \mathfrak{R}_{ij'}^{\text{coll}} * \mathfrak{R}_{ij}^{\text{coll}}. \quad (4.59)$$

From this, $\mathcal{R}_{ij}^{\text{soft}}$ and $\mathcal{R}_i^{\text{coll}}$ can be evaluated:

$$\mathcal{R}_{jj'}^{\text{soft}}(q_i, \{p\}) = \frac{(q_{i\perp}^{(jj')})^2 p_{j'} \cdot p_j}{2q_i \cdot (p_{j'} + p_j) (p_j \cdot q_i)} \mathcal{J}_{ij} + (j \leftrightarrow j'), \quad \mathcal{R}_j^{\text{coll}}(q_i, \{p\}) = \mathcal{J}_{ij}. \quad (4.60)$$

We can now go ahead and determine the subtraction functions used to define variant B. Using (4.37) and (4.38) we get

$$\mathcal{F}_{jj'}(q_i, \{p\}) = 1 - \frac{dq_{i\perp}^{(j\bar{n})}}{dq_{i\perp}^{(jj')}} \frac{q_{i\perp}^{(jj')} \theta_j(q_i)}{q_{i\perp}^{(j\bar{n})} \theta_{jj'}(q_i)} \frac{\mathcal{J}_{ij}}{\mathcal{R}_{jj'}^{\text{soft}}}. \quad (4.61)$$

Before moving on we want to comment on the discussion in [17], which shows that the dipole recoil scheme, as implemented in a dipole shower, fails at the level of the NLL even at LC due to incorrectly assigning the longitudinal recoil after multiple emissions. It remains to be seen whether this is also true in the scheme discussed here.

4.3.4.1 A LL_Σ recoil prescription

We can now consider constructing a recoil prescription where we only keep the parts contributing at LL_Σ . Firstly note that in the strictly leading soft limit

$$\mathfrak{R}_{ij}^{\text{coll}} * \mathfrak{R}_{ij}^{\text{coll}} = \mathfrak{R}_{ij'}^{\text{soft}} * \mathfrak{R}_{ij}^{\text{soft}} = \prod_k \delta^4(p_k - \tilde{p}_k).$$

We can use this fact with variant B restricted to LL_Σ accuracy and find

$$\mathfrak{f}_{jj'}(q_i, \{p\}, \{\tilde{p}\}) = \mathcal{F}_{jj'}(q_i, p_j, p_{j'}) = 1 - \frac{dq_{i\perp}^{(j\bar{n})}}{dq_{i\perp}^{(jj')}} \frac{q_{i\perp}^{(jj')} \theta_j(q_i)}{q_{i\perp}^{(j\bar{n})} \theta_{jj'}(q_i)}. \quad (4.62)$$

Using the naive recoil prescription,

$$\begin{aligned} \mathfrak{R}_{ij}^{\text{coll}} * \mathfrak{R}_{ij}^{\text{coll}} &= \left(\delta^4(p_j - z_i^{-1} \tilde{p}_j) \delta_j^{\text{final}} + \delta^4(p_j - z_i \tilde{p}_j) \delta_j^{\text{initial}} \right) \prod_{k \neq j} \delta^4(p_k - \tilde{p}_k), \\ \mathfrak{R}_{ij'}^{\text{soft}} * \mathfrak{R}_{ij}^{\text{soft}} &= \prod_k \delta^4(p_k - \tilde{p}_k), \quad \mathcal{R}_{ij'}^{\text{soft}} = \mathcal{R}_i^{\text{coll}} = 1, \end{aligned} \quad (4.63)$$

with (4.62), variant B fully captures the correct DGLAP evolution as longitudinal recoil is now included in the soft-collinear region. This is not the case for variant A. We stress that this observation is not a reflection of any fundamental difference between A and B since, with a complete recoil prescription, A and B are equivalent. Indeed, we can use the Catani-Seymour dipole factorisation [46], as previously discussed, to extend the naive recoil prescription so that it does generate longitudinal recoil with variant A, i.e.

$$\begin{aligned}\mathfrak{N}_{ij}^{\text{coll}*}\mathfrak{N}_{ij}^{\text{coll}} &= \left(\delta^4(p_j - z_i^{-1}\tilde{p}_j)\delta_j^{\text{final}} + \delta^4(p_j - z_i\tilde{p}_j)\delta_j^{\text{initial}} \right) \prod_{k \neq j} \delta^4(p_k - \tilde{p}_k), \\ \mathfrak{N}_{ij'}^{\text{soft}*}\mathfrak{N}_{ij'}^{\text{soft}} &= \frac{(q_{i\perp}^{(jj')})^2 \tilde{p}_{j'} \cdot \tilde{p}_j}{2q_i \cdot (\tilde{p}_{j'} + \tilde{p}_j)(\tilde{p}_j \cdot q_i)} \mathfrak{N}_{ij}^{\text{coll}*}\mathfrak{N}_{ij}^{\text{coll}} + \frac{(q_{i\perp}^{(jj')})^2 \tilde{p}_{j'} \cdot \tilde{p}_j}{2(\tilde{p}_{j'} \cdot q_i)(\tilde{p}_{j'} + \tilde{p}_j) \cdot q_i} \mathfrak{N}_{ij'}^{\text{coll}*}\mathfrak{N}_{ij'}^{\text{coll}}.\end{aligned}\tag{4.64}$$

With this, variant A also captures the correct DGLAP evolution.

4.3.5 A manifestly infra-red finite reformulation

It is possible to re-cast both variants of our algorithm such that the IR divergences, other than those renormalised into parton distribution and fragmentation functions, explicitly cancel at each iteration of the algorithm. We will demonstrate this for variant A, though the procedure is pretty much identical for variant B. Our method closely follows that in [27].

We begin by expressing a generalised measurement function in the soft and collinear limits as follows

$$u_m(q_1, \dots, q_m) \stackrel{q_j \text{ soft}}{=} u(q_j, \{q_1, \dots, q_{j-1}, q_{j+1}, \dots, q_m\})u_{m-1}(q_1, \dots, q_{j-1}, q_{j+1}, \dots, q_m), \tag{4.65}$$

and

$$u_m(q_1, \dots, q_m) \stackrel{q_j \parallel q_i}{=} u(q_j, \{q_1, \dots, q_i + q_j, \dots, q_m\})u_{m-1}(q_1, \dots, q_i + q_j, \dots, q_m), \tag{4.66}$$

where $u(q_j, \{q\}) \rightarrow 1$ as j becomes exactly soft or collinear. For many observables, it is possible to further pull apart the measurement function by defining an ‘out’ region, where there is total inclusivity over radiation. For such observables we can write

$$u(q_j, \{q\}) = \Theta_{\text{out}}(q_j) + \Theta_{\text{in}}(q_j)u_{\text{in}}(q_j, \{q\}), \tag{4.67}$$

where $\Theta_{\text{in/out}}(q_j) = 1$ when q_j is in the in/out region and zero otherwise. For a global

observable, the out region has zero extent and so $\Theta_{\text{out}}(q_j) = 0$. First we define

$$\begin{aligned}
\mathbf{\Gamma} &= \mathbf{\Gamma}_u + \bar{\mathbf{\Gamma}}_u, \\
\bar{\mathbf{\Gamma}}_u &= \int \frac{dS_2}{4\pi} (1 - u(k, \{q\})) \frac{1}{2} \mathbf{D}_k^2 + \sum_{i < j} \mathbb{T}_i^g \cdot \mathbb{T}_j^g i\pi \tilde{\delta}_{ij}, \quad dS_2 = dy d\phi = \frac{dz d\phi}{(1-z)}, \\
\frac{1}{2} \mathbf{D}_k^2 &= \sum_{i < j} (-\mathbb{T}_i^g \cdot \mathbb{T}_j^g) (k_\perp^{(ij)})^2 \frac{p_i \cdot p_j}{(p_i \cdot k)(p_j \cdot k)} \theta_{ij}(k) \mathcal{R}_{ij}^{\text{soft}} + \frac{(1-z)}{2} \sum_{i,v} \mathbb{T}_i^{\bar{v}2} \bar{\mathcal{P}}_{vv_i}^\circ \theta_i(k) \mathcal{R}_i^{\text{coll}}, \\
\bar{\mathbf{V}}_{a,b} &= \text{Pexp} \left(-\frac{\alpha_s}{\pi} \int_a^b \frac{dk_\perp}{k_\perp} \bar{\mathbf{\Gamma}}_u \right). \tag{4.68}
\end{aligned}$$

After a simple path-ordered operator expansion,

$$\begin{aligned}
\mathbf{V}_{a,b} &= \bar{\mathbf{V}}_{a,b} - \int d\Pi_1 u(k_1, \{q\}) \bar{\mathbf{V}}_{a,k_1\perp} \frac{1}{2} \mathbf{D}_1^2 \bar{\mathbf{V}}_{k_1\perp,b} \\
&\quad + \int d\Pi_1 d\Pi_2 \Theta(k_{1\perp} - k_{2\perp}) u(k_1, \{q\}) u(k_2, \{q\}) \bar{\mathbf{V}}_{a,k_2\perp} \frac{1}{2} \mathbf{D}_2^2 \bar{\mathbf{V}}_{k_2\perp,k_1\perp} \frac{1}{2} \mathbf{D}_1^2 \bar{\mathbf{V}}_{k_1\perp,b} - \dots \tag{4.69}
\end{aligned}$$

the observable, Σ , can be expressed as

$$\Sigma(\mu) = \int \sum_n \left(\prod_{i=1}^n d\Pi_i \right) \text{Tr} \mathbf{B}_n(\mu; \{p\}_n) \Phi_n(q_1, \dots, q_n), \tag{4.70}$$

where

$$\begin{aligned}
\mathbf{B}_n(q_\perp; \{\tilde{p}\}_{n-1} \cup q_n) &= \bar{\mathbf{V}}_{q_\perp, q_n\perp} \left[\int \prod_i d^4 p_i \delta_n^R \mathbf{D}_n \mathbf{B}_{n-1}(q_n\perp; \{p\}_{n-1}) \mathbf{D}_n^\dagger \right. \\
&\quad \left. - \delta_n^V \left\{ \mathbf{B}_{n-1}(q_n\perp; \{\tilde{p}\}_{n-1}), \frac{1}{2} \mathbf{D}_n^2 \right\} u(q_n, \{\tilde{p}\}_{n-1}) \right] \bar{\mathbf{V}}_{q_\perp, q_n\perp}^\dagger \Theta(q_n\perp - q_\perp), \tag{4.71}
\end{aligned}$$

with $\mathbf{B}_0(q_\perp) = \bar{\mathbf{V}}_{q_\perp, Q} \mathbf{H}(Q) \bar{\mathbf{V}}_{q_\perp, Q}^\dagger$. We define $\delta_n^R = 1$ when parton n is real and $\delta_n^R = 0$ when parton n is virtual, and similarly $\delta_n^V = 1 - \delta_n^R$. $\Phi_n(q_1, \dots, q_n)$ is a measurement function on the phase-space of real particles. We refer to [27] for its precise definition and here just present an illustrative example:

$$\begin{aligned}
&(\delta_3^R \delta_2^V \delta_1^V + \delta_3^V \delta_2^R \delta_1^R + \delta_3^R \delta_2^V \delta_1^R + \delta_3^V \delta_2^V \delta_1^V) \Phi_3(q_1, q_2, q_3) \\
&= \delta_3^R \delta_2^V \delta_1^V u_1(q_3) + \delta_3^V \delta_2^R \delta_1^R u_2(q_1, q_2) + \delta_3^R \delta_2^V \delta_1^R u_2(q_1, q_3) + \delta_3^V \delta_2^V \delta_1^V. \tag{4.72}
\end{aligned}$$

Written in this form, each \mathbf{B}_n is explicitly infra-red finite provided the measurement function is infra-red-collinear safe, and that the evolution is not convoluted with parton distribution or fragmentation functions. In this case μ can be safely taken to zero. In the case that the evolution is convoluted with parton distribution or fragmentation functions,

collinear poles remain (one for each hadron). These poles are removed by renormalisation of the parton distribution functions or fragmentation functions, generating their μ dependence. Finally, note that for recursively-infra-red-safe continuously-global observables [9] in e^+e^- collisions $\mathbf{B}_n = 0$ for $n \geq 1$ at single-log accuracy. If the observable depends on fragmentation functions the $n \geq 1$ contributions give rise to the DGLAP evolution of the fragmentation functions (see Section 4.4).

4.4 Collinear factorisation

Up to this point we have been interleaving the emission of soft and collinear partons to build up the complete amplitude. As is well known, it is possible to factorise the collinear emissions into the evolution of parton distribution and fragmentation functions. In this section, our aim is to explore collinear factorisation within the context of our algorithm.

The plan is as follows. First, we will derive the factorisation of collinear physics into jet functions; one for each parton in the initial hard process. At first we do this ignoring the presence of Coulomb exchanges. This result is sufficient to derive DGLAP evolution (which we do in Section 4.5). After this, we go on to construct the complete factorisation of collinear physics into jet functions on every hard or soft leg. Finally, we use a path-ordered expansion of our Sudakov operators, $\mathbf{V}_{a,b}$, to re-insert Coulomb exchanges one-by-one into the previous results. The result is that collinear evolution below the scale of the last Coulomb exchange can be factorised. The outcome of which is the general factorisation of collinear poles into parton distribution functions, as anticipated after the work of Collins, Soper and Sterman [33].

We provide diagrammatic proofs where possible and only sketch in the text the algebra that is going on behind the scenes. Throughout this section we leave aside the recoil functions $\mathfrak{R}^{\text{soft}}$, $\mathfrak{R}^{\text{coll}}$, and the integrals corresponding to the momentum maps between each iteration of the algorithm. This is to reduce the length of the algebra that remains, and it is certainly valid to LL_Σ accuracy since tracking longitudinal recoil is sufficiently simple. We also drop the inclusion of measurement functions since they too have no affect on the discussion. That said, in Sections 4.4.1.1 and 4.4.1.2, we present a summary of the results with all of these functions re-instated (for both of variants A and B).

4.4.1 Factorisation on hard legs without Coulomb interactions

The main result of this subsection is the factorisation of collinear physics into jet functions; one for each leg emerging from the hard scatter. We do this with Coulomb gluons removed ($\tilde{\delta}_{ij} = 0$) and will discuss their re-introduction in Section 4.4.3. The following manipulations can equally well be performed using either variant A or B of the algorithm. For concreteness

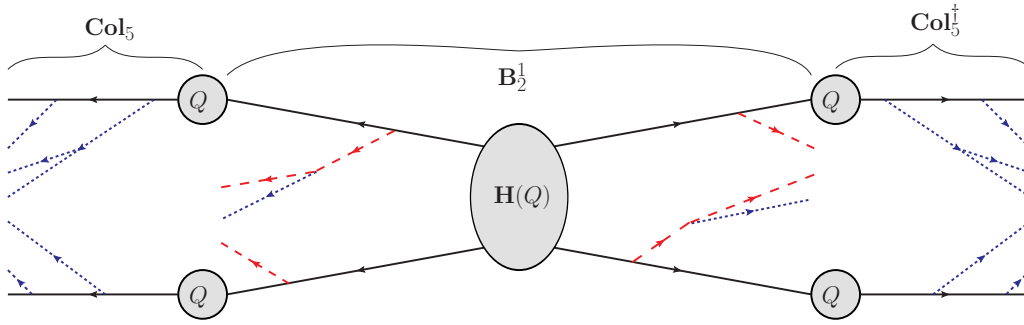


Figure 4.3: Illustrating hard-leg factorisation. Red dashed lines represent the emission of soft gluons and collinear emissions are represented by blue dotted lines. Circles indicate the hard scale from which subsequent evolution proceeds. Loops (Sudakov factors) have been neglected to avoid clutter.

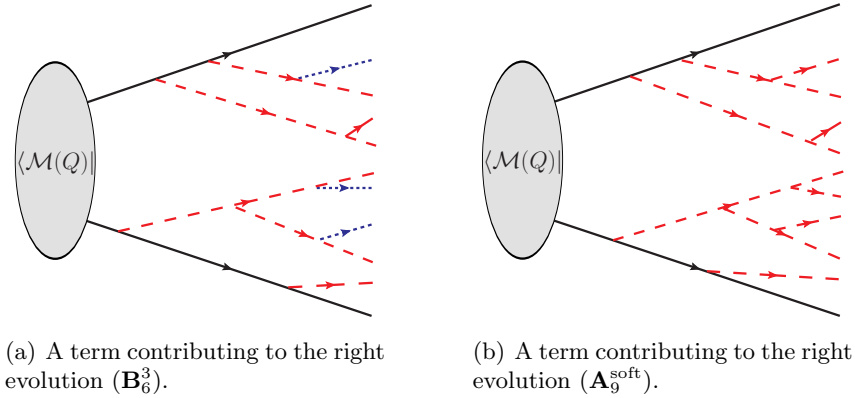


Figure 4.4: The right evolution (the evolution of the conjugate amplitude) of a hard process after 9 emissions. Red dashed lines represent the emission of soft gluons and collinear emissions are represented by blue dotted lines. Loops (Sudakov factors) have been neglected to avoid clutter.

we will use variant B whenever an operator needs to be given an explicit definition¹³. Let us begin by simply stating the result:

$$\Sigma(\mu) = \int \sum_n \left(\prod_{i=1}^n d\Pi_i \right) \sum_{m=0}^n \sum_{p=0}^{n-m} \text{Tr} \left(\mathbf{Col}_m^\dagger(\mu) \circ \mathbf{Col}_m(\mu) \mathbf{B}_{n-m-p}^p(\mu) \right). \quad (4.73)$$

Figure 4.3 illustrates what is going on diagrammatically (it shows a contribution with $n = 8$, $m = 5$ and $p = 1$). The collinear evolution operators for hard legs, which provide an operator description of a jet function, are constructed iteratively according to

$$\begin{aligned} \mathbf{Col}_0(q_\perp) &= \mathbf{V}_{q_\perp, Q}^{\text{col}}, \\ \mathbf{Col}_m(q_\perp) &= \mathbf{V}_{q_\perp, q_{m\perp}}^{\text{col}} \bar{\mathbf{C}}_m \mathbf{Col}_{m-1}(q_{m\perp}) \Theta(q_\perp \leq q_{m\perp}), \end{aligned} \quad (4.74)$$

¹³In the case of variant A, for the most part, all that must be done is exchange \mathbf{P}_{ij} and $\mathcal{P}_{v_i v_j}$ with the overlined versions $\bar{\mathbf{P}}_{ij}$ and $\bar{\mathcal{P}}_{v_i v_j}$.

where

$$\begin{aligned} \mathbf{V}_{a,b}^{\text{col}} &= \exp \left[-\frac{\alpha_s}{\pi} \sum_j \int_a^b \frac{dk_{\perp}^{(j\vec{n})}}{k_{\perp}^{(j\vec{n})}} \sum_v \mathbb{T}_j^{\vec{v}2} \int \frac{dz d\phi}{8\pi} \mathcal{P}_{vv_j}^{\circ} \right], \\ \bar{\mathbf{C}}_i &= \sum_j \frac{q_{i\perp}^{(j\vec{n})}}{2\sqrt{z_i}} \Delta_{ij} \mathbf{P}_{ij}. \end{aligned} \quad (4.75)$$

In both operators j sums only over hard partons. The circle operation, \circ , indicates the sharing of partons between $\mathbf{Col}_m(\mu)$ and $\mathbf{Col}_m^{\dagger}(\mu)$, i.e.

$$\mathbf{Col}_m(q_{\perp}) \circ \mathbf{Col}_m^{\dagger}(q_{\perp}) = \mathbf{V}_{q_{\perp}, q_{m\perp}}^{\text{col}} \bar{\mathbf{C}}_m \mathbf{Col}_{m-1}(q_{m\perp}) \circ \mathbf{Col}_{m-1}^{\dagger}(q_{m\perp}) \bar{\mathbf{C}}_m^{\dagger} \mathbf{V}_{q_{\perp}, q_{m\perp}}^{\text{col}\dagger}. \quad (4.76)$$

$\mathbf{B}_{n-m-p}^p(\mu)$ are the scattering matrices evolved using the algorithm, modified so that all collinear emissions from hard legs have been removed. Specifically,

$$\tilde{\mathbf{A}}_{n-m}(\mu) = \sum_{p=0}^{n-1} \mathbf{B}_{n-p-m}^p(\mu), \quad (4.77)$$

where $\tilde{\mathbf{A}}_{n-m}(\mu)$ is computed using (4.12) with the collinear evolution off hard legs removed, i.e. with the replacements $\mathbf{D}_i \mapsto \mathbf{D}_i - \bar{\mathbf{C}}_i$ and $\mathbf{V}_{a,b} \mapsto \mathbf{V}_{a,b}(\mathbf{V}_{a,b}^{\text{col}})^{-1}$. The number of collinear emissions not off hard legs is indexed by p and $n-p-m$ is the number of soft emissions (in equation (4.73), m is the number of collinear emissions off hard legs). An example term, contributing to $\mathbf{B}_6^3(\mu)$, is presented in Figure 4.4(a).

It may be helpful to contrast $\mathbf{B}_n^p(\mu)$ with scattering matrices evolved using the FKS algorithm [27]. We denote the FKS matrices as $\mathbf{A}_n^{\text{soft}}(\mu)$ and they can be evaluated using variant A with $\bar{\mathcal{P}}_{v_i v_j} = 0$; an example is shown in Figure 4.4(b). Note that $\mathbf{B}_n^0(\mu) \neq \mathbf{A}_n^{\text{soft}}(\mu)$ for $n \geq 1$ since $\mathbf{B}_n^0(\mu)$ still contains the collinear Sudakov factors ‘attached’ to soft partonic legs. Also note that $\mathbf{B}_0^0(\mu) = \mathbf{A}_0^{\text{soft}}(\mu)$ and $\mathbf{B}_0^i(\mu) = 0$ for all $i > 0$. In Section 4.4.2 we will generalise the arguments presented here so that we can factorise collinear physics into jet functions that multiply $\mathbf{A}_n^{\text{soft}}(\mu)$. However, in this section we will not make any further use of $\mathbf{A}_n^{\text{soft}}(\mu)$.

Equation (4.73) can be written more simply by combining the collinear evolution operators (which are proportional to unit operators in colour space) into a single cross-section level jet function, $\mathbf{Col}_m^{\dagger}(\mu) \circ \mathbf{Col}_m(\mu) = \mathbb{1} \otimes \mathbf{Col}_m(\mu)$. Doing this enables (4.73) to be written as

$$\Sigma(\mu)|_{u_n=1} = \int \sum_n \left(\prod_{i=1}^n d\Pi_i \right) \sum_{m=0}^n \sum_{p=0}^{n-m} \text{Tr}_s (\mathbf{Col}_m(\mu) \text{Tr}_c \mathbf{B}_{n-m-p}^p(\mu)), \quad (4.78)$$

where the traces are over colour, c , and helicity, s . However, we avoid working with collinear factorisation in this form because it does not apply when Coulomb exchanges are present.

Having stated the result, let us now proceed to show how it is derived. The following commutation relations are important:

$$\begin{aligned} [\mathbf{D}_i - \overline{\mathbf{C}}_i, \overline{\mathbf{C}}_j] &\simeq 0, & [\mathbf{V}_{a,b}(\mathbf{V}_{a,b}^{\text{col}})^{-1}, \overline{\mathbf{C}}_j] &\simeq 0, \\ [\mathbf{V}_{a,b}(\mathbf{V}_{a,b}^{\text{col}})^{-1}, \mathbf{V}_{c,d}^{\text{col}}] &\simeq 0, & [\mathbf{D}_i - \overline{\mathbf{C}}_i, \mathbf{V}_{a,b}^{\text{col}}] &\simeq 0. \end{aligned} \quad (4.79)$$

Here \simeq denotes equality when the operator acts on a matrix element, which is all we ever encounter.

$[\mathbf{V}_{a,b}(\mathbf{V}_{a,b}^{\text{col}})^{-1}, \mathbf{V}_{c,d}^{\text{col}}] \simeq 0$ and $[\mathbf{D}_i - \overline{\mathbf{C}}_i, \mathbf{V}_{a,b}^{\text{col}}] \simeq 0$ are trivial to show as $\mathbf{V}_{a,b}^{\text{col}}$ is proportional to the identity in colour-helicity space. Diagrammatically, proving

$$[\mathbf{V}_{a,b}(\mathbf{V}_{a,b}^{\text{col}})^{-1}, \mathbf{V}_{c,d}^{\text{col}}] \simeq 0$$

reduces to showing

$$\text{Diagrammatic equation (4.80)} \quad (4.80)$$

and $[\mathbf{D}_i - \overline{\mathbf{C}}_i, \mathbf{V}_{a,b}^{\text{col}}] \simeq 0$ to showing

$$\text{Diagrammatic equation (4.81)} \quad (4.81)$$

As ever, a red dashed line is used to represent a soft parton and a blue dotted line represents a collinear parton. The black dashed line indicates a cut (cut lines are on shell).

$[\mathbf{V}_{a,b}(\mathbf{V}_{a,b}^{\text{col}})^{-1}, \overline{\mathbf{C}}_j] \simeq 0$ and $[\mathbf{D}_i - \overline{\mathbf{C}}_i, \overline{\mathbf{C}}_j] \simeq 0$ can be shown by factorising kinematic factors from the colour and helicity operators, then carefully tracking the action of the colour operators so that colour conservation can be applied. Proving the commutators also requires noting that both soft real emissions and soft Sudakov factors are identity operators in helicity space, and that helicity states are orthogonal. $[\mathbf{V}_{a,b}(\mathbf{V}_{a,b}^{\text{col}})^{-1}, \overline{\mathbf{C}}_j] \simeq 0$ presents the biggest challenge. The derivation follows closely the discussion in [13]. It is most easily illustrated by expressing the operators diagrammatically. Doing so reduces the problem to

showing

$$\begin{aligned}
 & \langle \mathcal{M} | \text{[diagram 1]} + \langle \mathcal{M} | \text{[diagram 2]} + \langle \mathcal{M} | \text{[diagram 3]} \\
 &= \langle \mathcal{M} | \text{[diagram 4]} . \tag{4.82}
 \end{aligned}$$

Also note that

$$[\mathbf{V}_{a,b}(\mathbf{V}_{a,b}^{\text{col}})^{-1}, \bar{\mathbf{C}}_j] \simeq 0$$

implies $[\mathbf{D}_i - \bar{\mathbf{C}}_i, \bar{\mathbf{C}}_j] \simeq 0$ since

$$\langle \mathcal{M} | \text{[diagram 1]} + \langle \mathcal{M} | \text{[diagram 2]} = \langle \mathcal{M} | \text{[diagram 3]} , \tag{4.83}$$

which trivially follows from (4.82). Using these commutation relations, reconstructing the separate strong orderings of collinear and soft physics in (4.73) is simply a case of careful combinatorics and relabelling of momenta. For instance

$$\begin{aligned}
 & \left[\langle \mathcal{M} | \text{[diagram 1]} + \langle \mathcal{M} | \text{[diagram 2]} \right] \Theta(q_{j\perp} - q_{i\perp})\Theta(q_{i\perp} - \mu)\Theta(Q - q_{j\perp}) \\
 & + \langle \mathcal{M} | \text{[diagram 3]} \Theta(q_{i\perp} - q_{j\perp})\Theta(q_{j\perp} - \mu)\Theta(Q - q_{i\perp}) \\
 & = \langle \mathcal{M} | \text{[diagram 4]} \Theta(q_{i\perp} - \mu)\Theta(Q - q_{i\perp})\Theta(q_{j\perp} - \mu)\Theta(Q - q_{j\perp}). \tag{4.84}
 \end{aligned}$$

For the sake of completeness, in the next section we will go ahead and put back $\mathfrak{R}^{\text{soft}}$, $\mathfrak{R}^{\text{coll}}$, and the measurement functions. However, we have only proven correctness at LL_Σ accuracy. As such, Sections 4.4.1.1 and 4.4.1.2 are conjectures. It might be the case that only certain classes of recoil prescription factorise in this way. We will focus on variant A in

Section 4.4.1.1 and turn to variant B in Section 4.4.1.2, where we show how to re-instate the plus prescription in the collinear splitting functions. We caution that both these versions of the algorithm will not produce super-leading logarithms because Coulomb interactions have been neglected. Therefore they are only suitable for processes with fewer than two coloured particles in either the initial or final state of the hard process, i.e. e^+e^- , deep-inelastic scattering and Drell-Yan.

4.4.1.1 The details

Now we summarise the results of the previous section and make a conjecture regarding the inclusion of recoils (recall we left these out of the discussions in the previous section). For concreteness we use variant A. The evolution has two phases. In the first phase soft gluons are emitted:

$$\begin{aligned}
\sigma(0,0) &= \tilde{\mathbf{V}}_{\mu,Q} \mathbf{H}(Q; \{p\}) \tilde{\mathbf{V}}_{\mu,Q}^\dagger = \tilde{\mathbf{A}}_0(\mu; \{p\}), \\
\mathbf{d}\sigma(1,0) &= \int \prod_i d^4 p_i \tilde{\mathbf{V}}_{\mu,q_{1\perp}} \tilde{\mathbf{D}}_1 \tilde{\mathbf{A}}_0(q_{1\perp}; \{p\}) \tilde{\mathbf{D}}_1^\dagger \tilde{\mathbf{V}}_{\mu,q_{1\perp}}^\dagger d\Pi_1 \\
&= \tilde{\mathbf{A}}_1(\mu; \{p\}_1) d\Pi_1 \equiv \mathbf{B}_1^0(\mu; \{p\}_1) d\Pi_1, \\
\mathbf{d}\sigma(2,0) &= \int \prod_i d^4 p_i \tilde{\mathbf{V}}_{\mu,q_{2\perp}} \tilde{\mathbf{D}}_2 \tilde{\mathbf{A}}_1(q_{2\perp}; \{p\}) \tilde{\mathbf{D}}_2^\dagger \tilde{\mathbf{V}}_{\mu,q_{2\perp}}^\dagger d\Pi_1 d\Pi_2 \\
&= \tilde{\mathbf{A}}_2(\mu; \{p\}_2) d\Pi_1 d\Pi_2 \equiv (\mathbf{B}_2^0(\mu) + \mathbf{B}_1^1(\mu)) d\Pi_1 d\Pi_2, \\
\mathbf{d}\sigma(n,0) &= \tilde{\mathbf{A}}_n(\mu; \{p\}_n) \prod_{i=1}^n d\Pi_i \equiv \sum_{p=0}^n \mathbf{B}_{n-p}^p(\mu) \prod_{i=1}^n d\Pi_i, \tag{4.85}
\end{aligned}$$

where $\tilde{\mathbf{D}}_i = \mathbf{D}_i - \bar{\mathbf{C}}_i$ and

$$\bar{\mathbf{C}}_i = \sum_l \frac{q_{i\perp}^{(l\vec{n})}}{2\sqrt{z_i}} \Delta_{il} \bar{\mathbf{P}}_{il} \mathfrak{R}_{ij}^{\text{coll}}(\{p\}, \{\tilde{p}\}, q_i), \tag{4.86}$$

where l sums only over hard partons. And $\tilde{\mathbf{V}}_{a,b} = \mathbf{V}_{a,b}(\bar{\mathbf{V}}_{a,b})^{-1}$ and

$$\bar{\mathbf{V}}_{a,b} = \exp \left[-\frac{\alpha_s}{\pi} \sum_l \int_a^b \frac{dk_\perp^{(l\vec{n})}}{k_\perp^{(l\vec{n})}} \sum_v \mathbb{T}_l^{\bar{v}2} \int \frac{dz d\phi}{8\pi} \bar{\mathcal{P}}_{vv_l}^\circ \mathcal{R}_l^{\text{coll}} \right]. \tag{4.87}$$

Again, the sum over l only includes hard partons. In $\mathbf{d}\sigma(n,m)$, n indicates the number of soft emissions, which occur during the first phase of the evolution, and m indicates the number of collinear emissions, which occur during the second phase of the evolution.

The second phase of the evolution dresses the hard legs with collinear emissions:

$$\begin{aligned}
d\sigma(n, 0) &= \text{Tr} \left(\overline{\mathbf{V}}_{\mu, Q} d\sigma(n, 0) \overline{\mathbf{V}}_{\mu, Q}^\dagger \right) = \text{Tr} \left(\tilde{\mathbf{A}}_{n+0}^n(\mu; \{p\}_n) \right) \\
&\equiv \sum_{p=0}^n \text{Tr}(\mathbf{Col}_0^\dagger(\mu) \circ \mathbf{Col}_0(\mu) \mathbf{B}_{n-p}^p(\mu)), \\
d\sigma(n, 1) &= \int \prod_i d^4 p_i \text{Tr} \left(\overline{\mathbf{V}}_{\mu, q_{n+1\perp}} \overline{\mathbf{C}}_{n+1} \overline{\mathbf{V}}_{q_{n+1\perp}, Q} d\sigma(n, 0) \right. \\
&\quad \left. \times \overline{\mathbf{V}}_{q_{n+1\perp}, Q}^\dagger \overline{\mathbf{C}}_{n+1}^\dagger \overline{\mathbf{V}}_{\mu, q_{n+1\perp}}^\dagger \right) d\Pi_{n+1} = \text{Tr} \left(\tilde{\mathbf{A}}_{n+1}^n(\mu; \{p\}_{n+1}) \right) d\Pi_{n+1} \\
&\equiv \sum_{p=0}^n \text{Tr}(\mathbf{Col}_1^\dagger(\mu) \circ \mathbf{Col}_1(\mu) \mathbf{B}_{n-p}^p(\mu)) d\Pi_{n+1}, \\
d\sigma(n, m) &= \text{Tr} \left(\tilde{\mathbf{A}}_{n+m}^n(\mu; \{p\}_{n+m}) \right) \prod_{i=1}^m d\Pi_{n+i} \\
&\equiv \sum_{p=0}^n \text{Tr}(\mathbf{Col}_m^\dagger(\mu) \circ \mathbf{Col}_m(\mu) \mathbf{B}_{n-p}^p(\mu)) \prod_{i=1}^m d\Pi_{n+i}, \tag{4.88}
\end{aligned}$$

where $\tilde{\mathbf{A}}_{n+m}^n$ obeys the recurrence relation

$$\begin{aligned}
\tilde{\mathbf{A}}_{n+m}^n(q_\perp; \{\tilde{p}\}_{n+m-1} \cup q_{n+m}) &= \int \prod_i d^4 p_i \overline{\mathbf{V}}_{q_\perp, q_{n+m\perp}} \overline{\mathbf{C}}_{n+m} \tilde{\mathbf{A}}_{n+m-1}^n(q_{n+m\perp}; \{p\}_{n+m-1}) \\
&\quad \times \overline{\mathbf{C}}_{n+m}^\dagger \overline{\mathbf{V}}_{q_\perp, q_{n+m\perp}}^\dagger \Theta(q_\perp \leq q_{n+m\perp}).
\end{aligned}$$

An observable can be calculated using

$$\Sigma(\mu) = \sum_n \int d\sigma_n u_n(q_1, \dots, q_n), \tag{4.89}$$

where $d\sigma_n = \sum_{m=0}^n d\sigma(n-m, m)$.

4.4.1.2 Recovering the ‘plus prescription’

Now let us turn to variant B. Recall that, in this variant of the algorithm collinear evolution proceeds using the full DGLAP splitting functions. Things are precisely as in the last subsection except that we now use the splitting operators without overlines (\mathbf{P}_{il}) and the functions \mathfrak{f} and \mathcal{F} are to be included in the soft terms. We can go a little further and expand out the Sudakov factors in order to recover the familiar DGLAP plus prescription. To that end, we expand the collinear Sudakov factors ($\overline{\mathbf{V}}$) that appear in the second phase of the evolution:

$$\overline{\mathbf{V}}_{a,b} = \mathbb{1} - \int_a^b \frac{dk_{1\perp}}{k_{1\perp}} \Gamma_1 + \int_a^b \frac{dk_{2\perp}}{k_{2\perp}} \Gamma_1 \int_{k_1}^b \frac{dk_{2\perp}}{k_{2\perp}} \Gamma_2 - \dots \tag{4.90}$$

where

$$\Gamma_i = \frac{\alpha_s}{\pi} \sum_l \sum_v \mathbb{T}_l^{\bar{v}2} \int \frac{dz_i d\phi_i}{8\pi} \bar{\mathcal{P}}_{vv_i}^\circ \mathcal{R}_l^{\text{coll}}. \quad (4.91)$$

Once again, the sum over l is only over hard partons. Using this, we can regroup terms in the same way as Section 4.3.5 to generate the plus prescription:

$$\begin{aligned} d\sigma(n, 0) &= \text{Tr}(\mathbf{d}\sigma(n, 0)) = \text{Tr} \tilde{\mathbf{A}}_{n+0}^n, \\ d\sigma(n, 1) &= \int \prod_i d^4 p_i \text{Tr} \left(\bar{\mathbf{D}}_{n+1} \mathbf{d}\sigma(n, 0) \bar{\mathbf{D}}_{n+1}^\dagger \right) d\bar{\Pi}_{n+1} \\ &= \text{Tr} \tilde{\mathbf{A}}_{n+1}^n(\mu; \{p\}_{n+1}) d\bar{\Pi}_{n+1}, \\ d\sigma(n, m) &= \text{Tr} \tilde{\mathbf{A}}_{n+m}^n(\mu; \{p\}_{n+m}) \prod_{i=1}^m d\bar{\Pi}_{n+i} \\ &\equiv \sum_{p=0}^n \text{Tr} \left(\left[\mathbf{Col}_m^\dagger(\mu) \circ \mathbf{Col}_m(\mu) + \mathcal{O}(\alpha_s^{m+1}) \right] \mathbf{B}_{n-p}^p(\mu) \right) \prod_{i=1}^m d\bar{\Pi}_{n+i}, \end{aligned} \quad (4.92)$$

where

$$\tilde{\mathbf{A}}_{n+m}^n(q_\perp; \{\tilde{p}\}_{n+m-1} \cup q_{n+m}) = \bar{\mathbf{D}}_{n+m} \tilde{\mathbf{A}}_{n+m-1}^n(q_{n+m\perp}; \{p\}_{n+m-1}) \bar{\mathbf{D}}_{n+m}^\dagger \Theta(q_\perp \leq q_{n+m\perp}),$$

using the boundary condition that

$$\tilde{\mathbf{A}}_{n+1}^n(q_\perp) = \bar{\mathbf{D}}_{n+1} \tilde{\mathbf{A}}_{n+0}^n \bar{\mathbf{D}}_{n+1}^\dagger \Theta(q_\perp \leq q_{n+1\perp}) \Theta(q_{n+1\perp} \leq Q), \quad (4.93)$$

and

$$\bar{\mathbf{D}}_i = \sum_{\bar{l}} \frac{q_{i\perp}}{2} \Delta_{i\bar{l}} \mathbf{P}_{i\bar{l}}^+ \mathfrak{R}_{ij}^{\text{coll}}(\{p\}, \{\tilde{p}\}, q_i). \quad (4.94)$$

The sum over \bar{l} only includes hard partons. $\mathbf{P}_{i\bar{l}}$ has been redefined to include the plus prescription and labelled $\mathbf{P}_{i\bar{l}}^+$. The plus prescription is defined in Appendix 4.7. Observables are computed using (4.89).

4.4.2 Complete collinear factorisation without Coulomb interactions

Now we are going to go ahead and factorise the collinear physics completely. Once again, the manipulations are essentially the same for either variant of our algorithm. To be concrete, we will use variant B whenever an exact definition must be given. As before, we will begin by stating the final result:

$$\Sigma(\mu) = \int \sum_n \left(\prod_{i=1}^n d\Pi_i \right) \sum_{m=0}^n \text{Tr} \left(\mathbf{tCol}_m^\dagger(\mu) \circ \mathbf{tCol}_m(\mu) \mathbf{A}_{n-m}^{\text{soft}}(\mu) \right), \quad (4.95)$$

where have we defined the following operators:

$$\begin{aligned}
\mathbf{tCol}_0(q_\perp) &= \mathbf{V}_{q_\perp, Q}^{\text{tcol}}, \\
\mathbf{tCol}_m(q_\perp) &= \mathbf{V}_{q_\perp, q_{m\perp}}^{\text{tcol}} \tilde{\mathbf{C}}_m \mathbf{tCol}_{m-1}(q_{m\perp}) \Theta(q_\perp \leq q_{m\perp}), \\
\mathbf{V}_{a,b}^{\text{tcol}} &= \exp \left[-\frac{\alpha_s}{\pi} \sum_j \int_a^b \frac{dk_\perp^{(j\vec{n})}}{k_\perp^{(j\vec{n})}} \Theta(q_{i\perp}^{(j\vec{n})} \leq p_{j\perp}) \sum_v \mathbb{T}_j^{\bar{v}2} \int \frac{dz d\phi}{8\pi} \mathcal{P}_{vv_j}^\circ \right], \\
\tilde{\mathbf{C}}_i &= \sum_j \frac{q_{i\perp}^{(j\vec{n})}}{2\sqrt{z_i}} \Delta_{ij} \mathbf{P}_{ij} \Theta(q_{i\perp}^{(j\vec{n})} \leq p_{j\perp}),
\end{aligned} \tag{4.96}$$

and the index j runs over all partons (hard, collinear and soft). We continue to leave aside the functions $\mathfrak{R}^{\text{soft}}$, $\mathfrak{R}^{\text{coll}}$, from emission operators and Sudakov factors. These can readily be re-instated as in Sections 4.4.1.1 and 4.4.1.2. $\mathbf{A}_n^{\text{soft}}(\mu)$ is as defined in Section 4.4.1 and evolves the same as $\mathbf{A}_n(\mu)$ except that $\mathbf{C}_i \mapsto 0$ and $\mathbf{V}_{a,b} \mapsto \mathbf{V}_{a,b}(\mathbf{V}_{a,b}^{\text{tcol}})^{-1} \equiv \mathbf{V}_{a,b}^{\text{soft}}$, i.e. it corresponds to summing over diagrams such as the one in Figure 4.4(b). Ignoring the effects of recoil (and Coulomb exchanges) and using variant A, $\mathbf{A}_n^{\text{soft}}(\mu)$ corresponds to FKS evolution [27]. One of the possible contributions to \mathbf{tCol}_4^\dagger is represented in Figure 4.5. In the figure, we have sacrificed the intuitive picture of a parton cascade in lieu of providing more detail on the evolution. To construct Figure 4.5, we have employed the Casimir structure of $\mathbf{V}_{a,b}^{\text{tcol}}$ to split it apart as

$$\mathbf{V}_{a,b}^{\text{tcol}} = \prod_j \mathbf{U}_{a,b}^j$$

where

$$\mathbf{U}_{a,b}^j = \exp \left[-\frac{\alpha_s}{\pi} \int_a^b \frac{dk_\perp^{(j\vec{n})}}{k_\perp^{(j\vec{n})}} \Theta(q_{i\perp}^{(j\vec{n})} \leq p_{j\perp}) \sum_v \mathbb{T}_j^{\bar{v}2} \int \frac{dz d\phi}{8\pi} \mathcal{P}_{vv_j}^\circ \right], \tag{4.97}$$

and the product over j is over all partons. In the figures we will be explicit with the labelling so that it is clear whether $\mathbf{U}_{a,b}^j$ is associated with a hard parton (labelled by Q), a soft parton or a collinear parton, i.e. $j \in \{Q, 1^{\text{soft}}, 2^{\text{soft}}, \dots, (n-m)^{\text{soft}}, 1^{\text{coll}}, 2^{\text{coll}}, \dots, m^{\text{coll}}\}$. Something more in the style of our previous diagrams is illustrated in Figure 4.6.

We will now prove (4.95) by induction. First, we assume that

$$\text{Tr } \mathbf{A}_n(\mu) = \sum_{m=0}^n \text{Tr} \left(\mathbf{tCol}_m^\dagger(\mu) \circ \mathbf{tCol}_m(\mu) \mathbf{A}_{n-m}^{\text{soft}}(\mu) \right), \tag{4.98}$$

where \mathbf{A}_n is computed as usual from (4.12). We can see that this is true for $n = 1$ by

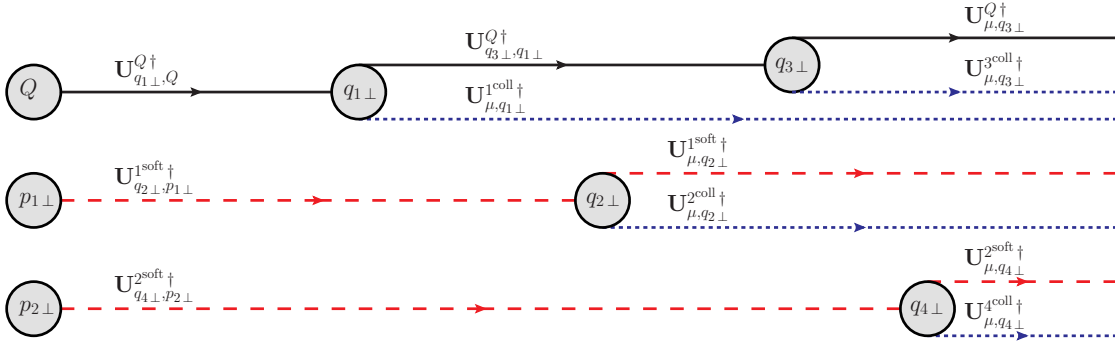


Figure 4.5: One of the possible contributions to \mathbf{tCol}_4^\dagger . Red dashed lines represent soft gluons and blue dotted lines represent collinear partons. Each line is associated with a Sudakov factor and circles indicate the scale from which the subsequent evolution proceeds. Circles from which two lines leave indicate the action of the operator $\tilde{\mathbf{C}}$. Circles from which one line leaves indicate the scales inherited from the soft evolution phase (not shown). Collinear scales $\{q_{i\perp}\}$ are ordered with respect to each other, as are soft scales $\{p_{i\perp}\}$. Scales connected along lines are also ordered, with the largest to the left and smallest to the right.

expanding out the \mathbf{tCol} operators and \mathbf{A}^{soft} :

$$\begin{aligned}
& \sum_{m=0}^1 \text{Tr} \left(\mathbf{tCol}_m^\dagger(\mu) \circ \mathbf{tCol}_m(\mu) \mathbf{A}_{n-m}^{\text{soft}}(\mu) \right) \\
&= \text{Tr} \left(\mathbf{V}_{\mu, q_{1\perp}}^{\text{tcol}} \tilde{\mathbf{C}}_1 \mathbf{V}_{q_{1\perp}, Q}^{\text{tcol}} \mathbf{V}_{\mu, Q}^{\text{soft}} \mathbf{H}(Q) \mathbf{V}_{\mu, Q}^{\text{soft}\dagger} \mathbf{V}_{q_{1\perp}, Q}^{\text{tcol}\dagger} \tilde{\mathbf{C}}_1^\dagger \mathbf{V}_{\mu, q_{1\perp}}^{\text{tcol}\dagger} \right. \\
&\quad \left. + \mathbf{V}_{\mu, Q}^{\text{tcol}} \mathbf{V}_{\mu, q_{1\perp}}^{\text{soft}} \mathbf{S}_1 \mathbf{V}_{q_{1\perp}, Q}^{\text{soft}} \mathbf{H}(Q) \mathbf{V}_{q_{1\perp}, Q}^{\text{soft}\dagger} \mathbf{S}_1^\dagger \mathbf{V}_{\mu, q_{1\perp}}^{\text{soft}\dagger} \mathbf{V}_{\mu, Q}^{\text{tcol}\dagger} \right) \\
&= \text{Tr} \left(\mathbf{V}_{\mu, q_{1\perp}}^{\text{soft}} \mathbf{V}_{\mu, q_{1\perp}}^{\text{tcol}} \mathbf{C}_1 \mathbf{V}_{q_{1\perp}, Q}^{\text{tcol}} \mathbf{V}_{q_{1\perp}, Q}^{\text{soft}} \mathbf{H}(Q) \mathbf{V}_{\mu, Q}^{\text{soft}\dagger} \mathbf{V}_{q_{1\perp}, Q}^{\text{tcol}\dagger} \mathbf{C}_1^\dagger \mathbf{V}_{\mu, q_{1\perp}}^{\text{tcol}\dagger} \right. \\
&\quad \left. + \mathbf{U}_{\mu, q_{1\perp}}^1 \mathbf{V}_{\mu, q_{1\perp}}^{\text{col}} \mathbf{V}_{\mu, q_{1\perp}}^{\text{soft}} \mathbf{S}_1 \mathbf{V}_{q_{1\perp}, Q}^{\text{col}} \mathbf{V}_{q_{1\perp}, Q}^{\text{soft}} \mathbf{H}(Q) \mathbf{V}_{q_{1\perp}, Q}^{\text{soft}\dagger} \mathbf{S}_1^\dagger \mathbf{V}_{\mu, q_{1\perp}}^{\text{soft}\dagger} \mathbf{V}_{\mu, Q}^{\text{tcol}\dagger} \right) \\
&= \text{Tr} \left(\mathbf{V}_{\mu, q_{1\perp}} \mathbf{D}_1 \mathbf{V}_{q_{1\perp}, Q} \mathbf{H}(Q) \mathbf{V}_{q_{1\perp}, Q}^\dagger \mathbf{D}_1^\dagger \mathbf{V}_{\mu, q_{1\perp}}^\dagger \right), \tag{4.99}
\end{aligned}$$

where we have used $\tilde{\mathbf{C}}_1 \equiv \bar{\mathbf{C}}_1 \equiv \mathbf{C}_1$ as it only acts on hard legs. We have also used the commutators $[\mathbf{V}_{a,b}(\mathbf{V}_{a,b}^{\text{col}})^{-1}, \mathbf{V}_{c,d}^{\text{col}}] \simeq 0$ and $[\mathbf{V}_{a,b}(\mathbf{V}_{a,b}^{\text{col}})^{-1}, \bar{\mathbf{C}}_j] \simeq 0$, derived in the previous section, and $\mathbf{V}_{c,a} = \mathbf{V}_{c,b} \mathbf{V}_{b,a}$. Notice in the above expressions the theta functions present in $\tilde{\mathbf{C}}_1$ and $\mathbf{V}_{q_{1\perp}, Q}^{\text{tcol}}$ are always unity on hard legs as the ordering guarantees their argument is satisfied. We will now show that if (4.98) is true for \mathbf{A}_n , it is also true for \mathbf{A}_{n+1} . We begin by noting that from the Markovian way our algorithm evolves, we can write $\mathbf{A}_{n+1} \equiv \hat{\mathbf{A}}_n(\mu, q_{1\perp})$ where $\hat{\mathbf{A}}_n(\mu, q_{1\perp})$ is computed using our algorithm (as described in (4.12)) however with the evolution initiated by $\hat{\mathbf{H}}(q_{1\perp}) = \mathbf{D}_1 \mathbf{V}_{q_{1\perp}, Q} \mathbf{H}(Q) \mathbf{V}_{q_{1\perp}, Q}^\dagger \mathbf{D}_1^\dagger$ and

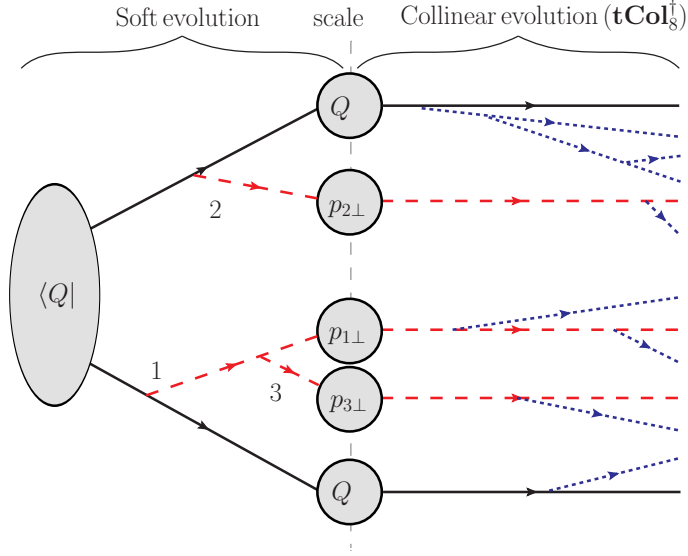


Figure 4.6: A diagram illustrating factorised parton evolution. Red dashed lines represent the emission of soft gluons and blue dotted lines represent collinear emissions. Circles represent the hard scale from which the subsequent evolution proceeds. Loops (Sudakov factors) have not been drawn.

with the parton momentum indexed as 2, 3, 4, From this we can use (4.98) to write

$$\text{Tr } \mathbf{A}_{n+1}(\mu) = \text{Tr } \hat{\mathbf{A}}_n(\mu, q_{1\perp}) = \sum_{m=0}^n \text{Tr} \left(\mathbf{t}\hat{\mathbf{C}}\mathbf{ol}_m^\dagger(\mu, q_{1\perp}) \circ \mathbf{t}\hat{\mathbf{C}}\mathbf{ol}_m(\mu, q_{1\perp}) \hat{\mathbf{A}}_{n-m}^{\text{soft}}(\mu, q_{1\perp}) \right), \quad (4.100)$$

where $\hat{\mathbf{A}}_{n-m}^{\text{soft}}(\mu, q_{1\perp})$ are generated by the same algorithm as $\mathbf{A}_{n-m}^{\text{soft}}(\mu)$ however using $\hat{\mathbf{H}}(q_{1\perp})$ as the initial condition. $\mathbf{t}\hat{\mathbf{C}}\mathbf{ol}_m(\mu, q_{1\perp})$ are generated using the iterative relation in (4.96) but with an initial condition $\mathbf{t}\hat{\mathbf{C}}\mathbf{ol}_0(q_{1\perp}, q_{1\perp}) = \mathbf{V}_{q_{1\perp}, q_{1\perp}}^{\text{tcol}}$. Next we split apart $\hat{\mathbf{H}}(q_{1\perp})$ as

$$\begin{aligned} \hat{\mathbf{H}}(q_{1\perp}) = & \mathbf{S}_1 \mathbf{V}_{q_{1\perp}, Q}^{\text{tcol}} \mathbf{V}_{q_{1\perp}, Q}^{\text{soft}} \mathbf{H}(Q) \mathbf{V}_{q_{1\perp}, Q}^{\text{soft}\dagger} \mathbf{V}_{q_{1\perp}, Q}^{\text{tcol}\dagger} \mathbf{S}_1^\dagger \\ & + \tilde{\mathbf{C}}_1 \mathbf{V}_{q_{1\perp}, Q}^{\text{tcol}} \mathbf{V}_{q_{1\perp}, Q}^{\text{soft}} \mathbf{H}(Q) \mathbf{V}_{q_{1\perp}, Q}^{\text{soft}\dagger} \mathbf{V}_{q_{1\perp}, Q}^{\text{tcol}\dagger} \tilde{\mathbf{C}}_1^\dagger. \end{aligned} \quad (4.101)$$

Using the commutation relations from Section 4.4.1, we can move the collinear operators in $\hat{\mathbf{H}}(q_{1\perp})$ past the soft operators which construct $\hat{\mathbf{A}}_{n-m}^{\text{soft}}(\mu, q_{1\perp})$ to arrive at

$$\begin{aligned} \text{Tr } \mathbf{A}_{n+1}(\mu) = & \sum_{m=0}^n \text{Tr} \left(\mathbf{V}_{q_{1\perp}, Q}^{\text{tcol}\dagger} \mathbf{t}\hat{\mathbf{C}}\mathbf{ol}_m^\dagger(\mu, q_{1\perp}) \circ \mathbf{t}\hat{\mathbf{C}}\mathbf{ol}_m(\mu, q_{1\perp}) \mathbf{V}_{q_{1\perp}, Q}^{\text{tcol}} \mathbf{A}_{n+1-m}^{\text{soft}}(\mu, Q) \right) \\ & + \sum_{m=0}^n \text{Tr} \left(\mathbf{V}_{q_{1\perp}, Q}^{\text{tcol}\dagger} \tilde{\mathbf{C}}_1^\dagger \mathbf{t}\hat{\mathbf{C}}\mathbf{ol}_m^\dagger(\mu, q_{1\perp}) \circ \mathbf{t}\hat{\mathbf{C}}\mathbf{ol}_m(\mu, q_{1\perp}) \tilde{\mathbf{C}}_1 \mathbf{V}_{q_{1\perp}, Q}^{\text{tcol}} \mathbf{A}_{n-m}^{\text{soft}}(\mu, Q) \right). \end{aligned} \quad (4.102)$$

We can now combine the collinear operators using

$$\mathbf{t}\hat{\mathbf{C}}\mathbf{ol}_m(\mu, q_{1\perp}) \tilde{\mathbf{C}}_1 \mathbf{V}_{q_{1\perp}, Q}^{\text{tcol}} = \mathbf{t}\mathbf{C}\mathbf{ol}_{m+1}(\mu) \theta(q_{1\perp}^{\text{coll}} > q_{1\perp}^{\text{soft}})$$

and

$$\mathbf{t}\hat{\mathbf{C}}\mathbf{ol}_m(\mu, q_{1\perp})\mathbf{V}_{q_{1\perp}, Q}^{\text{tcol}} = \mathbf{t}\mathbf{C}\mathbf{ol}_m(\mu)\theta(q_{1\perp}^{\text{coll}} < q_{1\perp}^{\text{soft}}),$$

where in the second equality we need to relabel the momenta of collinear partons again so that they are indexed as 1, 2, 3, ... We have denoted the momentum of the hardest collinear emission generated by the collinear operators, $\mathbf{t}\mathbf{C}\mathbf{ol}$, as $q_{1\perp}^{\text{coll}}$ and the hardest soft momentum in $\mathbf{A}_{n-m}^{\text{soft}}(\mu, Q)$ as $q_{1\perp}^{\text{soft}}$. Combining the two sums and theta functions, we arrive at

$$\text{Tr } \mathbf{A}_{n+1}(\mu) = \sum_{m=0}^{n+1} \text{Tr} \left(\mathbf{t}\mathbf{C}\mathbf{ol}_m^\dagger(\mu) \circ \mathbf{t}\mathbf{C}\mathbf{ol}_m(\mu) \mathbf{A}_{n+1-m}^{\text{soft}}(\mu) \right). \quad (4.103)$$

Thus we have proven that (4.95) holds for $n \rightarrow n+1$. It is important to note the role of the theta functions in the definitions of $\tilde{\mathbf{C}}_i$ and $\mathbf{V}_{a,b}^{\text{tcol}}$. These ensure that the commutation relations from Section 4.4.1 can always be applied. They do this by squeezing to zero the phase space of any collinear partons generated by $\tilde{\mathbf{C}}_1$ and $\mathbf{V}_{q_{1\perp}, Q}^{\text{tcol}}$ from not-hard legs. To illustrate this point, we will consider the relevant Feynman diagrams:

$$\begin{aligned} & \left[\begin{array}{c} \langle \mathcal{M} | \text{---} \text{---} \text{---} | \mathcal{M} \rangle + \langle \mathcal{M} | \text{---} \text{---} \text{---} | \mathcal{M} \rangle \end{array} \right] \Theta(q_{j\perp} - q_{i\perp})\Theta(q_{i\perp} - \mu)\Theta(Q - q_{j\perp}) \\ & + \left[\begin{array}{c} \langle \mathcal{M} | \text{---} \text{---} \text{---} | \mathcal{M} \rangle + \langle \mathcal{M} | \text{---} \text{---} \text{---} | \mathcal{M} \rangle \end{array} \right] \Theta(q_{i\perp} - q_{j\perp})\Theta(q_{j\perp} - \mu)\Theta(Q - q_{i\perp}) \\ & = \langle \mathcal{M} | \text{---} \text{---} \text{---} | \mathcal{M} \rangle \Theta(q_{i\perp} - \mu)\Theta(Q - q_{i\perp})\Theta(q_{j\perp} - \mu)\Theta(Q - q_{j\perp}) \\ & + \langle \mathcal{M} | \text{---} \text{---} \text{---} | \mathcal{M} \rangle \Theta(q_{i\perp} - q_{j\perp})\Theta(q_{j\perp} - \mu)\Theta(Q - q_{i\perp}). \end{aligned} \quad (4.104)$$

Note that the last term on either side of the equation cannot be manipulated using our commutators and there are no more diagrams we could include which they may cancel against. Nevertheless terms of this form are generated by our algorithm. They represent a collinear parton, emitted from a soft parton, restricted so that its transverse momentum is smaller than the transverse momentum of the soft parton. Using $\tilde{\mathbf{C}}_i$, equation (4.104) reduces to

$$\begin{aligned} & \langle \mathcal{M} | \mathbf{D}_1^\dagger \mathbf{D}_2^\dagger \mathbf{D}_2 \mathbf{D}_1 | \mathcal{M} \rangle \Theta(q_{1\perp} - q_{2\perp})\Theta(q_{2\perp} - \mu)\Theta(Q - q_{1\perp}) \\ & = \langle \mathcal{M} | \mathbf{S}_1^\dagger \tilde{\mathbf{C}}_2^\dagger \tilde{\mathbf{C}}_2 \mathbf{S}_1 | \mathcal{M} \rangle \Theta(Q > q_{1\perp} > \mu)\Theta(Q > q_{2\perp} > \mu). \end{aligned} \quad (4.105)$$

4.4.3 Partial collinear factorisation with Coulomb interactions

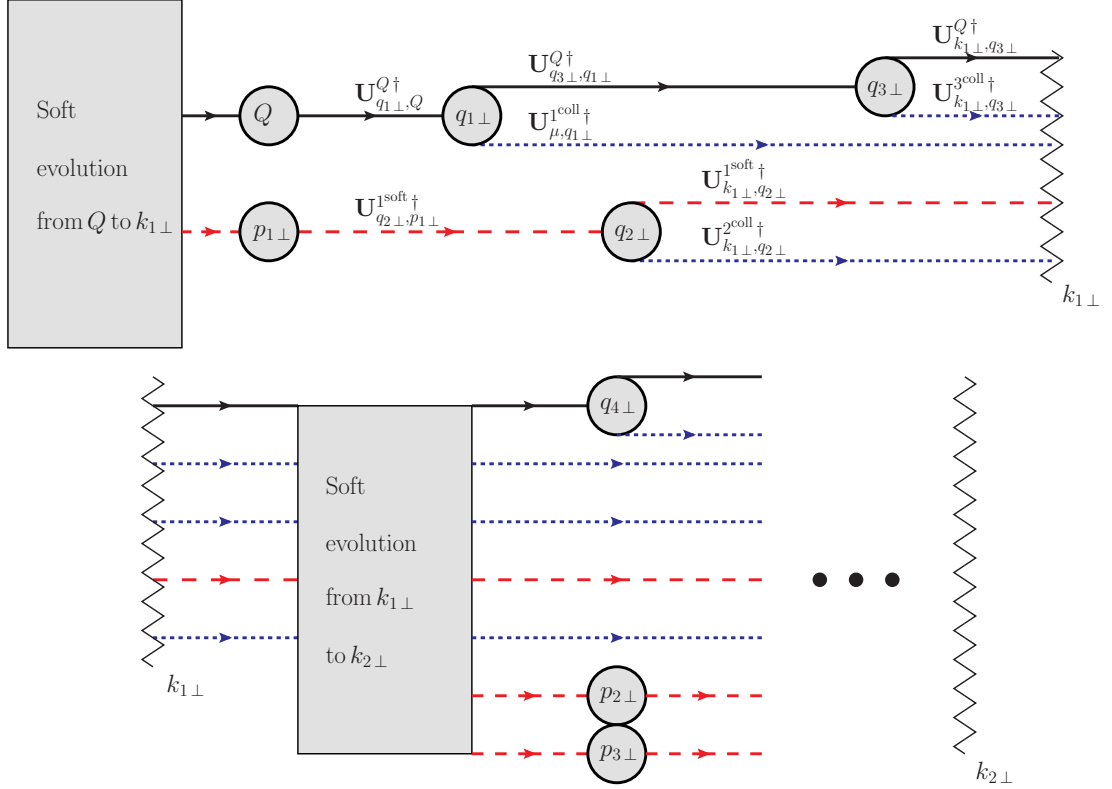


Figure 4.7: A diagram illustrating factorised parton evolution including Coulomb exchanges. Red dashed lines represent soft gluons and blue dotted lines represent collinear partons. Each line is associated with a Sudakov factor. Circles represent the scale from which the subsequent evolution proceeds. Circles from which two lines leave represent the action of the operator $\tilde{\mathbf{C}}$. Circles from which one line leaves contain the scale information from the preceding soft evolution. Coulomb exchanges are indicated by vertical zig-zag lines. Momenta are ordered from ‘left to right’, as in Figure 4.5, including Coulomb exchanges. (The top half of the diagram lies to the ‘left’ of the bottom half.)

Though it is not possible to use the identities in (4.79) to factorise collinear physics past a Coulomb exchange ($i\pi$ term), it is possible to perform a partial factorisation. Our approach is to expand each Sudakov operator as a series in the number of Coulomb exchanges it resums. Consequently, this enables \mathbf{A}_n to be expanded as a series in the number of Coulomb exchanges. We can then factorise soft physics from collinear physics either side of a Coulomb exchange, using our work in the previous section. The partial factorisation is illustrated in

Figure 4.7. We begin by expanding the Sudakov operator:

$$\begin{aligned}
\mathbf{V}_{a,b} = & \hat{\mathbf{V}}_{a,b} - \frac{\alpha_s}{\pi} \sum_{i_1 < j_1} \int_a^b \frac{dk_{1\perp}^{(i_1 j_1)}}{k_{1\perp}^{(i_1 j_1)}} \hat{\mathbf{V}}_{a,k_{1\perp}}(\mathbb{T}_{i_1}^g \cdot \mathbb{T}_{j_1}^g) i\pi \tilde{\delta}_{i_1 j_1} \hat{\mathbf{V}}_{k_{1\perp},b} \\
& + \left(\frac{\alpha_s}{\pi}\right)^2 \sum_{i_2 < j_2} \int_a^b \frac{dk_{1\perp}^{(i_1 j_1)}}{k_{1\perp}^{(i_1 j_1)}} \sum_{i_1 < j_1} \int_a^{k_{1\perp}^{(i_1 j_1)}} \frac{dk_{2\perp}^{(i_2 j_2)}}{k_{2\perp}^{(i_2 j_2)}} \hat{\mathbf{V}}_{a,k_{2\perp}}(\mathbb{T}_{i_2}^g \cdot \mathbb{T}_{j_2}^g) i\pi \tilde{\delta}_{i_2 j_2} \\
& \quad \times \hat{\mathbf{V}}_{k_{2\perp},k_{1\perp}}(\mathbb{T}_{i_1}^g \cdot \mathbb{T}_{j_1}^g) i\pi \tilde{\delta}_{i_1 j_1} \hat{\mathbf{V}}_{k_{1\perp},b} - \dots, \tag{4.106}
\end{aligned}$$

where $\hat{\mathbf{V}}_{a,b}$ is equal to $\mathbf{V}_{a,b}$ with $\tilde{\delta}_{ij} = 0$. Consider using this expanded Sudakov in a parton cascade. The theta functions describing the integral limits on each $i\pi$ term can be used to constrain the limits on the transverse momenta of subsequent emissions (after the $i\pi$). For instance

$$\begin{aligned}
& \mathbf{D}_3 \mathbf{V}_{q_{3\perp}, q_{2\perp}} \mathbf{D}_2 \mathbf{V}_{q_{2\perp}, q_{1\perp}} \mathbf{D}_1 \\
& = \dots + \mathbf{D}_3 \int_{q_{3\perp}}^{q_{2\perp}} \frac{dk_{2\perp}}{k_{2\perp}} \hat{\mathbf{V}}_{q_{3\perp}, k_{2\perp}} \sum_{i_2 < j_2} (\mathbb{T}_{i_2}^g \cdot \mathbb{T}_{j_2}^g) i\pi \hat{\mathbf{V}}_{k_{2\perp}, q_{2\perp}} \\
& \quad \times \mathbf{D}_2 \int_{q_{2\perp}}^{q_{1\perp}} \frac{dk_{1\perp}}{k_{1\perp}} \hat{\mathbf{V}}_{q_{2\perp}, k_{1\perp}} \sum_{i_1 < j_1} (\mathbb{T}_{i_1}^g \cdot \mathbb{T}_{j_1}^g) i\pi \hat{\mathbf{V}}_{k_{1\perp}, q_{1\perp}} \mathbf{D}_1 + \dots, \\
& \equiv \dots + \mathbf{D}_3 \int_{\mu}^Q \frac{dk_{2\perp}}{k_{2\perp}} \hat{\mathbf{V}}_{q_{3\perp}, k_{2\perp}} \sum_{i_2 < j_2} (\mathbb{T}_{i_2}^g \cdot \mathbb{T}_{j_2}^g) i\pi \hat{\mathbf{V}}_{k_{2\perp}, q_{2\perp}} \\
& \quad \times \mathbf{D}_2 \int_{\mu}^Q \frac{dk_{1\perp}}{k_{1\perp}} \hat{\mathbf{V}}_{q_{2\perp}, k_{1\perp}} \sum_{i_1 < j_1} (\mathbb{T}_{i_1}^g \cdot \mathbb{T}_{j_1}^g) i\pi \hat{\mathbf{V}}_{k_{1\perp}, q_{1\perp}} \mathbf{D}_1 \\
& \quad \times \Theta(k_{2\perp} > q_{3\perp}) \Theta(k_{1\perp} > q_{2\perp} > k_{1\perp}) \Theta(q_{1\perp} > k_{1\perp}) + \dots. \tag{4.107}
\end{aligned}$$

Therefore, we can treat each Coulomb scale as hard relative to the emissions that follow it and soft relative to the emission before it. Thus we can perform a factorised evolution on a hard process up to the scale of the first $i\pi$ term ($k_{1\perp}$). We can take the output from this evolution,

$$\begin{aligned}
\sum_n \mathbf{A}_n(k_{1\perp}) = & -\frac{\alpha_s}{\pi} \sum_{i_2 < j_2} \frac{dk_{1\perp}^{(i_1 j_1)}}{k_{1\perp}^{(i_1 j_1)}} i\pi \tilde{\delta}_{i_1 j_1} \sum_n \sum_{m=0}^n \\
& \times \text{Tr} \left(\mathbf{A}_{n-m}^{\text{soft}}(k_{1\perp}) \sum_{i_1 < j_1} \mathbf{Col}_m^\dagger(k_{1\perp}) \circ (\mathbb{T}_{i_1}^g \cdot \mathbb{T}_{j_1}^g) \mathbf{Col}_m(k_{1\perp}) \right), \tag{4.108}
\end{aligned}$$

and use it as a new hard process $\mathbf{H}(k_{1\perp})$ from which a second factorised evolution can be initiated. This process can be iterated for each $i\pi$ term in the expansion, as illustrated in Figure 4.7. To complete the computation of Σ , each $k_{i\perp}$ must be integrated over the range $[\mu, Q]$. Interestingly, note that any term in the evolution terminating on a $i\pi$ term to the

left of the hard process will cancel against an equivalent term terminating with an $i\pi$ term to the right. Hence collinear emissions can always be factorized below the scale of the last Coulomb exchange. This is consistent with the collinear factorisation shown by Collins, Soper and Sterman [32, 33].

4.4.4 Observations on factorisation

Before we leave our discussion on factorisation a few comments are in order. Firstly, we have not been able to achieve factorisation of collinear emissions past Coulomb exchanges. This is to be expected and there is already extensive literature exploring this subject [13, 15, 16, 33, 47–51]. That said, it should be possible to factorise more completely than we have done, by re-expressing the evolution so that all Coulomb terms are only attached to the initial state partons [16], i.e. so we would have complete factorisation on all final state legs.

Secondly, in order to factorise the collinear physics on all legs we had to keep track of intermediate soft scales, from which to initialise the collinear evolution. The number of scales required is equal to the number of soft emissions that occurred prior to factorisation. This means the fully factorised algorithm is no-longer Markovian. We anticipate that our attempts to factorise the collinear physics should bring us in to contact with exact resummations and soft-collinear effective theory (SCET).

It also should be noted that by factorising collinear emissions from the soft evolution, the soft evolution can be explicitly seen to be independent of spin. This is less evident in the interleaved variants of the algorithm. Soft gluons, and subsequent collinear partons, trapped between Coulomb exchanges might conceivably contribute non-trivial spin correlations. This is because, despite equal probabilities for the probability of emission of positive and negative helicity gluons, a collinear emission originating from a soft gluon may depend on its helicity (specifically $g \rightarrow qq$ splitting). This has also been explored in the literature, where it has been noted that soft gluons in the presence of Coulomb/Glauber exchanges can generate spin asymmetries [50]. Further discussions on the spin evolution of the algorithm after factorisation can be found in Appendix 4.8.

It is also interesting to consider the consequences of factorisation in the case of variant B with a universal recoil. A universal recoil allows B to be partitioned in terms of colour-diagonal evolution generated by \mathbf{C}_i and colour off-diagonal evolution generated by \mathbf{S}_i . Hence, provided the recoil prescription does not change the commutators in (4.79), the proofs of collinear factorisation we have presented become proofs of the complete factorisation of colour-diagonal physics from colour off-diagonal. This is for observables insensitive to the presence of Coulomb exchanges. Since we know that Coulomb exchanges can be

factorised onto the initial state [16], this means that there is a complete factorisation of colour-diagonal from colour off-diagonal physics in lepton-lepton, deep-inelastic and Drell-Yan scattering.

Finally, we should remark that it is possible to write down infra-red finite versions of each of the factorised versions of our algorithm, using the procedure in Section 4.3.5.

4.5 Phenomenology and resummations

In this section we will first demonstrate how DGLAP evolution emerges. After that, we illustrate the use of the algorithm by calculating thrust at LL_Σ accuracy, the hemisphere jet mass and gaps-between-jets in e^+e^- at LL_Σ with the leading non-global logarithms.

4.5.1 DGLAP evolution

We will now show how our algorithm can be used to generate DGLAP evolution, which resums the collinear physics into the running of parton distribution functions. We focus on unpolarised incoming hadrons that collide and produce some high- p_T system of interest. We will neglect threshold effects as sub-leading, which is shown carefully in [52–54]. The methods employed in this section can readily be extended to other processes, including those dependent on fragmentation functions.

DGLAP evolution [36, 38] states that

$$\mu \frac{\partial f_i(x, \mu)}{\partial \mu} = \frac{\alpha_s}{\pi} \sum_j \int_x^1 \frac{dz}{z} P_{ij}(z) f_j(x/z, \mu), \quad (4.109)$$

where $f_i(x, \mu)$ is the parton distribution function for partons of type i . $P_{ij}(z)$ are the regularised splitting functions defined at the end of Appendix 4.7. Iterative solutions can be found by expanding the parton distributions:

$$f_i(x, Q) = f_i^{(0)}(x) + \sum_{n=1}^{\infty} \left(\frac{\alpha_s}{\pi}\right)^n f_i^{(n)}(x, Q), \quad (4.110)$$

where $f_i^{(n)}(x, \mu) = 0$ for all $n \geq 1$. This gives

$$f_i^{(n+1)}(x, q_{m-1\perp}) = \int_{\mu}^{q_{m-1\perp}} \frac{dq_{m\perp}}{q_{m\perp}} \sum_j \int_x^1 \frac{dz_m}{z_m} P_{ij}(z_m) f_j^{(n)}(x/z_m, q_{m\perp}), \quad (4.111)$$

which has a separable solution of the form $f_i^{(n)}(x, Q) = f_i^{(n)}(x) \frac{1}{n!} \ln^n(Q/\mu)$, where $f_i^{(n)}(x)$ satisfies

$$f_i^{(n+1)}(x) = \sum_j \int_x^1 \frac{dz_m}{z_m} P_{ij}(z_m) f_j^{(n)}(x/z_m). \quad (4.112)$$

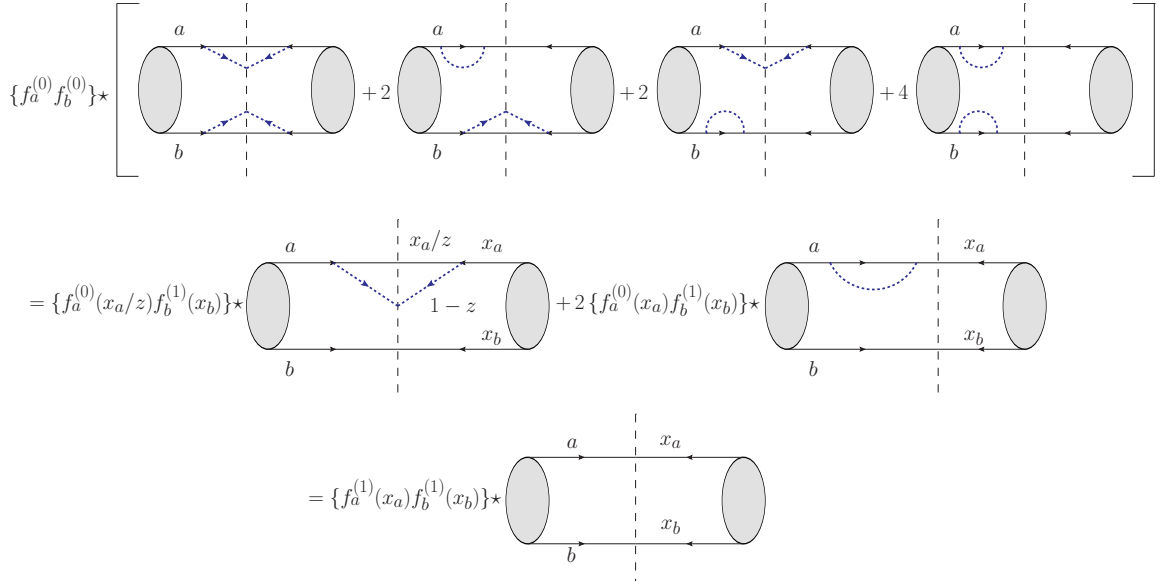


Figure 4.8: How DGLAP and fragmentation evolution can be constructed from the α_s expansion of our algorithm. The vertical dashed lines here correspond to a cut on all external legs (incoming and outgoing) and the grey blobs represent the hard process, i.e. the amplitude evolves from the right grey blob to the vertical dashed line and the conjugate amplitude evolves from the left grey blob to the vertical dashed line. Solid lines indicate hard partons and blue lines collinear partons.

We can write this in terms of the unregularised splitting functions (e.g. see [38])

$$f_i^{(n+1)}(x) = \sum_j \int_0^1 \frac{dz_m}{z_m} \left(\mathcal{P}_{ij}(z_m) f_j^{(n)}(x/z_m) - z_m^2 \mathcal{P}_{ji}(z_m) f_i^{(n)}(x) \right), \quad (4.113)$$

where $f_j^{(n)}(x) = 0$ for $x > 1$ and we have removed factors of n_f from \mathcal{P}_{qg} .

For hadron-hadron collisions, we label the two incoming partons as a and b and their momentum fractions in the hard process as x_a and x_b . We can take the factorised expression corresponding to variant B of our algorithm (4.73) and attach parton distribution functions:

$$\begin{aligned} \Sigma = \int \sum_n \left(\prod_{i=1}^n d\Pi_i \right) \sum_{m=0}^n \sum_{p=0}^{n-m} \int dx_a dx_b \text{Tr} \left(\mathbf{Col}_m^\dagger(\mu) \circ \mathbf{Col}_m(\mu) \right. \\ \left. \times \mathbf{B}_{n-m-p}^p(\mu) \right) \star \left\{ f_a^{(0)}(x_{a_m}) f_b^{(0)}(x_{b_m}) \right\}. \end{aligned} \quad (4.114)$$

x_{a_m} and x_{b_m} are the momentum fractions of partons a and b respectively after m collinear emissions generated by $\mathbf{Col}_m^\dagger(\mu) \circ \mathbf{Col}_m(\mu)$; they can be related back to x_a and x_b by momentum conservation along the collinear cascade. The \star operator acts to attach parton distributions of the correct flavour/species to partons a and b . There is a technicality relating to parton flavour. That is because DGLAP evolution cares about quark flavour

whilst we have defined the splitting operators to sum over quark flavours (in the case $g \rightarrow q\bar{q}$). We could have avoided this technicality by defining the splitting operators per flavour (i.e. set $n_f = 1$ throughout Appendix 4.7). Then we would have to sum over quark flavours throughout the rest of the paper. Instead, we choose to handle quark flavour by keeping track of flavour along the evolution chain, and whenever a $g \rightarrow q\bar{q}$ splitting occurs we label the subsequent parton flavour generically, i.e. for two-flavours the relevant set of parton flavours would be $\{u, \bar{u}, d, \bar{d}, q, g\}$. Note that since we evolve *away from* the hard scattering, a $g \rightarrow q\bar{q}$ branching from an incoming g actually corresponds to a $q \rightarrow qg$ (or $\bar{q} \rightarrow \bar{q}g$) splitting in the usual DGLAP sense. This can be seen in (4.132), where the terms involving $\delta_j^{\text{initial}}$ and $s_j = \pm 1$ involve the \mathcal{P}_{gq} splitting function (the \mathcal{P}_{qq} splitting function appears in the corresponding δ^{initial} terms). With this in mind we have that

$$d\sigma \star \{f^A f^B\} = \sum_{\alpha, \beta} d\sigma_{\alpha, \beta} f_{\alpha}^A f_{\beta}^B, \quad (4.115)$$

where α and β label parton type. For $n_f = 2$, we would have $\alpha, \beta \in \{u, \bar{u}, d, \bar{d}, q, g\}$, and $2n_f f_q$ is the singlet distribution function, i.e. $f_q = (u + \bar{u} + d + \bar{d})/(2n_f)$ for $n_f = 2$. For completeness, we here also attach labels A and B to indicate the type of hadron (we will drop that label elsewhere in this section).

After expanding $\mathbf{Col}_m^{\dagger}(\mu) \circ \mathbf{Col}_m(\mu)$ in powers of α_s , then spin averaging at every vertex, substituting for (4.112) and evaluating the transverse momentum integrals, we find

$$\begin{aligned} \Sigma &= \int \sum_n \sum_{m=0}^n \sum_{p=0}^{n-m} \left(\prod_{i=1}^{n-m} d\Pi_i \right) \\ &\times \int dx_a dx_b \text{Tr} \left(\mathbf{B}_{n-m-p}^p(\mu) \right) \star \{f_a(x_a, Q) f_b(x_b, Q) + \mathcal{O}(\alpha_s^{m+1})\}. \end{aligned} \quad (4.116)$$

Figure 4.8 illustrates how terms in our algorithm should be grouped in order to generate the iterative relation in (4.113) and so arrive at (4.116). Hence we see that variant B iteratively generates DGLAP evolution up to the hard scale. The derivation of fragmentation function evolution of final-state partons proceeds similarly.

For processes where Coulomb exchanges are relevant, DGLAP evolution is generated up to the scale of the last Coulomb exchange. Also note that, in the infra-red finite reformulations of A and B, DGLAP can be found in the \mathbf{B}_n for $n \geq 1$.

4.5.2 Example resummations

In this subsection we show how to resum a number of observables in $e^+e^- \rightarrow$ hadrons. The idea is to use well-known results to illustrate the use of the algorithm and how to handle its colour structures. The simplicity of the hard process means we can use $\mathbf{H}(Q) = N_c^{-1} \sigma_H \mathbb{1}$ for

the hard-scattering matrix. We perform all calculations using the LL $_{\Sigma}$ recoil from Section 4.3.4.1.

4.5.2.1 Thrust

The resummed thrust distribution was initially computed at LL accuracy in [55], then at NLL in [56]. The current state-of-the-art computation is at N³LL [57]. Thrust is defined as

$$T = \max_{\mathbf{n}} \frac{\sum_{\forall \mathbf{p}} |\mathbf{p} \cdot \mathbf{n}|}{\sum_{\forall \mathbf{p}} |\mathbf{p}|}, \quad (4.117)$$

where the thrust axis \mathbf{n} points along the initial hard parton axis at leading-order in the soft and collinear limits; see Section 3.1 in [56]. We will only need to define thrust for 3 partons; of which 2 are hard (p_1 and p_2) and one is soft (k). We can work in the dipole zero-momentum frame using $p_q = E_q(1, 0, 0, 1)$, $p_{\bar{q}} = E_{\bar{q}}(1, 0, 0, -1)$, $k = (k_{\perp} \cosh y, \vec{k}_{\perp}, k_{\perp} \sinh y)$, and we can fix $2E_q = 2E_{\bar{q}} = Q$. Thrust is evaluated as

$$T = 1 - \frac{k_{\perp} \cosh |y| - k_{\perp} \sinh |y|}{Q} + \mathcal{O}\left(\frac{k_{\perp}^2}{Q^2}\right). \quad (4.118)$$

When calculated in the hard-collinear limit, we can let $T = 1 + \mathcal{O}(k_{\perp}^2)$ as all partons lie on the thrust axis up to sub-leading contributions. The thrust distribution R_T is defined as

$$R_T = \int dT' \frac{1}{\text{Tr}(\mathbf{H}(Q))} \frac{d\Sigma}{dT'}. \quad (4.119)$$

As thrust is global, the calculation is most readily performed using the manifestly infrared finite version of variant A (see Section 4.3.5). Using this, all terms with one or more emissions cancel exactly. The measurement function $u(k, \{\emptyset\})$ is

$$u(k, \{\emptyset\}) = \Theta\left(1 - \frac{k_{\perp}^{(q\bar{q})} \cosh |y| - k_{\perp}^{(q\bar{q})} \sinh |y|}{Q} - T\right). \quad (4.120)$$

This is unity for a hard-collinear emission, since $|y| \rightarrow \infty$ at LL accuracy. This kills the hard-collinear terms, since they contain a factor $(1 - u(k, \{\emptyset\})) = 0$, which is as expected since they contribute no double logarithms. Thus we can immediately write

$$\begin{aligned} \Sigma(T) &= \text{Tr}(\bar{\mathbf{V}}_{0,Q} \bar{\mathbf{V}}_{0,Q}^{\dagger}) \sigma_{\text{H}} \\ &= \text{Tr} \left(\exp \left[\frac{2\alpha_s}{\pi} \mathbb{T}_q^g \cdot \mathbb{T}_{\bar{q}}^g \int_0^Q \frac{dk_{\perp}^{(q\bar{q})}}{k_{\perp}^{(q\bar{q})}} \int \frac{dS_2}{4\pi} \theta_{ij}(k) \right. \right. \\ &\quad \left. \left. \times \Theta \left(T - 1 + \frac{k_{\perp}^{(q\bar{q})} \cosh |y| - k_{\perp}^{(q\bar{q})} \sinh |y|}{Q} \right) k_{\perp}^2 \frac{p_q \cdot p_{\bar{q}}}{(p_q \cdot k)(p_{\bar{q}} \cdot k)} \right] \right) N_c^{-1} \sigma_{\text{H}}. \end{aligned} \quad (4.121)$$

After integrating

$$\begin{aligned}\Sigma(T) &= \text{Tr} \left(\exp \left[\frac{2\alpha_s}{\pi} \mathbb{T}_q^g \cdot \mathbb{T}_{\bar{q}}^g \int_0^Q \frac{dk_{\perp}^{(q\bar{q})}}{k_{\perp}^{(q\bar{q})}} 2 \int_0^{\infty} dy \theta_{ij}(k) \Theta \left(\frac{k_{\perp}}{Q} e^{-y} - (1-T) \right) \right] \right) N_c^{-1} \sigma_{\text{H}}, \\ &= \text{Tr} \left(\exp \left[\frac{\alpha_s}{\pi} \mathbb{T}_q^g \cdot \mathbb{T}_{\bar{q}}^g \ln^2 \left(\frac{1}{1-T} \right) \right] \right) N_c^{-1} \sigma_{\text{H}}.\end{aligned}\quad (4.122)$$

Here we used the fact that $\theta_{ij}(k)$ restricts the integration so that $k_0 < Q$. The colour trace can be evaluated to give

$$\begin{aligned}\frac{\Sigma(T)}{N_c^{-1} \sigma_{\text{H}}} &= \text{Tr}(\mathbb{1}) + \frac{\alpha_s}{\pi} \ln^2 \left(\frac{1}{1-T} \right) \text{Tr}(\mathbb{T}_q^g \cdot \mathbb{T}_{\bar{q}}^g) \\ &\quad + \frac{1}{2!} \left[\frac{\alpha_s}{\pi} \ln^2 \left(\frac{1}{1-T} \right) \right]^2 \text{Tr}(\mathbb{T}_q^g \cdot \mathbb{T}_{\bar{q}}^g \mathbb{T}_{\bar{q}}^g \cdot \mathbb{T}_q^g) + \dots \\ &= \text{Tr}(\mathbb{1}) - \frac{\alpha_s}{\pi} \ln^2 \left(\frac{1}{1-T} \right) \text{Tr}(\mathbb{T}_q^g \cdot \mathbb{T}_q^g) \\ &\quad + \frac{1}{2!} \left[\frac{\alpha_s}{\pi} \ln^2 \left(\frac{1}{1-T} \right) \right]^2 \text{Tr}(\mathbb{T}_q^g \cdot \mathbb{T}_{\bar{q}}^g \mathbb{T}_{\bar{q}}^g \cdot \mathbb{T}_q^g) + \dots \\ &= \text{Tr}(\mathbb{1}) - \frac{\alpha_s}{\pi} \mathcal{C}_{\text{F}} \ln^2 \left(\frac{1}{1-T} \right) \text{Tr}(\mathbb{1}) + \left[\frac{\alpha_s}{\pi} \mathcal{C}_{\text{F}}^2 \ln^2 \left(\frac{1}{1-T} \right) \right]^2 \text{Tr}(\mathbb{1}) + \dots \\ &= N_c \exp \left[-\frac{\alpha_s}{\pi} \mathcal{C}_{\text{F}} \ln^2 \left(\frac{1}{1-T} \right) \right].\end{aligned}\quad (4.123)$$

And so we obtain the familiar result:

$$\begin{aligned}R_T &= \int dT' \frac{1}{\text{Tr}(\mathbf{H}(Q))} \frac{d\Sigma}{dT'} \\ &= -\frac{\alpha_s}{\pi} \mathcal{C}_{\text{F}} \int dT' \frac{\ln(1-T')}{1-T'} \exp \left[-\frac{\alpha_s}{\pi} \mathcal{C}_{\text{F}} \ln^2 \left(\frac{1}{1-T'} \right) \right].\end{aligned}\quad (4.124)$$

4.5.2.2 Hemisphere jet mass

The hemisphere jet mass is subject to non-global logarithms, which greatly increase the challenge of resummation. It was first resummed at LL and LC in [58]. The current state-of-the-art is split between fixed-order computation (α_s^5 with leading colour [59] and α_s^4 with full colour [60]) and resummation using numerical techniques to introduce full colour dependence with sub-leading logarithms [61]. The measurement function corresponding to the hemisphere jet mass in $e^+e^- \rightarrow \text{hadrons}$ is

$$u_{\pm}(\{q_i\}) = \prod_{q \in \{q_i\}} \left(\Theta(q \in S_2^{\mp}) + \Theta(q \in S_2^{\pm}) \Theta(\rho - m_{\pm}) \right), \quad (4.125)$$

where S_2^+ and S_2^- are the hemispheres centred on the two primary jets. m_{\pm} is the total invariant mass in the S_2^{\pm} hemisphere and ρ is the cut on hemisphere mass. The measurement

function can be simplified by considering m_{\pm}

$$m_{\pm}^2 = \sum_{q_i, q_j \in S_2^{\pm}} 2q_i \cdot q_j = \sum_{q_i, q_j \in S_2^{\pm}} 2E_i E_j \left(1 - \sqrt{1 - \frac{q_{i\perp}^2}{E_i^2}} \right). \quad (4.126)$$

At the order we will perform the calculation we only need to consider one emission, hence

$$\begin{aligned} u_{\pm}(q_1) &= \Theta(q_1 \in S_2^{\mp}) + \Theta(q_1 \in S_2^{\pm}) \Theta \left(\rho^2 - 2E_1 E_{\pm} + 2E_1 E_{\pm} \sqrt{1 - q_{1\perp}^2 / E_1^2} \right), \\ &= \begin{cases} \Theta(q_1 \in S_2^{\mp}) + \Theta(q_1 \in S_2^{\pm}) \Theta \left(\rho^2 - Q(q_{1\perp} \cosh y - q_{1\perp} \sinh y) \right) & \text{for } E_1 \ll E_{\pm}, \\ \Theta(q_1 \in S_2^{\mp}) + \Theta(q_1 \in S_2^{\pm}) \Theta \left(\rho^2 - \frac{E_{\pm}}{E_1} q_{1\perp}^2 \right) & \text{for } q_{1\perp} \ll E_1, \end{cases} \end{aligned}$$

where E_{\pm} is the energy of the quark/anti-quark defining the S_2^{\pm} hemisphere and $Q = 2E_{\pm}$. Note the similarity between this and the measurement function for thrust, which is expected since it is well known that, at lowest-order, thrust can be expressed as the sum over the two hemisphere jet masses defined by the thrust axis.

Again, we can use the manifestly infra-red finite version of A to find $\Sigma(\rho)$:

$$\begin{aligned} \Sigma(\rho) &= \text{Tr}(\bar{\mathbf{V}}_{0,Q} \bar{\mathbf{V}}_{0,Q}^{\dagger}) N_c^{-1} \sigma_H + \int d\Pi_1 \text{Tr} \left[\bar{\mathbf{V}}_{0,q_{1\perp}} \mathbf{D}_1 \bar{\mathbf{V}}_{q_{1\perp},Q} \bar{\mathbf{V}}_{q_{1\perp},Q}^{\dagger} \mathbf{D}_1^{\dagger} \bar{\mathbf{V}}_{0,q_{1\perp}}^{\dagger} u(q_1) \right. \\ &\quad \left. \bar{\mathbf{V}}_{0,q_{1\perp}} \left\{ \bar{\mathbf{V}}_{q_{1\perp},Q} \bar{\mathbf{V}}_{q_{1\perp},Q}^{\dagger}, \frac{1}{2} \mathbf{D}_1^2 \right\} \bar{\mathbf{V}}_{0,q_{1\perp}}^{\dagger} u(q_1, \{\emptyset\}) \right] \Theta(Q - q_{1\perp}) N_c^{-1} \sigma_H + \dots \end{aligned} \quad (4.127)$$

From the calculation in the previous section, we can immediately write

$$\text{Tr}(\bar{\mathbf{V}}_{0,Q} \bar{\mathbf{V}}_{0,Q}^{\dagger}) = N_c \exp \left[-\frac{2\alpha_s}{\pi} \mathcal{C}_F \ln^2 \left(\frac{Q}{\rho} \right) \right]. \quad (4.128)$$

This gives the global contribution. The non-global contributions are found by evaluating the remaining terms (corresponding to summing over real emissions in (4.70)). This calculation can be found in [27], where the non-global terms are evaluated using the FKS algorithm, which is entirely sufficient in this case. Hence we find

$$\begin{aligned} \Sigma(\rho) &= \sigma_H \exp \left[-\frac{2\alpha_s}{\pi} \mathcal{C}_F \ln^2(Q/\rho) \right] \left(1 - \mathcal{C}_A \mathcal{C}_F \zeta(2) \left(\frac{\alpha_s}{\pi} \right)^2 \frac{\ln(Q/\rho)^2}{2} \right. \\ &\quad \left. - \mathcal{C}_A^2 \mathcal{C}_F \zeta(3) \left(\frac{\alpha_s}{\pi} \right)^3 \frac{\ln(Q/\rho)^3}{3!} + \dots \right). \end{aligned} \quad (4.129)$$

4.5.2.3 Gaps-between-jets

The LL_{Σ} measurement function in the case of gaps-between-jets is

$$u_n(q_1, \dots, q_n) = \prod_{m=1}^n (\Theta_{\text{out}}(q_m) + \Theta_{\text{in}}(q_m) \Theta(Q_0 - q_{m,\perp})), \quad (4.130)$$

where the ‘in’ region corresponds to two cones centred on the two leading jets and the ‘out’ region is the region between these cones. The observable vetoes emissions in the out region that have transverse momentum greater than Q_0 . At order α_s^5 this observable is sensitive to super-leading logarithms [12, 13]. These will be correctly calculated using variants A, B and their manifestly infra-red finite versions, but not their factorised form unless Coulomb exchanges are interleaved as in Section 4.4.3). Using the manifestly infra-red finite version of variant A we correctly find that

$$\Sigma(\mu) = \sigma_H \exp \left[-\frac{2\alpha_s \mathcal{C}_F}{\pi} Y \ln(Q/Q_0) \right] (1 + \mathcal{O}(\alpha_s^2)), \quad (4.131)$$

where Y is the rapidity range of the out region and the $(1 + \mathcal{O}(\alpha_s^2))$ factor is the stack of non-global logarithms, which can be computed by considering real gluon emission into the out region, as encoded in (4.70). These were calculated up to $\mathcal{O}(\alpha_s^5)$ in [12, 13, 62]. We note a kinematic maximum on the rapidity of an emitted gluon, i.e. $2|y| < Y_{\max} = \ln\left(\frac{Q}{2Q_0} + \sqrt{\frac{Q}{2Q_0} - 1}\right)$. This means that as $Y \rightarrow Y_{\max}$ all soft radiation goes into the in region. At leading-order in the soft approximation $Y_{\max} = \ln(Q/Q_0)$, i.e. for $Y \geq Y_{\max}$ the observable becomes doubly logarithmic.

4.6 Conclusions

Our primary goal in writing this paper is to provide the theoretical basis for the future development of a computer code that is able systematically to resum enhanced logarithms due to soft and/or collinear partons including quantum mechanical interference effects. The algorithm we present, and its variants, are (mostly) Markovian and their recursive nature makes them well suited for the task. First steps towards this goal are under development, using the `CVolver` code to perform the colour evolution [63–65].

The algorithms in this paper correctly account for the leading soft and/or collinear logarithms, though we have been careful to try and present them in such a way as to make the extension beyond leading order. For example, we have taken account of the momentum re-mappings that are necessary in order to account for energy-momentum conservation and we have included $g \rightarrow q\bar{q}$ transitions which are strictly single logarithmic.

4.7 Appendix: Splitting functions

The splitting operator \mathbf{P}_{ij} (see Figure 4.2), which is explicitly used in variant B of our algorithm, is built from the spin dependent DGLAP splitting functions [40, 66]. It is an operator in colour and helicity spaces and is defined using the spinor-helicity formalism [41]. We use the convention $v(p, \lambda) = C\bar{u}^T(p, \lambda)$ where $C = i\gamma^2\gamma^0$, which defines our crossing

symmetry to have no global minus sign. Using rotational symmetry and parity invariance one generally can write $\mathcal{M}(\{\lambda_i\}) = \mathcal{M}^*(\{-\lambda_i\})$ where \mathcal{M} is a matrix element and $\{\lambda_i\}$ the set of helicity states on which \mathcal{M} depends. Together these define the correct treatment for antiparticles, which should evolve as if they are particles with the opposite helicity. Thus \mathbf{P}_{ij} is

$$\begin{aligned}
\mathbf{P}_{ij} = & \delta_{s_j, \frac{1}{2}} \delta_j^{\text{final}} \left(\sqrt{\frac{\mathcal{P}_{qq}}{2\mathcal{C}_F(1+z_i^2)}} \frac{1}{\langle q_i \tilde{p}_j \rangle} (\mathbb{T}_j^g \otimes \mathbb{S}^{+1_i}) + \sqrt{\frac{z_i^2 \mathcal{P}_{qq}}{2\mathcal{C}_F(1+z_i^2)}} \frac{1}{[\tilde{p}_j q_i]} (\mathbb{T}_j^g \otimes \mathbb{S}^{-1_i}) \right. \\
& + \sqrt{\frac{\mathcal{P}_{gg}}{2\mathcal{C}_F(2-2z_i+z_i^2)}} \frac{1}{\langle \tilde{p}_j q_i \rangle} \mathbb{W}^{ij} (\mathbb{T}_j^g \otimes \mathbb{S}^{+1_i}) + \sqrt{\frac{(1-z_i)^2 \mathcal{P}_{gg}}{2\mathcal{C}_F(2-2z_i+z_i^2)}} \frac{1}{[q_i \tilde{p}_j]} \mathbb{W}^{ij} (\mathbb{T}_j^g \otimes \mathbb{S}^{-1_i}) \left. \right) \\
& + \delta_{s_j, -\frac{1}{2}} \delta_j^{\text{final}} \left(\sqrt{\frac{\mathcal{P}_{qq}}{2\mathcal{C}_F(1+z_i^2)}} \frac{1}{[\tilde{p}_j q_i]} (\mathbb{T}_j^g \otimes \mathbb{S}^{-1_i}) + \sqrt{\frac{z_i^2 \mathcal{P}_{qq}}{2\mathcal{C}_F(1+z_i^2)}} \frac{1}{\langle q_i \tilde{p}_j \rangle} (\mathbb{T}_j^g \otimes \mathbb{S}^{+1_i}) \right. \\
& + \sqrt{\frac{\mathcal{P}_{gg}}{2\mathcal{C}_F(2-2z_i+z_i^2)}} \frac{1}{[q_i \tilde{p}_j]} \mathbb{W}^{ij} (\mathbb{T}_j^g \otimes \mathbb{S}^{-1_i}) + \sqrt{\frac{(1-z_i)^2 \mathcal{P}_{gg}}{2\mathcal{C}_F(2-2z_i+z_i^2)}} \frac{1}{\langle \tilde{p}_j q_i \rangle} \mathbb{W}^{ij} (\mathbb{T}_j^g \otimes \mathbb{S}^{+1_i}) \left. \right) \\
& + \delta_{s_j, 1} \delta_j^{\text{final}} \left(\sqrt{\frac{(1-z_i)^2 \mathcal{P}_{qq}}{2T_R(1-2z_i(1-z_i))}} \frac{1}{[\tilde{p}_j q_i]} (\mathbb{W}^{ij} - \mathbb{1}) (\mathbb{T}_j^q \otimes \mathbb{P}_j^1 \mathbb{P}_j^2 \mathbb{S}^{+\frac{1}{2}_i}) \right. \\
& + \sqrt{\frac{z_i^2 \mathcal{P}_{qq}}{2T_R(1-2z_i(1-z_i))}} \frac{1}{[\tilde{p}_j q_i]} (\mathbb{W}^{ij} - \mathbb{1}) (\mathbb{T}_j^q \otimes \mathbb{P}_j^2 \mathbb{S}^{-\frac{1}{2}_i}) \\
& + \sqrt{\frac{\mathcal{P}_{gg}}{2\mathcal{C}_A(1-z_i+z_i^2)^2}} \frac{1}{\langle q_i \tilde{p}_j \rangle} (\mathbb{T}_j^g \otimes \mathbb{S}^{+1_i}) \\
& + \sqrt{\frac{z_i^4 \mathcal{P}_{gg}}{2\mathcal{C}_A(1-z_i+z_i^2)^2}} \frac{1}{[q_i \tilde{p}_j]} (\mathbb{T}_j^g \otimes \mathbb{S}^{-1_i}) + \sqrt{\frac{\mathcal{P}_{gg}(1-z_i)^4}{2\mathcal{C}_A(1-z_i+z_i^2)^2}} \frac{1}{[\tilde{p}_j q_i]} (\mathbb{T}_j^g \otimes \mathbb{P}_j^1 \mathbb{S}^{+1_i}) \left. \right) \\
& + \delta_{s_j, -1} \delta_j^{\text{final}} \left(\sqrt{\frac{(1-z_i)^2 \mathcal{P}_{qq}}{2T_R(1-2z_i(1-z_i))}} \frac{1}{\langle q_i \tilde{p}_j \rangle} (\mathbb{W}^{ij} - \mathbb{1}) (\mathbb{T}_j^q \otimes \mathbb{P}_j^1 \mathbb{P}_j^2 \mathbb{S}^{-\frac{1}{2}_i}) \right. \\
& + \sqrt{\frac{z_i^2 \mathcal{P}_{qq}}{2T_R(1-2z_i(1-z_i))}} \frac{1}{\langle q_i \tilde{p}_j \rangle} (\mathbb{W}^{ij} - \mathbb{1}) (\mathbb{T}_j^q \otimes \mathbb{P}_j^2 \mathbb{S}^{+\frac{1}{2}_i}) \\
& + \sqrt{\frac{\mathcal{P}_{gg}}{2\mathcal{C}_A(1-z_i+z_i^2)^2}} \frac{1}{[\tilde{p}_j q_i]} (\mathbb{T}_j^g \otimes \mathbb{S}^{-1_i}) \\
& + \sqrt{\frac{z_i^4 \mathcal{P}_{gg}}{2\mathcal{C}_A(1-z_i+z_i^2)^2}} \frac{1}{\langle \tilde{p}_j q_i \rangle} (\mathbb{T}_j^g \otimes \mathbb{S}^{+1_i}) + \sqrt{\frac{\mathcal{P}_{gg}(1-z_i)^4}{2\mathcal{C}_A(1-z_i+z_i^2)^2}} \frac{1}{\langle q_i \tilde{p}_j \rangle} (\mathbb{T}_j^g \otimes \mathbb{P}_j^1 \mathbb{S}^{-1_i}) \left. \right)
\end{aligned}$$

$$\begin{aligned}
& + \delta_{s_j, \frac{1}{2}} \delta_j^{\text{initial}} \sqrt{\frac{1}{z_i}} \left(\sqrt{\frac{\mathcal{P}_{qq}}{\mathcal{C}_F(1+z_i^2)}} \frac{1}{\langle q_i p_j \rangle} (\mathbb{T}_j^g \otimes \mathbb{S}^{+1_i}) + \sqrt{\frac{z_i^2 \mathcal{P}_{qq}}{\mathcal{C}_F(1+z_i^2)}} \frac{1}{[p_j q_i]} (\mathbb{T}_j^g \otimes \mathbb{S}^{-1_i}) \right. \\
& \quad + \sqrt{\frac{(1-z_i)^2 \mathcal{P}_{qq}}{n_f \mathcal{C}_F(1-2z_i(1-z_i))}} \frac{1}{[p_j q_i]} \mathbb{W}^{ij} (\mathbb{T}_j^g \otimes \mathbb{S}^{+1_i}) \\
& \quad \left. + \sqrt{\frac{z_i^2 \mathcal{P}_{qq}}{n_f \mathcal{C}_F(1-2z_i(1-z_i))}} \frac{1}{\langle q_i p_j \rangle} \mathbb{W}^{ij} (\mathbb{T}_j^g \otimes \mathbb{S}^{-1_i}) \right) \\
& + \delta_{s_j, -\frac{1}{2}} \delta_j^{\text{initial}} \sqrt{\frac{1}{z_i}} \left(\sqrt{\frac{\mathcal{P}_{qq}}{\mathcal{C}_F(1+z_i^2)}} \frac{1}{[p_j q_i]} (\mathbb{T}_j^g \otimes \mathbb{S}^{-1_i}) + \sqrt{\frac{z_i^2 \mathcal{P}_{qq}}{\mathcal{C}_F(1+z_i^2)}} \frac{1}{\langle q_i p_j \rangle} (\mathbb{T}_j^g \otimes \mathbb{S}^{+1_i}) \right. \\
& \quad + \sqrt{\frac{(1-z_i)^2 \mathcal{P}_{qq}}{n_f \mathcal{C}_F(1-2z_i(1-z_i))}} \frac{1}{\langle q_i p_j \rangle} \mathbb{W}^{ij} (\mathbb{T}_j^g \otimes \mathbb{S}^{-1_i}) \\
& \quad \left. + \sqrt{\frac{z_i^2 \mathcal{P}_{qq}}{n_f \mathcal{C}_F(1-2z_i(1-z_i))}} \frac{1}{[p_j q_i]} \mathbb{W}^{ij} (\mathbb{T}_j^g \otimes \mathbb{S}^{+1_i}) \right) \\
& + \delta_{s_j, 1} \delta_j^{\text{initial}} \sqrt{\frac{1}{z_i}} \left(\sqrt{\frac{2n_f \mathcal{P}_{gg}}{T_R(2-2z_i+z_i^2)}} \frac{1}{\langle p_j q_i \rangle} (\mathbb{T}_j^g \otimes \mathbb{P}_j^2 \mathbb{S}^{+\frac{1}{2}i}) \right. \\
& \quad + \sqrt{\frac{2n_f(1-z_i)^2 \mathcal{P}_{gg}}{T_R(2-2z_i+z_i^2)}} \frac{1}{[q_i p_j]} (\mathbb{T}_j^g \otimes \mathbb{P}_j^1 \mathbb{P}_j^2 \mathbb{S}^{-\frac{1}{2}i}) + \sqrt{\frac{\mathcal{P}_{gg}}{\mathcal{C}_A(1-z_i+z_i^2)^2}} \frac{1}{\langle q_i p_j \rangle} (\mathbb{T}_j^g \otimes \mathbb{S}^{+1_i}) \\
& \quad \left. + \sqrt{\frac{z_i^4 \mathcal{P}_{gg}}{\mathcal{C}_A(1-z_i+z_i^2)^2}} \frac{1}{[q_i p_j]} (\mathbb{T}_j^g \otimes \mathbb{S}^{-1_i}) + \sqrt{\frac{\mathcal{P}_{gg}(1-z_i)^4}{\mathcal{C}_A(1-z_i+z_i^2)^2}} \frac{1}{\langle q_i p_j \rangle} (\mathbb{T}_j^g \otimes \mathbb{P}_j^1 \mathbb{S}^{-1_i}) \right) \\
& + \delta_{s_j, -1} \delta_j^{\text{initial}} \sqrt{\frac{1}{z_i}} \left(\sqrt{\frac{2n_f \mathcal{P}_{gg}}{T_R(2-2z_i+z_i^2)}} \frac{1}{[q_i p_j]} (\mathbb{T}_j^g \otimes \mathbb{P}_j^2 \mathbb{S}^{-\frac{1}{2}i}) \right. \\
& \quad + \sqrt{\frac{2n_f(1-z_i)^2 \mathcal{P}_{gg}}{T_R(2-2z_i+z_i^2)}} \frac{1}{\langle p_j q_i \rangle} (\mathbb{T}_j^g \otimes \mathbb{P}_j^1 \mathbb{P}_j^2 \mathbb{S}^{+\frac{1}{2}i}) + \sqrt{\frac{\mathcal{P}_{gg}}{\mathcal{C}_A(1-z_i+z_i^2)^2}} \frac{1}{[p_j q_i]} (\mathbb{T}_j^g \otimes \mathbb{S}^{-1_i}) \\
& \quad \left. + \sqrt{\frac{z_i^4 \mathcal{P}_{gg}}{\mathcal{C}_A(1-z_i+z_i^2)^2}} \frac{1}{\langle p_j q_i \rangle} (\mathbb{T}_j^g \otimes \mathbb{S}^{+1_i}) + \sqrt{\frac{\mathcal{P}_{gg}(1-z_i)^4}{\mathcal{C}_A(1-z_i+z_i^2)^2}} \frac{1}{[p_j q_i]} (\mathbb{T}_j^g \otimes \mathbb{P}_j^1 \mathbb{S}^{+1_i}) \right). \tag{4.132}
\end{aligned}$$

Here s_j is the spin/helicity of parton j and z_i is the momentum fraction between parton i and its parent parton, j (as in (4.19)). \mathbb{T}_j^g are the basis-independent colour-charge operators for the emission of a gluon [27, 67]. \mathbb{T}_j^q is the colour charge operator for the emission of a $q\bar{q}$ pair from a gluon. In the colour flow basis it is

$$\mathbb{T}_j^q = \sqrt{T_R} \mathbb{1} - \frac{\sqrt{T_R}}{N} \tau_j, \tag{4.133}$$

where τ_j exchanges the anti-colour lines associated with the colour line of parton j . For example, let parton j have colour line c_2 and anti-colour \bar{c}_5 , τ_j would exchange anti-colour lines \bar{c}_2 and \bar{c}_5 . A full definition of τ_j , and other colour flow operators, can be found in [27],

where τ_j is written $\mathbf{s}_{\alpha,\beta}$. Note $\mathbb{T}_j^q \cdot \mathbb{T}_j^q = T_R \mathbb{1}$.¹⁴ We have defined \mathbb{S}^s as the operator that adds a parton with helicity s . Just as $\mathbb{T}_i^g \cdot \mathbb{T}_i^g = C_i \mathbb{1}$, it can be shown that $\mathbb{S}^s \cdot \mathbb{S}^s = \mathbb{1}$. We have also defined a ‘swap’ operator, \mathbb{W}^{ij} , which swaps the colour and helicity of particles i and j . Finally, we defined \mathbb{P}_i^1 as the operator that flips the helicity of parton i and \mathbb{P}_i^2 that halves the helicity of i . There is some freedom in how we introduce operators to keep track of the evolving helicity state (for example one could have instead made use of $(\mathbb{S}^s)^\dagger$, which deletes a parton of helicity s). Examples to illustrate the use of these helicity operators can be found in Appendix 4.8. The (unregularised) collinear splitting functions are

$$\begin{aligned}\mathcal{P}_{qq} &= C_F \frac{1+z^2}{1-z}, \\ \mathcal{P}_{gq} &= C_F \frac{1+(1-z)^2}{z}, \\ \mathcal{P}_{qg} &= n_f T_R (1-2z(1-z)), \\ \mathcal{P}_{gg} &= 2C_A \left(z(1-z) + \frac{z}{1-z} + \frac{1-z}{z} \right).\end{aligned}\quad (4.134)$$

It should be understood that \mathbf{P}_{ij} always acts as

$$\mathbf{P}_{ij} \mathcal{O} \mathbf{P}_{ij}^\dagger = \sum_{v, s_i, s'_i} S_{s_i, s'_i}^{(v_j \rightarrow v)} \mathbb{T}_j^{\bar{v}} \otimes S_{s_i}^{(v_j \rightarrow v)} \mathcal{O} \mathbb{T}_j^{\bar{v}^\dagger} \otimes S_{s'_i}^{(v_j \rightarrow v)^\dagger}, \quad (4.135)$$

where $S_{s_i}^{(v_j \rightarrow v)}$ is a generalised spin operator and $S_{s_i, s'_i}^{(v_j \rightarrow v)}$ is a c-number coefficient corresponding to a $v_j \rightarrow v$ splitting. For example, when j is a quark

$$\begin{aligned}\mathbf{P}_{ij} \mathcal{O} \mathbf{P}_{ij}^\dagger &= S_{1,1}^{(q \rightarrow q)} \mathbb{T}_j^q \otimes S^{1_i} \mathcal{O} \mathbb{T}_j^{q^\dagger} \otimes S^{1_i} + S_{1,-1}^{(q \rightarrow q)} \mathbb{T}_j^q \otimes S^{1_i} \mathcal{O} \mathbb{T}_j^{q^\dagger} \otimes S^{-1_i} \\ &+ S_{-1,1}^{(q \rightarrow q)} \mathbb{T}_j^q \otimes S^{-1_i} \mathcal{O} \mathbb{T}_j^{q^\dagger} \otimes S^{1_i} + S_{-1,-1}^{(q \rightarrow q)} \mathbb{T}_j^q \otimes S^{-1_i} \mathcal{O} \mathbb{T}_j^{q^\dagger} \otimes S^{-1_i} \\ &+ S_{1,1}^{(q \rightarrow g)} \mathbb{T}_j^g \otimes \mathbb{W}^{ij} S^{1_i} \mathcal{O} \mathbb{T}_j^{g^\dagger} \otimes S^{1_i} \mathbb{W}^{ij} + S_{1,-1}^{(q \rightarrow g)} \mathbb{T}_j^g \otimes \mathbb{W}^{ij} S^{1_i} \mathcal{O} \mathbb{T}_j^{g^\dagger} \otimes S^{-1_i} \mathbb{W}^{ij} \\ &+ S_{-1,1}^{(q \rightarrow g)} \mathbb{T}_j^g \otimes \mathbb{W}^{ij} S^{-1_i} \mathcal{O} \mathbb{T}_j^{g^\dagger} \otimes S^{1_i} \mathbb{W}^{ij} + S_{-1,-1}^{(q \rightarrow g)} \mathbb{T}_j^g \otimes \mathbb{W}^{ij} S^{-1_i} \mathcal{O} \mathbb{T}_j^{g^\dagger} \otimes S^{-1_i} \mathbb{W}^{ij},\end{aligned}\quad (4.136)$$

where

$$\sum_{v, s_i} S_{s_i, s_i}^{(q \rightarrow v)} = \mathcal{P}_{qq} C_F^{-1} \left(\frac{\delta_j^{\text{final}}}{4 q_i \cdot \tilde{p}_j} + \frac{\delta_j^{\text{initial}}}{2 z_i q_i \cdot p_j} \right) + \mathcal{P}_{gq} C_F^{-1} \left(\frac{\delta_j^{\text{final}}}{4 q_i \cdot \tilde{p}_j} + \frac{\delta_j^{\text{initial}}}{2 z_i q_i \cdot p_j} \right). \quad (4.137)$$

The Sudakov factors in variant B can be written in a variety of ways using

$$\int_x^{1-x} dz \mathcal{P}_{gg} = 2 \int_x^{1-x} dz z \mathcal{P}_{gg} \quad \text{and} \quad \int_x^{1-x} dz (\mathcal{P}_{qq} + \mathcal{P}_{gq}) = 2 \int_x^{1-x} dz z \mathcal{P}_{qq}.$$

Note also that there is a subtle factor of two difference between initial state and final state splittings in \mathbf{P}_{ij} . The factor arises as partons in the initial state must be convoluted with

¹⁴Strictly speaking this is only valid when acting on a physical matrix element.

PDFs which changes the pole structure of splittings and increases the number of diagrams that must be summed over relative to splittings in the final state. In the final state (without fragmentation function dependence), soft poles from real emissions can be found at both $z = 1$ and $z = 0$. These poles cancel the poles from loop diagrams. For real emissions in the initial state, the $z = 0$ poles are absent due to kinematics whilst the $z = 1$ poles cancel the poles from loops. The factor of 2 ensures the correct pattern of cancellations.

Finally, we also note the factors of n_f , the number of quark flavours, in \mathbf{P}_{ij} . They are present since we sum democratically over flavours whenever there is a $g \rightarrow q\bar{q}$ branching. Note that since we always evolve away from the hard process this means that we sum over quark flavours in the case of an initial-state $q \rightarrow gq$ branching. Care must be taken however, since if the branching cascade terminates with an initial-state quark (or anti-quark) then it is necessary to divide by a factor of n_f before convoluting with the corresponding parton distribution function. The same holds in the case where fragmentation functions are needed. In Section 4.5, we introduced the \star notation to handle this. Of course, one could set $n_f = 1$ in the above splitting operators, after which it would be necessary to sum over flavours as appropriate.

For variant A, we need the hard-collinear emission operator $\bar{\mathbf{P}}_{ij}$. This operator is defined at cross-section level through the relation

$$\begin{aligned}
\bar{\mathbf{P}}_{ij}\mathcal{O}\bar{\mathbf{P}}_{ij}^\dagger &= \mathbf{P}_{ij}\mathcal{O}\mathbf{P}_{ij}^\dagger - \delta_j^{\text{final}}\mathbb{T}_j^g \otimes \left(\frac{\mathbb{S}^{1_i}}{\sqrt{1-z_i}\langle q_i\tilde{p}_j \rangle} + \frac{\mathbb{S}^{-1_i}}{\sqrt{1-z_i}\langle \tilde{p}_j q_i \rangle} + \frac{\mathbb{W}^{ij}\mathbb{S}^{1_i}}{\sqrt{z_i}\langle \tilde{p}_j q_i \rangle} + \frac{\mathbb{W}^{ij}\mathbb{S}^{-1_i}}{\sqrt{z_i}\langle q_i\tilde{p}_j \rangle} \right) \\
&\quad \times \mathcal{O}\mathbb{T}_j^{g\dagger} \otimes \left(\frac{\mathbb{S}^{1_i}}{\sqrt{1-z_i}\langle q_i\tilde{p}_j \rangle} + \frac{\mathbb{S}^{-1_i}}{\sqrt{1-z_i}\langle \tilde{p}_j q_i \rangle} + \frac{\mathbb{W}^{ij}\mathbb{S}^{1_i}}{\sqrt{z_i}\langle \tilde{p}_j q_i \rangle} + \frac{\mathbb{W}^{ij}\mathbb{S}^{-1_i}}{\sqrt{z_i}\langle q_i\tilde{p}_j \rangle} \right)^\dagger \\
&\quad - 2\delta_j^{\text{initial}}\mathbb{T}_j^g \otimes \left(\frac{\mathbb{S}^{1_i}}{\sqrt{1-z_i}\langle q_i p_j \rangle} + \frac{\mathbb{S}^{-1_i}}{\sqrt{1-z_i}\langle p_j q_i \rangle} \right) \\
&\quad \times \mathcal{O}\mathbb{T}_j^{g\dagger} \otimes \left(\frac{\mathbb{S}^{1_i}}{\sqrt{1-z_i}\langle q_i p_j \rangle} + \frac{\mathbb{S}^{-1_i}}{\sqrt{1-z_i}\langle p_j q_i \rangle} \right)^\dagger, \tag{4.138}
\end{aligned}$$

where \mathcal{O} is a generalised operator. Note that $\dots\mathbf{P}_{ij}\mathcal{O}\mathbf{P}_{ij}^\dagger\dots$ is not necessarily Casimir in colour. However, as we observed in section 4.4, ignoring Coulomb contributions, the collinear physics can be factorised and becomes colour-diagonal after taking the trace. Therefore, for processes where Coulomb terms do not contribute (e.g. e^+e^- and DIS) we could use the emergent colour-diagonal structure to greatly simplify the \mathbf{P}_{ij} and $\bar{\mathbf{P}}_{ij}$ operators. For example, we could redefine $\bar{\mathbf{P}}_{ij}$ with a simpler amplitude-level statement.

To this end, we can introduce the hard-collinear splitting functions;

$$\begin{aligned}
\bar{\mathcal{P}}_{qq} &= \mathcal{P}_{qq} - 2\mathcal{C}_F \frac{1}{1-z} = -\mathcal{C}_F(1+z), \\
\bar{\mathcal{P}}_{gg}^{\text{initial}} &= \mathcal{P}_{gg} - 2\mathcal{C}_A \frac{1}{1-z} = 2\mathcal{C}_A \left(\frac{1}{z} + z(1-z) - 2 \right) \\
\bar{\mathcal{P}}_{gg}^{\text{final}} &= \mathcal{P}_{gg} - 2\mathcal{C}_A \frac{1}{1-z} - 2\mathcal{C}_A \frac{1}{z} = 2\mathcal{C}_A (z(1-z) - 2) \\
\bar{\mathcal{P}}_{gq}^{\text{final}} &= \mathcal{P}_{gq} - 2\mathcal{C}_F \frac{1}{z} = \mathcal{C}_F \left(\frac{1 + (1-z)^2}{z} - \frac{2}{z} \right), \quad \bar{\mathcal{P}}_{gq}^{\text{initial}} = \mathcal{P}_{gq}, \\
\bar{\mathcal{P}}_{qg} &= \mathcal{P}_{qg}.
\end{aligned} \tag{4.139}$$

The newly simplified $\bar{\mathbf{P}}_{ij}$ is equal to the operator found by substituting $\mathcal{P} \mapsto \bar{\mathcal{P}}$ inside \mathbf{P}_{ij} , i.e.

$$\delta_j^{\text{final}} \mathcal{P}_{gq} \mapsto \delta_j^{\text{final}} \bar{\mathcal{P}}_{gq}^{\text{final}} \quad \text{and} \quad \delta_j^{\text{initial}} \mathcal{P}_{gq} \mapsto \delta_j^{\text{initial}} \bar{\mathcal{P}}_{gq}^{\text{initial}}.$$

This new $\bar{\mathbf{P}}_{ij}$ operator is constructed so that when used in the LHS of (4.138) the expression becomes exact after a trace is taken. Additionally, it correctly computes spin correlations after collinear factorisation. Simplifying the collinear emission operators would be very pertinent to an efficient computational implementation of our algorithm.

$\bar{\mathcal{P}}_{v_i v_j}^\circ$ and $\mathcal{P}_{v_i v_j}^\circ$ are splitting functions used exclusively in our Sudakov factors and they are defined with all colour factors removed:

$$\begin{aligned}
\bar{\mathcal{P}}_{qq}^\circ &= \mathcal{P}_{qq}^\circ - \frac{1}{1-z} = -\frac{1}{2}(1+z), \\
\bar{\mathcal{P}}_{gq}^\circ &= \mathcal{P}_{gq}^\circ - \frac{1}{z} = \frac{1 + (1-z)^2}{2z} - \frac{1}{z}, \\
\bar{\mathcal{P}}_{qg}^\circ &= \mathcal{P}_{qg}^\circ = n_f(1 - 2z(1-z)), \\
\bar{\mathcal{P}}_{gg}^\circ &= \mathcal{P}_{gg}^\circ - \frac{1}{1-z} - \frac{1}{z} = (z(1-z) - 2).
\end{aligned} \tag{4.140}$$

In Section 4.4.1.2 and Section 4.5 we make use of the plus prescription (see (4.94)). Applying the plus prescription means

$$\int_0^1 dx f(x)_+ g(x) = \int_0^1 dx [f(x)g(x) - f(x)g(1)]. \tag{4.141}$$

The plus prescription is, in our case, is defined by

$$\begin{aligned}
\int dx \mathbf{P}(x)_+ \mathcal{O} \mathbf{P}^\dagger(x)_+ u(x) &= \int dx \left[\mathbf{P}(x) \mathcal{O} \mathbf{P}^\dagger(x) u(x) \right. \\
&\quad \left. - \mathbf{P}_V^\dagger(x) \mathbf{P}_V(x) \mathcal{O} \frac{u(1)}{2} - \mathcal{O} \mathbf{P}_V^\dagger(x) \mathbf{P}_V(x) \frac{u(1)}{2} \right],
\end{aligned} \tag{4.142}$$

where the structure of the subtraction terms is determined by the corresponding structure of the virtual corrections and this simply means that \mathbf{P}_V is determined using (4.132) but

with parton j always treated as if it is final state. The two splitting functions affected by the plus prescription are

$$\begin{aligned} P_{qq} &= \mathcal{C}_F \left(\frac{1+z^2}{1-z} \right)_+ \equiv \mathcal{C}_F \left[\frac{1+z^2}{(1-z)_+} + \frac{3}{2} \delta(1-z) \right], \\ P_{gg} &= 2\mathcal{C}_A \left(\frac{z}{(1-z)_+} + z(1-z) + \frac{1-z}{z} \right) + \frac{1}{6} (11\mathcal{C}_A - 4n_f T_R) \delta(1-z). \end{aligned} \quad (4.143)$$

For the other parton branchings, $P_{ij} = \mathcal{P}_{ij}$ where i, j labels parton type.

4.8 Appendix: Connecting to other work on spin

Our goal in this appendix is to show how our treatment of spin connects with the work of others, specifically that of Collins [68] and Knowles [69]. We will begin by re-capping the calculation of the tree-level $q \rightarrow qg$ collinear splitting using the standard notation. The matrix element is

$$\mathcal{M}_{s_1 \dots s_i \lambda_j}^{n+1}(\dots, p_i, p_j) = ig T_f^a \epsilon_{\lambda_j \mu}^* (p_j) \bar{u}_{s_i}(p_i) \gamma^\mu \frac{i \not{p}_{ij}}{p_{ij}^2 + i\epsilon} \hat{\mathcal{M}}_{s_1 \dots}^n(\dots, p_{ij}), \quad (4.144)$$

where $p_{ij} = p_i + p_j$. $\mathcal{M}_{s_1 \dots s_n}^n$ is the spin-dependent n -particle matrix element, carrying n spin indices. $\hat{\mathcal{M}}^n$ is defined so that $\bar{u}_{s_{ij}}(p_{ij}) \hat{\mathcal{M}}_{s_1 \dots}^n(\dots, p_{ij}) = \mathcal{M}_{s_1 \dots s_{ij}}^n(\dots, p_{ij})$. In the collinear limit, \not{p}_{ij} is on shell and so we can express it as a product of on-shell spinors, i.e. $\not{p}_{ij} = \sum_{s_{ij}} u_{s_{ij}}(p_{ij}) \bar{u}_{s_{ij}}(p_{ij})$. We can then further simplify by replacing Dirac spinors with massless Weyl spinors, defined in the chiral basis as $u_s = (x_{s\alpha}, y_s^{\dagger\dot{\alpha}})^T$. To avoid clutter, we will temporarily drop colour factors, factors of g and the denominator of the propagator. We find

$$\begin{aligned} \mathcal{M}_{s_1 \dots s_i \lambda_j}^{n+1}(\dots, p_i, p_j) &\propto \epsilon_{\lambda_j \mu}^* (p_j) y_{\frac{1}{2}}^\alpha(p_i) \sigma_{\alpha\beta}^\mu y_{\frac{1}{2}}^{\dagger\beta}(p_{ij}) \mathcal{M}_{s_1 \dots \frac{1}{2}}^n(\dots, p_{ij}) \delta_{s_i \frac{1}{2}} \\ &+ \epsilon_{\lambda_j \mu}^* (p_j) x_{-\frac{1}{2}\dot{\alpha}}^\dagger(p_i) \bar{\sigma}^{\mu\dot{\alpha}\beta} x_{-\frac{1}{2}\beta}(p_{ij}) \mathcal{M}_{s_1 \dots -\frac{1}{2}}^n(\dots, p_{ij}) \delta_{s_i -\frac{1}{2}}. \end{aligned} \quad (4.145)$$

We can now employ the spinor-helicity formalism [41]. Also applying a Sudakov decomposition, as defined in Section 4.3.2, the matrix element becomes

$$\begin{aligned} \mathcal{M}_{s_1 \dots s_i \lambda_j}^{n+1}(\dots, p_i, p_j) &= g T_f \sqrt{\frac{\mathcal{P}_{qq}}{\mathcal{C}_F(1+z^2)}} \frac{1}{\langle p_j p_i \rangle} \mathcal{M}_{s_1 \dots \frac{1}{2}}^n(\dots, p_{ij}) \delta_{s_i, \frac{1}{2}} \delta_{\lambda_j, 1} \\ &+ g T_f \sqrt{\frac{z^2 \mathcal{P}_{qq}}{\mathcal{C}_F(1+z^2)}} \frac{1}{\langle p_j p_i \rangle} \mathcal{M}_{s_1 \dots -\frac{1}{2}}^n(\dots, p_{ij}) \delta_{s_i, -\frac{1}{2}} \delta_{\lambda_j, 1} \\ &+ g T_f \sqrt{\frac{z^2 \mathcal{P}_{qq}}{\mathcal{C}_F(1+z^2)}} \frac{1}{[p_i p_j]} \mathcal{M}_{s_1 \dots \frac{1}{2}}^n(\dots, p_{ij}) \delta_{s_i, \frac{1}{2}} \delta_{\lambda_j, -1} \\ &+ g T_f \sqrt{\frac{\mathcal{P}_{qq}}{\mathcal{C}_F(1+z^2)}} \frac{1}{[p_i p_j]} \mathcal{M}_{s_1 \dots -\frac{1}{2}}^n(\dots, p_{ij}) \delta_{s_i, -\frac{1}{2}} \delta_{\lambda_j, -1}. \end{aligned} \quad (4.146)$$

Therefore, for each fixed value of λ_j there is an amplitude level decay matrix $\mathcal{D}_{s_i s_{ij}}^{(\lambda_j)}$ describing the transition of a quark with spin s_{ij} to two partons with spin s_i and λ_s so that $\mathcal{M}_{s_1 \dots s_i \lambda_j}^{n+1} = \mathcal{D}_{s_i s_{ij}}^{(\lambda_j)} \mathcal{M}_{s_1 \dots s_{ij}}^n$, which can be determined from the above expression. Equivalent calculations lead to decay matrices for each possible collinear splitting. When computed for initial-state collinear splittings, these matrices are amplitude-level spin-density matrices and we denote them with an \mathcal{S} instead of a \mathcal{D} .

Current parton showers deal with spin by algorithmically evaluating cross-section level spin density matrices. Consider a $2 \rightarrow 2$ scattering, where each hard parton is coloured. Then

$$d\sigma \propto \rho_{s_1 s'_1}^{(1)} \rho_{s_2 s'_2}^{(2)} \mathcal{M}_{s_1 s_2 s_3 s_4} \mathcal{M}_{s'_1 s'_2 s'_3 s'_4}^* D_{s_3 s'_3}^{(3)} D_{s_4 s'_4}^{(4)}, \quad (4.147)$$

where \mathcal{M} is the full spin-dependent hard matrix element. Summation over spin indices is implicit in this expression. $\rho_{s_1 s'_1}^{(1)}$ and $\rho_{s_2 s'_2}^{(2)}$ are cross-section level spin-density matrices. $D_{s_3 s'_3}^{(3)}$ and $D_{s_4 s'_4}^{(4)}$ are cross-section level decay matrices. D and ρ are calculated from products of amplitude level matrices, \mathcal{D} and \mathcal{S} respectively. For instance, after n emissions from parton 1:

$$\rho_{s_1 s'_1}^{(1)} = \sum_{\{\lambda\}} [\mathcal{S}^{\lambda_1} \mathcal{S}^{\lambda_2} \mathcal{S}^{\lambda_3} \dots \mathcal{S}^{\lambda_n} \mathcal{S}^{\lambda_n \dagger} \dots \mathcal{S}^{\lambda_3 \dagger} \mathcal{S}^{\lambda_2 \dagger} \mathcal{S}^{\lambda_1 \dagger}]_{s_1 s'_1},$$

where usual matrix multiplication is implied. The algorithm of Collins and Knowles is able to determine the spin density and decay matrices such that computational time only grows linearly with the number of partons [68–70].

Now let us turn to the calculation of splitting functions in our notation. We write $\mathcal{M}_{s_1 \dots s_n}^n = \langle s_1 \dots s_n | n \rangle$, which ignores colour since it is not our focus here, i.e. more correctly we should write $\mathcal{M}_{c_1 \dots c_n, s_1 \dots s_n}^n = \langle (c_1 \dots c_n) \otimes (s_1 \dots s_n) | n \rangle$. We wish to define an operator $\mathbf{P}_{k \rightarrow ij}$ that adds a new (collinear) particle (j) to $|n\rangle$ that is emitted off leg k , i.e. $|n + 1_{\text{col}}\rangle = \sum_{k \in \{n\}} \mathbf{P}_{k \rightarrow ij} |n\rangle$.

As before, we will focus on the $q \rightarrow qg$ collinear splitting. Note that $\mathcal{M}_{s_1 \dots s_i, \lambda_j}^{n+1} = \langle s_1 \dots s_i, \lambda_j | \mathbf{P}_{k \rightarrow ij} |n\rangle$. Inserting the identity gives

$$\begin{aligned} \mathcal{M}_{s_1 \dots s_i, \lambda_j}^{n+1} &= \langle s_1 \dots s_i, \lambda_j | \mathbf{P}_{k \rightarrow ij} \sum_{s'_1 \dots s'_k} |s'_1 \dots s'_k\rangle \langle s'_1 \dots s'_k | n \rangle \\ &= \sum_{s'_k} \langle s_1 \dots s_i, \lambda_j | \mathbf{P}_{k \rightarrow ij} |s_1 \dots s'_k\rangle \mathcal{M}_{s_1 \dots s'_k}^n. \end{aligned} \quad (4.148)$$

Comparing to (4.146), it follows that $\mathbf{P}_{k \rightarrow ij}$ is (for $q \rightarrow qq$)

$$\begin{aligned}
\langle s_1 \dots s_i, \lambda_j | \mathbf{P}_{k \rightarrow ij} | s_1 \dots s'_k \rangle &= gT_f \sqrt{\frac{\mathcal{P}_{qq}}{\mathcal{C}_F(1+z^2)}} \frac{1}{\langle p_j p_i \rangle} \langle s_1 \dots s_i, 1_j | \mathbb{S}^{1_j} | s_1 \dots s'_k \rangle \delta_{s_i, \frac{1}{2}} \delta_{\lambda_j, 1} \\
&+ gT_f \sqrt{\frac{z^2 \mathcal{P}_{qq}}{\mathcal{C}_F(1+z^2)}} \frac{1}{\langle p_j p_i \rangle} \langle s_1 \dots s_i, 1_j | \mathbb{S}^{1_j} | s_1 \dots s'_k \rangle \delta_{s_i, -\frac{1}{2}} \delta_{\lambda_j, 1} \\
&+ gT_f \sqrt{\frac{z^2 \mathcal{P}_{qq}}{\mathcal{C}_F(1+z^2)}} \frac{1}{[p_i p_j]} \langle s_1 \dots s_i, -1_j | \mathbb{S}^{-1_j} | s_1 \dots s'_k \rangle \delta_{s_i, \frac{1}{2}} \delta_{\lambda_j, -1} \\
&+ gT_f \sqrt{\frac{\mathcal{P}_{qq}}{\mathcal{C}_F(1+z^2)}} \frac{1}{[p_i p_j]} \langle s_1 \dots s_i, -1_j | \mathbb{S}^{-1_j} | s_1 \dots s'_k \rangle \delta_{s_i, -\frac{1}{2}} \delta_{\lambda_j, -1}.
\end{aligned} \tag{4.149}$$

\mathbb{S}^{s_j} must satisfy $\langle s_1 \dots s_i, s_j | \mathbb{S}^{s_j} | s_1 \dots s'_k \rangle = \delta_{s_i, s'_k}$. More generally, we require

$$\langle s_1 \dots s_i, s_j | \mathbb{S}^{s'_j} | s'_1 \dots s'_k \rangle = \delta_{s_1, s'_1} \dots \delta_{s_i, s'_i} \delta_{s_j, s'_j}.$$

This is the definition for \mathbb{S}^s presented in Appendix 4.7¹⁵.

We will now construct a decay matrix $D_{s_j s'_j}^{(j)}$, for a final-state hard parton j using the spin operators we have just introduced. Let us first consider the situation where there are no soft interactions and only include emissions from the initial primary leg, j :

$$\begin{aligned}
d\sigma &\propto \\
&\sum_n \sum_{\{i\}} \langle n; j | \mathbf{V}_{1,Q}^\dagger \mathbf{P}_{i_1 j}^\dagger \mathbf{V}_{2,1}^\dagger \dots \mathbf{V}_{n,n-1}^\dagger \mathbf{P}_{i_n j}^\dagger \mathbf{V}_{0,n}^\dagger \mathbf{V}_{0,n} \mathbf{P}_{i_n j} \mathbf{V}_{2,1} \dots \mathbf{V}_{2,1} \mathbf{P}_{i_1 j} \mathbf{V}_{1,Q} | n; j \rangle, \tag{4.150}
\end{aligned}$$

where the partons in the set $\{i\}$ are transverse momentum ordered. $\mathbf{V}_{a,b}$ is a Sudakov factor:

$$\mathbf{V}_{a,b}^\dagger = \exp \left[-\frac{\alpha_s}{\pi} \int_{q_{a\perp}}^{q_{b\perp}} \frac{dk_\perp}{k_\perp} \sum_v \mathbb{T}_j^{\bar{v}2} \int \frac{dz d\phi}{8\pi} \mathcal{P}_{vv_j}^\circ \right]. \tag{4.151}$$

We can evaluate (4.150) by inserting identity operators and extracting Sudakov factors, which are proportional to identity operators, into a single numerical factor. Hence

$$d\sigma \propto \sum_n \sum_{\{i\}} \sum_{s_j s'_j} \#_{i_1 \dots i_n i'_1 \dots i'_n}^{s_j s'_j} \langle n; j | s_j \rangle \langle s_j | \mathbf{P}_{i_1}^\dagger \dots \mathbf{P}_{i_n}^\dagger \mathbf{P}_{i'_n} \dots \mathbf{P}_{i'_1} | s'_j \rangle \langle s'_j | n; j \rangle, \tag{4.152}$$

where each \mathbf{P}_i^\dagger is a ‘pure’ colour-helicity operator with no scalar pre-factor. For instance $\mathbf{P}_i = \mathbb{T}_j^g \otimes \mathbb{S}^{1_i}$ in the case of a $q^{+\frac{1}{2}} \rightarrow q^{+\frac{1}{2}} g^{+1}$ splitting or $\mathbf{P}_i = \mathbb{T}_j^q \otimes \mathbb{P}_j^1 \mathbb{P}_j^2 \mathbb{S}^{-1_i}$ in the case of a $g^{-1} \rightarrow q^{+\frac{1}{2}} q^{-\frac{1}{2}}$ splitting. $\#_{i_1 \dots i_n i'_1 \dots i'_n}^{s_j s'_j}$ is a c-number coefficient built from helicity

¹⁵Repeating this procedure for the other splitting operators leads us to introduce the operators \mathbb{W}^{ij} , \mathbb{P}_i^1 and \mathbb{P}_i^2 used in Appendix A.

dependent splitting functions and expanded Sudakov factors. We can now make the link with the previous approach, i.e.

$$D_{s_j s'_j}^{(j)} = \sum_n \sum_{\{i\}} \#_{i_1 \dots i_n i'_1 \dots i'_n}^{s_j s'_j} \langle s_j | \mathbf{P}_{i_1}^\dagger \dots \mathbf{P}_{i_n}^\dagger \mathbf{P}_{i'_n} \dots \mathbf{P}_{i'_1} | s'_j \rangle. \quad (4.153)$$

The expectation value is calculable and equals a product of n Casimir co-coefficients, e.g. if parton j is a gluon and each operator \mathbf{P}_i corresponds to a $g \rightarrow gg$ splitting then the expectation value equals \mathcal{C}_A^n (up to a normalisation for the colour evolution).

Following this procedure, spin-density and decay matrices can be derived using the algorithm presented in this paper. Let's see this explicitly. Knowles' algorithm calculates spin-density and decay matrices using other intermediate matrices ρ' , ρ'' , D' and D'' [69]. We will calculate ρ' using the factorised form of variant B (which we refer to as B-f), with LL recoil. $\rho'_{ss'}$ describes the distribution of spin states for a give parton after a single collinear emission. It is normalised by the trace of itself so that it maintains a probabilistic interpretation. Knowles begins by defining

$$\rho'_{ss'} = \frac{\sum_{s_1, s'_1, s_2, s'_2} \rho_{s_1 s'_1} V_{s_1 s_2 s} V_{s'_1 s'_2 s'}^* \delta_{s_2 s'_2}}{\sum_{s, s_1, s'_1, s_2, s'_2} \rho_{s_1 s'_1} V_{s_1 s_2 s} V_{s'_1 s'_2 s'}^* \delta_{s_2 s'_2}}, \quad (4.154)$$

where ρ is a spin density matrix for a parton in the hard process that is to be inherited by a forwardly evolving shower. In the language of this paper $\rho_{s_1 s'_1} \propto \langle s_1 | \mathbf{H}(Q) | s'_1 \rangle$ ¹⁶. $V_{s_1 s_2 s}$ is the spin-dependent collinear splitting function for the transition $s_1 \rightarrow s s_2$ with parton type indices suppressed. Importantly, parton type indices are not summed over in $V_{s_1 s_2 s}$. When using Knowles' algorithm, it is assumed that the structure of a cascade has already been fully decided; all except the spin that is.

Consider a term from B-f corresponding to one collinear emission from a final-state hard parton. Labelling this term P' , we have

$$\begin{aligned} P'_{ss'} &= \frac{\sum_{s_2 s'_2} \left\langle s, s_2 \left| \bar{\mathbf{V}}_{\mu, q_{n+1 \perp}} \bar{\mathbf{D}}_{n+1} \bar{\mathbf{V}}_{q_{n+1 \perp}, Q} \mathbf{d}\sigma(n, 0) \bar{\mathbf{V}}_{q_{n+1 \perp}, Q}^\dagger \bar{\mathbf{D}}_{n+1}^\dagger \bar{\mathbf{V}}_{\mu, q_{n+1 \perp}}^\dagger \right| s', s'_2 \right\rangle \delta_{s_2 s'_2}}{\text{Tr}(\bar{\mathbf{V}}_{\mu, q_{n+1 \perp}} \bar{\mathbf{D}}_{n+1} \bar{\mathbf{V}}_{q_{n+1 \perp}, Q} \mathbf{d}\sigma(n, 0) \bar{\mathbf{V}}_{q_{n+1 \perp}, Q}^\dagger \bar{\mathbf{D}}_{n+1}^\dagger \bar{\mathbf{V}}_{\mu, q_{n+1 \perp}}^\dagger)}, \\ &= \frac{\sum_{s_2 s'_2} \left\langle s, s_2 \left| \mathbf{P}_{21} \mathbf{H}(Q) \mathbf{P}_{21}^\dagger \right| s', s'_2 \right\rangle \delta_{s_2 s'_2}}{\text{Tr}(\mathbf{P}_{21} \mathbf{H}(Q) \mathbf{P}_{21}^\dagger)}. \end{aligned} \quad (4.155)$$

We have used the LL recoil with variant B and so integrals over the recoil functions were trivial. In the second line, we have labelled the collinear parton as parton 2 and the hard

¹⁶For simplicity we suppose $\mathbf{H}(Q)$ to contain a single propagating particle. If we were to introduce more particles we would have more indices/states to keep track of. This is because collinear emissions do not involve interference terms.

parton as parton 1. We can insert identity operators and evaluate the trace explicitly to find

$$P'_{ss'} = \frac{\sum_{s_1, s'_1, s_2, s'_2} \langle s, s_2 | \mathbf{P}_{21} | s_1 \rangle \langle s'_1 | \mathbf{P}_{21}^\dagger | s', s'_2 \rangle \rho_{s_1 s'_1} \delta_{s_2 s'_2}}{\sum_{s, s_1, s'_1, s_2, s'_2} \langle s, s_2 | \mathbf{P}_{21} | s_1 \rangle \langle s'_1 | \mathbf{P}_{21}^\dagger | s, s'_2 \rangle \rho_{s_1 s'_1} \delta_{s_2 s'_2}}. \quad (4.156)$$

Now note that $\langle s s_2 | \mathbf{P}_{21} | s_1 \rangle = V_{s_1 s_2 s}$, with the possibilities of parton 2 being a gluon or quark summed over. Hence

$$P'_{ss'} = \frac{\sum_{2 \in \{q, g\}} \sum_{s_1, s'_1, s_2, s'_2} \rho_{s_1 s'_1} V_{s_1 s_2 s} V_{s'_1 s'_2 s'}^* \delta_{s_2 s'_2}}{\sum_{2 \in \{q, g\}} \sum_{s, s_1, s'_1, s_2, s'_2} \rho_{s_1 s'_1} V_{s_1 s_2 s} V_{s'_1 s'_2 s}^* \delta_{s_2 s'_2}}. \quad (4.157)$$

Thus, we have made the link to Collins and Knowles. If we pick either the quark or gluon term in the numerator and set it 0, then renormalise $P'_{ss'}$ against the trace of itself, we find

$$P'_{ss'}{}^{(1 \rightarrow 23)} = \frac{\sum_{s_1, s'_1, s_2, s'_2} \rho_{s_1 s'_1} V_{s_1 s_2 s} V_{s'_1 s'_2 s'}^* \delta_{s_2 s'_2}}{\sum_{s, s_1, s'_1, s_2, s'_2} \rho_{s_1 s'_1} V_{s_1 s_2 s} V_{s'_1 s'_2 s}^* \delta_{s_2 s'_2}} = \rho'_{ss'}.$$

When comparing with Collins and Knowles it was necessary for us to pick a species for parton 2 as their algorithm is defined for pre-determined decay chains. This is why $\rho'_{ss'}$ is typically used without a label specifying the species of the partons involved, as their species is always provided by context.

We will finish off by calculating $\rho'_{ss'}$ for a $q \rightarrow qg$ splitting. $\rho_{s_1 s'_1}$ is hermitian and so can be expressed as $\rho_{s_1 s'_1} = \mathbb{1} + \rho_i \sigma_i$ where σ_i are the Pauli matrices. Using (4.156) and normalising correctly gives

$$\begin{aligned} P'_{++}{}^{(q \rightarrow qg)} &= \frac{2q \cdot \tilde{p}_i \sqrt{\frac{\mathcal{P}_{qq}}{1+z^2}} \rho_{+++} + 2q \cdot \tilde{p}_i \sqrt{\frac{z^2 \mathcal{P}_{qq}}{1+z^2}} \rho_{+++}}{\left(2q \cdot \tilde{p}_i \sqrt{\frac{\mathcal{P}_{qq}}{1+z^2}} + 2q \cdot \tilde{p}_i \sqrt{\frac{z^2 \mathcal{P}_{qq}}{1+z^2}} \right) (\rho_{+++} + \rho_{---})} = \frac{1}{2} (1 + \rho_3), \\ P'_{+-}{}^{(q \rightarrow qg)} &= \frac{2q \cdot \tilde{p}_i \sqrt{\frac{\mathcal{P}_{qq}}{1+z^2}} \sqrt{\frac{z^2 \mathcal{P}_{qq}}{1+z^2}} \rho_{+++} + 2q \cdot \tilde{p}_i \sqrt{\frac{\mathcal{P}_{qq}}{1+z^2}} \sqrt{\frac{z^2 \mathcal{P}_{qq}}{1+z^2}} \rho_{+++}}{\left(2q \cdot \tilde{p}_i \sqrt{\frac{\mathcal{P}_{qq}}{1+z^2}} + 2q \cdot \tilde{p}_i \sqrt{\frac{z^2 \mathcal{P}_{qq}}{1+z^2}} \right) (\rho_{+++} + \rho_{---})} = \frac{z}{1+z^2} (\rho_1 - i\rho_2), \end{aligned} \quad (4.158)$$

where q is the momentum of the gluon and $1-z$ is its momentum fraction. We also used $\langle q \tilde{p}_i \rangle \langle q \tilde{p}_i \rangle^* = [q \tilde{p}_i] [q \tilde{p}_i]^* = 2q \cdot \tilde{p}_i$. It follows that

$$P^{(q \rightarrow qg)} = \frac{1}{2} \begin{pmatrix} 1 + \rho_3 & \frac{2z}{1+z^2} (\rho_1 - i\rho_2) \\ \frac{2z}{1+z^2} (\rho_1 + i\rho_2) & 1 - \rho_3 \end{pmatrix} = \rho'^{(q \rightarrow qg)}.$$

Similarly, matrices for the other collinear splittings can be found. The most algebraically complex is the $g \rightarrow gg$ splitting (as usual). In that case

$$P'_{++}{}^{(g \rightarrow gg)} = 1 + \frac{\left(\frac{z}{1-z} + 2(1-z) \right) \rho_3}{\frac{1}{2} P_{gg} + z(1-z)(\cos(2\phi)\rho_1 + \sin(2\phi)\rho_2)} = \rho'_{++}{}^{(g \rightarrow gg)}, \quad (4.159)$$

where ϕ is the azimuthal angle to the plane of the splitting. The exact angular dependence depends on the definition of the Weyl spinor products. We have chosen the definition so as to match with the matrices defined in [69], where a factor $e^{i(s_1-s_2-s)\phi}$ has been pulled out from the definitions of $V_{s_1 s_2 s}$.

References

- [1] C. W. Bauer, S. Fleming, M. E. Luke, “Summing Sudakov logarithms in $B \rightarrow X_s + \gamma$ in effective field theory”, *Phys. Rev.* **2000**, *D63*, 014006, arXiv: [hep-ph/0005275 \[hep-ph\]](#).
- [2] C. W. Bauer, S. Fleming, D. Pirjol, I. W. Stewart, “An Effective field theory for collinear and soft gluons: Heavy to light decays”, *Phys. Rev.* **2001**, *D63*, 114020, arXiv: [hep-ph/0011336 \[hep-ph\]](#).
- [3] C. W. Bauer, D. Pirjol, I. W. Stewart, “Soft collinear factorization in effective field theory”, *Phys. Rev.* **2002**, *D65*, 054022, arXiv: [hep-ph/0109045 \[hep-ph\]](#).
- [4] T. Becher, A. Broggio, A. Ferroglia, “Introduction to Soft-Collinear Effective Theory”, *Lect. Notes Phys.* **2015**, *896*, pp.1–206, arXiv: [1410.1892 \[hep-ph\]](#).
- [5] L. Lönnblad, “ARIADNE version 4: A Program for simulation of QCD cascades implementing the color dipole model”, *Comput. Phys. Commun.* **1992**, *71*, 15–31.
- [6] S. Plätzer, S. Gieseke, “Dipole Showers and Automated NLO Matching in Herwig++”, *Eur. Phys. J.* **2012**, *C72*, 2187, arXiv: [1109.6256 \[hep-ph\]](#).
- [7] S. Gieseke, P. Stephens, B. Webber, “New formalism for QCD parton showers”, *JHEP* **2003**, *12*, 045, arXiv: [hep-ph/0310083 \[hep-ph\]](#).
- [8] S. Höche, S. Prestel, “The midpoint between dipole and parton showers”, *Eur. Phys. J.* **2015**, *C75*, 461, arXiv: [1506.05057 \[hep-ph\]](#).
- [9] A. Banfi, G. P. Salam, G. Zanderighi, “Principles of general final-state resummation and automated implementation”, *JHEP* **2005**, *03*, 073, arXiv: [hep-ph/0407286 \[hep-ph\]](#).
- [10] T. Sjöstrand, P. Z. Skands, “Transverse-momentum-ordered showers and interleaved multiple interactions”, *Eur. Phys. J.* **2005**, *C39*, 129–154, arXiv: [hep-ph/0408302 \[hep-ph\]](#).
- [11] T. Sjöstrand, S. Ask, J. R. Christiansen, R. Corke, N. Desai, P. Ilten, S. Mrenna, S. Prestel, C. O. Rasmussen, P. Z. Skands, “An Introduction to PYTHIA 8.2”, *Comput. Phys. Commun.* **2015**, *191*, 159–177, arXiv: [1410.3012 \[hep-ph\]](#).
- [12] J. R. Forshaw, A. Kyrieleis, M. H. Seymour, “Super-leading logarithms in non-global observables in QCD”, *JHEP* **2006**, *08*, 059, arXiv: [hep-ph/0604094 \[hep-ph\]](#).
- [13] J. R. Forshaw, A. Kyrieleis, M. H. Seymour, “Super-leading logarithms in non-global observables in QCD: Colour basis independent calculation”, *JHEP* **2008**, *09*, 128, arXiv: [0808.1269 \[hep-ph\]](#).
- [14] A. Banfi, G. P. Salam, G. Zanderighi, “Phenomenology of event shapes at hadron colliders”, *JHEP* **2010**, *06*, 038, arXiv: [1001.4082 \[hep-ph\]](#).

- [15] S. Catani, D. de Florian, G. Rodrigo, “Space-like (versus time-like) collinear limits in QCD: Is factorization violated?”, *JHEP* **2012**, *07*, 026, arXiv: [1112.4405 \[hep-ph\]](#).
- [16] J. R. Forshaw, M. H. Seymour, A. Siódmok, “On the Breaking of Collinear Factorization in QCD”, *JHEP* **2012**, *11*, 066, arXiv: [1206.6363 \[hep-ph\]](#).
- [17] M. Dasgupta, F. A. Dreyer, K. Hamilton, P. F. Monni, G. P. Salam, “Logarithmic accuracy of parton showers: a fixed-order study”, *JHEP* **2018**, *09*, 033, arXiv: [1805.09327 \[hep-ph\]](#).
- [18] M. Dasgupta, F. A. Dreyer, K. Hamilton, P. F. Monni, G. P. Salam, G. Soyez, “Parton showers beyond leading logarithmic accuracy”, **2020**, arXiv: [2002.11114 \[hep-ph\]](#).
- [19] J. R. Forshaw, J. Holguin, S. Plätzer, “Building a consistent parton shower”, *JHEP* **2020**, *09*, 014, arXiv: [2003.06400 \[hep-ph\]](#).
- [20] K. Hamilton, R. Medves, G. P. Salam, L. Scyboz, G. Soyez, “Colour and logarithmic accuracy in final-state parton showers”, **2020**, arXiv: [2011.10054 \[hep-ph\]](#).
- [21] S. Plätzer, M. Sjödahl, J. Thorén, “Color matrix element corrections for parton showers”, *JHEP* **2018**, *11*, 009, arXiv: [1808.00332 \[hep-ph\]](#).
- [22] S. Plätzer, M. Sjödahl, “Subleading N_c improved Parton Showers”, *JHEP* **2012**, *07*, 042, arXiv: [1201.0260 \[hep-ph\]](#).
- [23] Z. Nagy, D. E. Soper, “What is a parton shower?”, *Phys. Rev.* **2018**, *D98*, 014034, arXiv: [1705.08093 \[hep-ph\]](#).
- [24] Z. Nagy, D. E. Soper, “Parton showers with quantum interference: Leading color, with spin”, *JHEP* **2008**, *07*, 025, arXiv: [0805.0216 \[hep-ph\]](#).
- [25] Z. Nagy, D. E. Soper, “Parton shower evolution with subleading color”, *JHEP* **2012**, *06*, 044, arXiv: [1202.4496 \[hep-ph\]](#).
- [26] Z. Nagy, D. E. Soper, “Effects of subleading color in a parton shower”, *JHEP* **2015**, *07*, 119, arXiv: [1501.00778 \[hep-ph\]](#).
- [27] R. Ángeles Martínez, M. De Angelis, J. R. Forshaw, S. Plätzer, M. H. Seymour, “Soft gluon evolution and non-global logarithms”, *JHEP* **2018**, *05*, 044, arXiv: [1802.08531 \[hep-ph\]](#).
- [28] Z. Nagy, D. E. Soper, “Parton showers with more exact color evolution”, **2019**, arXiv: [1902.02105 \[hep-ph\]](#).
- [29] R. Ángeles-Martínez, J. R. Forshaw, M. H. Seymour, “Coulomb gluons and the ordering variable”, *JHEP* **2015**, *12*, 091, arXiv: [1510.07998 \[hep-ph\]](#).
- [30] R. Ángeles Martínez, J. R. Forshaw, M. H. Seymour, “Ordering multiple soft gluon emissions”, *Phys. Rev. Lett.* **2016**, *116*, 212003, arXiv: [1602.00623 \[hep-ph\]](#).
- [31] A. Banfi, G. Marchesini, G. Smye, “Away from jet energy flow”, *JHEP* **2002**, *08*, 006, arXiv: [hep-ph/0206076 \[hep-ph\]](#).
- [32] J. C. Collins, D. E. Soper, “The Theorems of Perturbative QCD”, *Ann. Rev. Nucl. Part. Sci.* **1987**, *37*, 383–409.
- [33] J. C. Collins, D. E. Soper, G. F. Sterman, “Soft Gluons and Factorization”, *Nucl. Phys.* **1988**, *B308*, 833–856.

- [34] Y. L. Dokshitzer, “Calculation of the Structure Functions for Deep Inelastic Scattering and e^+e^- Annihilation by Perturbation Theory in Quantum Chromodynamics.”, *Sov. Phys. JETP* **1977**, *46*, [Zh. Eksp. Teor. Fiz.73,1216(1977)], 641–653.
- [35] V. N. Gribov, L. N. Lipatov, “Deep inelastic e p scattering in perturbation theory”, *Sov. J. Nucl. Phys.* **1972**, *15*, [Yad. Fiz.15,781(1972)], 438–450.
- [36] G. Altarelli, G. Parisi, “Asymptotic freedom in parton language”, *Nuclear Physics B* **1977**, *126*, 298–318.
- [37] Y. L. Dokshitzer, V. A. Khoze, A. H. Mueller, S. I. Troian, *Basics of perturbative QCD*, **1991**.
- [38] Y. Dokshitzer, D. Dyakonov, S. Troyan, “Hard processes in quantum chromodynamics”, *Physics Reports* **1980**, *58*, 269–395.
- [39] A. Bassetto, M. Ciafaloni, G. Marchesini, “Jet Structure and Infrared Sensitive Quantities in Perturbative QCD”, *Phys. Rept.* **1983**, *100*, 201–272.
- [40] Z. Bern, V. Del Duca, W. B. Kilgore, C. R. Schmidt, “The infrared behavior of one loop QCD amplitudes at next-to-next-to leading order”, *Phys. Rev.* **1999**, *D60*, 116001, arXiv: [hep-ph/9903516](#) [hep-ph].
- [41] H. K. Dreiner, H. E. Haber, S. P. Martin, “Two-component spinor techniques and Feynman rules for quantum field theory and supersymmetry”, *Phys. Rept.* **2010**, *494*, 1–196, arXiv: [0812.1594](#) [hep-ph].
- [42] G. Bewick, S. Ferrario Ravasio, P. Richardson, M. H. Seymour, “Logarithmic Accuracy of Angular-Ordered Parton Showers”, **2019**, arXiv: [1904.11866](#) [hep-ph].
- [43] Y. L. Dokshitzer, G. Marchesini, “Hadron collisions and the fifth form-factor”, *Phys. Lett.* **2005**, *B631*, 118–125, arXiv: [hep-ph/0508130](#) [hep-ph].
- [44] S. Schumann, F. Krauss, “A Parton shower algorithm based on Catani-Seymour dipole factorisation”, *JHEP* **2008**, *03*, 038, arXiv: [0709.1027](#) [hep-ph].
- [45] S. Plätzer, S. Gieseke, “Coherent Parton Showers with Local Recoils”, *JHEP* **2011**, *01*, 024, arXiv: [0909.5593](#) [hep-ph].
- [46] S. Catani, M. H. Seymour, “A General algorithm for calculating jet cross-sections in NLO QCD”, *Nucl. Phys.* **1997**, *B485*, [Erratum: Nucl. Phys.B510,503(1998)], 291–419, arXiv: [hep-ph/9605323](#) [hep-ph].
- [47] M. L. Mangano, S. J. Parke, “Multiparton amplitudes in gauge theories”, *Phys. Rept.* **1991**, *200*, 301–367, arXiv: [hep-th/0509223](#) [hep-th].
- [48] F. Berends, W. Giele, “Recursive calculations for processes with n gluons”, *Nuclear Physics B* **1988**, *306*, 759–808.
- [49] T. C. Rogers, P. J. Mulders, “No Generalized TMD-Factorization in Hadro-Production of High Transverse Momentum Hadrons”, *Phys. Rev.* **2010**, *D81*, 094006, arXiv: [1001.2977](#) [hep-ph].
- [50] T. C. Rogers, “Extra spin asymmetries from the breakdown of transverse-momentum-dependent factorization in hadron-hadron collisions”, *Phys. Rev.* **2013**, *D88*, 014002, arXiv: [1304.4251](#) [hep-ph].
- [51] S. M. Aybat, G. F. Sterman, “Soft-Gluon Cancellation, Phases and Factorization with Initial-State Partons”, *Phys. Lett.* **2009**, *B671*, 46–50, arXiv: [0811.0246](#) [hep-ph].

- [52] P. Z. Skands, S. Weinzierl, “Some remarks on dipole showers and the DGLAP equation”, *Phys. Rev.* **2009**, *D79*, 074021, arXiv: [0903.2150 \[hep-ph\]](#).
- [53] Z. Nagy, D. E. Soper, “Final state dipole showers and the DGLAP equation”, *JHEP* **2009**, *05*, 088, arXiv: [0901.3587 \[hep-ph\]](#).
- [54] Y. L. Dokshitzer, G. Marchesini, “Monte Carlo and large angle gluon radiation”, *JHEP* **2009**, *03*, 117, arXiv: [0809.1749 \[hep-ph\]](#).
- [55] P. Binetruy, “Summing Leading Logs in Thrust Distributions”, *Phys. Lett.* **1980**, *91B*, 245–248.
- [56] S. Catani, L. Trentadue, G. Turnock, B. Webber, “Resummation of large logarithms in e^+e^- event shape distributions”, *Nucl. Phys.* **1993**, *B407*, 3.
- [57] T. Becher, M. D. Schwartz, “A precise determination of α_s from LEP thrust data using effective field theory”, *JHEP* **2008**, *07*, 034, arXiv: [0803.0342 \[hep-ph\]](#).
- [58] M. Dasgupta, G. P. Salam, “Resummation of nonglobal QCD observables”, *Phys. Lett.* **2001**, *B512*, 323–330, arXiv: [hep-ph/0104277 \[hep-ph\]](#).
- [59] M. D. Schwartz, H. X. Zhu, “Nonglobal logarithms at three loops, four loops, five loops, and beyond”, *Phys. Rev.* **2014**, *D90*, 065004, arXiv: [1403.4949 \[hep-ph\]](#).
- [60] K. Khelifa-Kerfa, Y. Delenda, “Non-global logarithms at finite N_c beyond leading order”, *JHEP* **2015**, *03*, 094, arXiv: [1501.00475 \[hep-ph\]](#).
- [61] Y. Hagiwara, Y. Hatta, T. Ueda, “Hemisphere jet mass distribution at finite N_c ”, *Phys. Lett.* **2016**, *B756*, 254–258, arXiv: [1507.07641 \[hep-ph\]](#).
- [62] J. Keates, M. H. Seymour, “Super-leading logarithms in non-global observables in QCD: Fixed order calculation”, *JHEP* **2009**, *04*, 040, arXiv: [0902.0477 \[hep-ph\]](#).
- [63] S. Plätzer, “Summing Large- N Towers in Colour Flow Evolution”, *Eur. Phys. J.* **2014**, *C74*, 2907, arXiv: [1312.2448 \[hep-ph\]](#).
- [64] M. De Angelis, Non-global Logarithms beyond Leading Colour, talk at <https://indico.cern.ch/event/662485/>, **2018**.
- [65] J. R. Forshaw, S. Plätzer, Soft Gluon Evolution beyond Leading Colour, talks at <https://indico.cern.ch/event/729453/>, **2018**.
- [66] L. J. Dixon in QCD and beyond. Proceedings, Theoretical Advanced Study Institute in Elementary Particle Physics, TASI-95, Boulder, USA, June 4-30, 1995, **1996**, pp. 539–584, arXiv: [hep-ph/9601359 \[hep-ph\]](#).
- [67] W. Kilian, T. Ohl, J. Reuter, C. Speckner, “QCD in the Color-Flow Representation”, *JHEP* **2012**, *10*, 022, arXiv: [1206.3700 \[hep-ph\]](#).
- [68] J. C. Collins, “Spin Correlations in Monte Carlo Event Generators”, *Nucl. Phys.* **1988**, *B304*, 794–804.
- [69] I. Knowles, “A linear algorithm for calculating spin correlations in hadronic collisions”, *Computer Physics Communications* **1990**, *58*, 271–284.
- [70] P. Richardson, “Spin correlations in Monte Carlo simulations”, *Journal of High Energy Physics* **2001**, *2001*, 029–029.

Chapter 5

Publication: Comments on a new ‘full colour’ parton shower

“There’s always a bigger fish.”

— Qui-Gon Jinn, Star Wars: The Phantom Menace

5.1 Preface

The research presented in the previous Chapter combined with that in [1] provides the backbone to a full-colour parton shower known as CVolver [2]. Full-colour parton shower Monte-Carlos are difficult to formulate as the number of colour flows the shower must sample grows factorially with the parton multiplicity. This causes problems with numerical convergence. Not only do real emissions increase the number of colour flows but loops can re-arrange them. This re-arranging is a key reason for why the colour evolution cannot easily be simplified.

Building on recent developments in the Monte-Carlo evaluation of colour algebra in the colour flow basis [1, 3, 4], a new proposal for a full-colour parton shower was made public [5]. In the following work, we highlight how errors can easily appear in the construction of ‘full-colour’ parton showers. What follows is a short and self contained analysis, focused on highlighting the incorrect computation of full colour loops in [5]. After this analysis was made public, the authors of [5] corrected their paper with an appropriate acknowledgement.

References

- [1] R. Ángeles Martínez, M. De Angelis, J. R. Forshaw, S. Plätzer, M. H. Seymour, “Soft gluon evolution and non-global logarithms”, *JHEP* **2018**, *05*, 044, arXiv: [1802.08531 \[hep-ph\]](#).
- [2] M. D. Angelis, J. R. Forshaw, S. Plätzer, “Resummation and simulation of soft gluon effects beyond leading colour”, **2020**, arXiv: [2007.09648 \[hep-ph\]](#).

- [3] F. Maltoni, K. Paul, T. Stelzer, S. Willenbrock, “Color Flow Decomposition of QCD Amplitudes”, *Phys. Rev. D* **2003**, *67*, 014026, arXiv: [hep-ph/0209271](#).
- [4] S. Plätzer, M. Sjödal, “Subleading N_c improved Parton Showers”, *JHEP* **2012**, *07*, 042, arXiv: [1201.0260 \[hep-ph\]](#).
- [5] S. Höche, D. Reichelt, “Numerical resummation at sub-leading color in the strongly ordered soft gluon limit”, **2020**, arXiv: [2001.11492 \[hep-ph\]](#).

Declaration

The subsequent work is mine and my collaborators. It is without plagiarism. Each section in the paper is my own research.

The authors want to thank the Erwin Schrödinger Institute for support during the period when this and related work has been carried out. This work has received funding from the UK Science and Technology Facilities Council (grant no. ST/P000800/1), the European Union's Horizon 2020 research and innovation programme as part of the Marie Skłodowska-Curie Innovative Training Network MCnetITN3 (grant agreement no. 722104), and in part by the by the COST actions CA16201 "PARTICLEFACE" and CA16108 "VBSCAN". JH thanks the UK Science and Technology Facilities Council for the award of a studentship.

Comments on a new ‘full colour’ parton shower

Authors: Jack Holguin, Jeffrey Forshaw, Simon Plätzer

Abstract

A new parton shower algorithm has been presented with the claim of providing soft-gluon resummation at ‘full colour’ [1]. In this paper we show that the algorithm does not succeed in this goal. We show that full colour accuracy requires the Sudakov factors to be defined at amplitude level and that the simple parton-shower unitarity argument employed in [1] is not sufficient.

5.2 Introduction

Over recent years much attention has been devoted to the development of parton showers with ‘full colour’ evolution [2–7]. The study of these has multiple motivations: most importantly, reducing theoretical uncertainties in parton showers will be crucial for precision phenomenology at future colliders. Currently, parton showers provide some of the largest sources of uncertainty in experimental analyses, e.g. [8]. There has also been a growth in interest towards developing tools for the formal resummation of observables sensitive to the complexity of the non-abelian structure of the strong interaction, specifically observables with non-global or super-leading logarithms [9–14]. These will play an important role in advancing parton shower algorithms. In this context, a widely available ‘full colour’ parton shower would be a powerful tool.

In this letter we comment on the formalism for resumming complex colour structures employed recently in [1]. A similar approach was previously put forward by one of the present authors and collaborators [3, 5]. The authors of [1] describe their formalism as being capable of producing “numerical resummation at full color in the strongly ordered soft gluon limit.” We will examine this claim in what follows.

Let us be clear on what we mean by leading and sub-leading colour. A general observable can be written

$$\Sigma(L) = \sum_{n=0}^{\infty} (N_c \alpha_s)^n \sum_{m=0}^{n+1} C_{n,m}(L), \quad (5.1)$$

where L is some large logarithm. The coefficients $C_{n,m}$ can be expanded:

$$C_{n,m} = \underbrace{C_{n,m}^{(0)}}_{\text{LC}_{\Sigma}} + \underbrace{\frac{1}{N_c} C_{n,m}^{(1)}}_{\text{NLC}_{\Sigma}} + \underbrace{\frac{1}{N_c^2} C_{n,m}^{(2)}}_{\text{NNLC}_{\Sigma}} + \dots \quad (5.2)$$

and a ‘full colour’ shower should be able to compute all of the $C_{n,m}^{(i)}$ at a stated logarithmic accuracy.¹ We will show that the formalism of [1] generally fails to compute the NNLC $_{\Sigma}$ terms, even in the strongly-ordered soft gluon approximation. Note also that, for many observables, the NLC $_{\Sigma}$ term vanishes, so that the dominant sub-leading colour corrections occur at NNLC $_{\Sigma}$. It is also important to appreciate that the colour expansion defined in Eq. (5.2) is very weak in its ambition. Just as in the case of logarithmic resummation, more ambitious would be to perform a resummation of towers of enhanced corrections. In which case an expansion of the form of Eq. (5.2) would be exponentiated.

5.3 Summary of the new ‘full colour’ parton shower

We will briefly summarize the algorithm advocated in [1] and we largely follow their notation. The amplitude for an n -parton hard process is $|M_n\rangle$ and $|m_{n+k}\rangle$ is the amplitude after dressing with k soft gluons. Real emissions are accounted for recursively according to

$$\langle m_{n+k} | m_{n+k} \rangle = \langle m_{n+k-1} | \mathbf{\Gamma}_{n+k-1}(\mathbf{1}) | m_{n+k-1} \rangle = \langle M_n | \mathbf{\Gamma}_n(\dots \mathbf{\Gamma}_{n+k-2}(\mathbf{\Gamma}_{n+k-1}(\mathbf{1})) \dots) | M_n \rangle, \quad (5.3)$$

where

$$\mathbf{\Gamma}_n(\mathbf{\Gamma}) = - \sum_{\substack{i,j=1 \\ i \neq j}}^n \mathbf{T}_i \mathbf{\Gamma} \mathbf{T}_j \omega_{ij}, \quad \omega_{ij} = \frac{s_{ij}}{s_{iq} s_{qj}} \quad (5.4)$$

and $s_{ij} = 2p_i \cdot p_j$ in terms of the momenta of the partons i and j . The radiation pattern for a single emission, q , is then determined by

$$\frac{d\sigma_{n+k+1}}{\sigma_{n+k}} = d\Phi_{+1} 8\pi\alpha_s \frac{\langle m_{n+k} | \mathbf{\Gamma}_{n+k}(\mathbf{1}) | m_{n+k} \rangle}{\langle m_{n+k} | m_{n+k} \rangle}, \quad (5.5)$$

where $d\Phi_{+1}$ is a phase-space measure and parametrises the momentum map from a state of $n+k$ partons to a state of $n+k+1$ partons. Its details are not needed for our discussion.

¹Or in a specified kinematic limit, e.g. the strongly-ordered soft gluon limit.

Virtual corrections are encoded via a no-emission probability, i.e. via a typical parton-shower cross-section-level Sudakov factor, defined though unitarity as

$$\int_{t'}^t \frac{d\kappa_{ij}^2}{\sigma_{n+k}} \int \frac{d\sigma_{n+k+1}}{d\kappa_{ij}^2} \Pi(\kappa_{ij}^2, t) = 1 - \Pi(t', t), \quad (5.6)$$

where $\kappa_{ij}^2 = \omega_{ij}^{-1}$ plays the role of the ordering variable. This equation has the solution

$$\Pi^{(k)}(t', t) = \prod_{\substack{i,j=1 \\ i \neq j}}^{n+k} \Pi_{ij}(t', t), \quad (5.7)$$

where

$$\Pi_{ij}(t', t) = \exp \left(- \int_{t'}^t \frac{d\kappa_{ij}^2}{\kappa_{ij}^2} \int \frac{8\pi d\Phi_{+1}}{d\kappa_{ij}^2} \alpha_s \frac{\langle m_{n+k} | \mathbf{T}_i \mathbf{T}_j | m_{n+k} \rangle}{\langle m_{n+k} | m_{n+k} \rangle} \right), \quad (5.8)$$

is the no-emission probability for a single dipole (i, j) . The overall no-emission probability dresses the real emission matrix elements defined in Eq. (5.3) according to

$$\langle m_{n+k}; t | m_{n+k}; t \rangle = \Pi^{(k)}(t, t_k) \dots \Pi^{(1)}(t_2, t_1) \Pi^{(0)}(t_1, Q^2) \langle m_{n+k} | m_{n+k} \rangle, \quad (5.9)$$

where t_i is the ordering variable associated with the i th emission and Q^2 is the hard scale.

5.4 The problem with Sudakovs

In this section we show that defining Sudakov factors through cross-section-level unitarity gives rise to two compounding errors in colour. The first error is in the computation of loops, the second is in the computation of the interplay between loops and real emissions. These errors make the inclusion of Coulomb terms impossible, since they always appear as a pure (abelian) phase in the amplitude. Firstly, we address the computation of loops (resummed into Sudakov factors). The role of Sudakov factors in full-colour evolution of amplitudes has been extensively studied [4, 6, 7, 13–17]. Ignoring Coulomb terms (including them only makes matters more complicated), Sudakov factors² should dress a general amplitude as

$$\begin{aligned} & \langle m_{n+k}; t' | m_{n+k}; t' \rangle \\ &= \langle m_{n+k}; t | e^{-\int_{t'}^t d\kappa^2 \int \frac{4\pi d\Phi_{+1}}{d\kappa^2} \alpha_s \mathbf{\Gamma}_{n+k}(\mathbf{1})} e^{-\int_{t'}^t d\kappa^2 \int \frac{4\pi d\Phi_{+1}}{d\kappa^2} \alpha_s \mathbf{\Gamma}_{n+k}^\dagger(\mathbf{1})} | m_{n+k}; t \rangle, \\ &= \frac{\langle m_{n+k}; t | e^{-\int_{t'}^t d\kappa^2 \int \frac{8\pi d\Phi_{+1}}{d\kappa^2} \alpha_s \mathbf{\Gamma}_{n+k}(\mathbf{1})} | m_{n+k}; t \rangle}{\langle m_{n+k}; t | m_{n+k}; t \rangle} \langle m_{n+k}; t | m_{n+k}; t \rangle, \\ & \neq \Pi^{(k)}(t', t) \langle m_{n+k}; t | m_{n+k}; t \rangle. \end{aligned} \quad (5.10)$$

²The argument of the Sudakov exponent is the real part of the one-loop cusp anomalous dimension [13, 14]. Depending on the choice of ordering variable, path ordering should be implied. See Section 2 of [6] for more details.

The not equals to sign represents the first error in [1].

We will now attempt to explicate this error and its consequences by giving it two different interpretations. Firstly, we will show how this error can be thought of as a straightforward linear algebra error. Secondly, we will present some fixed-order calculations that show this error corresponds to miscalculating NNLC $_{\Sigma}$ diagrams with two or more loops. To begin the linear algebra interpretation, let us rewrite the pertinent term from Eq. (5.10) as

$$\begin{aligned} & \frac{\langle m_{n+k}; t | e^{-\int_{t'}^t d\kappa^2 \int \frac{8\pi d\Phi_{+1}}{d\kappa^2} \alpha_s \mathbf{\Gamma}_{n+k}(\mathbf{1})} | m_{n+k}; t \rangle}{\langle m_{n+k}; t | m_{n+k}; t \rangle} \\ &= \frac{\text{Tr}(|m_{n+k}; t\rangle \langle m_{n+k}; t| e^{\mathbf{V}})}{\text{Tr}(|m_{n+k}; t\rangle \langle m_{n+k}; t|)} \equiv \text{Tr}_{\text{norm}}(e^{\mathbf{V}}), \end{aligned} \quad (5.11)$$

where Tr_{norm} is a normalised trace, such that $\text{Tr}_{\text{norm}} \mathbf{1} = 1 \neq N$ where N is the dimension of the matrix. In this notation we can write

$$\Pi^{(k)}(t', t) = e^{\text{Tr}_{\text{norm}}(\mathbf{V})}. \quad (5.12)$$

This definition is the source of the error. Motivated by cross-section-level arguments of unitarity, it is implicitly assumed that

$$\text{Tr}_{\text{norm}}(e^{\mathbf{V}}) = e^{\text{Tr}_{\text{norm}}(\mathbf{V})}, \quad (5.13)$$

which is wrong.

As a trivial example of how this sort of error could give problems, consider $\text{Tr} e^{\mathbf{1}N} = Ne$ whereas $e^{\text{Tr} \mathbf{1}N} = e^N$. However, the error from using a normalised trace is more subtle, since $\text{Tr}_{\text{norm}} e^{\mathbf{1}N} = e^{\text{Tr}_{\text{norm}} \mathbf{1}N} = e$. To see where the actual problem arises, consider a toy model where $\mathbf{V} = \alpha_s N_c (\mathbf{1} + N_c^{-1} \delta \mathbf{V})$ and $\delta \mathbf{V}$ is not diagonal. In this case, the $\alpha_s N_c \mathbf{1}$ piece plays the role of the leading colour part of the Sudakov and $\alpha_s \delta \mathbf{V}$ the sub-leading colour part. The result is that

$$\text{Tr}_{\text{norm}}(e^{\mathbf{V}}) = e^{\text{Tr}_{\text{norm}}(\mathbf{V})} + \sum_{n \geq 2} \mathcal{O}(\alpha_s^n N_c^{n-2} (\text{Tr}_{\text{norm}} \delta \mathbf{V}^2 - (\text{Tr}_{\text{norm}} \delta \mathbf{V})^2)). \quad (5.14)$$

The important difference arises because $(\text{Tr}_{\text{norm}} \delta \mathbf{V})^n \neq \text{Tr}_{\text{norm}}(\delta \mathbf{V}^n)$ for $n \geq 2$. From this argument it is clear that errors will occur, starting with the computation of NNLC $_{\Sigma}$.

Now let us now give a physical interpretation of the error by expanding Eq. (5.11) to $\mathcal{O}(\alpha_s^2)$. The $\mathcal{O}(\alpha_s^2)$ term corresponds to dressing a general hard process at fixed order with two strongly ordered soft loops. The correct amplitude is

$$\begin{aligned} & \sum_{\substack{i,j=1 \\ i \neq j}}^n \int_{t'}^t d\kappa_{ij}^2 \int \frac{8\pi d\Phi_{+1}}{d\kappa_{ij}^2} \alpha_s \sum_{\substack{k,l=1 \\ k \neq l}}^n \int_{\kappa_{ij}^2}^t d\kappa_{kl}^2 \int \frac{8\pi d\Phi_{+1}}{d\kappa_{kl}^2} \alpha_s \\ & \times \text{Tr}_{\text{norm}}(\mathbf{T}_i \cdot \mathbf{T}_j \mathbf{T}_k \cdot \mathbf{T}_l) \langle m_{n+k}; t | m_{n+k}; t \rangle. \end{aligned} \quad (5.15)$$

Now, we can expand $\Pi^{(k)}(t', t) \langle m_{n+k}; t | m_{n+k}; t \rangle$ to the same order. We find

$$\begin{aligned} & \frac{1}{2} \sum_{\substack{i,j=1 \\ i \neq j}}^n \int_{t'}^t d\kappa_{ij}^2 \int \frac{8\pi d\Phi_{+1}}{d\kappa_{ij}^2} \alpha_s \text{Tr}_{\text{norm}}(\mathbf{T}_i \cdot \mathbf{T}_j) \sum_{\substack{k,l=1 \\ k \neq l}}^n \int_{t'}^t d\kappa_{kl}^2 \int \frac{8\pi d\Phi_{+1}}{d\kappa_{kl}^2} \alpha_s \\ & \times \text{Tr}_{\text{norm}}(\mathbf{T}_k \cdot \mathbf{T}_l) \langle m_{n+k}; t | m_{n+k}; t \rangle. \end{aligned} \quad (5.16)$$

These two expressions are only equal when $n+k \leq 3$ because the colour matrices are then proportional to identity matrices. However, for multiplicities of coloured partons greater than 3 they differ by NNLC_Σ pieces. This error occurs because writing a matrix element in the form of Eq. (5.16) implicitly assumes that $[\mathbf{T}_i \cdot \mathbf{T}_j, \mathbf{T}_i \cdot \mathbf{T}_k] \approx 0$, which is only correct up to NLC_Σ terms. For example, consider the case of $e^+e^- \rightarrow q\bar{q}g_1g_2$ (for which the NLC_Σ term is zero). To illustrate the point consider the limit that both gluons were emitted from the quark. In this limit a NNLC_Σ error emerges due to the non-vanishing of

$$\begin{aligned} & \alpha_s^2 \text{Tr}_{\text{norm}}(\mathbf{T}_q \cdot \mathbf{T}_{g_1} \mathbf{T}_{g_1} \cdot \mathbf{T}_{g_2}) - \alpha_s^2 \text{Tr}_{\text{norm}}(\mathbf{T}_q \cdot \mathbf{T}_{g_1}) \text{Tr}_{\text{norm}}(\mathbf{T}_{g_1} \cdot \mathbf{T}_{g_2}) \\ & = \alpha_s^2 \frac{N_c^6 + 3N_c^4 - 14N_c^2 + 2}{4N_c^2(N_c^2 - 1)^2} = \frac{(N_c \alpha_s)^2}{4} \left(\frac{1}{N_c^2} + \frac{5}{N_c^4} + \dots \right). \end{aligned} \quad (5.17)$$

Similar errors arise from other emission topologies. The non-vanishing commutator is also the reason why Coulomb terms do not cancel and, as a result, underpins the origin of super-leading logarithms [9].

The second error compounds the first. Let us now consider the evolution of an amplitude to a new scale whilst emitting a single gluon:

$$\begin{aligned} & \langle m_{n+k+1}; t'' | m_{n+k+1}; t'' \rangle \\ & = \int_{t''}^{t'} d\kappa^2 \int \frac{8\pi d\Phi_{+1}}{d\kappa^2} \alpha_s \langle m_{n+k}; t | e^{-\int_{t''}^t d\kappa^2} \int \frac{4\pi d\Phi_{+1}}{d\kappa^2} \alpha_s \mathbf{\Gamma}_{n+k}(\mathbf{1}) \mathbf{\Gamma}_{n+k}(\mathbf{1}) \\ & \times e^{-\int_{t''}^t d\kappa^2} \int \frac{4\pi d\Phi_{+1}}{d\kappa^2} \alpha_s \mathbf{\Gamma}_{n+k}^\dagger(\mathbf{1}) | m_{n+k}; t \rangle. \end{aligned} \quad (5.18)$$

In order to recombine the two exponentials into a single Sudakov that builds $\Pi^{(k)}(t', t)$ one must assume $[\mathbf{\Gamma}_{n+k}(\mathbf{1}), e^{\mathbf{V}}] \approx 0$. For the same reasons as those described above, this is again a NNLC_Σ error. Where the previous error was in the higher order colour of loop diagrams (≥ 2 loops), this error is in the higher order colour from the interplay between (≥ 1) loops and emissions. Consequently, the algorithm does correctly generate real emissions in the absence of any loop corrections. It also correctly generates one-loop contributions that dress the softest real emission but fails thereafter.

5.5 Conclusions

QCD colour dynamics beyond leading colour is highly non-trivial and its correct inclusion generally requires an amplitude-level approach that goes beyond the simple treatment of virtual corrections presented in [1].

References

- [1] S. Höche, D. Reichelt, “Numerical resummation at sub-leading color in the strongly ordered soft gluon limit”, **2020**, arXiv: [2001.11492 \[hep-ph\]](#).
- [2] Z. Nagy, D. E. Soper, “Parton shower evolution with subleading color”, *JHEP* **2012**, *06*, 044, arXiv: [1202.4496 \[hep-ph\]](#).
- [3] S. Plätzer, M. Sjö Dahl, “Subleading N_c improved Parton Showers”, *JHEP* **2012**, *07*, 042, arXiv: [1201.0260 \[hep-ph\]](#).
- [4] R. Ángeles Martínez, M. De Angelis, J. R. Forshaw, S. Plätzer, M. H. Seymour, “Soft gluon evolution and non-global logarithms”, *JHEP* **2018**, *05*, 044, arXiv: [1802.08531 \[hep-ph\]](#).
- [5] S. Plätzer, M. Sjö Dahl, J. Thorén, “Color matrix element corrections for parton showers”, *JHEP* **2018**, *11*, 009, arXiv: [1808.00332 \[hep-ph\]](#).
- [6] J. R. Forshaw, J. Holguin, S. Plätzer, “Parton branching at amplitude level”, *JHEP* **2019**, *08*, 145, arXiv: [1905.08686 \[hep-ph\]](#).
- [7] Z. Nagy, D. E. Soper, “Parton showers with more exact color evolution”, **2019**, arXiv: [1902.02105 \[hep-ph\]](#).
- [8] P. Azzi et al., “Report from Working Group 1”, *CERN Yellow Rep. Monogr.* **2019**, *7*, 1–220, arXiv: [1902.04070 \[hep-ph\]](#).
- [9] J. R. Forshaw, A. Kyrieleis, M. H. Seymour, “Super-leading logarithms in non-global observables in QCD: Colour basis independent calculation”, *JHEP* **2008**, *09*, 128, arXiv: [0808.1269 \[hep-ph\]](#).
- [10] A. Banfi, G. Corcella, M. Dasgupta, “Angular ordering and parton showers for non-global QCD observables”, *JHEP* **2007**, *03*, 050, arXiv: [hep-ph/0612282 \[hep-ph\]](#).
- [11] J. R. Forshaw, M. H. Seymour, A. Siódmok, “On the Breaking of Collinear Factorization in QCD”, *JHEP* **2012**, *11*, 066, arXiv: [1206.6363 \[hep-ph\]](#).
- [12] Y. Hagiwara, Y. Hatta, T. Ueda, “Hemisphere jet mass distribution at finite N_c ”, *Phys. Lett.* **2016**, *B756*, 254–258, arXiv: [1507.07641 \[hep-ph\]](#).
- [13] S. Caron-Huot, “Resummation of non-global logarithms and the BFKL equation”, *JHEP* **2018**, *03*, 036, arXiv: [1501.03754 \[hep-ph\]](#).
- [14] T. Becher, M. Neubert, L. Rothen, D. Y. Shao, “Factorization and Resummation for Jet Processes”, *JHEP* **2016**, *11*, [Erratum: *JHEP*05,154(2017)], 019, arXiv: [1605.02737 \[hep-ph\]](#).
- [15] Z. Nagy, D. E. Soper, “Parton showers with quantum interference: Leading color, with spin”, *JHEP* **2008**, *07*, 025, arXiv: [0805.0216 \[hep-ph\]](#).

- [16] S. Plätzer, “Summing Large- N Towers in Colour Flow Evolution”, *Eur. Phys. J.* **2014**, *C74*, 2907, arXiv: [1312.2448 \[hep-ph\]](#).
- [17] Z. Nagy, D. E. Soper, “Effects of subleading color in a parton shower”, *JHEP* **2015**, *07*, 119, arXiv: [1501.00778 \[hep-ph\]](#).

Chapter 6

Publication: Building a consistent parton shower

“All’s well that ends better.”

— The Gaffer, J.R.R. Tolkien, *The Return of the King*

6.1 Preface

Following the completion of our parton branching algorithm several questions opened up. Of primary concern were: what are the immediate phenomenological applications of our algorithm, and how does our algorithmic framework fit into the broader literature on QCD radiation? Parton shower Monte Carlos form the basis for most modern phenomenological studies of QCD radiation [1–15]. Therefore, we were motivated to link our work to current parton shower models by deriving the current models from our algorithm. We hoped that by deriving parton shower models, from a single unifying framework, we might identify the weaknesses of each model and learn how to improve them.

In the publication that follows we derive the two most common parton shower models: an angular ordered shower and a dipole shower. The derivation links our understanding of these two showers, enabling us to find improvements to the dipole shower framework required by consistency with an angular ordered shower.

Additional comment on context and PanScales

The following paper was published in 2020. Whilst this paper was being finalised, a study of NLL accuracy in parton showers was released by the PanScales collaboration [7]. There is a fair degree of similarity between the dipole shower we derive and the PanGlobal shower with $\beta = 0$ presented in [7]. Our recoil schemes in particular are similar in how they handle transverse momentum. The dipole partitioning they employ also obeys the same

basic properties as ours: a rapid rise to 1 in the region that the emitted parton becomes collinear (and a rapid drop to 0 in the anti-collinear region), summing the two halves of the partitioning gives unity at all points in the phase-space of emission, and in the limit that both partons in the dipole have the similar energy the partitioning divides the dipole symmetrically in the event ZMF. The solutions to LC NLL accuracy proposed by [7] and the solution we propose in the following paper have been broadly accepted, this is in large part due to the extensive phenomenological work presented by [7].

References

- [1] T. Sjöstrand, P. Z. Skands, “Transverse-momentum-ordered showers and interleaved multiple interactions”, *Eur. Phys. J.* **2005**, *C39*, 129–154, arXiv: [hep-ph/0408302](#) [[hep-ph](#)].
- [2] T. Sjöstrand, S. Ask, J. R. Christiansen, R. Corke, N. Desai, P. Ilten, S. Mrenna, S. Prestel, C. O. Rasmussen, P. Z. Skands, “An Introduction to PYTHIA 8.2”, *Comput. Phys. Commun.* **2015**, *191*, 159–177, arXiv: [1410.3012](#) [[hep-ph](#)].
- [3] S. Gieseke, P. Stephens, B. Webber, “New formalism for QCD parton showers”, *JHEP* **2003**, *12*, 045, arXiv: [hep-ph/0310083](#) [[hep-ph](#)].
- [4] S. Plätzer, S. Gieseke, “Dipole Showers and Automated NLO Matching in Herwig++”, *Eur. Phys. J.* **2012**, *C72*, 2187, arXiv: [1109.6256](#) [[hep-ph](#)].
- [5] S. Schumann, F. Krauss, “A Parton shower algorithm based on Catani-Seymour dipole factorisation”, *JHEP* **2008**, *03*, 038, arXiv: [0709.1027](#) [[hep-ph](#)].
- [6] M. Dasgupta, F. A. Dreyer, K. Hamilton, P. F. Monni, G. P. Salam, “Logarithmic accuracy of parton showers: a fixed-order study”, *JHEP* **2018**, *09*, 033, arXiv: [1805.09327](#) [[hep-ph](#)].
- [7] M. Dasgupta, F. A. Dreyer, K. Hamilton, P. F. Monni, G. P. Salam, G. Soyez, “Parton showers beyond leading logarithmic accuracy”, **2020**, arXiv: [2002.11114](#) [[hep-ph](#)].
- [8] M. D. Angelis, J. R. Forshaw, S. Plätzer, “Resummation and simulation of soft gluon effects beyond leading colour”, **2020**, arXiv: [2007.09648](#) [[hep-ph](#)].
- [9] Z. Nagy, D. E. Soper, “Parton showers with quantum interference: Leading color, with spin”, *JHEP* **2008**, *07*, 025, arXiv: [0805.0216](#) [[hep-ph](#)].
- [10] Z. Nagy, D. E. Soper, “What is a parton shower?”, *Phys. Rev.* **2018**, *D98*, 014034, arXiv: [1705.08093](#) [[hep-ph](#)].
- [11] S. Catani, M. H. Seymour, “A General algorithm for calculating jet cross-sections in NLO QCD”, *Nucl. Phys.* **1997**, *B485*, [Erratum: *Nucl. Phys.*B510,503(1998)], 291–419, arXiv: [hep-ph/9605323](#) [[hep-ph](#)].
- [12] B. Cabouat, J. R. Gaunt, K. Ostrolenk, “A Monte-Carlo Simulation of Double Parton Scattering”, *JHEP* **2019**, *11*, 061, arXiv: [1906.04669](#) [[hep-ph](#)].
- [13] G. Bewick, S. Ferrario Ravasio, P. Richardson, M. H. Seymour, “Logarithmic Accuracy of Angular-Ordered Parton Showers”, **2019**, arXiv: [1904.11866](#) [[hep-ph](#)].
- [14] Y. L. Dokshitzer, G. Marchesini, “Monte Carlo and large angle gluon radiation”, *JHEP* **2009**, *03*, 117, arXiv: [0809.1749](#) [[hep-ph](#)].

- [15] R. K. Ellis, W. J. Stirling, B. R. Webber, “QCD and collider physics”, *Camb. Monogr. Part. Phys. Nucl. Phys. Cosmol.* **1996**, 8, 1–435.

Declaration

The subsequent work is mine and my collaborators. It is without plagiarism. Each section in the paper is my own research.

The authors want to thank the Erwin Schrödinger Institute Vienna for support while this work was carried out. This work has received funding from the UK Science and Technology Facilities Council (grant no. ST/P000800/1), the European Union’s Horizon 2020 research and innovation programme as part of the Marie Skłodowska-Curie Innovative Training Network MCnetITN3 (grant agreement no. 722104), and in part by the by the COST actions CA16201 “PARTICLEFACE” and CA16108 “VBSCAN”. JH thanks the UK Science and Technology Facilities Council for the award of a studentship. Thanks also to Jack Helliwell, Mike Seymour and Andy Pilkington for comments and discussions. Finally we would also like to thank the organisers of the “Taming the accuracy of event generators” workshop (2020) for facilitating enlightening discussions. We especially want to thank to Pier Monni and Gavin Salam for useful exchange on the subject.

Building a consistent parton shower

Authors: Jack Holguin, Jeffrey R. Forshaw, Simon Plätzer

Abstract

Modern parton showers are built using one of two models: dipole showers or angular ordered showers. Both have distinct strengths and weaknesses. Dipole showers correctly account for wide-angle, soft gluon emissions and track the leading flows in QCD colour charge but they are known to mishandle partonic recoil. Angular ordered showers keep better track of partonic recoil and correctly include large amounts of wide-angle, soft physics but azimuthal averaging means they are known to mishandle some correlations. In this paper, we derive both approaches from the same starting point; linking our understanding of the two showers. This insight allows us to construct a new dipole shower that has all the strengths of a standard dipole shower together with the collinear evolution of an angular-ordered shower. We show that this new approach corrects the next-to-leading-log errors previously observed in parton showers and improves their sub-leading-colour accuracy.

6.2 Introduction

Parton showers simulate the particle content of scattering events at collider experiments and provide the backbone to modern experimental analyses [1–7]. Yet questions over their accuracy and on how best to improve them remain. In this paper we present a unified analysis of the two main approaches to formulating parton showers: dipole showers [2–4, 8] and angular ordered showers [5, 6, 9]. As a result, we are able to construct a new dipole shower that does not suffer from the next-to-leading logarithm (NLL) problems suffered by existing parton showers and has increased next-to-leading colour (NLC) accuracy [10].

In our previous papers [11, 12] we introduced an algorithm for amplitude-level parton branching (the PB algorithm). The PB algorithm was designed to capture both the soft and collinear logarithms associated with the leading infra-red singularities of scattering amplitudes without making any approximations on the spin and colour. In [12] we showed how the PB algorithm can be used to derive the resummation of observables at leading-logarithmic

accuracy (it has the capacity to be extended to include next-to-leading-logarithms) and we showed that it gives rise to the collinear factorisation of parton density and fragmentation functions. In [11] we showed that the colour evolution is equivalent to that of other approaches [13–16]. The PB algorithm is the starting point for the analysis presented here.

In the next section, we present a brief overview of the algorithm (recapping Chp. 4 and introducing some new notation) before going on to use it to derive both dipole and angular ordered showers. In these derivations we keep close track of the approximations made, with the goal of gaining a solid understanding of the sources for errors in these showers. We focus on deriving showers in e^+e^- , though much of the machinery necessary to derive showers for hadron-hadron processes is also present in this paper. The full discussion of our derivations is technical and largely handled in Appendix 6.6.

More specifically, in Section 6.3.2, we derive an angular ordered shower starting from the PB algorithm. In doing so we are able to constrain the recoil functions in the original PB algorithm, since angular ordered showers provide clear constraints on how momentum longitudinal to a jet must be conserved in order to get NLL physics correct. In Section 6.3.3 we then derive a dipole shower from the PB algorithm, taking particular care over the constraints observed from our angular ordered derivation. The result is a dipole shower that reduces the doubly-logarithmic NLC errors noted in [10] (complete removal of NLC errors at a given logarithmic accuracy generally requires amplitude-level evolution). Having pinned down longitudinal recoil, in Section 6.4 we present a scheme (inspired by [17]) for the transverse recoil. This completes the specification of our shower. We then go on to recreate the fixed order analysis of [10] and show that our shower corrects the NLL errors from incorrect transverse recoil previously observed in dipole showers. In Appendix 6.9 we go further and show that our new shower is sufficient for the correct leading-colour NLL resummations of thrust and the generating functions for jet multiplicity.

6.3 Evolution equations

6.3.1 Amplitude evolution overview

What follows is a review of the algorithm presented in Chp. 4 introducing some new notation that is of use throughout this paper. The PB algorithm defines a sequence of transitions in a Markov chain of amplitude density matrices: $\mathbf{A}_0(q_{0\perp}; \{p\}_0) \mapsto \mathbf{A}_1(q_{1\perp}; \{p\}_1) \mapsto \dots \mapsto \mathbf{A}_n(q_{n\perp}; \{p\}_n)$. The sequence is illustrated in Figure 6.1. We use n to index the number of partons dressing the hard process. Each amplitude is defined at a given scale (parametrised by an ordering variable), this is its first argument. The second argument, after a semi-colon, specifies its full dependence on the relevant parton momenta (which we often choose

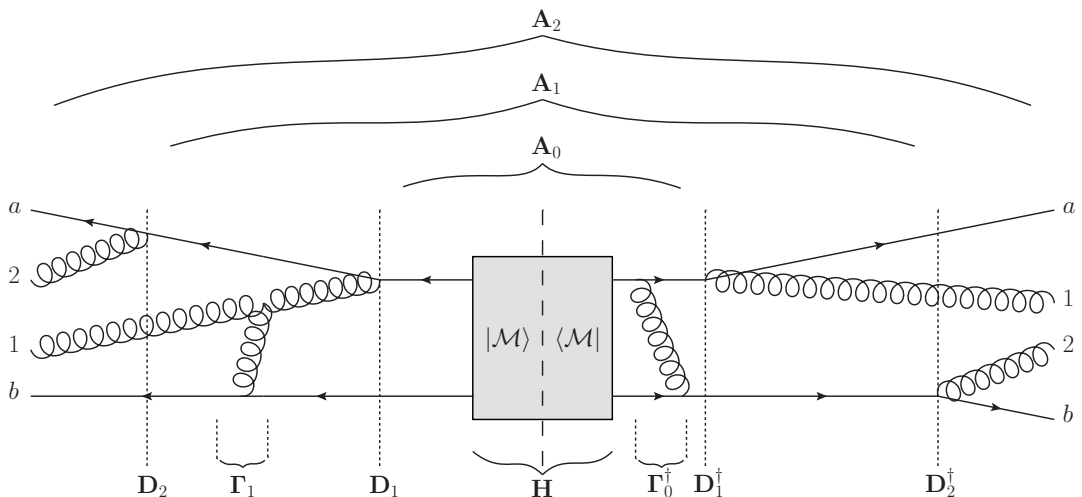


Figure 6.1: A general term in the Markov chain of amplitude density matrices, \mathbf{A}_n , constructed by the PB algorithm. $\mathbf{H} \equiv |\mathcal{M}\rangle \langle \mathcal{M}|$ is the initial hard process; in this case it has two hard coloured legs, a and b . \mathbf{D}_n dresses an amplitude with the n th emission that is either soft or collinear. Collinear emissions are emitted symmetrically from the amplitude and conjugate amplitude, such as gluon 1. Soft emissions appear as interference terms, such as gluon 2. $\mathbf{\Gamma}_n$ dresses the amplitude after n soft or collinear emissions with a loop.

to omit). The Markov chain uses the initial condition $\mathbf{A}_0(Q; \{p\}_0) = \mathbf{H}(Q; P_1, \dots, P_{n_H})$, where $\mathbf{H} \equiv |\mathcal{M}\rangle \langle \mathcal{M}|$ is the hard process density matrix for a process of hard scale Q and with n_H hard partons. The hard partons' momenta form the set $\{P_1, \dots, P_{n_H}\} \equiv \{p\}_0$. The Markov chain terminates on the amplitudes $\mathbf{A}_n(\mu; \{p\}_n)$; μ is an infra-red cut-off and $\{p\}_n = \{P_1, \dots, P_{n_H}, q_1, \dots, q_n\}$ where q_1, \dots, q_n are the momenta of the n partons that dress the hard process. Steps in the Markov chain are constructed from the action of two operators, \mathbf{D}_n and $\mathbf{\Gamma}_n$. The \mathbf{D}_n operators are emission operators; they act as maps from a state $\mathbf{A}_{n-1}(q_\perp; \{p\}_{n-1})$ to a state $\mathbf{A}_n(q_\perp; \{p\}_n)$, and they describe the emission of the n th parton. Operators $\mathbf{\Gamma}_n$ provide a map from a state $d\mathbf{A}_n(q_\perp; \{p\}_n)/dq_\perp$ onto some other $d\tilde{\mathbf{A}}_n(q_\perp; \{p\}_n)/dq_\perp$. Physically, they dress the density operator with (iterated) virtual corrections. The path-ordered exponent of $\mathbf{\Gamma}_n$ is an amplitude level Sudakov factor/operator which we call $\mathbf{V}_{a,b}$:

$$\mathbf{V}_{a,b} = \text{Pexp} \left(- \int_a^b \frac{dq_\perp}{q_\perp} \mathbf{\Gamma}_n(q_\perp) \right). \quad (6.1)$$

$\mathbf{V}_{a,b}$ evolves a state $\mathbf{A}_n(b; \{p\}_n)$ to a state at a lower scale $\tilde{\mathbf{A}}_n(a; \{p\}_n)$; for a complete discussion of $\mathbf{V}_{a,b}$ see [12]. In [12] we presented the PB algorithm in the following form:

$$\mathbf{A}_n(q_\perp; \{p\}_n) = \int dR_n \mathbf{V}_{q_\perp, q_{n\perp}} \mathbf{D}_n \mathbf{A}_{n-1}(q_{n\perp}; \{p\}_{n-1}) \mathbf{D}_n^\dagger \mathbf{V}_{q_\perp, q_{n\perp}}^\dagger \Theta(q_\perp \leq q_{n\perp}). \quad (6.2)$$

The algorithm maps the set of partonic momenta prior to the n th emission ($\{p_{n-1}\}$) onto a new set ($\{p_n\}$), by adding a parton (q_n). In order to conserve energy-momentum, the set of momenta prior to the emission are adjusted after each emission, i.e. $\{p_{n-1}\} \rightarrow \{\tilde{p}_{n-1}\}$ and $\{p_n\} = \{\tilde{p}_{n-1} \cup q_n\}$. We achieve this by integrating over delta functions relating the two sets of momenta. This is all hidden inside $\int dR_n$, which we describe in Appendix 6.6.1 and give examples of in Section 6.4. We also provide definitions of each operator involved in the evolution in Appendix 6.6.1.

In this paper, it better suits our purposes to work with the PB algorithm expressed as an evolution equation, i.e. working differentially in the ordering variable, q_\perp . Broadly speaking, $q_{n\perp}$ is the transverse momentum of the n th parton and it is a function of the n -parton phase-space. The precise definition of $q_{n\perp}$ is context dependent and is given in Appendix 6.6.1. The evolution equation is

$$q_\perp \frac{\partial \mathbf{A}_n(q_\perp; \{p\}_n)}{\partial q_\perp} = \mathbf{\Gamma}_n(q_\perp) \mathbf{A}_n(q_\perp; \{p\}_n) + \mathbf{A}_n(q_\perp; \{p\}_n) \mathbf{\Gamma}_n^\dagger(q_\perp) - \int dR_n \mathbf{D}_n(q_{n\perp}) \mathbf{A}_{n-1}(q_{n\perp}; \{p\}_{n-1}) \mathbf{D}_n^\dagger(q_{n\perp}) q_\perp \delta(q_\perp - q_{n\perp}). \quad (6.3)$$

It is from this equation that we will derive generalised dipole and angular ordered showers.

The phase-space measure for the n th parton emitted in the cascade is variously written as

$$\frac{d^3 q_n}{2E_{q_n}} = \frac{q_{n\perp}^2 dq_{n\perp}}{2q_{n\perp}} dS_2^{(q_n)} = \frac{\pi^2 q_{n\perp}^2}{2\alpha_s} d\Pi_n. \quad (6.4)$$

We typically parametrise the evolution so that real emissions use the phase-space measure $d\Pi_n$ and loops $d \ln q_{n\perp} dS_2^{(q_n)}$. From each \mathbf{A}_n we can compute the differential $n_H + n$ parton cross section:

$$d\sigma_n(\mu) = \left(\prod_{i=1}^n d\Pi_i \right) \text{Tr} \mathbf{A}_n(\mu), \quad (6.5)$$

where μ is either an infra-red regulator that should be taken to zero or the shower cut-off scale. We will focus on e^+e^- hard matrix elements, in which case observables are computed using

$$\Sigma(\mu; \{p\}_0, \{v\}) = \int \sum_n d\sigma_n(\mu) u(\{p\}_n, \{v\}), \quad (6.6)$$

where $u(\{p\}_n, \{v\})$ is a measurement function for an observable defined by the set of parameters $\{v\}$.¹ The formula for processes involving incoming hadrons is given in Appendix 6.6.1.1.

¹ $\Sigma(\mu; \{p\}_0, \{v\})$ is $\sum_\delta \frac{d\sigma_\delta}{dB} f_{B,\delta}(v)$ in [18].

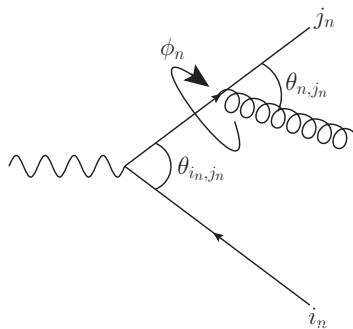


Figure 6.2: The angles used to derive angular ordering by azimuthal averaging. ϕ_n is the azimuth that is averaged over. In some equations two azimuths are present, in these situations we give ϕ_n a second index, e.g. ϕ_{n, j_n} . Angular ordering corresponds to $\theta_{i_n, j_n} > \theta_{n, j_n}$.

6.3.2 Angular ordered shower

In this section we give an overview of the derivation of an angular ordered shower, starting from Eq. (6.3). The unabridged derivation is given in Appendix 6.6.2. Angular ordering is derived after averaging over the azimuth of each emitted parton, as measured relative to their parent parton (and neglecting all subsequent azimuthal correlations). After performing this averaging in Eq. (6.3), the colour structures can be greatly simplified (a manifestation of QCD coherence). We exploit this to re-write the evolution in terms of squared matrix elements, $|\mathcal{M}_n|^2$. What follows is a little more detail of the key steps.

1. The \mathbf{D}_n operators in Eq. (6.3) describe the emission of soft gluons from dipoles (via eikonal currents) and the emission of hard-collinear partons. The probability for the emission of a soft gluon is partitioned as

$$\frac{n_{i_n} \cdot n_{j_n}}{n_{i_n} \cdot n \ n_{j_n} \cdot n} = P_{i_n j_n} + P_{j_n i_n}, \quad \text{where} \quad 2P_{i_n j_n} = \frac{n_{i_n} \cdot n_{j_n} - n_{i_n} \cdot n}{n_{i_n} \cdot n \ n_{j_n} \cdot n} + \frac{1}{n_{i_n} \cdot n},$$

$n_{i_n} = p_{i_n}/E_{i_n}$ and $n = q_n/E_{q_n}$, and E is an energy in the event zero-momentum frame. Note that $P_{i_n j_n}$ only has a pole when the emission is parallel to i_n . When integrated, this term gives rise to a theta function that enforces angular ordering.

2. We average over the emitted parton's azimuth, $\langle \dots \rangle_{1, \dots, n}$, such that (for some quantity f)

$$\langle f \rangle_{1, \dots, n} = \int \frac{d\phi_n}{2\pi} \dots \int \frac{d\phi_1}{2\pi} f(\phi_1, \dots, \phi_n).$$

The relevant angles are defined in Figure 6.2. We use this operation on both sides of Eq. (6.3) and spin-average, see Appendices 6.6.2 and 6.7 for details. It is at this point we see that $\langle P_{i_n j_n} \rangle_n \propto \Theta(\theta_{j_n, i_n} - \theta_{n, i_n})$.

3. We perform a change of variables, $q_{n\perp} \rightarrow \zeta_{n,j_n} = 1 - \cos \theta_{n,j_n}$, so as to make the angular ordering explicit. We merge the soft and hard-collinear emission kernels; expressing them in terms of collinear splitting functions. We also must sort out recoil so that the longitudinal component of the total momentum in a $1 \rightarrow 2$ splitting is conserved. Finally, using kinematic variables defined in the event zero-momentum frame² allows us to saturate the $\Theta(\theta_{j_n,i_n} - \theta_{n,i_n})$ angular ordering constraint for emissions originating from the primary hard partons (which are anti-parallel to each other). For all other emissions, it is necessary to approximate $\Theta(\theta_{j_n,i_n} - \theta_{n,i_n}) \approx 1$. This approximation (which corresponds to strong ordering in angles) is equivalent to assuming the angle of the current emission is smaller than the opening angle of every other dipole, not just the opening angle of its parent dipole. This is the familiar angular ordering used in both resummations [19, 20] and parton showers when showering from an $e^+e^- \rightarrow q\bar{q}$ hard process [5]. Strong ordering in angles simplifies the colour structures, so that all colour-charge operators can be reduced to Casimir, i.e. \mathcal{C}_F for a quark and \mathcal{C}_A for a gluon. The simplified colour reduces the evolution equation to an evolution of matrix elements, $|\mathcal{M}_n|^2$.

The final result is

$$\begin{aligned} & \zeta \frac{\partial \langle |\mathcal{M}_n(\zeta)|^2 \rangle_{1,\dots,n}}{\partial \zeta} \approx \\ & \sum_{j_{n+1}} \sum_v \frac{\alpha_s}{\pi} \int dz \mathcal{P}_{vv_{j_{n+1}}}(z) \langle \Theta_{\text{on shell}} \rangle_{n+1} \langle |\mathcal{M}_n(\zeta)|^2 \rangle_{1,\dots,n} - \sum_v \frac{\alpha_s}{\pi} \mathcal{P}_{vv_{j_n}}(z_n) \\ & \times \langle \Theta_{\text{on shell}} \rangle_n \int d^4 p_{j_n} \delta^4(p_{j_n} - z_n^{-1} \tilde{p}_{j_n}) \langle |\mathcal{M}_{n-1}(\zeta_{n,j_n})|^2 \rangle_{1,\dots,n-1} \zeta_{n,j_n} \delta(\zeta - \zeta_{n,j_n}). \end{aligned} \quad (6.7)$$

The angular ordering variable $\zeta_{n,j_n} = 1 - \cos \theta_{n,j_n}$. $\mathcal{P}_{vv_{j_n}}(z_n)$ are the usual collinear splitting functions, e.g. $\mathcal{P}_{qq}(z_n) = \mathcal{C}_F \frac{1+z_n^2}{1-z_n}$. Here we have used v_{j_n} to label the species of parton j_n and v to label the species j_n transitions to; if $v_{j_n} = q$ then $v = q$ and if $v_{j_n} = g$ then $v = q, g$. z_n is the momentum fraction of parton n , i.e. if we have a collinear splitting that induces $j_{n-1} \rightarrow j_n n$ then $p_{j_n} \approx z_n p_{j_{n-1}}$ and $q_n \approx (1 - z_n) p_{j_{n-1}}$. $\Theta_{\text{on shell}}$ is a product of theta functions that ensures each parton is integrated over the phase space corresponding to a real particle (see Section 6.6.2.2). In the first term, $\Theta_{\text{on shell}}$ is a function of ζ , z and the n -parton phase space. In the second term $\Theta_{\text{on shell}}$ is a function of ζ_{n,j_n} , z_n and the $(n-1)$ -parton phase space. $\langle |\mathcal{M}_n(\zeta; \{P_1, \dots, P_{n_H}, (z_1, \zeta_{1,j_1}), \dots, (z_n, \zeta_{n,j_n})\})|^2 \rangle_{1,\dots,n}$ is the azimuthally averaged, squared matrix element for a hard process dressed with n strongly-ordered partons with a unique branching topology; each emitted parton is specified by a

²i.e. for $e^+e^- \rightarrow q\bar{q}$, $z_n = \tilde{p}_{i_n} \cdot n / p_{i_n} \cdot n$ and n is chosen so that $n \parallel P_{\bar{q}}$ for all emissions in the quark jet and vice versa for the anti-quark jet.

pair (z_m, ζ_{m,j_m}) and parton j_m is the corresponding parent. The delta function enforces longitudinal momentum conservation; $|\mathcal{M}_n|^2$ depends on the momentum after the emission, \tilde{p}_{j_n} , and $|\mathcal{M}_{n-1}|^2$ depends on the momentum before the emission, p_{j_n} .

Observables in e^+e^- are computed after summing over emission topologies:

$$\Sigma(\mu; \{p\}_0, \{v\}) \approx \int \sum_n \sum_{j_1, \dots, j_n} \left(\prod_{m=1}^n \frac{d\zeta_{m,j_m} dz_i d\phi_i}{\zeta_{m,j_m} 2\pi} \right) \langle |\mathcal{M}_n(\mu)|^2 \rangle_{1, \dots, n} u(\{p\}_n, \{v\}), \quad (6.8)$$

where μ should be taken to zero (or the shower cutoff) and for hadron-hadron collisions see Appendix 6.6.1.1.³

There are several noteworthy points involved in this derivation:

- In order to reduce the colour structures to being diagonal, we made the approximation $\Theta(\theta_{j_n, i_n} - \theta_{n, i_n}) \approx 1$ for emissions from partons other than the two primary hard particles. The approximation is generally only good to LL accuracy (though angular ordered showers are able to go beyond this when combined with the CMW running of the coupling [20], e.g. to compute thrust at NLL [19]). Moreover, modern angular ordered showers retain information on the hard-process, leading N_c colour flows by working in the dipole frames of initially colour-connected partons. This improves the approximation for hard processes with greater than two hard jets, since it is then only required to assume $\Theta(\theta_{j_n, i_n} - \theta_{n, i_n}) \approx 1$ for emissions from partons other than the primary hard partons. During the subsequent evolution, traditional angular ordered showers lose the information on QCD colour flows⁴, while dipole showers retain it to all orders at leading N_c . We will exploit this in our dipole shower construction. Appendix 6.6.2 and 6.6.3 give more details on this point.
- The shower does not yet fully conserve energy and momentum. Rather it only conserves energy-momentum longitudinal to a jet. Accounting fully for energy-momentum conservation is formally sub-leading in many observables. However, it is phenomenologically important and necessary for shower unitarity. Furthermore, if total energy-momentum conservation is handled incorrectly it can spoil the NLL accuracy of a shower for some observables [10]. We will return to this in Section 6.4.
- We averaged the azimuthal dependence of the matrix elements. However, this ignores possible azimuthal dependence of the observable. Really one should compute $\langle |\mathcal{M}_n|^2 u(\{p\}_n, \{v\}) \rangle_{1, \dots, n}$. It is therefore important to ask whether

$$\langle |\mathcal{M}_n|^2 u(\{p\}_n, \{v\}) \rangle_{1, \dots, n} \approx \langle |\mathcal{M}_n|^2 \rangle_{1, \dots, n} \langle u(\{p\}_n, \{v\}) \rangle_{1, \dots, n}$$

³In the appendix, we sum over branching topologies: $\sum_{j_1, \dots, j_n} \langle |\mathcal{M}_n|^2 \rangle_{1, \dots, n} = \langle |\mathcal{M}_n|^2 \rangle_{1, \dots, n}$.

⁴Some azimuthal correlations due to colour correlations can be re-instantiated in coherent branching algorithms [21, 22].

is a good approximation. In other words, are the azimuthal dependencies of the matrix element and the observable correlated? This is clearly an observable dependent statement. Despite this we can make some progress; we can remove the approximation and find

$$\begin{aligned} \langle |\mathcal{M}_n|^2 u(\{p\}_n) \rangle_{1,\dots,n} &= \langle |\mathcal{M}_n|^2 \rangle_{1,\dots,n} \langle u(\{p\}_n) \rangle_{1,\dots,n} \\ &+ \sum_{m=1}^n \sigma_m(\langle |\mathcal{M}_n|^2 \rangle_{1,\dots,n}) \sigma_m(\langle u(\{p\}_n) \rangle_{1,\dots,n}) \text{Cor}_m(\langle |\mathcal{M}_n|^2 \rangle_{1,\dots,n}, \langle u(\{p\}_n) \rangle_{1,\dots,n}) \\ &+ \text{higher order correlations,} \end{aligned} \quad (6.9)$$

where $\sigma_n(x) = \sqrt{\langle x^2 \rangle_n - \langle x \rangle_n^2}$ and $\text{Cor}_n(x, y) = \frac{\langle (x - \langle x \rangle_n)(y - \langle y \rangle_n) \rangle_n}{\sigma_n(x)\sigma_n(y)}$. The first order correlation term (the second line of Eq. (6.9)) acts as a switch. If it is suppressed relative to the uncorrelated term then all higher correlations will be too. If it is not suppressed then higher order correlations may not be. In Appendix 6.3.2 we show that the higher order correlations are subdominant in the computation of NLL thrust. This is because the observable is two-jet dominated⁵ and exponentiates, and so at NLL accuracy $\sigma_m(\langle u(\{p\}_n) \rangle_{1,\dots,n}) \approx 0$. However, we also find that the correlation term can provide a formally leading contribution to non-global logarithms. In Appendix 6.6.2 we observe that the correlation terms contribute leading logarithms to observables like gaps-between-jets, for which $\alpha_s^n L^n$ logs are leading. The miscalculation of non-global logarithms by angular ordered showers has previously been subject to numerical study in [24, 25], where it was observed that leading non-global logarithms are incorrectly computed by angular ordered showers. However, [24, 25] also observed the error to be a phenomenologically small effect.

6.3.3 Dipole shower

In the PB algorithm, the mechanism for energy-momentum conservation is unspecified. This is because interference terms make it difficult to see how recoil should be distributed. There are no such issues in angular ordered showers. In this case, the naive guess for how to conserve momentum longitudinal to a jet is correct and is sufficient for the computation of NLL DGLAP evolution and jet physics [26–31]. We can exploit this to constrain the form of the recoil ($\int dR_n$) so that the PB algorithm is consistent with an angular ordered shower. In this section, we will derive a dipole shower with this constraint in place from the outset. The resulting dipole shower is very similar to the dipole showers that are commonplace in

⁵Observables, such as thrust, for which the leading logarithms quantify small deviations from the two-jet limit or, more generally, the n -jet limit in the case of n -jettiness [23]

event generators [2, 3]. However, it has a crucial difference: it does not use Catani-Seymour dipole factorisation [32].

To derive the dipole shower proceed as follows.

1. Expand Eq. (6.3) in powers of the number of colours N_c and keep only the leading terms, which go as $\alpha_s^n N_c^n$, see [11, 33]. This is necessary as only in the leading colour limit can we write evolution equations for $|\mathcal{M}_n|^2$. For the same purpose, spin average the evolution, see Appendix 6.7 for details.
2. The colour expansion reduces the evolution equation so that it only depends on dipoles formed by colour connected partons. We use the form of $\int dR_n$ to partition each dipole into two parts, introducing longitudinal momentum conservation to each part of the dipole in such a way that it is exactly consistent with the angular ordered shower. This is similar to how dipoles are usually partitioned using Catani-Seymour dipole factorisation. This partitioning allows us to exchange the sum over dipoles with a sum over emitting parton colour lines.
3. Use the dipole partitioning to restore the (full-colour) hard-collinear physics that is correctly computed by an angularly ordered shower. This is uniquely determined by how longitudinal recoil is assigned. The result is a dipole shower that does not suffer the NLC errors in radiation ordered in angle noted in [10].

In Appendix 6.6.3 the complete proof is presented. The final result, expressed in the colour flow basis, is

$$\begin{aligned}
& q_\perp \frac{\partial |\mathcal{M}_n^{(\sigma)}(q_\perp)|^2}{\partial q_\perp} \\
& \approx \frac{\alpha_s}{\pi} \sum_{i_{n+1}^c} \int dq_\perp^{(i_{n+1}^c, \bar{i}_{n+1}^c)} \delta(q_\perp^{(i_{n+1}^c, \bar{i}_{n+1}^c)} - q_\perp) \int dz \Theta_{\text{on shell}} P_{v_{i_{n+1}} v_{i_{n+1}}}(z) |\mathcal{M}_n^{(\sigma)}(q_\perp)|^2 \\
& - \frac{\alpha_s}{\pi} \int \left(\prod_{j_n} d^4 p_{j_n} \right) \mathfrak{A}_{i_n^c}^{\text{dipole}} P_{v_{i_n} v_{i_n}}(z_n) q_\perp \delta(q_{n\perp}^{(i_n^c, \bar{i}_n^c)} - q_\perp) |\mathcal{M}_{n-1}^{(\sigma/n)}(q_{n\perp}^{(i_n^c, \bar{i}_n^c)})|^2, \quad (6.10)
\end{aligned}$$

where σ is a colour flow and σ/n is the same colour flow but with the n th colour line removed. We use i_n^c to index the (anti-)colour line(s) of parton i in a final state dressed with n soft or collinear partons, i.e. if parton i is a quark it has a single colour line and so $i_n^c = i_n^q$, if parton i is a gluon it will have a colour and an anti-colour line so $i_n^c = i_n^g, \bar{i}_n^g$ respectively. \bar{i}_n^c is the (anti-)colour line connected to i_n^c . Momenta with colour line indices are the momenta of the partons associated to that colour line, i.e. $p_{i_n^c} = p_{i_n}$. The shower is ordered in dipole p_T , defined as

$$(q_{n\perp}^{(i_n^c, \bar{i}_n^c)})^2 = \frac{2(p_{i_n^c} \cdot q_n)(p_{\bar{i}_n^c} \cdot q_n)}{p_{i_n^c} \cdot p_{\bar{i}_n^c}}. \quad (6.11)$$

The dipole splitting functions are

$$P_{qq}(z_n) = C_F \frac{1+z_n^2}{1-z_n}, \quad P_{gg}(z_n) = \frac{C_A}{2} \frac{1+z_n^3}{1-z_n}.$$

These splitting functions are related to those in the previous section according to $\mathcal{P}_{gg}(z) = P_{gg}(z) + P_{gg}(1-z)$, and $\mathcal{P}_{qq}(z) = P_{qq}(z)$. Note that to simplify Eq. (6.10) we have omitted the possibility of $g \rightarrow qq$ transitions, which is sub-leading in colour and only contributes a leading logarithm to single-logarithm, collinear-sensitive observables or at NLL for double-logarithmic observables. In Appendix 6.3.3 we present Eq. (6.10) with this splitting included. Being explicit, we would write the squared matrix element as

$$|\mathcal{M}_n^{(\sigma)}(q_\perp; \{P_1, \dots, P_{n_H}, (z_1, q_{1\perp}^{(i_1^c, \bar{i}^{c_1})}, \phi_1), \dots, (z_n, q_{n\perp}^{(i_n^c, \bar{i}^{c_n})}, \phi_n)\})|^2.$$

As for the angular ordered shower, this is the squared matrix element for a hard process dressed with n strongly-ordered partons with a unique branching topology, i.e. each emitted parton is specified by a triplet $(z_m, q_{m\perp}^{(i_m^c, \bar{i}^{c_m})}, \phi_m)$ and is emitted from the parton with colour line i_m^c . The dipole recoil function is given by

$$\mathfrak{R}_{i_n^c}^{\text{dipole}} = \left(\frac{1}{2} + \text{Asym}_{i_n^c \bar{i}^{c_n}}(q_n) \right) \mathfrak{R}_{i_n^c}, \quad (6.12)$$

where

$$\mathfrak{R}_{i_n^c} = \delta^4(p_{i_n} - z_n^{-1} \tilde{p}_{i_n}) \prod_{i_n \neq j_n} \delta^4(p_{j_n} - \tilde{p}_{j_n}) + \mathcal{O}(q_\perp/Q), \quad (6.13)$$

and where

$$\text{Asym}_{i_n^c \bar{i}^{c_n}}(q_n) = \left[\frac{T \cdot p_{i_n^c} (q_{n\perp}^{(i_n^c, \bar{i}^{c_n})})^2}{4T \cdot q_n p_{i_n^c} \cdot q_n} - \frac{T \cdot p_{\bar{i}^{c_n}} (q_{n\perp}^{(i_n^c, \bar{i}^{c_n})})^2}{4T \cdot q_n p_{\bar{i}^{c_n}} \cdot q_n} \right], \quad \text{and} \quad T = \sum_{i_n} p_{i_n}. \quad (6.14)$$

Note, in the limit that q_n is collinear to $p_{i_n^c}$, $\text{Asym}_{i_n^c \bar{i}^{c_n}}(q_n) = 1/2$. Thus, in this limit $\mathfrak{R}_{i_n^c}^{\text{dipole}} \rightarrow \mathfrak{R}_{i_n^c}$, as required. Our expression for $\mathfrak{R}_{i_n^c}^{\text{dipole}}$ should be compared to the recoil function one would find using Catani-Seymour dipole factorisation:

$$\mathfrak{R}_{i_n^c}^{\text{C.S.}}(q_n) = \left(\frac{(q_{n\perp}^{(i_n^c, \bar{i}^{c_n})})^2 p_{\bar{i}^{c_n}} \cdot p_{i_n^c}}{2p_{i_n^c} \cdot q_n (p_{\bar{i}^{c_n}} + p_{i_n^c}) \cdot q_n} \right) \mathfrak{R}_{i_n^c}. \quad (6.15)$$

$\mathfrak{R}_{i_n^c}^{\text{dipole}} \rightarrow \mathfrak{R}_{i_n^c}^{\text{C.S.}}$ if we were to make the replacement $T \rightarrow p_{i_n^c} + p_{\bar{i}^{c_n}}$. Observables are computed after summing over emission topologies:

$$\Sigma(\mu; \{p\}_0, \{v\}) \approx \int \sum_n \sum_\sigma \sum_{i_1^c, \dots, i_n^c} \left(\prod_{m=1}^n \frac{dq_{m\perp}^{(i_m^c, \bar{i}^{c_m})}}{q_{m\perp}^{(i_m^c, \bar{i}^{c_m})}} \frac{dz_i d\phi_i}{2\pi} \right) |\mathcal{M}_n^{(\sigma)}(\mu)|^2 u(\{p\}_n, \{v\}). \quad (6.16)$$

There are several noteworthy points involved in this derivation:

- This shower was built around preserving the beneficial features of an angular ordered shower. In fact, azimuthally averaging the dipole shower reinstates an angular ordering. Angular ordered showers provide a sufficient framework to resum global two-jet dominated observables, such as thrust, up to $\alpha_s^n L^{2n-1}$ terms with full colour. Radiation consecutively ordered in angle generated by the dipole shower presented here will also achieve this accuracy (radiation unordered in angle will differ at sub-leading N_c). This reduces the doubly logarithmic NLC errors noted in [10], where the particular example of errors in the thrust observable was given.
- Traditional angular ordered showers fail to correctly compute $\alpha_s^n L^{2n-1}$ logarithms for $n > 2$ jet observables. This is because soft, wide-angle physics is miscalculated because of the $\Theta(\theta_{j_n, i_n} - \theta_{n, i_n}) \approx 1$ approximation, as previously discussed.⁶ It is never necessary to make this approximation in the dipole shower since we can use the underlying colour flows to define variables in the relevant dipole frame, for which $\Theta(\theta_{j_n, i_n} - \theta_{n, i_n}) = 1$ is always true. Thus we expect the dipole shower to have the capacity to re-sum $\alpha_s^n L^{2n-1}$ logarithms at leading colour.⁷
- In the soft limit the dipole shower generates iterative solutions to the BMS equation [16, 34] (the proof is as in Section 3 of [11]). This demonstrates that the shower computes non-global logarithms at leading colour correctly.
- At this point in our theoretical development, the dipole shower does not completely conserve energy and momentum. Rather it only conserves momentum longitudinal to the emitting parton. Accounting for total energy-momentum conservation is not needed to compute some observables to NLL accuracy, e.g. thrust. Regardless, it is an important effect that if handled incorrectly can spoil the NLL accuracy of the shower [10]. Addressing this is the focus of the next section.

6.4 Improving recoil in dipole showers

In this section we will address the problem of energy-momentum conservation in a dipole shower, though our approach is simple to map onto an angular ordered shower. The mechanism for energy-momentum conservation (or recoil scheme) we present lacks a formal derivation. Rather it is inspired by the study of recoil by Bewick et al. [17]. Bewick et

⁶Modern implementations of angular ordered showers do use colour flow information from the hard process, allowing them to compute $\alpha_s^n L^{2n-1}$ terms at leading colour for global $n > 2$ jet dominated observables by deriving appropriate initial conditions from the respective large- N colour flows of the hard process [5].

⁷Eq. (6.10) as it stands only provides a sufficient framework for this resummation. It is not yet sufficient in itself: one would need to enhance the shower with a running coupling and, possibly, higher order splitting functions.

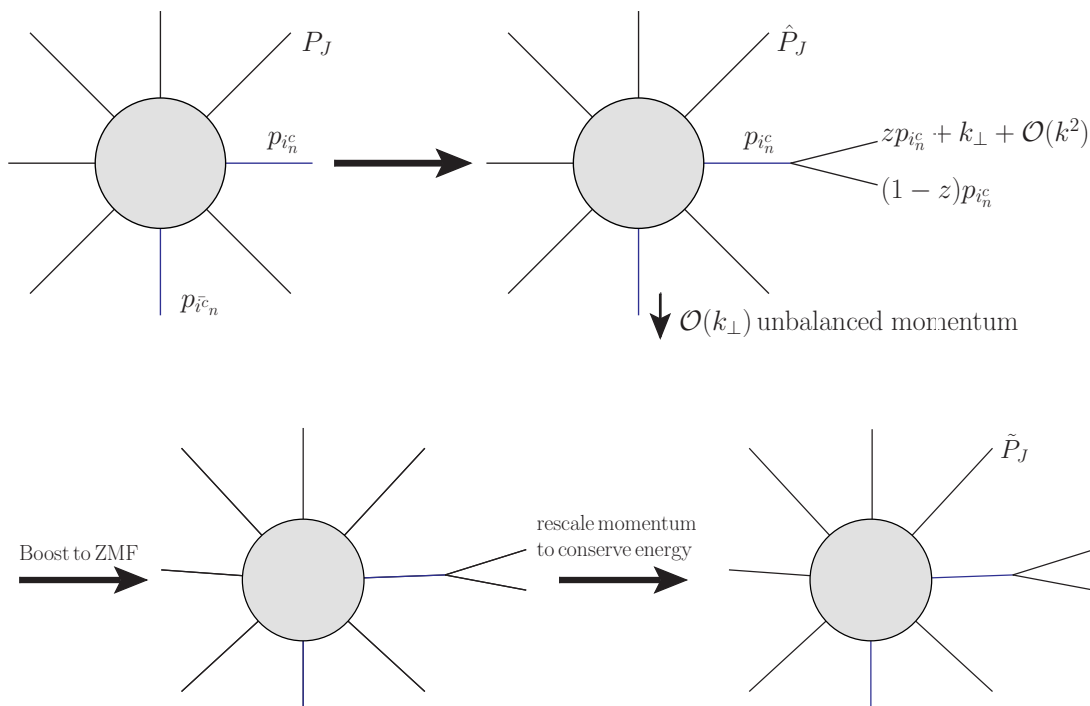


Figure 6.3: A summary of the dipole shower global recoil scheme (a scheme for energy-momentum conservation). In words: A new particle is emitted which leaves some momentum unbalanced (in the direction of the colour connected parton and in the plane transverse to the dipole); perform a Lorentz boost to the new ZMF, and re-scale the jet momenta in such a way that the rescaling does not change the k_\perp of the emission. This leaves an n -parton ensemble with the same total energy and total momentum as the $n - 1$ -parton ensemble.

al. analysed several approaches to recoil in angular ordered showers, reproducing some of the fixed-order checks of [10] and performing further numerical checks. They observed that among the better performing recoil schemes are globally defined schemes; schemes that redistribute momentum across an entire jet or event. From our perspective, a global scheme is also preferable, as it is more simply implemented in a dipole shower. Momentum conservation on an emission-by-emission basis is also desirable when it comes to matching to fixed-order and merging of hard processes of different jet multiplicity. In the two-jet limit, our scheme becomes that which is analysed in [17] and implemented in HERWIG’s angular ordered shower [5]. For comparison, in Appendix 6.8 we summarise the implementation and limitations of a spectator recoil scheme, as implemented in [2, 3, 35].

We start with an observation that is key to all global recoil schemes: when a parton is emitted from another, the parent parton must have been off-shell. We parametrise the amount by which it is off shell by giving it a virtual mass. A parton shower approximates the sum over the multiplicities of QCD radiation dressing a given hard process. Each term

in the sum should have the same total energy and the same zero-momentum frame (ZMF). Naively adding a parton to an $n - 1$ on-shell parton state changes the total energy and ZMF. We will redistribute parton momenta as simply as possible in order to restore the ZMF and total energy. We will do this using a single global Lorentz boost and a single rescaling that preserves the transverse momentum ordering. This procedure is illustrated in Figure 6.3. Below we will spell out how to implement this recoil scheme. The simplicity of the scheme can get lost in its mathematical definition and so we encourage the reader to keep Figure 6.3 in mind.

Let us now make Figure 6.3 quantitative. We require that energy is conserved, $E_{\text{before}} = E_{\text{after}} = Q$ where

$$\begin{aligned} \sum_{i_n}^{n-1} \sqrt{\mathbf{p}_{i_n}^2 + m_{i_n}^2} &\equiv \sum_{J=1}^{n-1} \sqrt{\mathbf{P}_J^2 + m_J^2} = E_{\text{before}}, \\ \sum_{i_n}^{n-1} \sqrt{\tilde{\mathbf{p}}_{i_n}^2 + m_{i_n}^2} + \sqrt{\mathbf{q}_n^2 + m_{q_n}^2} &\equiv \sum_{J=1}^{n-1} \sqrt{\tilde{\mathbf{P}}_J^2 + \tilde{P}_J^2} = E_{\text{after}}, \end{aligned} \quad (6.17)$$

and that momentum is conserved

$$\sum_{J=1}^{n-1} \mathbf{P}_J = \sum_{J=1}^{n-1} \tilde{\mathbf{P}}_J = 0, \quad (6.18)$$

where, in the ZMF, \mathbf{P}_J is the 3-momentum of J th jet amongst the $n - 1$ jets constructed from an $n - 1$ parton ensemble, i.e. $\mathbf{P}_J = \mathbf{p}_{i_n}$ for $J = i_n$ (recall that i_n labels parton i in an n -parton ensemble). We introduce the extra notation because it is the momentum of jets that we particularly focus on conserving. $\tilde{\mathbf{P}}_J$ is what we wish to find; it is the momentum of the J th jet now constructed from an n parton ensemble after the necessary redistribution of momenta (all jets contain a single parton except for one which contains two partons; the original parton and the newly added parton). m_i is the mass of parton i , and $m_i = 0$ since we consider only massless partons. \tilde{P}_J^2 is the virtual mass squared of the J th jet, it also is zero for all jets other than the jet built of two partons. We can achieve our desired redistribution by a Lorentz boost, Λ_{ν}^{μ} , from the ZMF of the $n - 1$ parton ensemble to the ZMF of the n parton ensemble. Once in this frame, we re-scale all the jet momenta by a global factor $\kappa_{i_n^c}$ (the index will prove necessary later on) so as to preserve the centre-of-mass energy. In all, we wish to find $\tilde{P}_{J\mu} = \kappa_{i_n^c} \Lambda_{\mu}^{\nu} \hat{P}_{j\nu}$ where \hat{P}_j is the four-momentum of the J th jet constructed from the n parton ensemble *before* the redistribution of momenta. We place a hat on all intermediary kinematic variables (i.e. those after the emission but before redistribution of momenta). We denote the 3-momentum of \tilde{P}_J as $\tilde{\mathbf{P}}_J = \kappa_{i_n^c} \mathbf{\Lambda} \hat{\mathbf{P}}_J$.

Λ_ν^μ is specified by solving Eq. (6.18) and $\kappa_{i_n^c}$ is specified by solving

$$Q = \sum_{J=1}^{n-1} \sqrt{\tilde{\mathbf{P}}_J^2 + \tilde{P}_J^2} = \sum_{J=1}^{n-1} \kappa_{i_n^c} \sqrt{(\Lambda \hat{\mathbf{P}}_J)^2 + \hat{P}_J^2}, \quad (6.19)$$

which comes from requiring $E_{\text{before}} = E_{\text{after}} = Q$.

We will express this recoil scheme in terms of the shower kinematics and solve for $\tilde{\mathbf{P}}_J$. We use the following Sudakov decomposition for a $1 \rightarrow 2$ ($p_{i_n^c} \rightarrow \hat{p}_{i_n^c} \hat{q}_n$) parton transition:

$$\begin{aligned} \hat{q}_n &= (1 - z_n) p_{i_n^c} + k_\perp + \frac{(q_{n\perp}^{(i_n^c \bar{i}_n^c)})^2}{1 - z_n} \frac{p_{\bar{i}_n^c}}{2p_{i_n^c} \cdot p_{\bar{i}_n^c}}, \\ \hat{p}_{i_n^c} &= z_n p_{i_n^c}, \quad (q_{n\perp}^{(i_n^c \bar{i}_n^c)})^2 = -k_\perp^2, \quad k_\perp \cdot p_{i_n^c} = k_\perp \cdot p_{\bar{i}_n^c} = 0. \end{aligned} \quad (6.20)$$

We label the jet in which the splitting takes place as $P_{J \text{ emit}}$, so that $P_{J \text{ emit}} = p_{i_n^c}$. From Eq. (6.20):

$$\hat{P}_{J \text{ emit}}^2 = \frac{z_n (q_{n\perp}^{(i_n^c \bar{i}_n^c)})^2}{(1 - z_n)}, \quad \hat{\mathbf{P}}_{J \text{ emit}} = \mathbf{P}_{J \text{ emit}} + \mathbf{k}_\perp + \frac{(q_{n\perp}^{(i_n^c \bar{i}_n^c)})^2}{(1 - z_n) 2p_{i_n^c} \cdot p_{\bar{i}_n^c}} \mathbf{P}_{\bar{i}_n^c}.$$

For all jets other than “ J emit” $\hat{\mathbf{P}}_J = \mathbf{P}_J$ and $\hat{P}_J^2 = 0$. The Lorentz boost, $\Lambda_\nu^\mu(i_n^c, \bar{i}_n^c)$, can now be found. The boost is in the direction of $\mathbf{p}_{\bar{i}_n^c}$ and is given by the boost velocity

$$\beta_{\text{ZMF}} = \frac{\hat{\mathbf{P}}_{J \text{ emit}} - \mathbf{P}_{J \text{ emit}}}{\sum_J \sqrt{\hat{\mathbf{P}}_J^2 + \hat{P}_J^2} + \sqrt{|\hat{\mathbf{P}}_{J \text{ emit}} - \mathbf{P}_{J \text{ emit}}|^2 + k_\perp^2}}. \quad (6.21)$$

Finally we must solve for $\kappa_{i_n^c}$ using Eq. (6.19),

$$\kappa_{i_n^c} = \frac{\sum_{J=1}^{n-1} \sqrt{\mathbf{P}_J^2 + P_J^2}}{\sum_{J=1}^{n-1} \sqrt{(\Lambda \hat{\mathbf{P}}_J)^2 + \hat{P}_J^2}}. \quad (6.22)$$

Note that in both the soft and collinear limits $\kappa_{i_n^c} \rightarrow 1$.

So now we have everything we need to compute $\tilde{\mathbf{P}}_J = \kappa_{i_n^c} \Lambda \hat{\mathbf{P}}_J$. We can put this in the dipole shower by introducing a recoil function

$$\mathfrak{R}_{i_n^c} = \delta_{\mathcal{J}}^4(\tilde{p}_{i_n^c} - z_n \kappa_{i_n^c} \Lambda(i_n^c, \bar{i}_n^c) p_{i_n^c}) \prod_{j_n \neq i_n} \delta_{\mathcal{J}}^4(\kappa_{i_n} \Lambda(i_n^c, \bar{i}_n^c) p_{j_n} - \tilde{p}_{j_n}), \quad (6.23)$$

where $\delta_{\mathcal{J}}^4(f(p_{i_n^c}))$ is a delta function normalised against its Jacobi factor:

$$\delta_{\mathcal{J}}^4(f(p_{i_n^c})) = \delta^4(p_{i_n^c} - X),$$

where X is the (unique) solution to $f(X) = 0$. Note that in an implementation of the algorithm there is never any need to invert the argument of the delta function to solve for $p_{i_n^c}$ since $\tilde{p}_{i_n^c}$ is what is needed going forwards. In Eq. (6.10), the delta functions simply

kill all of the integrals over p_{jn} . For the sake of being explicit, the emitted parton has momentum

$$q_n = (1 - z_n)\kappa_{i_n^c} \Lambda(i_n^c, \bar{i}_n^c) p_{i_n^c} + k_\perp + \frac{(q_{n\perp}^{(i_n^c \bar{i}_n^c)})^2}{\kappa_{i_n^c} (1 - z_n)} \frac{\Lambda(i_n^c, \bar{i}_n^c) p_{\bar{i}_n^c}}{2p_{i_n^c} \cdot p_{\bar{i}_n^c}}. \quad (6.24)$$

Note that both z_n and $dq_{n\perp}^{(i_n^c \bar{i}_n^c)}/q_{n\perp}^{(i_n^c \bar{i}_n^c)}$ are Lorentz and jet scaling invariants. This means that all of the emission kernels remain unchanged and so the implementation of this recoil scheme only enters so as to ensure that the real emissions continue to be integrated over the correct phase-space (and through the corresponding $\Theta_{\text{on shell}}$ for the virtuals).

In order to implement the proposed shower computationally we must specify the phase-space boundary for real emissions. In our previous papers, [11, 12, 35], we gave general formulae for the computation of phase-space boundaries, derived by ensuring the emitted parton is on-shell and has less energy than its parent. Applying these to the recoil prescription we present here, we find that

$$z_n \in \left(0, 1 - \frac{(q_{n\perp}^{(i_n^c \bar{i}_n^c)})^2}{2p_{i_n^c} \cdot p_{\bar{i}_n^c}} \right), \quad \phi \in [0, 2\pi), \quad (6.25)$$

up to terms of the order $(1 - \kappa_{i_n^c})$; in the following section, we show that these terms are negligible at NLL accuracy. Here ϕ is the trivial azimuth in the dipole frame. Thus, the complete dipole shower is defined by Eq. (6.10)⁸, Eq. (6.12), Eq. (6.23), and Eq. (6.25).

6.4.1 NLC and NLL accuracy of the global recoil

In this section we will discuss the colour accuracy of our new dipole shower and test its logarithmic accuracy.

Firstly, the sub-leading colour contained in the shower is inherited from its link to angular ordered showers. In fact, when next-to-leading order splitting functions and the CMW running coupling are introduced the collinear radiation generated by the dipole shower is equivalent (after azimuthal averaging) to that generated by the coherent branching algorithm of [19, 20] up to the handling of transverse recoil. We discuss this in more detail in Appendix 6.9.1 where we argue that differences due to transverse recoil do not effect next-to-leading logarithmic accuracy in the angular-ordered limit. This means that the dipole shower can be used to compute the leading-colour NLL resummation of thrust, again see Appendix 6.9.1. Correct colour factors will also be assigned to the leading logarithms associated with a broad class of observables that can be computed fully at LL accuracy in the angular-ordered approach (for which radiation unordered in angle generate NLLs).

⁸Or better still, Eq. (6.83), which also includes $g \rightarrow qq$ transitions.

Outside of this limit, only leading colour accuracy is guaranteed. This is an improvement on existing dipole showers, which have been noted to incorrectly compute NLC at LL accuracy [10], even including errors in logarithms originating from radiation ordered in angle. Further improvements on sub-leading colour, for more general observables, require amplitude evolution. We doubt that substantial further improvements in the accuracy of sub-leading-colour effects can be achieved in either the dipole shower or coherent branching frameworks. There is already a body of literature exploring possible resolutions to the NLC errors in dipole showers [36–38]. Our approach of using angular ordering to improve dipole evolution is similar to that of [36, 37], though there it was largely explored only in the context of hadronisation and the computation of jet multiplicity observables. We also note that, by partitioning dipoles so as to identify a unique parent, we expect the sub-leading logarithms associated with unresolved soft and collinear radiation to be captured using the CMW scheme for the running coupling [18, 20].

We will now proceed to evaluate the logarithmic accuracy of the recoil scheme discussed in the previous section. We do so in two ways. Firstly by re-creating the analysis of Section 4.2 in [10]. In this analysis, several event shape observables, defined by functions $V(\{p\})$, are considered at fixed order. The analysis tests the sub-leading contributions from the soft region found in the limit that the transverse momentum of the second emission is of similar magnitude to that of the first but both are small relative to the hard scale. This limit is considered because it is the limit where dipole showers have previously been shown to mishandle recoil. Specifically, we calculate the difference between the α_s^2 LC, NLL contribution to the observable using the fixed-order amplitude, and the shower contribution: $\delta\Sigma(L) = \Sigma_{\text{shower}}^{(\alpha_s^2)}(L) - \Sigma_{\text{FO}}^{(\alpha_s^2)}(L)$. As the observables exponentiate, we are looking for differences of the form $\alpha_s^2 N_c^2 L^2$ at fixed coupling since these terms contribute to the NLL exponent.

Our second check of logarithmic accuracy is to compare against two known NLL resummations: Thrust and generating functions for jet multiplicity. This is done in Appendix 6.9.

Let us proceed to compute $\delta\Sigma(L)$ in the doubly-soft limit in $e^+e^- \rightarrow q\bar{q}$. We label the quark as parton a and the anti-quark as parton b . In the same way that we label partons with indices i_n , each parton label is given a subscript stating the ‘current’ multiplicity of radiated partons (since a parton’s momentum changes to conserve momentum as more

partons are radiated). From Eq. (6.10) we can compute the first two soft emissions and find

$$\begin{aligned} \delta\Sigma(L) &= \mathcal{C}_F^2 \sigma_{n_H} \int d\Pi_2 d\Pi_1 \int dq_{2\perp}^{(a_2,1_2)} \delta(q_{2\perp}^{(a_2,1_2)} - q_{2\perp}) \int dq_{1\perp}^{(a_1,b_1)} \delta(q_{1\perp}^{(a_1,b_1)} - q_{1\perp}) \\ &\times \Theta(q_{1\perp} - q_{2\perp}) \left[\int \prod_{n=1}^2 \prod_{k_n} d^4 p_{k_n} \mathfrak{R}_{a_2 1_2}^{\text{soft}} \theta_{a_2 1_2} \mathfrak{R}_{a_1 b_1}^{\text{soft}} \theta_{a_1 b_1} \Theta(e^{-L} - V(\{p\}_2)) \right. \\ &\quad \left. - \theta_{a_2 1_2}^{\text{correct}} \theta_{a_1 b_1}^{\text{correct}} \Theta(e^{-L} - V(\{p\}_{\text{correct}})) \right], \end{aligned} \quad (6.26)$$

where σ_{n_H} is the hard process cross section. $\theta_{i_n j_n}$ is the product of theta functions defining the on-shell requirements for emission from dipole $i_n j_n$ (previously given without indices as $\Theta_{\text{on-shell}}$). $\{p\}_{\text{correct}}$ are the momenta used to compute $\Sigma_{\text{FO}}^{(\alpha_s^2)}(L)$ and $\theta_{i_n j_n}^{\text{correct}} = \theta_{i_n j_n}(\{p\}_{\text{correct}})$. $\mathfrak{R}_{i_n j_n}^{\text{soft}}$ is the combined dipole recoil function, $\mathfrak{R}_{i_n j_n}^{\text{soft}} = \mathfrak{R}_{i_n}^{\text{dipole}} + \mathfrak{R}_{j_n}^{\text{dipole}}$. Before considering any specific event shape, we can simplify our expressions further by using the recoil delta functions to perform some of the integrals. These fix the final state momenta:

$$\begin{aligned} \{p\}_2 &= \{\tilde{p}_a, \tilde{p}_b, \tilde{q}_1, q_2\}, \quad \text{where} \quad \tilde{p}_a = \kappa_{a_2} \kappa_{a_1} \Lambda(a_2, 1_2) \Lambda(a_1, b_1) p_a, \\ &\quad \tilde{p}_b = \kappa_{a_2} \kappa_{a_1} \Lambda(a_2, 1_2) \Lambda(a_1, b_1) p_b, \\ &\quad \tilde{q}_1 = \kappa_{a_2} \Lambda(a_2, 1_2) q_1, \quad q_2 \text{ unmodified}, \\ &\quad \tilde{Q} = \kappa_{a_2} \kappa_{a_1} Q, \quad \tilde{Q} = \kappa_{a_1} Q, \quad Q = \mathcal{O}(2p_a \cdot p_b). \end{aligned} \quad (6.27)$$

q_1 and q_2 are defined with respect to the rescaled momenta \tilde{p}_a, \tilde{p}_b and so have appropriately modified limits on their phase space. We employ the ‘equally soft’ limit ($Q \gg q_{1\perp}, q_{2\perp}$; $q_{1\perp} \gtrsim q_{2\perp}$) which reduces the complexity of the phase space limits and removes dependence on longitudinal recoil. In total, we find that

$$\begin{aligned} \delta\Sigma(L) &\approx \frac{4\alpha_s^2 \mathcal{C}_F^2 \sigma_{n_H}}{\pi^2} \int_0^Q \frac{dq_{2\perp}^{(a_2,1_2)}}{q_{2\perp}^{(a_2,1_2)}} \int_0^Q \frac{dq_{1\perp}^{(a_1,b_1)}}{q_{1\perp}^{(a_1,b_1)}} \int_{-\ln \tilde{Q}/q_{1\perp}^{(a_1,b_1)}}^{\ln \tilde{Q}/q_{1\perp}^{(a_1,b_1)}} dy_1 \int_{-\ln \tilde{Q}/\tilde{q}_{2\perp}^{(a_2,1_2)}}^{\ln \tilde{Q}/\tilde{q}_{2\perp}^{(a_2,1_2)}} dy_2 \\ &\quad \times \int_0^{2\pi} \frac{d\phi_2}{2\pi} \Theta(e^{-L} - V(\{p\}_2)) \Theta(Q - q_{1\perp}^{(a_1,b_1)}) \Theta(\kappa_{a_2}^{-1} q_{1\perp}^{(a_1,b_1)} - q_{2\perp}^{(a_2,1_2)}) \\ &\quad - \frac{4\alpha_s^2 \mathcal{C}_F^2 \sigma_{n_H}}{\pi^2} \int_0^Q \frac{dq_{1\perp}^{(a_1,b_1)}}{q_{1\perp}^{(a_1,b_1)}} \int_0^{q_{1\perp}^{(a_1,b_1)}} \frac{dq_{2\perp}^{(a_2,1_2)}}{q_{2\perp}^{(a_2,1_2)}} \int_{-\ln Q/q_{1\perp}^{(a_1,b_1)}}^{\ln Q/q_{1\perp}^{(a_1,b_1)}} dy_1 \int_{-\ln Q/q_{2\perp}^{(a_2,1_2)}}^{\ln Q/q_{2\perp}^{(a_2,1_2)}} dy_2 \\ &\quad \times \int_0^{2\pi} \frac{d\phi_2}{2\pi} \Theta(e^{-L} - V(\{p\}_{\text{correct}})). \end{aligned} \quad (6.28)$$

In the ‘equally soft’ limit we are considering

$$\kappa_{i_n} \approx 1 - \mathcal{O}(q_{\perp}^2/2Q^2). \quad (6.29)$$

The κ dependence in the shower integrals (lines 1 and 2 of Eq. (6.28)) causes potentially incorrect $\mathcal{O}(q_\perp^2/2Q^2)$ terms in the phase space limits.⁹ These integrate to give dilogarithms in $q_\perp^2/2Q^2$ which do not contribute $\alpha_s^2 L^2$ terms but rather $\alpha_s^2 L^0$ terms that go to zero in both soft and collinear limits.¹⁰ Thus, with NLL accuracy, Eq. (6.28) reduces to

$$\begin{aligned} \delta\Sigma(L) \approx & \frac{4\alpha_s^2 \mathcal{C}_F^2 \sigma_{n_H}}{\pi^2} \int_0^Q \frac{dq_{1\perp}^{(a_1, b_1)}}{q_{1\perp}^{(a_1, b_1)}} \int_{-\ln Q/q_{1\perp}^{(a_1, b_1)}}^{\ln Q/q_{1\perp}^{(a_1, b_1)}} dy_1 \int_0^{q_{1\perp}^{(a_1, b_1)}} \frac{dq_{2\perp}^{(a_2, 1_2)}}{q_{2\perp}^{(a_2, 1_2)}} \int_{-\ln Q/q_{2\perp}^{(a_2, 1_2)}}^{\ln Q/q_{2\perp}^{(a_2, 1_2)}} dy_2 \\ & \times \int_0^{2\pi} \frac{d\phi_2}{2\pi} [\Theta(e^{-L} - V(\{p\}_2)) - \Theta(e^{-L} - V(\{p\}_{\text{correct}}))]. \end{aligned} \quad (6.30)$$

Note that $\delta\Sigma(L)$ is only non-zero because $\{p\}_2 \neq \{p\}_{\text{correct}}$.

We will now consider several specific observables, still following [10]. Dasgupta et al. first consider the two-jet rate in the Cambridge algorithm. They argue that for this observable $V(\{p_i\}) = \max_i \{p_{i\perp}\}$. We notice that $q_{n\perp}^{(a_n, b_n)}$ is a Lorentz invariant. As a consequence $q_{n\perp}^{(a_n, b_n)}$ is always larger than $q_{n+1\perp}^{(a_{n+1}, b_{n+1})}$ for our recoil scheme, up to the neglected dilogarithmic piece. Therefore we find $V(\{p\}_{\text{correct}}) = V(\{p\}_2) = q_{1\perp}^{(a_1, b_1)}$ and that the $\alpha_s^2 N_c^2 L^2$ terms are correctly computed. Similarly, $V(\{p\}_2)$ is also equal to the correct measurement function (up to neglected poly-logs) for the ‘fractal moment of energy-energy correlation’ (FC₁) which, in the soft-collinear limit, is given by $V(\{p_i\}_{\text{correct}}) = \sum_i p_{i\perp}$. In the limit we are studying $V(\{p_i\}_2) = \kappa_{a_2} q_{1\perp}^{(a_1, b_1)} + q_{2\perp}^{(a_2, 1_2)} \approx q_{1\perp}^{(a_1, b_1)} + q_{2\perp}^{(a_2, 1_2)} = V(\{p_i\}_{\text{correct}})$. In fact, it will be the case that for all observables built from Lorentz invariant and jet rescaling insensitive quantities¹¹ our recoil scheme is sufficient for the computation of $\alpha_s^2 N_c^2 L^2$ terms. This being because the scheme is constructed by a Lorentz boost and a formally sub-leading reweighting. We expect that for suitably simple observables this accuracy will also extend to higher orders, see the resummations in Appendix 6.9. This discussion should be contrasted with that in Appendix 6.8, where we perform the same tests with a spectator recoil scheme [2–4]. In agreement with [10], we find that with such a recoil scheme these observables return $V(\{p_i\}_2) \not\approx V(\{p_i\}_{\text{correct}})$. This generates NLL errors.

⁹The algebra to show this is awkward but as κ_{i_n} is simply a ratio of energies, we can argue that it must be an even polynomial when expanded in small q_\perp .

¹⁰The recoil terms in these integrals are reducible to a few general forms. One such form is

$$\begin{aligned} & \int_a^1 \frac{dx}{x} \ln^2 x \ln \left(x \left(1 - \frac{x^2 \epsilon}{2} \right) \right) \\ & = \frac{1}{4} \left(\text{Li}_4 \left(\frac{a^2 \epsilon}{2} \right) + 2 \ln^2(a) \text{Li}_2 \left(\frac{a^2 \epsilon}{2} \right) - 2 \ln(a) \text{Li}_3 \left(\frac{a^2 \epsilon}{2} \right) - \ln^4(a) - \text{Li}_4 \left(\frac{\epsilon}{2} \right) \right) \end{aligned}$$

where a parametrises the observable, $x \sim q_\perp/Q$ and ϵ parametrises the coefficients to the $\mathcal{O}(q_\perp^2/2Q^2)$ effects from our recoil scheme; $\epsilon = 0$ gives the leading log result. Note that all terms other than the LL result are not enhanced in the $a \rightarrow 0$ limit. See Appendix 6.9.1 for more details.

¹¹Observables not sensitive to the absolute magnitude of energy deposited in a part of a detector.

6.5 Conclusions

Starting from a general algorithm designed to capture both the soft and collinear logarithms associated with the leading infra-red singularities of scattering amplitudes, we have derived an angular ordered shower and a dipole shower. Our dipole shower is novel in the way that it partitions each dipole in order to account for longitudinal momentum conservation. This partitioning is constructed so as to ensure that the shower implements longitudinal momentum conservation in precisely the same way as the angular ordered shower does. This new dipole partitioning is similar to, but not the same as, Catani-Seymour partitioning. We complete our dipole shower by specifying the transverse recoil and phase-space. The result is a new dipole shower that formally represents an increase in accuracy when compared to the traditional parton shower models employed by many current event generators [2–6, 8, 39, 40]. For example it will compute radiation ordered in angle at full-colour, and the leading-colour contribution associated with non-global logarithms, i.e. it will reproduce the correct leading-colour, wide-angle, soft radiation pattern beyond the two, three, and four-jet limits whilst retaining complete leading-colour, global NLLs in the two-jet limit. To our knowledge this is not achieved by other parton shower models.

However, our shower still has substantial limitations. In large part that is because it is based on a cross-section-level, semi-classical picture. Operating at cross-section level necessitates that the shower generally be defined only at leading-colour. General full-colour resummation means a more complicated, amplitude-level, approach [12–15, 41–43]. Certainly it would be of considerable interest to compare a parton shower defined at amplitude level, such as the CVolver shower that is currently under construction [44, 45] or the Deductor shower [46], with the improved dipole shower we present here.

6.6 Appendix: The evolution equations supplementary material

6.6.1 Amplitude evolution detailed definitions

Before we proceed with the technical details of the PB evolution, it is necessary that we properly introduce the notation we will later be relying on. In these appendices we will often find ourselves manipulating expressions relating states of differing parton multiplicities (for instance Eq. (6.3) relates an $n_H + n - 1$ state to a $n_H + n$ state). We must label partons and the multiplicity of state they come from carefully since the state's multiplicity determines both the dimension of the colour-helicity space in which the state resides and the momenta of the constituent partons. To this end, we label partons with indices i_n, j_n, k_n, \dots which run as $i_n, j_n, \dots \in \{1_H, 2_H, \dots, n_H\} \cup \{1, 2, \dots, n - 1\}$, where $\{1_H, 2_H, \dots, n_H\}$ is the set

of hard partons and $\{1, 2, \dots, n-1\}$ the set of partons emitted during the evolution. We use $v_{i_n} \in \{q, g\}$ to label the species of a parton i_n . The momentum of the i^{th} parton in a state of multiplicity $n_{\text{H}} + n - 1$ is $p_{i_n} \in \{p\}_{n-1} = \{P_1, P_2, \dots, P_{n_{\text{H}}}, q_1, \dots, q_{n-1}\}$. The emission operator, \mathbf{D}_n , adds a new (n th) parton, of four-momentum q_n , to the state. After considering energy-momentum conservation, the parton momentum, q_n , is added to the set $\{p\}_{n-1}$, to produce the set $\{p\}_n$. dR_n acts in conjunction with \mathbf{D}_n to map $\{p\}_{n-1}$ to a new set, $\{\tilde{p}\}_{n-1}$. The difference between these two sets is determined by the way we implement energy-momentum conservation (i.e. the recoil prescription). Following this, $\{p\}_n = \{\tilde{p}\}_{n-1} \cup \{q_n\}$ is the set of n momenta including the last emission, q_n .

Many of the objects used in this paper carry complicated dependencies. To simplify some lengthy expressions, we will only provide the full list of arguments in an object's definition. In definitions, we will write every object as some $f(x; \{y\})$, where x is the evolution variable on which f depends and the set $\{y\}$ itemises the complete dependences of f . In all expressions subsequent to the definition we will drop the $\{y\}$ dependence and only write $f(x)$. We can do this safely as, following the initial definition of an object, each object can always be uniquely determined by the subscripts and superscripts we provide.

In Section 6.3.1 we gave an overview of the roles of \mathbf{D}_n , $\int dR_n$ and $\mathbf{\Gamma}_n$. Let us now define these operators more carefully¹²

$$\begin{aligned} \mathbf{D}_n(q_{n\perp}; q_n \cup \{\tilde{p}\}_{n-1}) \mathbf{O} \mathbf{D}_n^\dagger(q_{n\perp}; q_n \cup \{\tilde{p}\}_{n-1}) = \\ \sum_{i_n, j_n} \int \delta q_{n\perp}^{(i_n, j_n)}(q_{n\perp}) \mathbf{S}_n^{i_n} \mathbf{O} \mathbf{S}_n^{j_n \dagger} + \sum_{i_n} \int \delta q_{n\perp}^{(i_n, \vec{n})}(q_{n\perp}) \mathbf{C}_n^{i_n} \mathbf{O} \mathbf{C}_n^{i_n \dagger}, \end{aligned} \quad (6.31)$$

where \mathbf{O} is some operator in the colour-helicity space and where we have used a shorthand notation to help save space

$$\delta x(y) \equiv dx \delta(x - y). \quad (6.32)$$

Delta functions of this form are used to carry the frame dependence of the ordering variable in a compact form. Physically, $\mathbf{S}_n^{i_n}$ emits a soft parton from the parton labelled i_n . These soft partons take the form of interference terms in the evolution. Note that, due to our choice of ordering variable, $\mathbf{S}_n^{i_n}$ cannot completely factorise from $\mathbf{S}_n^{j_n \dagger}$ as both depend on the momenta $(q_{n\perp}^{(i_n, j_n)})^2$ (defined below). They have been written in this separated form to reflect their operator structure in the colour-helicity space. $\mathbf{C}_n^{i_n}$ emits a collinear parton from the parton labelled i_n . The following two definitions for transverse momenta are used as ordering variables for soft and collinear emissions respectively,

$$(q_{n\perp}^{(i_n, j_n)})^2 = \frac{2(p_{i_n} \cdot q_n)(p_{j_n} \cdot q_n)}{p_{i_n} \cdot p_{j_n}}, \quad \text{and} \quad (q_{n\perp}^{(i_n, \vec{n})})^2 = \frac{2(p_{i_n} \cdot q_n)(n \cdot q_n)}{p_{i_n} \cdot n}, \quad (6.33)$$

¹²For pedagogical reviews of the colour-helicity operators relevant in the definition of these operators see [11, 12, 47].

where n is a light-like reference vector. The choice of n is determined by how recoil is handled in the evolution and is often taken to be in the backwards direction relative to p_{i_n} . Strictly speaking, recoil cannot be entirely factorised from each \mathbf{D}_n however the way in which it acts in each \mathbf{D}_n follows a simple pattern. Thus we have used the recoil measure dR_n as an abridged notation. It is defined to act by the following rules

$$\begin{aligned} dR_n \mathbf{S}_n^{i_n} \mathbf{O} \mathbf{S}_n^{j_n \dagger} &\equiv \left(\prod_{i_n} d^4 p_{i_n} \right) \mathfrak{R}_{i_n j_n}^{\text{soft}} \mathbf{S}_n^{i_n} \mathbf{O} \mathbf{S}_n^{j_n \dagger}, \\ dR_n \mathbf{C}_n^{i_n} \mathbf{O} \mathbf{C}_n^{i_n \dagger} &\equiv \left(\prod_{i_n} d^4 p_{i_n} \right) \mathfrak{R}_{i_n}^{\text{coll}} \mathbf{C}_n^{i_n} \mathbf{O} \mathbf{C}_n^{i_n \dagger}. \end{aligned} \quad (6.34)$$

$\mathfrak{R}_{i_n j_n}^{\text{soft}}$ and $\mathfrak{R}_{i_n}^{\text{coll}}$ contain the necessary delta functions and kinematic pre-factors needed to account for energy-momentum conservation. They are discussed in Section 6.4 and further examples are given in [12].¹³ Explicit expressions defining $\mathbf{S}_n^{i_n}$ and $\mathbf{C}_n^{i_n}$ are lengthy and can be found in [12]. Finally,

$$\begin{aligned} \mathbf{\Gamma}_n(q_\perp; \{p\}_n) &= \frac{\alpha_s}{\pi} \int \frac{dS_2^{(q)}}{4\pi} \frac{1}{2} \mathbf{D}_n^2(q_\perp) \Theta_{\text{on shell}} + \frac{\alpha_s}{2\pi} \sum_{i_{n+1}, j_{n+1}} \mathbb{T}_{i_{n+1}}^g \cdot \mathbb{T}_{j_{n+1}}^g i\pi \tilde{\delta}_{i_{n+1} j_{n+1}}, \\ \frac{1}{2} \mathbf{D}_n^2(q_\perp; q \cup \{p\}_n) &= \int dR_{n+1} \frac{1}{2} \text{Final}[\mathbf{D}_{n+1}(q_\perp) \cdot \mathbf{D}_{n+1}(q_\perp)]. \end{aligned} \quad (6.35)$$

Final[...] indicates that the enclosed operators should act on any incoming partons as if they were in the final state (see Eq. A.1 in [12], which defines the operators from which \mathbf{D}_{n+1} is constructed, in this context $\text{Final}[\delta_j^{\text{initial}}] = 0$ and $\text{Final}[\delta_j^{\text{final}}] = 1$ for all j). $\Theta_{\text{on shell}}$ is our short-hand notation for the inclusion of the theta functions necessary for restricting the range of integration to the phase-space for an on-shell parton. These are also specified fully in [12] (see functions θ_{ij} and θ_i in Section 2). $\tilde{\delta}_{i_{n+1} j_{n+1}} = 1$ if both partons i, j are incoming or both outgoing and $\tilde{\delta}_{ij} = 0$ otherwise.

We ought to remark on the fact that $q_{n\perp}$ is not equivalent to the dipole transverse momentum derived in [48, 49]. The latter was derived using fixed-order perturbation theory and is an amplitude-level object that acts to determine the limits on loop integrals. We have not yet figured out a way to include this physics within our algorithm, though we note that it is a higher-order effect.

¹³In [12] $\mathfrak{R}_{i_n j_n}^{\text{soft}}$ and $\mathfrak{R}_{i_n}^{\text{coll}}$ are written as $\mathfrak{R}_{n j_n}^{\text{soft}} * \mathfrak{R}_{n i_n}^{\text{soft}}$ and $\mathfrak{R}_{n i_n}^{\text{coll}} * \mathfrak{R}_{n i_n}^{\text{coll}}$ respectively.

6.6.1.1 Computing observables

In the main text our focus is on dressing $e^+e^- \rightarrow q\bar{q}$. The formalism is more general and can be used to compute observables in hadron-hadron collisions using

$$\begin{aligned} d\sigma_n &= \left(\prod_{i=1}^n d\Pi_i \right) \text{Tr } \mathbf{A}_n(\mu; \{p\}_n), \\ \Sigma(\mu; \{p\}_0, \{v\}) &= \int \sum_n d\sigma_n \star \left\{ \prod_{i \in \text{initial}} f_{v_i} \left(\frac{x_i}{z_{i_1} z_{i_2} \dots}, \mu \right) \right\} u_n(\{p\}_n, \{v\}), \end{aligned} \quad (6.36)$$

where $f_{v_i}(x_i, \mu)$ are the parton distribution functions (PDFs) with momentum fractions x_i and $u_n(\{p\}_n, \{v\})$ is the $(n_H + n)$ -body measurement function for an observable described by parameters $v_i \in \{v\}$. Note that Σ is differential in hard process momenta, and that it should be multiplied by the necessary flux factors as necessary. The star operation is defined in Section 4 of [12] but in essence assigns PDF type to a given partonic leg (gluon or quark). In this paper, every concrete use of our formalism concerns the showering of an e^+e^- hard process and so we will not expand further on the treatment of DGLAP evolution.

6.6.2 Derivation of the angular ordered shower

This section derives an angular ordered shower from Eq. (6.3). It is split in three parts. Part one forms the main derivation, however it will state some results without proof (when these results are themselves laborious to prove). The subsection following presents the limitations of this derivation. Finally the last subsection fills in the gaps. We will focus on $e^+e^- \rightarrow q\bar{q}$ as the hard processes, and at the end we will sketch the extension to other hard processes.

We begin with the amplitude evolution equation, Eq. (6.3), and introduce an azimuthal averaging operation $\langle \rangle_{1, \dots, n}$ which averages the lab frame dipole azimuths of partons 1 to n , i.e.

$$\langle f \rangle_{1, \dots, n} = \int \frac{d\phi_n}{2\pi} \dots \int \frac{d\phi_1}{2\pi} f(\phi_1, \dots, \phi_n).$$

Implicit in this operation is also spin averaging when acting on spin-dependent operators, as discussed in Appendix 6.7. To keep things simple, we will proceed in this section without discussing any dependence on the observable, which means we are implicitly assuming the observable is not a function of the parton azimuths. We devote the next sub-section to

addressing this. After averaging, Eq. (6.3) becomes

$$\begin{aligned}
q_\perp \frac{\partial \langle \mathbf{A}_n(q_\perp) \rangle_{1,\dots,n}}{\partial q_\perp} &= \mathbf{\Gamma}_n(q_\perp) \langle \mathbf{A}_n(q_\perp) \rangle_{1,\dots,n} + \langle \mathbf{A}_n(q_\perp) \rangle_{1,\dots,n} \mathbf{\Gamma}_n^\dagger(q_\perp) \\
&- \int \prod_{i_n} d^4 p_{i_n} \sum_{i_n, j_n} \int \delta q_{n\perp}^{(i_n j_n)}(q_n \perp) \langle s_{i_n, j_n} \rangle_n \mathbb{T}_{i_n} \langle \mathbf{A}_{n-1}(q_n \perp) \rangle_{1,\dots,n-1} \mathbb{T}_{j_n}^\dagger q_\perp \delta(q_\perp - q_n \perp) \\
&- \int \prod_{i_n} d^4 p_{i_n} \sum_{j_n} \int \delta q_{n\perp}^{(j_n, \vec{n})}(q_n \perp) \langle c_{j_n} \rangle_n \mathbb{T}_{j_n} \langle \mathbf{A}_{n-1}(q_n \perp) \rangle_{1,\dots,n-1} \mathbb{T}_{j_n}^\dagger q_\perp \delta(q_\perp - q_n \perp),
\end{aligned} \tag{6.37}$$

where s_{i_n, j_n} and c_{j_n} are the spin-averaged kinematic factors associated with a soft or collinear emission respectively (they will be manipulated into the form of collinear splitting functions shortly). They are defined through the relations

$$\begin{aligned}
s_{i_n, j_n} \mathbb{T}_{j_n} \cdot \mathbb{T}_{i_n} &\equiv \frac{1}{2} \sum_{h_{i_n}} \langle h_{i_n} | \mathbf{S}_n^{j_n} \cdot \mathbf{S}_n^{i_n} | h_{i_n} \rangle \mathfrak{R}_{i_n j_n}^{\text{soft}}, \\
c_{j_n} \mathbb{T}_{i_n} \cdot \mathbb{T}_{i_n} &\equiv \frac{1}{2} \sum_{h_{i_n}} \langle h_{i_n} | \mathbf{C}_n^{i_n} \cdot \mathbf{C}_n^{i_n} | h_{i_n} \rangle \mathfrak{R}_{i_n}^{\text{coll}}.
\end{aligned} \tag{6.38}$$

We observe that $c_{j_n} = \langle c_{j_n} \rangle_n$ provided $\mathfrak{R}_{i_n}^{\text{coll}}$ is independent of the emission's azimuth (spin correlations provide the only azimuthal dependence for collinear emissions). In Section 6.6.2.2 we show that¹⁴

$$\begin{aligned}
&\int \delta q_{n\perp}^{(i_n j_n)}(q_n \perp) \langle s_{i_n, j_n} \rangle_n = \\
&- \int \prod_{i_n} d^4 p_{i_n} \left(\langle P_{i_n j_n} \rangle_{\phi_{n, i_n}} \langle \Theta_{\text{on shell}} \rangle_{\phi_{n, i_n}} + \langle P_{j_n i_n} \rangle_{\phi_{n, j_n}} \langle \Theta_{\text{on shell}} \rangle_{\phi_{n, j_n}} \right) \mathfrak{R}_{i_n j_n}^{\text{soft}} + \mathcal{O}(1),
\end{aligned} \tag{6.39}$$

where

$$\langle P_{i_n j_n} \rangle_{\phi_{n, i_n}} = \frac{\Theta(\theta_{j_n, i_n} - \theta_{n, i_n})}{1 - \cos \theta_{n, i_n}}. \tag{6.40}$$

The angles in Eq. (6.40) are defined in Figure 6.2. $\langle \Theta_{\text{on shell}} \rangle_{\phi_{n, i_n}}$ contains the necessary theta functions to constrain the phase-space of parton q_n so that it is real and on-shell, encoding the phase-space limits for energy conservation. Its lengthy definition can also be found in Section 6.6.2.2. The presence of the functions $\langle P_{i_n j_n} \rangle_{\phi_{n, i_n}}$ enforces an angular ordering, secondary to the k_\perp ordering. To bring this ordering to the fore, we now change variables:

$$q_\perp^2 = E_n^2 \sin^2 \theta = E_n^2 (1 - (1 - \zeta)^2), \quad q_\perp \frac{\partial}{\partial q_\perp} = \frac{\zeta(2 - \zeta)}{1 - \zeta} \frac{\partial}{\partial \zeta}$$

¹⁴Under the assumption that $\mathfrak{R}_{i_n j_n}^{\text{soft}}$ is independent of the azimuth up to $\mathcal{O}(1)$ terms, which is true for the two recoil schemes we discuss in this paper.

and define $\zeta_{n,i_n} = 1 - \cos \theta_{n,i_n}$. In these new variables Eq. (6.37) becomes¹⁵

$$\begin{aligned}
\zeta \frac{\partial \langle \mathbf{A}_n(\zeta) \rangle_{1,\dots,n}}{\partial \zeta} &\approx \mathbf{\Gamma}_n(\zeta) \langle \mathbf{A}_n(\zeta) \rangle_{1,\dots,n} + \langle \mathbf{A}_n(\zeta) \rangle_{1,\dots,n} \mathbf{\Gamma}_n^\dagger(\zeta) \\
&+ \int \prod_{i_n} d^4 p_{i_n} \sum_{i_n, j_n} 2 \langle P_{i_n j_n} \rangle_{\phi_{n,i_n}} \langle \Theta_{\text{on shell}} \rangle_{\phi_{n,i_n}} \mathfrak{R}_{i_n j_n}^{\text{soft}} \mathbb{T}_{i_n} \langle \mathbf{A}_{n-1}(q_{n\perp}) \rangle_{1,\dots,n-1} \mathbb{T}_{j_n}^\dagger \zeta_{n,i_n} \delta(\zeta - \zeta_{n,i_n}) \\
&- \int \prod_{i_n} d^4 p_{i_n} \sum_{j_n} \langle P_{j_n} \rangle_n \langle \Theta_{\text{on shell}} \rangle_{\phi_{n,j_n}} \mathfrak{R}_{j_n}^{\text{col}} \mathbb{T}_{j_n} \langle \mathbf{A}_{n-1}(q_{n\perp}) \rangle_{1,\dots,n-1} \mathbb{T}_{j_n}^\dagger \zeta_{n,j_n} \delta(\zeta - \zeta_{n,j_n}).
\end{aligned} \tag{6.41}$$

Here we have used

$$\langle c_{j_n} \rangle_n \approx \langle P_{j_n} \rangle_n \langle \Theta_{\text{on shell}} \rangle_{\phi_{n,j_n}} \mathfrak{R}_{j_n}^{\text{col}},$$

where $\langle P_{j_n} \rangle_n$ is a sum over collinear splitting functions with the soft divergences subtracted away, e.g. when j_n is a quark, $\langle P_{j_n} \rangle_n(z) = (1-z)\bar{\mathcal{P}}_{qq}/2$ where $\bar{\mathcal{P}}_{qq}(z) = -(1+z)$. The details can be found in Appendix A of [12]. We will formulate the evolution in terms of the full splitting functions once equations have been reduced enough that it becomes convenient to do so.

Using the strongly ordered approximation, $\zeta_1 \gg \zeta_2 \gg \dots$ ¹⁶,

$$\langle P_{ij} \rangle_{\phi_{n,i_n}} = \frac{\Theta(\theta_{j_n,i_n} - \theta_{n,i_n}) E_q E_i}{q \cdot p_i} \approx \frac{1}{\zeta_{q,i}}. \tag{6.42}$$

Also using strong ordering, the leading part of $\langle \Theta_{\text{on shell}} \rangle_{\phi_{n,i_n}}$ does not depend on j_n and $\mathfrak{R}_{i_n j_n}^{\text{soft}}$ can be chosen so that its leading part can be factorised from the sum over j_n as

$$\frac{1}{\zeta_{n,i_n}} \langle \Theta_{\text{on shell}} \rangle_{\phi_{n,i_n}} \mathfrak{R}_{i_n j_n}^{\text{soft}} \approx \frac{1}{\zeta_{n,i_n}} \langle \Theta_{\text{on shell}} \rangle_{\phi_{n,i_n}} \mathfrak{R}_{i_n}^{\text{col}}.$$

Using these simplifications we can apply colour conservation and, by re-labelling indices, write

$$\begin{aligned}
\zeta \frac{\partial \langle \mathbf{A}_n(\zeta) \rangle_{1,\dots,n}}{\partial \zeta} &\approx \mathbf{\Gamma}_n(\zeta) \langle \mathbf{A}_n(\zeta) \rangle_{1,\dots,n} + \langle \mathbf{A}_n(\zeta) \rangle_{1,\dots,n} \mathbf{\Gamma}_n^\dagger(\zeta) - \int \prod_{i_n} d^4 p_{i_n} \\
&\times \sum_{j_n} \left(\langle P_{j_n} \rangle_n \langle \Theta_{\text{on shell}} \rangle_{\phi_{n,j_n}} + 2 \frac{1}{\zeta_{n,j_n}} \langle \Theta_{\text{on shell}} \rangle_{\phi_{n,j_n}} \right) \mathfrak{R}_{j_n}^{\text{col}} \\
&\times \mathbb{T}_{j_n} \langle \mathbf{A}_{n-1}(q_{n\perp}) \rangle_{1,\dots,n-1} \mathbb{T}_{j_n}^\dagger \zeta_{n,j_n} \delta(\zeta - \zeta_{n,j_n}).
\end{aligned} \tag{6.43}$$

¹⁵ $\mathbf{\Gamma}_n(\zeta)$ is defined as $\mathbf{\Gamma}_n(q_\perp)$ after the change of variables has been made rather than naively swapping out the argument.

¹⁶When working in a frame that ensures i and j are back to back, the theta function is saturated without approximation. In this derivation we are concerned with $e^+e^- \rightarrow q\bar{q}$. Thus we can saturate the theta function for emissions from the primary hard partons, so that they are handled without approximation. This means we pick the backwards direction (n) (used to define kinematic variables for emissions in a jet) to be in the direction of the other jet. This in turn fixes the definition for the momentum fraction used in later equations: $z_n = \frac{\bar{p}_{j\cdot n}}{p_{j\cdot n}}$. When working beyond the two-jet limit, tricks can be played to further saturate the theta function using knowledge of the hard process colour flows.

By recognising the evolution will become entirely colour-diagonal once the trace is taken, we can diagonalise the colour structures. In turn this allows us to group the soft evolution kernels and the collinear ones into splitting functions. We find

$$\begin{aligned} \zeta \frac{\partial \text{Tr} \langle \mathbf{A}_n(\zeta) \rangle_{1,\dots,n}}{\partial \zeta} &\approx 2\Gamma_n(\zeta) \text{Tr} \langle \mathbf{A}_n(\zeta) \rangle_{1,\dots,n} - \int \prod_{i_n} d^4 p_{i_n} \frac{(1-z_n)}{2} \sum_{j_n} \sum_{v \in \{q,g\}} \mathcal{P}_{vv_{j_n}}(z_n) \\ &\times \langle \Theta_{\text{on shell}} \rangle_{\phi_{n,j_n}} \mathfrak{R}_{j_n}^{\text{col}} \text{Tr} \langle \mathbf{A}_{n-1}(q_{n\perp}) \rangle_{1,\dots,n-1} \zeta_{n,j_n} \delta(\zeta - \zeta_{n,j_n}). \end{aligned} \quad (6.44)$$

$\mathcal{P}_{vv_{j_n}}(z_n)$ are the usual DGLAP splitting functions, e.g. $\mathcal{P}_{qq}(z_n) = \mathcal{C}_F \frac{1+z_n^2}{1-z_n}$. Here we have used v_{j_n} to label the species of parton j_n and v to label the state j_n transitions to; if $v_{j_n} = q$ then $v = q$ and if $v_{j_n} = g$ then $v = q, g$. z_n is the momentum fraction of parton n , i.e. if we have a collinear splitting that induces $j_{n-1} \rightarrow j_n n$ then $p_{j_n} \approx z_n p_{j_{n-1}}$ and $q_n \approx (1-z_n)p_{j_{n-1}}$. We specifically require that $z_n = \frac{\tilde{p}_{j_n \cdot n}}{p_{j_n \cdot n}}$ where n is a light-like vector pointing along the primary axis of the jet from which parton j_n does not stem.

We can make connection to squared matrix elements by letting

$$\langle |M_n|^2 \rangle_{1,\dots,n} = \left(\frac{2\alpha_s}{\pi} \right)^n \prod_{i=1}^n (1-z_i)^{-1} \text{Tr} \langle \mathbf{A}_n(\zeta) \rangle_{1,\dots,n}, \quad (6.45)$$

from which we find the evolution equation for a final-state angular ordered shower with a conventional phase-space for a coherent shower in dz . After which, Eq. (6.44) can be written as in Eq. (6.7) after $\langle |M_n|^2 \rangle_{1,\dots,n} \rightarrow \sum_{j_1,\dots,j_n} \langle |\mathcal{M}_n|^2 \rangle_{1,\dots,n}$.

6.6.2.1 Observable dependence and logarithmic accuracy

In the previous discussion we derived $\langle |M_n|^2 \rangle_{1,\dots,n}$ from Eq. (6.3). However, as we highlighted at the beginning, a full treatment should compute $\langle |M_n|^2 u(\{p\}_n, \{v\}) \rangle_{1,\dots,n}$ where $u(\{p\}_n; \{v\})$ is the measurement function for an observable defined by parameters $v \in \{v\}$.

We want to know to what accuracy is

$$\langle |M_n|^2 u(\{p\}_n) \rangle_{1,\dots,n} \approx \int \prod_{i=1}^n \frac{d\phi_i}{2\pi} \langle |M_n|^2 \rangle_{1,\dots,n} u(\{p\}_n) = \langle |M_n|^2 \rangle_{1,\dots,n} \langle u(\{p\}_n) \rangle_{1,\dots,n}. \quad (6.46)$$

We can start by considering the effects of only averaging over the n th parton and use the following identity

$$\begin{aligned} \langle |M_n|^2 u(\{p\}_n) \rangle_n &= \langle |M_n|^2 \rangle_n \langle u(\{p\}_n) \rangle_n \\ &+ \sigma_n(|M_n|^2) \sigma_n(u(\{p\}_n)) \text{Cor}_n(|M_n|^2, u(\{p\}_n)), \end{aligned} \quad (6.47)$$

where $\sigma_n(x) = \sqrt{\langle x^2 \rangle_n - \langle x \rangle_n^2}$ and $\text{Cor}_n(x(\phi_n), y(\phi_n))$ is the correlation function of x and y under the variation of ϕ_n . Both $|\text{Cor}_n(|M_n|^2, u(\{p\}_n))|$ and $\sigma_n(u(\{p\}_n))$ are smaller than unity¹⁷. Next we can consider averaging over both the n th and $(n-1)$ th partons:

$$\begin{aligned} \langle |M_n|^2 u(\{p\}_n) \rangle_{n-1,n} &= \langle \langle |M_n|^2 \rangle_n \langle u(\{p\}_n) \rangle_n \rangle_{n-1} \\ &\quad + \langle \sigma_n(|M_n|^2) \sigma_n(u(\{p\}_n)) \text{Cor}_n(|M_n|^2, u(\{p\}_n)) \rangle_{n-1}, \end{aligned} \quad (6.48)$$

where

$$\begin{aligned} \langle \langle |M_n|^2 \rangle_n \langle u(\{p\}_n) \rangle_n \rangle_{n-1} &= \langle |M_n|^2 \rangle_{n-1,n} \langle u(\{p\}_n) \rangle_{n-1,n} \\ &\quad + \sigma_{n-1}(\langle |M_n|^2 \rangle_n) \sigma_{n-1}(\langle u(\{p\}_n) \rangle_n) \text{Cor}_n(\langle |M_n|^2 \rangle_n, \langle u(\{p\}_n) \rangle_n). \end{aligned} \quad (6.49)$$

This can be iterated to give

$$\begin{aligned} \langle |M_n|^2 u(\{p\}_n) \rangle_{1,\dots,n} &= \langle |M_n|^2 \rangle_{1,\dots,n} \langle u(\{p\}_n) \rangle_{1,\dots,n} \\ &\quad + \sum_{m=1}^n \sigma_m(\langle |M_n|^2 \rangle_{1,\dots,n}) \sigma_m(\langle u(\{p\}_n) \rangle_{1,\dots,n}) \text{Cor}_m(\langle |M_n|^2 \rangle_{1,\dots,n}, \langle u(\{p\}_n) \rangle_{1,\dots,n}) \\ &\quad + \text{higher order correlations.} \end{aligned} \quad (6.50)$$

We have been slightly lazy with notation; it is implicit that

$$\sigma_m(\langle x \rangle_{1,\dots,n}) \equiv \sigma_m(\langle x \rangle_{1,\dots,m-1,m+1,\dots,n}).$$

The important question is whether the correlations can provide a logarithmic enhancement to the observable. This is obviously an observable dependent statement. To progress we will place some assumptions on the observable. If the observable is such that the correlation term's contribution to the cross section is suppressed relative to $\langle |M_n|^2 \rangle_m \langle u(\{p\}_n) \rangle_m$, we can approximate $\langle |M_n|^2 u(\{p\}_n) \rangle_{1,\dots,n}$ by only keeping the first order correlations, since second order correlations will necessarily be even further suppressed. The approximation assumed by coherent branching is to neglect correlation terms altogether. Let us look at the $n = m = 1$ term for thrust. At this order $u(\{p\}_n)$ is not a function of the azimuth and so $\sigma_1(u(\{p\}_1)) = 0$. As the observable exponentiates [18, 19], this is sufficient to guarantee that it can be computed to NLL using the coherent branching formalism (these last two sentences are an abridged form of the argument in [19]). For contrast, let us look at the $n = m = 2$ term in the computation of gaps-between-jets, with the same hard process. The pertinent measurement functions are

$$u_n(\{p\}_n) = \prod_{m=1}^n (\Theta_{\text{out}}(q_m) + \Theta_{\text{in}}(q_m) \Theta(Q_0 - q_{m,\perp})), \quad (6.51)$$

¹⁷This makes the weak assumption that the measurement function, $u(\{p\}_n)$ is bounded.

where $\Theta_{\text{in/out}}(q_m)$ is unity when parton m is in/out the rapidity region between the two highest p_T jets and zero otherwise. In the following subsection, we compute all the ingredients for $\sigma_2(\langle |M_2|^2 \rangle_1)$. It is reasonably easy to argue (though less easy to compute) that, unless suppressed by multiplicative factors in $\sigma_2(\langle u(\{p\}_2) \rangle_1)$ and correlation functions, $\sigma_2(\langle |M_2|^2 \rangle_1)$ terms can contribute fourth-order, infra-red poles and with them leading logarithms. By considering the variation of ϕ_2 , it is also simple to convince oneself that the correlation function must be finite and positive. So, if angular ordering is to adequately describe this observable, it must be the role of $\sigma_2(\langle u(\{p\}_2) \rangle_1)$ to screen against contaminating logarithms. This means we only need to test to see if $\sigma_2(\langle u(\{p\}_2) \rangle_1)$ is non-zero:

$$\begin{aligned} \sigma_2(\langle u(\{p\}_2) \rangle_1) &= \sqrt{\langle u(\{p\}_2) \rangle_{1,2} \left(1 - \frac{\langle u(\{p\}_2) \rangle_{1,2}}{\langle u(\{p\}_1) \rangle_1} \right)}, \\ &= (\Theta_{\text{out}}(q_1) + \Theta_{\text{in}}(q_1)\Theta(Q_0 - q_{1,\perp})) \\ &\quad \times \sqrt{\langle \Theta_{\text{out}}(q_2) + \Theta_{\text{in}}(q_2)\Theta(Q_0 - q_{2,\perp}) \rangle_2 \left(1 - \langle \Theta_{\text{out}}(q_2) + \Theta_{\text{in}}(q_2)\Theta(Q_0 - q_{2,\perp}) \rangle_2 \right)} \neq 0. \end{aligned} \tag{6.52}$$

Furthermore, not only is this non-zero but it contains non-vanishing terms in $\Theta_{\text{in}}(q_1)\Theta_{\text{out}}(q_2)$. While these terms do screen against fourth order poles and logarithms, they are crucial for the computation of the $\alpha_s^2 L^2$ non-global logarithms. As such, a coherence branching algorithm (that makes usage of azimuthal averaging) cannot compute the leading logarithms to gaps-between-jets, as it certainly gets the numerical coefficient to non-global pieces incorrect. This is a general feature: coherent branching will fail to capture leading, non-global logarithms (though in most cases these logarithms are sub-leading in the computation of the overall cross section). This has been previously observed in [24, 25], where the effect of the missing correlations was computed numerically to all-orders. They found that, though the missing correlations are a formally leading effect, phenomenologically their effect is $< 10\%$. As is widely known, we observe that coherent branching is always capable of calculating logarithms up to $\alpha_s^n L^{2n-1}$ in observables for which $\alpha_s^n L^{2n}$ is the leading logarithm.

6.6.2.2 Azimuthal averaging

In this appendix we will fill in the details on the azimuthal averaging of the evolution kernels. The general procedure for azimuthal averaging is well known [20] textbook material [26, 50]. However, the procedure is less widely discussed taking into account phase-space limits and momentum maps. In this section we provide a more careful treatment than the textbook one. We begin by looking at the following integral (which corresponds to the integrated

soft emission spectrum),

$$\begin{aligned} \int \frac{dS_2^{(q_n)}}{4\pi} \frac{1}{2} \mathbf{S}_n^{j_n} \cdot \mathbf{S}_n^{i_n} &\propto \int \frac{dS_2^{(q_n)}}{4\pi} \int \frac{\delta q_{n\perp}^{(i_n, j_n)}(q_\perp)}{q_\perp} 2 \Theta_{\text{on shell}} \\ &= \int \frac{d\Omega_{q_n}}{4\pi} \int \frac{dE_{q_n}}{E_{q_n}} E_{q_n}^2 \frac{\tilde{p}_{i_n} \cdot \tilde{p}_{j_n}}{\tilde{p}_{i_n} \cdot q_n \tilde{p}_{j_n} \cdot q_n} \Theta_{\text{on shell}} \delta(q_{n\perp}^{(i_n, j_n)} - q_\perp), \end{aligned} \quad (6.53)$$

where E_{q_n} is the energy of parton q and $d\Omega_{q_n}$ is solid angle in the frame which E_{q_n} is measured. We can regroup the dipole kinematics as

$$\begin{aligned} \text{Eq. (6.53)} &= \int \frac{d\Omega_{q_n}}{4\pi} \int \frac{dE_{q_n}}{E_{q_n}} (P_{i_n j_n} + P_{j_n i_n}) \Theta_{\text{on shell}} \delta(q_{n\perp}^{(i_n, j_n)} - q_\perp), \\ 2P_{i_n j_n} &= \frac{n_{i_n} \cdot n_{j_n} - n_{i_n} \cdot n}{n_{i_n} \cdot n \, n_{j_n} \cdot n} + \frac{1}{n_{i_n} \cdot n}, \end{aligned} \quad (6.54)$$

where $n_{i_n} = p_{i_n}/E_{i_n}$. The two terms in this integral are symmetric under the exchange of i and j and so we shall focus only on the first:

$$\begin{aligned} \int \frac{dE_{q_n}}{E_{q_n}} \int \frac{d\Omega_{q_n}}{4\pi} P_{i_n j_n} \Theta_{\text{on shell}} \delta(q_{n\perp}^{(i_n, j_n)} - q_\perp) \\ = \int \frac{dE_{q_n}^2}{2E_{q_n}^2} \int \frac{\sin \theta_{n, i_n} d\theta_{n, i_n} d\phi_{n, i_n}}{4\pi} P_{i_n j_n} \Theta_{\text{on shell}} 2q_\perp \delta\left((q_{n\perp}^{(i_n, j_n)})^2 - q_\perp^2\right). \end{aligned} \quad (6.55)$$

To compute this the integral we take $n_{i_n} = (1, 0, 0, 1)$, $n_{j_n} = (1, \sin \theta_{j_n, i_n}, 0, \cos \theta_{j_n, i_n})$, and $n = (1, \sin \theta_{n, i_n} \cos \phi_{n, i_n}, \sin \theta_{n, i_n} \sin \phi_{n, i_n}, \cos \theta_{n, i_n})$. In this basis

$$\begin{aligned} (q_{n\perp}^{(i_n, j_n)})^2 &= E_{q_n}^2 \frac{2(1 - \cos \theta_{n, i_n})(1 - \sin \theta_{n, i_n} \cos \phi_{n, i_n} \sin \theta_{j_n, i_n} - \cos \theta_{j_n, i_n} \cos \theta_{n, i_n})}{1 - \cos \theta_{j_n, i_n}} \\ &\equiv E_{q_n}^2 \kappa_{i, j, n}, \end{aligned} \quad (6.56)$$

and

$$\begin{aligned} \text{Eq. (6.55)} &= \int \frac{\sin \theta_{n, i_n} d\theta_{n, i_n} d\phi_{n, i_n}}{4\pi} \int \frac{d(\kappa_{i, j, n} E_{q_n}^2)}{2\kappa_{i, j, n} E_{q_n}^2} P_{i_n j_n} \Theta_{\text{on shell}} 2q_\perp \delta(E_{q_n}^2 \kappa_{i, j, n} - q_\perp^2) \\ &= \frac{1}{q_\perp} \int \frac{\sin \theta_{n, i_n} d\theta_{n, i_n} d\phi_{n, i_n}}{4\pi} P_{i_n j_n} \Theta_{\text{on shell}}. \end{aligned} \quad (6.57)$$

The textbook treatment would set $\Theta_{\text{on shell}} = 1$ here. For us,

$$\begin{aligned} \Theta_{\text{on shell}} &= \Theta(p_{i_n} \cdot p_{j_n} - q_n \cdot (p_{j_n} + p_{i_n})) \\ &= \Theta\left(E_{i_n} E_{j_n} (1 - \cos \theta_{j_n, i_n}) - \frac{q_\perp E_{j_n}}{\sqrt{\kappa_{i, j, n}}} (1 - \sin \theta_{n, i_n} \cos \phi_{n, i_n} \sin \theta_{j_n, i_n} - \cos \theta_{j_n, i_n} \cos \theta_{n, i_n}) \right. \\ &\quad \left. - \frac{q_\perp E_{i_n}}{\sqrt{\kappa_{i, j, n}}} (1 - \cos \theta_{n, i_n})\right), \end{aligned} \quad (6.58)$$

which bounds the ϕ_{n,i_n} integration to the range $|\phi_{n,i_n}| \in [\phi_{q,i}^-, \phi_{q,i}^+]$. The solutions for the boundaries, $\phi_{q,i}^\pm$ are given by

$$\begin{aligned}
\cos \phi_{q,i}^\pm &= \pm \min(|\alpha^\pm|, 1) \quad \text{for } \alpha^\pm > 0 \quad \text{and } \cos \phi_{q,i}^\pm = 0 \text{ otherwise,} \\
\alpha^\pm &= \frac{\pm \sqrt{AF^2(AF^2 - 2DGH) + AF^2 - DG(H + CG)}}{(\sin \theta_{n,i_n} \sin \theta_{j_n,i_n})(1 - \cos \theta_{j_n,i_n})q_\perp^2 E_{j_n}^2} \\
F &= E_{i_n} E_{j_n} (1 - \cos \theta_{j_n,i_n}) = E_{i_n} E_{j_n} D, \quad D = 1 - \cos \theta_{j_n,i_n}, \\
H &= q_\perp E_{i_n} (1 - \cos \theta_{n,i_n}) = q_\perp E_{i_n} A, \quad A = 1 - \cos \theta_{n,i_n}, \\
B &= \sin \theta_{n,i_n} \sin \theta_{j_n,i_n}, \\
C &= 1 - \cos \theta_{j_n,i_n} \cos \theta_{n,i_n}, \\
G &= q_\perp E_{j_n}.
\end{aligned} \tag{6.59}$$

Note that the expression under the square root is always positive. The usual approach to azimuthal averaging is to employ the soft limit and set $\Theta_{\text{on shell}} = 1$, after which the ϕ_{n,i_n} integral can be performed by contour integration. However, in our case this is not viable, due to the boundaries on the ϕ_{n,i_n} integral. Instead we will write the integral as

$$\begin{aligned}
\text{Eq. (6.55)} &= \frac{1}{q_\perp} \int \frac{\sin \theta_{n,i_n} d\theta_{n,i_n}}{2} \langle P_{i_n j_n} \Theta_{\text{on shell}} \rangle_{\phi_{n,i_n}} \\
&= \frac{1}{q_\perp} \int \frac{\sin \theta_{n,i_n} d\theta_{n,i_n}}{2} \left[\langle P_{i_n j_n} \rangle_{\phi_{n,i_n}} \langle \Theta_{\text{on shell}} \rangle_{\phi_{n,i_n}} \right. \\
&\quad \left. + \sigma_{P_{i_n j_n}} \sqrt{\langle \Theta_{\text{on shell}} \rangle_{\phi_{n,i_n}} (1 - \langle \Theta_{\text{on shell}} \rangle_{\phi_{n,i_n}})} \text{Cor}(P_{i_n j_n}, \Theta_{\text{on shell}}) \right],
\end{aligned} \tag{6.60}$$

where $\text{Cor}(x, y)$ is the correlation function between two variables x and y , in context the correlation over variation of the azimuth. Firstly note that

$$\langle P_{i_n j_n} \rangle_{\phi_{n,i_n}} = \frac{\Theta(\theta_{j_n,i_n} - \theta_{n,i_n})}{1 - \cos \theta_{n,i_n}},$$

the usual result from azimuthal averaging. We can also note that $\langle \Theta_{\text{on shell}} \rangle_{\phi_{n,i_n}} \in [0, 1]$ and $|\text{Cor}(P_{i_n j_n}, \Theta_{\text{on shell}})| \in [0, 1]$. By brute-force evaluation and noting $\Theta_{\text{on shell}}$ is binomially valued, we find

$$\begin{aligned}
\langle \Theta_{\text{on shell}} \rangle_{\phi_{n,i_n}} &= \frac{|\phi_{q,i}^+ - \phi_{q,i}^-|}{\pi} \bar{\theta}_{\text{on shell}}, \\
\text{where } \bar{\theta}_{\text{on shell}} &= \Theta_{\text{on shell}} \Big|_{\phi_{n,i_n} = \phi^{\text{crit}}}, \quad \text{and} \quad \cos \phi^{\text{crit}} = \text{sign}(f) \min(|f|, 1), \\
f(\theta_{n,i_n}, \theta_{j_n,i_n}, E_{i_n}, E_{j_n}, q_\perp) &= \frac{1 - (1 - \cos \theta_{n,i_n}) E_{i_n} / E_{j_n} - 4 \frac{1 - \cos \theta_{n,i_n}}{1 - \cos \theta_{j_n,i_n}} (1 - \cos \theta_{j_n,i_n} \cos \theta_{n,i_n})}{1 - 4 \frac{\sin \theta_{n,i_n} \sin \theta_{j_n,i_n}}{1 - \cos \theta_{n,i_n}}}.
\end{aligned} \tag{6.61}$$

The exact angular ordered result is obtained when $\langle \Theta_{\text{on shell}} \rangle_{\phi_{n,i_n}} = \bar{\theta}_{ij} = 1$, which is the case in the strongly ordered, $q_{\perp}/Q \rightarrow 0$, and collinear, $\theta_{n,i_n} \rightarrow 0$, limits (here Q stands in for any other harder invariant). The remainder of this section is used to show that the correlation term can be neglected at least at $\alpha_s^n L^{2n-1}$ accuracy (and for NLL thrust). It can be skipped if the reader does not need convincing.

Now we must compute $\sigma_{P_{i_n j_n}}^2 = \langle P_{i_n j_n}^2 \rangle_{\phi_{n,i_n}} - \langle P_{i_n j_n} \rangle_{\phi_{n,i_n}}^2$

$$\begin{aligned} \langle P_{i_n j_n}^2 \rangle_{\phi_{n,i_n}} &= \int \frac{d\phi_{n,i_n}}{2\pi} P_{i_n j_n}^2 = \int \frac{d\phi_{n,i_n}}{8\pi} \left(\frac{n_{i_n} \cdot n_{j_n} - n_{i_n} \cdot n}{n_{i_n} \cdot n \, n_{j_n} \cdot n} + \frac{1}{n_{i_n} \cdot n} \right)^2, \\ &= \frac{1}{(n_{i_n} \cdot n)^2} \int \frac{d\phi_{n,i_n}}{8\pi} \left(\frac{\cos \theta_{n,i_n} - \cos \theta_{j_n,i_n}}{1 - \sin \theta_{n,i_n} \cos \phi_{n,i_n} \sin \theta_{j_n,i_n} - \cos \theta_{j_n,i_n} \cos \theta_{n,i_n}} + 1 \right)^2, \end{aligned} \quad (6.62)$$

using the substitution $z = \exp(i\phi_{n,i_n})$ this integral equals

$$\begin{aligned} \langle P_{i_n j_n}^2 \rangle_{\phi_{n,i_n}} &= \frac{1}{(n_{i_n} \cdot n)^2} \oint_{S^1} \frac{z \, dz}{2\pi i} \left(\frac{\cos \theta_{n,i_n} - \cos \theta_{j_n,i_n}}{2z - \sin \theta_{n,i_n} (z^2 + 1) \sin \theta_{j_n,i_n} - 2z \cos \theta_{j_n,i_n} \cos \theta_{n,i_n}} + \frac{1}{2z} \right)^2, \\ &= \frac{1}{(n_{i_n} \cdot n)^2} \oint_{S^1} \frac{dz}{2\pi i} \left(\frac{z(\cos \theta_{n,i_n} - \cos \theta_{j_n,i_n})}{\sin^2 \theta_{n,i_n} \sin^2 \theta_{j_n,i_n} (z - z_+)^2 (z - z_-)^2} \right. \\ &\quad \left. + \frac{\cos \theta_{n,i_n} - \cos \theta_{j_n,i_n}}{\sin \theta_{n,i_n} \sin \theta_{j_n,i_n} (z - z_+)(z - z_-)} + \frac{1}{4z} \right), \end{aligned} \quad (6.63)$$

where

$$z_{\pm} = \frac{1 - \cos \theta_{j_n,i_n} \cos \theta_{n,i_n}}{\sin \theta_{n,i_n} \sin \theta_{j_n,i_n}} \pm \sqrt{\left(\frac{1 - \cos \theta_{j_n,i_n} \cos \theta_{n,i_n}}{\sin \theta_{n,i_n} \sin \theta_{j_n,i_n}} \right)^2 - 1}. \quad (6.64)$$

Only the $z = z_-$ and $z = 0$ poles are in the unit circle:

$$\begin{aligned} &\frac{1}{(n_{i_n} \cdot n)^2} \oint_{S^1} \frac{dz}{2\pi i} \left(\frac{\cos \theta_{n,i_n} - \cos \theta_{j_n,i_n}}{\sin \theta_{n,i_n} \sin \theta_{j_n,i_n} (z - z_+)(z - z_-)} + \frac{1}{4z} \right) \\ &= \begin{cases} \frac{3}{4(1 - \cos \theta_{n,i_n})^2} & \text{when } \theta_{n,i_n} < \theta_{j_n,i_n}, \\ -\frac{1}{4(1 - \cos \theta_{n,i_n})^2} & \text{otherwise,} \end{cases} \end{aligned} \quad (6.65)$$

and

$$\begin{aligned} &\frac{1}{(n_{i_n} \cdot n)^2} \oint_{S^1} \frac{dz}{2\pi i} \left(\frac{z(\cos \theta_{n,i_n} - \cos \theta_{j_n,i_n})}{\sin^2 \theta_{n,i_n} \sin^2 \theta_{j_n,i_n} (z - z_+)^2 (z - z_-)^2} \right) \\ &= \frac{1}{(1 - \cos \theta_{n,i_n})^2 (\cos \theta_{n,i_n} - \cos \theta_{j_n,i_n})} \left(1 - \frac{2z_- \text{sign}(\cos \theta_{n,i_n} - \cos \theta_{j_n,i_n})}{(\cos \theta_{n,i_n} - \cos \theta_{j_n,i_n})^2} \right). \end{aligned} \quad (6.66)$$

Thus

$$\langle P_{i_n j_n}^2 \rangle_{\phi_{n,i_n}} = \begin{cases} \frac{1 - \frac{2z_-}{(\cos \theta_{n,i_n} - \cos \theta_{j_n,i_n})^2}}{(1 - \cos \theta_{n,i_n})^2 (\cos \theta_{n,i_n} - \cos \theta_{j_n,i_n})} + \frac{3}{4(1 - \cos \theta_{n,i_n})^2} & \text{when } \theta_{n,i_n} < \theta_{j_n,i_n}, \\ \frac{1 + \frac{2z_-}{(\cos \theta_{n,i_n} - \cos \theta_{j_n,i_n})^2}}{(1 - \cos \theta_{n,i_n})^2 (\cos \theta_{n,i_n} - \cos \theta_{j_n,i_n})} - \frac{1}{4(1 - \cos \theta_{n,i_n})^2} & \text{otherwise,} \end{cases} \quad (6.67)$$

and so

$$\sigma_{P_{injn}}^2 = \begin{cases} \frac{1 - \frac{2z_-}{(\cos \theta_{n,in} - \cos \theta_{jn,in})^2}}{(1 - \cos \theta_{n,in})^2 (\cos \theta_{n,in} - \cos \theta_{jn,in})} + \frac{1}{4(1 - \cos \theta_{n,in})^2} & \text{when } \theta_{n,in} < \theta_{jn,in}, \\ \frac{1 + \frac{2z_-}{(\cos \theta_{n,in} - \cos \theta_{jn,in})^2}}{(1 - \cos \theta_{n,in})^2 (\cos \theta_{n,in} - \cos \theta_{jn,in})} - \frac{1}{4(1 - \cos \theta_{n,in})^2} & \text{otherwise.} \end{cases} \quad (6.68)$$

This has a collinear divergence that is suitably screened in Eq. (6.60) by the accompanying phase space factor,

$$\sqrt{\langle \Theta_{\text{on shell}} \rangle_{\phi_{n,in}} (1 - \langle \Theta_{\text{on shell}} \rangle_{\phi_{n,in}})},$$

as is the soft divergence from the q_{\perp} pre-factor in Eq. (6.55). $\text{Cor}(P_{injn}, \Theta_{\text{on shell}})$, is bounded above and below by 1 and -1 so at most further dampens the effect of the $\sigma_{P_{injn}}^2$ term. As a result it is a finite non-logarithmic correction at order α_s and its contribution is suppressed at higher orders (to be seen explicitly one could repeat the analysis of Appendix 6.9.1). Hence, for $\alpha_s^n L^{2n-1}$ accuracy, we need only take the first term on the right hand-side of Eq. (6.60).

6.6.3 Derivation of the dipole shower

In this section we will derive from Eq. (6.3) an evolution equation for a dipole shower for final-state coloured radiation in e^+e^- . The extension to an initial state shower does not add complexity but lengthens equations. To derive the dipole shower we will spin average the evolution and make the leading colour approximation. To approximate the colour, we express amplitude density matrices and colour charge operators in the colour-flow basis. We manipulate the colour-flow basis using the mathematical machinery introduced in [11].

Before we begin the derivation let us look at Eq. (6.3) in more detail and apply some of the knowledge we have gained from deriving an angular ordered shower. Angular ordering is most powerful when applied to the two-jet limit in e^+e^- , the mono-jet limit of DIS and Drell-Yan. In these cases, angular ordering does not approximate the soft radiation pattern at all. Instead, the soft radiation is colour diagonal. The diagonalisation of soft radiation renders the conservation of momentum longitudinal to a jet unambiguous. Matching to the angular ordered limit is sufficient to completely constrain the leading component of momentum conservation in Eq. (6.3) (it must respect the partitioning defined by P_{injn} as given in Appendix 6.6.2). It is required that

$$\begin{aligned} \mathfrak{R}_{injn}^{\text{soft}} &= \frac{(q_{n\perp}^{(injn)})^2}{2E_n^2} (P_{injn} \mathfrak{R}_{in} + P_{jnin} \mathfrak{R}_{jn}) \\ &= \frac{(q_{n\perp}^{(injn)})^2}{4} \left(\left[\frac{p_{in} \cdot p_{jn}}{p_{in} \cdot q_n p_{jn} \cdot q_n} - \frac{T \cdot p_{jn}}{T \cdot q_n} \frac{1}{p_{jn} \cdot q_n} + \frac{T \cdot p_{in}}{T \cdot q_n} \frac{1}{p_{in} \cdot q_n} \right] \mathfrak{R}_{in} + (i \leftrightarrow j) \right), \end{aligned} \quad (6.69)$$

where $T = \sum_{i_n} p_{i_n}$ is a vector for projecting out the energy of a parton in the event ZMF and where E_n is the energy of q_n in the ZMF. This can be rearranged to give

$$\mathfrak{R}_{i_n j_n}^{\text{soft}} = \frac{\mathfrak{R}_{i_n} + \mathfrak{R}_{j_n}}{2} + \text{Asym}_{i_n j_n}(q_n) \mathfrak{R}_{i_n} + \text{Asym}_{j_n i_n}(q_n) \mathfrak{R}_{j_n}, \quad (6.70)$$

$$\text{Asym}_{i_n j_n}(q_n) = \left[\frac{T \cdot p_{i_n}}{4T \cdot q_n} \frac{(q_{n\perp}^{(i_n j_n)})^2}{p_{i_n} \cdot q_n} - \frac{T \cdot p_{j_n}}{4T \cdot q_n} \frac{(q_{n\perp}^{(i_n j_n)})^2}{p_{j_n} \cdot q_n} \right]. \quad (6.71)$$

As previously stated in our discussions on angular ordering,

$$\mathfrak{R}_{j_n} = \delta^4(p_{j_n} - z_n^{-1} \tilde{p}_{j_n}) \prod_{i_n \neq j_n} \delta^4(p_{i_n} - \tilde{p}_{i_n}) + \mathcal{O}(q_\perp/Q).$$

This recoil function is ready to use in Eq. (6.3).

Now, let us begin computing the leading colour evolution of $\mathbf{A}_n(q_\perp)$. We intend to compute

$$\text{Leading}_{\tau\sigma}^{(0)}[\mathbf{A}_n(q_\perp)] \equiv A_n^{(0)\tau\sigma}(q_\perp) |\tau\rangle \langle\sigma|, \quad (6.72)$$

where $A_n^{(0)\tau\sigma}$ is the leading colour amplitude for colour flows τ and σ , see [11, 33] for details on this procedure. Term by term in Eq. (6.3) we can apply this operation and find

$$\text{Leading}_{\tau\sigma}^{(0)} \left[\Gamma_n(q_\perp) \mathbf{A}_n(q_\perp) + \mathbf{A}_n(q_\perp) \Gamma_n^\dagger(q_\perp) \right] = 2 \gamma_n^{(\sigma)}(q_\perp) \delta_{\tau\sigma} \text{Leading}_{\tau\sigma}^{(0)}[\mathbf{A}_n(q_\perp)], \quad (6.73)$$

where

$$\begin{aligned} \gamma_{n-1}^{(\sigma)}(q_\perp; q_\perp \cup \{p\}_{n-1}) &= \frac{\alpha_s}{2\pi} \int \frac{dS_2^{(q)}}{4\pi} \left(\sum_{i_n, j_n \text{ c.c. in } \sigma} \lambda_{i_n} \bar{\lambda}_{j_n} N_c \int \delta q_{n\perp}^{(i_n, j_n)}(q_\perp) \right. \\ &\times \mathcal{R}_{i_n j_n}^{\text{soft}} + \sum_{i_n, v_n} \bar{\mathcal{P}}_{v_{i_n} \rightarrow v, v_n}^{(\text{final})} (1 - z_n) \int \delta q_{n\perp}^{(i_n, \vec{n})}(q_\perp) \mathcal{R}_{i_n}^{\text{col}} \left. \right) \Theta_{\text{on shell}} \end{aligned} \quad (6.74)$$

and where

$$\mathcal{R}_{i_n j_n}^{\text{soft}} = \int \prod_{i_n} d^4 p_{i_n} \mathfrak{R}_{i_n j_n}^{\text{soft}} = 1 + \mathcal{O}(q_\perp/Q), \quad \mathcal{R}_{i_n}^{\text{col}} = \int \prod_{i_n} d^4 p_{i_n} \mathfrak{R}_{i_n}^{\text{coll}} = 1 + \mathcal{O}(q_\perp/Q). \quad (6.75)$$

The sum over “ i_n, j_n c.c. in σ ” standards for performing the sum over partons dipoles i_n, j_n which are colour connected in the colour state σ . $\bar{\mathcal{P}}_{v_{i_n} \rightarrow v, v_n} \equiv \bar{\mathcal{P}}_{v, v_{i_n}}$ are the hard-collinear splitting functions defined in Appendix A of [12]. They are the usual collinear splitting functions with soft poles subtracted away, i.e. $\bar{\mathcal{P}}_{qq} = -\mathcal{C}_F(1 + z_n)$. Note that as we are working in the strict leading colour limit $\mathcal{C}_F = N_c/2$. The constants λ_{i_n} and $\bar{\lambda}_{j_n}$ are defined in Table 1 of [11], in the situations we will use them (the LC limit) $\lambda_{i_n} \bar{\lambda}_{j_n} \rightarrow 1/2$. We can

observe that the first term on the RHS of Eq. (6.74) is of the same form as the standard dipole type term. Next we can take the leading colour part of the emission operators. We spin average emission kernels, see Appendix 6.7 for details, and place carats on objects to remind us that they are spin-averaged. We find

$$\text{Leading}_{\mathcal{G}\tau\sigma}^{(0)} \left[\hat{\mathbf{D}}_n(q_{n\perp}) \hat{\mathbf{A}}_{n-1}(q_{n\perp}) \hat{\mathbf{D}}_n^\dagger(q_{n\perp}) \right] = \hat{W}_n^{(\sigma)}(q_{n\perp}) \delta_{\tau\sigma} \text{Leading}_{\mathcal{G}\tau\backslash n\sigma\backslash n}^{(0)} \left[\hat{\mathbf{A}}_{n-1}(q_{n\perp}) \right], \quad (6.76)$$

where

$$\begin{aligned} \hat{W}_n^{(\sigma)}(q_{n\perp}; q_n \cup \{\tilde{p}\}_{n-1}) &= \sum_{i_n, j_n \text{ c.c. in } \sigma} \lambda_{i_n} \bar{\lambda}_{j_n} N_c \int \delta q_{n\perp}^{(i_n, j_n)}(q_{n\perp}) \mathfrak{R}_{i_n j_n}^{\text{soft}} \\ &+ \sum_{\substack{i_n \in \text{final} \\ v_n}} \bar{\mathcal{P}}_{v_{i_n} \rightarrow v, v_n}^{(\text{final})} (1 - z_n) \int \delta q_{n\perp}^{(i_n, \bar{n})}(q_{n\perp}) \mathfrak{R}_{i_n}^{\text{col}}. \end{aligned} \quad (6.77)$$

Note that $\hat{\gamma}^{(\sigma)} = \gamma^{(\sigma)}$ as the loops do not depend on spin.

For now we will ignore the single logarithmic, hard-collinear pieces as they are easy to introduce later on (they are uniquely attributed to delta functions of the form $\delta^4(p_{j_n} - z_n^{-1} \tilde{p}_{j_n})$ in the recoil). This means that for now our final state will simply be the $q\bar{q}$ pair plus n gluons. It is also typical in the strict LLA to let $\mathcal{R}_{i_n j_n}^{\text{soft}} = 1$; this will prove to be exact with the recoil scheme given in Section 6.4 though only approximately so with the spectator scheme in Appendix 6.8. Thus the evolution equation is

$$\begin{aligned} q_\perp \text{Leading}_{\mathcal{G}\tau\sigma}^{(0)} \left[\frac{\partial \hat{\mathbf{A}}_n(q_\perp)}{\partial q_\perp} \right] &\approx \frac{\alpha_s}{\pi} \int \frac{dS_2^{(q_{n+1})}}{4\pi} \sum_{i_{n+1}, j_{n+1} \text{ c.c. in } \sigma} \\ &\times 4\lambda_{i_{n+1}} \bar{\lambda}_{j_{n+1}} N_c \int \delta q_{n+1\perp}^{(i_{n+1}, j_{n+1})}(q_\perp) \Theta_{\text{on shell}} \delta_{\tau\sigma} \text{Leading}_{\mathcal{G}\tau\sigma}^{(0)} \left[\hat{\mathbf{A}}_n(q_\perp) \right] \\ &- \int \left(\prod_{i_n} d^4 p_{i_n} \right) \sum_{i_n, j_n \text{ c.c. in } \sigma} \lambda_i \bar{\lambda}_j N_c \int \delta q_{n\perp}^{(i_n, j_n)}(q_{n\perp}) \mathfrak{R}_{i_n j_n}^{\text{soft}} \\ &\times \delta_{\tau\sigma} \text{Leading}_{\mathcal{G}\tau\backslash n\sigma\backslash n}^{(0)} \left[\hat{\mathbf{A}}_{n-1}(q_{n\perp}) \right] q_\perp \delta(q_\perp - q_{n\perp}). \end{aligned} \quad (6.78)$$

This is a modified version of the equation for dipole evolution found in [11] that was shown to reproduce BMS evolution [16]. It has been modified to allow for the possibility of kinematic recoil and to account for the phase-space effects from energy conservation.

By taking the leading colour limit, the colour evolution has been made diagonal. We can trivially make the connection with squared spin-averaged matrix elements; for a given colour flow, σ ,

$$|\hat{M}_n^{(\sigma)}(q_\perp)|^2 |\sigma\rangle \langle \sigma| = \left(\frac{2\alpha_s}{\pi} \right)^n \text{Leading}_{\mathcal{G}\sigma\sigma}^{(0)} \left[\hat{\mathbf{A}}_n(q_\perp) \right], \quad (6.79)$$

where \hat{M} is a dimensionless, spin-averaged and leading-colour matrix element, up to global factors of 2 and π which have been absorbed into the definition of our phase-space measure¹⁸.

Thus

$$\begin{aligned}
& q_{\perp} \frac{\partial |\hat{M}_n^{(\sigma)}(q_{\perp})|^2}{\partial q_{\perp}} \\
& \approx \frac{\alpha_s}{\pi} \int \frac{dS_2^{(q_{n+1})}}{4\pi} \sum_{i_{n+1}, j_{n+1} \text{ c.c. in } \sigma} 4\lambda_{i_{n+1}} \bar{\lambda}_{j_{n+1}} N_c \int \delta q_{n+1\perp}^{(i_{n+1}, j_{n+1})}(q_{\perp}) \Theta_{\text{on shell}} |\hat{M}_n^{(\sigma)}(q_{\perp})|^2 \\
& - \frac{2\alpha_s}{\pi} \sum_{i_n, j_n \text{ c.c. in } \sigma} \lambda_i \bar{\lambda}_j N_c \int \left(\prod_{i_n} d^4 p_{i_n} \right) \delta q_{n\perp}^{(i_n, j_n)}(q_{n\perp}) \mathfrak{R}_{i_n j_n}^{\text{soft}} |\hat{M}_{n-1}^{(\sigma/n)}(q_{n\perp})|^2 q_{\perp} \delta(q_{\perp} - q_{n\perp}).
\end{aligned} \tag{6.80}$$

This is a generalised leading-colour dipole shower evolution equation with fixed coupling. Commonly one would introduce a running coupling with q_{\perp} as its argument. At this point this would be a simple extension. We have omitted the running coupling as it does not effect our discussion. From this point on we drop the carat denoting spin averaging, leaving it implicit that the equations are spin averaged.

To manipulate our new dipole construction into the more usual form we now define a recoil function based on colour flows:

$$\mathfrak{R}_{i_n^c}^{\text{dipole}} = \left(\frac{1}{2} + \text{Asym}_{i_n^c \bar{i}_n^c}(q_n) \right) \mathfrak{R}_{i_n^c}, \tag{6.81}$$

where, just as in Section 6.3.3, we use i_n^c to index the (anti)-colour line(s) of parton i in a final state dressed with n soft or collinear partons. Using this we can now return to Eq. (6.80) and manipulate the dipoles so that emissions from each half of a dipole are separated:

$$\begin{aligned}
& q_{\perp} \frac{\partial |M_n^{(\sigma)}|^2}{\partial q_{\perp}} \\
& \approx \frac{\alpha_s}{\pi} \int \frac{dS_2^{(q_{n+1})}}{4\pi} \sum_{i_{n+1}^c} \mathcal{C}_{i_{n+1}^c} \int \delta q_{n+1\perp}^{(i_{n+1}^c, \bar{i}_{n+1}^c)}(q_{\perp}) 2 \Theta_{\text{on shell}} |M_n^{(\sigma)}|^2 \\
& - \frac{\alpha_s}{\pi} \sum_{i_n^c} \mathcal{C}_{i_n^c} \int \left(\prod_{j_n} d^4 p_{j_n} \right) \delta q_{n\perp}^{(i_n^c, \bar{i}_n^c)}(q_{n\perp}) \mathfrak{R}_{i_n^c}^{\text{dipole}} |M_{n-1}^{(\sigma/n)}|^2 q_{\perp} \delta(q_{\perp} - q_{n\perp}).
\end{aligned} \tag{6.82}$$

We can now include the sub-leading logarithms from the hard-collinear limit along with full-colour Casimir invariants. The Casimir invariants and collinear logarithms are each uniquely associated with longitudinal recoil and so a single $\mathfrak{R}_{i_n^c}^{\text{dipole}}$. We note that $\text{Asym}_{i_n^c \bar{i}_n^c}(q_n)$ gives no logarithmic enhancement in the hard-collinear region, rendering the inclusion of hard-collinear pieces simple (including the re-inclusion of $g \rightarrow qq$ transitions). Thus we arrive at

¹⁸The usual dimensionful matrix element is retrieved by multiplying with a factor $\prod_{i_{n+1}} 2\pi^{-1} q_{i_{n+1}\perp}^{-2}$.

Eq. (6.10).¹⁹ We can explicitly include the $g \rightarrow qq$ transitions by extending Eq. (6.10):

$$\begin{aligned}
& q_{\perp} \frac{\partial |M_n^{(\sigma)}|^2}{\partial q_{\perp}} \\
& \approx \frac{\alpha_s}{\pi} \sum_{i_{n+1}^c} \int dq_{\perp}^{(i_{n+1}^c, \bar{i}_{n+1}^c)} \delta(q_{\perp}^{(i_{n+1}^c, \bar{i}_{n+1}^c)} - q_{\perp}) \int dz \Theta_{\text{on shell}} P_{v_{i_n} v_{i_n}}(z) |M_n^{(\sigma)}|^2 \\
& - \frac{\alpha_s}{\pi} \sum_{i_n^c} \int \left(\prod_{j_n} d^4 p_{j_n} \right) \mathfrak{R}_{i_n^c}^{\text{dipole}} P_{v_{i_n} v_{i_n}}(z_n) q_{\perp} \delta(q_{n\perp}^{(i_n^c, \bar{i}_n^c)} - q_{\perp}) |M_{n-1}^{(\sigma/n)}|^2 \\
& - \frac{\alpha_s}{\pi} \sum_{i_n^c} \int \left(\prod_{j_n} d^4 p_{j_n} \right) \mathfrak{R}_{i_n^c}^{\text{dipole}} \delta_{v_{i_n} g} P_{qg}(z_n) q_{\perp} \delta(q_{n\perp}^{(i_n^c, \bar{i}_n^c)} - q_{\perp}) |M_{n-1}^{(\sigma)}|^2, \quad (6.83)
\end{aligned}$$

where $P_{qg}(z_n) = n_f T_R z_n^2$. The inclusion of Casimir factors and collinear physics in this fashion ensures our shower correctly computes everything an angular ordered shower can compute, in the angular-ordered limit. There will however be NLC errors for radiation not ordered in angle. At the same time, the usual LC accuracy of a dipole shower is preserved. Also note that at no point in this derivation did we restrict ourselves to a $q\bar{q}$ final state for the hard process. In Section 6.3.3 we made this restriction as it allows Eq. (6.16) to be written more simply. For more complex hard-process topologies one should sum over showers originating from each distinct hard-process colour flow (dipole).

So far we have still not constrained the $\mathcal{O}(q_{\perp}/Q)$ pieces in the recoil function associated with recoil in the backwards direction. These pieces are important for the computation of NLLs. Specifying them is the purpose of Section 6.4 and Appendix 6.8. In these sections we study their effect on NLLs. For contrast, in Section 2 of [12] we considered various recoil functions that specify the $\mathcal{O}(q_{\perp}/Q)$ pieces. We ensured each possible recoil prescription would consistently produce all leading physics, however we did not check sub-leading effects. One of the prescriptions we considered was based on the spectator recoil commonly employed in modern dipole showers [2, 35]. This approach involves partitioning the dipole using Catani-Seymour dipole factorisation [32] and distributing the longitudinal recoil in accordance with this partitioning. The remaining transverse recoil is then given to a third parton, not in the dipole but colour connected to the emitting parton. In [12] we give the functional form of $\mathfrak{R}_{i_n j_n}^{\text{soft}}$ necessary to implement this recoil. Using this recoil function instead of the one we present here gives us an evolution equation similar to that governing Pythia8 [2].

In [10] it was shown that the standard spectator recoil prescriptions used in conjunction with Catani-Seymour dipole type showers are subject to errors computing NLLs and

¹⁹When constructing Eq. (6.10) we chose to multiply each matrix element by a phase-space factor so that $|M_n^{(\sigma)}|^2 \rightarrow \prod_i 1/(1-z_i) |M_n^{(\sigma)}|^2$ and separate sums over emission topologies, $|M_n^{(\sigma)}|^2 \rightarrow \sum_{i_1^c, \dots, i_n^c} |M_n^{(\sigma)}|^2$. This ensures the standard dipole shower phase space can be used [2–4, 10].

miscalculate next-to-leading colour. The errors in NLC occur because of the misattribution of longitudinal components of recoil and so colour factors. The errors in NLLs occur as unphysical artefacts from the shower construction do not cancel when one properly considers the effects of recoil after multiple emissions. It is for this reason that we have taken so much care to ensure consistency between our dipole shower and angular ordered showers, and why we take great care implementing recoil in Section 6.4.

6.7 Appendix: Spin averaging

In the derivation of an angular ordered shower and a dipole shower we had to spin average the evolution from Eq. (6.3). We can introduce spin averaging safe in the knowledge that the spin-correlated evolution can be computed from the spin averaged by re-weighting with the algorithm of Collins, Knowles et al [22, 51]. In our previous paper [12] we showed that, given collinear factorisation, the evolution of our algorithm is consistent with that of Collins and Knowles et al. We also showed that complete collinear factorisation can be achieved in the PB algorithm (neglecting Coulomb exchanges, which cancel in the leading colour limit). In this appendix we will summarise the spin averaging procedure. We will do so in the leading colour limit, as this is the limit of interest in the dipole shower case and this limit reduces the number of indices on objects. Real emissions in the leading colour limit without spin averaging give rise to

$$\int dR_n \text{Leading}_{\tau\sigma}^{(0)} \left[\mathbf{D}_n(q_{n\perp}) \mathbf{A}_{n-1}(q_{n\perp}) \mathbf{D}_n^\dagger(q_{n\perp}) \right] = \int dR_n W_n^{(\sigma), h_n^L, h_n^R}(q_{n\perp}) \delta_{\tau\sigma} \text{Leading}_{\mathcal{S}_\tau \setminus n \sigma \setminus n}^{(0)} [\mathbf{A}_{n-1}(q_{n\perp})], \quad (6.84)$$

where

$$W_n^{(\sigma), h_n^L, h_n^R}(q_{n\perp}; q_n \cup \{\tilde{p}\}_{n-1}, \{h^L\}, \{h^R\}) = \sum_{i_n, j_n \text{ c.c. in } \sigma} 2\lambda_{i_n} \bar{\lambda}_{j_n} N_c \int \delta q_{n\perp}^{(i_n, j_n)}(q_{n\perp}) s_n^{j_n, h_n^R \dagger} s_n^{i_n, h_n^L} \mathfrak{R}_{i_n j_n}^{\text{soft}} + \sum_{i_n} \int \delta q_{n\perp}^{(i_n, \bar{n})}(q_{n\perp}) C_{i_n} c_n^{i_n, h_n^L \dagger}(h_{i_n}^L) c_n^{i_n, h_n^R}(h_{i_n}^R) \mathfrak{R}_{i_n}^{\text{col}}, \quad (6.85)$$

and where $s_n^{i_n, h_n^L}$ and $c_n^{i_n, h_n^L}(h_{i_n}^L)$ are the kinematic factors associated with a soft or collinear emission respectively, for a fixed spin state. We have unpacked some of the recoil factors from $\int dR_n$ and placed them next to the appropriate emission kernels, these are the $\mathfrak{R}_{i_n j_n}^{\text{soft}}$ and $\mathfrak{R}_{i_n}^{\text{col}}$ factors. $s_n^{i_n, h_n^L}$ and $c_n^{i_n, h_n^L}(h_{i_n}^L)$ are defined through the relations

$$s_n^{j_n, h_n^R \dagger} s_n^{i_n, h_n^L} \mathbb{T}_{j_n} \cdot \mathbb{T}_{i_n} = \langle h_{j_n}^R | \mathbf{S}_n^{j_n \dagger} | h_{j_n}^R, h_n^R \rangle \langle h_{i_n}^L, h_n^L | \mathbf{S}_n^{i_n} | h_{i_n}^L \rangle, \\ c_n^{i_n, h_n^R \dagger}(h_{i_n}^R) c_n^{i_n, h_n^L}(h_{i_n}^L) \mathbb{T}_{i_n} \cdot \mathbb{T}_{i_n} = \sum_{h_{i_n}^R, h_{i_n}^L} \langle h_{i_n}^R | \mathbf{C}_n^{i_n \dagger} | h_{i_n}^R, h_n^R \rangle \langle h_{i_n}^L, h_n^L | \mathbf{C}_n^{i_n} | h_{i_n}^L \rangle, \quad (6.86)$$

where $h_i^{L/R}$ is the helicity of the parton with label i on the left/right hand side of the amplitude. In Eq. (6.85) we again used the abbreviation “ i_n, j_n c.c. in σ ” to mean that we sum over pairs i_n, j_n that are colour connected in σ . Note we have been a little sloppy by omitting sums over trivial spin indices of partons not involved in the splittings induced by $\mathbf{C}_n^{i_n}$ and $\mathbf{S}_n^{i_n}$ in Eq. (6.84). Spin averaging is achieved by setting $\{h^L\} = \{h^R\} = \{h\}$ and performing all trivial sums over spin states in Eq. (6.84). This is equivalent to replacing

$$\begin{aligned} \mathbf{A}_n &\mapsto \hat{\mathbf{A}}_n, & W_n^{(\sigma), h_n^L, h_n^R}(q_{n\perp}) &\mapsto \hat{W}_n^{(\sigma)}(q_{n\perp}), \\ s_n^{j_n, h_n^R \dagger} s_n^{i_n, h_n^L} \mathbb{T}_{j_n} \cdot \mathbb{T}_{i_n} &\mapsto \hat{s}_n^{j_n i_n} \mathbb{T}_{j_n} \cdot \mathbb{T}_{i_n} = \frac{1}{2} \sum_{h_{i_n}} \langle h_{i_n} | \mathbf{S}_n^{j_n} \cdot \mathbf{S}_n^{i_n} | h_{i_n} \rangle, \\ c_n^{i_n, h_n^R \dagger}(h_{i_n}^R) c_n^{i_n, h_n^L}(h_{i_n}^L) \mathbb{T}_{i_n} \cdot \mathbb{T}_{i_n} &\mapsto \hat{c}_n^{i_n} \mathbb{T}_{i_n} \cdot \mathbb{T}_{i_n} = \frac{1}{2} \sum_{h_{i_n}} \langle h_{i_n} | \mathbf{C}_n^{i_n} \cdot \mathbf{C}_n^{i_n} | h_{i_n} \rangle, \end{aligned} \quad (6.87)$$

where we denoted the spin averaged objects with a caret. We have assumed $\mathfrak{R}_{i_n j_n}^{\text{soft}}$ and $\mathfrak{R}_{i_n}^{\text{col}}$ are chosen such that they are not spin dependent, otherwise they too should be averaged in the same fashion.

6.8 Appendix: Dipole shower with spectator recoil

It is commonplace to use local ‘spectator’ recoils in dipole showers rather than the global approach we have opted for [2, 3]. In this appendix we introduce one such recoil scheme and show that, despite the other improvements to our dipole shower, it suffers the NLL errors pointed out in [10].

Following the approach of [35], we can treat each transition from an $n-1$ to an n parton matrix element as being generated by a $2 \rightarrow 3$ parton splitting which locally conserves momentum. The splitting is defined such that the parton with colour line i_n under goes a primary decay into two partons, the amplitude for which is given by a collinear splitting function. The parton with colour line \bar{i}_n acts as a spectator and under goes a secondary $1 \rightarrow 1$ transition where it absorbs the residual recoil from the primary decay. To this end we introduce the following Sudakov decomposition

$$\begin{aligned} \tilde{p}_{i_n} &= z_n p_{i_n} - k_\perp + \frac{(q_{n\perp}^{(i_n \bar{i}_n)})^2}{z_n} \frac{p_{\bar{i}_n}}{2p_{i_n} \cdot p_{\bar{i}_n}}, & (q_{n\perp}^{(i_n \bar{i}_n)})^2 &= -k_\perp^2, \\ q_n &= (1 - z_n) p_{i_n} + k_\perp + \frac{(q_{n\perp}^{(i_n \bar{i}_n)})^2}{1 - z_n} \frac{p_{\bar{i}_n}}{2p_{i_n} \cdot p_{\bar{i}_n}}, \\ \tilde{p}_{\bar{i}_n} &= \left(1 - \frac{(q_{n\perp}^{(i_n \bar{i}_n)})^2}{z_n(1 - z_n)} \frac{1}{2p_{i_n} \cdot p_{\bar{i}_n}} \right) p_{\bar{i}_n}, & k_\perp \cdot p_{i_n} &= k_\perp \cdot p_{\bar{i}_n} = 0, \end{aligned} \quad (6.88)$$

which conserves momentum as $p_{i_n} + p_{\bar{i}_n} = \tilde{p}_{i_n} + \tilde{p}_{\bar{i}_n} + q_n$. This decomposition defines the kinematics of the $2 \rightarrow 3$ splitting. Enforcing this local recoil scheme implies that

$$\begin{aligned} \mathfrak{R}_{i_n} = & \left(1 - \frac{(q_{n\perp}^{(i_n\bar{i}_n)})^2}{z_n(1-z_n)2p_{i_n} \cdot p_{\bar{i}_n}} \right) \delta_{\mathcal{J}}^4 \left(\tilde{p}_{\bar{i}_n} - p_{\bar{i}_n} + \frac{(q_{n\perp}^{(i_n\bar{i}_n)})^2}{z_n(1-z_n)} \frac{p_{\bar{i}_n}}{2p_{i_n} \cdot p_{\bar{i}_n}} \right) \\ & \times \delta_{\mathcal{J}}^4 \left(\tilde{p}_{i_n} - z_n p_{i_n} + k_{\perp} - \frac{(q_{n\perp}^{(i_n\bar{i}_n)})^2}{z_n} \frac{p_{\bar{i}_n}}{2p_{i_n} \cdot p_{\bar{i}_n}} \right) \prod_{j_n \neq i_n, \bar{i}_n} \delta^4(p_{j_n} - \tilde{p}_{j_n}), \end{aligned} \quad (6.89)$$

where

$$\delta_{\mathcal{J}}(f(x)) = f'(x_i)\delta(f(x)) = \delta(x - x_i),$$

and x_i is the single root of $f(x)$ inside the range of x over which the delta function has support.

6.8.1 NLC and NLL accuracy of the spectator recoil

Let us begin by filling in some of the derivation of Eq. (6.26) with the local dipole recoil specified in previous section. Starting from Eq. (6.80),

$$\begin{aligned} \delta\Sigma(L) = & \sigma_{n\text{H}} \prod_{n=1}^2 \left(\int d\Pi_n \sum_{i_n, j_n \text{ c.c. in } \sigma} \int \prod_{k_n} d^4 p_{k_n} \delta q_{n\perp}^{(i_n, j_n)}(q_{n\perp}) \lambda_i \bar{\lambda}_j N_c \mathfrak{R}_{i_n j_n}^{\text{soft}} \theta_{i_n j_n} \right) \\ & \times \Theta(q_{1\perp} - q_{2\perp}) \Theta(e^{-L} - V(\{p\}_2)) \\ & - \sigma_{n\text{H}} \prod_{n=1}^2 \left(\int d\Pi_n \sum_{i_n, j_n \text{ c.c. in } \sigma} \int \delta q_{n\perp}^{(i_n, j_n)}(q_{n\perp}) \lambda_i \bar{\lambda}_j N_c \theta_{i_n j_n}^{\text{correct}} \right) \\ & \times \Theta(q_{1\perp} - q_{2\perp}) \Theta(e^{-L} - V(\{p\}_{\text{correct}})), \\ = & \mathcal{C}_F \sigma_{n\text{H}} \int d\Pi_2 d\Pi_1 \int \delta q_{2\perp}^{(a_2, 1_2)}(q_{2\perp}) \int \delta q_{1\perp}^{(a_1, b_1)}(q_{1\perp}) \Theta(q_{1\perp} - q_{2\perp}) \\ & \times \left[\int \prod_{n=1}^2 \prod_{k_n} d^4 p_{k_n} \mathfrak{R}_{a_2 1_2}^{\text{soft}} \theta_{a_2 1_2} \mathfrak{R}_{a_1 b_1}^{\text{soft}} \theta_{a_1 b_1} \Theta(e^{-L} - V(\{p\}_2)) \right. \\ & \left. - \theta_{a_2 1_2}^{\text{correct}} \theta_{a_1 b_1}^{\text{correct}} \Theta(e^{-L} - V(\{p\}_{\text{correct}})) \right], \end{aligned} \quad (6.90)$$

where $\{p\}_{\text{correct}}$ is the set of correct momenta for the 4-body system and where $\theta_{i_n j_n}^{\text{correct}} = \theta_{i_n j_n}(\{p\}_{\text{correct}})$. From this we find

$$\begin{aligned} \delta\Sigma(L) \approx & \frac{4\alpha_s^2 \mathcal{C}_F^2 \sigma_{n\text{H}}}{\pi^2} \int_0^Q \frac{dq_{1\perp}^{(a_1, b_1)}}{q_{1\perp}^{(a_1, b_1)}} \int_{-\ln Q/q_{1\perp}^{(a_1, b_1)}}^{\ln Q/q_{1\perp}^{(a_1, b_1)}} dy_1 \int_0^{q_{1\perp}^{(a_1, b_1)}} \frac{dq_{2\perp}^{(a_2, 1_2)}}{q_{2\perp}^{(a_2, 1_2)}} \int_{-\ln Q/q_{2\perp}^{(a_2, 1_2)}}^{\ln Q/q_{2\perp}^{(a_2, 1_2)}} dy_2 \\ & \times \int_0^{2\pi} \frac{d\phi_2}{2\pi} [\Theta(e^{-L} - V(\{p\}_2)) - \Theta(e^{-L} - V(\{p\}_{\text{correct}}))]. \end{aligned} \quad (6.91)$$

The kinematics are encapsulated by $\{p\}_2$, just as in the global scheme given in Section 6.4. They are in fact exactly the same kinematics as those specified in Section 3.3 of [10] and we have arrived at the same expression as B.5 of [10]. Thus, we can follow their argument from Appendix A and Section 4 and conclude that our local dipole prescription does suffer the same NLL errors as other local dipole prescriptions. For example, we can consider the two-jet rate using the Cambridge algorithm, for which $V(\{p_i\}) = \max_i\{p_{i\perp}\}$. In the limit we have considered, this reduces to $V(\{p\}_{\text{correct}}) = q_{1\perp}^{(a_1, b_1)}$ whereas $V(\{p\}_2) = \max(q_{1\perp}^{(a_1, b_1)}, q_{2\perp}^{(a_2, 1_2)})$ since the recoil scheme does not ensure that $q_{1\perp}^{(a_1, b_1)} > q_{2\perp}^{(a_2, 1_2)}$ at all points in the phase-space for parton 2's emission. [10] show that this error generates an incorrect NLL ($N_c^2 \alpha_s^2 L^2$). This was expected, as in our local dipole scheme we have only made modifications to fix the NLC of the usual dipole shower procedure. It would be unexpectedly fortuitous if this also fixed the NLL problems.

6.9 Appendix: Further checks

6.9.1 Thrust with NLL accuracy using global recoil

Thrust has a long history. It was first resummed to leading log accuracy in 1980 [52] and then later at next-to-leading in 1993 [19]. More recently, it was resummed to N³LL [53]. In this section we will analyse the consistency of the dipole shower and recoil scheme we present in Sections 6.3.3 and 6.4 with the NLL computation found in [19]. Crucially, the calculation of NLL thrust was performed using a coherent branching algorithm [20] (or equivalently by analytic computation of an angular ordered shower). The coherent branching algorithm employed in the resummation was not strictly momentum conserving and effectively only conserved the momentum longitudinal to the two back-to-back jets. In [19] they show that neglecting the other components is a valid approximation in the computation of NLLs for thrust (see their ϵ expansion of the correct phase-space). However, in [10] it was observed that incorrect handling of transverse momentum in dipole showers can induce NLL errors in thrust from $\mathcal{O}(\alpha_s^3)$ onwards. These two papers are not inconsistent with each other, the situation is simply that the incorrect inclusion of momentum conserving terms can induce NLL errors.

Our dipole shower algorithm was built around consistency with an angular ordered shower. Its collinear radiation pattern reproduces that of an angular ordered shower with the correct longitudinal momentum conservation after azimuthally averaging. At NLL accuracy, it is also consistent at leading-colour with the angular ordered shower (restricted to leading-colour since our dipole shower only has leading-colour accuracy for radiation unordered in angle). Notwithstanding those NLC terms, there is one other main difference between

the coherent branching resummed in [19] and our algorithm after azimuthal averaging; ours conserves momentum completely. Thus the only remaining question is whether our approach to momentum conservation breaks the full-colour collinear evolution and leading-colour NLL accuracy of our dipole shower. We can compute the difference between our algorithm's computation of thrust and [19]. As thrust is dominated by the two-jet limit, we initially focus on emissions from the primary hard legs (which is sufficient for NLL accuracy in the approach of [19] by assuming inclusivity over jets from secondary jets). Afterwards we will briefly consider the effects of secondary emissions, i.e. possible recoil effects from the multi-jet limit. Firstly note that thrust can be defined as

$$T(\{p\}_n) = \max_{\mathbf{n}} \frac{\sum_{\forall p \in \{p\}_n} |\mathbf{p} \cdot \mathbf{n}|}{\sum_{\forall p \in \{p\}_n} |\mathbf{p}|} \stackrel{\text{NLL}}{\simeq} 1 - \frac{P_n^2 + P_{\bar{n}}^2}{Q^2},$$

where P_n ($P_{\bar{n}}$) is the total four-momentum in the hemisphere centred on the forwards (backwards) thrust axis. From this definition, it is clear that thrust is invariant under boosts along the thrust axis and is invariant under global jet energy rescaling. Following the notation of Section 6.4, the difference in the two-jet limit between our dipole algorithm and the NLL result due to recoil is of the general form

$$\begin{aligned} \delta\Sigma(L) \sim \sum_n \alpha_s^n C_n & \left(\int_0^Q \frac{dq_{n\perp}}{q_{n\perp}} \dots \int_0^Q \frac{dq_{1\perp}}{q_{1\perp}} \int_{-\ln(\kappa_n Q/q_{n\perp})}^{\ln(\kappa_n Q/q_{n\perp})} dy_n \dots \int_{-\ln(\kappa_1 Q/q_{1\perp})}^{\ln(\kappa_1 Q/q_{1\perp})} dy_1 \right. \\ & \times \Theta(Q - q_{1\perp}) \dots \Theta(\kappa_n^{-1} q_{n-1\perp} - q_{n\perp}) \\ & - \int_0^Q \frac{dq_{n\perp}}{q_{n\perp}} \dots \int_0^Q \frac{dq_{1\perp}}{q_{1\perp}} \int_{-\ln(Q/q_{n\perp})}^{\ln(Q/q_{n\perp})} dy_n \dots \int_{-\ln(Q/q_{1\perp})}^{\ln(Q/q_{1\perp})} dy_1 \\ & \left. \times \Theta(Q - q_{1\perp}) \dots \Theta(q_{n-1\perp} - q_{n\perp}) \right) \Theta(e^{-L} - (1 - T(\{p\}_n))), \quad (6.92) \end{aligned}$$

where each transverse momentum is defined relative to the thrust axis and C_n is a constant coefficient.

It is most beneficial to us if we evaluate the logarithmic order of $\delta\Sigma(L)$ by starting more generally and then applying the result to thrust. As previously stated, each $\kappa_n = 1 - \mathcal{O}(q_{n\perp}^2/2Q^2)$. We will parametrise this as $\kappa_n = 1 - \epsilon q_{n\perp}^2/2Q^2$ where ϵ is order unity. Note that when $\epsilon = 0$, $\delta\Sigma(L) = 0$. Eq. (6.92) is built from repeated sums over elementary integrals of the following type

$$\mathcal{I}_n = \int_a^1 \frac{dx_n}{x_n} \dots \int_{x_2}^1 \frac{dx_1}{x_1} \left[\prod_{i=1}^n \ln \left(x_i \left(1 - \frac{\epsilon x_i^2}{2} \right) \right) - \prod_{i=1}^n \ln(x_i) \right] \Theta(f(a, \{x_i\})), \quad (6.93)$$

where a parametrises the observable dependence (for thrust $a \sim 1 - T$), $x_i \sim q_{i\perp}/Q$ and $\Theta(f(a, \{x_i\}))$ parametrises any residual more complex observable dependence. Note that both terms in the square bracket are monotonically decreasing as $x_i \rightarrow 0$ and that the

second is always of smaller magnitude than the first. Thus \mathcal{I} evaluates to having the largest possible magnitude when $\Theta(f(a, \{x_i\})) = 1$, as every point in the domain of the integrand adds constructively to the integral. Therefore we will work assuming $\Theta(f(a, \{x_i\})) = 1$ in order to place an upper limit on the order of logarithms produced. With this assumption applied, \mathcal{I} is dominated by the term

$$\mathcal{I}_n \approx \int_a^1 \frac{dx_n}{x_n} \dots \int_{x_2}^1 \frac{dx_1}{x_1} \left[\sum_{j=1}^n \ln \left(x_j \left(1 - \frac{\epsilon x_j^2}{2} \right) \right) \prod_{i \neq j}^n \ln(x_i) - \prod_{i=1}^n \ln(x_i) \right], \quad (6.94)$$

which is in turn proportional to $g_{2n-2}(a, \epsilon) - g_{2n-2}(a, 0)$ where

$$g_n(a, \epsilon) = \int_a^1 \frac{dx}{x} \ln \left(x \left(1 - \frac{\epsilon x^2}{2} \right) \right) \ln(x)^n. \quad (6.95)$$

For large n , g_n is difficult to evaluate. However we can navigate this by constructing a generating function for g_n ,

$$GF(a, \epsilon, \nu) = \int_a^1 dx x^{\nu-1} \ln \left(x \left(1 - \frac{\epsilon x^2}{2} \right) \right), \quad (6.96)$$

so that $g_n = (\partial_\nu)^n GF|_{\nu=0}$ and

$$GF(a, \epsilon, \nu) = \frac{a^\nu - 1}{\nu^2} + \frac{\epsilon \left({}_2F_1 \left(1, \frac{\nu}{2} + 1; \frac{\nu}{2} + 2; \frac{\epsilon}{2} \right) - a^{\nu+2} {}_2F_1 \left(1, \frac{\nu}{2} + 1; \frac{\nu}{2} + 2; \frac{a^2 \epsilon}{2} \right) \right)}{\nu(\nu+2)} + \frac{\ln(2)a^\nu - \ln(2) + \ln(2-\epsilon) - a^\nu \ln(2a - a^3 \epsilon)}{\nu}. \quad (6.97)$$

The Taylor series in ν of $GF(a, \epsilon, \nu)$ can be computed. The series is expressible in the form

$$GF(a, \epsilon, \nu) - GF(a, 0, \nu) = \sum_{n=0}^{\infty} \left(\sum_{i=0}^n A_{i,n} \ln(a)^{n-i} \text{Li}_{2+i} \left(\frac{a\epsilon}{2} \right) + B_n \text{Li}_{2+n} \left(\frac{\epsilon}{2} \right) \right) \frac{\nu^n}{n!}, \quad (6.98)$$

where $A_{i,n}$ and B_n are order unity constants that we do not need. Thus

$$\delta\Sigma(L) \lesssim \sum_{n=2}^{\infty} \frac{\alpha_s^n}{(2n-2)!} \left(\sum_{i=0}^{2n-2} \tilde{A}_{i,n} \ln(1-T)^{2n-2-i} \text{Li}_{2+i} \left(\frac{(1-T)\epsilon}{2} \right) + \tilde{B}_n \text{Li}_{2n} \left(\frac{\epsilon}{2} \right) \right), \quad (6.99)$$

where $L = \ln(1-T)$, and $\tilde{A}_{i,n}$ and \tilde{B}_n are order unity constants. Hence for $T \approx 1$, the limit in which we resum, $\delta\Sigma(L) \ll \sum_n \frac{\alpha_s^n C_n}{n!} \ln(1-T)^{2n-2}$ where C_n are also order unity coefficients. Also note that the first logarithmic enhancement from our recoil scheme occurs as $\sim \alpha_s^4 L^2$. Finally, we note that this argument applies to recoil distributed along any chain of strongly ordered emissions. Therefore recoil from emissions off secondary legs also contributes terms to $\delta\Sigma(L)$ that are much less than $\sum_n \frac{\alpha_s^n C_n}{n!} \ln(1-T)^{2n-2}$.²⁰

²⁰In fact, following the epsilon expansion arguments of [19], recoil from secondary legs will contribute terms less dominant than $\sum_n \frac{\alpha_s^n C_n}{n!} \ln(1-T)^{2n-4}$.

We have shown that the recoil scheme for the dipole shower presented in Section 6.4 does not introduce incorrect next-to-leading logarithms into the resummation of thrust in e^+e^- . We did this using a very general approach, leading us to believe that for other exponentiating two-jet dominated observables the same result will also be found. Thus, one would only need to add a running coupling and the shower could be used to compute the NLL resummation of thrust. In summary, we expect our formalism to be capable of leading-colour NLL accuracy in observables that can be resummed at NLL accuracy using the coherent branching approach and will capture much of the full-colour LL contributions.

6.9.2 Generating functions for jet multiplicity using global recoil

We will now use our algorithm with our new recoil scheme (as presented in Section 6.4) to compute the integral equation defining the spin-uncorrelated generating function for the multiplicity of subjects in the final state of $e^+e^- \rightarrow$ hadrons. The generating function was first computed at NLL accuracy (i.e. including all $\alpha_s^n L^{2n-1}$ terms) in [54]. The methodology has since seen a variety of applications [28, 31] (and references therein) and can be found in graduate texts [26, 50]. We will compute the generating function at LL accuracy, though taking care to include all $\alpha_s^n L^{2n-1}$ logs from recoil.

The generating function is defined by

$$\phi_\Sigma(u, Q) = \sum_{n=0}^{\infty} u^n P_\Sigma(n, Q) = F \sum_{n=0}^{\infty} u^{n+N} \int d\Pi_{\text{Born}} \int d\sigma_n(Q). \quad (6.100)$$

It can be used for the computation of the moments of the subjet multiplicity distribution for a process Σ :

$$\langle n_\Sigma(n_\Sigma - 1) \dots (n_\Sigma - n + 1) \rangle = \left. \frac{d^n \phi_\Sigma(u, Q)}{du^n} \right|_{u=1}. \quad (6.101)$$

Here F is some flux factor for the hard process and $P_\Sigma(n, Q)$ is the probability of finding n partons/subjects in the final state of a process with centre-of-mass energy (or hard-scale) Q . N is the number of partons in the hard process and $\langle n_\Sigma \rangle$ is the mean number of subjects in Σ .

For $e^+e^- \rightarrow q\bar{q}$, i.e. computing $\phi_{q\bar{q}}(u, Q)$, it is a textbook result that at our accuracy generating functions factorise as $\phi_{q\bar{q}}(u, Q) = \phi_q(u, \tau)\phi_{\bar{q}}(u, \tau)$ where $\phi_a(u, \tau)$ is the generating function for subjet multiplicity within the jet from a single parton a . $\tau = 2E \sin(\theta/2)$ is the scale of an individual jet and can be thought of as its maximum transverse momentum, E is the energy of each jet and θ the opening angle of the jet, e.g. $\phi_{q\bar{q}}(u, Q) = \phi_q(u, Q)\phi_{\bar{q}}(u, Q)$ as $\theta = \pi$ and $E = Q/2$ [28, 50].

We will now construct an integral equation for $\phi_a(u, \tau)$. To do so consider also computing $\phi_{e^+e^- \rightarrow q\bar{q}[g]}(u, q_{\perp 1})$, where the next hardest jet (if one occurs) is a gluon jet of scale

$q_{\perp 1}$. For the computation of $\phi_{e^+e^- \rightarrow q\bar{q}[g]}(u, q_{\perp 1})$, the hard process can be approximated as $\mathbf{H}^{(e^+e^- \rightarrow q\bar{q}[g])}(q_{\perp 1}) = \mathbf{A}_0(q_{\perp 1}) + u\mathbf{A}_1(q_{\perp 1})$. Hence

$$\phi_{e^+e^- \rightarrow q\bar{q}[g]}(u, q_{\perp 1}) = F \sum_{n=0}^{\infty} u^n \int d\Pi_{\text{Born}} \left(u^2 \int d\sigma_n^{(\mathbf{A}_0)}(q_{\perp 1}) + u^3 \int d\Pi_1 \int d\sigma_n^{(\mathbf{A}_1)}(q_{\perp 1}) \right), \quad (6.102)$$

where $d\Pi_{\text{Born}} \equiv d\Pi_{\text{Born}}^{(q)} d\Pi_{\text{Born}}^{(\bar{q})}$ is the Born phase-space for the $q\bar{q}$ pair²¹. We can rewrite this as

$$\begin{aligned} \phi_{e^+e^- \rightarrow q\bar{q}[g]}(u, q_{\perp 1}) &= \phi_q(u, q_{\perp 1}) \phi_{\bar{q}}(u, q_{\perp 1}) \text{Tr}(\mathbf{V}_{q_{\perp 1}, Q} \cdot \mathbf{V}_{q_{\perp 1}, Q}) + \int d\Pi_{\text{Born}} \int d\Pi_1 \\ &\times \int dR_1 \int d^4 P_g \frac{d\phi_q(u, q_{\perp 1})}{d^4 P_q} \frac{d\phi_{\bar{q}}(u, q_{\perp 1})}{d^4 P_{\bar{q}}} \frac{d\phi_g(u, q_{\perp 1})}{d^4 P_g} \\ &\times \text{Tr} \left(\mathbf{V}_{q_{\perp 1}, Q} \cdot \mathbf{V}_{q_{\perp 1}, Q} \left\langle \mathbf{D}_1^\dagger \cdot \mathbf{D}_1 \right\rangle_1 \right) \delta^4(P_g - q_1), \end{aligned} \quad (6.103)$$

where we have employed azimuthally averaged result of Appendix 6.6.2 since the equation is independent of the azimuth of the gluon. We have also spin averaged at this step. We also note that Eq. (6.103) is equal to $\phi_{q\bar{q}}(u, Q)$ by necessity, i.e. $\phi_{q\bar{q}}(u, Q) = \phi_{e^+e^- \rightarrow q\bar{q}[g]}(u, q_{\perp 1})$ as within the strong ordering approximation the next hardest jet of an $e^+e^- \rightarrow q\bar{q}$ process must be a gluon jet. After a little work,

$$\begin{aligned} \phi_{q\bar{q}}(u, Q) &= \frac{1}{2} \phi_q(u, q_{\perp 1}) \Delta_q(q_{\perp 1}, Q) \phi_{\bar{q}}(u, q_{\perp 1}) \Delta_{\bar{q}}(q_{\perp 1}, Q) \\ &+ \phi_{\bar{q}}(u, q_{\perp 1}) \Delta_{\bar{q}}(q_{\perp 1}, Q) \frac{\alpha_s}{2\pi} \int_{q_{\perp 1}}^Q \frac{dq_{\perp}}{q_{\perp}} \Delta_q(q_{\perp}, Q) \int_{\frac{q_{\perp}}{2Q}}^{1-\frac{q_{\perp}}{2Q}} dz \mathcal{P}_{qq}(z) \tilde{\phi}_q(u, q_{\perp}) \tilde{\phi}_g(u, q_{\perp}) \\ &+ (q \leftrightarrow \bar{q}), \end{aligned} \quad (6.104)$$

where

$$\begin{aligned} \tilde{\phi}_q(u, q_{\perp}) &= \int d\Pi_{\text{Born}}^{(q)} d^4 P_q \frac{d\phi_q(u, q_{\perp})}{d^4 P_q} \mathfrak{R}_{q_1}^{\text{primary}} \approx \phi_q(u, zq_{\perp}), \\ \tilde{\phi}_{\bar{q}}(u, q_{\perp}) &= \int d\Pi_{\text{Born}}^{(\bar{q})} d^4 P_{\bar{q}} \frac{d\phi_{\bar{q}}(u, q_{\perp})}{d^4 P_{\bar{q}}} \mathfrak{R}_{q_1}^{\text{secondary}} \approx \phi_{\bar{q}}(u, q_{\perp}), \\ \tilde{\phi}_g(u, q_{\perp}) &= \int \frac{d\phi_1}{2\pi} d^4 P_g \frac{d\phi_g(u, q_{\perp 1})}{d^4 P_g} \delta^4(P_g - q_1) \approx \phi_q(u, (1-z)q_{\perp}), \end{aligned} \quad (6.105)$$

and where the recoil functions, using the same definitions as Section 6.4, are given by

$$\begin{aligned} \mathfrak{R}_{q_1}^{\text{primary}} &= \delta_{\mathcal{J}}^4 \left(\tilde{P}_{q_1} - z\kappa_q \Lambda(q, \bar{q}) p_q \right), \\ \mathfrak{R}_{q_1}^{\text{secondary}} &= \delta_{\mathcal{J}}^4 \left(\kappa_{q_1} \Lambda(q, \bar{q}) P_{j_n} - \tilde{P}_{j_n} \right), \end{aligned}$$

²¹The Born phase-space on the momenta of partons after momentum conservation has been taken into account and includes the momentum conserving delta function $\delta^4(P_{\bar{q}} + P_q)$ as well as a delta function fixing the energy.

i.e. each $\tilde{\phi}$ is simply related to each ϕ by momentum conservation. At our accuracy, momentum conservation simply maps $E_q \rightarrow z_1 E_q$ and $E_g = (1 - z_1) E_q$ since κ_{q_1} and the Lorentz boost are unity at our desired accuracy (noting the argument for neglecting the changes in phase-space due to our recoil scheme given in the previous subsection also holds for this resummation as the measurement function is unity and we are resumming logs up to $\alpha_s^n L^{2n-1}$ accuracy). The limits on the z integrals partition the phase-space in the lab frame (replacing the dipole partition at NLL accuracy) whilst still using a k_\perp ordering variable. $\Delta_c(a, b)$ is a Sudakov factor

$$\Delta_c(a, b) = \exp \left(-\frac{\alpha_s}{2\pi} \int_a^b \frac{dk_\perp^{(c\bar{n})}}{k_\perp^{(c\bar{n})}} \int_{\frac{k_\perp^{(c\bar{n})}}{2Q}}^{1 - \frac{k_\perp^{(c\bar{n})}}{2Q}} dz \mathcal{P}_{cc}(z) \right). \quad (6.106)$$

We can factorise Eq. (6.104) as

$$\begin{aligned} \phi_{q\bar{q}}(u, Q) &= \left(\phi_q(u, q_{\perp 1}) \Delta_q(q_{\perp 1}, Q) \right. \\ &\quad \left. + \frac{\alpha_s}{2\pi} \int_{q_{\perp 1}}^Q \frac{dq_\perp}{q_\perp} \Delta_q(q_\perp, Q) \int_{\frac{q_\perp}{2Q}}^{1 - \frac{q_\perp}{2Q}} dz \mathcal{P}_{qq}(z) \tilde{\phi}_q(u, q_\perp) \tilde{\phi}_g(u, q_\perp) \right) \\ &\quad \times (q \leftrightarrow \bar{q}) + \mathcal{O}(\alpha_s^2). \end{aligned} \quad (6.107)$$

keeping only terms first order in α_s ²². From this, we can identify

$$\begin{aligned} \phi_q(u, Q) &= \phi_q(u, q_{\perp 1}) \Delta_q(q_{\perp 1}, Q) \\ &\quad + \frac{\alpha_s}{2\pi} \int_{q_{\perp 1}}^Q \frac{dq_\perp}{q_\perp} \Delta_q(q_\perp, Q) \int_{\frac{q_\perp}{2Q}}^{1 - \frac{q_\perp}{2Q}} dz \mathcal{P}_{qq}(z) \tilde{\phi}_q(u, q_\perp) \tilde{\phi}_g(u, q_\perp). \end{aligned} \quad (6.108)$$

This expression is correct at LL accuracy with complete colour and only requires the coupling to run as $\alpha_s(z(1-z)q_\perp)$ in order to capture the full NLL ($\alpha_s^n L^{2n-1}$) result. We also can note that the correct NLL resummation might not have been achieved using the local dipole prescription presented in Appendix 6.8. This is because the recoil could introduce a correction in the $n > 3$ jet limit of the form $\phi_{\bar{q}}(u, q_{\perp 1}) \rightsquigarrow \phi_{\bar{q}}(u, |\mathbf{q}_{\perp 1} - \mathbf{q}_{\perp 2}|)$ (the wavy arrow implying that it will approximately go to). This correction prevents both the usage of naive azimuthal averaging and the factorisation $\phi_{q\bar{q}} \equiv \phi_q \phi_{\bar{q}}$ (which naturally emerged between Eq. (6.104) and Eq. (6.107)), though it is possible that these features could re-emerge once the phase space of each jet has been inclusively integrated over. Due to the other known NLL limitations of this recoil scheme, we did not think it worthwhile further proceeding to evaluate the order of these errors but rather conjecture that NLL errors will also be likely here.

²²The $\mathcal{O}(\alpha_s^2)$ terms can be computed by instead starting with $\mathbf{H}^{(e^+e^- \rightarrow q\bar{q}[g][g])}(q_{2\perp}) = \mathbf{A}_0(q_{2\perp}) + u\mathbf{A}_1(q_{2\perp}) + u^2\mathbf{A}_2(q_{2\perp})$ and proceeding as above.

References

- [1] T. Sjöstrand, P. Z. Skands, “Transverse-momentum-ordered showers and interleaved multiple interactions”, *Eur. Phys. J.* **2005**, *C39*, 129–154, arXiv: [hep-ph/0408302](#) [[hep-ph](#)].
- [2] T. Sjöstrand, S. Ask, J. R. Christiansen, R. Corke, N. Desai, P. Ilten, S. Mrenna, S. Prestel, C. O. Rasmussen, P. Z. Skands, “An Introduction to PYTHIA 8.2”, *Comput. Phys. Commun.* **2015**, *191*, 159–177, arXiv: [1410.3012](#) [[hep-ph](#)].
- [3] S. Plätzer, S. Gieseke, “Dipole Showers and Automated NLO Matching in Herwig++”, *Eur. Phys. J.* **2012**, *C72*, 2187, arXiv: [1109.6256](#) [[hep-ph](#)].
- [4] S. Höche, S. Prestel, “The midpoint between dipole and parton showers”, *Eur. Phys. J.* **2015**, *C75*, 461, arXiv: [1506.05057](#) [[hep-ph](#)].
- [5] S. Gieseke, P. Stephens, B. Webber, “New formalism for QCD parton showers”, *JHEP* **2003**, *12*, 045, arXiv: [hep-ph/0310083](#) [[hep-ph](#)].
- [6] T. Gleisberg, S. Hoeche, F. Krauss, M. Schonherr, S. Schumann, F. Siegert, J. Winter, “Event generation with SHERPA 1.1”, *JHEP* **2009**, *02*, 007, arXiv: [0811.4622](#) [[hep-ph](#)].
- [7] W. T. Giele, D. A. Kosower, P. Z. Skands, “A simple shower and matching algorithm”, *Phys. Rev.* **2008**, *D78*, 014026, arXiv: [0707.3652](#) [[hep-ph](#)].
- [8] L. Lönnblad, “ARIADNE version 4: A Program for simulation of QCD cascades implementing the color dipole model”, *Comput. Phys. Commun.* **1992**, *71*, 15–31.
- [9] G. Marchesini, B. Webber, “Simulation of QCD Jets Including Soft Gluon Interference”, *Nucl.Phys.B* **1984**, *238*, 1–29.
- [10] M. Dasgupta, F. A. Dreyer, K. Hamilton, P. F. Monni, G. P. Salam, “Logarithmic accuracy of parton showers: a fixed-order study”, *JHEP* **2018**, *09*, 033, arXiv: [1805.09327](#) [[hep-ph](#)].
- [11] R. Ángeles Martínez, M. De Angelis, J. R. Forshaw, S. Plätzer, M. H. Seymour, “Soft gluon evolution and non-global logarithms”, *JHEP* **2018**, *05*, 044, arXiv: [1802.08531](#) [[hep-ph](#)].
- [12] J. R. Forshaw, J. Holguin, S. Plätzer, “Parton branching at amplitude level”, *JHEP* **2019**, *08*, 145, arXiv: [1905.08686](#) [[hep-ph](#)].
- [13] T. Becher, M. Neubert, L. Rothen, D. Y. Shao, “Factorization and Resummation for Jet Processes”, *JHEP* **2016**, *11*, [Erratum: *JHEP*05,154(2017)], 019, arXiv: [1605.02737](#) [[hep-ph](#)].
- [14] S. Caron-Huot, “Resummation of non-global logarithms and the BFKL equation”, *JHEP* **2018**, *03*, 036, arXiv: [1501.03754](#) [[hep-ph](#)].
- [15] S. Caron-Huot, M. Herranen, “High-energy evolution to three loops”, *JHEP* **2018**, *02*, 058, arXiv: [1604.07417](#) [[hep-ph](#)].
- [16] A. Banfi, G. Marchesini, G. Smye, “Away from jet energy flow”, *JHEP* **2002**, *08*, 006, arXiv: [hep-ph/0206076](#) [[hep-ph](#)].
- [17] G. Bewick, S. Ferrario Ravasio, P. Richardson, M. H. Seymour, “Logarithmic Accuracy of Angular-Ordered Parton Showers”, **2019**, arXiv: [1904.11866](#) [[hep-ph](#)].

- [18] A. Banfi, G. P. Salam, G. Zanderighi, “Principles of general final-state resummation and automated implementation”, *JHEP* **2005**, *03*, 073, arXiv: [hep-ph/0407286](#) [[hep-ph](#)].
- [19] S. Catani, B. Webber, Y. Dokshitzer, F. Fiorani, “Average multiplicities in two- and three-jet e^+e^- annihilation events”, *Nuclear Physics B* **1992**, *383*, 419–441.
- [20] S. Catani, B. Webber, G. Marchesini, “QCD coherent branching and semi-inclusive processes at large x ”, *Nuclear Physics B* **1991**, *349*, 635–654.
- [21] I. G. Knowles, “Angular Correlations in QCD”, *Nucl. Phys.* **1988**, *B304*, 767–793.
- [22] I. Knowles, “A linear algorithm for calculating spin correlations in hadronic collisions”, *Computer Physics Communications* **1990**, *58*, 271–284.
- [23] I. W. Stewart, F. J. Tackmann, W. J. Waalewijn, “N-Jettiness: An Inclusive Event Shape to Veto Jets”, *Phys. Rev. Lett.* **2010**, *105*, 092002, arXiv: [1004.2489](#) [[hep-ph](#)].
- [24] M. Dasgupta, G. P. Salam, “Accounting for coherence in interjet $E(t)$ flow: A Case study”, *JHEP* **2002**, *03*, 017, arXiv: [hep-ph/0203009](#) [[hep-ph](#)].
- [25] A. Banfi, G. Corcella, M. Dasgupta, “Angular ordering and parton showers for non-global QCD observables”, *JHEP* **2007**, *03*, 050, arXiv: [hep-ph/0612282](#) [[hep-ph](#)].
- [26] Y. L. Dokshitzer, V. A. Khoze, A. H. Mueller, S. I. Troian, *Basics of perturbative QCD*, **1991**.
- [27] Y. L. Dokshitzer, “Calculation of the Structure Functions for Deep Inelastic Scattering and e^+e^- Annihilation by Perturbation Theory in Quantum Chromodynamics.”, *Sov. Phys. JETP* **1977**, *46*, [Zh. Eksp. Teor. Fiz.73,1216(1977)], 641–653.
- [28] Y. L. Dokshitzer, M. Olsson, “Jet cross-sections and multiplicities in the modified leading logarithmic approximation”, *Nucl. Phys.* **1993**, *B396*, 137–160.
- [29] V. N. Gribov, L. N. Lipatov, “Deep inelastic $e p$ scattering in perturbation theory”, *Sov. J. Nucl. Phys.* **1972**, *15*, [Yad. Fiz.15,781(1972)], 438–450.
- [30] G. Altarelli, G. Parisi, “Asymptotic freedom in parton language”, *Nuclear Physics B* **1977**, *126*, 298–318.
- [31] J. R. Forshaw, M. H. Seymour, “Subjet rates in hadron collider jets”, *JHEP* **1999**, *09*, 009, arXiv: [hep-ph/9908307](#) [[hep-ph](#)].
- [32] S. Catani, M. H. Seymour, “A General algorithm for calculating jet cross-sections in NLO QCD”, *Nucl. Phys.* **1997**, *B485*, [Erratum: Nucl. Phys.B510,503(1998)], 291–419, arXiv: [hep-ph/9605323](#) [[hep-ph](#)].
- [33] S. Plätzer, “Summing Large- N Towers in Colour Flow Evolution”, *Eur. Phys. J.* **2014**, *C74*, 2907, arXiv: [1312.2448](#) [[hep-ph](#)].
- [34] A. J. Larkoski, I. Moulton, D. Neill, “The Analytic Structure of Non-Global Logarithms: Convergence of the Dressed Gluon Expansion”, *JHEP* **2016**, *11*, 089, arXiv: [1609.04011](#) [[hep-ph](#)].
- [35] S. Plätzer, S. Gieseke, “Coherent Parton Showers with Local Recoils”, *JHEP* **2011**, *01*, 024, arXiv: [0909.5593](#) [[hep-ph](#)].
- [36] P. Eden, G. Gustafson, “Energy and virtuality scale dependence in quark and gluon jets”, *JHEP* **1998**, *09*, 015, arXiv: [hep-ph/9805228](#) [[hep-ph](#)].

- [37] C. Friberg, G. Gustafson, J. Hakkinen, “Color connections in $e^+ e^-$ annihilation”, *Nucl. Phys.* **1997**, *B490*, 289–305, arXiv: [hep-ph/9604347](#) [[hep-ph](#)].
- [38] W. T. Giele, D. A. Kosower, P. Z. Skands, “Higher-Order Corrections to Timelike Jets”, *Phys. Rev.* **2011**, *D84*, 054003, arXiv: [1102.2126](#) [[hep-ph](#)].
- [39] F. Krauss, A. Schalicke, G. Soff, “APACIC++ 2.0: A Parton cascade in C++”, *Comput. Phys. Commun.* **2006**, *174*, 876–902, arXiv: [hep-ph/0503087](#) [[hep-ph](#)].
- [40] R. Kuhn, F. Krauss, B. Ivanyi, G. Soff, “APACIC++: A Parton Cascade In C++, version 1.0”, *Comput. Phys. Commun.* **2001**, *134*, 223–266, arXiv: [hep-ph/0004270](#) [[hep-ph](#)].
- [41] Z. Nagy, D. E. Soper, “Effects of subleading color in a parton shower”, *JHEP* **2015**, *07*, 119, arXiv: [1501.00778](#) [[hep-ph](#)].
- [42] Z. Nagy, D. E. Soper, “What is a parton shower?”, *Phys. Rev.* **2018**, *D98*, 014034, arXiv: [1705.08093](#) [[hep-ph](#)].
- [43] D. Neill, V. Vaidya, “Soft evolution after a hard scattering process”, **2018**, arXiv: [1803.02372](#) [[hep-ph](#)].
- [44] M. De Angelis, Non-global Logarithms beyond Leading Colour, talk at <https://indico.cern.ch/event/662485/>, **2018**.
- [45] J. R. Forshaw, S. Plätzer, Soft Gluon Evolution beyond Leading Colour, talks at <https://indico.cern.ch/event/729453/>, **2018**.
- [46] Z. Nagy, D. E. Soper, “Parton showers with more exact color evolution”, **2019**, arXiv: [1902.02105](#) [[hep-ph](#)].
- [47] W. Kilian, T. Ohl, J. Reuter, C. Speckner, “QCD in the Color-Flow Representation”, *JHEP* **2012**, *10*, 022, arXiv: [1206.3700](#) [[hep-ph](#)].
- [48] R. Angeles-Martínez, J. R. Forshaw, M. H. Seymour, “Coulomb gluons and the ordering variable”, *JHEP* **2015**, *12*, 091, arXiv: [1510.07998](#) [[hep-ph](#)].
- [49] R. Angeles Martínez, J. R. Forshaw, M. H. Seymour, “Ordering multiple soft gluon emissions”, *Phys. Rev. Lett.* **2016**, *116*, 212003, arXiv: [1602.00623](#) [[hep-ph](#)].
- [50] R. K. Ellis, W. J. Stirling, B. R. Webber, “QCD and collider physics”, *Camb. Monogr. Part. Phys. Nucl. Phys. Cosmol.* **1996**, *8*, 1–435.
- [51] J. C. Collins, “Spin Correlations in Monte Carlo Event Generators”, *Nucl. Phys.* **1988**, *B304*, 794–804.
- [52] P. Binetruy, “Summing Leading Logs in Thrust Distributions”, *Phys. Lett.* **1980**, *91B*, 245–248.
- [53] T. Becher, M. D. Schwartz, “A precise determination of α_s from LEP thrust data using effective field theory”, *JHEP* **2008**, *07*, 034, arXiv: [0803.0342](#) [[hep-ph](#)].
- [54] S. Catani, B. R. Webber, Y. L. Dokshitzer, F. Fiorani, “Average multiplicities in two and three jet $e^+ e^-$ annihilation events”, *Nucl. Phys.* **1992**, *B383*, 419–441.

Chapter 7

Publication: Improvements on dipole shower colour

“The greatest teacher, failure is”

— Yoda, Star Wars: The Last Jedi

7.1 Preface

In the previous chapter we presented improvements to the dipole shower framework. In particular we addressed NLL errors due to mistreatment of momentum conservation and corrected colour factors for emissions that are concurrently order in k_t and angle. In the work that follows we address the assignment of colour factors for emissions not concurrently ordered in k_t and angle.

Before presenting the solution, let us first sketch a review of why our work in the previous section did not correct these disordered colour factors. We derived angular ordered and dipole showers from our amplitude level evolution equation:

$$q_{\perp} \frac{\partial \mathbf{A}_n(q_{\perp})}{\partial q_{\perp}} = \mathbf{E}(\{\mathbf{A}_i(q_{\perp}) | i \leq n\}; q_{\perp}). \quad (7.1)$$

Here we’ve introduced a very abridged notation $\mathbf{E}(\dots; q_{\perp})$ which is an evolution kernel which is a linear operator on the set of amplitude density matrices $\{\mathbf{A}_i(q_{\perp}) | i \leq n\}$, defined at a scale q_{\perp} . We have dropped the explicit particle momentum dependence of $\mathbf{A}_n(q_{\perp})$ which can be restored as $\mathbf{A}_n(q_{\perp}) \rightarrow \mathbf{A}_n(\{p\}_n; q_{\perp})$. \mathbf{E} is defined so that it returns the variation of $\mathbf{A}_n(q_{\perp})$ in a logarithmic slice of the scale q_{\perp} :

$$d\mathbf{A}_n(q_{\perp}) = \mathbf{E}(\{\mathbf{A}_i(q_{\perp}) | i \leq n\}; q_{\perp}) d \ln q_{\perp}. \quad (7.2)$$

\mathbf{E} can be read off at a given perturbative order from Eq.(4.7). There were two main steps to deriving an angular ordered shower, described by an evolution equation

$$\theta \frac{\partial \text{Tr} \langle \mathbf{A}_n(\theta) \rangle}{\partial \theta} = K(\{\text{Tr} \langle \mathbf{A}_i(\theta) \rangle | i \leq n\}; \theta), \quad (7.3)$$

where we've used the same abridged notation for the evolution kernel. The angled brackets $\langle \rangle$ imply azimuthal averaging and θ is an angular resolution scale. It is important to note that $\mathbf{A}_n(\theta) \neq \mathbf{A}_n(q_\perp)$ as the former is \mathbf{A}_n viewed at a given angular resolution (i.e. all partons are separated on the momentum-space celestial sphere at least by the characteristic scale θ) whilst the later is \mathbf{A}_n viewed at a given k_t resolution (all transverse momenta are large than q_\perp).¹

When deriving the angular ordered shower, we showed that after azimuthal averaging and in the ‘mostly collinear’ limit²,

$$\begin{aligned} q_\perp \frac{\partial \text{Tr} \langle \mathbf{A}_n(q_\perp) \rangle}{\partial q_\perp} &= \text{Tr} \langle \mathbf{E}(\{\mathbf{A}_i(q_\perp) | i \leq n\}; q_\perp) \rangle \\ &\approx K(\{\text{Tr} \langle \mathbf{A}_i(q_\perp) \rangle | i \leq n\}; q_\perp). \end{aligned} \quad (7.4)$$

In words, the trace of the evolution kernel \mathbf{E} in the ‘mostly collinear’ limit after azimuthal averaging is equal to the evolution kernel for an angular ordered shower, K , viewed at a fixed k_t resolution scale. Next we changed ordering variables. Note that inclusivity over radiation at all scales requires that

$$\begin{aligned} &\int_{q'_\perp}^Q K(\{\text{Tr} \langle \mathbf{A}_i(q_\perp) \rangle | i \leq n\}; q_\perp) d \ln q_\perp \\ &= \int_{\theta'}^\pi K(\{\text{Tr} \langle \mathbf{A}_i(\theta) \rangle | i \leq n\}; \theta) d \ln \theta + \mathcal{O}\left(\frac{\theta'}{\pi}\right) + \mathcal{O}\left(\frac{q'_\perp}{Q}\right). \end{aligned} \quad (7.5)$$

Thus, we change change ordering variables by applying

$$\lim_{q'_\perp \rightarrow 0} \frac{\partial}{\partial \ln \theta} \int_{q'_\perp}^Q d \ln q_\perp,$$

where θ is the smallest angular separation between partons in $\mathbf{A}_n(q_\perp)$, to both sides of Eq. (7.4):

$$\begin{aligned} \lim_{q'_\perp \rightarrow 0} \theta \frac{\partial \text{Tr} \langle \mathbf{A}_n(q'_\perp) \rangle}{\partial \theta} &= K(\{\text{Tr} \langle \mathbf{A}_i(\theta) \rangle | i \leq n\}; \theta) + \mathcal{O}\left(\frac{\theta}{\pi}\right) \\ &= \theta \frac{\partial \text{Tr} \langle \mathbf{A}_n(\theta) \rangle}{\partial \theta} + \mathcal{O}\left(\frac{\theta}{\pi}\right). \end{aligned} \quad (7.6)$$

¹Of course it is necessarily true that, when computed at equivalent accuracies, $\lim_{\theta \rightarrow 0} \mathbf{A}_n(\theta) = \lim_{q_\perp \rightarrow 0} \mathbf{A}_n(q_\perp)$.

²Up to one parton is allowed to be emitted at arbitrary angle whilst every other particle is assumed to be collinear, picking up a collinear log.

In this way we derived angular ordering.

The ‘moral’ of this discussion is that we only had to show

$$\text{Tr} \langle \mathbf{E}(\{\mathbf{A}_i(q_\perp) | i \leq n\}; q_\perp) \rangle \approx K(\{\text{Tr} \langle \mathbf{A}_i(q_\perp) \rangle | i \leq n\}; q_\perp), \quad (7.7)$$

to know that the two formulations were equivalent at the accuracy we were considering. Let us now look at the dipole shower, here we found an evolution equation of the form

$$\begin{aligned} q_\perp \frac{\partial \text{Leading}(\mathbf{A}_n(q_\perp))}{\partial q_\perp} &= \text{Leading}(\mathbf{E}(\{\mathbf{A}_i(q_\perp) | i \leq n\}; q_\perp)) \\ &\equiv L(\{\text{Leading}(\mathbf{A}_i(q_\perp)) | i \leq n\}; q_\perp), \end{aligned} \quad (7.8)$$

where Leading is an operation for taking the leading colour piece. L is a dipole shower evolution kernel derived from the soft limit. Importantly, we found that L had to be greatly constrained so that

$$\langle L(\{\text{Leading}(\mathbf{A}_i(q_\perp)) | i \leq n\}; q_\perp) \rangle \approx \text{Leading}(K(\{\text{Tr} \langle \mathbf{A}_i(q_\perp) \rangle | i \leq n\}; q_\perp)), \quad (7.9)$$

else the dipole shower is inconsistent with the angular ordered shower in the ‘mostly collinear’ limit. This informed us how recoil and hard-collinear physics should be implemented into L . The problem is that both sides of the expression are still in the leading colour approximation. To extend L past leading colour we made the following observation, assigning Casimir colour factors in-accordance with the presence of collinear poles and letting $C_F = 4/3$ in L guarantees that

$$\langle L_{C_F=4/3}(\{\text{Leading}(\mathbf{A}_i(\{p\}_i; q_\perp)) | i \leq n\}; \theta) \rangle \approx K(\{\text{Tr} \langle \mathbf{A}_i(\{p\}_i; \theta) \rangle | i \leq n\}; \theta), \quad (7.10)$$

where θ is the smallest angular separation between partons in $\mathbf{A}_n(\{p\}_n; q_\perp)$. We therefore set $C_F = 4/3$ throughout the dipole shower. However, this only correctly introduces full colour accuracy to $L(\dots; q_\perp)$ for particles separated by the angular scale θ (where $\langle L \rangle$ coincides with K). Therefore, setting $C_F = 4/3$ throughout the dipole shower we achieved the following

$$\begin{aligned} \langle L_{C_F=4/3}(\{\text{Leading}(\mathbf{A}_i(q_\perp)) | i \leq n\}; q_\perp) \rangle \\ \approx K(\{\text{Tr} \langle \mathbf{A}_i(q_\perp) \rangle | i \leq n\}; q_\perp) \text{ for } q_\perp/E \sim \theta, \end{aligned} \quad (7.11)$$

where E is the energy of the softest parton in \mathbf{A}_n , and

$$\begin{aligned} \text{Leading}(\langle L_{C_F=4/3}(\text{Leading}(\mathbf{A}_i(q_\perp)) | i \leq n\}; q_\perp) \rangle) \\ \approx \text{Leading}(K(\{\text{Tr} \langle \mathbf{A}_i(q_\perp) \rangle | i \leq n\}; q_\perp)) \text{ for } q_\perp/E \gg \theta. \end{aligned} \quad (7.12)$$

However

$$\begin{aligned} & \langle L_{C_F=4/3}(\{\text{Leading}(\mathbf{A}_i(q_\perp))|i \leq n\}; q_\perp) \rangle \\ & \not\approx K(\{\text{Tr} \langle \mathbf{A}_i(q_\perp) \rangle |i \leq n\}; q_\perp) \text{ for } q_\perp/E \gg \theta. \end{aligned} \quad (7.13)$$

Thus sub-leading colour errors may appear in wide angle radiation for which their angular scale is ordered differently to their k_t scale.

In the work that follows we introduce new dynamic colour factors, defined so that

$$\begin{aligned} & \langle L_{\text{dynamic}}(\{\text{Leading}(\mathbf{A}_i(q_\perp))|i \leq n\}; q_\perp) \rangle \\ & \approx K(\{\text{Tr} \langle \mathbf{A}_i(q_\perp) \rangle |i \leq n\}; q_\perp) \text{ for } q_\perp/E \gg \theta. \end{aligned} \quad (7.14)$$

We initially motivate the dynamic colour factors by fixed order calculations with two soft gluons dressing a hard process. Two are required since for one soft gluon $q_\perp/E \approx \theta$, thus Eq. (7.11) holds and there isn't a sub-leading colour error. We then generalise the dynamic colour factors to all orders.

Additional note on context

The following paper was released at the begin of 2021. As the paper was being concluded, reference [1] was also released. One solution that [1] provides to improve dipole shower colour, by dividing the emission phase-space and subsequently assigning colour factors C_F or $C_A/2$ in accordance with QCD coherence, appears to be similar to the solution presented here. The authors of [1] state that their method for correctly assigning colour factors "... can be applied to almost any dipole or antenna shower." As of August 2021, the following chapter and [1] remain state of the art.

References

- [1] K. Hamilton, R. Medves, G. P. Salam, L. Scyboz, G. Soyez, "Colour and logarithmic accuracy in final-state parton showers", **2020**, arXiv: [2011.10054](https://arxiv.org/abs/2011.10054) [[hep-ph](https://arxiv.org/abs/2011.10054)].

Declaration

The subsequent work is mine and my collaborators. It is without plagiarism. Each section in the paper is my own research.

This work has received funding from the UK Science and Technology Facilities Council (grant no. ST/P000800/1), the European Union's Horizon 2020 research and innovation programme as part of the Marie Skłodowska-Curie Innovative Training Network MCnetITN3 (grant agreement no. 722104), and in part by the by the COST actions CA16201 "PARTICLEFACE" and CA16108 "VBSCAN". JH thanks the UK Science and Technology Facilities Council for the award of a studentship. We would also like to thank the organisers of the "Taming the accuracy of event generators" workshop (2020) for facilitating enlightening discussions. We especially want to thank Gavin Salam for valuable discussions.

Improvements on dipole shower colour

Authors: Jack Holguin, Jeffrey R. Forshaw, Simon Plätzer

Abstract

The dipole formalism provides a powerful framework from which parton showers can be constructed. In a recent paper [1], we proposed a dipole shower with improved colour accuracy and in this paper we show how it can be further improved. After an explicit check at $\mathcal{O}(\alpha_s^2)$ we confirm that our original shower performs as it was designed to, i.e. inheriting its handling of angular-ordered radiation from a coherent branching algorithm. We also show how other dipole shower algorithms fail to achieve this. Nevertheless, there is an $\mathcal{O}(\alpha_s^2)$ topology where it differs at sub-leading N_c from a coherent branching algorithm. This erroneous topology can contribute a leading logarithm to some observables and corresponds to emissions that are ordered in k_t but not angle. We propose a simple, computationally efficient way to correct this and assign colour factors in accordance with the coherence properties of QCD to all orders in α_s .

7.2 Introduction

Parton showers typically are constructed using one of two basic approaches: angular-ordered showers (based on the coherent branching formalism) and dipole showers. Angular ordering is a very powerful approach, providing next-to-leading logarithmic (NLL) accuracy in some observables,³ but it fails to capture physics salient to the description of multi-jet final states in hadron colliders and non-global observables. By comparison, dipole showers are typically restricted to leading-colour accuracy but they can be applied across the board. In recent literature, much attention has been focused on improving the framework upon which dipole showers are constructed [4–14]. Substantial progress has been made demonstrating

³Many e^+e^- observables share the property that their distributions exponentiate:

$$\Sigma(\alpha_s, L) = (1 + C(\alpha_s)) \exp(L g_1(\alpha_s L) + g_2(\alpha_s L) + \dots),$$

where Σ is the fraction of events for which the observable is less than some value, $v = e^{-L}$. NLL accuracy corresponds to correctly computing the functions g_1 and g_2 [2, 3].

their capacity for NLL resummation [1, 15] and methods for partially addressing sub-leading colour have also been proposed, by extending dipole showers beyond leading- N_c colour flows [16–19]. In a recent paper [1], we constructed a dipole shower that has the virtue of inheriting some of the colour dynamics of an angular-ordered shower, which improved sub-leading colour accuracy. In this paper we perform a fixed-order cross-check of that approach. We do so by comparing the improved shower’s assignment of colour factors to the corresponding exact e^+e^- matrix elements, computed with second-order QCD corrections. Motivated by these calculations, we are able to further improve our dipole shower’s description of colour, in a way that is applicable to evolution with an arbitrary number of emissions.

In [1] we derived an improved dipole shower in the context of $e^+e^- \rightarrow q\bar{q}$ collisions⁴, starting from an algorithm for the evolution of QCD amplitudes first presented in [20]. The shower can be understood by considering a few key features of angular-ordered and dipole showers. When a shower emits a parton, three new degrees of freedom (DoF) are introduced, describing the new parton’s energy and direction. Angular-ordered showers average over one of the DoF (a contextually defined azimuth) which allows the effects of QCD coherence to become manifest. In turn, this reduces the shower to a Markovian sequence of parton decays ($1 \rightarrow 2$ transitions). Thus the final-state partons produced by the shower have a unique branching history with colour factors assigned in accordance with QCD coherence. The angular-ordered approach is very powerful; by harnessing QCD coherence, NLL resummation can be achieved for a broad class of global observables [2]. However, averaging a DoF limits the approach.

In contrast to angular ordering, the dipole approach retains full dependence on the DoF of each emitted parton. Instead it approximates the colour structures in the shower by emitting partons from colour-connected dipoles. This restricts a basic dipole shower to leading-colour accuracy. Thus a dipole shower is built from a Markovian sequence of $2 \rightarrow 3$ transitions and, as a result, dipole showers lack a unique branching history of parent partons and their decay products. However, a branching history can be constructed by introducing a dipole partitioning, which probabilistically assigns the emitted parton to one of the two parent partons in the dipole. Modern dipole showers use this partitioning to assign colour factors and momentum conservation, and to facilitate hard-process matching. In effect, our approach in [1] was to define a partitioning so that, after averaging over azimuths, each branching history and its relative weight matches with a corresponding branching history generated by an angular-ordered shower. Through this link, we could assign colour factors beyond leading colour in the dipole shower. As we show in this paper, when applied naively (as was done in [1]) this procedure does not completely eliminate sub-leading colour errors

⁴Though the framework to extend the shower beyond e^+e^- was presented in the appendices of [1].

in the dipole shower for some observables, even at LL accuracy. The problem arises since the k_t -ordered dipole shower necessarily involves branching histories disordered in angle: soft, large-angle emissions can appear anywhere in the branching history. These particular branching histories complicate any attempt to assign colour factors in a dipole shower (a point previously noted in [21]) and were not completely accounted for in our original approach. In this paper, we solve this problem by introducing dynamical colour factors, i.e. we fix the LL, sub-leading colour errors in event shape observables and increase the shower’s sensitivity to full-colour NLLs (falling short of full-colour NLL resummation).

The rest of the paper is structured as follows. After a review of the double emission matrix element in Section 7.3, we repeat the calculation for our original dipole shower in Section 7.4 and compare the two. We find that the shower works as intended, i.e. the colour factors assigned to partons whose emissions are ordered in angle agree with those of the fixed-order result. However, for emissions unordered in angle, the shower has only leading-colour accuracy. The understanding brought about by the fixed-order analysis allows us to construct a new method for the correct assignment of dynamical colour factors for emissions unordered in angle. The specific partitioning we introduced in [1] plays a crucial role in the construction of the new colour factors. The approach we take involves altering shower kernels by introducing a dynamic colour factor that is a function of the branching history. This method involves a computational complexity that asymptotically grows logarithmically with the parton multiplicity. Finally, to illustrate the importance of the dipole partitioning, we compute the $\mathcal{O}(\alpha_s^2)$ difference between exact squared matrix elements and those calculated using a dipole shower employing a different (Catani-Seymour [22]) partitioning. We find that, in the limit the emissions are strongly ordered in energy and angle, the $\mathcal{O}(\alpha_s^2)$ difference does not vanish, with the possibility of a LL, sub-leading colour error, as was noted in [21]. For specific observables (e.g. thrust) this error may be removed at order $\mathcal{O}(\alpha_s^2)$ from a dipole shower employing a Catani-Seymour-type dipole partitioning by using our dynamic colour factors. However, the error will likely re-emerge at higher-orders.

7.3 A recap of the $\mathcal{O}(\alpha_s^2)$ QCD squared matrix element

First we recap the calculation of the $\mathcal{O}(\alpha_s^2)$ $e^+e^- \rightarrow q\bar{q}gg$ squared matrix element when the gluons are either soft or collinear. Figure 7.1 illustrates our labelling of the partons and the angles between them. This calculation is essentially a recap of Section 5.5 in Ellis, Stirling and Webber [23] and Chapter 4 in Dokshitzer, Khoze, Mueller and Troyan [24]. To start, we will only take the limit that lab-frame energies satisfy $E_q \ll E_j, E_i, E_k$ (i.e. the pure

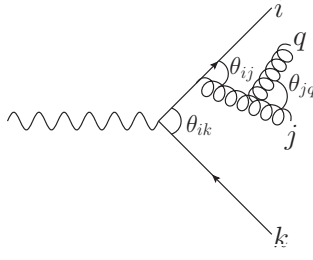


Figure 7.1: One of the Feynman diagrams contributing to the $\mathcal{O}(\alpha_s^2)$ $e^+e^- \rightarrow q\bar{q}gg$ matrix element used to compute Eq. (7.15). In the present work we calculate these in the soft approximation for which the second gluon is assumed to have energy much less than the first emission.

soft limit for q). Thus our starting point is⁵

$$|\mathcal{M}_2|^2 \frac{d^3\vec{p}_q}{2E_q} \approx -\frac{2\alpha_s}{\pi} \text{Tr}(\mathbf{T}_i \cdot \mathbf{T}_j w_{ij} + \mathbf{T}_j \cdot \mathbf{T}_k w_{jk} + \mathbf{T}_k \cdot \mathbf{T}_i w_{ki}) \frac{dE_q}{E_q} \frac{d\Omega_q}{4\pi} |\mathcal{M}_1(\vec{p}_i, \vec{p}_j, \vec{p}_k)|^2, \quad (7.15)$$

where

$$w_{ab} = \frac{E_q^2 p_a \cdot p_b}{p_a \cdot p_q p_b \cdot p_q}. \quad (7.16)$$

and where $|\mathcal{M}_1(\vec{p}_i, \vec{p}_j, \vec{p}_k)|^2$ is the $\mathcal{O}(\alpha_s)$ squared matrix element. At leading colour (LC) we have

$$|\mathcal{M}_2|^2 \frac{d^3\vec{p}_q}{2E_q} \approx \frac{\alpha_s N_c}{\pi} (w_{ij} + w_{jk}) \frac{dE_q}{E_q} \frac{d\Omega_q}{4\pi} |\mathcal{M}_1(\vec{p}_i, \vec{p}_j, \vec{p}_k)|^2. \quad (7.17)$$

This can be interpreted as a sum of emissions from two independent dipoles, (ij) and (jk) , and is the basic result on which dipole showers and the Banfi-Marchesini-Smye (BMS) equation [3] are built, see also the discussion in [25] for a more detailed analysis in the case of more general processes.

Without approximating colour, we can simplify the matrix element by only keeping terms which are logarithmically enhanced in the two-jet limit (i.e. terms that diverge as $\theta_{ij}/\theta_{ik} \rightarrow 0$). To do this, we write each w_{ab} as

$$w_{ab} = P_{ab} + P_{ba}, \quad (7.18)$$

where

$$2P_{ab} = w_{ab} + \frac{E_a E_q}{p_a \cdot p_q} - \frac{E_b E_q}{p_b \cdot p_q} \quad (7.19)$$

⁵In this case, as the three-parton matrix element is diagonal in colour, we have $\langle \mathcal{M}_1(\dots) | \mathbf{T}_i \cdot \mathbf{T}_j | \mathcal{M}_1(\dots) \rangle = \text{Tr}[\mathbf{T}_i \cdot \mathbf{T}_j] |\mathcal{M}_1(\dots)|^2$.

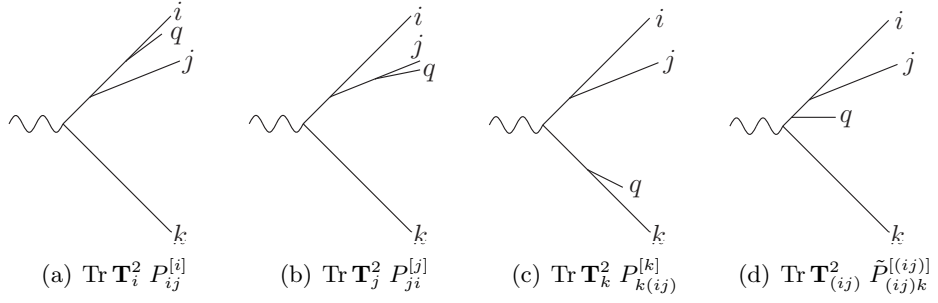


Figure 7.2: Diagrams illustrating the angular-ordered interpretation of the four terms in Eq. (7.23). The relative lengths of lines depict the relative energies. Likewise, the relative angles between lines are indicative.

and

$$\int_0^{2\pi} \frac{d\phi_q^{(a)}}{2\pi} P_{ab} = \frac{1}{1 - \cos \theta_{aq}} \Theta(\theta_{aq} < \theta_{ab}). \quad (7.20)$$

Here $\phi_q^{(a)}$ is the azimuth as measured around the direction of p_a . We define the following shorthand for averaging the azimuths:

$$P_{ab}^{[a]} = \frac{(\text{d} \cos \theta_{aq}) \text{d}\phi_q^{(a)}}{4\pi} \int_0^{2\pi} \frac{d\phi_q^{(a)}}{2\pi} P_{ab}. \quad (7.21)$$

Importantly, $P_{ab}^{[a]}$ only depends on parton b via the theta function constraining the angle of emission. We now consider the limit $\theta_{ij} \ll \theta_{ik} = \pi$, whence we can assume

$$P_{ki}^{[k]} \approx P_{kj}^{[k]} \approx P_{k(ij)}^{[k]}, \quad (7.22)$$

where (ij) refers to the momentum $p_{(ij)} = p_i + p_j$, which is approximately on-shell in the collinear limit we consider. By employing this and similar relations we can simplify the matrix element:

$$|\mathcal{M}_2|^2 \frac{d^3 \vec{p}_q}{2E_q} \approx \frac{2\alpha_s}{\pi} \text{Tr} \left(\mathbf{T}_i^2 P_{ij}^{[i]} + \mathbf{T}_j^2 P_{ji}^{[j]} + \mathbf{T}_k^2 P_{k(ij)}^{[k]} + \mathbf{T}_{(ij)}^2 \tilde{P}_{(ij)k}^{[(ij)]} \right) \frac{dE_q}{E_q} |\mathcal{M}_1(\vec{p}_i, \vec{p}_j, \vec{p}_k)|^2, \quad (7.23)$$

where $\tilde{P}_{(ij)k}^{[(ij)]} = P_{(ij)k}^{[(ij)]} \Theta(\theta_{(ij)q} > \theta_{ij})$. The four contributions are illustrated in Figure 7.2 and Table 7.1 tabulates each term in Eq. (7.23) across the entire emission phase-space for q .

It is important to note that when deriving Eq. (7.23), terms such as

$$\Delta = \frac{1}{2} \left(P_{ik}^{[i]} - P_{ij}^{[i]} - P_{jk}^{[j]} + P_{ji}^{[j]} \right), \quad (7.24)$$

were set to zero by approximating the direction of i and j with a combined direction (ij) . For finite θ_{ij} , these terms are only subject to energy divergences and therefore are negligible so

$\frac{\theta_{iq}}{\theta_{ij}}$	$\frac{\theta_{jq}}{\theta_{ij}}$	$\text{Tr } \mathbf{T}_i^2 P_{ij}^{[i]}$	$\text{Tr } \mathbf{T}_j^2 P_{ji}^{[j]}$	$\text{Tr } \mathbf{T}_k^2 P_{k(ij)}^{[k]}$	$\text{Tr } \mathbf{T}_{(ij)}^2 \tilde{P}_{(ij)k}^{[(ij)]}$
< 1	< 1	$C_F P_{ij}^{[i]}$	$C_A P_{ji}^{[j]}$	$C_F P_{k(ij)}^{[k]}$	0
< 1	> 1	<u>$C_F P_{ij}^{[i]}$</u>	<u>0</u>	<u>$C_F P_{k(ij)}^{[k]}$</u>	<u>0</u>
> 1	< 1	<u>0</u>	<u>$C_A P_{ji}^{[j]}$</u>	<u>$C_F P_{k(ij)}^{[k]}$</u>	<u>0</u>
> 1	> 1	<u>0</u>	<u>0</u>	<u>$C_F P_{k(ij)}^{[k]}$</u>	<u>$C_F \tilde{P}_{(ij)k}^{[(ij)]}$</u>

Table 7.1: The contributions to Eq. (7.23), the azimuthally-averaged squared matrix element in the limit $\theta_{ij} \ll \theta_{ik}$. Terms where wide-angle, soft physics has been lost as a result of the collinear approximation are underlined.

long as we insist that a collinear logarithm is picked up. However, because we azimuthally averaged and neglected these pieces, some wide-angle physics is lost which is otherwise captured at LC in Eq. (7.17) (and consequently in dipole showers and BMS evolution). These soft poles are crucial to a complete description of non-global logarithms. Regions of phase-space for which some wide-angle physics has been set to zero are underlined in Table 7.1. Crucially, all wide-angle soft physics is included in the limit $\theta_{ij} \rightarrow 0$.

Eq. (7.23) can be generalised to include the situation where the parton energies are no longer strongly ordered by introducing hard-collinear physics:

$$\frac{dE_q}{E_q} \mapsto \frac{dE_q}{E_q} (1 + \text{hard-collinear}). \quad (7.25)$$

For instance, in the limits defining the rows 1 through 3 of Table 7.1, Eq. (7.23) with hard-collinear physics is

$$|\mathcal{M}_2|^2 \frac{d^3 \vec{p}_q}{2E_q} \approx \frac{2\alpha_s}{\pi} \left(P_{ij}^{[i]} dz_i \mathcal{P}_{qq} + P_{ji}^{[j]} dz_j \mathcal{P}_{gg} + P_{k(ij)}^{[k]} dz_k \mathcal{P}_{qq} \right) |\mathcal{M}_1(\vec{p}_i, \vec{p}_j, \vec{p}_k)|^2, \quad (7.26)$$

where \mathcal{P}_{ab} is an unregularised splitting function and $1 - z_m \approx E_q/E_m$ with E_m the energy of parton m before the emission⁶. Likewise, Eq. (7.23) in the limit defined in the last row of Table 7.1 becomes

$$|\mathcal{M}_2|^2 \frac{d^3 \vec{p}_q}{2E_q} \approx \frac{2\alpha_s}{\pi} \left(P_{(ij)k}^{[(ij)]} dz_{(ij)} \mathcal{P}_{qq} + P_{k(ij)}^{[k]} dz_k \mathcal{P}_{qq} \right) |\mathcal{M}_1(\vec{p}_i, \vec{p}_j, \vec{p}_k)|^2. \quad (7.27)$$

7.4 Computing the squared matrix element with the dipole shower

Now we want to compute the same squared matrix element using our k_t -ordered dipole shower. We wish to test that it correctly reproduces the terms in Table 7.1 and the hard-

⁶We have ignored the recoil. See Section 7.5.1 for a discussion on its inclusion.

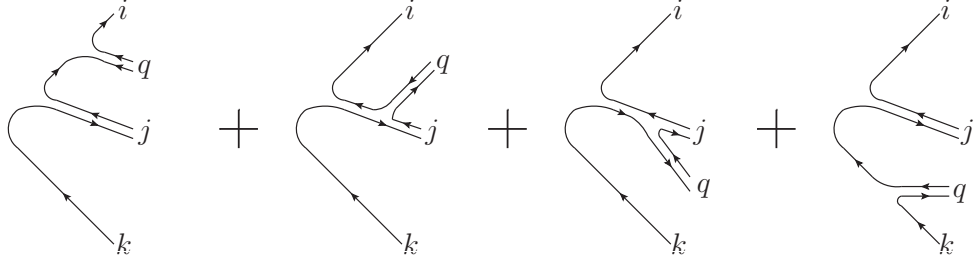


Figure 7.3: The relevant colour topologies in a dipole shower corresponding to Eq. (7.23).

collinear physics in Eqs. (7.26) and (7.27). The relevant contributions are pictured in Figure 7.3.

Consider a generic k_t -ordered dipole shower, for which emission from a dipole (a, b) at a given slice in k_t is generated by an emission probability of

$$\frac{d\text{Prob}}{\ln k_{\perp}^{ab}} = \int \frac{d\phi}{2\pi} \frac{\alpha_s}{\pi} \left(C_a g_{ab} \mathcal{P}_{a \rightarrow aq}^d(z^{ab}) dz^{ab} + C_b g_{ba} \mathcal{P}_{b \rightarrow bq}^d(z^{ba}) dz^{ba} \right), \quad (7.28)$$

where $\mathcal{P}_{q \rightarrow qq}^d(z) = \mathcal{P}_{qq}^d(z)$ and $\mathcal{P}_{g \rightarrow gg}^d(z) = \mathcal{P}_{gg}^d(z)$. We neglect $g \rightarrow q\bar{q}$ transitions, which are sub-leading in colour and only contribute a NLL for doubly-logarithmic observables⁷. $\mathcal{P}_{qq}^d(z)$ and $\mathcal{P}_{gg}^d(z)$ are the usual dipole splitting functions, stripped of their colour factors:

$$\begin{aligned} C_F \mathcal{P}_{qq}^d(z) &= \mathcal{P}_{qq}(z), \\ \frac{C_A}{2} \mathcal{P}_{gg}^d(z) + \frac{C_A}{2} \mathcal{P}_{gg}^d(1-z) &= \mathcal{P}_{gg}(z), \end{aligned} \quad (7.29)$$

and where $C_a = C_F$ or $C_A/2$ if parton a is a quark or gluon. The g_{ab} are dipole partitioning functions, they define how colour factors and momentum conservation should be distributed across the two members of a dipole and are functions of the momenta of all partons emitted so far. Functions g_{ab} can be smooth or discontinuous functions of the parton momenta. Since we are neglecting momentum conservation in this section, $g_{ab} + g_{ba} = 1$. The relevant kinematic variables are

$$\begin{aligned} (k_{\perp}^{ab})^2 &= \frac{2 p_a \cdot p_q p_b \cdot p_q}{p_a \cdot p_b}, & 1 - z^{ab} &= \frac{p_q \cdot p_b}{p_a \cdot p_b}, \\ (k_{\perp})^2 &= \frac{2 p_i \cdot p_j p_k \cdot p_j}{p_i \cdot p_k}, \end{aligned} \quad (7.30)$$

and ϕ is an azimuth so that $\vec{k}_{\perp}^{ab} = k_{\perp}^{ab}(\sin \phi \vec{n}_1 + \cos \phi \vec{n}_2)$ where $\vec{n}_{1,2}$ are two mutually orthogonal and normalised transverse vectors in the (a, b) dipole zero-momentum frame.

⁷For single-logarithm, collinear-sensitive observables they contribute a leading logarithm at sub-leading colour.

After two emissions, the shower gives

$$\begin{aligned}
|\mathcal{M}_2|^2 \frac{d^3 \vec{p}_q}{2E_q} &\approx \frac{\alpha_s}{\pi} \left[\left(C_F g_{ij} \mathcal{P}_{qq}^d(z^{ij}) dz^{ij} + \frac{C_A}{2} g_{ji} \mathcal{P}_{gg}^d(z^{ji}) dz^{ji} \right) \frac{dk_{\perp}^{ij}}{k_{\perp}^{ij}} \frac{d\phi}{2\pi} \Theta(k_{\perp}^{ij} < k_{\perp}) \right. \\
&\quad \left. + \left(\frac{C_A}{2} g_{jk} \mathcal{P}_{gg}^d(z^{jk}) dz^{jk} + C_F g_{kj} \mathcal{P}_{qq}^d(z^{kj}) dz^{kj} \right) \frac{dk_{\perp}^{jk}}{k_{\perp}^{jk}} \frac{d\phi}{2\pi} \Theta(k_{\perp}^{jk} < k_{\perp}) \right] |\mathcal{M}_1(\vec{p}_i, \vec{p}_j, \vec{p}_k)|^2.
\end{aligned} \tag{7.31}$$

7.4.1 $\mathcal{O}(\alpha_s^2)$ with emissions ordered in angle

We will first consider whether our dipole shower can recreate the physics in rows 1 through 3 of Table 7.1. The diagrams contributing to this limit will be produced in our shower when the parton transverse momenta and angles are concurrently ordered. For now we will neglect recoil and hard-collinear pieces. Keeping only the soft parts, we have

$$\begin{aligned}
|\mathcal{M}_2|^2 \frac{d^3 \vec{p}_q}{2E_q} &\approx \frac{2\alpha_s}{\pi} \left[\left(C_F g_{ij} w_{ij} + \frac{C_A}{2} g_{ji} w_{ij} \right) \frac{dE_q}{E_q} \frac{d^2 \Omega_q}{4\pi} \Theta(k_{\perp}^{ij} < k_{\perp}) \right. \\
&\quad \left. + \left(\frac{C_A}{2} g_{jk} w_{jk} + C_F g_{kj} w_{jk} \right) \frac{dE_q}{E_q} \frac{d^2 \Omega_q}{4\pi} \Theta(k_{\perp}^{jk} < k_{\perp}) \right] |\mathcal{M}_1(\vec{p}_i, \vec{p}_j, \vec{p}_k)|^2.
\end{aligned} \tag{7.32}$$

Our dipole shower is built using the partitioning

$$g_{ab} = \frac{1}{2} + \text{Asym}_{a,b}, \tag{7.33}$$

where [1]

$$\text{Asym}_{a,b} = \left[\frac{T \cdot p_a}{4T \cdot p_q} \frac{(k_{\perp}^{(ab)})^2}{p_a \cdot p_q} - \frac{T \cdot p_b}{4T \cdot p_q} \frac{(k_{\perp}^{(ab)})^2}{p_b \cdot p_q} \right], \quad \text{and} \quad T = \sum_i p_i, \tag{7.34}$$

where the sum over i is a sum over all partons in the event. T plays the role of projecting the lab frame energy when it is contracted with a momentum vector. Roughly speaking, this way of partitioning a dipole corresponds to splitting the dipole in half in the laboratory frame; it is defined specifically to ensure

$$g_{ab} w_{ab} = P_{ab}, \tag{7.35}$$

and therefore

$$\begin{aligned}
|\mathcal{M}_2|^2 \frac{d^3 \vec{p}_q}{2E_q} &\approx \frac{2\alpha_s}{\pi} \left[\left(C_F P_{ij} + \frac{C_A}{2} P_{ji} \right) \frac{dE_q}{E_q} \frac{d^2 \Omega_q}{4\pi} \Theta(k_{\perp}^{ij} < k_{\perp}) \right. \\
&\quad \left. + \left(\frac{C_A}{2} P_{jk} + C_F P_{kj} \right) \frac{dE_q}{E_q} \frac{d^2 \Omega_q}{4\pi} \Theta(k_{\perp}^{jk} < k_{\perp}) \right] |\mathcal{M}_1(\vec{p}_i, \vec{p}_j, \vec{p}_k)|^2.
\end{aligned} \tag{7.36}$$

After azimuthal averaging:

$$|\mathcal{M}_2|^2 \frac{d^3 \vec{p}_q}{2E_q} \approx \frac{2\alpha_s}{\pi} \left[\left(C_F P_{ij}^{[i]} + \frac{C_A}{2} P_{ji}^{[j]} \right) \frac{dE_q}{E_q} \Theta(k_{\perp}^{ij} < k_{\perp}) \right. \\ \left. + \left(\frac{C_A}{2} P_{jk}^{[j]} + C_F P_{kj}^{[k]} \right) \frac{dE_q}{E_q} \Theta(k_{\perp}^{jk} < k_{\perp}) \right] |\mathcal{M}_1(\vec{p}_i, \vec{p}_j, \vec{p}_k)|^2. \quad (7.37)$$

As we are working in the limits defined in rows 1 through 3 of Table 7.1, and in the soft limit for q , the k_t ordering theta functions all saturate and can be removed. Thus, we find

$$|\mathcal{M}_2|^2 \frac{d^3 \vec{p}_q}{2E_q} \approx \frac{2\alpha_s}{\pi} \left(C_F P_{ij}^{[i]} + C_A P_{ji}^{[j]} + C_F P_{k(ij)}^{[k]} \right) \frac{dE_q}{E_q} |\mathcal{M}_1(\vec{p}_i, \vec{p}_j, \vec{p}_k)|^2. \quad (7.38)$$

This is the same as the fixed-order result given in the previous section.

We will now relax the soft approximation and check whether our dipole shower correctly includes the hard-collinear physics too, i.e. that it reconstructs Eq. (7.26). We can once again start from Eq. (8.6):

$$C_a g_{ab} \mathcal{P}_{a \rightarrow aq}^d(z^{ab}) \frac{dk_{\perp}^{ab}}{k_{\perp}^{ab}} dz^{ab} \frac{d\phi}{2\pi} = C_a g_{ab} w_{ab} \frac{dE_q}{E_q} \frac{d^2 \Omega_q}{2\pi} (1 + \text{hard pieces}) \\ = C_a P_{ab} \frac{dE_q}{E_q} \frac{d^2 \Omega_q}{2\pi} (1 + \text{hard pieces}), \quad (7.39)$$

where the ‘hard pieces’ part depends on the splitting function:

$$\mathcal{P}_{a \rightarrow aq}^d = \mathcal{P}_{qq}^d : \quad \text{hard pieces} = (z^{ab})^2, \\ \mathcal{P}_{a \rightarrow aq}^d = \mathcal{P}_{gg}^d : \quad \text{hard pieces} = (z^{ab})^3. \quad (7.40)$$

Since the collinear limit requires θ_{iq} or $\theta_{jq} \ll \theta_{ij} \ll \theta_{ik}$, we can let $z^{ab} \approx z_a$ where $1 - z_a \approx E_q/E_a$ and where E_a is the energy of parton a before the emission is generated. Thus ‘hard pieces’ does not have any azimuthal dependence⁸ and so azimuthal averaging proceeds as before. We find that

$$|\mathcal{M}_2|^2 \frac{d^3 \vec{p}_q}{2E_q} \approx \frac{2\alpha_s}{\pi} \left(\left[P_{ij}^{[i]} dz_i \mathcal{P}_{qq} + P_{ji}^{[j]} dz_j \frac{C_A}{2} \mathcal{P}_{gg}^d(z_j) \right] \Theta(k_{\perp}^{ij} < k_{\perp}) \right. \\ \left. + \left[P_{jk}^{[j]} dz_j \frac{C_A}{2} \mathcal{P}_{gg}^d(1 - z_j) + P_{k(ij)}^{[k]} dz_k \mathcal{P}_{qq} \right] \Theta(k_{\perp}^{jk} < k_{\perp}) \right) |\mathcal{M}_1(\vec{p}_i, \vec{p}_j, \vec{p}_k)|^2. \quad (7.41)$$

Once again, the collinear limit results in $P_{ji}^{[j]} = P_{jk}^{[j]}$. The small-angle approximation for q saturates the ordering theta functions and so

$$|\mathcal{M}_2|^2 \frac{d^3 \vec{p}_q}{2E_q} \approx \frac{2\alpha_s}{\pi} \left(P_{ij}^{[i]} dz_i \mathcal{P}_{qq} + P_{ji}^{[j]} dz_j \mathcal{P}_{gg}(z_j) + P_{k(ij)}^{[k]} dz_k \mathcal{P}_{qq} \right) |\mathcal{M}_1(\vec{p}_i, \vec{p}_j, \vec{p}_k)|^2. \quad (7.42)$$

⁸‘hard pieces’ do contain azimuthal dependence if we include spin correlations. In [20], we discussed using the Collins and Knowles algorithm [26, 27] to re-introduce spin correlations by re-weighting after the shower has terminated.

This is equivalent to the fixed-order result of Eq. (7.26).

An important part of this section was to assume we can neglect recoil and that further emissions do not modify momenta in such a way that these correctly computed matrix elements are destroyed. As we showed explicitly in Section 3.1 of [1], our global recoil does not mess the computation of NLLs at this order. This is further discussed in Section 7.5.1.

7.4.2 $\mathcal{O}(\alpha_s^2)$ with emissions unordered in angle

In the previous section we validated our dipole shower's ability to reproduce rows 1 through 3 of Table 7.1. In this section we wish to test the shower's ability to reproduce the last row of Table 7.1 and the LC limit in Eq. (7.17), which is applicable across all the limits considered in the table and also when $\theta_{ij} \ll \theta_{ik}$. To start we will test our dipole shower in the limit that q is soft whilst $\theta_{ij} \ll \theta_{ik}$ but $\theta_{iq} \approx \theta_{jq} > \theta_{ij}$ (i.e. we will compare against row 4 in Table 7.1). We describe these emissions as unordered in angle since they are produced in the shower with angles out of order; the k_t and angle of these emissions are not concurrently ordered. However, these emissions can still have a strong angular hierarchy allowing them to produce a LL, i.e. $\theta_{ij} \ll \theta_{iq} \approx \theta_{jq} \ll \theta_{ik}$. The region of phase-space which has this hierarchy is highly restricted, due to the opposing k_t ordering, but is nevertheless present and its mistreatment can induce a (small) LL error in some observables, for instance thrust [21]. At the end of this section we will check the crucial soft, wide-angle limit, where parton q is soft but all angles are unconstrained.

We will begin from Eq. (7.37), which was derived from our shower by only assuming parton q is soft. Employing $\theta_{ij} \ll \theta_{ik}$ allows us to replace $P_{ki}^{[k]} \approx P_{kj}^{[k]} \approx P_{k(ij)}^{[k]}$, i.e.

$$|\mathcal{M}_2|^2 \frac{d^3 \vec{p}_q}{2E_q} \approx \frac{2\alpha_s}{\pi} \left[\left(C_F P_{ij}^{[i]} + \frac{C_A}{2} P_{ji}^{[j]} \right) \frac{dE_q}{E_q} \Theta(k_{\perp}^{ij} < k_{\perp}) + \left(\frac{C_A}{2} P_{jk}^{[j]} + C_F P_{k(ij)}^{[k]} \right) \frac{dE_q}{E_q} \Theta(k_{\perp}^{jk} < k_{\perp}) \right] |\mathcal{M}_1(\vec{p}_i, \vec{p}_j, \vec{p}_k)|^2. \quad (7.43)$$

Now we take the limit that $\theta_{iq}, \theta_{jq} \gg \theta_{ij}$, thus $P_{ij}^{[i]} = P_{ji}^{[j]} = 0$ and $P_{jk}^{[j]} \approx P_{(ij)k}^{[(ij)]}$ which gives rise to

$$|\mathcal{M}_2|^2 \frac{d^3 \vec{p}_q}{2E_q} \approx \frac{2\alpha_s}{\pi} \left(\frac{C_A}{2} P_{(ij)k}^{[(ij)]} + C_F P_{k(ij)}^{[k]} \right) \frac{dE_q}{E_q} \Theta(k_{\perp}^{(ij)k} < k_{\perp}) |\mathcal{M}_1(\vec{p}_i, \vec{p}_j, \vec{p}_k)|^2. \quad (7.44)$$

We should add to this the contribution where parton q is emitted first. Doing so gives

$$|\mathcal{M}_2|^2 \frac{d^3 \vec{p}_q}{2E_q} \approx \frac{2\alpha_s}{\pi} \left[\left(\frac{C_A}{2} \Theta(k_{\perp}^{(ij)k} < k_{\perp}) + C_F \Theta(k_{\perp}^{(ij)k} > k_{\perp}) \right) P_{(ij)k}^{[(ij)]} + C_F P_{k(ij)}^{[k]} \right] \frac{dE_q}{E_q} |\mathcal{M}_1(\vec{p}_i, \vec{p}_j, \vec{p}_k)|^2. \quad (7.45)$$

Comparing with row 4 of Table 7.1 we see an N_c^{-2} suppressed error in the colour factor of the $P_{(ij)k}^{[(ij)]}$ term. This error is due to the parton angles being disordered and is not present in an angular-ordered shower. However, in our dipole shower the disordered configuration is present and important, since it is required to get the correct wide-angle, soft physics beyond the two-jet limit.

Following the same logic as before, it is simple to show that our dipole shower includes the hard-collinear physics in Eq. (7.27) with the same N_c^{-2} suppressed error as in Eq. (7.45).

Finally, a good dipole shower should encode Eq. (7.17) and therein BMS evolution in the limit that the emission is soft. Starting from Eq. (7.36) and taking the leading colour limit:

$$|\mathcal{M}_2|^2 \frac{d^3 \vec{p}_q}{2E_q} \approx \frac{\alpha_s N_c}{\pi} \left[(P_{ij} + P_{ji}) \frac{dE_q}{E_q} \frac{d^2 \Omega_q}{4\pi} \Theta(k_{\perp}^{ij} < k_{\perp}) + (P_{jk} + P_{kj}) \frac{dE_q}{E_q} \frac{d^2 \Omega_q}{4\pi} \Theta(k_{\perp}^{jk} < k_{\perp}) \right] |\mathcal{M}_1(\vec{p}_i, \vec{p}_j, \vec{p}_k)|^2. \quad (7.46)$$

This is equal to

$$|\mathcal{M}_2|^2 \frac{d^3 \vec{p}_q}{2E_q} \approx \frac{\alpha_s N_c}{\pi} \left[w_{ij} \Theta(k_{\perp}^{ij} < k_{\perp}) + w_{jk} \Theta(k_{\perp}^{jk} < k_{\perp}) \right] \frac{dE_q}{E_q} \frac{d^2 \Omega_q}{4\pi} |\mathcal{M}_1(\vec{p}_i, \vec{p}_j, \vec{p}_k)|^2, \quad (7.47)$$

which is equal to Eq. (7.17), modulo the use of k_t instead of energy as the ordering variable, which does not hinder the logarithmic accuracy [28, 29]. Hence the dipole shower correctly handles wide-angle soft radiation in the LC approximation. To go beyond the LC approximation generally requires amplitude-level evolution [20, 25, 30–33].

7.4.3 Summary

In this section we have evaluated the accuracy at which our original dipole shower recreates the squared matrix elements summarised in Section 7.3. In summary, when parton q is emitted from parton i or k the matrix element is reproduced without error. When parton q is emitted from parton j there is an N_c^{-2} suppressed error. We can look at different limits of the phase-space for partons j and q and evaluate the colour accuracy of our shower in each limit as follows:

1. $\theta_{ij} \ll 1$:
 - (a) $\theta_{jq} \ll \theta_{ij}$: in this region an angular-ordered shower has full colour accuracy and our shower agrees with an angular-ordered shower (see rows 1 and 3 of Table 7.1).

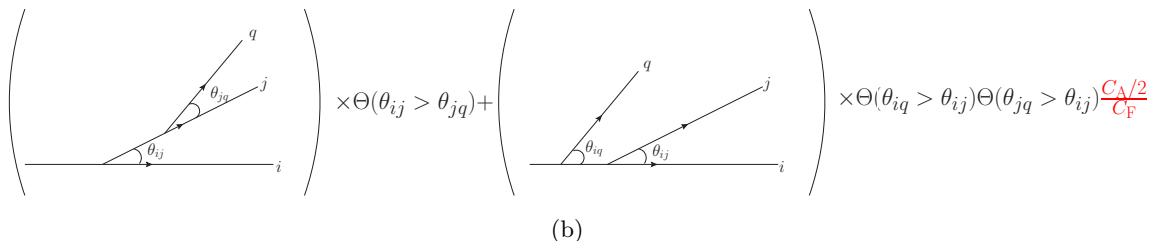
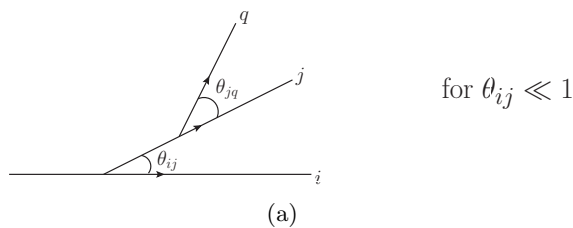


Figure 7.4: Diagram (a) is generated using our dipole shower, after partitioning. This topology is where the N_c^{-2} error emerges. Diagram (b) represents the re-arrangements of (a) that can be made in the limit $\theta_{ij} \ll 1$. These diagrams correspond to those of an angular-ordered shower. The red factor is the N_c^{-2} suppressed error produced by our original dipole shower.

- (b) $\theta_{jq} \sim \theta_{ij}$: in this region an angular-ordered shower cannot recreate the complete matrix element and our shower only guarantees LC accuracy in the soft limit. This region does not contain a strong angular hierarchy so at most can contribute a NLL and is suppressed further in event shape observables only sensitive to perturbations from the two-jet limit, for instance thrust.
- (c) $\theta_{jq} \approx \theta_{iq} \gg \theta_{ij}$: in this region an angular-ordered shower has full colour accuracy and our shower currently lacks complete agreement with an angular-ordered shower beyond LC (row 4 of Table 7.1). This is the region we will address in Section 7.5.

2. $\theta_{ij} \sim 1$: angular ordering cannot describe this region and our shower only guarantees LC accuracy.⁹

In Figure 7.4 we illustrate the origin of the N_c^{-2} suppressed error: the erroneous factor is shown in red. The diagram in this figure is sufficient to enable us to read off the correct colour factor, and we make heavy use of this perspective in what follows.

⁹In this limit (which is potentially subject to all manner of soft and non-global logarithms), it is difficult to make statements on the logarithmic accuracy of the shower beyond the leading accuracy of soft logarithms achievable through the BMS equation [34], which is embedded in the dipole shower approach. Though, with this in mind, Dasgupta et al. [15] have demonstrated LC NLL accuracy in non-global observables for dipole showers with carefully constructed global recoils and lab-frame based dipole partitionings. Our shower has both these properties and our fixed-order tests of the shower [1] are consistent with their results. Note that Dasgupta et al.'s definition of NLL accuracy encompasses NLL in the exponent but is also applicable to logs that do not resum into an exponential form such as non-global logs.

7.5 Colour factors for emissions unordered in angle

In the previous section we computed the double-emission matrix elements squared corresponding to $e^+e^- \rightarrow q\bar{q}gg$, comparing the result from our dipole shower formalism with the relevant limits of the exact matrix element. We showed that, when the two emissions are strongly ordered in angle (with one emission collinear in the direction of one of the hemispheres), the matrix elements calculated from our dipole shower were correct except when a gluon is emitted with an angle larger than the opening angle of its parent dipole. In such a configuration, the coherent branching calculation would correctly assign a colour factor C_F , whilst the dipole shower gives $C_A/2$ (see Eq. (7.45)). At this order, we can correct the colour factor by replacing C_i in Eq. (7.28) with a dynamic colour factor of

$$C_{ij}(\theta_{iq}, \theta_{ij}) = \left(C_F \delta_i^{(q)} + \frac{C_A}{2} \delta_i^{(g)} \right) \theta(\theta_{iq} < \theta_{ij}) + \left(\frac{C_A}{2} (\delta_i^{(q)} \delta_j^{(q)} + \delta_i^{(g)} \delta_j^{(g)}) + C_F (\delta_i^{(q)} \delta_j^{(g)} + \delta_i^{(g)} \delta_j^{(q)}) \right) \theta(\theta_{iq} > \theta_{ij}), \quad (7.48)$$

where $\delta_i^{(q)}$ ($\delta_i^{(g)}$) is one when the parton i is a quark (gluon), and zero otherwise. We stress that this correction leads to the correct result only because our way of partitioning is able to encode angular ordering via

$$\frac{(d \cos \theta_{aq}) d\phi_q^{(a)}}{4\pi} \int_0^{2\pi} \frac{d\phi_q^{(a)}}{2\pi} g_{ab} w_{ab} = P_{ab}^{[a]}, \quad (7.49)$$

which ensures that the error is localized in the colour factor of Eq. (7.45). Our partitioning satisfies this requirement exactly.¹⁰

It is not too difficult to generalize to higher orders, and the solution is particularly straightforward in the absence of $g \rightarrow q\bar{q}$ branchings, which will be discussed at the end of this section (see also [35]). Figures 7.5 and 7.6 illustrate errors that occur in the case of three emissions. They highlight a key feature: the colour factor of the last emission is incompatible with coherence only when it is emitted at an angle larger than the angular extent of the colour charge distribution of the chain of partons leading to the emission.

Figure 7.7 shows the generalisation to an arbitrary fixed order¹¹. As a consequence of using a partitioning which defines a unique branching history of $1 \rightarrow 2$ transitions, the collection of partons in an event can be divided into m branches for an m parton hard process. Each branch contains one of the hard-process partons and the radiation emitted from it. Each parton in the branch can also be assigned a unique sub-branch consisting of the parton and its “parental chain”, see Figure 7.8. We only need to modify colour

¹⁰In 7.9 we discuss tests for checking whether other partitionings are consistent with the requirement at NLL accuracy.

¹¹In 7.8 we show that the planar diagrams arising after azimuthal averaging do generalise to higher orders

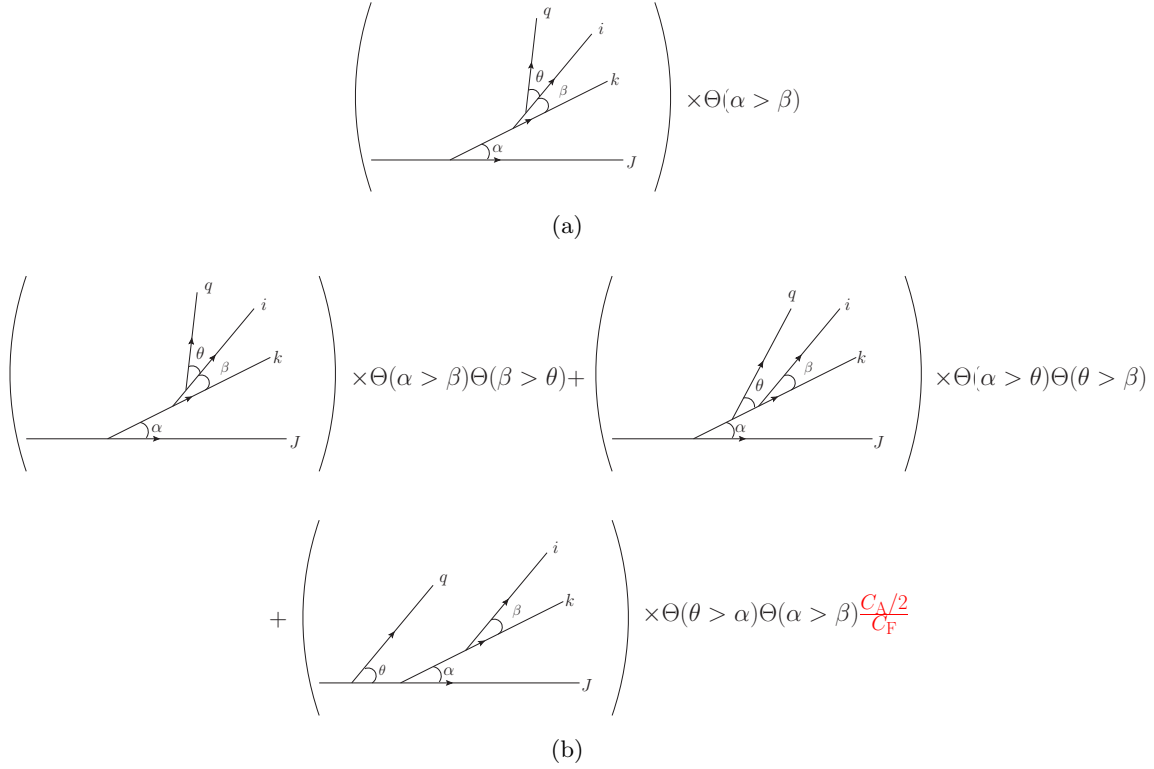


Figure 7.5: Diagram (a) is generated by our dipole shower and is chosen because it contains an incorrect colour factor. Diagram (b) represents the re-arrangements of (a) corresponding to an angular-ordered shower. The red colour factor is the N_c^{-2} suppressed error produced by our original dipole shower.

factors for gluons which cannot probe the largest angle in their sub-branch. We do this by extending the definition of \mathcal{C}_{ij} to

$$\mathcal{C}_{iJ}(\theta_{iq}, \theta_{LJ}) = \left(C_F \delta_i^{(q)} + \frac{C_A}{2} \delta_i^{(g)} \right) \theta(\theta_{iq} < \theta_{LJ}) + \left(\frac{C_A}{2} \delta_J^{(g)} + C_F \delta_J^{(q)} \right) \theta(\theta_{iq} > \theta_{LJ}), \quad (7.50)$$

where J is the hard parton in the sub-branch and L is the parton in the sub-branch emitted at the largest angle. θ_{LJ} is the angle between L and J .¹² One should use these newly defined dynamic colour factors in both emissions and in the Sudakov form factors, i.e. so that the two are related by unitarity.¹³ The computation of the dynamic colour factor grows at most linearly as the shower progresses and on average logarithmically.¹⁴

In summary we have constructed a dipole shower which encodes the physics of QCD coherence just as in an angular-ordered shower. The resulting dipole shower, at LC, reproduces BMS evolution and, after using the CMW running coupling [37], will match the

¹² $\theta_{LJ} = \pi$ for an emission with a sub-branch of length 2.

¹³All current dipole shower implementations [4, 6, 36] could directly employ our algorithm using existing methods such as the Sudakov veto algorithm.

¹⁴The average sub-branch length for a multiplicity, n , of partons in the branch is $\sum_{i=1}^n \frac{1}{i} \leq \ln n + 1$.

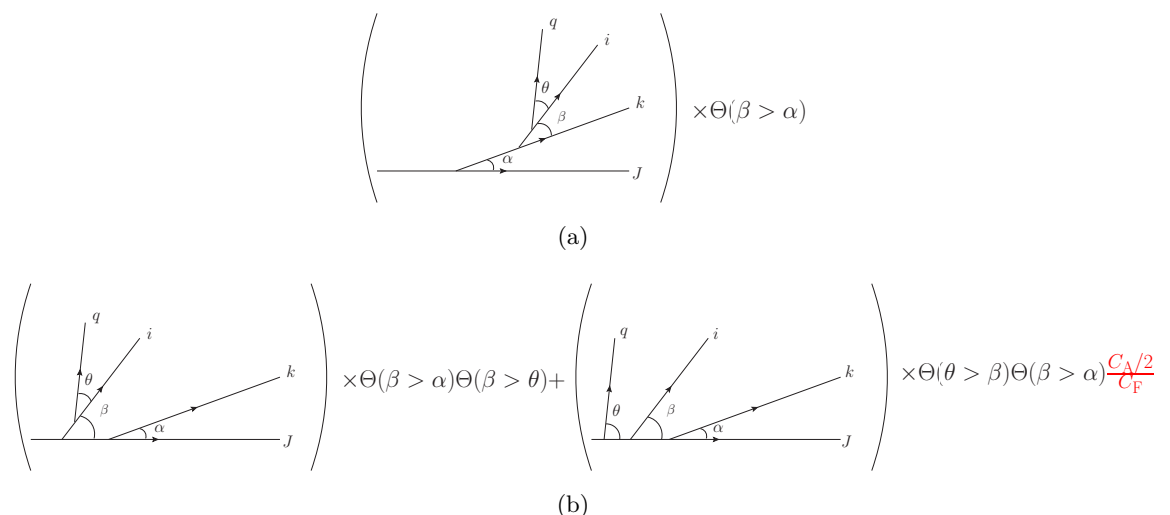


Figure 7.6: A second possible ordering of angles that also leads to an incorrect colour factor.

NLL-accurate dipole showers with global recoils discussed in [15]. In all, we expect our dipole shower to achieve full colour LL accuracy in any observable for which an angular-ordered shower can also be used to resum LLs. In the case of $e^+e^- \rightarrow q\bar{q}$, the NLLs of some observables (i.e. thrust) do not directly depend on $g \rightarrow q\bar{q}$ transitions¹⁵ in which case our shower is accurate to NLL at full colour. Our methodology of assigning colour factors by mapping branching histories onto those of an angular-ordered shower could be generalised to assign the correct colour factors after including $g \rightarrow q\bar{q}$ transitions.¹⁶ However, because these transitions introduce more quark lines into the parton cascade, there would be the need to correct incorrect factors of $2C_F$. This would worsen the computational efficiency. Whether the decreased efficiency is mitigated by the relative infrequency of $g \rightarrow q\bar{q}$ transitions in a typical shower is beyond the scope of this paper.

7.5.1 The effects of momentum conservation

In the paper so far we only briefly mentioned momentum conservation, which is vital for any implementation in an event generator, and needs to be treated very carefully. Bad implementations of momentum conservation have the potential to modify the phase-space boundaries of partons in the cascade or the matrix elements, leading to NLL errors [21]. In a dipole shower, emissions are on-shell and their momentum is typically expressed using three components: momentum longitudinal to the emitter, momentum transverse to the

¹⁵Such transitions are restricted to secondary branchings, the remnants of which can be resummed into the CMW coupling and are otherwise rendered trivial by the angular-ordering constraint [2].

¹⁶Furthermore, our arguments also generalise to a hard process with more than two coloured, hard legs provided each of the dipoles found in the colour flow for the hard process is evolved in its back-to-back frame as is done in an angular ordered shower [38]. See Appendix A of [1] for a more complete discussion on generalising our shower beyond $e^+e^- \rightarrow q\bar{q}$.

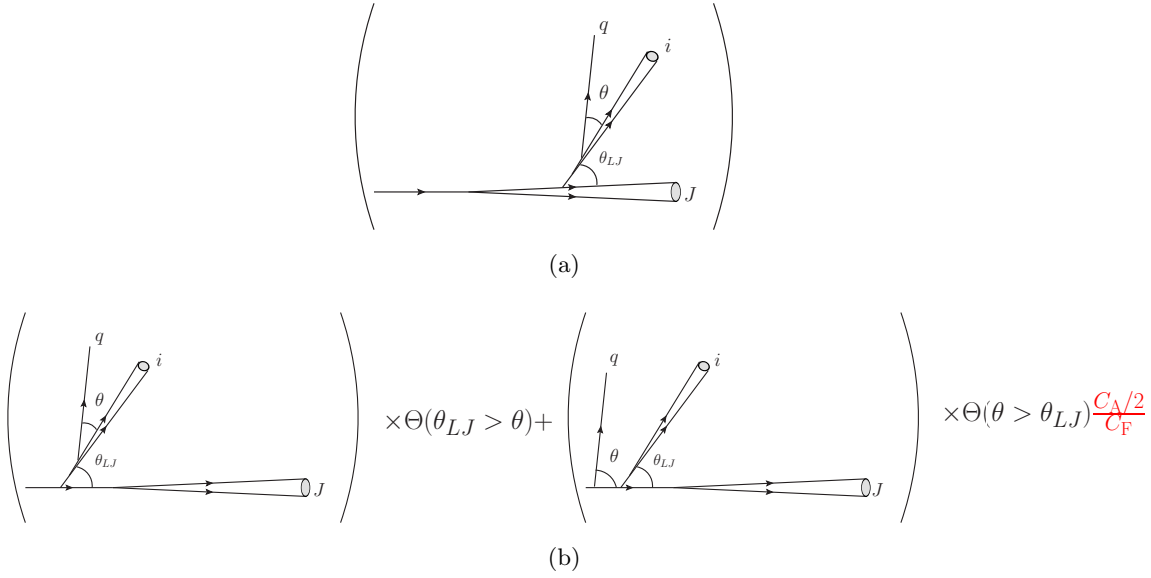


Figure 7.7: The generalisation of Figures 7.5 and 7.6 to an arbitrary fixed order. Cones i and J represent a unspecified number of parton branchings, each at angles smaller than θ_{LJ} , which is the largest angle in q 's sub-branch. As before, diagram (a) is generated by our dipole shower and contains an incorrect colour factor associated with the emission of q . Diagram (b) represents the re-arrangements of (a) corresponding to an angular-ordered shower. The red colour factor is the N_c^{-2} suppressed error produced by our original dipole shower.

emitting dipole and momentum in the ‘backwards’ direction (collinear to the other parton in the dipole). A momentum map is used after an emission to ensure energy-momentum conservation in the shower by distributing ‘recoil’ across the partons in an event whilst keeping the partons are on-shell.

In [1] we presented a momentum map with the idea of being as simple as possible whilst preserving the matrix elements computed by the shower. In the map, longitudinal recoil is trivially handled correctly (it is conserved between the emission and the parent parton as dictated by the dipole partitioning) and does not spoil anything. The other components are handled by a Lorentz boost and a global re-scaling of every momentum in the event after the emission. The emission kernels are invariant under both of these (as both z^{ab} and $dk_{\perp}^{ab}/k_{\perp}^{ab}$ are invariant under boosts and re-scalings). Thus only the phase-space is modified by the momentum map, not matrix elements. In Section 3.1 of [20] we showed that the changes to the phase-space due to recoil will generally not produce a log-enhanced term at $\mathcal{O}(\alpha_s^2)$ and that, for global two-jet observables such as thrust, artifacts in the phase-space from the recoil after iterated emissions produce terms beyond NLL. Alternative global momentum maps with similar constructions have also been studied in [15] where the NLL accuracy of the maps was demonstrated for a wide range of observables. The momentum maps in [15]

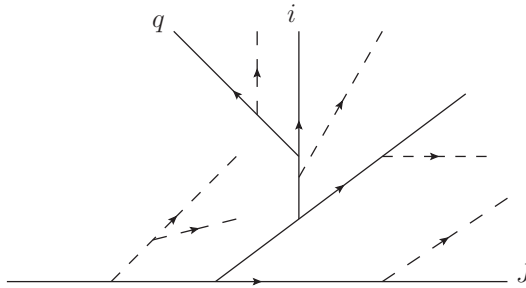


Figure 7.8: An illustration of a branch containing hard parton J . The sub-branch for parton q contains the partons with solid lines, these form parton q 's 'parental chain'. Partons with dashed lines are in J 's branch but are not in q 's sub-branch. The sub-branch length is the number of partons in a sub-branch: parton q 's sub-branch has a length 4 whilst parton i 's sub-branch has a length 3.

were designed so that their action preserved key features of the Lund plane [39, 40] (for instance preserving the separation between emissions on the plane). They have the added benefit of conserving 'backwards' components of momentum locally in a dipole, minimising the affect of the map on the phase-space available to partons in the shower. Any of these global prescriptions could be implemented into our shower without effecting the results in this paper.

7.6 Errors in other dipole showers

In this section we want to emphasize the role of the dipole partitioning to our findings. To eliminate sub-leading colour errors, the partitioning function g_{ab} must satisfy

$$\frac{(d \cos \theta_{aq}) d\phi_q^{(a)}}{4\pi} \int_0^{2\pi} \frac{d\phi_q^{(a)}}{2\pi} g_{ab} w_{ab} = P_{ab}^{[a]} + \text{negligible}. \quad (7.51)$$

In 7.9 we discuss the term labelled 'negligible'; the remainder after azimuthal averaging when compared to the strict angular ordering result. Our dipole algorithm was carefully constructed to not produce such a contribution at all. Note that the demand of $P_{ab}^{[a]}$ being proportional to a theta function cannot be satisfied with a zero remainder if g_{ab} is positive definite and only zero at a finite number of points in the phase-space. On top of this, since $P_{ab}^{[a]}$ has no dependence on the energies of the partons in the dipole, any partitioning that retains such a dependence after azimuthal averaging will result in a non-zero contribution remainder.

An interesting example to illustrate how wrong results can be obtained is that of Catani-Seymour (CS) dipole factorisation. The errors due to using a CS factorisation to construct the dipole partitioning have been previously noted in [21]. Here we give a complementary

discussion. The CS partitioning contains both the issues described in the previous paragraph; the partitioning function is positive definite and has strong dependence on parton energies after azimuthal averaging. The partitioning that generates Catani-Seymour dipole factorisation is

$$g_{ab} = \frac{(k_{\perp}^{ab})^2 p_a \cdot p_b}{2p_a \cdot p_q (p_a + p_b) \cdot p_q} \equiv \frac{e^{2\eta}}{1 + e^{2\eta}}, \quad (7.52)$$

where η is the dipole-frame rapidity of parton q ($\eta \rightarrow \infty$ as $p_q/E_q \rightarrow p_a/E_a$ and $\eta \rightarrow -\infty$ as $p_q/E_q \rightarrow p_b/E_b$). We must compute

$$\int_0^{2\pi} \frac{d\phi_q^{(a)}}{2\pi} g_{ab} w_{ab} = \int_0^{2\pi} \frac{d\phi_q^{(a)}}{2\pi} \frac{E_q^2 p_a \cdot p_b}{p_a \cdot p_q (p_a + p_b) \cdot p_q}. \quad (7.53)$$

Using the basis

$$\begin{aligned} p_a &= E_a(1, 0, 0, 1), \\ p_b &= E_b(1, \sin \theta_{ab}, 0, \cos \theta_{ab}), \\ p_q &= E_q(1, \sin \theta_{aq} \cos \phi_q^{(a)}, \sin \theta_{aq} \sin \phi_q^{(a)}, \cos \theta_{aq}) \end{aligned}$$

gives

$$\int_0^{2\pi} \frac{d\phi_q^{(a)}}{2\pi} g_{ab} w_{ab} = \int_0^{2\pi} \frac{d\phi_q^{(a)}}{2\pi} \frac{(1 - \cos \theta_{ab})}{(1 - \cos \theta_{aq}) (D - \sin \theta_{ab} \sin \theta_{aq} \sin \phi_q^{(a)})}, \quad (7.54)$$

where

$$E_b D = E_a + E_b - E_a \cos \theta_{aq} - E_b \cos \theta_{ab} \cos \theta_{aq}.$$

Note $D > \sin \theta_{ab} \sin \theta_{aq}$ for all momentum configurations. It is therefore easily shown that

$$\int_0^{2\pi} \frac{d\phi_q^{(a)}}{2\pi} g_{ab} w_{ab} = \frac{(1 - \cos \theta_{ab})}{(1 - \cos \theta_{aq}) \sqrt{D^2 - \sin^2 \theta_{ab} \sin^2 \theta_{aq}}}. \quad (7.55)$$

For all momentum configurations other than $\theta_{ab} = \pi$ and $E_b = E_a$ this results in

$$W_{ab}^{[a]} = \frac{(d \cos \theta_{aq}) d\phi_q^{(a)}}{4\pi} \int_0^{2\pi} \frac{d\phi_q^{(a)}}{2\pi} g_{ab} w_{ab} \not\approx P_{ab}^{[a]}. \quad (7.56)$$

Using this azimuthal averaging of the Catani-Seymour partitioning we can compute the azimuthally-averaged squared matrix element in the limit that emissions are strongly ordered in angle and energy:

$$\begin{aligned} |\mathcal{M}_2|^2 \frac{d^3 \vec{p}_q}{2E_q} &\approx \frac{2\alpha_s}{\pi} \left[\left(C_F W_{ij}^{[i]} + \frac{C_A}{2} W_{ji}^{[j]} \right) \frac{dE_q}{E_q} \Theta(k_{\perp}^{ij} < k_{\perp}) \right. \\ &\quad \left. + \left(\frac{C_A}{2} W_{jk}^{[j]} + C_F W_{kj}^{[k]} \right) \frac{dE_q}{E_q} \Theta(k_{\perp}^{jk} < k_{\perp}) \right] |\mathcal{M}_1(\vec{p}_i, \vec{p}_j, \vec{p}_k)|^2. \end{aligned} \quad (7.57)$$

As $k_{\perp}^{ab} \approx k_{\perp}^{ca} \approx E_q \theta_{aq}$ in this limit and since energies are strongly ordered, the k_t ordering theta functions are saturated and we find:

$$|\mathcal{M}_2|^2 \frac{d^3 \vec{p}_q}{2E_q} \approx \frac{2\alpha_s}{\pi} \left[C_F W_{ij}^{[i]} + \frac{C_A}{2} \left(W_{ji}^{[j]} + W_{jk}^{[j]} \right) + C_F W_{kj}^{[k]} \right] \frac{dE_q}{E_q} |\mathcal{M}_1(\vec{p}_i, \vec{p}_j, \vec{p}_k)|^2. \quad (7.58)$$

We can subtract this from the correct result (for rows 1 through 3 of Table 7.1) to find the error:

$$\begin{aligned} \delta |\mathcal{M}_2|^2 \frac{d^3 \vec{p}_q}{2E_q} &\approx \\ \frac{2\alpha_s C_F}{\pi} \left[(P_{ij}^{[i]} - W_{ij}^{[i]} + P_{kj}^{[k]} - W_{kj}^{[k]}) + \frac{C_A}{2C_F} \left(2P_{ji}^{[j]} - W_{ji}^{[j]} - W_{jk}^{[j]} \right) \right] \frac{dE_q}{E_q} |\mathcal{M}_1(\vec{p}_i, \vec{p}_j, \vec{p}_k)|^2 &\neq 0. \end{aligned} \quad (7.59)$$

Of course the error vanishes if $C_F = C_A/2$. The error becomes large when $E_j \ll E_i \approx E_k$. In this limit

$$W_{jb}^{[j]} \approx \frac{(d \cos \theta_{jq}) d\phi_q^{(j)}}{4\pi} \frac{(1 - \cos \theta_{jb})}{(1 - \cos \theta_{jq}) |\cos \theta_{jb} - \cos \theta_{jq}|}, \quad (7.60)$$

when $\theta_{ij} \neq \theta_{jq}$ and $\theta_{jk} \neq \theta_{jq}$ ¹⁷, and where $b = i, k$. Also in this limit

$$W_{bj}^{[b]} \approx \frac{(d \cos \theta_{iq}) d\phi_q^{(i)}}{4\pi} \frac{E_b(1 - \cos \theta_{bj})}{E_a(1 - \cos \theta_{bq})^2}, \quad (7.61)$$

once again this is only valid when $\theta_{ij} \neq \theta_{jq}$ and $\theta_{jk} \neq \theta_{jq}$ (equivalently $\theta_{iq} \neq 0$ and $\theta_{kq} \neq 0$). Thus

$$\begin{aligned} \delta |\mathcal{M}_2|^2 \frac{d^3 \vec{p}_q}{2E_q} &\approx \frac{2\alpha_s C_F}{\pi} \left[\frac{(d \cos \theta_{iq}) d\phi_q^{(i)}}{4\pi} \left(\frac{\Theta(\theta_{iq} < \theta_{ij})}{1 - \cos \theta_{iq}} - \frac{E_b(1 - \cos \theta_{ij})}{E_a(1 - \cos \theta_{iq})^2} \right) + (i \leftrightarrow k) \right] \\ &+ \frac{C_A}{2C_F} \left(2 \frac{\Theta(\theta_{jq} < \theta_{ij})}{1 - \cos \theta_{jq}} - \frac{(1 - \cos \theta_{ij})}{(1 - \cos \theta_{jq}) |\cos \theta_{ij} - \cos \theta_{jq}|} - \frac{(1 - \cos \theta_{jk})}{(1 - \cos \theta_{jq}) |\cos \theta_{jk} - \cos \theta_{jq}|} \right) \\ &\times \frac{(d \cos \theta_{jq}) d\phi_q^{(j)}}{4\pi} \frac{dE_q}{E_q} |\mathcal{M}_1(\vec{p}_i, \vec{p}_j, \vec{p}_k)|^2. \end{aligned} \quad (7.62)$$

Note that the C_A/C_F piece contains a non-cancelling collinear pole when $\theta_{jq} \rightarrow 0$ and so is capable of generating logarithms in observables that probe secondary emissions even in the limit of a strong angular hierarchy, where $\theta_{jq} \ll \theta_{ij} \ll \theta_{(ij)k}$, since the numerator of $W_{ji}^{[j]}$ goes as $\mathcal{O}(\theta_{ij}^2)$ whilst the numerator of $P_{ji}^{[j]}$ goes as $\mathcal{O}(1)$. Also note that this error cannot be fixed by using the dynamic colour factors $\mathcal{C}_{iJ}(\theta_{iq}, \theta_{LJ})$ since in the limit we are considering the dynamic colour factors reduce exactly to the usual colour factors already present in Eq. (7.62).

¹⁷In the region where $\theta_{ij} \neq \theta_{jq}$ terms in E_j/E_i are not negligible as they screen the divergence $\theta_{ij} = \theta_{jq}$.

We can also compare the error made using a CS-partitioned dipole shower with row 4 from Table 7.1. Here we find

$$\delta|\mathcal{M}_2|^2 \frac{d^3\vec{p}_q}{2E_q} = \frac{2\alpha_s C_F}{\pi} \left[(P_{(ij)k}^{[(ij)]} - W_{ij}^{[i]} + P_{k(ij)}^{[k]} - W_{k(ij)}^{[k]}) - \frac{C_A}{2C_F} (W_{ji}^{[j]} + W_{jk}^{[j]}) \right] \frac{dE_q}{E_q} |\mathcal{M}_1(\vec{p}_i, \vec{p}_j, \vec{p}_k)|^2 \neq 0. \quad (7.63)$$

This error is potentially LL, since with a strong hierarchy in emission energies and angles the functions W are singular and so capable of generating double logarithms. Of course this too vanishes if $C_F = C_A/2$. If the dipole shower instead used colour factors $\mathcal{C}_{iJ}(\theta_{iq}, \theta_{LJ})$ this limit would be improved since the error would instead become

$$\delta|\mathcal{M}_2|^2 \frac{d^3\vec{p}_q}{2E_q} = \frac{2\alpha_s C_F}{\pi} \left[(P_{(ij)k}^{[(ij)]} - W_{ij}^{[i]} + P_{k(ij)}^{[k]} - W_{k(ij)}^{[k]}) + \Theta(\theta_{jq} > \theta_{LJ})(W_{ji}^{[j]} + W_{jk}^{[j]}) - \frac{C_A \Theta(\theta_{jq} < \theta_{LJ})}{2C_F} (W_{ji}^{[j]} + W_{jk}^{[j]}) \right] \frac{dE_q}{E_q} |\mathcal{M}_1(\vec{p}_i, \vec{p}_j, \vec{p}_k)|^2 \approx 0. \quad (7.64)$$

However, this improvement may not extend to higher orders since θ_{LJ} as computed with the CS dipole shower branching history will not necessarily equal θ_{LJ} as computed from a branching history matched to the angular-ordered description. This problem, combined with Eq. (7.59), is sufficient for us to assert that CS dipole showers employing the dynamic colour factors $\mathcal{C}_{iJ}(\theta_{iq}, \theta_{LJ})$ will still be subject to LL errors in some observables that angular-ordering can completely describe at LL.

7.7 Conclusions

We have performed a fixed-order cross-check of the dipole shower presented in [1] and shown that the shower performs as it was designed to: the shower inherits its handling of collinear radiation from an angular-ordered shower whilst improving over angular ordering in the case of the leading colour, wide-angle soft radiation. We also highlight a limitation of our original approach, showing how the dipole shower will not assign correct colour factors to emissions disordered in angle, though they will be correct at leading colour. We then introduced a new method for correcting these colour factors. The new method is efficient: the computation time on average grows logarithmically with parton multiplicity. Using this method, our shower will match the LL accuracy of an angular-ordered shower in cases where an angular-ordered shower has LL accuracy. When enhanced with the CMW running coupling [37], our shower will include all leading logarithms and leading-colour, next-to-leading logarithms in the two-jet limit for continuously-global observables. As it stands, the shower will not be capable of the full-colour NLL resummation of global observables, due to the absence of full

colour $g \rightarrow q\bar{q}$ transitions. These transitions could be included as described in [1] but would generate sub-leading colour NLL errors: however, they could be included at full colour by extending the methods outlined in Section 7.5.

7.8 Appendix: Drawing planar diagrams at arbitrary order

In this appendix we demonstrate that the planar diagrams representing re-arrangements of our dipole shower into an angular ordered shower, in Figure 7.4, are not just a feature of our dipole shower at $\mathcal{O}(\alpha_s^2)$ but rather can continue to be used at higher orders if we continue to assume that the branching history produced by our shower has a strong hierarchy in angles. We do not assume a hierarchy in angles that is concurrently ordered with their k_t . At a scale k_\perp , a given n -parton state produced by our dipole shower has a weight at a point in the n -parton phase-space $d\mathcal{S}_n(k_\perp)$. We consider dressing this state with one further gluon, q , produced by the shower. This gives an $(n+1)$ -parton state:

$$d\mathcal{S}_{n+1}(k_\perp) \frac{d^3\vec{p}_q}{2E_q} = \frac{\alpha_s}{\pi} \sum_{a,b \text{ c.c.}} \left(\mathcal{C}_{aJ}(\theta_{aq}, \theta_{LJ}) g_{ab} \mathcal{P}_{a \rightarrow aq}^d(z^{ab}) dz^{ab} + (a \leftrightarrow b) \right) \frac{d \ln k_\perp^{ab} d\phi}{2\pi} \delta(k_\perp^{ab} - k_\perp) d\mathcal{S}_n(k_\perp), \quad (7.65)$$

where c.c. means a and b are colour connected in the n -parton state and J is the hard parton that initiated a 's branch. All other symbols have the same definitions as in the previous sections. We can azimuthally average exactly as in Section 7.4, and find

$$d\mathcal{S}_{n+1}(k_\perp) \frac{d^3\vec{p}_q}{2E_q} = \frac{\alpha_s}{\pi} \sum_{a,b \text{ c.c.}} \left(\mathcal{C}_{aJ}(\theta_{aq}, \theta_{LJ}) P_{ab}^{[a]} \mathcal{P}_{a \rightarrow aq}^d(z^{ab}) dz^{ab} + (a \leftrightarrow b) \right) \delta(k_\perp^{ab} - k_\perp) d\mathcal{S}_n(k_\perp). \quad (7.66)$$

Just as we have already demonstrated at $\mathcal{O}(\alpha_s^2)$, the weight assigned to the $(n+1)$ -state after azimuthal averaging uses the same LC emission kernels as an angular-ordered approach. We can make this very explicit by exchanging the sum over colour lines with a sum over parton indices. To illustrate this, at LC we find

$$d\mathcal{S}_{n+1}(k_\perp) \frac{d^3\vec{p}_q}{2E_q} = \frac{\alpha_s}{\pi} \sum_a \left(\frac{C_A}{2} P_{ab}^{[a]} \mathcal{P}_{a \rightarrow aq}^d(z^{ab}) dz^{ab} \delta(k_\perp^{ab} - k_\perp) + \delta_a^{(g)} \frac{C_A}{2} P_{ac}^{[a]} \mathcal{P}_{a \rightarrow aq}^d(z^{ac}) dz^{ac} \delta(k_\perp^{ac} - k_\perp) \right) d\mathcal{S}_n(k_\perp). \quad (7.67)$$

We can exchange the non-singular dependence on b and c in Eqs. (7.66) and (7.67) with that of J (or the other hard parton J' if either b or c are in the opposing hemisphere). Similarly,

for the non-singular region $\theta_{aq} \gg \theta_{aJ}$ we can exchange the dependence on a with J so that $\theta_{aq} \approx \theta_{Jq}$. Thus, just as in an angular-ordered framework, emissions are generated with a weight

$$C P_{aJ}^{[a]} \mathcal{P}_{a \rightarrow aq}^d(z^{aJ})$$

when they can probe the jet and

$$C P_{JJ'}^{[J]} \mathcal{P}_{J \rightarrow Jq}^d(z^{JJ'})$$

when they cannot. At LC, $C = C_A/2$ when a is a quark and, when a is a gluon, $C = C_A$ if q can probe the jet (determined by the angular ordering constraint embedded in $P_{aJ}^{[a]}$ ¹⁸) and $C = C_A/2$ when q cannot. It is these properties that our planar diagrams are defined to encapsulate, validating their usage at arbitrary higher orders. The planar diagrams led us to define $\mathcal{C}_{aJ}(\theta_{aq}, \theta_{LJ})$ so that the sub-leading N_c terms are included in accordance with Figure 7.7.

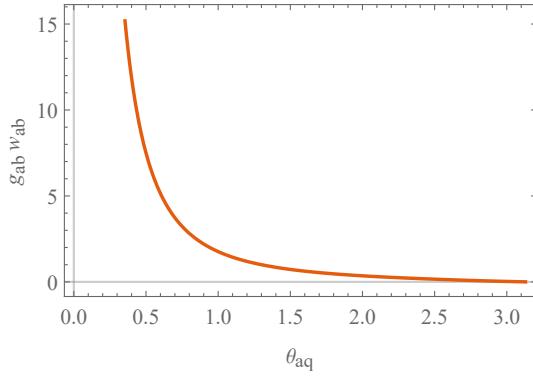
7.9 Appendix: Current limitations of our dipole shower

An important part of our dipole shower is its partitioning. However, the form of our partitioning, g_{ab} (defined through Eqs. (7.33) and (7.35)), might cause complications in a computational implementation of our shower. In this appendix we will discuss the issues and possible solutions.

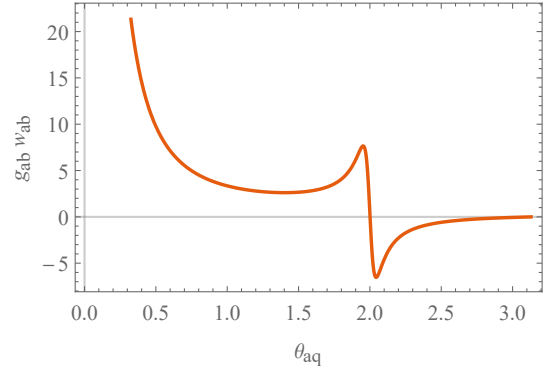
A dipole shower is fully differential in the parton phase-space and so emits by sampling from the distribution $g_{ab}w_{ab}$ to populate a 3-dimensional phase-space for each parton.¹⁹ However, $g_{ab}w_{ab}$ has two undesirable properties (illustrated in Figure 7.9): firstly $g_{ab}w_{ab}$ is negative in some portions of the emission phase-space, introducing negative weights into the shower; secondly $g_{ab}w_{ab}$ contains an integrable singularity when $\theta_{aq} = \theta_{ab} < \pi$ and $\phi_q^{(a)} = 0$ (i.e. q is in the plane of partons a and b). Both of these features can be handled in a modern dipole shower: the Herwig dipole shower already contains all the necessary machinery [6], as do others [41]. However, both features will hinder numerical convergence. Fortunately the two features counter balance each other: $g_{ab}w_{ab}$ is most negative when $\theta_{aq} = (1 + \varepsilon)\theta_{ab}$, for $\varepsilon \ll 1$ whilst strictly positive, and $\phi_q^{(a)} = 0$. The negative weights and integrable singularity are linked such that, when $\theta_{aq} = \theta_{ab}$, $g_{ab}w_{ab}$ azimuthally averages to

¹⁸This constraint is saturated by using an angular ordering variable in an angular-ordered shower and so would typically be omitted if one were to write Eq. (7.66) specifically for such a shower.

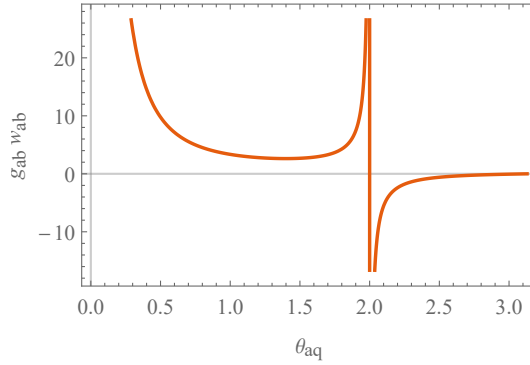
¹⁹Including hard-collinear physics, the shower samples from $g_{ab}\mathcal{P}_{ab}^d$ where \mathcal{P}_{ab}^d is a dipole splitting function but this does not effect our discussion here.



(a) $\theta_{ab} = 2$ and $\phi_q^{(a)} = 2$, i.e. q is out of the plane of the dipole (a, b) . The choice of $\phi_q^{(a)} = 2$ is indicative of the majority of the emission phase-space for which $\phi_q^{(a)} \not\approx 0$.



(b) $\theta_{ab} = 2$ and $\phi_q^{(a)} = 0.05$, i.e. q is only slightly out of the plane of the dipole (a, b) . Negative weights are starting to emerge, as are the peaks that become an integrable divergence for $\phi_q^{(a)} = 0$.



(c) $\theta_{ab} = 2$ and $\phi_q^{(a)} = 0$, i.e. q is in the plane of the dipole (a, b) . For $\theta_{aq} < \theta_{ab}$, q is 'inside' the dipole. The negative weights and integrable divergence are present when $\theta_{aq} = \theta_{ab}$.

Figure 7.9: Graphs of $g_{ab}w_{ab}$ as a function of $\theta_{ab}, \theta_{aq}, \phi_q^{(a)}$ as measured in the lab frame.

a well behaved quantity,

$$\int_0^{2\pi} \frac{d\phi_q^{(a)}}{2\pi} g_{ab}w_{ab} \Big|_{\theta_{aq}=\theta_{ab}} = \frac{1}{2(1 - \cos \theta_{aq})}. \quad (7.68)$$

A simple solution to the two issues would be, in regions bounded by $\theta_{aq} = \theta_{ab} \pm \delta\theta$ (for $\delta\theta/\theta_{ab} \ll 1$), to sample emissions according to the azimuthally averaged distribution, Eq. (7.68). This would entail sampling emissions from a discontinuous distribution but would alleviate the undesirable features whilst only introducing a power correction in $\delta\theta$ to azimuthal correlations in the shower.

Alternatively, one might use an alternative partitioning, \tilde{g}_{ab} , free from negative weights

and integrable singularities, that satisfies

$$\frac{(d \cos \theta_{aq}) d\phi_q^{(a)}}{4\pi} \int_0^{2\pi} \frac{d\phi_q^{(a)}}{2\pi} \tilde{g}_{ab} w_{ab} \approx P_{ab}^{[a]}. \quad (7.69)$$

This \tilde{g}_{ab} would be suitable for use with our proposed dynamic colour factors and retain our shower’s accuracy concerning LC NLL physics. It is possible that a pre-existing partitioning employed by another parton shower might already achieve this. We have demonstrated that the Catani-Seymour partitioning [22] does not satisfy this requirement but there are others on the market that we have not tested [15, 41–43]. An acceptable partitioning should at least satisfy

$$\frac{(d \cos \theta_{aq}) d\phi_q^{(a)}}{4\pi} \int_0^{2\pi} \frac{d\phi_q^{(a)}}{2\pi} (g_{ab} - \tilde{g}_{ab}) w_{ab} = \frac{(d \cos \theta_{aq}) d\phi_q^{(a)}}{4\pi(1 - \cos \theta_{aq})} \Theta(\theta_{aq} < \theta_{ab}) f(E_q/E_a, \theta_{aq}, \theta_{ab}; \dots), \quad (7.70)$$

where the ellipses denote all other kinematic quantities on which f depends but q ’s emission kernel otherwise does not, and where

$$\left[\int_{\tau Q}^Q \ln^n \frac{E_a}{Q} \frac{dE_a}{E_a} \int_{E_a}^Q \frac{dE_q}{E_q} + \int_{\tau Q}^Q \frac{dE_q}{E_q} \int_{E_q}^Q \ln^{2n-2} \frac{E_a}{Q} \frac{dE_a}{E_a} \right] \times \int_{\tau}^1 \frac{d\theta_{aq}}{\theta_{aq}} f(E_q/E_a, \theta_{aq}, \theta_{ab}; \dots) \Theta(\nu_q < \nu_a) = \mathcal{O}(\ln^{n+1} \tau), \quad (7.71)$$

$$\left[\int_{\tau}^1 \ln^n \theta_{ab} \frac{d\theta_{ab}}{\theta_{ab}} \int_{\theta_{ab}}^1 \frac{d\theta_{aq}}{\theta_q} + \int_{\tau}^1 \frac{d\theta_q}{\theta_{aq}} \int_{\theta_{aq}}^1 \ln^{2n-2} \theta_{ab} \frac{d\theta_{ab}}{\theta_{ab}} \right] \times \int_{\tau Q}^Q \frac{dE_q}{E_q} f(E_q/E_a, \theta_{aq}, \theta_{ab}; \dots) \Theta(\nu_q < \nu_a) = \mathcal{O}(\ln^{n+1} \tau), \quad (7.72)$$

where $\nu_{q,a}$ is the shower ordering variable. These ensure that f at most contributes logarithms of the form $\alpha_s^n L^{2n-2}$ to the expansion of an observable. In most two-jet event shape observables, towers of $\alpha_s^n L^{2n-2}$ logarithms which first appear for $n = 1$ are NNLLs in the resummed observable. If one were to perform these tests using the Catani-Seymour partitioning, each of Eqs. (7.71) and (7.72) evaluates to $\mathcal{O}(\ln^{n+3} \tau)$; a LL error (the calculation of which follows almost exactly the same structure as the thrust calculation in [21]).

References

- [1] J. R. Forshaw, J. Holguin, S. Plätzer, “Building a consistent parton shower”, *JHEP* **2020**, 09, 014, arXiv: [2003.06400](https://arxiv.org/abs/2003.06400) [[hep-ph](https://arxiv.org/abs/2003.06400)].
- [2] S. Catani, L. Trentadue, G. Turnock, B. Webber, “Resummation of large logarithms in e^+e^- event shape distributions”, *Nucl. Phys.* **1993**, *B407*, 3.

- [3] A. Banfi, G. P. Salam, G. Zanderighi, “Principles of general final-state resummation and automated implementation”, *JHEP* **2005**, *03*, 073, arXiv: [hep-ph/0407286 \[hep-ph\]](#).
- [4] T. Sjöstrand, S. Ask, J. R. Christiansen, R. Corke, N. Desai, P. Ilten, S. Mrenna, S. Prestel, C. O. Rasmussen, P. Z. Skands, “An Introduction to PYTHIA 8.2”, *Comput. Phys. Commun.* **2015**, *191*, 159–177, arXiv: [1410.3012 \[hep-ph\]](#).
- [5] T. Gleisberg, S. Hoeche, F. Krauss, M. Schonherr, S. Schumann, F. Siegert, J. Winter, “Event generation with SHERPA 1.1”, *JHEP* **2009**, *02*, 007, arXiv: [0811.4622 \[hep-ph\]](#).
- [6] S. Plätzer, S. Gieseke, “Dipole Showers and Automated NLO Matching in Herwig++”, *Eur. Phys. J.* **2012**, *C72*, 2187, arXiv: [1109.6256 \[hep-ph\]](#).
- [7] S. Höche, S. Prestel, “Triple collinear emissions in parton showers”, *Phys. Rev. D* **2017**, *96*, 074017, arXiv: [1705.00742 \[hep-ph\]](#).
- [8] S. Höche, F. Krauss, S. Prestel, “Implementing NLO DGLAP evolution in Parton Showers”, *JHEP* **2017**, *10*, 093, arXiv: [1705.00982 \[hep-ph\]](#).
- [9] B. Cabouat, T. Sjöstrand, “Some Dipole Shower Studies”, *Eur. Phys. J. C* **2018**, *78*, 226, arXiv: [1710.00391 \[hep-ph\]](#).
- [10] F. Dulat, S. Höche, S. Prestel, “Leading-Color Fully Differential Two-Loop Soft Corrections to QCD Dipole Showers”, *Phys. Rev. D* **2018**, *98*, 074013, arXiv: [1805.03757 \[hep-ph\]](#).
- [11] T. Sjöstrand, “The PYTHIA Event Generator: Past, Present and Future”, *Comput. Phys. Commun.* **2020**, *246*, 106910, arXiv: [1907.09874 \[hep-ph\]](#).
- [12] B. Cabouat, J. R. Gaunt, K. Ostrolenk, “A Monte-Carlo Simulation of Double Parton Scattering”, *JHEP* **2019**, *11*, 061, arXiv: [1906.04669 \[hep-ph\]](#).
- [13] B. Cabouat, J. R. Gaunt, “Combining single and double parton scatterings in a parton shower”, *JHEP* **2020**, *10*, 012, arXiv: [2008.01442 \[hep-ph\]](#).
- [14] S. Alioli et al., “Monte Carlo event generators for high energy particle physics event simulation”, **2019**, (Eds.: A. Buckley, F. Krauss, S. Plätzer, M. Seymour), arXiv: [1902.01674 \[hep-ph\]](#).
- [15] M. Dasgupta, F. A. Dreyer, K. Hamilton, P. F. Monni, G. P. Salam, G. Soyez, “Parton showers beyond leading logarithmic accuracy”, **2020**, arXiv: [2002.11114 \[hep-ph\]](#).
- [16] S. Plätzer, M. Sjöstrand, “Subleading N_c improved Parton Showers”, *JHEP* **2012**, *07*, 042, arXiv: [1201.0260 \[hep-ph\]](#).
- [17] S. Plätzer, M. Sjöstrand, J. Thorén, “Color matrix element corrections for parton showers”, *JHEP* **2018**, *11*, 009, arXiv: [1808.00332 \[hep-ph\]](#).
- [18] J. Isaacson, S. Prestel, “Stochastically sampling color configurations”, *Phys. Rev. D* **2019**, *99*, 014021, arXiv: [1806.10102 \[hep-ph\]](#).
- [19] S. Höche, D. Reichelt, “Numerical resummation at sub-leading color in the strongly ordered soft gluon limit”, **2020**, arXiv: [2001.11492 \[hep-ph\]](#).
- [20] J. R. Forshaw, J. Holguin, S. Plätzer, “Parton branching at amplitude level”, *JHEP* **2019**, *08*, 145, arXiv: [1905.08686 \[hep-ph\]](#).

- [21] M. Dasgupta, F. A. Dreyer, K. Hamilton, P. F. Monni, G. P. Salam, “Logarithmic accuracy of parton showers: a fixed-order study”, *JHEP* **2018**, *09*, 033, arXiv: [1805.09327 \[hep-ph\]](#).
- [22] S. Catani, M. H. Seymour, “A General algorithm for calculating jet cross-sections in NLO QCD”, *Nucl. Phys.* **1997**, *B485*, [Erratum: Nucl. Phys.B510,503(1998)], 291–419, arXiv: [hep-ph/9605323 \[hep-ph\]](#).
- [23] R. K. Ellis, W. J. Stirling, B. R. Webber, *QCD and Collider Physics*, Cambridge University Press, **1996**.
- [24] Y. L. Dokshitzer, V. A. Khoze, A. H. Mueller, S. I. Troian, *Basics of perturbative QCD*, **1991**.
- [25] R. Ángeles Martínez, M. De Angelis, J. R. Forshaw, S. Plätzer, M. H. Seymour, “Soft gluon evolution and non-global logarithms”, *JHEP* **2018**, *05*, 044, arXiv: [1802.08531 \[hep-ph\]](#).
- [26] J. C. Collins, “Spin Correlations in Monte Carlo Event Generators”, *Nucl. Phys.* **1988**, *B304*, 794–804.
- [27] I. Knowles, “A linear algorithm for calculating spin correlations in hadronic collisions”, *Computer Physics Communications* **1990**, *58*, 271–284.
- [28] R. Ángeles-Martínez, J. R. Forshaw, M. H. Seymour, “Coulomb gluons and the ordering variable”, *JHEP* **2015**, *12*, 091, arXiv: [1510.07998 \[hep-ph\]](#).
- [29] R. Ángeles Martínez, J. R. Forshaw, M. H. Seymour, “Ordering multiple soft gluon emissions”, *Phys. Rev. Lett.* **2016**, *116*, 212003, arXiv: [1602.00623 \[hep-ph\]](#).
- [30] M. D. Angelis, J. R. Forshaw, S. Plätzer, “Resummation and simulation of soft gluon effects beyond leading colour”, **2020**, arXiv: [2007.09648 \[hep-ph\]](#).
- [31] Z. Nagy, D. E. Soper, “Effects of subleading color in a parton shower”, *JHEP* **2015**, *07*, 119, arXiv: [1501.00778 \[hep-ph\]](#).
- [32] Z. Nagy, D. E. Soper, “What is a parton shower?”, *Phys. Rev.* **2018**, *D98*, 014034, arXiv: [1705.08093 \[hep-ph\]](#).
- [33] Z. Nagy, D. E. Soper, “Parton showers with more exact color evolution”, **2019**, arXiv: [1902.02105 \[hep-ph\]](#).
- [34] A. Banfi, G. Marchesini, G. Smye, “Away from jet energy flow”, *JHEP* **2002**, *08*, 006, arXiv: [hep-ph/0206076 \[hep-ph\]](#).
- [35] C. Friberg, G. Gustafson, J. Hakkinen, “Color connections in e+ e- annihilation”, *Nucl. Phys.* **1997**, *B490*, 289–305, arXiv: [hep-ph/9604347 \[hep-ph\]](#).
- [36] S. Schumann, F. Krauss, “A Parton shower algorithm based on Catani-Seymour dipole factorisation”, *JHEP* **2008**, *03*, 038, arXiv: [0709.1027 \[hep-ph\]](#).
- [37] S. Catani, M. H. Seymour, “A General algorithm for calculating jet cross-sections in NLO QCD”, *Nucl. Phys.* **1997**, *B485*, [Erratum: Nucl. Phys.B510,503(1998)], 291–419, arXiv: [hep-ph/9605323 \[hep-ph\]](#).
- [38] S. Gieseke, P. Stephens, B. Webber, “New formalism for QCD parton showers”, *JHEP* **2003**, *12*, 045, arXiv: [hep-ph/0310083 \[hep-ph\]](#).
- [39] B. Andersson, P. Dahlkvist, G. Gustafson, “An infrared stable multiplicity measure on QCD parton states”, *Phys. Lett. B* **1988**, *214*, 604–608.

- [40] G. Gustafson, “Multiplicity distributions in QCD cascades”, *Nucl. Phys. B* **1993**, *392*, 251–280.
- [41] S. Höche, S. Prestel, “The midpoint between dipole and parton showers”, *Eur. Phys. J.* **2015**, *C75*, 461, arXiv: [1506.05057 \[hep-ph\]](#).
- [42] Z. Nagy, D. E. Soper, “Parton showers with quantum interference: Leading color, with spin”, *JHEP* **2008**, *07*, 025, arXiv: [0805.0216 \[hep-ph\]](#).
- [43] L. Lönnblad, “ARIADNE version 4: A Program for simulation of QCD cascades implementing the color dipole model”, *Comput. Phys. Commun.* **1992**, *71*, 15–31.

Chapter 8

Publication: Coulomb gluons will generally destroy coherence

“Well, I’m a hair’s breath from investigating bunnies at the moment, so I’m open to anything.”

— Rupert Giles, Buffy the Vampire Slayer Season 6

8.1 Preface

In our publication “Parton branching at amplitude level” (Chapter 4) we carefully study the factorisation properties of our parton branching algorithm. The factorisation of QCD amplitudes is of broad interest [1–7] and underpins the application of DGLAP evolution to phenomenological studies of protons at the LHC. In the following publication we use the insight gained from the factorisation properties of our parton branching algorithm to evaluate corrections to DGLAP evolution due to factorisation violating logarithms.

References

- [1] J. C. Collins, D. E. Soper, “The Theorems of Perturbative QCD”, *Ann. Rev. Nucl. Part. Sci.* **1987**, *37*, 383–409.
- [2] J. C. Collins, D. E. Soper, G. F. Sterman, “Soft Gluons and Factorization”, *Nucl. Phys.* **1988**, *B308*, 833–856.
- [3] A. Banfi, G. P. Salam, G. Zanderighi, “Principles of general final-state resummation and automated implementation”, *JHEP* **2005**, *03*, 073, arXiv: [hep-ph/0407286](#) [[hep-ph](#)].
- [4] J. R. Forshaw, A. Kyrieleis, M. H. Seymour, “Super-leading logarithms in non-global observables in QCD: Colour basis independent calculation”, *JHEP* **2008**, *09*, 128, arXiv: [0808.1269](#) [[hep-ph](#)].

- [5] A. Banfi, G. P. Salam, G. Zanderighi, “Phenomenology of event shapes at hadron colliders”, *JHEP* **2010**, *06*, 038, arXiv: [1001.4082 \[hep-ph\]](#).
- [6] J. R. Forshaw, M. H. Seymour, A. Siódmok, “On the Breaking of Collinear Factorization in QCD”, *JHEP* **2012**, *11*, 066, arXiv: [1206.6363 \[hep-ph\]](#).
- [7] R. Ángeles-Martínez, J. R. Forshaw, M. H. Seymour, “Coulomb gluons and the ordering variable”, *JHEP* **2015**, *12*, 091, arXiv: [1510.07998 \[hep-ph\]](#).

Declaration

The subsequent work is mine own. It is without plagiarism. Each section in the paper is my own research undertaken in collaboration with my PhD supervisor Prof. Jeff Forshaw.

JRF thanks the Mainz Institute for Theoretical Physics (MITP) (Project ID 39083149) for its hospitality and support. JH thanks the UK Science and Technology Facilities Council for the award of a postgraduate studentship. We would like to thank Simon Plätzer, Mike Seymour and Gavin Salam for insightful discussions. We would also like to thank Jack Helliwell, Matthew De Angelis and the Manchester QCD theory group for broad and helpful discussions.

Coulomb gluons will generally destroy coherence

Authors: Jack Holguin, Jeffrey R. Forshaw

Abstract

Coherence violation is an interesting and counter-intuitive phenomenon in QCD. We discuss the circumstances under which violation occurs in observables sensitive to soft radiation and arrive at the conclusion that almost all such observables at hadron colliders will violate coherence to some degree. We illustrate our discussion by considering the gaps-between-jets observable, where coherence violation is super-leading, then we generalise to other observables. We end with a general discussion on the logarithmic order of coherence violation.

8.2 Introduction

The collinear evolution of hadronic parton densities is accounted for using the equations of Dokshitzer, Gribov, Lipatov, Altarelli & Parisi (DGLAP) [1–3]. It is often assumed that, as a result of QCD coherence, this collinear evolution can be factorized from any wide-angle, soft-gluon emissions [4]. However, Coulomb/Glauber exchanges can destroy coherence and invalidate the factorisation [5, 6]. In this letter, we explore the circumstances under which this happens.

8.2.1 Case study: gaps between jets

Oderda & Sterman (OS) [7–9] presented the first calculations of the rate for the production of two or more jets subject to the restriction that there should be no additional jets located in the rapidity interval between the two highest p_T jets (the dijets) with transverse momentum (or energy) bigger than some value, Q_0 . This observable is sensitive to logarithmically enhanced, wide-angle, soft-gluon emissions. According to OS, the leading logarithmic (LL) contribution to the gaps-between-jets cross-section at a hadron collider is

$$\frac{d\sigma_{\text{OS}}}{dx_a dx_b d\mathcal{B}} = f_A(x_a, Q) f_B(x_b, Q) \text{Tr}(\mathbf{V}_{Q_0, Q} \mathbf{H} \mathbf{V}_{Q_0, Q}^\dagger), \quad (8.1)$$

where $\mathbf{H} = |M_0\rangle\langle M_0|$ is the QCD hard scattering matrix ($|M_0\rangle$ is the lowest-order, QCD hard-process amplitude for dijet production), $d\mathcal{B} \equiv dy d^2\mathbf{p}_\perp/16\pi^2\hat{s}$ is the measure for the on-shell (Born) kinematics of the final state dijets, $f_{A/B}$ are parton distribution functions for the incoming hadrons A and B , Q is the jet transverse momentum and

$$\mathbf{V}_{Q_0,Q} \approx \exp\left(-\frac{\alpha_s}{\pi} \ln \frac{Q}{Q_0} (Y\mathbf{T}_t^2 - i\pi\mathbf{T}_s^2)\right). \quad (8.2)$$

The rapidity separation between the dijets is Y , \mathbf{T}_t^2 is the colour-space operator corresponding to the colour exchanged in the t -channel and \mathbf{T}_s^2 corresponds to the colour exchanged in the s -channel. For example, if the hard process is $ab \rightarrow cd$ then $\mathbf{T}_s^2 = (\mathbf{T}_a + \mathbf{T}_b)^2 = (\mathbf{T}_c + \mathbf{T}_d)^2$ and $\mathbf{T}_t^2 = (\mathbf{T}_a + \mathbf{T}_c)^2 = (\mathbf{T}_b + \mathbf{T}_d)^2$. The Sudakov operator $\mathbf{V}_{Q_0,Q}$ corresponds to no soft-gluon emission directly into the region between the dijets with transverse momentum greater than Q_0 . Eq. (8.2) is a good approximation for $Y \gg 1$ (the terms we have neglected are proportional to the unit matrix in colour space, which means their neglect does not affect what follows).

Following the discovery of non-global logarithms by Dasgupta & Salam [10], it became clear that the OS analysis was incomplete because it did not account for the Sudakov suppression associated with partons originally radiated into the out-of-gap region. Including this physics makes the problem considerably more complicated/interesting. Notwithstanding the role of this non-global radiation, our focus here is on the collinear evolution of the incoming partons and for that we will continue to neglect the non-global corrections. We do so for pedagogical reasons, fully aware that non-global corrections are important. That said, let us return to Eq. (8.1) and notice that it is still not quite right.

To see what is wrong, let us consider only the order α_s correction to the collinear evolution of the parton densities above the veto scale Q_0 . For simplicity, we only consider quark evolution from hadron A . The result is

$$\begin{aligned} \frac{d\sigma_1}{dx_a dx_b d\mathcal{B}} &= \frac{\alpha_s}{\pi} \int_{Q_0}^Q \frac{dk_T}{k_T} \int_0^{1-k_T/Q} \frac{dz}{z} P_{qq}(z) f_B(x_b, Q) \\ &\times \left[\Theta(z - x_a) f_A(x_a/z, Q_0) \frac{1}{\mathbf{T}_a^2} \text{Tr}(\mathbf{V}_{Q_0,k_T} \mathbf{T}_a \mathbf{V}_{k_T,Q} \mathbf{H} \mathbf{V}_{k_T,Q}^\dagger \mathbf{T}_a^\dagger \mathbf{V}_{Q_0,k_T}^\dagger) \right. \\ &\quad \left. - z f_A(x_a, Q_0) \text{Tr}(\mathbf{V}_{Q_0,Q} \mathbf{H} \mathbf{V}_{Q_0,Q}^\dagger) \right]. \quad (8.3) \end{aligned}$$

Here $\mathbf{T}_a^2 = C_F$ since we are supposing that parton a is a quark and we are following convention in writing

$$P_{qq} = C_F \frac{1+z^2}{1-z}. \quad (8.4)$$

In the case of no jet veto we have the familiar result for the dijet cross-section including the evolution of the parton distribution functions in terms of the plus prescription [1–3, 11],

$$\begin{aligned}
\frac{d\sigma_1}{dx_a dx_b d\mathcal{B}} &= \frac{\alpha_s}{\pi} \int_{Q_0}^Q \frac{dk_T}{k_T} \int_0^{1-k_T/Q} \frac{dz}{z} P_{qq}(z) [\Theta(z-x_a) f_A(x_a/z, Q_0) \\
&\quad - z f_A(x_a, Q_0)] \text{Tr}(\mathbf{V}_{Q_0, Q} \mathbf{H} \mathbf{V}_{Q_0, Q}^\dagger) f_B(x_b, Q), \\
&= \frac{\alpha_s}{\pi} \int_{Q_0}^Q \frac{dk_T}{k_T} \int_{x_a}^1 \frac{dz}{z} C_F \left(\frac{1+z^2}{1-z} \right)_+ f_A(x_a/z, Q_0) f_B(x_b, Q) \text{Tr}(\mathbf{V}_{Q_0, Q} \mathbf{H} \mathbf{V}_{Q_0, Q}^\dagger).
\end{aligned} \tag{8.5}$$

In the first line, it is safe to set the upper limit of the z integral to unity, which allows us to write the second line in terms of the plus prescription.

The problem in Eq. (8.3) is the non-commutativity of the colour emission operator \mathbf{T}_a with the Sudakov operator, which can be traced to the Coulomb/Glauber $i\pi$ term in Eq. (8.2). In the case of the gaps-between-jets observable, expanding Eq. (8.3) order-by-order in α_s reveals an unexpected double logarithmic enhancement starting at

$$\sim \pi^2 N_c^2 Y \alpha_s^4 \log^5(Q/Q_0)$$

relative to the inclusive dijet cross section. These are the super-leading logarithms first reported in [12]. Notice that the $i\pi$ terms do not cancel because $[\mathbf{T}_t^2, \mathbf{T}_s^2] \neq 0$. This is what spoils our ability to factorize the collinear evolution into the parton distribution functions since, in the absence of any $i\pi$ terms, we would recover Eq. (8.5) due to the fact that $[\mathbf{T}_a, \mathbf{T}_t^2] = 0$. The problem is also entirely a problem with emissions collinear to one of the two incoming partons; emissions collinear to the outgoing partons do factorize since $[\mathbf{T}_{c,d}, \mathbf{T}_s^2] = 0$ and $[\mathbf{T}_{c,d}, \mathbf{T}_t^2] = 0$.

8.3 General considerations

We now consider more general pure QCD processes in hadron-hadron collisions (we will consider electroweak processes later). We continue to neglect non-global logs and other important sources of logarithms, for instance from the running coupling and recoil. We begin with a generalisation of Eq. (8.3):

$$\begin{aligned}
\frac{d\sigma_1}{dx_a dx_b d\mathcal{B}} &= \frac{\alpha_s}{\pi} \int_{\mu_F}^Q \frac{dk_T}{k_T} \int_0^{1-k_T/Q} \frac{dz}{z} P_{qq}(z) u_1(k) f_B(x_b, Q) \\
&\quad \times \left[\Theta(z-x_a) f_A(x_a/z, \mu_F) \frac{1}{\mathbf{T}_a^2} \text{Tr}(\mathbf{V}_{\mu_F, k_T} \mathbf{T}_a \mathbf{V}_{k_T, Q} \mathbf{H} \mathbf{V}_{k_T, Q}^\dagger \mathbf{T}_a^\dagger \mathbf{V}_{\mu_F, k_T}^\dagger) \right. \\
&\quad \left. - z f_A(x_a, \mu_F) \text{Tr}(\mathbf{V}_{\mu_F, Q} \mathbf{H} \mathbf{V}_{\mu_F, Q}^\dagger) \right], \tag{8.6}
\end{aligned}$$

where Q is the hard scale and

$$\mathbf{V}_{a,b} \approx \text{Pexp} \left(\frac{\alpha_s}{\pi} \left[\sum_{i \neq j} \mathbf{T}_i \cdot \mathbf{T}_j \int_a^b \frac{dq_{\perp}^{(ij)}}{q_{\perp}^{(ij)}} \int_{-\ln Q/q_{\perp}^{(ij)}}^{\ln Q/q_{\perp}^{(ij)}} dy^{(ij)} \int_0^{2\pi} \frac{d\phi^{(ij)}}{4\pi} (1 - u_n(q, \{q\}_{n-1})) \right. \right. \\ \left. \left. + i\pi \mathbf{T}_s^2 \ln \frac{b}{a} \right] \right). \quad (8.7)$$

The measurement function corresponding to n emissions with respect to the Born process is $u(q, \{q\}_{n-1})$, where q is the most recent emission momentum and $\{q\}_{n-1}$ is the set of all previous emission momenta. In Eq. (8.6) we only need $u(q, \{q\}) \equiv u_1(q)$ and $u(q, k) \equiv u_2(q, k)u_1(k)$. In Eq. (8.7),

$$(q_{\perp}^{(ij)})^2 = \frac{2p_i \cdot q p_j \cdot q}{p_i \cdot p_j}$$

is the transverse momentum defined in the zero momentum frame of partons i and j ; $y^{(ij)}$ and $\phi^{(ij)}$ are the rapidity and azimuth in the same frame. The sum over i and j in Eq. (8.7) is over all prior real emissions and as such it is context dependent.

Eq. (8.6) will generate coherence violating terms at some perturbative order if the Coulomb terms do not entirely cancel. For this cancellation to occur we require

$$[\text{Re}(\ln \mathbf{V}_{\mu, k_{\perp}}), \mathbf{T}_s^2] = 0. \quad (8.8)$$

This is because if Eq. (8.8) is satisfied we can write $\mathbf{V}_{\mu, k_{\perp}} = \mathbf{V}_{\mu, k_{\perp}}^{\text{Re}} \mathbf{V}_{\mu, k_{\perp}}^{\text{Im}}$ where $\mathbf{V}_{\mu, k_{\perp}}^{\text{Im}} = e^{\text{Im}(\ln \mathbf{V}_{\mu, k_{\perp}})}$ and $(\mathbf{V}_{\mu, k_{\perp}}^{\text{Im}})^{\dagger} = (\mathbf{V}_{\mu, k_{\perp}}^{\text{Im}})^{-1}$. This permits the cancellation of the outermost Coulomb terms and then, since

$$[\text{Re}(\ln \mathbf{V}_{\mu, k_{\perp}}), \mathbf{T}_a] = 0, \quad (8.9)$$

a cascade effect leads to the cancellation of all other Coulomb terms [4, 13, 14].

Eq. (8.8) can be generalized to a statement that there be no coherence violation in σ_n , i.e. for any number of collinear emissions, thereby allowing all-orders DGLAP evolution up to the hard scale Q . For this to be so, it is necessary that

$$[\text{Re}(\ln \mathbf{V}_{a,b}), \mathbf{T}_s^2] \left| \mathcal{M}_0^{(n)} \right\rangle = 0, \quad (8.10)$$

where $\left| \mathcal{M}_0^{(n)} \right\rangle$ is the Born amplitude dressed with n soft or collinear partons. Eq. (8.10) means that

$$\left[\sum_{i \neq j} \mathbf{T}_i \cdot \mathbf{T}_j \Omega_{ij}, \mathbf{T}_s^2 \right] = \left[\left(\sum_{i=a,b} + \sum_{i \neq a,b} \right) \left(\sum_{j=a,b} + \sum_{j \neq a,b} \right) \mathbf{T}_i \cdot \mathbf{T}_j \Omega_{ij}, \mathbf{T}_s^2 \right] \\ = 2 \left[\sum_{i=a,b} \sum_{j \neq a,b} \mathbf{T}_i \cdot \mathbf{T}_j \Omega_{ij}, \mathbf{T}_s^2 \right] = 0, \quad (8.11)$$

and it is understood that the commutators are to act on $|\mathcal{M}_0^{(n)}\rangle$. In other words, we only need to check the commutativity of a Coulomb exchange with any soft interference term between an initial and a final state parton in order to check for coherence violation.

For topologies with fewer than two coloured incoming particles Eq. (8.11) is automatically satisfied since \mathbf{T}_s^2 is a Casimir. For all other processes, the commutator in Eq. (8.11) only vanishes if $\Omega_{aj} = \Omega_{bj}$ ¹. Quite generally,

$$\begin{aligned} \Omega_{aj} &= \int_{\alpha}^{\beta} \frac{dq_{\perp}^{(ab)}}{q_{\perp}^{(ab)}} \int \frac{dy^{(ab)} d\phi^{(ab)}}{8\pi} (q_{\perp}^{(ab)})^2 \frac{p_a \cdot p_j}{p_a \cdot q p_j \cdot q} (1 - u_n(q, \{q\}_{n-1})) \\ &\quad \times \Theta \left(\alpha < \sqrt{\frac{p_a \cdot p_j}{p_j \cdot q} \frac{p_b \cdot q}{p_a \cdot p_b}} q_{\perp}^{(ab)} < \beta \right), \end{aligned} \quad (8.12)$$

where j labels a final-state particle. Written this way, we see that $\Omega_{aj} = \Omega_{bj}$ only when $p_a \cdot p_j = p_b \cdot p_j$. This must hold true for all j , which restricts all final-state partons to be at 90 degrees in the (ab) zero-momentum frame. This means that all observables at hadron-hadron colliders that have any sensitivity to soft gluon emission will violate coherence to some degree. As pointed out in [15], this includes Drell-Yan and $gg \rightarrow H$ hard-processes, since their colour can become sufficiently involved after emitting two or more gluons into the final state (i.e. coherence violation will first appear in $\frac{d\sigma_2}{dx_a dx_b}$).

8.4 The logarithmic order of coherence violation

For the majority of pure QCD observables, coherence violation will emerge for the first time at $\mathcal{O}(\alpha_s^4)$ in the fixed order expansion (relative to the order of the Born process). That's because one needs at least one soft gluon, one collinear emission and two Coulomb exchanges.

The logarithmic order at which coherence violation will occur is process dependent. We consider a general measurement function which produces logarithms $\ln v^{-1} \equiv L$:

$$u(\{p\}) = \sum_j F_j(\{p\}) \Theta(v - V_j(\{p\})). \quad (8.13)$$

Observables for which $F_j = 1$ are known as event-shape observables [16–18] and observables for which $F_j \neq 1$ are weighted cross-sections [18–22]. We will give specific examples of the functions F_j and V_j below. To get the leading coherence-violating logarithm we must take the $z \rightarrow 1$ limit of Eq. (8.6). As anticipated, the first potentially non-vanishing term occurs

¹Alternatively, the commutator will vanish if $\Omega_{ij} = \Omega_{ij'}$ for all $j, j' \notin \{a, b\}$ and $i \in \{a, b\}$. However this is kinematically impossible when j is hard and j' is soft.

at $\mathcal{O}(\alpha_s^4)$ relative to the Born result:

$$\begin{aligned} & \frac{d\sigma_1}{dx_a dx_b d\mathcal{B}} \\ & \approx \sum_{\substack{i=a,b \\ j \neq a,b}} A_{ij} \int_{\mu_F}^Q \frac{dk_{4\perp}}{k_{4\perp}} \int_{k_{4\perp}}^Q \frac{dk_{3\perp}^{(ab)}}{k_{3\perp}^{(ab)}} \left(\int_{-\infty}^{\infty} dy_3 \int_0^{2\pi} \frac{d\phi_3}{2\pi} w_{ij} \right) \int_{k_{3\perp}^{(ab)}}^Q \frac{dk_{2\perp}}{k_{2\perp}} \int_{k_{2\perp}}^Q \frac{dk_{1\perp}}{k_{1\perp}} \int_0^1 \frac{d\theta_2}{\theta_2} \\ & \quad \times (u(k_2) - u(k_3, k_2)) \Theta(k_{2\perp} < Q\theta_2) + (1 \leftrightarrow 2) + (3 \leftrightarrow 4) + (1 \leftrightarrow 2, 3 \leftrightarrow 4), \end{aligned} \quad (8.14)$$

where the collinear parton is parton 2. Parton 3 is a real soft wide-angle gluon and partons 1 and 4 are Coulomb exchanges, $w_{ij} = (k_{3\perp}^{(ab)}/k_{3\perp}^{(ij)})^2$ and

$$A_{ij} = \left(\frac{\alpha_s}{\pi}\right)^4 C_{ij} f_A(x_a, \mu_F) f_B(x_b, Q) \frac{d\sigma_0}{dx_a dx_b d\mathcal{B}},$$

where C_{ij} is a non-zero constant built from the colour algebra and numerical factors:

$$C_{ij} = (i\pi)^2 \text{Tr} \left([\mathbf{T}_s^2, \mathbf{T}_i \cdot \mathbf{T}_j] (\mathbf{T}_a [\mathbf{T}_s^2, \mathbf{h}] \mathbf{T}_a^\dagger - \mathbf{T}_a^2 [\mathbf{T}_s^2, \mathbf{h}]) \right),$$

and where $\frac{d\sigma_0}{dx_a dx_b d\mathcal{B}} \mathbf{h} = \mathbf{H}$. $i \leftrightarrow j$ indicates swapping partons i and j in the k_t ordering and likewise altering the order of colour charges in C_{ij} . As parton 3 is a wide-angle gluon its angular integrals, which are bracketed in Eq. (8.14), produce observable dependent, finite not-logarithmically enhanced terms when restricted by the two parton measurement function, $1 - u_2(k_3, k_2)$. Though these terms may not factorise from Eq. (8.14), they can be ignored in the subsequent discussion as they do not effect the logarithmic power counting. In Eq. (8.14) we have used that in the soft-collinear limit $k_{2\perp}/E_a \approx (1 - z_2)\theta_2$. The theta-function defines the available phase-space for the collinear parton. μ_F is the factorisation scale, below which proton evolution is completely DGLAP. It is optimally chosen to have the largest value such that for all k_3 with $k_{3\perp}^{(ab)} < \mu_F$ or k_2 with $k_{2\perp} < \mu_F$, $u(k_2) - u(k_3, k_2) \approx 0$ whilst $u(k_2) \not\approx 0$.

There are three scenarios that we must study when evaluating Eq. (8.14). Firstly we can consider when $\max(k_{2\perp}) \gg \mu_F$, where $\max(k_{2\perp})$ is the smallest value of $k_{2\perp}$ such that for all k_2 with $k_{2\perp} > \max(k_{2\perp})$ both $u(k_2) \approx 0$ and $u(k_3, k_2) \approx 0$. In this situation, each of the 5 nested integrals generates a logarithm (the infra-red safety of the functions F_i means they do not alter the logarithmic counting in this limit). As a result, $\frac{d\sigma_1}{dx_a dx_b} \sim \alpha_s^4 L^5$. Secondly we have the case $\max(k_{2\perp}) \approx w \mu_F$, where $w \gtrsim 1$. This means that the observable restricts the phase-space in the collinear region such that upper limit on $k_{2\perp}$ in Eq. (8.14) can be exchanged with $w \mu_F$. Consequently integrals over $dk_{4\perp} dk_{3\perp}^{(ab)} dk_{2\perp}$ generate a term proportional to $(\ln w)^3 \sim \mathcal{O}(1)$. However, in this scenario logarithms requiring resummation are still generated, though the $(1 \leftrightarrow 2)$ terms are sub-leading and thus the logarithms are produced with smaller numerical prefactors since fewer topologies

contribute. Logarithms are still produced since either the $dk_{1\perp}^{(ab)}$ integral generates a single logarithm or both the $dk_{1\perp}^{(ab)}$ and the $d\theta_2$ integrals generate logarithms. As a result, $\frac{d\sigma_1}{dx_a dx_b} \sim \alpha_s^4 L$ or $\frac{d\sigma_1}{dx_a dx_b} \sim \alpha_s^4 L^2$ respectively. Examples of both $\alpha_s^4 L$ and $\alpha_s^4 L^2$ observables are given in the following paragraph. Finally, there is the case $\mu_F = \max(k_{2\perp})$. This can only occur if $u(k_2) - u(k_3, k_2) = 0$ for all $k_{3\perp}^{(ab)} \sim k_{2\perp}$, which means the observable is completely insensitive to wide-angle radiation and so the hadron evolution can be completely described using DGLAP evolution without soft resummation. In other words, the observable is trivially without coherence violating logarithms. Observables of this form include the modified massdrop tagger [23] and N -point energy correlators [22].

To illustrate matters, we will review coherence violation in event shape observables that are continuously-global. The effects of coherence violation on continuously-global observables was first evaluated in [24]. For these, the measurement function can be written $u = \Theta(v - V(\{p\}))$, where $V(\{p\})$ is the value of the event shape,² and [25]

- for a single, soft emission, k , that is collinear to hard parton i ,

$$V(\{p\}) = d_i \left(\frac{k_{\perp}^{(in)}}{Q} \right)^h e^{-l_i y_k} g_i(\phi_k),$$

where d_i, h, l_i are constants, and $g_i(\phi_k)$ can be any function of the azimuth for which the integral $\int d \ln \phi_k g_i(\phi_k)$ exists. $k_{\perp}^{(in)}$ is the transverse momentum relative to parton i and any other arbitrary direction given by the unit vector \vec{n} . In the limit that k is both soft and collinear to i , the choice of \vec{n} is sub-leading. To be global, all of the $d_i \neq 0$.

- for a single, soft emission, k , that is not collinear to any hard parton,

$$V(\{p\}) \sim \left(k_{\perp}^{(ab)} \right)^h,$$

where h has the same value as in the collinear case above. This ensures the observable's scaling in transverse momentum is continuous across all logarithmically enhanced regions of phase-space.

The continuous scaling in transverse momentum of these observables allows us to set $\mu_F \approx Q e^{-\frac{L}{h}}$ and $u_2(k_3, k_2) \rightarrow 0$. If the collinear parton is soft and collinear to parton a and $V(k_2) \sim k_{2\perp}^h \theta_2^{l_a}$, we can replace

$$u(k_2) \rightarrow \Theta(k_{2\perp} \theta_2^{\frac{l_a}{h}} \lesssim Q e^{-\frac{L}{h}}).$$

²Here we have let $F_i \rightarrow 1$ but the argument is easily generalised provided F_i are infra-red and collinear safe polynomial functions of the parton momenta, as is typical of observables built from weighted cross-sections [21, 22].

Thus Eq. (8.14) gives $\frac{d\sigma_1}{dx_a dx_b} \sim \alpha_s^4 L$ for $l_a/h < 0$, and $\frac{d\sigma_1}{dx_a dx_b} \sim \alpha_s^4 L^2$ for $l_a/h = 0$. When $l_a/h > 0$ both terms contribute and $\frac{d\sigma_1}{dx_a dx_b} \sim \alpha_s^4 L^5$. In [24] it was identified that $l_a/h \leq 0$ is the case for ‘standard’ rIRC observables (such as transverse-thrust, for which $l_{a,b} = 0$), whereas $l_a/h > 0$ typically occurs in ‘exponentially-suppressed’ rIRC observables.

Now we consider all other (i.e. not continuously-global) observables. These observables cannot be written in the form

$$u(\{p\}) \approx F(\{p\})\Theta(v - V(\{p\})), \quad (8.15)$$

where $\ln V \sim h \ln k_{\perp}^{(ab)}$ and $F \sim A(1 + (k_{\perp}^{(ab)}/Q)^{h'})$, for constant h , A , and h' , over the entire phase space of a soft parton with momentum k . Therefore the phase-space of an emission can be divided into, at least, two regions, c and s , between which the scaling of the observable differs (i.e. gaps-between-jets where in the jet regions $h = 0$ but in the gap region V can be approximated by letting $h = 1$). Each region has an inclusivity scale, μ_c or μ_s respectively, such that the observable is insensitive to radiation emitted into that region with $k_t \lesssim \mu_{c,s}$. The inclusivity scales are functions of the parameter(s) defining the observable in the given phase-space region. As the observable is not continuously-global, μ_c and μ_s do not scale proportionally to each other under variation of the observable’s parameter(s) ($\mu_c \not\sim \mu_s$). Let c contain the region collinear to parton a , thus $u(k_2) - u(k_3, k_2) \approx 0$ for $k_{2\perp} < \mu_c$ and for $k_{3\perp}^{(ab)} < \min(\mu_c, \mu_s)$. Hence $\mu_F = \min(\mu_c, \mu_s)$. By construction $\max(k_{2\perp}) \approx \mu_c$ (this is a consequence of unitarity in the collinear region around parton a). Therefore either $\max(k_{2\perp}) \gg \mu_F = \mu_s$ or $\max(k_{2\perp}) = \mu_F = \mu_c$. When $\max(k_{2\perp}) \gg \mu_F$, $\frac{d\sigma_1}{dx_a dx_b} \sim \alpha_s^4 L^5$ and so the observable suffers coherence violating logarithms. This is typical of a non-global observable, for instance gaps-between-jets where $\mu_F \approx Q_0$ and $\max(k_{2\perp}) \approx Q$. As previously discussed, when $\max(k_{2\perp}) = \mu_F$ the observable is trivially insensitive to soft radiation and so is not of interest to us in this paper. We note that some observables only become not continuously-global after a particular multiplicity of partons has been reached; these are known as dynamically, not-continuously-global observables [26]. We can extrapolate the argument given in this paragraph to higher multiplicities of radiation. The value of μ_F should be fixed independently of the order of perturbation theory at which the observable is computed; thus either $\mu_F = \mu_c$ for all multiplicities of radiation in the regions s and c , or $\mu_F \ll \mu_c$ due to not continuously-global effects (even if they only appear at higher multiplicities). As we have stressed, if $\mu_F \ll \mu_c$ then the observable will suffer $\alpha_s^4 L^5$ coherence violating logarithms.

8.5 Conclusions

Our analysis shows that in hadron colliders all observables with sensitivity to wide-angle soft radiation dressing the initial state hadrons will suffer coherence violation. In the previous section, we computed the logarithmic order of this violation at fixed order in α_s . We see no arguments for why our analysis cannot be extrapolated to n th order in perturbation theory. Provided the observable under consideration has leading logarithms of the form $\alpha_s^n L^{2n}$, we expect coherence violating logarithms of the form:

- $\alpha_s^n L^{2n-6}$ or $\alpha_s^n L^{2n-7}$ in standard continuously-global observables [16, 25].
- $\alpha_s^n L^{2n-3}$ in ‘forward suppressed’ continuously-global observables (with $l_a/h > 0$ as defined in the previous section or $a_{1,2}/b_{1,2} > 0$ in the notation of [24]). Though, as these logarithms first emerge at $\mathcal{O}(\alpha_s^4)$ they will formally contribute to the LL exponent if they can be exponentiated.
- $\alpha_s^n L^{2n-3}$ for not continuously-global observables. When a not continuously-global observable has leading logarithms of the form $\alpha_s^n L^n$, coherence violating logarithms will become superleading.

A remark on the role of electroweak hard processes. In [5, 6] it was noted that two Coulomb exchanges are not needed to ensure real coherence-violating terms emerge in re-summations dressing electroweak hard-processes with non-trivial colour flows (for instance the hard process is the sum of s and t channel amplitudes for $qq' \rightarrow qq'$ hard processes mediated by W or Z bosons). This is because the hard process itself can supply a complex phase, which allows terms with a single Coulomb exchange to contain a real piece that can contribute to the cross-section. Thus for such hard-processes there is a possibility for $\mathcal{O}(\alpha_s^3)$ coherence-violating logs to emerge as well as the $\mathcal{O}(\alpha_s^4)$ and $\mathcal{O}(\alpha_s^5)$ we have studied. By repeating the analysis of the previous section, we see that coherence violation could contribute logarithms of the form $\alpha_s^n L^{2n-2}$ in the case of an electroweak hard process.

References

- [1] Y. Dokshitzer, D. Dyakonov, S. Troyan, “Hard processes in quantum chromodynamics”, *Physics Reports* **1980**, 58, 269–395.
- [2] V. N. Gribov, L. N. Lipatov, “Deep inelastic e p scattering in perturbation theory”, *Sov. J. Nucl. Phys.* **1972**, 15, [Yad. Fiz.15,781(1972)], 438–450.
- [3] G. Altarelli, G. Parisi, “Asymptotic freedom in parton language”, *Nuclear Physics B* **1977**, 126, 298–318.
- [4] J. C. Collins, D. E. Soper, “The Theorems of Perturbative QCD”, *Ann. Rev. Nucl. Part. Sci.* **1987**, 37, 383–409.

- [5] S. Catani, D. de Florian, G. Rodrigo, “Space-like (versus time-like) collinear limits in QCD: Is factorization violated?”, *JHEP* **2012**, *07*, 026, arXiv: [1112.4405 \[hep-ph\]](#).
- [6] J. R. Forshaw, M. H. Seymour, A. Siódmok, “On the Breaking of Collinear Factorization in QCD”, *JHEP* **2012**, *11*, 066, arXiv: [1206.6363 \[hep-ph\]](#).
- [7] N. Kidonakis, G. Oderda, G. F. Sterman, “Evolution of color exchange in QCD hard scattering”, *Nucl. Phys.* **1998**, *B531*, 365–402, arXiv: [hep-ph/9803241 \[hep-ph\]](#).
- [8] G. Oderda, G. F. Sterman, “Energy and color flow in dijet rapidity gaps”, *Phys. Rev. Lett.* **1998**, *81*, 3591–3594, arXiv: [hep-ph/9806530 \[hep-ph\]](#).
- [9] G. Oderda, “Dijet rapidity gaps in photoproduction from perturbative QCD”, *Phys. Rev.* **2000**, *D61*, 014004, arXiv: [hep-ph/9903240 \[hep-ph\]](#).
- [10] M. Dasgupta, G. P. Salam, “Resummation of nonglobal QCD observables”, *Phys. Lett.* **2001**, *B512*, 323–330, arXiv: [hep-ph/0104277 \[hep-ph\]](#).
- [11] Y. L. Dokshitzer, V. A. Khoze, A. H. Mueller, S. I. Troian, *Basics of perturbative QCD*, **1991**.
- [12] J. R. Forshaw, A. Kyrieleis, M. H. Seymour, “Super-leading logarithms in non-global observables in QCD”, *JHEP* **2006**, *08*, 059, arXiv: [hep-ph/0604094 \[hep-ph\]](#).
- [13] J. C. Collins, D. E. Soper, G. F. Sterman, “Soft Gluons and Factorization”, *Nucl. Phys.* **1988**, *B308*, 833–856.
- [14] J. R. Forshaw, J. Holguin, S. Plätzer, “Parton branching at amplitude level”, *JHEP* **2019**, *08*, 145, arXiv: [1905.08686 \[hep-ph\]](#).
- [15] T. Becher, M. Neubert, D. Y. Shao, “Resummation of Super-Leading Logarithms”, **2021**, arXiv: [2107.01212 \[hep-ph\]](#).
- [16] A. Banfi, G. P. Salam, G. Zanderighi, “Resummed event shapes at hadron - hadron colliders”, *JHEP* **2004**, *08*, 062, arXiv: [hep-ph/0407287 \[hep-ph\]](#).
- [17] S. Catani, L. Trentadue, G. Turnock, B. Webber, “Resummation of large logarithms in e^+e^- event shape distributions”, *Nucl. Phys.* **1993**, *B407*, 3.
- [18] G. P. Korchemsky, G. F. Sterman, “Power corrections to event shapes and factorization”, *Nucl. Phys. B* **1999**, *555*, 335–351, arXiv: [hep-ph/9902341](#).
- [19] N. Sveshnikov, F. Tkachov, “Jets and quantum field theory”, *Phys. Lett. B* **1996**, *382*, (Eds.: B. Levchenko, V. Savrin), 403–408, arXiv: [hep-ph/9512370](#).
- [20] F. V. Tkachov, “Measuring multi - jet structure of hadronic energy flow or What is a jet?”, *Int. J. Mod. Phys. A* **1997**, *12*, 5411–5529, arXiv: [hep-ph/9601308](#).
- [21] D. M. Hofman, J. Maldacena, “Conformal collider physics: Energy and charge correlations”, *JHEP* **2008**, *05*, 012, arXiv: [0803.1467 \[hep-th\]](#).
- [22] H. Chen, I. Moutl, X. Zhang, H. X. Zhu, “Rethinking jets with energy correlators: Tracks, resummation, and analytic continuation”, *Phys. Rev. D* **2020**, *102*, 054012, arXiv: [2004.11381 \[hep-ph\]](#).
- [23] M. Dasgupta, A. Fregoso, S. Marzani, G. P. Salam, “Towards an understanding of jet substructure”, *JHEP* **2013**, *09*, 029, arXiv: [1307.0007 \[hep-ph\]](#).
- [24] A. Banfi, G. P. Salam, G. Zanderighi, “Phenomenology of event shapes at hadron colliders”, *JHEP* **2010**, *06*, 038, arXiv: [1001.4082 \[hep-ph\]](#).

- [25] A. Banfi, G. P. Salam, G. Zanderighi, “Principles of general final-state resummation and automated implementation”, *JHEP* **2005**, *03*, 073, arXiv: [hep-ph/0407286](#) [[hep-ph](#)].
- [26] M. Dasgupta, G. P. Salam, “Resummed event shape variables in DIS”, *JHEP* **2002**, *08*, 032, arXiv: [hep-ph/0208073](#) [[hep-ph](#)].

Chapter 9

Conclusions and outlook

“True education is a kind of never ending story — a matter of continual beginnings, of habitual fresh starts, of persistent newness.”

— J.R.R. Tolkien

QCD dynamics in the infra-red limit is highly non-trivial. This thesis has concerned itself with the development of new algorithmic techniques for computing infra-red and collinear QCD radiation from inelastic hard processes with large momentum transfers. The parton branching algorithm this thesis introduces in Chapter 4 accurately computes full colour matrix elements for QCD radiation in the neighbourhood of the leading soft and/or collinear divergences. We have been careful to try and present the algorithm in such a way as to make the extension beyond leading-order possible. We have studied the properties of the algorithm, most notably we deduced how collinear factorisation is manifest in the algorithm in the presence of Coulomb/Glauber gluons.

The parton branching algorithm provides the theoretical basis for the development of new computer codes that systematically resum enhanced logarithms due to soft and/or collinear partons. The algorithm reduces the computation of complicated distributions of QCD radiation to a Markov chain of amplitude density matrices. The Markovian nature of the algorithm makes it well suited to numerical evaluation. The parton branching algorithm provides the backbone to CVolver [1–4], an amplitude level code for the computation of QCD radiation including interference effects at full colour. Indirectly, the algorithm provides the theoretical motivation for improvements we have proposed to the dipole parton shower formalism. We arrived at these improvements by deriving evolution equations, starting from our parton branching algorithm, for the radiation in both dipole and angular-ordered showers. We found that consistency between the two approaches, over regions of phase-space where both shower formalisms should be accurate, constrained the dipole shower. The newly constrained dipole shower differs from current models [5–7] in a few key ways: in

how it conserves momentum (the focus of Chapter 6), and in how it assigns colour factors (the focus of Chapter 7). We found that accurately handling both these features hinges on using a dipole partition which is symmetrical in the event centre of mass frame, not the dipole frame of an emission as is most commonly used. We studied the accuracy of our new dipole shower model and found it did not suffer from the errors plaguing common dipole showers, highlighted in [8]. Our findings are in agreement with, and are complementary to, those in [9, 10] where similar conclusions were arrived at by studying the phenomenology of the Lund plane [11] for QCD radiation.

Our final chapter looks at the phenomenological relevance of coherence violating logarithms (CVLs). CVLs originate from the breakdown of the complete collinear factorisation of QCD amplitudes due to Coulomb/Glauber gluons. They appear as corrections to the DGLAP evolution of a proton due to soft wide-angle radiation. As we have mentioned, in Chapter 4 we studied the factorisation properties of the parton branching algorithm in the presence of Coulomb/Glauber gluons. We found a general form for corrections to DGLAP evolution arising from the lowest order CVL. From this general form, we studied the logarithmic order at which CVL appear in the resummation of various classes of observables. We found that in many observables studied at the LHC, which are sensitive to soft radiation, CVLs will contribute to the leading logarithmic exponent if they resum into an exponential form.

There are many open questions which stem from the completion of the work presented in this thesis. Two immediate potential research projects are:

1. Extending the parton branching algorithm to next-to-leading accuracy. This would entail computing the next-to-leading order corrections to Eq. (4.7) and then solving for the amplitude density matrices \mathbf{A}_n . Next-to-leading corrections take two forms: next-to-leading power corrections to the leading operators, and next-to-leading ($\mathcal{O}(\alpha_s^2)$) operators. Many of the ingredients for this already exist in the literature: next-to-eikonal soft gluons [12], next-to-leading differential anomalous dimension matrices [13], next-to-leading collinear splitting operators [14, 15], and the running coupling [16]. However, combining every component is undoubtedly a large task (perhaps aided by a better choice of ordering variable [17, 18] though this too is an open question). Concurrently, it would be pertinent to understand the formal accuracy in the resummation that the next-to-leading algorithm would achieve. We can compare the ingredients needed for the next-to-leading algorithm against those needed for other approaches to the resummation of selected classes of observable [19] and notice that, at least superficially, the next-to-leading algorithm might be capable of NNLL

resummation for some observables. However, broad statements on accuracy across classes of resummed observables are well known to be difficult to make [9].

2. Optimising the current leading order parton branching algorithm. This is likely more easy to achieve than extending the algorithm to next-to-leading order but also constitutes a more loosely defined project. What do we want from an optimised version of the algorithm? By fusing the work presented in Chapters 4 and 6, it could be possible to improve the algorithm by using the dipole partitioning and global recoil to merge the operators for soft partons (\mathbf{S}_n) with the operators for collinear partons (\mathbf{C}_n). Such aesthetic improvements could also lead to increased computational efficiency. The only obviously non-trivial element to this task is correctly handling the spin correlations carried by hard-collinear partons in the presence of Coulomb/Glauber gluons (which prevent the use of the algorithm by Collins and Knowles [20, 21]). More practically, there could be great benefit to recasting the algorithm as a functional Fokker-Planck equation (such an equivalence has already been demonstrated for the soft physics contained in the algorithm [22]). It is known that such equations can be solved by the stochastic integration of an associated Langevin equation, and the resummation of soft gluons via this approach has recently seen a great deal of success [23, 24].

In Chapters 6 and 7 we derived current popular parton shower models from the parton branching algorithm. This proved a fruitful task, since our derivations highlighted ways in which the accuracy of these models could be improved. In the same spirit, it would also be interesting to formalise links between our parton branching algorithm and soft-collinear effective theory [25]. Whilst we could not state the immediate phenomenological benefit of this task, a dictionary for translating between the methodology of perturbative QCD and soft-collinear effective theories would be interesting.

References

- [1] J. R. Forshaw, J. Holguin, S. Plätzer, “Building a consistent parton shower”, *JHEP* **2020**, 09, 014, arXiv: [2003.06400 \[hep-ph\]](#).
- [2] S. Plätzer, “Summing Large- N Towers in Colour Flow Evolution”, *Eur. Phys. J.* **2014**, *C74*, 2907, arXiv: [1312.2448 \[hep-ph\]](#).
- [3] M. De Angelis, Non-global Logarithms beyond Leading Colour, talk at <https://indico.cern.ch/event/662485/>, **2018**.
- [4] J. R. Forshaw, S. Plätzer, Soft Gluon Evolution beyond Leading Colour, talks at <https://indico.cern.ch/event/729453/>, **2018**.
- [5] T. Sjöstrand, P. Z. Skands, “Transverse-momentum-ordered showers and interleaved multiple interactions”, *Eur. Phys. J.* **2005**, *C39*, 129–154, arXiv: [hep-ph/0408302 \[hep-ph\]](#).

- [6] T. Sjöstrand, S. Ask, J. R. Christiansen, R. Corke, N. Desai, P. Ilten, S. Mrenna, S. Prestel, C. O. Rasmussen, P. Z. Skands, “An Introduction to PYTHIA 8.2”, *Comput. Phys. Commun.* **2015**, *191*, 159–177, arXiv: [1410.3012 \[hep-ph\]](#).
- [7] S. Schumann, F. Krauss, “A Parton shower algorithm based on Catani-Seymour dipole factorisation”, *JHEP* **2008**, *03*, 038, arXiv: [0709.1027 \[hep-ph\]](#).
- [8] M. Dasgupta, F. A. Dreyer, K. Hamilton, P. F. Monni, G. P. Salam, “Logarithmic accuracy of parton showers: a fixed-order study”, *JHEP* **2018**, *09*, 033, arXiv: [1805.09327 \[hep-ph\]](#).
- [9] M. Dasgupta, F. A. Dreyer, K. Hamilton, P. F. Monni, G. P. Salam, G. Soyez, “Parton showers beyond leading logarithmic accuracy”, **2020**, arXiv: [2002.11114 \[hep-ph\]](#).
- [10] K. Hamilton, R. Medves, G. P. Salam, L. Scyboz, G. Soyez, “Colour and logarithmic accuracy in final-state parton showers”, **2020**, arXiv: [2011.10054 \[hep-ph\]](#).
- [11] G. Gustafson, “Multiplicity distributions in QCD cascades”, *Nucl. Phys. B* **1993**, *392*, 251–280.
- [12] E. Laenen, L. Magnea, G. Stavenga, C. D. White, “Next-to-Eikonal Corrections to Soft Gluon Radiation: A Diagrammatic Approach”, *JHEP* **2011**, *01*, 141, arXiv: [1010.1860 \[hep-ph\]](#).
- [13] S. Plätzer, I. Ruffa, “Towards Colour Flow Evolution at Two Loops”, **2020**, arXiv: [2012.15215 \[hep-ph\]](#).
- [14] S. Catani, M. Grazzini, “Collinear factorization and splitting functions for next-to-next-to-leading order QCD calculations”, *Phys. Lett. B* **1999**, *446*, 143–152, arXiv: [hep-ph/9810389](#).
- [15] S. Catani, D. de Florian, G. Rodrigo, “Space-like (versus time-like) collinear limits in QCD: Is factorization violated?”, *JHEP* **2012**, *07*, 026, arXiv: [1112.4405 \[hep-ph\]](#).
- [16] S. Catani, B. Webber, G. Marchesini, “QCD coherent branching and semi-inclusive processes at large x ”, *Nuclear Physics B* **1991**, *349*, 635–654.
- [17] R. Ángeles-Martínez, J. R. Forshaw, M. H. Seymour, “Coulomb gluons and the ordering variable”, *JHEP* **2015**, *12*, 091, arXiv: [1510.07998 \[hep-ph\]](#).
- [18] R. Ángeles Martínez, J. R. Forshaw, M. H. Seymour, “Ordering multiple soft gluon emissions”, *Phys. Rev. Lett.* **2016**, *116*, 212003, arXiv: [1602.00623 \[hep-ph\]](#).
- [19] A. Banfi, H. McAslan, P. F. Monni, G. Zanderighi, “A general method for the re-summation of event-shape distributions in e+e- annihilation”, *JHEP* **2015**, *05*, 102, arXiv: [1412.2126 \[hep-ph\]](#).
- [20] J. C. Collins, “Spin Correlations in Monte Carlo Event Generators”, *Nucl. Phys.* **1988**, *B304*, 794–804.
- [21] I. Knowles, “A linear algorithm for calculating spin correlations in hadronic collisions”, *Computer Physics Communications* **1990**, *58*, 271–284.
- [22] R. Ángeles Martínez, M. De Angelis, J. R. Forshaw, S. Plätzer, M. H. Seymour, “Soft gluon evolution and non-global logarithms”, *JHEP* **2018**, *05*, 044, arXiv: [1802.08531 \[hep-ph\]](#).
- [23] Y. Hagiwara, Y. Hatta, T. Ueda, “Hemisphere jet mass distribution at finite N_c ”, *Phys. Lett.* **2016**, *B756*, 254–258, arXiv: [1507.07641 \[hep-ph\]](#).

- [24] Y. Hatta, T. Ueda, “Non-global logarithms in hadron collisions at $N_c = 3$ ”, *Nucl. Phys. B* **2021**, *962*, 115273, arXiv: [2011.04154 \[hep-ph\]](#).
- [25] I. Z. Rothstein, I. W. Stewart, “An Effective Field Theory for Forward Scattering and Factorization Violation”, *JHEP* **2016**, *08*, 025, arXiv: [1601.04695 \[hep-ph\]](#).

Appendix A

Definitions and identities

“The true work of improving things is in the little achievements of the day, and that’s what you need to enjoy.”

— Celine, Before Sunset

A.1 Dirac algebra and polarisation sums

In this section we provide some identities useful in the computation of Feynman diagrams. The proofs of these identities are widely available [1–3] and so won’t be given here.

Spinor identities:

$$\begin{aligned} u^s(p)\bar{u}^s(p) &= \frac{1}{2}(1 + 2s\gamma_5)\not{p}, & v^s(p)\bar{v}^s(p) &= \frac{1}{2}(1 - 2s\gamma_5)\not{p}, \\ \sum_s u^s(p)\bar{u}^s(p) &= \not{p} + m, & \sum_s v^s(p)\bar{v}^s(p) &= \not{p} - m. \end{aligned} \quad (1.1)$$

Polarisation identities for massless vector bosons:

$$\begin{aligned} \sum_\lambda \epsilon_\mu^\lambda(k)\epsilon_\nu^{*\lambda}(k) &= -g_{\mu\nu} + \frac{k_\nu n_\mu + n_\nu k_\mu}{k \cdot n} & \text{when } k^2 = 0, \\ &= -g_{\mu\nu} + \frac{k_\nu n_\mu + n_\nu k_\mu}{k \cdot n} - k^2 \frac{n^\mu n^\nu}{(k \cdot n)^2} & \text{when } k^2 \neq 0. \end{aligned} \quad (1.2)$$

The latter equality for when $k^2 \neq 0$ is an analytic continuation for unphysical polarisations of off-shell vector bosons. Clifford algebra identities:

$$\begin{aligned} \gamma_\mu \not{p} \gamma^\mu &= -2\not{p}, & \gamma_\mu \not{p} \not{k} \gamma^\mu &= 4p \cdot k, & \gamma_\mu \not{p} \not{k} \not{q} \gamma^\mu &= -2\not{q} \not{k} \not{p}, & \not{p} \not{p} &= p^2, \\ \text{tr}(\not{p} \not{k} \not{q} \not{l}) &= 4[(p \cdot k)(q \cdot l) - (p \cdot q)(k \cdot l) + (p \cdot l)(q \cdot k)], & \text{tr}(\not{p} \not{k}) &= 4p \cdot k, \\ \text{tr} \left(\prod_{\text{odd } n} \not{p}_n \right) &= 0. \end{aligned} \quad (1.3)$$

A.2 Spinor-helicity identities

Here listed are identities useful for the spin-helicity formalism. We employ the following short hand notation so that identities can be written in a compact fashion:

$$\begin{aligned} |p\rangle &\equiv |p+\rangle, & |p] &\equiv |p-\rangle, & \langle p| &\equiv \langle p-|, & [p| &\equiv \langle p+|, \\ \sigma^\mu &\equiv \sigma_+^\mu, & \bar{\sigma}^\mu &\equiv \sigma_-^\mu. \end{aligned} \quad (1.4)$$

In this notation:

$$|p\pm\rangle \langle p\pm| = p \cdot \sigma_\mp, \quad (1.5)$$

$$\langle p\pm| \sigma_\pm^\mu |p\pm\rangle = 2p^\mu, \quad (1.6)$$

$$\langle p\pm| q\mp\rangle = -\langle q\pm| p\mp\rangle, \quad (1.7)$$

$$\langle p\pm| \sigma_\pm^\mu |q\pm\rangle = \langle q\mp| \sigma_\mp^\mu |p\mp\rangle, \quad (1.8)$$

$$\langle p\pm| \sigma_\pm^\mu \sigma_\mp^\nu |q\mp\rangle = -\langle q\pm| \sigma_\pm^\nu \sigma_\mp^\mu |p\mp\rangle. \quad (1.9)$$

Note that to retain covariance with the dotted and undotted indices, a bra/ket state should always be contracted with a σ_\pm of the same sign and a σ_\pm should always be contracted with a σ_\pm of the opposite sign. For example, the above identities are allowed contractions whereas $\langle p+| \sigma_-^\mu \sigma_-^\nu |q+\rangle$ is not allowed as it contains two incorrect contractions. A consequence of identity (1.7) is $\langle pp\rangle = [pp] = 0$. Identities (1.8) and (1.9) can be generalised for odd and even numbers of σ s respectively

$$\begin{aligned} \langle p\pm| \sigma_\pm^{\mu_1} \sigma_\mp^{\mu_2} \dots \sigma_\pm^{\mu_{2n+1}} |q\pm\rangle &= \langle q\mp| \sigma_\mp^{\mu_{2n+1}} \dots \sigma_\pm^{\mu_2} \sigma_\mp^{\mu_1} |p\mp\rangle, \\ \langle p\pm| \sigma_\pm^{\mu_1} \sigma_\mp^{\mu_2} \dots \sigma_\mp^{\mu_{2n}} |q\mp\rangle &= -\langle q\pm| \sigma_\pm^{\mu_{2n}} \dots \sigma_\pm^{\mu_2} \sigma_\mp^{\mu_1} |p\mp\rangle. \end{aligned} \quad (1.10)$$

As is indicative of the bra-ket notation $\langle p\pm| A |q\rangle^* = \langle q| A |p\pm\rangle$ where A is any hermitian operator, such as the σ matrices. As previously stated in Section 3.1.3,

$$|\langle pq\rangle|^2 = |[pq]|^2 = 2p \cdot q, \quad (1.11)$$

which is easily shown using the identities above,

$$|\langle pq\rangle|^2 = \text{Tr}(|p-\rangle \langle p-| |q+\rangle \langle q+|) = p_\mu q_\nu \text{Tr}(\sigma_-^\mu \sigma_+^\nu) = 2p \cdot q. \quad (1.12)$$

An extension of identity (1.11) is

$$\begin{aligned} \langle p_1 p_2\rangle [p_2 p_3] \langle p_3 p_4\rangle [p_4 p_1] &= \text{Tr}(|p_1-\rangle \langle p_1-| |p_2+\rangle \langle p_2+| |p_3-\rangle \langle p_3-| |p_4+\rangle \langle p_4+|), \\ &= p_1^\mu p_2^\nu p_3^\rho p_4^\tau \text{Tr}(\sigma_+^\mu \sigma_-^\nu \sigma_+^\rho \sigma_-^\tau), \\ &= 2(g_{\mu\nu} g_{\rho\tau} - g_{\mu\rho} g_{\nu\tau} + g_{\mu\tau} g_{\nu\rho} + i\epsilon_{\mu\rho\nu\tau}) p_1^\mu p_2^\nu p_3^\rho p_4^\tau. \end{aligned} \quad (1.13)$$

Finally there are the Fierz identities, which are useful when combining multiple matrix elements:

$$\langle p_1 p_2 \rangle \langle p_3 p_4 \rangle = \langle p_1 p_3 \rangle \langle p_2 p_4 \rangle + \langle p_1 p_4 \rangle \langle p_3 p_2 \rangle, \quad (1.14)$$

$$[p_1 p_2] [p_3 p_4] = [p_1 p_3] [p_2 p_4] + [p_1 p_4] [p_3 p_2], \quad (1.15)$$

$$\langle p_1 + | \sigma_+^\mu | p_2 + \rangle \langle p_3 + | \sigma_{+\mu} | p_4 + \rangle = 2 [p_1 p_3] \langle p_4 p_2 \rangle, \quad (1.16)$$

$$\langle p_1 - | \sigma_-^\mu | p_2 - \rangle \langle p_3 - | \sigma_{-\mu} | p_4 - \rangle = 2 \langle p_1 p_3 \rangle [p_4 p_2], \quad (1.17)$$

$$\langle p_1 + | \sigma_+^\mu | p_2 + \rangle \langle p_3 - | \sigma_{-\mu} | p_4 - \rangle = 2 [p_1 p_4] \langle p_3 p_2 \rangle, \quad (1.18)$$

which when applied to the polarisation vectors gives

$$\begin{aligned} \sigma_\pm \cdot \epsilon(k, \pm 1) &= \frac{\sqrt{2} |n\mp\rangle \langle k\mp|}{\langle k\pm | n\mp\rangle}, & \sigma_\pm \cdot \epsilon^*(k, \pm 1) &= \frac{\sqrt{2} |k\mp\rangle \langle n\mp|}{\langle n\mp | k\pm\rangle}, \\ \sigma_\mp \cdot \epsilon(k, \pm 1) &= \frac{\sqrt{2} |k\pm\rangle \langle n\pm|}{\langle k\pm | n\mp\rangle}, & \sigma_\mp \cdot \epsilon^*(k, \pm 1) &= \frac{\sqrt{2} |n\pm\rangle \langle k\pm|}{\langle n\mp | k\pm\rangle}. \end{aligned} \quad (1.19)$$

A.3 Sudakov decompositions, kinematic variables and phase-space measures

It is often desirable to express a 4-vector into terms of two reference vectors and a vector transverse to the plane of the reference vectors (for this Appendix these are P^μ , Q^μ , and k^μ respectively). In Section 3.1.1 we employed a light-cone decomposition which was of this form. A general decomposition for n vectors is given by

$$\begin{aligned} p_1^\mu &= \alpha_1 P^\mu + \beta_1 Q^\mu + k_1^\mu, \\ &\vdots \\ p_i^\mu &= \alpha_i P^\mu + \beta_i Q^\mu + k_i^\mu, \\ &\vdots \\ p_n^\mu &= \alpha_n P^\mu + \beta_n Q^\mu + k_n^\mu, \end{aligned} \quad (1.20)$$

where $k_i^\mu P_\mu = k_i^\mu Q_\mu = 0$ for all i . If P and Q are light-like this is referred to as a light-cone decomposition (LCD). In an LCD, k_i is space-like and so it is typical to define $k_i^2 = -k_{i\perp}^2$ where $k_{i\perp}^2$ is positive.¹ Some more useful relations in a LCD are:

$$\alpha_i = \frac{p_i \cdot Q}{P \cdot Q}, \quad \beta_i = \frac{p_i \cdot P}{P \cdot Q}. \quad (1.21)$$

¹It is also common to use $k_t \equiv k_\perp$, particularly if P and Q are back-to-back in the lab frame and define a beam/jet axis in which case k_{it} is the transverse momentum from the axis.

If p_i is light-like, then its pseudo-rapidity in the frame where P and Q are back to back (known as the PQ dipole frame) is given by

$$y_i = \frac{1}{2} \ln \frac{\alpha_i}{\beta_i}, \quad (1.22)$$

where P defines the $+\infty$ pseudo-rapidity axis. In this decomposition, the phase-space measure for a particle with momentum p_i is given by

$$d^4 p_i = \frac{(P+Q)^2}{2} d\alpha_i d\beta_i d^2 \vec{k}_i \equiv \frac{(P+Q)^2}{2} d\alpha_i d\beta_i dk_{i\perp} d\phi, \quad (1.23)$$

where ϕ is an azimuth in the plane transverse to P and Q .

When looking at a $1 \rightarrow 2$ particle transition (with momentum $p_{ij} \rightarrow p_i + p_j$ where p_i and p_j are massless and on-shell) it is common to use a LCD of the following form

$$\begin{aligned} p_i^\mu &= zP^\mu + \frac{k_\perp^2}{z2P \cdot Q} Q^\mu + k^\mu, \\ p_j^\mu &= (1-z)P^\mu + \frac{k_\perp^2}{(1-z)2P \cdot Q} Q^\mu - k^\mu, \end{aligned} \quad (1.24)$$

where

$$p_{ij} = P + \frac{k_\perp^2}{z(1-z)2P \cdot Q} Q.$$

This is known as a Sudakov decomposition. In the limit that p_j goes collinear to p_i , with the scaling given in Section 3.1.1,

$$p_i^\mu = zP^\mu + \mathcal{O}(\lambda), \quad p_j^\mu = (1-z)P^\mu + \mathcal{O}(\lambda), \quad p_{ij} = P + \mathcal{O}(\lambda^2). \quad (1.25)$$

Note that complete momentum conservation in the transition is $\mathcal{O}(\lambda^2)$ and so is typically not relevant at leading (and often next-to-leading) order. With this Sudakov decomposition, the Lorentz invariant phase-space measure is decomposed as

$$\frac{d^3 p_j}{2E_j} = k_\perp^2 \pi \frac{dk_\perp}{k_\perp} \frac{dz}{1-z} \frac{d\phi}{2\pi} = k_\perp^2 \pi \frac{dk_\perp}{k_\perp} \frac{dy d\phi}{2\pi}, \quad (1.26)$$

where ϕ is an azimuth in the plane transverse to P and Q , and y is a pseudo-rapidity in the P, Q dipole frame. Typically the $k_\perp^2 \pi$ pre-factor is absorbed into the integral kernel so that the phase-space is dimensionless and the azimuth is normalised.

A.4 Dimensional regularisation

Integrals can be regularised via a variety of methods. Often, the most intuitive of which is to introduce a cut-off scale that limits the domain of integration so that divergences are avoided (for instance limits of the momentum which can be transferred). However, one of the most useful but less intuitive regularisation procedures is that of dimensional

regularisation (dim reg). This thesis does not find much need for an extensive discussion of regulators, as they are mostly only required when presenting introductory material in Chapters 2 and 3. However, as we do make use of dim reg in those chapters, we will now collate some basic results found in the application of the procedure (we follow the overview in [4]).

Dim reg regularises integrals by allowing the space-time dimension to be a variable. For instance,

$$\int_1^\infty \frac{d^d \vec{x}}{\vec{x}^2} \quad (1.27)$$

diverges for dimensions $d \geq 2$ and otherwise converges. The most popular dimension to use in modern day particle physics is $d = 4 - 2\epsilon$ for $|\epsilon| \ll 1$, which regularises all integrals which diverge logarithmically in $d = 4$ dimensions.² Using this regulator, UV diverges, such as

$$\int_1^\infty \frac{d^{4-2\epsilon} \vec{x}}{\vec{x}^4},$$

are regularised for $\epsilon > 0$ and IR divergences, such as

$$\int_0^1 \frac{d^{4-2\epsilon} \vec{x}}{\vec{x}^4},$$

are regularised for $\epsilon < 0$. Often the regulator is analytically continued so that it is simultaneously positive and negative, regulating both UV and IR diverges. In which case, scaleless integrals evaluate to zero since UV poles are allowed to cancel the IR poles. We can demonstrate this by making the substitution $\vec{x} = \lambda \vec{y}$ for a constant λ :

$$\int_0^\infty \frac{d^{4-2\epsilon} \vec{x}}{\vec{x}^4} = \lambda^{-2\epsilon} \int_0^\infty \frac{d^{4-2\epsilon} \vec{y}}{\vec{y}^4}, \quad (1.28)$$

hence the scaleless integral must be equal to zero.

Integrals in dim reg are most commonly evaluated by using an analytic continuation of spherical polar coordinates: $d^{4-2\epsilon} \vec{x} \mapsto |\vec{x}|^{3-2\epsilon} d|\vec{x}| d\Omega_{4-2\epsilon}$ where Ω_d is a solid angle in d dimensions, defined by the relation

$$\Omega_d = \frac{2\pi^{d/2}}{\Gamma(d/2)}, \quad (1.29)$$

where $\Gamma(d/2)$ is the Euler gamma-function. If \vec{x} is Lorentzian it must be Wick rotated ($x^0 \rightarrow -ix_E^0$), so as to become Euclidean, for spherical polar coordinates to be used. The prototypical integral for dimensional regularisation is

$$\int \frac{d^d \vec{k}}{(2\pi)^{d_i}} \frac{1}{(\vec{k}^2 - 2\vec{p} \cdot \vec{k} - \vec{r}^2 + i0)^\alpha} = \frac{(-1)^\alpha}{(4\pi)^{d/2}} \frac{\Gamma(\alpha - d/2)}{\Gamma(\alpha)} \frac{1}{(\vec{p}^2 + \vec{r}^2 - i0)^{\alpha - d/2}}, \quad (1.30)$$

²The factor of 2 is included to cancel factors of 1/2 which commonly appear in calculations.

where we have replaced the usual $i\epsilon$ from the Feynman propagator with $i0$ to avoid confusion. The additional factor of i on the left hand side is to account for Wick rotating the vectors. Integrals with polynomials of \vec{k} in the numerator can be found by taking derivatives with respect to \vec{p} :

$$\int \frac{d^d \vec{k}}{(2\pi)^d i} \frac{\vec{k}}{(\vec{k}^2 - 2\vec{p} \cdot \vec{k} - \vec{r}^2 + i0)^\alpha} = \frac{(-1)^\alpha \Gamma(\alpha - d/2)}{(4\pi)^{d/2} \Gamma(\alpha)} \frac{\vec{p}}{(\vec{p}^2 + \vec{r}^2 - i0)^{\alpha - d/2}}. \quad (1.31)$$

Most divergent integrals over propagators in loops can be reduced to one of these fundamental forms by using Feynman parameters and completing the square. For more on this we point the reader to more comprehensive sources in the literature [1, 2, 4]. Additionally, for more information on computing generalised integrals over solid angles in d dimensions we direct the reader to the Appendices in the seminal paper [5].

References

- [1] M. E. Peskin, D. V. Schroeder, *An Introduction to quantum field theory*, Addison-Wesley, Reading, USA, **1995**.
- [2] M. D. Schwartz, “Quantum Field Theory and the Standard Model”, *Cam. Press* **2014**.
- [3] H. K. Dreiner, H. E. Haber, S. P. Martin, “Two-component spinor techniques and Feynman rules for quantum field theory and supersymmetry”, *Phys. Rept.* **2010**, *494*, 1–196, arXiv: [0812.1594](https://arxiv.org/abs/0812.1594) [[hep-ph](#)].
- [4] B. L. Ioffe, V. S. Fadin, L. N. Lipatov, *Quantum chromodynamics: Perturbative and nonperturbative aspects*, Vol. 30, Cambridge Univ. Press, **2010**.
- [5] W. Beenakker, H. Kuijf, W. L. van Neerven, J. Smith, “QCD Corrections to Heavy Quark Production in p anti-p Collisions”, *Phys. Rev. D* **1989**, *40*, 54–82.